



The Effects of Surface Layer Proteins
Isolated from *Clostridium difficile* on TLR4
Signalling

A thesis submitted for the degree of Ph.D.

by

Kathy F. Kennedy M.Sc.

January 2016

Based on research carried out at

The School of Biotechnology

Dublin City University

Dublin 9

Under the supervision of Prof. Christine E. Loscher

Declaration

I hereby certify that this material, which I now submit for assessment on the programme of study leading to the award of Doctor of Philosophy is entirely my own work, and that I have exercised reasonable care to ensure that the work is original, and does not to the best of my knowledge breach any law of copyright, and has not been taken from the work of others save and to the extent that such work has been cited and acknowledged within the text of my work.

Signed: _____ (Candidate) ID No.: _____ Date: _____

Table of Contents

Declaration	I
Table of Contents	II
Acknowledgments.....	VI
Abbreviations	VIII
Publications	XIII
Presentations	XIII
List of Tables.....	XV
List of Figures	XVII
Abstract	XXIII
Chapter 1: General Introduction.....	1
1.1 <i>Clostridium difficile</i>	2
1.1.1 Toxin Production	3
1.1.2 <i>Clostridium difficile</i> Spores and Germination	5
1.1.3 Surface Layer Proteins.....	7
1.1.4 Cell Wall Proteins.....	9
1.2 Immune Response to <i>Clostridium difficile</i>	10
1.2.1 SLPs Activate Macrophage and Induce Bacterial Clearance	11
1.2.2 SLPs Induce the Maturation of Dendritic Cells.....	12
1.3 Pattern Recognition Receptors	13
1.3.1 Toll-Like Receptor 4	15
1.3.1.1 MyD88-Dependent Signalling Pathway	16
1.3.1.2 MyD88-Independent Signalling Pathway	18
1.3.2 NF- κ B	20
1.3.3 Interferon Regulatory Factor 3	21
1.4 MicroRNAs	24
1.4.1 MiRNAs Regulate TLRs	26
1.4.2 MiRNAs Regulate Signalling Proteins.....	28
1.4.3 MiRNAs Regulate Transcription Factors	29
1.4.4 MiRNAs Regulate Cytokines and Chemokines	30
1.4.5 MiRNAs Regulate Other Regulatory Molecules.....	30
1.5 Aims and Objectives.....	34
Chapter 2: Materials and Methods	35

2.1 Materials	36
2.2 Methods	41
2.2.1 Characterisation of SLPs	41
2.2.1.1 SDS-PAGE	42
2.2.1.2 Protein Concentration of SLPs	43
2.2.1.3 Endotoxin Assay	44
2.2.2 Cell Culture Techniques	44
2.2.2.1 Revival of Frozen Stocks	44
2.2.2.2 Cell Enumeration and Viability Assessment	45
2.2.2.3 Cryogenic Preservation of Cell Line Stocks	46
2.2.3 Bone Marrow Derived Dendritic Cell Isolation and Culture	46
2.2.4 Hek-293 and Hek TLR4/MD2/CD14 Cell Culture	47
2.2.5 JAWS II Dendritic Cell Line Culture	47
2.2.6 Cell Stimulation	48
2.2.7 Cytotoxicity Assay	48
2.2.8 Enzyme Linked Immunosorbent Assay (ELISA)	48
2.2.8.1 Detection of Murine/Human Cytokines & Chemokines	49
2.2.8.2 Detection of IL-1 β and IL-8	50
2.2.9 Flow Cytometry	50
2.2.9.1 Cell Surface Staining of BMDCs	50
2.2.10 Purification of Plasmid DNA	51
2.2.11 Transient Transfection of Cells	52
2.2.11.1 NF- κ B assays	53
2.2.11.2 IRF3 assays	53
2.2.11.3 MiRNA mimics	53
2.2.12 Luciferase Assays	54
2.2.13 RNA Isolation	55
2.2.13.1 Total Isolation from Cell Lines	55
2.2.13.2 Enrichment of Total RNA Derived from <i>C. difficile</i> Infection model	57
2.2.14 Agarose Gel Electrophoresis to Assess RNA Integrity	58
2.2.15 cDNA Synthesis	59
2.2.15.1 cDNA Synthesis for Pool A and B TLDA Cards	59
2.2.15.2 cDNA Synthesis for Custom TLDA Cards and Individual miRNA assays ..	60
2.2.16 Pre-amplification of cDNA	61
2.2.16.1 Pre-amplification Reaction for Pool A and pool B TLDA Cards	61

2.2.16.2	Pre-amplification for Custom TLDA Cards and Individual miRNA Assays	62
2.2.17	Running Taqman® Low Density Arrays (TLDA) cards	63
2.2.18	Running Custom TLDA cards	64
2.2.19	Running Individual Taqman miRNA Assays	65
2.2.20	MiRNA Data Analysis following qPCR	66
2.2.20.1	MiRNA Data Analysis of Targets from Pool A and B TLDA Cards	67
2.2.20.2	MiRNA Data Analysis of Targets from Custom TLDA Cards	68
2.2.20.3	MiRNA Analysis of Targets from Individual miRNA Assays	68
2.2.21	MiRNA Gene/Target/Pathway Predictions using Bioinformatics	69
Chapter 3: Characterising the Immune Response of SLPs from <i>C. difficile</i> in BMDCs		71
3.1	Introduction	72
3.2	Results	76
3.2.1	Characterisation of SLPs from <i>C. difficile</i>	76
3.2.2	SLPs Modulate Cell Surface Marker Expression on BMDCs	76
3.2.3	SLPs Induce Cytokine Production in BMDCs	78
3.2.4	SLPs from RT 027 Activate NF- κ B and IRF3	79
3.3	Discussion	100
Chapter 4: Profiling the MiRNAs Induced by SLPs from <i>C. difficile</i>		108
4.1	Introduction	109
4.2	Results	112
4.2.1	Optimising a Method for Profiling MiRNAs Induced by SLPs from <i>C. difficile</i>	112
4.2.2	TLDA Card Analysis Parameters	114
4.2.3	Profiling Studies Using TLDA Cards Revealed 16 MiRNAs were Differentially Regulated in Response to LPS and SLPs from RT 001	115
4.2.4	Additional MiRNAs of Interest were Chosen for Further Validation Following a Review of the Literature and Re-examination of the Profiling Study	116
4.2.5	Custom TLDA Card Analysis Parameters	117
4.2.6	Twenty-Four MiRNAs were Differentially Regulated by SLPs from RT 001 and RT 027	117
4.2.7	Further Validation Confirmed let-7e, miR-155, miR-145 and miR-146a were Differentially Regulated in Response to SLPs from RT 001 and RT 027	119
4.2.8	Let-7e, miR-155, miR-145 and miR-146a were Differentially Regulated in JAWS II Cells	120
4.3	Discussion	170

Chapter 5: Validation of miRNA Targets in a <i>C. difficile</i> Infection Model and Analysis of miRNA Functionality	178
5.1 Introduction	179
5.2 Results	183
5.2.1 Optimising miRNA Mimics for Luciferase Gene Reporter Assays	183
5.2.2 Mimics Over Expressing miR-146a, miR-145, miR-155 and let-7e Individually Target IRF3 Signalling in Response to LPS but not in Response to SLPs from RT 001 and RT 027	188
5.2.3 MiRNAs were Enriched from RNA Derived from Colonic Tissue from an <i>in vivo</i> <i>C. difficile</i> Infection Model	193
5.2.4 MiR-146a, miR-145, miR-155 and let-7e were Differentially Regulated in Colonic Tissue During <i>C. difficile</i> Infection with RT 001 and RT 027	194
5.2.5 Bioinformatics Analysis Reveals miRNAs Induced by SLPs from RT 001 and RT 027 Target Genes Involved in Essential Cell Signalling Pathways.....	196
5.2.6 Forty-nine Genes Crossed Two or More Pathways from the Top Five Analysed, Most Genes had Predicted Binding sites in the 3'UTR regions for the miRNAs of Interest according to TargetScan	199
5.2.7 Genes with Predicted Binding Sites for the miRNAs of Interest are found in Distinctive Groups, Examples from IL-6, NRAS, SMAD2, SOS1 and TRAF6..	201
5.3 Discussion.....	252
Chapter 6: General Discussion.....	262
6.1 General Discussion	263
Chapter 7: Bibliography	276
7.1 Bibliography	277
Appendices.....	311
Appendix A- Buffers and Solutions.....	312
Appendix B- SLP Characterisation.....	317
Appendix C- Plasmid DNA Constructs	319
Appendix D- RNA Quality Assurance.....	320
Appendix E- Taqman Assays.....	321
Appendix F- Endogenous Controls for qPCR.....	343
Appendix G- Bioinformatics.....	344

Acknowledgments

First and foremost I would like to thank my supervisor Prof. Christine Loscher. Your dedication, drive, passion and enthusiasm are truly inspiring. Thank you for encouraging and believing in me.

X181B became my second home and the Loscher lab my second family. Laura, Maja, Iza, Joey, Catherine, Mark, Fiona, Kim and Niamh I learnt from the very best. Thank you for helping to make me the scientist I am today and for all the support, friendship, guidance and laughs over the years. Iza, we went on many adventures together, these are memories I will never forget.

Thank you to the staff and students in the School of Biotechnology and everybody I have encountered in DCU on the way. Thank you Alisha for always having a kind word to say, I always looked forward to dropping in to your lab and having a catch up. Alli I can't thank you enough for your friendship and support. You have always been there for me, tea and chats with you in the nursing building kept me going.

Thank you to everybody involved in the BioAT programme, in particular Joan Kelly for looking after us all. Thank you to my fellow DCU BioAT's for the support and friendship.

To my wonderful friends, you guys have been amazing. In particular the girls, Kate, Germaine, Katie, Emma M, Elaine, Ro, Sammy, Michèle, Sarah, Caoimhe, Orlaith and Emma G, I can't thank you enough for all of the messages of support and pep talks when I needed it.

Thank you to my amazing family, to all of the Leonards and Kennedys. Nana Rose, my number one cheerleader, you will forever be in my heart. Mam, Dad and Paul, I could not have done this without you. You always told me to dream big and believe in myself. Thank you with all of my heart. Last but not least I would like to thank my partner Kevin for his love and support throughout, I am so excited we begin a new chapter of our lives together.

I dedicate this thesis to my family and in loving memory of my uncle Charlie Leonard
(1948-2014)

Abbreviations

ACHE	Acetyl Cholinesterase
ADP	Adenosine Diphosphate
Ago	Argonaute
APC	Allophycocyanin
AP-1	Activator protein 1
APS	Ammonium persulphate
ANOVA	Analysis of Variance
BCA	Bicinchoninic Acid
BMDC	Bone Marrow derived Dendritic Cell
BHI	Brain Heart Infusion
BSA	Bovine Serum Albumin
CaM-Kinase II	Calcium/calmodulin dependent protein Kinase II
CBP	cAMP responsive element Binding Protein
C/EBP β	CCAAT/Enhancer Binding Protein- β
cDNA	Complementary DNA
<i>C. difficile</i>	<i>Clostridium difficile</i>
CD	Cluster of Differentiation
CDI	<i>Clostridium difficile</i> Infection
CDT	<i>Clostridium difficile</i> Transferase
Ct	Threshold cycle
CTLA4	Cytotoxic T-lymphocyte-Associated protein 4
CWPs	Cell Wall Proteins
CXCL10	C-X-C motif Chemokine 10
CX3CR1	C-X-3-C Chemokine Receptor 1
DCs	Dendritic Cells
DBD	DNA-Binding Domain
DEPC	Diethylprocarbonate
DNA	Deoxyribonucleic Acid
DPA	Dipicolinic Acid
DTT	Dithiothreitol

ECM	Extracellular Matrix
EDTA	Ethylenediaminetetraacetic Acid
ELISA	Enzyme Linked Immunosorbent Assay
ETS-1	E26 Transformation specific Sequence 2
FADD	Fas-Associated Death Domain protein
FAE	Follicle-Associated Epithelium
FBS	Foetal Bovine Serum
FDR	False Discovery Rate
FITC	Fluorescein Isothiocyanate
FMT	Faecal microbiota transplantation
Foxp3	Forkhead box p3
FRET	Fluorescence Resonance Energy Transfer
GALT	Gut-Associated Lymphoid Tissue
GI	Gastrointestinal
G-proteins	Guanine nucleotide-binding proteins
GRs	Germinant Receptors
GTPases	Guanosine Triphosphatase
GM-CSF	Granulocyte-Macrophage Colony-Stimulating Factor
Hek-293	Human Embryonic Kidney 293
<i>H. pylori</i>	<i>Helicobacter pylori</i>
HMW	High Molecular Weight
ICAM	Intracellular Adhesion Molecule
IFNs	Interferons
IKK	Inhibitory- κ B Kinase
IL	Interleukin
iNOS	Inducible Nitric Oxide Synthase
IRAK	IL-R Associated Kinase
IRF3	Interferon Regulatory Factor 3
ISGF3	Interferon Stimulated Gene Factor 3
ISRE	Interferon-Stimulated Response Element
JNK	c-Jun N-terminal Kinases
K63	Lysine 63

Kb	Kilobase
kDa	Kilodaltons
KEGG	Kyoto Encyclopaedia of Genes and Genomes
LAL	Limulus Amebocyte Lysate
LB	Lysogeny Broth
LBP	LPS Binding Protein
LMW	Low Molecular Weight
LP	<i>Lamina propria</i>
LPS	Lipopolysaccharide
LRR	Leucine Rich Repeats
Mal	MyD88 adaptor like
MAPK	Mitogen Activated Protein Kinase
MAP2K	MAPK Kinase
MAP3K	MAPKK Kinase
MFI	Mean Fluorescence Intensity
MKK3	Mitogen activated protein Kinase Kinase 3
M-cells	Microfold cells
MCP-1	Monocyte Chemo attractant Protein 1
MD2	Myeloid Differentiation protein 2
MGB	Minor Groove Binding
MiRNAs	MicroRNAs
MiRISC	MiRNA-Induced Silencing Complex
MIP-2	Macrophage Inflammatory Protein 2
MLNs	Mesenteric Lymph Nodes
mRNA	Messenger RNA
MyD88	Myeloid Differentiation primary response gene 88
NAP1	NF- κ B Activating Kinase Associated Protein 1
NES	Nuclear Export Sequences
NK cells	Natural Killer cells
NLS	Nuclear Localisation Sequences
Ns	Not Significant
Nt	Nucleotide

NTC	No Template Control
NF- κ B	Nuclear Factor κ light chain enhancer of activated B cells
OD	Optical Density
ORFs	Open Reading Frames
oxLDL	Oxidized Low Density Lipoprotein
PaLoc	Pathogenicity Locus
PAMPs	Pattern Associated Molecular Patterns
PBS	Phosphate Buffered Saline
PCC	Pearson's product moment Correlation Coefficient
PDCD4	Protein Programmed Cell Death 4
PE	Phycoerythrin
PPAR γ	Peroxisome Proliferator-Activated Receptor
Poly-A	Poly Adenylated
PCR	Polymerase Chain Reaction
PG	Peptidoglycan
PI	Proprodium Iodide
PMT	Photomultiplier Tubes
PPs	Peyer's Patches
PRRs	Pattern Recognition Receptors
QC	Quality Control
qPCR	Quantitative real time PCR
RANTES	Regulated on Activation Normal T cell Expressed and Secreted
RHD	Rel Homology Domain
RIP-1	Receptor Interacting Protein 1
RIPK1	Receptor (TNFRSF)-Interacting Serine-Threonine Kinase 1
RNA	Ribonucleic Acid
RT	Ribotype
RQ	Fold change
dsRNA	Double stranded RNA
rRNA	Ribosomal RNA
SEM	Standard Error of the Mean
SDS	Sodium dodecylsulphate

SDS-PAGE	Sodium Dodecylsulphate-Polyacrylamide Electrophoresis
SHIP1	Src Homology 2 domain-containing Inositol-5'-Phosphatase 1
S-layer	Surface layer
SLPs	Surface Layer Proteins
SPF	Specific Pathogen Free
stRNA	Small temporal RNA
SOCS1	Suppressor of Cytokine Signalling 1
STAT	Signal Transducer and Activator of Transcription
TAB1	TAK1 Binding protein 1
TAK1	Transforming growth factor- β -Activated Kinase 1
TBK1	Tank Binding Kinase 1
TEMED	N,N,M'- Tetramethylethylenediamine
TGF- β	Transforming Growth Factor beta
Th cells	T helper cells
TIR	Toll/IL-1 receptor homology
TLDA	Taqman Low Density Arrays
TLR	Toll-like Receptors
TLR4	Toll-like Receptor 4
T(m)	Melting temperature
TMB	3,3',5,5'-tetramethyl-benzidine
TNFRSF	Tumour Necrosis Factor Receptor Superfamily
TNF α	Tumour Necrosis Factor alpha
Treg	Regulatory T-cells
TRAF3	TNF Receptor Associated Factor
TRAM	TRIF-Related Adapter Molecule
TRIF	TIR- domain containing adaptor inducing Interferon- β
Ubc13	Ubiquitin conjugating enzymes 13
Uev1a	Ubiquitin conjugating enzyme E2 variant 1 isoform A
UTR	Untranslated region
VCAM-1	Vascular Cellular Adhesion Molecule 1

Publications

***Clostridium difficile* Ribotype 027 Induces More Severe Infection *in vivo* Compared to Ribotype 001.**

M. Lynch, M. Kristek, J. DeCoursey, I. Marszalowska, K. Kennedy, P. Casey, M. MacAogáin, T. Rogers, C. E. Loscher
Manuscript in preparation

Presentations

MicroRNAs are Differentially Regulated by Surface Layer Proteins Isolated from *Clostridium difficile*

K. Kennedy, I. Marszalowska, M. Lynch, P. Moynagh, and C.E. Loscher
Irish Society for Immunology Annual Meeting
TBSI Dublin, September 2015
Poster Presentation

MicroRNAs are Differentially Regulated by Surface Layer Proteins Isolated from *Clostridium difficile*

K. Kennedy, I. Marszalowska, M. Lynch, P. Moynagh, and C.E. Loscher
BioAT Research Day
IT Tallaght Dublin, June 2015
Oral Presentation

MicroRNAs are Differentially Regulated by Surface Layer Proteins Isolated from *Clostridium difficile*

K. Kennedy, I. Marszalowska, M. Lynch, P. Moynagh, and C.E. Loscher
Keystone Symposia Meeting: “Gut Microbiota Modulation of Host Physiology: The Search for Mechanism”
Keystone, Colorado, USA, March 2015
Poster Presentation

Profiling Study Reveals microRNAs are Differentially Regulated by Surface Layer Proteins Isolated from *Clostridium difficile*

K. Kennedy, I. Marszalowska, M. Lynch, P. Moynagh, and C.E. Loscher
School of Biotechnology Annual Research Day
DCU Dublin, January 2015
Oral Presentation

Profiling Study Reveals microRNAs are Differentially Regulated by Surface Layer Proteins Isolated from *Clostridium difficile*

K. Kennedy, I. Marszalowska, M. Lynch, P. Moynagh, and C.E. Loscher
Irish Society for Immunology Annual Meeting
Crowne Plaza Dublin, September 2014
Poster Presentation

Profiling Study Reveals microRNAs are Differentially Regulated by Surface Layer Proteins Isolated from *Clostridium difficile*”

K. Kennedy, I. Marszalowska, M. Lynch, P. Moynagh, and C.E. Loscher
BioAT Research Day 2014
DCU Dublin, June 2014
Oral Presentation

Can microRNAs Help us Solve the Problem of Hospital Acquired Infection?

K. Kennedy, I. Marszalowska, M. Lynch, P. Moynagh, and C.E. Loscher
Pitch in 3 competition, School of Biotechnology Annual Research Day
DCU Dublin, February 2014
Oral Presentation

Surface Layer Proteins Isolated from *Clostridium difficile* Activate the MyD88-Dependent Signalling Pathway Downstream of TLR4

K. Kennedy, I. Marszalowska, M. Lynch, S. Gargan, P. Moynagh, and C.E. Loscher
School of Biotechnology Annual Research Day
DCU Dublin, February 2014
Poster Presentation

Surface Layer Proteins Isolated from *Clostridium difficile* Activate the MyD88-Dependent Signalling Pathway Downstream of TLR4

K. Kennedy, I. Marszalowska, M. Lynch, S. Gargan, P. Moynagh, and C.E. Loscher
Irish Society for Immunology Annual Meeting
Crowne Plaza Dublin, September 2013
Poster Presentation

The Effects of Surface Layer Proteins Isolated from *Clostridium difficile* on TLR4 Signalling

K. Kennedy, P. Moynagh, and C.E. Loscher
BioAT Research Day
NUI Maynooth Dublin, June 2013
Poster Presentation

The Effects of Surface Layer Proteins Isolated from *Clostridium difficile* on TLR4 Signalling

K. Kennedy, P. Moynagh, and C.E. Loscher
School of Biotechnology Annual Research Day
DCU Dublin, January 2013
Poster Presentation

Surface Layer Proteins as Important Virulence Factors in *Clostridium difficile* infection

M. Lynch, K. Kennedy, D. Kelleher, M. O’Connell & C. Loscher.
European Congress of Immunology
SECC Glasgow, September 2012
Poster Presentation

List of Tables

Table 1.4.1 Summary of miRNAs that regulate TLR4 signalling	32
Table 2.1.1 Tissue cell culture	36
Table 2.1.2 Characterisation of SLPs.....	36
Table 2.1.3 SDS-PAGE	37
Table 2.1.4 Enzyme Linked Immunosorbent Assay (ELISA)	37
Table 2.1.5 Flow Cytometry	38
Table 2.1.6 Plasmid DNA preparation and transfection	38
Table 2.1.7 Luciferase gene reporter assay	39
Table 2.1.8 RNA and DNA integrity by gel electrophoresis	39
Table 2.1.9 RNA isolation, cDNA synthesis and qPCR.....	40
Table 2.2.1 Accession numbers for the slpA gene for each ribotype used in this study, sequences from GenBank.....	42
Table 2.2.2 Recipe for cDNA synthesis for pool A and pool B TLDA cards	60
Table 2.2.3 Thermocycler conditions for cDNA synthesis for pool A and B TLDA cards	60
Table 2.2.4 Recipe for cDNA synthesis for custom TLDA cards and individual miRNA assays	61
Table 2.2.5 Thermocycler conditions for cDNA synthesis for custom TLDA cards and individual miRNA assays.....	61
Table 2.2.6 Recipe for pre-amplification master mix for pool A and B TLDA cards	62
Table 2.2.7 Thermocycler conditions for pre-amplification	62
Table 2.2.8 Recipe for pre-amplification master mix for custom TLDA cards and individual miRNA assays.....	63
Table 2.2.9 Recipe for cDNA with pre-amplification for running on pool A and B TLDA cards.....	64
Table 2.2.10 Recipe for cDNA without pre-amplification for running on pool A and B TLDA cards.....	64
Table 2.2.11 Default thermocycler parameters for running pool A and B TLDA cards	64
Table 2.2.12 Recipe for reaction mix for Custom TLDA cards.....	65
Table 2.2.13 Thermocycler conditions for custom TLDA cards	65

Table 2.2.14 Recipe for reaction mix for individual TaqMan® microRNA Assays	66
Table 2.2.15 Thermocycler conditions for Individual TaqMan® microRNA Assays....	66
Table 4.2.1 qPCR analysis detected 254 miRNAs in Hek TLR4/MD2/CD14 cells from the 756 miRNAs analysed using the TLDA pool A & B cards.	125
Table 4.2.2. Sixteen miRNAs have statistically significant fold changes when Hek TLR4/MD2/CD14 cells were stimulated with LPS and SLPs from RT 001.	151
Table 4.2.3. List of miRNAs to be included in custom TLDA cards based on a review of the literature and re-examination of the profiling study.	152
Table 4.2.4 qPCR data analysis detected 28 miRNAs in Hek TLR4/MD2/CD14 cells stimulated with LPS, SLPs from RT 001 and RT 027 from the 31 miRNAs analysed on custom TLDA cards.	155
Table 4.2.5 Four miRNAs of interest were chosen for further validation based on the differences between expression in response to SLPs from RT 001 and RT 027. .	165
Table 4.2.6 Expression of miR-146a, miR-145, miR-155 and let-7e in response to SLPs from RT 027 is similar in Hek TLR4/MD2/CD14 cells and JAWS II cells.	169
Table 5.2.1 MiRNAs differentially regulated by SLPs from RT 001 and RT 027 are involved in essential cell signalling pathways.	225
Table 5.2.2 Forty-nine genes crossed two or more of the top 5 KEGG pathways and not all genes had predicted binding sites for the 24 miRNAs of interest.	231
Table 5.2.3 Some genes in the PI3K-Akt signalling pathway had predicted binding sites for the 24 miRNAs of interest.	234
Table 5.2.4 Some genes in the TGF- β signalling pathway had predicted binding sites for the 24 miRNAs of interest.	238
Table 5.2.5 Some genes involved in Focal adhesion had predicted binding sites for the 24 miRNAs of interest.	241
Table 5.2.6 Some genes in the MAPK signalling pathway had predicted binding sites for the 24 miRNAs of interest.	243

List of Figures

Figure 1.1.1 Image of ‘volcano-like’ lesions as a result of the local inflammatory effects of <i>C. difficile</i> infection in the colon.....	3
Figure 1.1.2 Image illustrating the destruction of the cellular barriers by TcdA and TcdB release from <i>C. difficile</i> leading to the pathogenesis of CDI.....	4
Figure 1.1.3 3D model of the proposed structure and orientation of the HMW and LMW SLPs on the surface of <i>C. difficile</i>	8
Figure 1.3.1 Image showing TLRs and the patterns of microbial components they recognise	14
Figure 1.3.2 Two distinct signalling pathways are activated following activation of TLR4, the MyD88-dependent and MyD88-independent signalling pathway.....	15
Figure 1.3.3 Downstream signalling following activation of MyD88-dependent and MyD88-independent signalling pathways following TLR4 activation.....	19
Figure 1.3.4 Image showing the generalised structures of the two subfamilies Rel and NF- κ B and related signalling molecules.....	21
Figure 1.3.5 Illustration showing that IRF3 contributes to the balance between IL-12 family members in antigen presenting cells.....	23
Figure 1.4.1 Image showing the processing of pri-miRNA to pre-miRNA.....	25
Figure 1.4.2 Image illustrating the array of miRNAs involved in the regulation of the TLR4 signalling pathway at multiple levels involving multiple molecules	27
Figure 2.2.1 Representation of the Neubauer haemocytometer used to count cells.	45
Figure 2.2.2 Summary of the RNA Isolation procedure.	56
Figure 2.2.3 Image depicting RNA-specific stem-looped reverse transcription primers	59
Figure 2.2.4 Screen shot from ExpressionSuite software of quality control criteria for TLDA card data	67
Figure 2.2.5 Diagrammatic representation of the types of miRNA matches predicted in TargetScan	70
Figure 3.1.1 Illustration of the range of clinical symptoms associated with CDI, comparing ribotype 001 with ribotype 027	72

Figure 3.2.1 SLPs from RT 005, RT 027, RT 031, RT 078 and RT 001 contain a conserved HMW protein at 44kDA and variable LMW band ranging from 35-37 kDA.....	83
Figure 3.2.2 BMDCs stimulated with LPS and SLPs from RT 001 do not notably affect cell viability.....	84
Figure 3.2.3 CD11c ⁺ population of BMDCs range from 70-73% when stimulated with LPS and SLPs from RT 001.....	85
Figure 3.2.4 SLPs from RT 001 modulate the expression of CD40 and CD14 on BMDCs.	86
Figure 3.2.5 SLPs from RT 001 modulate the expression of CD80 and CD86 on BMDCs.	87
Figure 3.2.6 CD11c ⁺ population of BMDCs range from 70-75% when stimulated with LPS and SLPs from RT 005, RT 027 and RT 031.....	88
Figure 3.2.7 SLPs from RT 005, RT 031 and RT 027 modulate the expression of CD14 on BMDCs.	89
Figure 3.2.8 SLPs from RT 005, RT 031 and RT 027 modulate the expression of CD40 on BMDCs.	90
Figure 3.2.9 SLPs from RT 005, RT 031 and RT 027 modulate the expression of CD80 on BMDCs.	91
Figure 3.2.10 SLPs from RT 005, RT 031 and RT 027 modulate the expression of CD86 on BMDCs.	92
Figure 3.2.11 SLPs from RT 001, RT 005, RT 031 and RT 027 induce the production of murine IL-1 β , IL-6, IL-12p40, IL-10, IL-23, TNF α and IL-12p70 in BMDCs.....	93
Figure 3.2.12 Time course analysis shows that the optimal time point is after 12 hours for examining the expression of NF- κ B and IRF3 expression in Hek TLR4/MD2/CD14 cells stimulated with LPS.....	94
Figure 3.2.13 Time course analysis shows 18 hours is the optimal time for examining the expression of human IL-8 and RANTES expression in Hek TLR4/MD2/CD14 cells stimulated with LPS.....	95
Figure 3.2.14 SLPs from RT 001 activates NF- κ B but it does not activate IRF3 downstream of TLR4.	96

Figure 3.2.15 SLP from RT 001 activates NF- κ B but do not activate IRF3 downstream of TLR4.....	97
Figure 3.2.16 SLPs from RT 001, RT 014, RT 027 and RT 078 activate NF- κ B. SLPs do not activate IRF3 with the exception of SLPs from RT 027.....	98
Figure 3.2.17 SLPs from RT 001, RT 014, RT 027 and RT 078 activate NF- κ B downstream of TLR4. SLPs do not activate IRF3 downstream of TLR4 with the exception of RT 027.....	99
Figure 4.1.1 Stem loop primers for miRNA detection and PCR using TaqMan chemistry	111
Figure 4.2.1 SLPs from RT 001 and RT 027 induce IL-8 after 8 hours in Hek TLR4/MD2/CD14 cells, however SLPs from RT 001 fail to induce RANTES...	122
Figure 4.2.2 Starting RNA of 350 ng and a pre-amplification step are required for the detection of miRNA for use in this study.	123
Figure 4.2.3. Overall Ct values follow normal distribution in miRNA profiling study with pool A & B TLDA cards.....	124
Figure 4.2.4. Ct Scatter plot shows there are differences in miRNA profiles between Hek TLR4/MD2/CD14 cells stimulated with LPS and SLPs from RT 001.	148
Figure 4.2.5. Volcano plot showing four miRNAs are significantly differentially regulated when Hek TLR4/MD2/CD14 cells were stimulated with LPS.....	149
Figure 4.2.6. Volcano plot showing 12 miRNAs were significantly differentially regulated when Hek TLR4/MD2/CD14 cells were stimulated with SLPs from RT 001.....	150
Figure 4.2.7 Overall Ct values follow normal distribution in miRNAs detected in custom TLDA cards.....	154
Figure 4.2.8 Ct Scatter plot shows there are differences in miRNA profiles between Hek TLR4/MD2/CD14 cells stimulated with LPS, SLPs from RT 001 and RT 027 compared to the control.....	159
Figure 4.2.9 Ct Scatter plot shows there are differences in miRNA profiles between Hek TLR4/MD2/CD14 cells stimulated with LPS, SLPs from RT 001 and RT 027 compared to each other.	160

Figure 4.2.10 Visual representation of miRNAs differentially regulated when Hek TLR4/MD2/CD14 cells were stimulated with LPS and SLPs from RT 001 and RT 027.....	162
Figure 4.2.11 MiR-145 and miR-146a were significantly up regulated when Hek TLR4/MD2/CD14 cells were stimulated with SLPs from RT 001.....	163
Figure 4.2.12 Twenty three miRNAs were significantly down regulated when Hek TLR4/MD2/CD14 cells were stimulated with SLPs from RT 027.....	164
Figure 4.2.13 MiR-146a, miR-145, miR-155 and let-7e are differentially regulated in Hek TLR4/MD2/CD14 cells stimulated with SLPs from RT 001 and RT 027....	166
Figure 4.2.14 SLPs from RT 001 and RT 027 induce the production of murine IL-1 β , TNF α , MCP, IL-6, RANTES and MIP-2 in JAWS II cells.	167
Figure 4.2.15 MiR-146a and miR-145, miR-155 and let-7e are differentially regulated in JAWS II cells stimulated with SLPs from RT 001 and RT 027.	168
Figure 5.1.1 Diagram depicting seed match between miRNA and target mRNA	180
Figure 5.2.1 MiRNA mimic over expressing miR-146a decrease RANTES production in a dose dependent but do not effect IL-8 production in response to LPS.	205
Figure 5.2.2 MiRNA mimic over expressing miR-145 decrease RANTES production in a dose dependent manner but do not significantly affect IL-8 production in response to LPS.....	206
Figure 5.2.3 MiRNA mimic over expressing miR-155 decrease RANTES production in a dose dependent manner but does not affect IL-8 production in response to LPS.	207
Figure 5.2.4 1nM and 100 nM miRNA mimic over expressing let-7e decreases RANTES production but do not effect IL-8 production when stimulated with LPS.	208
Figure 5.2.5 Transfection of plasmid DNA, miRNA mimics and stimulation with LPS and SLPs from RT 001 and RT 027 do not notably affect viability of the Hek TLR4/MD2/CD14 cells.....	209
Figure 5.2.6 The positive control miRNA mimic decreased NF- κ B and IRF3 gene expression in response to LPS and SLPs from RT 001 and 027.....	210
Figure 5.2.7 The positive control miRNA mimic decreased IL-8 and RANTES cytokine production in response to LPS and SLPs from RT 001 and 027.	211

Figure 5.2.8 MiR-146a targets IRF3 signalling in response to LPS but not in response to SLPs from RT 001 and RT 027.	212
Figure 5.2.9 MiR-146a targets RANTES production in response to LPS but not in response to SLPs from RT 001 and RT 027.	213
Figure 5.2.10 MiR-145 targets IRF3 signalling in response to LPS but not in response to SLPs from RT 001 and RT 027.	214
Figure 5.2.11 MiR-145 targets RANTES production in response to LPS but not in response to SLPs from RT 001 and RT 027.	215
Figure 5.2.12 MiR-155 targets IRF3 signalling in response to LPS but not in response to SLPs from RT 001 and RT 027.	216
Figure 5.2.13 MiR-155 targets RANTES production in response to LPS but not in response to SLPs from RT 001 and RT 027.	217
Figure 5.2.14 Let-7e targets IRF3 signalling in response to LPS but not in response to SLPs from RT 001 and RT 027.	218
Figure 5.2.15 Let-7e targets RANTES production in response to LPS but not in response to SLPs from RT 001 and RT 027.	219
Figure 5.2.16 MiR-146a is differentially regulated in colonic tissue of mice treated with RT 027 at day 3 and day 7 of infection.	220
Figure 5.2.17 MiR-145 is differentially regulated in colonic tissue of mice treated with RT 027 at day 3 and day 7 of infection.	221
Figure 5.2.18 MiR-155 is differentially regulated in colonic tissue of mice treated with RT 001 at day 3 of infection.	222
Figure 5.2.19 Let-7e is differentially regulated in colonic tissue of mice treated with RT 001 at day 3 of infection.	223
Figure 5.2.20. Heat map showing pathways interactions from miRNAs differentially regulated by SLPs from RT 001 and RT 027.	224
Figure 5.2.21 MiRNAs differentially regulated by SLPs from RT 001 and RT 027 may modulate genes involved in ECM-receptor interaction.	226
Figure 5.2.22. MiRNAs differentially regulated by SLPs from RT 001 and RT 027 may modulate genes involved in TGF- β signalling pathway.	227
Figure 5.2.23 MiRNAs differentially regulated by SLPs from RT 001 and RT 027 may modulate genes involved in the MAPK signalling pathway.	228

Figure 5.2.24 MiRNAs differentially regulated by SLPs from RT 001 and RT 027 may modulate genes involved in the PI3K-Akt signalling.	229
Figure 5.2.25 MiRNAs differentially regulated by SLPs from RT 001 and RT 027 may modulate genes involved in focal adhesion.	230
Figure 5.2.26 The IL-6 receptor gene contains possible 3'UTR binding sites for miR-125, miR-590, miR-155, miR-9 and let-7 b/c/d/e which were differentially regulated by SLPs from RT 001 and RT 027. These miRNAs were clustered in three distinct groups.	247
Figure 5.2.27 The NRAS gene contains possible 3'UTR binding sites for miR-152, miR-148b, miR-146a, let-7 b/c/d/e and miR-145 which are differentially regulated by SLPs from RT 001 and RT 027. These miRNAs were clustered in three distinct groups and let-7 b/c/d/e had 2 possible binding sites.....	248
Figure 5.2.28 The SMAD2 gene contains possible 3'UTR binding sites for miR-132, miR-125a, let-7 b/c/d/e, miR-145, miR-152, miR-148b and miR-155 which are differentially regulated by SLPs from RT 001 and RT 027. These miRNAs were clustered in three distinct groups.	249
Figure 5.2.29 The SOS1 gene contains possible 3'UTR binding sites for miR-152, miR-148b, miR-9, miR-132 and miR-155 which are differentially regulated by SLPs from RT 001 and RT 027. These miRNAs were clustered in two distinct groups.	250
Figure 5.2.30 The TRAF6 gene contains possible 3'UTR binding sites for miR-146a and miR-125a which are differentially regulated by SLPs from RT 001 and RT 027. These miRNAs were clustered in one group and miR-146a has 3 possible binding sites.	251

Abstract

The Effects of Surface Layer Proteins Isolated from *Clostridium difficile* on TLR4 signalling- Kathy F. Kennedy M.Sc.

Clostridium difficile (*C. difficile*) is a gram-positive, spore-forming, pathogenic bacterium that results in a range of gastrointestinal diseases. The incidence of *C. difficile* infection (CDI) has increased dramatically and has a significant impact on healthcare settings worldwide. The severity of disease may be dependent on the ribotype (RT) of *C. difficile* present. Previous research from our laboratory has shown that Surface Layer Proteins (SLPs) from RT 001 activate Toll-like receptor 4 (TLR4), with subsequent activation of downstream signalling pathways known to be important in the clearance of CDI. In this study we demonstrate that SLPs from RT 001 fail to activate IRF3 signalling, while SLPs from RT 027 activate both arms of the TLR4 pathway. Evidence from the literature suggests that microRNAs (miRNAs) tightly regulate TLR4 signalling and have a role in orchestrating the host's immune response to infection. The profile of miRNAs regulated in response to SLPs from *C. difficile* has not been profiled before. Subsequently we identified novel miRNAs regulated in response to LPS, SLPs from RT 001 and RT 027 *in vitro*. We found 24 miRNAs were differentially regulated between SLPs in response to RT 001 and RT 027 and there was a global down regulation of miRNAs in response to SLPs from RT 027. These miRNAs may modulate TLR4 signalling. Data from colonic tissue, from an *in vivo* murine model show miR-146a, miR-145, miR-155 and let-7e may have a role in regulating the host's immune response during early and late stage CDI. The absence of miRNAs regulated in response to RT 027 may correlate to less efficient clearance by the host's immune response and more persistent infection. The miRNAs are predicted to target essential cell processes and the impact of the modulation of the immune response by these miRNAs may lead to biologically relevant changes at the cell level. Further work is needed to fully elucidate the complexities of these miRNAs in relation to the networks they modulate. The effectiveness of current treatments is limited by a lack of response in some patients and high recurrence rates. The data generated in this study may be used to develop miRNA based therapy for the treatment of persistent CDI, allowing bacterial clearance by the host's immune system without the need for antibiotics.

Chapter 1: General Introduction

1.1 *Clostridium difficile*

Clostridium difficile (*C. difficile*) is a gram-positive, spore-forming, rod-shaped anaerobic bacterium that causes a range of gastrointestinal diseases known as *Clostridium difficile* Infection (CDI) (Bartlett, 1994; Fagan et al., 2009; Kachrimanidou & Malisiovas, 2011). It is the leading cause of antibiotic-associated diarrhoea worldwide (Dawson, Valiente, & Wren, 2009; Dubberke, 2012). *C. difficile* can only colonise the gut if the normal intestinal microbiota is disturbed or absent, in most cases this is achieved by the administration of antibiotics (Calabi, Calabi, Phillips, & Fairweather, 2002; Denève, Janoir, Poilane, Fantinato, & Collignon, 2009; Rupnik, Wilcox, & Gerding, 2009). The bacterium's ability to grow in the presence of antibiotics in recent years has enabled its rapid spread among patients (Rupnik et al., 2009). Antibiotic treatment diminishes commensal micro-organisms in the gut and their ability to mediate innate immune responses and this enables the proliferation of the often antibiotic resistant *C. difficile* (Buffie & Pamer, 2013). The bacterium can then dominate the mucosal surfaces and destroy cellular barriers through toxin mediated destruction of the epithelial cells, leading to apoptosis and cell death (Buffie & Pamer, 2013; Denève et al., 2009).

C. difficile is potentially a very serious condition frequently effecting hospitalised patients and in particular the elderly (Ausiello et al., 2006). However, not all infections result in disease; outcomes range from asymptomatic colonisation to mild diarrhoea. More serious disease symptoms include abdominal pain, fever and leukocytosis. Severe manifestations of the disease are characterised by inflammatory lesions see **Figure 1.1.1** and the formation of pseudo-membranes in the colon which can lead to bowel perforation, sepsis, shock and death. The severity of disease may also be dependent on the strain of *C. difficile* present (Goorhuis et al., 2007; Rupnik et al., 2009). Since its confirmation as a pathogen in 1977 (Larson, 1978), *C. difficile* has been one of the most intensively typed pathogens (Dawson et al., 2009). The most widely accepted method is polymerase chain reaction (PCR) ribotyping, where more than 100 distinguishable groups have been identified based on mutations in the 16S and 23S ribosomal RNA (rRNA) intergenic spacer regions (Dawson et al., 2009; Stubbs, Brazier, O'Neill, & Duerden, 1999). A study carried out by Ní Eidhin *et al.* (2006) sequenced the *slpA* gene

and flanking deoxyribonucleic acid (DNA) from *C. difficile* isolated from patients in St James's Hospital, Dublin Ireland over a 16-month period. The most frequently occurring ribotypes found in this study were 001, 012 and 017 (Ní Eidhin, Ryan, Doyle, Walsh, & Kelleher, 2006). There is much evidence to suggest that *C. difficile* is evolving to occupy niche hospital populations and there has been rapid worldwide spread of ribotypes 027 and 078 (Dawson et al., 2009). Ribotypes 027 and 078 are known to be 'hypervirulent' and have been associated with more severe diarrhoea, higher mortality and more recurrences (Clements, Magalhães, Tatem, Paterson, & Riley, 2010; Dawson et al., 2009; Goorhuis et al., 2007; Loo et al., 2005).

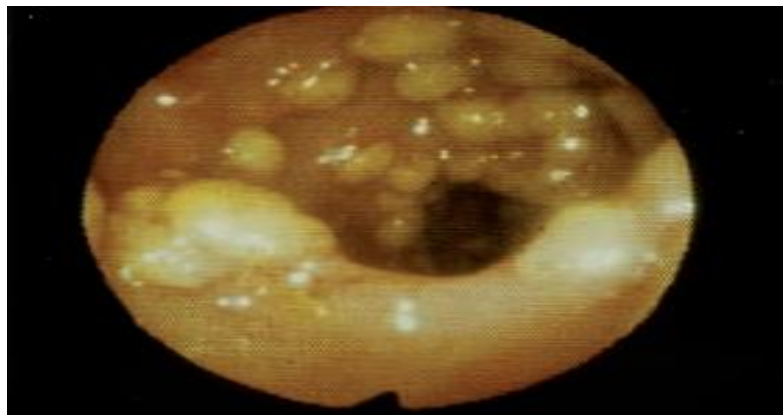


Figure 1.1.1 Image of 'volcano-like' lesions as a result of the local inflammatory effects of *C. difficile* infection in the colon (Rupnik, Wilcox and Gerding 2009)

1.1.1 Toxin Production

Treatment with broad-spectrum antibiotics alters the intestinal microbiota and this allows *C. difficile* to colonise the colon if present. After colonisation the bacterium produces and releases toxins. Toxin A (TcdA) encoded by *tcdA* and Toxin B (TcdB) encoded by *tcdB*, are the two main toxins released by *C. difficile*. These toxins are located in a 19.6 kilobase (Kb) pathogenicity locus (PaLoc) together with three additional *tcd* open reading frames (ORFs) *tcdC*, *tcdD* and *tcdE* (Braun, Hundsberger, Leukel, Sauerborn, & Von Eichel-Streiber, 1996; Dupuy, Govind, Antunes, & Matamouros, 2008; Hammond & Johnson, 1995). TcdA and TcdB are composed of three domains, the first being a carboxy-terminal domain which is responsible for binding to the host cell membrane (Eichel-streiber, Sauerborn, & Kuramitsu, 1992). The second domain

contains a hydrophobic centre which has been shown to be involved in translocation across the cellular membrane (Pfeifer et al., 2003) and finally the third domain contains an amino-terminal domain that enables glucosyltransferase to be catalysed (Hofmann, Busch, Just, Aktories, & Prepens, 1997; Jank, Giesemann, & Aktories, 2007; von Eichel-Streiber, Boquet, Sauerborn, & Thelestam, 1996). TcdA binds to the apical side of the cell where it is endocytosed and a pore in the membrane is formed see **Figure 1.1.2**. This triggers the activation of small molecular weight guanine nucleotide-binding proteins (G-proteins), resulting in disruption of the cytoskeleton (Reineke et al., 2007).

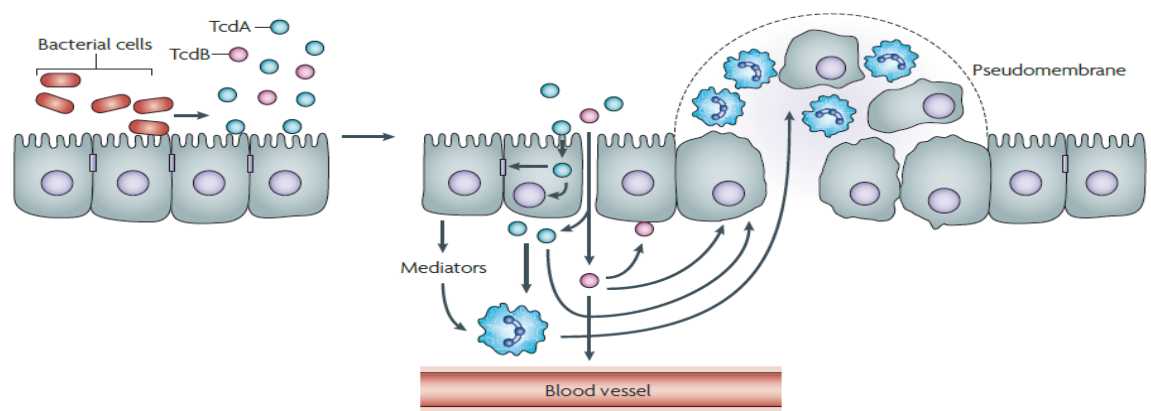


Figure 1.1.2 Image illustrating the destruction of the cellular barriers by TcdA and TcdB release from *C. difficile* leading to the pathogenesis of CDI (Rupnik et al., 2009)

Disruption of the cytoskeleton leads to the loosening of tight junctions in the epithelial barrier, enabling more toxins to cross the cell membrane (Rupnik et al., 2009). Cell death ensues and the dying cell produces inflammatory mediators that attract neutrophils. TcdB binds to the basolateral cell membrane where it acts on its cytosolic targets, the Guanosine Triphosphatase (GTPases) of the Rho/Rac family (Reineke et al., 2007). TcdB induces the release of more immunomodulatory mediators resulting in inflammation due to the accumulation of neutrophils, phagocytes and mast cells (Rupnik et al., 2009). Ultimately this leads to intestinal inflammation and the onset of the symptoms previously described. The majority of toxigenic *C. difficile* strains co-produce TcdA and TcdB (toxintype A+B+) while only a minority of *C. difficile* strains exclusively produce TcdB (toxintype A-B+); for instance the hypervirulent ribotype 017 has a truncated non-functional TcdA due to a deletion in the *tcdA* gene (Voth &

Ballard, 2005). Approximately 6–10% of *C. difficile* strains generate a binary actin-adenosine diphosphate (ADP) ribosylating toxin known as *C. difficile* transferase (CDT) in addition to the other toxins (Barth, Aktories, Popoff, & Stiles, 2004).

As mentioned earlier the PaLoc contains three additional ORFs, where sequencing and transcription analysis suggest that TcdC and TcdD are involved in the positive and negative regulation of TcdA and TcdB expression (Hammond & Johnson, 1995; Hundsberger et al., 1997). The TcdC region of ribotype 027 contains an 18 base pair (bp) deletion and it is thought that this modification may lead to an altered function of the protein contributing to the high level of toxin expression, in consequence causing ribotype 027 to be ‘hypervirulent’ (Spigaglia & Mastrantonio, 2002). However a variety of deletions have been observed in non-virulent strains, therefore deletions may not always result in the loss of function. Increased virulence is not solely due to toxin production (Drudy et al., 2004). While the toxins of *C. difficile* are clearly of great importance in the study of its pathogenesis, other virulence factors cannot be ignored.

1.1.2 *Clostridium difficile* Spores and Germination

C. difficile is extraordinary as it is highly transmissible between humans: this is key to its survival and persistence (Deakin et al., 2012). The main mode of transmission of CDI is through the ingestion of *C. difficile* spores, although the timing and signals triggered to initiate germination following ingestion are not well understood (Jump, Pultz, & Donskey, 2007). Signals that prompt *C. difficile* sporulation *in vivo* or *in vitro* have not been identified, but they could be related to environmental stimuli such as nutrient starvation, quorum sensing and other unidentified stress factors, as seen with other spore forming bacteria (Higgins & Dworkin, 2012). Unlike most pathogens, *C. difficile* produces a metabolically dormant spore that is excreted by infected patients (Lawley, Clare, et al., 2009). Infective spores persist in the environment and are resistant to a wide range of physical and chemical stresses, including environmental oxygen and the acidic environment of the stomach (Carlson et al., 2015; Paredes-Sabja, Shen, & Sorg, 2014). The spores can remain on environmental surfaces for many months as they are highly resistant to commonly used disinfectants (Kim et al., 1981; Paredes-Sabja et al., 2014). The spore surface is covered by an additional surface layer

called the exosporium (Pizarro-Guajardo et al., 2014). The morphology of the exosporium is dependent on the ribotype of *C. difficile*, some ribotypes have a compact exosporium on the surface of the spore while others have exosporium layers which resemble hair-like projections (Joshi, Phillips, Williams, Alyousef, & Baillie, 2012; Paredes-Sabja et al., 2014). Although the roles of the exosporium in CDI and pathogenesis are unclear, recent reports have shown that the exosporium interacts with unidentified surface receptors on intestinal epithelium cells (Paredes-Sabja, Cofre-Araneda, Brito-Silva, Pizarro-Guajardo, & Sarker, 2012).

In other bacterial species, spore germination is induced when specific germinant receptors (GRs) sense the presence of species specific small molecule germinants (Paredes-Sabja et al., 2014). The binding of the germinants to GRs triggers the release of monovalent cations and the spore core stores of dipicolinic acid (DPA), which in turn activates cortex hydrolases. Cortex hydrolases degrade the peptidoglycan (PG) cortex layer which allows the core to hydrate and metabolism can resume (Paredes-Sabja et al., 2014). *C. difficile* is unique, as it does not contain orthologs of the GerA family of GRs and it appears that commonly conserved germination and sporulation elements are differentially regulated in *C. difficile* compared to other spore-forming bacteria (Paredes-Sabja et al., 2012). *C. difficile* spores germinate in response to L-glycine, which acts as a co-germinant to specific bile salts such as Chololate and its derivatives Taurochololate, Glycochololate and Deoxychololate (Sorg & Sonenshein, 2008; Wheeldon, Worthington, & Lambert, 2011). The main components of the spore germination machinery of *C. difficile* have been identified, but further research is needed to define the exact signalling pathway elicited during germination. Studies have shown that the germination frequency of the hypervirulent ribotype 027 is different to that of a non-epidemic *C. difficile* strain (Burns, Heap, & Minton, 2010b). As spores represent the infectious stage of *C. difficile*, diversity in the germination characteristics of particular types may also contribute to the observed differences in disease severity (Burns, Heap, & Minton, 2010a).

1.1.3 Surface Layer Proteins

Calabi *et al.* (2002) found that the surface layer (S-layer) proteins play the biggest role in the binding of *C. difficile* to the host's gastrointestinal (GI) tract allowing bacterial adherence to the mucosa and the delivery of toxins (Calabi *et al.*, 2002). *C. difficile* expresses a crystalline S-layer encoded by the *slpA* gene, the product of which is cleaved to give two mature peptides which associate to form layers (Ausiello *et al.*, 2006; Ní Eidhin *et al.*, 2006). These layers are commonly known as Surface Layer Proteins (SLPs) and are found on the outer surface on *C. difficile*, facilitating interaction with the host enteric cells (Fagan *et al.*, 2009). SLPs have been previously described as virulence factors for *Aeromonas salmonicida* (Sara & Sleytr, 2000) and *Campylobacter fetus* (Grogono-Thomas, Dworkin, Blaser, & Newell, 2000) and as bacterial adhesions in *Lactobacillus acidophilus* (Schneitz, Nuotio, & Lounatma, 1993).

In most bacterial species the S-layer is composed of one major protein, which is modified by glycosylation (Sara & Sleytr, 2000). However *C. difficile* is unique in that a single gene encodes two SLPs which are derived from post-translational cleavage of a single precursor *slpA* gene (Fagan *et al.*, 2009). The *slpA* precursor protein contains a signal peptide that is 26 amino acids in length and it directs translocation across the cell membrane, after which cleavage occurs producing the mature SLPs (Calabi *et al.*, 2001; Karjalainen *et al.*, 2001). Mature SLPs contain a high molecular weight (HMW) protein (42 kDa) derived from the C-terminal portion of the precursor and a low molecular weight (LMW) partner protein (32–38 kDa) derived from the N-terminal portion of the precursor (Ní Eidhin *et al.*, 2006). Fagan *et al.* (2009) were the first to solve the crystal structure of SLP from a bacterial pathogen, they solved the structure of a LMW protein from *C. difficile* ribotype 012 and this provided an insight into the architecture of SLPs.

The HMW and LMW proteins were found to form a tightly associated non-covalent complex. Deletion analysis of the LMW protein demonstrated that the C-terminal residues are necessary for interaction with the HMW protein to form the HMW/LMW complex. The crystal structure of the LMW protein also revealed it had two domains, see **Figure 1.1.3**. Domain 1 adopts a two-layer sandwich architecture and domain 2 displays a novel protein fold which has not yet been classified (Fagan *et al.*, 2009).

HMW proteins contain Pfam (PF04122) which are cell wall binding motifs and they are predicted to mediate interactions with the underlying cell wall, where the HMW protein can attach to the cell wall and act as an anchor to display the LMW (Calabi et al., 2002; Fagan et al., 2009; Karjalainen et al., 2001). More recently it has been shown that the LMW protein has a role in adherence to the host cells (Merrigan et al., 2013), it was previously thought that the HMW protein bound to the gastrointestinal tissues and extracellular matrix (ECM) exclusively (Calabi et al., 2002).

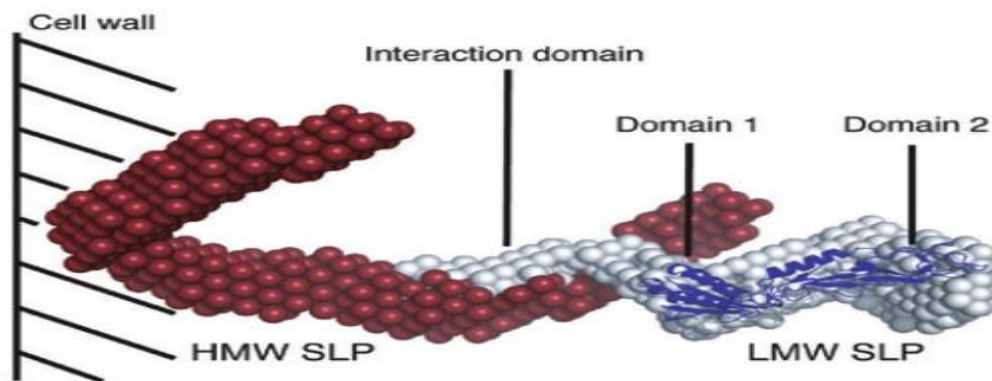


Figure 1.1.3 3D model of the proposed structure and orientation of the HMW and LMW SLPs on the surface of *C. difficile* (Fagan et al., 2009)

HMW proteins are highly conserved across strains of *C. difficile*, while the LMW proteins demonstrates considerable sequence diversity, and the latter have also been shown to be the dominant antigen (Drudy et al., 2004; Ní Eidhin et al., 2006; Sharp & Poxton, 1988). LMW protein on the outmost part of the bacteria may be exposed to the host immune system. Given the high sequence variability between strains and the fact that different strains induce different disease outcomes, it is plausible that this protein may be involved in masking the bacteria from the immune system (Lynch 2014, unpublished). High sequence variability may be a result of evolutionary selective pressures exerted by the host immune response acting on the bacteria to avoid a host response (Fagan et al. 2009). A change in structure or specific motifs in LMW proteins may result in host immune cells no longer being able to recognise *C. difficile* as a pathogen (Ausiello et al., 2006). Interestingly a recent study has shown a potential role for recombination in *slpA* between different strains (Dingle et al., 2013). Five main clades of *C. difficile*, along with twelve stable variants of a 10 Kb S-layer cassette,

containing *slpA*, were identified. The twelve S-layer cassette variants unexpectedly behaved as independent components of the genome, associating randomly with the five clades by horizontal genetic exchange. It was also shown that isolates sharing the same PCR ribotype can carry multiple distinct S-layer cassettes (Dingle et al., 2013).

1.1.4 Cell Wall Proteins

Pathogen attachment is a crucial early step in mucosal infections (Péchiné, Janoir, & Collignon, 2005). Cell wall proteins (CWPs) allow bacteria such as *C. difficile* to interact with the host and they can also facilitate adherence (Emerson et al., 2009). CWPs are not the only means by which *C. difficile* can attach to the mucosa, other adhesins such as the heat shock protein GroEL (Waligora, Hennequin, Mullany, & Bourlioux, 2001), the fibronectin-binding protein Fbp68 (Hennequin, 2003), the Flagellar cap proteins FliD and the flagellin FliC (Tasteyre, Barc, Collignon, Boureau, & Karjalainen, 2001) have been shown to play a role in the attachment of *C. difficile* to the mucosa. HMW SLPs and all CWPs each contain three Pfam motifs that appear to mediate non covalent binding to the underlying cell wall (de la Riva, Willing, Tate, & Fairweather, 2011). The majority of the CWPs have a second unique domain that specify a particular function (Emerson & Fairweather, 2009). CwpV contains a domain which allows for phase-variable protein expression (Emerson et al., 2009), while Cwp66 functions as an adhesin when the C-terminal domain is exposed to the cell surface- it can also act as an anchor to the cell wall via the N-terminal domain (Waligora et al., 2001). Cwp84 is a well characterised CWP that can degrade the host-cell ECM (Waligora et al., 2001), it also has an important role in the cleavage of the immature *slpA* into its HMW and LMW components (Dang et al., 2010). Inhibition of this protease results in accumulation of immature *slpA* on the cell wall, which leads to a decreased viability of the bacterium (Dang et al., 2010). Mutations of the *cwp84* gene were found to result in defective localisation of other CWPs and Cwp84 is itself regulated by Cwp13 (de la Riva et al., 2011). The high conservation of the SLP cleavage site between strains and low variability of Cwp84 implies a conserved process of SLPs maturation (Dang et al., 2010). CWPs have essential roles in the pathogenesis of *C. difficile* and are extremely important components of the S-layer.

1.2 Immune Response to *Clostridium difficile*

The GI tract is comprised of the small intestine, the large intestine also known as the colon and the rectum. Shortly after birth, the GI tract becomes colonised by vast amounts of non-pathogenic commensal bacteria collectively known as the microbiota, with the greatest number residing in the distal gut (Gill et al., 2006). The microbiota contribute to host nutrition and energy balance as they can synthesise essential amino acids and vitamins, they can also process products of the diet that are otherwise hard to digest (Gill et al., 2006; Ley, Peterson, & Gordon, 2006; Littman & Pamer, 2011). In turn, the host provides the microbes with essential nutrients, ensuring their transmission and retention within the host species (Littman & Pamer, 2011). Alongside the exposure to these commensal bacteria the GI tracts is also exposed to a variety of luminal elements such as food/commensal bacteria and it must be able to discriminate between these non-pathogenic elements and antigens from pathogenic organisms (Underdown & Schiff, 1986). This is achieved by the interaction of the intestinal epithelium with lymphoid cells in order to protect against infection but at the same time avoid unnecessary inflammatory responses to beneficial commensals and food (Jung, Hugot, & Barreau, 2010).

The Gut-Associated Lymphoid Tissue (GALT) consists of both isolated and aggregated lymphoid follicles and is one of the largest lymphoid organs, containing up to 70% of the body's immunocytes (Neutra, Mantis, & Kraehenbuhl, 2001). Aggregated lymphoid follicles were originally described by Marco Aurelio Severino in 1645 in Italy. They were named Peyer's Patches (PPs) after their detailed description by the Swiss pathologist Johann Conrad Peyer in 1677 (Jung et al., 2010). PPs are found in the small intestine and isolated lymphoid follicles which resemble PPs can be found in the colon. PPs are composed of aggregated lymphoid follicles surrounded by the follicle-associated epithelium (FAE), which forms the interface between the GALT and the luminal environment. The FAE contains specialised cells named microfold cells (M-cells) (Miller, Zhang, KuoLee, Patel, & Chen, 2007). These M-cells transport luminal antigens and bacteria toward the underlying immune cells, that activate or inhibit the immune response leading to either tolerance or systemic immune cell responses (Jung et al., 2010). The role of these tissues is in immune surveillance and the induction of the

immune response. Effector sites of the intestine are the mucosal epithelium and underlying *lamina propria* (LP). The LP contains various immune cells, including macrophages, dendritic cells (DCs), plasma cells, mast cells, neutrophils, T and B lymphocytes (Doe, 1989).

It is well known that antibiotic treatment diminishes commensal microorganisms in the gut and their ability to mediate innate immune responses (Buffie & Pamer, 2013). Once the normal flora is disturbed and *C. difficile* is present the bacterial spores - which are the infectious agent, germinate and vegetative cells multiply producing toxins (Fagan et al., 2009; Rupnik et al., 2009; von Eichel-Streiber et al., 1996). These toxins are internalised into epithelial cells where they inhibit small molecular weight G-proteins, resulting in disruption of the cytoskeleton, apoptosis and cell death (Buffie & Pamer, 2013; Denève et al., 2009; Just & Gerhard, 2004). The presence of *C. difficile* in the gut induces an acute inflammatory response and severe damage to the intestinal epithelium (Dawson et al., 2009). SLPs are found on the outer surface on *C. difficile* and facilitate the interaction with the host enteric cells (Fagan et al., 2009). SLPs can induce the production of pro-inflammatory cytokines in immune cells such as DCs, monocytes and macrophage (Ausiello et al., 2006; Bianco et al., 2011; Calabi et al., 2002; Collins et al., 2014; Madan & Petri Jr, 2012; Ryan et al., 2011; Vohra & Poxton, 2012). SLPs have been shown to elicit an immune response and they may have a role during infection (Drudy et al., 2004; Péchiné et al., 2005).

1.2.1 SLPs Activate Macrophage and Induce Bacterial Clearance

Research from our laboratory has shown that SLPs from *C. difficile* activate macrophages and induce bacterial clearance responses. SLPs from ribotype 001 induce pro-inflammatory cytokines such as Interleukin (IL)-6, IL-12p40 and tumour necrosis factor alpha (TNF α) as well as chemokines such as macrophage inflammatory protein 2-alpha (MIP-2) and monocyte chemo-attractant protein-1 (MCP-1). Co-stimulatory cell surface marker expression of CD40, CD14 and major histocompatibility complex (MHC) Class II were also increased, as well as the rate of phagocytosis when macrophages were stimulated with these SLPs (Collins et al., 2014). The highest numbers of intestinal macrophages are found in the colon, which is the largest reservoir

of macrophages in the body (Lee, Starkey, & Gordon, 1985). Intestinal macrophage express lower levels of co-stimulatory molecules CD80, CD86 and CD40 compared to their inflammatory macrophage counterparts (Rogler et al., 1998). Intestinal macrophage appear not to be responsive to many Toll-Like Receptor (TLRs) ligands, however they can express TLRs at a messenger RNA (mRNA) and protein level (Smith et al., 2011). They can also secrete high levels of TNF α without inducing an inflammatory response (Bain et al., 2013). Intestinal macrophages are capable of phagocytosing pathogens that display bacterial antigens (Smith et al., 2011). When intestinal macrophage are depleted there is an increase in inflammation (Qualls, Kaplan, Rooijen, & Cohen, 2006). It is now thought that the ability of SLPs to induce cell surface marker expression and induce cytokine production comes into effect when non-intestinal macrophages are recruited to the site of infection (Collins et al., 2014).

1.2.2 SLPs Induce the Maturation of Dendritic Cells

SLPs from *C. difficile* induce the maturation of DCs by inducing the expression of co-stimulatory cell surface markers: CD80, CD86 and MHCII, which leads to the induction of pro-inflammatory cytokines such as IL-1 β and IL-6 (Ausiello et al., 2006). Research from our group also showed that intact SLPs containing both the HMW and LMW proteins were required for DC activation and this subsequently generated T helper cells required for bacterial clearance via Toll-Like Receptor 4 (TLR4) (Ryan et al., 2011). DCs along with macrophages play an important role in immunity of the GI tract, where populations of both cells reside in the LP behind a wall of protective epithelial cells (Iwasaki, 2007; Sato & Iwasaki, 2005). DCs are known as the sentinels of the immune system and play an essential role in deciding when to mount the appropriate immune response by differentiating between invading pathogens and commensal bacteria (Banchereau & Steinman, 1998).

Resident mucosal DCs sample the environment *via* intestinal M-cells present in the epithelium of PPs: the antigen is taken from the lumen and transcytosed to the underlying DCs (Clark & Jepson, 2003; Coombes & Powrie, 2008). DCs can also sample antigen directly by forming tight junction structures with intestinal epithelial cells and extending dendrites into the lumen while preserving the epithelial barrier in

the mean time (Rescigno et al., 2001). This mechanism is active both with invasive and non-invasive bacteria and is regulated by the expression of CX3C chemokine receptor 1 (CX3CR1) (Niess et al., 2005). The number of epithelial dendrites is increased during infection and requires Myeloid Differentiation primary response gene 88 (MyD88)-dependent signalling through TLRs to function efficiently (Rescigno et al., 2001). Upon antigen uptake, intestinal DCs migrate to the mesenteric lymph nodes (MLNs), where they can interact with naïve T and B cells and display antigens (Sato & Iwasaki, 2005). In the absence of pathogens, mucosal DCs either ignore the antigen or induce regulatory responses, upon recognition of pathogens that invade the mucosal barrier they mount a robust protective immune response (Iwasaki, 2007).

1.3 Pattern Recognition Receptors

The first cellular barriers that pathogens face in the intestine are the intestinal epithelial cells, they form a monolayer between the lumen of the intestine and sub-epithelial tissue where immune cells are located (Peterson & Artis, 2014). Epithelial cells provide a physical barrier, but they can also interact with pathogens present in the lumen of the gut and the underlying host immune cells through Pattern Recognition Receptors (PRRs). These receptors recognise repeating patterns of conserved molecular structures found on invading pathogens, that are not present in host cells (Janeway, 1989). These patterns are collectively known as Pathogen Associated Molecular Patterns (PAMPs). Some PRRs recognise PAMPs directly while others recognise products generated by PAMP recognition. There are three types of PRRs; Secreted proteins, transmembrane receptors and intracellular receptors (Medzhitov & Janeway, 1997). Of particular interest are transmembrane PRRs known as TLRs, which play an important role in pathogen recognition and they have been extensively studied. TLRs derived their name based on homology to the *Drosophila melanogaster* Toll protein (Ruslan Medzhitov, Preston-hurlburt, & Janeway, 1997). TLRs are glycoproteins characterised by an extracellular or luminal ligand binding domain containing Leucine-Rich Repeats (LRRs) motifs and a cytoplasmic signalling Toll/IL-1 receptor homology (TIR) domain (O'Neill & Bowie, 2007). Ligand binding to TLRs through PAMP-TLR interactions induce receptor oligomerisation, which subsequently triggers intracellular signal transduction (Mogensen, 2009). There are ten functional TLRs in humans and twelve

known in mouse, each capable of recognising distinct PAMPs, see **Figure 1.3.1** (Kawai & Akira, 2006; Mogensen, 2009).

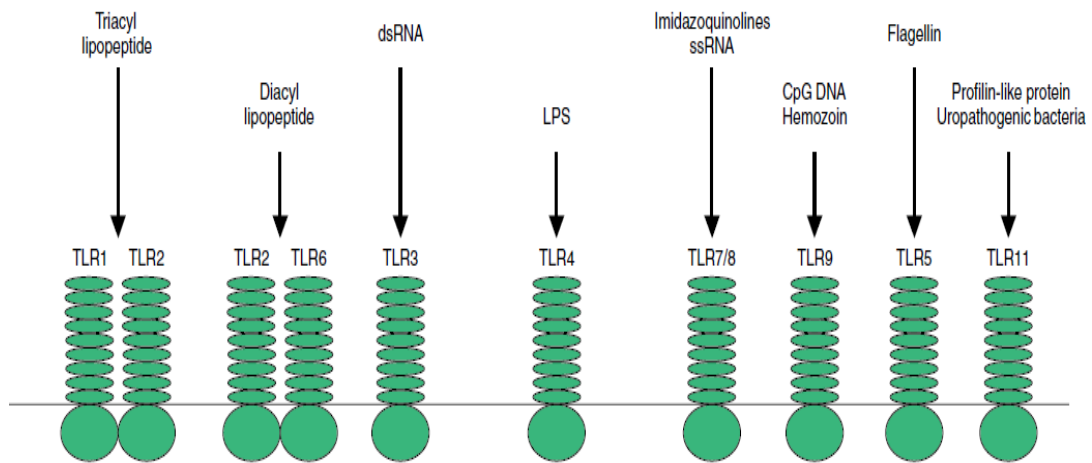


Figure 1.3.1 Image showing TLRs and the patterns of microbial components they recognise (Kawai & Akira, 2006)

TLR1, TLR2, TLR4, TLR5 and TLR6 are present on the cell surface. TLR2 forms heterodimers with TLR1 and TLR6 to recognise bacterial lipopeptides and lipoteichoic acid from gram positive cell walls (Akira & Takeda, 2004). TLR4 recognises lipopolysaccharide (LPS) on the outer layer of gram negative bacteria (Takeuchi et al., 1999). TLR5 recognises flagellated bacteria (Hayashi et al., 2001). TLR3 and TLR9 recognise PAMPs from intracellular pathogens. TLR3 recognises both single and double stranded viral Ribonucleic acid (RNA) (Alexopoulou, Holt, Medzhitov, & Flavell, 2001), while TLR9 recognises unmethylated CpG from DNA viruses (Hemmi et al., 2000). Nine human TLRs have been confirmed in epithelial cells of the small intestine to date (Otte, Cario, & Podolsky, 2004). The main TLR of interest in this thesis is TLR4. Despite recognising LPS in gram negative bacteria, TLR4 is the receptor responsible for recognising SLPs and mounting an immune response to *C. difficile*. It was also found that SLP from ribotype 001 can activate TLR4 signalling leading to the activation of nuclear factor κ light-chain-enhancer of activated B cells (NF- κ B) through the MyD88-dependent signalling pathway. However, SLPs failed to induce Interferon Regulatory Factor 3 (IRF3) through the MyD88-independent signalling pathway (Ryan et al., 2011).

1.3.1 Toll-Like Receptor 4

TLR4 was the first mammalian TLR to be discovered, it is expressed on the cell surface of innate immune cells such as macrophages, DCs, mast cells and on the surface of B lymphocytes (Gerondakis, Grumont, & Banerjee, 2007). TLR4 detects LPS which is one of the best studied components of bacteria that activates an immune response (Ruslan Medzhitov et al., 1997). LPS is an essential structural component of the cell wall of gram negative bacteria and consists of a core oligosaccharide, an O side chain and a highly conserved lipid A- which serves as the PAMP that activates TLR4 (Viswanathan, Sharma, & Hecht, 2004). Cellular recognition of LPS requires several different molecules including LPS Binding Protein (LBP), Cluster of Differentiation 14 (CD14), Myeloid Differentiation protein 2 (MD-2) and TLR4. LBP is present in the bloodstream and binds to LPS, it then transfers the LPS to the cell surface receptor CD14 (Wright, Ramos, Tobias, Ulevitch, & Mathison, 1990). CD14 is a glycoprotein expressed primarily on: macrophages, DCs and neutrophils, which contain multiple LRRs and are anchored to the cell membrane through phosphatidylinositol linkage (Haziot et al., 1988; Setoguchi et al., 1989). MD-2 is a small soluble protein that binds non-covalently to TLR4 and is essential for the recognition of LPS by TLR4 (Shimazu et al., 1999). The interaction of the CD14/LPS complex with TLR4/MD-2 causes receptor oligomerisation and initiates downstream signalling (Alexander & Rietschel, 2001).

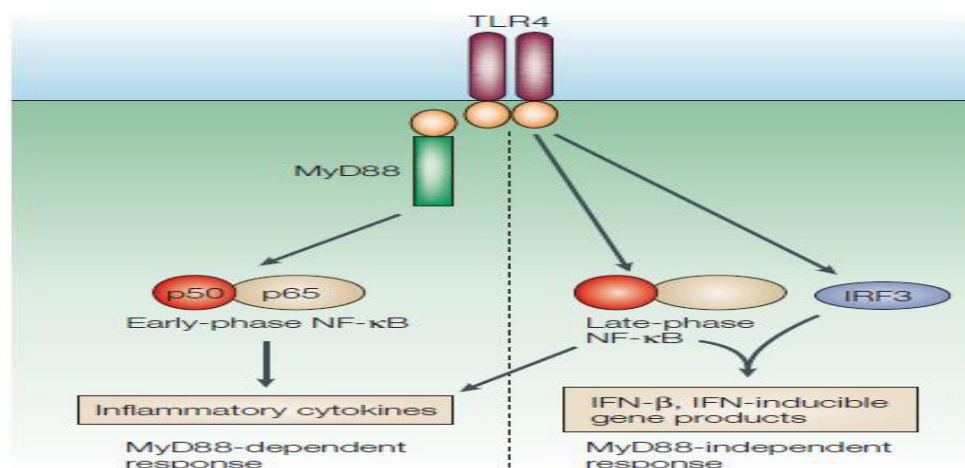


Figure 1.3.2 Two distinct signalling pathways are activated following activation of TLR4, the MyD88-dependent and MyD88-independent signalling pathway (Akira & Takeda, 2004)

TLR4 is distinctive among TLRs in that it activates two distinct signalling pathways see **Figure 1.3.2**. The adaptor protein recruited to the receptor dictates the signalling pathway which ensues. TLR4 is also unique as it utilises all four TIR domain-containing adaptor proteins. The signalling pathways activated by TLR4 are classified as the MyD88-dependent and MyD88-independent signalling pathways (Akira & Takeda, 2004). It was originally thought that these signalling pathways were initiated simultaneously following ligand recognition, however it was established that they are initiated sequentially (Kagan et al., 2008). Recognition of LPS by TLR4 initiates MyD88-dependent signalling and activation of transcription factors NF- κ B and AP-1. MyD88 is recruited to the receptor at the plasma membrane with the help of the bridging adaptor MyD88 adaptor-like (Mal), which can also be known as TIRAP (Yamamoto et al., 2002). The LPS-TLR4 complex is internalised into early endosomal structures in a process dependent on clatherin and the GTPase dynamin (Husebye et al., 2006). Once the LPS-TLR4 complex is endocytosed, MyD88-dependent signalling is abolished (Kagan et al., 2008). TIR-domain-containing adapter-inducing interferon- β (TRIF) is subsequently recruited to the receptor with the help of the bridging adaptor TRIF-related adapter molecule (TRAM) (Oshiumi et al., 2003). Recruitment of TRIF is dependent on endocytosis of the receptor which leads to downstream activation of members of the IRF family of transcription factors and the induction of Type I IFNs. Internalisation of TLR4 brings it into close proximity to TNF receptor associated 3 (TRAF3) and once they interact there is downstream activation (Kagan et al., 2008). The LPS-TLR4 complex is then trafficked to late endosomes or lysosomes for degradation and loading of associated antigens into MHCII molecules for presentation to helper T cells (Husebye et al., 2006). Activation of TLR4 induces the expression of co-stimulatory molecules and can lead to the maturation of DCs which activate cells of the adaptive immune system (Banchereau & Steinman, 1998).

1.3.1.1 MyD88-Dependent Signalling Pathway

MyD88-dependent signalling is activated when MyD88 is recruited to the receptor at the plasma membrane with the help of the bridging adaptor Mal (Yamamoto et al., 2002), see **Figure 1.3.3**. In addition to its TIR domain, MyD88 has an N-terminal death domain and upon recruitment it associates with members of the IL-1R associated kinase

(IRAK) family of protein kinases, through association of their death domains (Wesche, Henzel, Shillinglaw, Li, & Cao, 1997). IRAK4 is activated which in turn phosphorylates and activates IRAK1 through residues in the N-terminal (Shyun Li, Strelow, Fontana, & Wesche, 2009). After IRAK4 and IRAK1 have been sequentially phosphorylated, they dissociate from MyD88. In the mean time, IRAK2 becomes phosphorylated and dissociates from the complex. IRAK1 and IRAK2 then interact with the downstream adaptor, TNF-receptor associated-factor 6 (TRAF6) (Flannery & Bowie, 2010). TRAF6 is a RING domain containing E3 ubiquitin ligase and together with other molecules: E2 ubiquitin conjugating enzyme 13 (Ubc13) and ubiquitin conjugating enzyme E2 variant 1 isoform A (Uev1A), it promotes lysine 63 (K63) linked polyubiquitin of target proteins including itself and NEMO (IKK γ) chains (Adhikari, Xu, & Chen, 2007; Chen, Bhatia, Chang, & Castranova, 2006). Ubiquitinated NEMO and TRAF6 recruit transforming growth factor- β -activated kinase 1 (TAK1) and its regulators: TAK1 binding protein 1 (TAB1), TAB2 and TAB3 (Adhikari et al., 2007). Two further pathways are then activated, the mitogen-activated protein kinase (MAPK) pathway and also the inhibitory- κ B Kinase (IKK) complex.

MAPKs are a group of intracellular signal transducing enzymes that are phosphorylated and activated by a MAPK kinase (MAP2K), which are phosphorylated and activated by a MAPKK kinase (MAP3K). TAK1 is a MAP3K which can phosphorylate and activate mitogen-activated protein kinase kinase 3 (MKK3) and MKK6 (Moriguchi et al., 1996). MAP3Ks consecutively phosphorylate and activate the c-Jun N-terminal kinases (JNK) and p38 MAPK pathways. Activation of these MAPK pathways induces the transcription factor Activator Protein 1 (AP-1). AP-1 cooperates with NF- κ B to regulate gene expression. The IKK complex is made up of two protein kinases IKK α and IKK β along with a scaffolding protein NEMO which is essential for regulation and activation of the complex (Chen et al., 2006; Rothwarf, Zandi, Natoli, & Karin, 1998). Ubiquitinated TAK1 phosphorylates IKK β and activates the IKK complex (Wang et al., 2001). NF- κ B in its natural state associates with I κ B proteins, however when activated IKK complex phosphorylates I κ B, they mark them as targets for ubiquitination and degradation in the 26S proteasome (Hayden & Ghosh, 2004). NF- κ B then binds to κ B sites in the promoter regions of its target genes, including genes encoding pro-inflammatory cytokines and chemokines.

1.3.1.2 MyD88-Independent Signalling Pathway

NF- κ B and AP-1 can also be activated by a MyD88-independent pathway, involving the TIR domain containing adaptor protein TRIF where TRAM acts as a bridging adaptor between it and TLR4 (Oshiumi et al., 2003). TRIF interacts with Receptor Interacting Protein 1 (RIP1) following recruitment (Meylan et al., 2004). RIP1 interacts with the C-terminal domain of TRIF and the N-terminal region contains TRAF6 binding motifs. Poly-ubiquitination of RIP1 causes it to form a complex with TRAF6 and TAK1 (Taro Kawai & Akira, 2007). As in MyD88-dependent signalling TAK1 then activates the IKK complex and MAPKs as previously mentioned. However, MyD88-independent signalling also leads to the activation of IRF3 a member of the IRF family of transcription factors see **Figure 1.3.3**. TRIF is first recruited to the receptor which leads to the recruitment of TRAF3 (Kawai & Akira, 2007). This leads to succeeding recruitment and activation of Tank Binding Kinase 1 (TBK1) and inducible IKK which is also known as IKK ϵ . NF- κ B activating kinase associated protein 1 (NAP1) also plays a role in the recruitment of these kinases (Sasai et al., 2005). TBK1 and IKK ϵ phosphorylate key serine/threonine residues in the C-terminal region of IRF3 (Sharma et al., 2003). Phosphorylation of IRF3 promotes dimerisation and nuclear translocation that allows for interaction with the transcriptional co-activators cAMP responsive element binding protein (CBP)/p300 (Gauzzi, Del Cornò, & Gessani, 2010). CBP/p300 acetylates IRF3 homodimers, which causes a conformational change to unmask its DNA binding domain (Lin, Heylbroeck, Genin, Pitha, & Hiscott, 1999). IRF3 binds to the promoter region and up regulates the expression of genes encoding Type I IFNs.

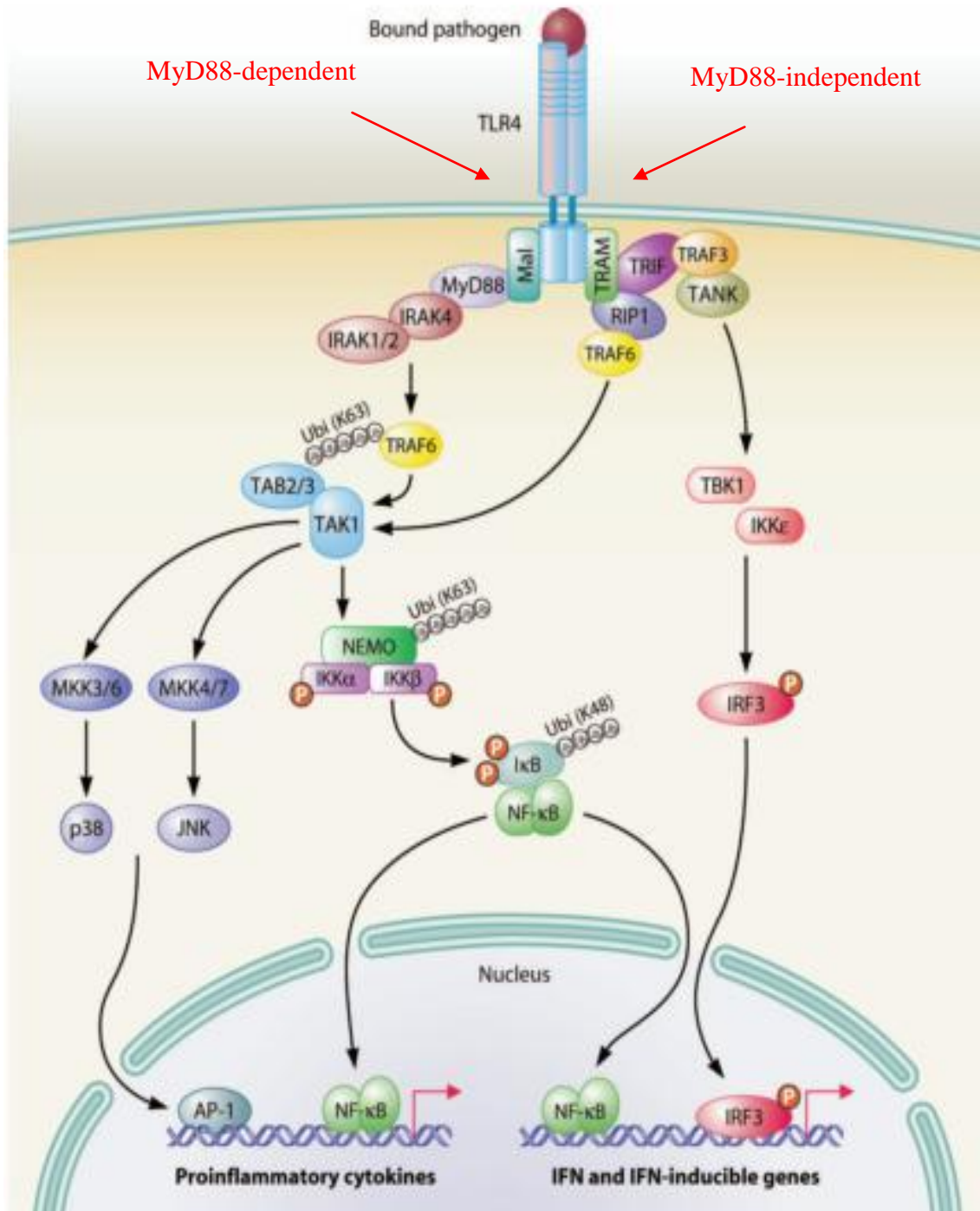


Figure 1.3.3 Downstream signalling following activation of MyD88-dependent and MyD88-independent signalling pathways following TLR4 activation. Ultimately leading to the activation of transcription factors such as AP-1, NF-κB and IRF3 and the induction of pro-inflammatory cytokines, IFN and IFN-inducible genes (Mogensen, 2009)

1.3.2 NF- κ B

NF- κ B was discovered in 1986 by the coincidental discovery of three proteins NF κ B, v-Rel and Dorsal (Baeuerle & Baltimore, 1988; Gilmore & Temin, 1986; Sen & Baltimore, 1986; Steward, Zusman, Huang, & Schedl, 1988). They have since been extensively studied and found to be members of the same protein family with distinct biological functions in immunity (NF- κ B), oncogenesis (v-Rel) and development (Dorsal) (Gilmore, 2006). The term NF- κ B can be used to describe the superfamily of Rel and NF- κ B proteins across species, the subfamily: p100, p105 and Relish or the specific p50- Rel A heterodimer, which is the foremost NF- κ B dimer in many cells. The larger NF- κ B family of proteins are composed of two subfamilies: the NF- κ B proteins and the Rel proteins. All of these proteins share a highly conserved 300 amino acid Rel homology domain (RHD) which is responsible for nuclear translocation, DNA-binding and dimerisation (Gilmore, 1990) see **Figure 1.3.4**.

The Rel subfamily includes c-Rel, Rel B, Rel A also known as p65, *Drosophila* Dorsal and Dif. While the NF- κ B subfamily includes p105, p100 and *Drosophila* Relish- which are distinguished by their long C-terminal domains that contain multiple copies of ankyrin repeats that act to inhibit proteins (Gilmore, 2006). The NF- κ B proteins p100 and p105 are processed to become shorter active DNA-binding proteins, resulting in the removal of their C-terminal ankyrin repeats. p105 is constitutively processed to p50 resulting in both p50 and p105 containing dimers, while p100 processing to p52 is stimulus dependent and preferentially binds to Rel B (Oeckinghaus & Ghosh, 2009). Due to the lack of a C-terminal trans activation domains p50 and p52 homodimeric complexes cannot activate transcription but instead act as transcriptional repressors (Hayden & Ghosh, 2004). Rel subunits form homo- or heterodimers and the various dimeric combinations that are formed, target slightly different DNA sequences allowing for distinct transcriptional activity of different NF- κ B dimers (Kunsch, Ruben, & Rosen, 1992).

The NF- κ B subfamily are generally not activators of transcription, except when they form dimers with members of the Rel subfamily, the predominant form of NF- κ B is a Rel A (p65) -p50 heterodimer (Gilmore, 2006). The p65-p50 heterodimer is bound by

I κ B and is rapidly degraded in response to NF- κ B activating stimuli. I κ B proteins bind to the NF- κ B dimer through multiple ankyrin repeats and inhibit their DNA binding activity (Whiteside & Israel, 1997). When activated IKK complex phosphorylate I κ B, they are marked for K48-linked ubiquitination and degradation in the 26S proteasome (Hayden & Ghosh, 2004). NF- κ B can then bind to κ B sites in the promoter regions of its target genes, including genes encoding pro-inflammatory cytokines and chemokines (Yamamoto et al., 2003). Active NF- κ B promotes the expression of I κ B α which is an important negative feedback regulatory mechanism which ensures termination of the NF- κ B response (Klement et al., 1996). NF- κ B regulates the expression of a range of proteins including pro-inflammatory cytokines, such as IL-1 β , IL-8, IL-6 and TNF α . They also regulate adhesion molecules such as intracellular adhesion molecule (ICAM)-1 and vascular cellular adhesion molecule (VCAM)-1 and inducible enzymes such as inducible nitric oxide synthase (iNOS) which mediate the innate immune response to the invading pathogen (Hayden & Ghosh, 2004; Pahl, 1999).

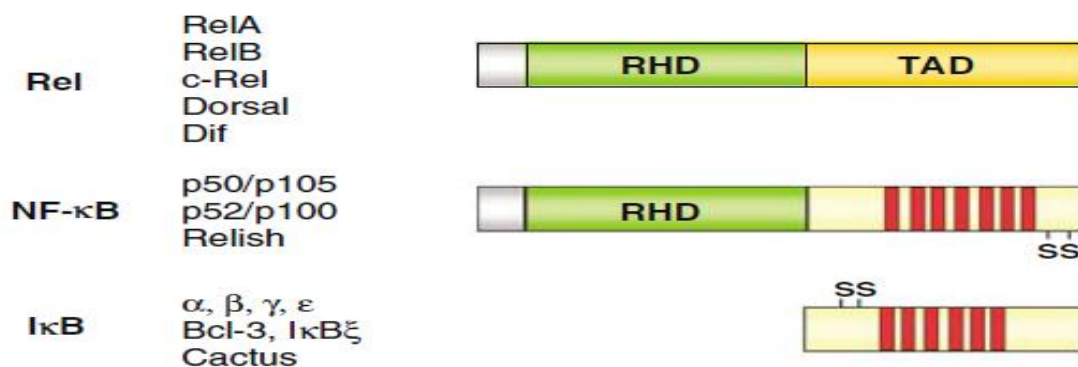


Figure 1.3.4 Image showing the generalised structures of the two subfamilies Rel and NF- κ B and related signalling molecules (Gilmore, 2006)

1.3.3 Interferon Regulatory Factor 3

IRF3 is a transcription factor belonging to the IRF family- which consists of nine members, it was discovered in 1995 as a regulatory component in cells infected with a virus and it has been shown to play an important role in type I IFN production (Au, Moore, Lowther, Juang, & Pitha, 1995; Honda, Takaoka, & Taniguchi, 2006). IRF3 was found to be a major component of the MyD88-independent pathway triggered

downstream of TLR4 in response to LPS (Doyle et al., 2002; Kawai et al., 2001). IRF3 is a transcription factor that is constitutively expressed in most cell types and displays both nuclear export sequences (NES) and nuclear localisation sequences (NLS). IRF3 possesses an amino N-terminal DNA-binding domain (DBD) that is characterised by a series of well conserved tryptophan-rich repeats (Honda & Taniguchi, 2006). The DBD forms a helix-turn-helix domain and can interact with interferon-stimulated response element (ISRE). IRF3 mainly resides in the cytoplasm due to the dominant NES but it is continuously shuttled between the cytoplasm and the nucleus in basal conditions (Kumar, McBride, Weaver, Dingwall, & Reich, 2000).

IRF3 is activated upon the recognition of specific PAMPS leading to the activation of the MyD88-independent signalling pathway as previously mentioned. Phosphorylation of IRF3 promotes dimerisation and nuclear translocation that allows for interaction with the transcriptional co-activators CBP/p300 (Gauzzi et al., 2010). CBP/p300 acetylates IRF3 homodimers, which causes a conformational change that unmask its DNA binding domain, promoting the transcription of its target genes (Lin et al., 1999). IRF3 binds to ISRE found in the promoters of Type I IFNs and other genes involved in immunity and oncogenesis (Honda & Taniguchi, 2006). IRF3 is central for the induction of IFN β , it is part of the enhanceosome that binds to the proximal promoter region and initiates local histone acetylation and nucleosomal repositioning (Agalioti et al., 2000). In macrophages and DCs stimulated with LPS, direct IRF3 binding is required for the recruitment of distinct sets of genes such as C-X-C motif chemokine 10 (CXCL10), regulated on activation normal T cell expressed and secreted (RANTES), IL-27a, IL-12a and IL-15 (Ramirez-Carrozzi et al., 2009). IFN β leads to the induction of specific genes that depend on other transcriptional regulators such as Interferon-stimulated gene factor 3 (ISGF3) and other downstream IRFs such as IRF1 and IRF5 (Ysebrant de Lendonck, Martinet, & Goriely, 2014).

IL-23 and IL-27 production is strongly dependent on the set of IRF family members that are activated with specific ligands. IRF3 is recruited to IL-12p35 and IL-27p28 promoter regions when DCs are stimulated with LPS (Goriely et al., 2008; Molle et al., 2007). Formation of the ISGF3 complex is critical for amplification of the IL-27p28 gene and may lead to late activation directly or through amplification of type I IFN

synthesis. The balance between IL-12, IL-23 and IL-27 production is strongly dependent on IRF3, which effects ensuing adaptive immune responses (Ysebrant de Lendonck et al., 2014). Polarization of CD4 T helper cells into distinct effector lineages are determined by the expression of master regulators: T-bet, Foxp3, GATA-3 or the orphan nuclear receptor ROR γ t, acting in close interaction with transcription factors from the signal transducer and activator of transcription (STAT) family. STAT4 is activated by IL-12, STAT6 is activated by IL-4, STAT3 is activated by IL-6, IL-21 or IL-23 and STAT5 is activated by IL-2. These are directly implicated in Th1, Th2, Th17 or Treg development (Zhu, Yamane, & Paul, 2010). Therefore IRF3 dependent pathway influences the polarization of CD4 T cells see **Figure 1.3.5**. Activation of IRF3 within APCs and subsequent autocrine type I IFNs signalling limits the induction of Th17 and Th1 responses. This can be favourable in the context of auto-immune inflammation or deleterious for the host in the context of bacterial infection (Ysebrant de Lendonck et al., 2014).

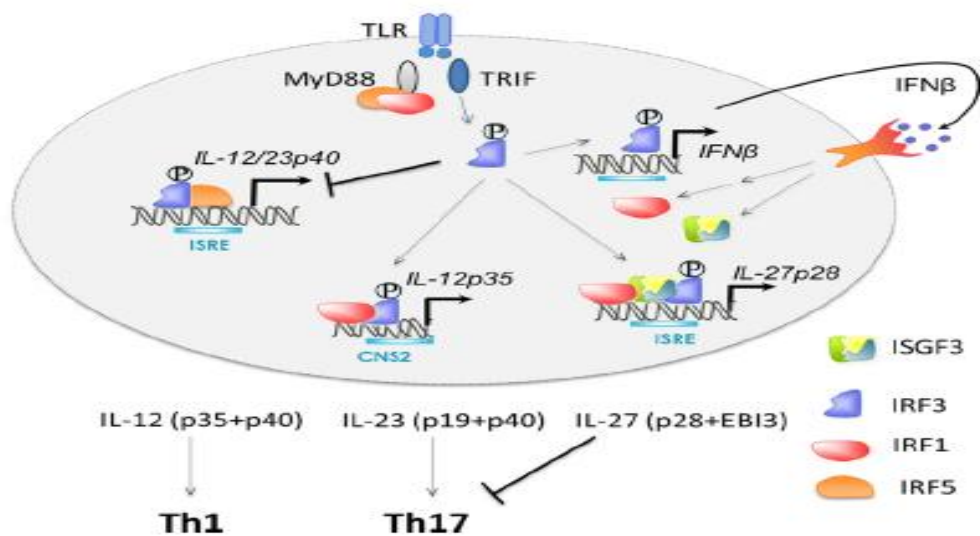


Figure 1.3.5 Illustration showing that IRF3 contributes to the balance between IL-12 family members in antigen presenting cells. Upon activation downstream of TLR4, IRF3 activates the transcription of IL-12p35 and IL-27p28 through direct recruitment to ISRE-binding sites within the promoter regions where IRF3 is recruited to the IL-12/23p40 promoter and enhancer regions (Ysebrant de Lendonck et al., 2014)

1.4 MicroRNAs

TLR signalling pathways are strictly and finely regulated by positive or negative modulators at various levels to prevent excessive inflammation, they can also regulate tissue maintenance and homeostasis (He, Jing, & Cheng, 2014). The mechanisms responsible include: physical interactions, conformational changes, phosphorylation, ubiquitination and proteasome mediated degradation involving various regulatory molecules (He, Jia, Jing, & Liu, 2013; Kondo, Kawai, & Akira, 2012; O'Neill, 2008). MicroRNAs (miRNAs) are a newly identified family of regulators involved in the fine tuning of TLR signalling (Yingke Li & Shi, 2013; Ma, Buscaglia, Barker, & Li, 2011; Nahid, Satoh, & Chan, 2011; O'Neill, Sheedy, & McCoy, 2011; Olivieri et al., 2013). MiRNAs were initially identified in 1993 in *C. elegans*, while examining the temporal regulation of a gene known as *lin-14*, by *lin-4* (Wightman, Ha, & Ruvkun, 1993). It was revealed that *lin-4* was expressed in two forms, a non-protein coding 22 nucleotide (nt) small RNA and a 61 nt precursor RNA molecule- also non-protein coding. The small 22 nt RNA molecules were found to have multiple "imperfect" complementary sites to the 3' Untranslated region (UTR) of *lin-14* mRNA. *Lin-4* was not found in any other species apart from *C. elegans* and this RNA interference mechanism was believed to be exclusive to this gene at the time (Lee, Feinbaum, & Ambros, 1993). Some time later it was discovered that a heterochronic gene *let-7* regulated the products of a gene known as *lin-41* and the regulation of this gene was similar to how *lin-4* regulated the products of *lin-14* (Reinhart et al., 2000). Unlike *lin-4*, the *let-7* gene homolog was found in other species such as *Drosophila* and humans (Hutvagner et al., 2001; Pasquinelli et al., 2000). These small RNA molecules were first defined as 'small temporal' RNA (stRNA) because of their roles in developmental timing, but as more small RNAs were identified in regulatory roles outside of development, they were defined more generally as miRNAs (Lagos-Quintana, Rauhut, Lendeckel, & Tuschl, 2001; Lau, Lim, Weinstein, & Bartel, 2001; Lee & Ambros, 2001).

Mature miRNAs are short double stranded RNA molecules approximately 19-23 nt in length. They are produced from full-length RNA polymerase II transcripts called pri-miRNA, after cleavage by two RNase III enzymes called Droscha and Dicer (Denli, Tops, Plasterk, Ketting, & Hannon, 2004; Lee et al., 2003; Zhang, Kolb, Jaskiewicz,

Westhof, & Filipowicz, 2004). Initial cleavage by Drosha within the nuclear compartment produces a hairpin RNA which is approximately 65 nt, known as pre-miRNA. Pre-miRNA is transported into the cytoplasm by exportin 5 and further processed by Dicer to produce the mature miRNA (Yi, Qin, Macara, & Cullen, 2003; Zhang et al., 2004). MiRNA actions are mediated by miRNA-induced silencing complex (miRISC), which is composed of many proteins including a member of the double-stranded RNA binding protein Argonaute (Ago) family (Liu et al., 2004; Meister et al., 2004). Using one strand of the miRNA called the guide strand, the miRISC either block mRNA translation, reduces mRNA stability or induces mRNA cleavage after imperfect binding to the miRNA recognition elements within the 3' and 5' UTR of target mRNA genes see **Figure 1.4.1** (Doench & Sharp, 2004; Lewis, Shih, Jones-Rhoades, Bartel, & Burge, 2003).

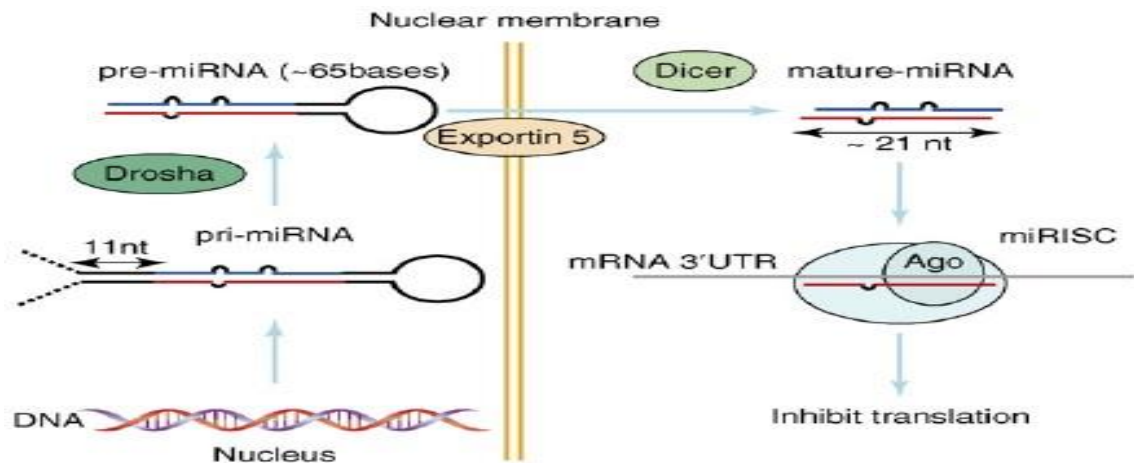


Figure 1.4.1 Image showing the processing of pri-miRNA to pre-miRNA. Mature miRNA recognises elements within the 3' and 5' UTR of target mRNA gene (Lindsay, 2008)

The discovery of the first miRNA initiated a large scale search to find other novel miRNAs in various organisms and cell types (Hutvagner et al., 2001). The mirBase database was created in 2002 to name, annotate and collate all published miRNA sequences (Griffiths-Jones, 2004). Newly discovered miRNAs are assigned official gene names after experimental isolation and verification, furthermore a manuscript describing the discovery must be accepted for publication before being entered in this

official miRNA database (Lhakhang & Chaudhry, 2012). MiRNA gene names consist of a three or four letter prefix used to designate the species e.g. hsa for human and mmu for *Mus musculus*, followed by a sequential numerical identifier. The mirBase database uses 'miR' to identify mature miRNA molecules, whereas 'mir' is used to designate the precursor hairpin subset (Griffiths-Jones, 2010). Additionally, paralogous miRNAs differing in only one or two positions are given lettered suffixes e.g. hsa-miR-146a and hsa-miR-146b. In cases where the miRNA products are identical but expressed from different genomic loci, the miRNA are given numerical suffixes e.g. hsa-mir-92a-1 and hsa-mir-92a-2 (Griffiths-Jones, Saini, Van Dongen, & Enright, 2008). In miRNA identification cloning studies, two mature products are often isolated from each arm of the double stranded miRNA hairpin. In many cases one is a non-functional by-product that is referred to as the 'star' sequence, and these miRNAs are designated with a '*' at the end of the gene name (Griffiths-Jones, Grocock, van Dongen, Bateman, & Enright, 2006). However, when there is insufficient evidence to determine the functional strand these miRNAs are given suffixes that signify the hairpin arm of origin, either -5p or -3p (Griffiths-Jones et al., 2008). To date there are 28,645 miRNA hairpin precursors, corresponding to 35,828 mature miRNAs in 223 species (miRBASE release June 2014); 2588 mature miRNAs are currently annotated in the human genome (Eulalio & Mano, 2015) and it has been estimated that up to 30% of all human genes are regulated by miRNAs in many cell types (Bartel, 2009; Fabian, Sonenberg, & Filipowicz, 2010; Yates, Norbury, & Gilbert, 2013).

1.4.1 MiRNAs Regulate TLRs

MiRNAs act as key regulators of gene expression and the regulation of TLRs may be one of the most effective points to alter signalling (He et al., 2014). Thus far, several miRNAs have been shown to regulate TLRs including the let-7 miRNA family. It has been shown that let-7e and let-7i regulate TLR4 expression, studies show the over expression of let-7e by miRNA mimics results in the down regulation of TLR4 in mouse peritoneal macrophages, and inhibition of let-7e leads to up regulation of TLR4 expression (Androulidaki et al., 2009). The myeloid-specific miR-223 is another TLR induced miRNA, it can regulate both TLR4 and TLR3 expression in granulocytes (Johnnidis et al., 2008). Another study found that miR-146a can also negatively regulate

TLR4, resulting in accumulation of oxidized low-density lipoprotein (oxLDL) and an inflammatory response in macrophages (Yang et al., 2011). In addition, miR-511 functions as a putative positive regulator of TLR4 under cell cycle arrest conditions, it is likely to inhibit TLR4 expression under similar conditions in monocytes and DCs (Tserel et al., 2011). These studies suggest that miRNAs may play an important role in the expression of TLRs and in particular TLR4. See **Figure 1.4.2** for a summary of miRNAs involved in the regulation of the TLR4 signalling pathway and their related regulatory molecules.

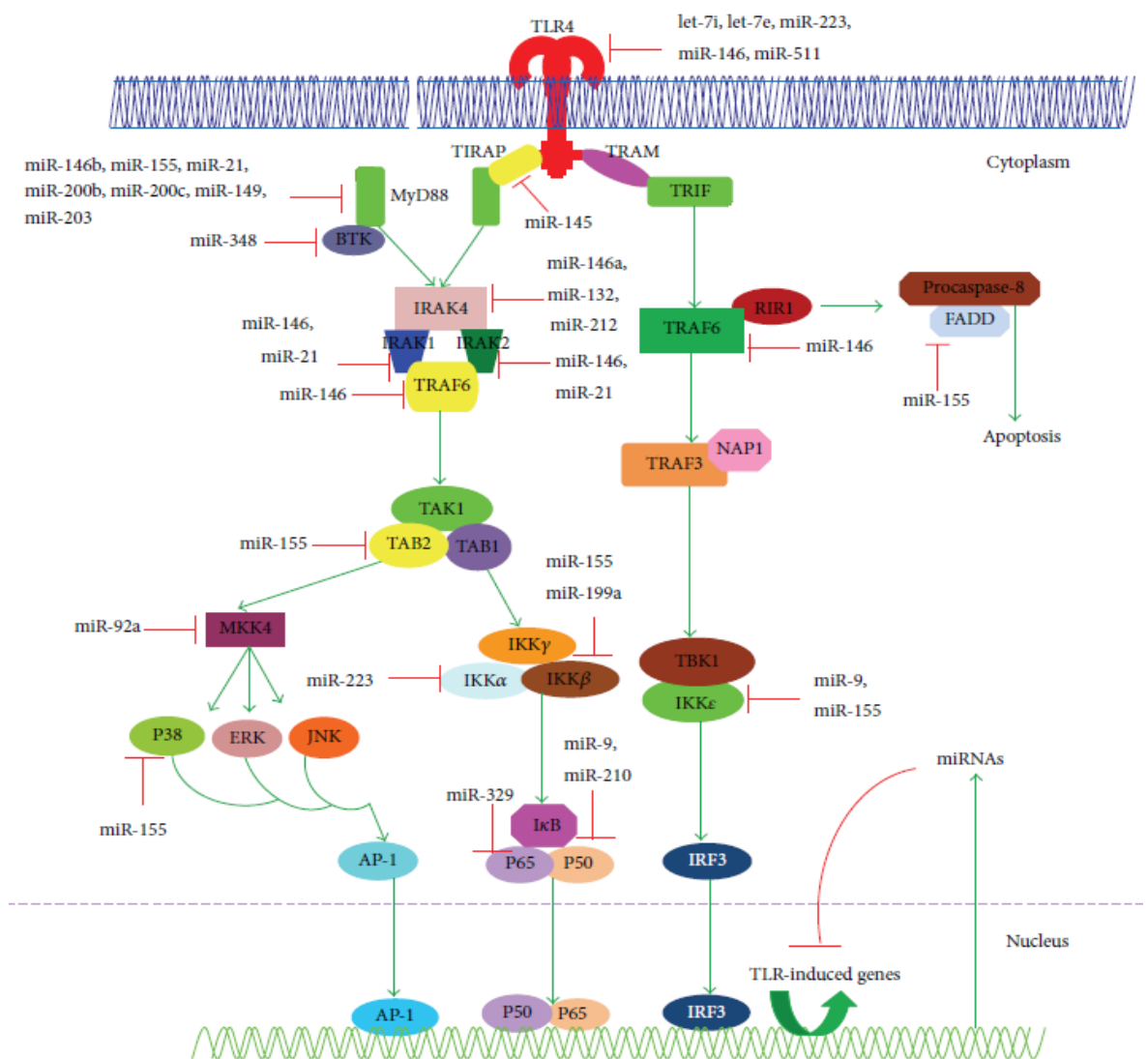


Figure 1.4.2 Image illustrating the array of miRNAs involved in the regulation of the TLR4 signalling pathway at multiple levels involving multiple molecules (He et al., 2014)

1.4.2 MiRNAs Regulate Signalling Proteins

TLR4 recruits many types of proteins upon ligand binding as mentioned earlier in this chapter. These proteins include various IRAKs, MKKs, TABs, IKKs, TRAFs and the adaptor molecules: MyD88, TRIF, mal and TRAM. Recently all of these molecules have also been shown to be targeted by miRNAs, especially when TLR4 is induced (Broz & Monack, 2013; He et al., 2013; Kondo et al., 2012; Yingke Li & Shi, 2013; Ma et al., 2011; Newton & Dixit, 2012; O'Neill et al., 2011; O'Neill, 2008; Olivieri et al., 2013). Among these miRNAs identified, miR-146a is one of the key TLR-induced miRNAs. MiR-146a inhibits TLR4 signalling by targeting IRAK1 kinase and TRAF6 ligase- components of the MyD88-dependent signalling pathway, in various cell types. IRAK2 another component of the MyD88-dependent pathway has also been shown to be regulated by miR-146a (Flannery & Bowie, 2010; Hou et al., 2009; Shuo Li, Yue, Xu, & Xiong, 2013; Lin et al., 2013; Nahid et al., 2011; Taganov, Boldin, Chang, & Baltimore, 2006; Tang et al., 2010). MiR-146b- another member of the miR-146 family, can modulate the TLR4 signalling pathway by directly targeting TLR4, MyD88, IRAK1, and TRAF6 (Curtale et al., 2013). MiR-132, miR-212, and miR-146a also target IRAK4 which leads to diminished production of inflammatory cytokines (Nahid et al., 2013).

MiR-155 another important TLR-induced miRNA, can target components of the NF- κ B pathway such as Fas-associated death domain protein (FADD), IKK β , IKK ϵ and Receptor (TNFRSF)-interacting serine-threonine kinase 1 (RIPK1) (Ceppi et al., 2009; Tili et al., 2007). MiR-155 has also been shown to inhibit the p38 MAPK signalling pathway and inflammatory cytokine production in human DCs in response to various microbial stimuli. In addition, miR-155 can regulate TAB2 in human monocyte-derived DCs (Ceppi et al., 2009). MyD88 has also been shown to be regulated by miR-155, miR-149, and miR-203 (Huang, Hu, Lin, Lin, & Sun, 2010; Tang et al., 2010; Wei et al., 2013; Xu et al., 2014). Another MyD88 adaptor-like protein mal has been identified as a target of miR-145 in hematopoietic stem/progenitor cells (Starczynowski et al., 2010). MiR-200b and miR-200c- members of the miR-200 family, can also regulate the expression of MyD88 and it has been shown that this regulation can modify the efficiency of the TLR4 signalling pathway effecting the host innate defences against

microbial pathogens (Wendlandt, Graff, Gioannini, McCaffrey, & Wilson, 2012). Collectively, some of the key components of TLR4 associated signalling proteins are regulated by miRNAs. These studies suggest that miRNA activation results in the timely and appropriate toning down and/or termination of TLR-signalling by targeting critical signalling proteins once they are activated (He et al., 2014).

1.4.3 MiRNAs Regulate Transcription Factors

Activation of transcription factors such as NF- κ B, AP-1, IRF and STAT are key functional steps following TLR activation (He et al., 2014). Studies have shown that miRNAs play a vital role in the negative feedback mechanisms that regulate these transcription factors (Filipowicz, Bhattacharyya, & Sonenberg, 2008; Martinez & Walhout, 2009). NF- κ B is considered one of the most important transcription factors and it has been shown that a miR-9 mediated feedback mechanisms directly targets NF- κ B1 mRNA to fine tune MyD88- dependent and NF- κ B signalling following activation with LPS (Bazzoni et al., 2009). Another study showed that miR-210 targets NF- κ B1 when induced by LPS in murine macrophages (Qi et al., 2012). Additionally, miR-329 plays a pivotal role in the inhibition of IL-6 mRNA expression by targeting the NF- κ B p65 complex (Garg, Potter, & Abrahams, 2013). MiR-223 has been shown to target STAT3, resulting in the inhibition of the pro-inflammatory cytokines IL-6 and IL-1 β production in macrophages (Chen et al., 2012). Furthermore, miR-17-5p and miR-20a target STAT3 to alleviate the suppressive function of myeloid-derived suppressor cells (Zhang et al., 2011). A transcriptional co-repressor CCAAT/enhancer binding protein- β (C/EBP β) has been identified as a target of miR-155 leading to decreased expression of granulocyte colony-stimulating factor and IL-6 in splenocytes (Costinean et al., 2009; Worm et al., 2009). Forkhead box p3 (Foxp3) - a transcription factor required for Tregs and E26 transformation specific sequence 2 (ETS-1) have also been identified as targets of miR-155 (Kohlhaas et al., 2009; Quinn et al., 2014). MiR-27b directly targets peroxisome proliferator-activated receptor (PPAR) γ when induced by NF- κ B and miR-27b can also inhibit TNF α secretion induced by LPS stimulation (Jennewein, von Knethen, Schmid, & Brüne, 2010).

1.4.4 MiRNAs Regulate Cytokines and Chemokines

Activation of TLR signalling through recognition of PAMPs leads to the transcriptional activation of genes that encode for pro-inflammatory cytokines, chemokines, and co-stimulatory molecules. These cytokines play an important role in eradicating infectious pathogens and recruiting inflammatory cells for an effective host defence (Kawai & Akira, 2006). Several key TLR induced cytokines including type I IFNs, TNF α , IL-6, IL-12, and IL-10 are regulated by miRNAs (Asirvatham, Gregorie, Hu, Magner, & Tomasi, 2008; Asirvatham, Magner, & Tomasi, 2009; Xiangde Liu & Rennard, 2011). MiR-146a sequentially suppresses the production of type I IFNs, TNF α , IL-1 β and IL-6 by targeting IRAK1, IRAK2, and TRAF6 in macrophages during LPS tolerance (Hou et al., 2009; Shuo Li et al., 2013; Xie et al., 2013). MiRNA-146a can also negatively regulate the release of the pro-inflammatory chemokines IL-8 and RANTES (Perry et al., 2008). MiR-26a, miR-34a, miR-145 and let-7b directly regulate the expression of IFN- β by targeting the 3'-UTR region (Witwer, Sisk, Gama, & Clements, 2010; Zhou, O'Hara, & Chen, 2011). Type I IFNs can also affect miRNA expression, it has been shown that the activation of IFN- β can suppress miR-378 and miR-30 which allows the release of cytolytic mRNAs resulting in augmented natural killer (NK) cell cytotoxicity (Wang et al., 2012). I κ B ξ , is a master regulator for the transcription of two key cytokines IL-6 and IL-12p40, it is indirectly targeted by miR-187, it was also shown that miR-187 directly targets TNF α mRNA (Rossato et al., 2012). When IL-6 is targeted by miRNAs including miR-16, miR-365 and miR-142-3p, there is a reduction in endotoxin induced mortality through a feedback mechanism (Sun et al., 2015; Xu et al., 2011; Zhou et al., 2011). IL-12p35 mRNA contains target sites for miR-21 in macrophages and DCs leading to restricted adaptive Th1 responses (Lu, Munitz, & Rothenberg, 2009). In contrast, miR-29 suppresses the immune response against intracellular pathogens by targeting IFN- γ (Ma et al., 2011).

1.4.5 MiRNAs Regulate Other Regulatory Molecules

MiRNAs can also target other regulatory molecules known to modulate TLR signalling pathways. MiR-132 targets acetyl cholinesterase (ACHE) which negatively regulates the TLR signalling pathway (Shaked et al., 2009). MiR-21 can target tumour suppressor

protein programmed cell death 4 (PDCD4), an inhibitor of eukaryotic translation initiation factor 4F in macrophages, thus enhancing innate immune responses in the early stages of infection by a pathogen. The inhibition of PDCD4 increases IL-10 secretion, suggesting a role for TLR induced cytokine production during infection (Loh et al., 2009; Sheedy et al., 2010; Yang et al., 2003). Src homology 2 domain-containing inositol-5'-phosphatase 1 (SHIP1), a negative regulator of TLR signalling and the inflammatory response, is a target of miR-155 (Costinean et al., 2009; Cremer et al., 2009). Studies have also shown that when macrophage are stimulated with LPS, there is a down regulation of SHIP1 and increased expression of miR-155 (Gabhann et al., 2010; Loh et al., 2009; Worm et al., 2009; Yang et al., 2003). MiR-155 has also been shown to target suppressor of cytokine signalling 1 (SOCS1), which is another negative regulator of TLR signalling. However, IL-10 can inhibit miR-155 expression leading to an increase in SHIP1 and SOCS1 expression, thus mitigating TLR signalling (Androulidaki et al., 2009; McCoy et al., 2010). Notch1 on the other hand is a known positive regulator of IL-12p70 production in DCs and miR-146a targets IL-12p70 in DCs stimulated with TLR9 (Bai et al., 2012). MiR-148a/b and miR-152 inhibit the expression of calcium/calmodulin dependent protein kinase II (CaM-kinase II) to regulate TLR signalling (Liu et al., 2010). Together these studies suggest that miRNAs are responsible for regulating regulatory molecules to fine tune TLR-signalling pathways and downstream events (He et al., 2014).

Table 1.4.1 Summary of miRNAs that regulate TLR4 signalling

Target mRNA	MiRNA(s)	Reference
Receptor		
TLR4	let-7i, let-7e miR-223, miR-146a, miR-146b, miR-511	Androulidaki et al., 2009; Curtale et al., 2013; Johnnidis et al., 2008; Tserel et al., 2011; Yang et al., 2011
Signalling Proteins		
IKK β	miR-155	Ceppi et al., 2009; Tili et al., 2007; Wendlandt et al., 2012
IKK ϵ	miR-155	Ceppi et al., 2009; Tili et al., 2007
IRAK1	miR-146a, miR-146b, miR-148b, miR-21	Curtale et al., 2013; Hou et al., 2009; Shuo Li et al., 2013; Lin et al., 2013; Liu et al., 2010; Taganov et al., 2006
IRAK2	miR-146a	Hou et al., 2009; Taganov et al., 2006
IRAK4	miR-146a, miR-132, miR-212	Nahid et al., 2013
Mal	miR-145	Starczynowski et al., 2010
MyD88	miR-146b, miR-155, miR-200b, miR-200c, miR-21, miR-203, miR-149	Curtale et al., 2013; Huang et al., 2010; Tang et al., 2010; Wei et al., 2013; Wendlandt et al., 2012
RIPK1	miR-155	Ceppi et al., 2009; Tili et al., 2007
TAB2	miR-155	Ceppi et al., 2009; Tili et al., 2007
TRAF6	miR-146a, miR-146b	Curtale et al., 2013; Hou et al., 2009; Liu et al., 2010; Taganov et al., 2006
Transcription Factors		
C/EBP β	miR-155	Costinean et al., 2009
ETS-1	miR-155	Quinn et al., 2014
Foxp3	miR-155	Kohlhaas et al., 2009
NF- κ B1	miR-9, miR-210	Bazzoni et al., 2009; Qi et al., 2012
NF- κ Bp65	miR-329	Garg et al., 2013

p38 MAPK	miR-155	Ceppi et al., 2009
PPAR γ	miR-27b	Jennewein et al., 2010
STAT3	miR-17-5p, miR-20a, miR-223	Chen et al., 2012; Zhang et al., 2011
Cytokines and Chemokines		
IFN- β	miR-26a, let-7b, miR-34a, miR-145, miR-378, miR-30	Witwer et al., 2010; Zhou et al., 2011
IFN- γ	miR-29	Ma et al., 2011
IL-10	miR-21, miR-155	Androulidaki et al., 2009; Loh et al., 2009; McCoy et al., 2010; Sheedy et al., 2010; H. Yang et al., 2003
IL-12p35	miR-21	Lu et al., 2009
IL-12p40	miR-187	Rossato et al., 2012
IL-1 β	miR-223	Chen et al., 2012
IL-6	miR-16, miR-365, miR-142-3p, miR- 187, miR-329, miR- 223	Chen et al., 2012; Garg et al., 2013; Sun et al., 2015; Xu et al., 2011; Zhou et al., 2011
IL-8	miR-146a	Jing et al., 2005; Perry et al., 2008
RANTES	miR-146a	Perry et al., 2008
TNF α	miR-187, miR-27b	Jennewein et al., 2010; Rossato et al., 2012
Regulatory Molecules		
ACHE	miR-132	Shaked et al., 2009
CaM-Kinase II	miR-148a/b, miR-152	Xingguang Liu et al., 2010
Notch1	miR-146a	Bai et al., 2012
PDCD4	miR-21	Loh et al., 2009; Yang et al., 2003
SHIP1	miR-155	Costinean et al., 2009; Cremer et al., 2009
SOCS1	miR-155	Androulidaki et al., 2009; McCoy et al., 2010

1.5 Aims and Objectives

C. difficile can induce severe inflammation in the gut and the severity of disease depends on the ribotype causing the infection. SLPs coat the outer layer of *C. difficile* and the LMW protein varies between ribotypes. Previous research focused on SLPs from ribotype 001 which activate innate and adaptive immunity suggesting an important role for SLPs in the recognition of *C. difficile* by the immune system. Given the differences in clinical symptoms between strains of *C. difficile*, SLPs may modulate the immune response and this may differ between ribotypes. SLPs from ribotype 001 activate TLR4 signalling with subsequent downstream activation of NF- κ B, however they fail to induce IRF3 signalling. MiRNAs are a newly identified family of regulators involved in the fine tuning of TLR4 signalling. There is mounting evidence that miRNAs orchestrate immune regulation and host responses to pathogens during infection. To date nobody has studied miRNAs regulated by SLPs from *C. difficile*. Our hypothesis states SLPs from various ribotypes of *C. difficile* may activate different immune responses to infection and signalling downstream of TLR4. MiRNAs may be expressed in response to SLPs, which perhaps modulate TLR4 signalling leading to the differences in severity of infection between ribotypes.

To address the above, the aims of this thesis were:

- To examine the immune response of various ribotypes of *C. difficile* and to determine downstream signalling following TLR4 activation with SLPs from the various ribotypes
- Establish and optimise a protocol to examine miRNAs
- Compare miRNA profiles regulated by SLPs from ribotype 001 and 027 *in vitro*
- Identify miRNAs switched on and off during infection by examining colonic tissue in a mouse model of *C. difficile in vivo*
- Analyse functionality of miRNAs induced by SLPs from ribotype 001 and 027 in TLR4 signalling
- Identify biologically relevant gene targets using bioinformatic target prediction tools

Chapter 2: Materials and Methods

2.1 Materials

Table 2.1.1 Tissue cell culture

Material	Source
15ml and 50ml centrifuge tubes	Sarstedt
Blasticidin	Invivogen™
Brightline Haemocytometer	Sigma-Aldrich®
Cell Titer® 96 AQueous One Solution	Promega
DMEM-6429	Gibco®
Foetal Bovine Serum (FBS)	Invitrogen™
GM-CSF expressing cell line	J558 GM-CSF
Hygrogold™	Invivogen™
LPS (<i>E. Coli</i> serotype R515)	Enzo Lifesciences
Mr. Frosty freezing container	Thermo Fisher Scientific
Penicillin Streptomycin/ Glutamine	Gibco®
Presept tablets	VWR International Ltd.
rGM-CSF(G0282)	Sigma-Aldrich®
RPMI-1640	Gibco®
Sterile dH ₂ O	Sigma-Aldrich®
Sterile petri dishes	Nunc™
Tissue culture flasks T-25cm ² and T-75cm ²	Nunc™
Tissue culture plates 6, 24 and 96-well	Nunc™
Trypan Blue (0.4% w/v)	Sigma-Aldrich®
Trypsin/ EDTA	Sigma-Aldrich®
α-MEM alpha	Invitrogen™

Table 2.1.2 Characterisation of SLPs

Material	Source
Bicinchoninic acid (BCA) Protein Assay Kit.	Pierce™
ToxinSensor™ Chromogenic LAL Endotoxin Assay Kit	Genscript

Table 2.1.3 SDS-PAGE

Material	Source
Acetic Acid CH ₃ CO ₂ H	Sigma-Aldrich®
Ammonium persulphate (APS)	Sigma-Aldrich®
Bicinchoninic acid (BCA) Protein Assay Kit.	Pierce™
Bis-acrylamide 30%	Sigma-Aldrich®
Bromo-blue	Sigma-Aldrich®
Coomassie Brilliant blue	Sigma-Aldrich®
Fermentas PageRuler™ plus Pre stain protein ladder	Thermo Fisher Scientific
Glycine	Sigma-Aldrich®
Methanol	Lennox
N,N,M'- Tetramethylethylenediamine (TEMED)	Sigma-Aldrich®
Propan-2-ol (Isopropanol)	VWR International Ltd.
Sodium dodecylsulphate (SDS)	Sigma-Aldrich®

Table 2.1.4 Enzyme Linked Immunosorbent Assay (ELISA)

Material	Source
96- well micro titre plate	Nunc™
Bovine serum albumin (BSA)	Sigma-Aldrich®
Dulbecco's Phosphate Buffered Saline (PBS)	Gibco®
DuoSet® ELISA kits	R&D systems
Streptavidin-HRP	R&D systems
Trizma base	Sigma-Aldrich®
VersaMax™ microplate reader	Molecular Devices
3,3',5,5'-tetramethyl-benzidine (TMB)	Sigma-Aldrich®
Tween® 20	Sigma-Aldrich®

Table 2.1.5 Flow Cytometry

Material	Source
APC hamster anti-mouse CD11c antibody	BD
BD buffer	BD
FACS Clean	BD
FACS flow	BD
FACS Rinse	BD
FACS tubes	Sarstedt
FITC rat anti-mouse CD14 antibody	eBioscience
FITC rat anti-mouse CD86 antibody	BD
PE rat anti-mouse CD40 antibody	BD
PE rat anti-mouse CD80 antibody	BD
Proprodium Iodide (PI)	BD
Sodium Azide (NaN ₃)	Sigma-Aldrich®
Wash buffer (PBS+ 0.1% Tween)	BD

Table 2.1.6 Plasmid DNA preparation and transfection

Material	Source
Ampicillin 100 mg/mL	Sigma-Aldrich®
hsa- let-7e mirVana miRNA mimic (MC 12304)	Ambion®
Empty Vector control construct pcDNA3.1	Invitrogen™
hsa-miR-145-5p mirVana miRNA mimic (MC11480)	Ambion®
hsa-miR-146a-5p mirVana miRNA mimic (MC10722)	Ambion®
hsa-miR-155-5p mirVana miRNA mimic (MC12601)	Ambion®
Inoculation Loops	Cruinn
Lipofectamine 2000 reagent	Thermo Fisher Scientific
Lysogeny broth (LB) Broth	Sigma-Aldrich®
mirVana miRNA mimic miR-1 positive control	Ambion®
mirVana miRNA negative control #1	Ambion®
NF-κB construct	Gift

Opti-Mem Reduced Serum Medium	Gibco®
pFA-IRF3 construct	Gift
pFR construct	Gift
Qiagen plasmid DNA Hi-speed midi kit	Qiagen
phRL-TK (TK renilla construct)	Gift

Table 2.1.7 Luciferase gene reporter assay

Material	Source
Acetyl Co Enzyme A (Lithium salt)	Sigma-Aldrich®
ATP	Sigma-Aldrich®
Coelenterazine	Biotium
Dithiothreitol (DTT)	Sigma-Aldrich®
D-Luciferin firefly	Sigma-Aldrich®
Ethylenediaminetetraacetic acid (EDTA)	Sigma-Aldrich®
GloMax® Microplate Luminometer	Promega
Luciferase cell culture lysis 5x reagent	Promega
Magnesium Carbonate Hydroxide Pentahydrate (MgCO ₃) ₄ Mg(OH) ₂ .5H ₂ O	Sigma-Aldrich®
Magnesium Sulfate Heptahydrate MgSO ₄ .7H ₂ O	Sigma-Aldrich®
Sodium Hydroxide NaOH	Sigma-Aldrich®
Tricine	Sigma-Aldrich®

Table 2.1.8 RNA and DNA integrity by gel electrophoresis

Material	Source
Agarose	Thermo Fisher Scientific
Fermentas 6X DNA Loading Dye	Thermo Fisher Scientific
Gene Ruler 1 kb Plus DNA ladder	Thermo Fisher Scientific
RNA Sample Loading Buffer	Sigma-Aldrich®
SYBR® Safe DNA Gel Stain	Invitrogen™
TAE	Sigma-Aldrich®

Table 2.1.9 RNA isolation, cDNA synthesis and qPCR. (Complete list of miRNA sequences and assays numbers see **Appendix E**)

Material	Source
96 well PCR plates	Applied Biosystems™
Diethyprocarbonate (DEPC) H ₂ O	Invitrogen™
DNA Zap	Invitrogen™
Megaplex PreAmp Primers, Human Set v2.0 (A & B)	Applied Biosystems™
Megaplex RT Primers Human Set v2.0 (A & B)	Applied Biosystems™
MicroAmp Optical Adhesive film	Applied Biosystems™
mirVana miRNA isolation kit	Ambion®
Taqman Array cards, 31 +1 MC format 32	Applied Biosystems™
TaqMan Array Human miRNA Cards Set v2.0 (A & B)	Applied Biosystems™
Taqman MicroRNA Individual Assays	Applied Biosystems™
TaqMan miRNA Reverse Transcription Kit	Applied Biosystems™
TaqMan Pre Amp Master Mix	Applied Biosystems™
Taqman Universal Master Mix II, no UNG	Applied Biosystems™

2.2 Methods

2.2.1 Characterisation of SLPs

C. difficile culture and the purification of all SLPs used in this project were carried out by Dr. Mark Lynch and Dr. Izabela Marszalowska- members of the Immunomodulation research group, DCU as part of their PhD research projects. SLPs were purified from frozen *C. difficile* spores from patient samples attending St. James hospital, Dublin. The *C. difficile* spores from the varying ribotypes were a gift from Prof. Thomas Rogers from the Department of Clinical Microbiology, School of Medicine, Trinity College, Dublin.

The strains used in this study included R13537 (ribotype 001) and R12885 (ribotype 014). The sequence of the *slpA* gene of these strains had been previously determined (accession numbers DQ060626 and DQ060638 respectively). To determine the *slpA* gene sequences of our clinical strains, whole-genome sequencing was performed. DNA was extracted from *C. difficile* using the Roche High-pure PCR template preparation kit (Roche, West Sussex, UK). Nextera XT library preparation reagents (Illumina, Eindhoven, The Netherlands) were used to generate multiplexed sequencing libraries of *C. difficile* genomic DNA, and resulting libraries were sequenced on an Illumina MiSeq®. Short-read data obtained has been deposited in the European Nucleotide Archive (ENA); project accession number PRJEB6566. Genome assemblies were performed using the Velvet short read assembler and *slpA* gene sequences were retrieved for each isolate using BLAST (Altschul, 1990).

All microbial cell culture was carried out using aseptic techniques in a BIOMat class II microbiological safety cabinet in the Institute of Molecular Medicine (Trinity College, Dublin), based in St. James hospital. The SLPs were purified from cultures grown anaerobically at 37°C in Brain Heart Infusion (BHI) broth/0.05% Sodium thioglycolate with 0.5% Hemin and 0.1% Vitamin K. Cultures were harvested and the S-Layer protein was purified from the surface of the bacteria. Crude extracts were dialysed and samples applied to MonoQ HR10/10 anion exchange column attached to an AKTA FPLC. SLPs were eluted with a linear gradient of 0–0.3 mol/L NaCl at a flow rate of 4 mL/min. Fractions containing pure SLPs were collected and concentrated down to a

volume of approximately 200 μ L using an Amicon Ultra- 4 filter unit centrifuge tubes. Samples were collected and exposed to a UV light for 15 min to ensure sterilisation. SLPs were then aliquoted and stored at -20°C until ready for use (Lynch 2014, unpublished; Marszalowska 2015, unpublished).

Table 2.2.1 Accession numbers for the *slpA* gene for each ribotype used in this study, sequences from GenBank

Ribotype	Accession number	Length of sequence
RT 001	DQ060626	AA: 756 Nuc: 2271
RT 005	DQ060630	AA: 610 Nuc: 1833
RT 027	R20291	AA: 758 Nuc: 2277
RT 031	DQ060641	AA: 739 Nuc: 2220
RT 078	DQ060643	AA: 726 Nuc: 2181
RT 014	DQ060638	AA: 732 Nuc: 2199

2.2.1.1 SDS-PAGE

Sodium Dodecylsulphate-Polyacrylamide Electrophoresis (SDS-PAGE) was carried out to visualise the HMW and LMW SLPs that were extracted from the *C. difficile* cultures. The loading buffer containing SDS applies a uniform negative charge to the samples which migrate in an electrical field towards the positive electrode. The proteins are separated primarily by size as a result of the mass to charge ratio following binding of the SDS. Pure and crude samples of each of the SLPs from the differing ribotypes were diluted in 5x Loading Buffer (see **Appendix A**) which was supplemented with Dithiothreitol (DTT) and heated to 96°C for 5 min to denature any protein structures. The samples were allowed to cool to room temperature. Acrylamide resolving gels (12%) and stacking gels (5%) (see **Appendix A**) were made - the APS (10%) and

TEMED were added last and swirled gently to induce setting. The Acrylamide gels were cast between a pair of 10 x 100 mm glass plates. Once set the gels were fixed to the electrophoresis unit using a spring clamp. Gels were submerged in 1X electrode running buffer (**see Appendix A**), 15 μ L of sample was loaded into each well. PageRuler Plus Prestained Protein ladder is a molecular weight protein ladder ranging from 10-250 kDa, it was added to lanes either side of the SLPs as a size indicator. Gels were run at 30 mA per gel for approximately one hour or until the dye front reached the base of the gel. Once electrophoresis was complete, the gels were washed with dH₂O and submerged in 10 mL of Coomassie Blue stain (**see Appendix A**). The gels were left on a rocker for one hour to stain any protein bands present. Following staining the gel was washed briefly with dH₂O and 10 mL of destain solution (**see Appendix A**) was added to the gels. The gels were placed on the rocker for 10 min before replacing the buffer with fresh destain, this was repeated four times. The gels were then left to agitate gently in destain overnight at 4°C. Gels were examined for the presence of SLPs. The HMW band was expected to be seen at 44 kDa while the LMW band was expected to be seen between 32-35kDa.

2.2.1.2 Protein Concentration of SLPs

The total protein concentration of the SLPs was determined using a Bicinchoninic Acid (BCA) protein assay kit (Pierce). The assay uses the well documented reduction of Cu⁺² to Cu⁺¹ by protein in a base, where colorimetric detection of Cu⁺¹ can be measured. A purple colour is observed in the presence of protein- darker colours signify a higher concentration of protein. Standards ranging from 0-2,000 μ g/mL were made from Bovine Serum Albumin (BSA). Each standard and sample was added to a 96 well plate in triplicate. BCA working reagent was added to each well and the plate was covered and incubated at 37°C for 30 min. Samples were allowed to cool to room temperature and absorbance was read at 562 nm on the VersaMax™ microplate reader (Molecular Devices). A standard curve was constructed using the blank corrected absorbance values for each standard (**see Appendix B**).

2.2.1.3 Endotoxin Assay

SLPs were tested for the presence of endotoxin, to ensure any observed immune response was not due to contaminants. The ToxinSensor™ Chromogenic LAL Endotoxin Assay Kit (GenScript) was used and instructions were followed according to manufacturer's specifications. Limulus amoebocyte lysate (LAL) reacts with bacterial endotoxin and lipopolysaccharide (LPS). A synthetic colour producing substrate is used to detect this endotoxin chromogenically. A series of standards were made from 1 EU/mL (endotoxin unit/mL) endotoxin stock solution ranging from 0.01-0.1 EU/mL. Subsequently 100 µL of standards and samples were placed in specific endotoxin-free vials in triplicate. A blank of LAL reagent water was also prepared. LAL was added to each vial and the samples were incubated at 37°C for 10 min. Chromogenic substrate solution was then added, the samples were gently mixed and incubated for 6 min. Stop solution and colour stabiliser were added and samples were gently swirled to avoid generation of bubbles. Samples were transferred to a 96 well plate and the absorbance was read at 545 nm on the VersaMax™ microplate reader (Molecular Devices). A standard curve was constructed using the absorbance values for each standard where 4 EU/mL equates to 1 ng/mL therefore the concentrations of endotoxin present in the unknown samples could be calculated (**see Appendix B**).

2.2.2 Cell Culture Techniques

All cell culture was carried out using aseptic technique in a class II laminar airflow unit (Holten 2010-ThermoElectron Corporation, OH, USA). Cell cultures were maintained in a 37°C incubator with 5% CO₂ and 95% humidified air (Model 381- Thermo Electron Corporation OH USA). Cell cultures were maintained in media supplemented with heat inactivated (HI) Fetal Bovine Serum (FBS) at 56°C for 30 min where stated. Cells were visualised with an inverted microscope (Olympus CKX31, Olympus Corporation, Toyko, Japan).

2.2.2.1 Revival of Frozen Stocks

A cryovial was removed from liquid nitrogen and thawed rapidly by gentle agitation in a 37°C water bath. As soon as contents were thawed, the vial was sprayed with 70%

ethanol and the contents were removed under aseptic conditions. The cells were transferred into 9 mL complete medium (depending on the cell line used) and centrifuged for 5 min at 250 x g. The pellet was re-suspended in 10 mL complete medium and placed in a pre-warmed T25 cm² culture flask. The flask was incubated at 37°C and 5% CO₂.

2.2.2.2 Cell Enumeration and Viability Assessment

Cell viability was assessed using trypan blue dye exclusion analysis. This test is based on the principle that viable cells maintain intact cell membranes and they can exclude trypan blue dye from entering the cell. In contrast dead cells cannot maintain intact cell membranes and allow the dye to enter the cell. Viable and non-viable cells can be visualised under the microscope. We placed 100 µl of cells in suspension were mixed with 150 µl PBS and 250 µl trypan blue solution (0.4% (v/v)). A glass coverslip was mounted onto the shoulders of a Brightline Neubauer Haemocytometer and 10 µL of the mixture was applied at the edge of the coverslip and drawn across the counting chamber underneath by capillary action. Cells were examined under high power magnification (x40) and cells were counted in the areas marked 1-4 see **Figure 2.2.1**. The number of cells in the 16 squares equates to the number of cells x 10⁴/mL, therefore the total number of cells was calculated using the following formula: Cell/mL = N x D x 10⁴ Where, N = average cell number counted in each square , D = dilution factor of cells in PBS.

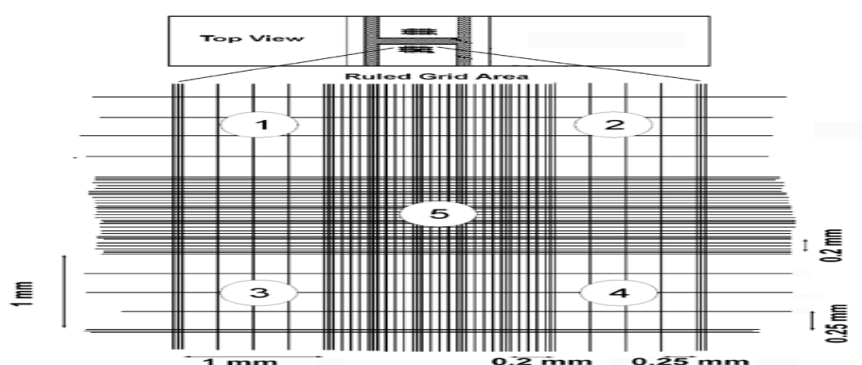


Figure 2.2.1 Representation of the Neubauer haemocytometer used to count cells. Areas 1-4 on the diagram show where cells were counted. Cells touching the left or top boundary were not counted

2.2.2.3 Cryogenic Preservation of Cell Line Stocks

To maintain reserves of cell lines, the cells were cryogenically preserved in liquid nitrogen. Cells were grown to a state of sub-confluency and counted (**see Section 2.2.2.2**) and re-suspended at 5×10^6 cells/mL in of complete medium with 5% (v/v) DMSO. Aliquots of 1 mL were transferred to labelled cryovials and placed in a Mr Frosty freezing container in a -80°C freezer. Mr Frosty freezing container provides a $1^\circ\text{C}/\text{min}$ cooling rate which is required for successful cryopreservation of cells. After three hours the cryovials were then transferred for storage to the liquid nitrogen vessel.

2.2.3 Bone Marrow Derived Dendritic Cell Isolation and Culture

Lutz *et al.* (1999) developed a technique to isolate large quantities of pure bone marrow-derived dendritic cells (BMDCs) from mouse bone marrow (Lutz et al., 1999). Bone marrow was isolated aseptically from the tibiae and femurs of BALB/c mice purchased from Charles River (U.K.) aged 10–14 weeks. The animals had *ad libitum* access to animal chow/water and were housed in a Specific Pathogen Free (SPF) unit in the licensed Bioresource facility at Dublin City University. The mice were culled in accordance with European Union (Protection of Animals used for scientific purposes regulations 2012) S.I No.543 of 2012 & directive 2010/63/EU of the European Parliament. The hind legs were removed and flesh/muscle was carefully removed from the leg bones, the bones were stored in RPMI media on ice. The femur was cut above the knee and below the hip to expose the bone marrow. A syringe with a 27.5 G needle was filled with RPMI and used to flush the bone marrow out of the femur into a sterile 50 mL falcon. The same process was repeated for the tibia. All bone marrow was collected together and a sterile 10 mL syringe with a 19 G needle was used to break up the bone marrow. The 50 mL falcon was centrifuged at $250 \times g$ for 5 min and the pellets were re-suspended in 1 mL media for every bone used in the experiment e.g. 2 legs equals 4 bones therefore cells re-suspended in 4 mL media. Enough complete RPMI media (**see Appendix A**) supplemented with Granulocyte macrophage colony-stimulating factor (GM-CSF) was added to the cells to load 10 mL of total media per sterile petri dish: 1 mL of cells to 9 mL RPMI. Cells were incubated at 7°C in 5% CO_2 in a humidified incubator. After 3 days 7 mL of media was removed from each petri

dish and 10 mL of fresh RPMI/GM-CSF was added. Cells were incubated for a further four days before being removed from the petri dishes, a sterile cell scraper was used to detach any adherent cells. The cells were collected in a sterile 50 mL centrifuge tube and centrifuged at 250 x g for 5 min. Cells were counted (see **Section 2.2.2.2**) and plated at 1×10^6 cells/mL for experiments.

2.2.4 Hek-293 and Hek TLR4/MD2/CD14 Cell Culture

Human Embryonic Kidney 293 (Hek-293) and human Hek-293 TLR4/MD2/CD14 cell lines were a gift from Prof. Paul Moynagh, The Institute of Immunology, National University of Ireland Maynooth, Maynooth Co. Kildare. The cells were maintained in complete DMEM (see **Appendix A**) in T-75 cm² flasks. The human Hek TLR4/MD2/CD14 cells are derived from Hek-293 cells but have the machinery for TLR4 signalling, as they are stably co-transfected with the pUNO-TLR4 that express human TLR4 genes and the pDUO2-MD2-CD14 plasmid which express human MD2 with CD14 genes. Cell monolayers were passaged at a confluency of 80% (every 4-5 days). Cells were detached from the flask surface by scraping with sterile cell scrapers in the presence of PBS. For subculture cells were split 1:3 in complete medium. Cells were counted (see **Section 2.2.2.2**) and plated at 1×10^6 cells/mL for experiments.

2.2.5 JAWS II Dendritic Cell Line Culture

The Murine JAWS II DC cell line (CRL-11904) were bought from the ATCC and maintained in complete α -MEM (see **Appendix A**) in T75cm² flasks. JAWS II DCs are an immature dendritic cell line derived from p53 growth suppressor gene deficient C57BL/6 mice. The cell line can be induced to become an activated dendritic cell line with the ability to stimulate T cells to proliferate (MacKay & Moore, 1997). JAWS II DCs are a mixed culture of attached and suspension cells. After seven days of growth the suspension cells were transferred to a 50 mL falcon before adherent cells were washed with PBS and detached with 0.25% trypsin-0.53 mM EDTA. All cells were pooled and centrifuged at 200 x g for 10 min and sub cultured at a 1:5 ratio in T75cm² flasks and incubated at 37°C in 5% CO₂. Cells were counted (see **Section 2.2.2.2**) and plated at 1×10^6 cells/mL for experiments.

2.2.6 Cell Stimulation

Cells were seeded at 1×10^6 cells/mL and incubated overnight or until adherent cells adhered to the base of each well. Cells were stimulated with 20 $\mu\text{g/mL}$ SLPs which were isolated from various ribotypes (RT) of *C. difficile*. Cells were also stimulated with 100 ng/mL LPS from a 1 mg/mL stock of *E. coli* serotype R515 as a positive control. Control cells were incubated in media alone. The cells were incubated for a period of time ranging from 1-24 hours depending on the experimental set up.

2.2.7 Cytotoxicity Assay

Cell titer 96 Aqueous One solution contains (3- 4,5-dimethylthiazol-2-yl)-5-(3-carboxymethoxyphenyl)-2-(4-sulfophenyl)-2H- tetrazolium, known as MTS. This compound can be used to measure the quantity of formazan produced by cells, to measure cell viability. The quantity of formazan produced is directly proportional to the number of living cells in culture. Hek TLR4/MD2/CD14 cells were counted and plated at 0.1×10^6 cells/100 μL in complete DMEM media in a 96 well plate overnight (see **Section 2.2.2.2**). Cells were transfected with miRNA mimics, NF- κB and IRF3 plasmid DNA constructs (see **Section 2.2.11**). Post transfection (18 hours) cells were stimulated with LPS and SLPs (see **Section 2.2.6**). We placed 20 μL of Cell Titer96 Aqueous One Solution to each well and incubated at 37°C in 5% CO_2 . After 4 hours the absorbance was read at 490 nm on the VersaMax™ microplate reader (Molecular Devices). The cell viability of each sample was expressed as a percentage of the control cells and compared to cells treated with 10% DMSO which is known to effect cell viability.

2.2.8 Enzyme Linked Immunosorbent Assay (ELISA)

Enzyme linked Immunosorbent assay (ELISA) was used to quantify numerous cytokines and chemokines in cell supernatants from both murine and human cells depending on the experiment. DuoSet ELISA kits from R&D Systems with antibodies specific for murine or human samples were used according to the manufacturer's specifications (see **Appendix A**). Capture antibody (100 μl) specific for the cytokine of interest was bound to each well in a 96 well plate by incubation overnight at room temperature. Excess or unbound antibodies were removed by washing with wash buffer.

Assay diluent (300 µl) was added to each well and incubated for one hour before being washed, the diluent acts as a blocking buffer preventing non-specific binding. A stock solution of standards at a known concentration of the cytokine/chemokine in question was prepared and a 1:2 serial dilution was carried out to make a range of known standards. Samples were prepared and diluted in reagent diluent where required. We placed 100 µl samples and standards into the 96 well plate and incubated at room temperature for 2 hours. The plates were washed again to remove any unbound sample and 100 µl biotinylated detection antibody specific for the assay of interest was added to each well on the plate. Streptavidin has a high affinity for biotin, therefore 100 µl streptavidin-HRP was added to each well. After 20 min the plate was washed with wash buffer to remove any excess and 100 µl Tetramethylbenzidine (TMB) was added to each well on the plate. The colour was allowed to develop as Streptavidin catalyses the oxidation of TMB which forms a blue colour, the intensity of colour is proportional to the concentration of the cytokine/chemokine being measured. The reaction was stopped after approximately 20 min by the addition of 50 µl sulphuric acid 2N H₂SO₄ (see **Appendix A**) which turns the colour of the assay from blue to a yellow. The absorbance of each of the samples and standards was read at 450 nm on the VersaMax™ microplate reader (Molecular Devices). The optical density (OD) at 450 nm of the set of known standards was plotted against their corresponding known concentrations, making a standard curve. The absorbance of samples being tested was calculated by interpolating the absorbance readings into the standard curve equation to determine the concentration of cytokine/chemokine in the cell supernatant.

2.2.8.1 Detection of Murine/Human Cytokines & Chemokines

The cytokines, murine (m) IL-6, mIL-10, mTNF α , mIL-12p40, mIL-12p70, mIL-23, mIL-27p28 and chemokines mRANTES, human (h) RANTES, mMCP-1 and mMIP-2 were quantified according to manufacturer's recommendations. 1% (w/v) BSA/PBS was used as a blocking buffer and reagent diluent. Washing buffer consisted of 0.05% Tween-20 in PBS made from 10X PBS (see **Appendix A**).

2.2.8.2 Detection of IL-1 β and IL-8

The cytokines mIL-1 β and hIL-8 were quantified according to manufacturer's recommendations. BSA/PBS 1% (w/v) was used as a blocking buffer and 0.1% BSA/TBS + 0.05% (v/v) Tween-20 were used as reagent diluent. Washing buffer consisted of 0.05% Tween-20 in PBS made from 10X PBS.

2.2.9 Flow Cytometry

Flow cytometry is a technique that allows the analysis of multiple parameters of cells in a heterogeneous cell population. Cells in suspension are passed through a 100 μ m nozzle which allows one cell at a time to pass through a laser light. The light scattered and the fluorescence emitted from positively stained cells can be read by detectors. The detector in front of the laser beam measures the forward scatter which determines cell size and the detector to the side measures side scatter which determines the granularity. When cells have been stained by fluorochemicals, light will be emitted at a certain wavelength when excited by a laser at the corresponding excitation. The emitted light is detected by photomultiplier tubes (PMTs) which convert the energy of a photon into an electrical signal called a voltage. Each voltage pulse equates to an "event" and 100,000 of these are recorded on average. In order to investigate an antigen on the surface of a cell, the cell is incubated with a fluorescently labelled monoclonal antibody specific to the antigen of interest. These fluorochemicals are excited by a laser and emit light at specific wavelengths. In this study we used three-colour polychromatic flow cytometry using the following fluorochemicals; Fluorescein Isothiocyanate (FITC), Phycoerythrin (PE) and Allophycocyanin (APC). FITC excites at 495 nm and emits at 520 nm. PE excites at 465 nm and emits at 578 nm. APC excites at 635 nm and emits at 660 nm.

2.2.9.1 Cell Surface Staining of BMDCs

The bone marrow from BALB/C mice were isolated (**See Section 2.2.3**) and grown for 7 days in the presence of GM-CSF. The cells were counted (**see Section 2.2.2.2**) and seeded at 2×10^6 cells in 2 mL of media on 6 well plates. The cells were then stimulated with LPS and SLPs for 24 hours (**see Section 2.2.6**). The supernatants were aspirated from each well and collected for further analysis by ELISA (**see Section 2.2.8**). The

cells were washed with 2 mL of sterile PBS and a cell scraper was used to gently detach cells from each well. The cells were transferred to 15 mL centrifuge tubes. An equal amount of FBS was added to each tube to block non-specific binding and cells were incubated at room temperature for 15 min. Cells were centrifuged at 250 x g for 5 min and re-suspended in FACS buffer (see **Appendix A**). We used 1 mL of buffer per 2×10^6 cells. We transferred 200 μ L of each sample to a round bottom 96-well plate. Plates were centrifuged at 250 x g for 5 min. The relevant antibody was added to each well at a concentration of 0.5 μ g/ 1×10^6 cells. Antibody stock was diluted in FACS buffer as required. Cells were incubated at 4°C for 30 min. Cells were then washed with 200 μ L FACS buffer, and centrifuged at 250 x g for 5 min. This was repeated three times. Cells were re-suspended in FACS buffer and transferred to labelled FACS tubes for analysis. Samples were then acquired immediately on the Becton Dickinson (BD) FACSAria™ I Cell Sorter and analysed using FlowJo software (Tree Star) with cells gates applied to CD11c⁺ BMDC population.

2.2.10 Purification of Plasmid DNA

Glycerol stocks of chemically competent DH5 α *E. coli* transformed with NF- κ B, pFA-IRF3, pFR phRL-TK renilla and pcDNA3.1 empty vector ligated DNA (see **Appendix C**) were a gift from Prof. Paul Moynagh, The Institute of Immunology, National University of Ireland Maynooth, Maynooth, Co. Kildare and all plasmids were authenticated by sequencing. Plasmid DNA from the individual glycerol stocks were inoculated into separate conical flasks containing 500 mL LB broth supplemented with 100 μ g/mL Ampicillin and grown overnight at 37 °C in a shaking incubator. Further glycerol stocks were made by aseptically mixing 930 μ L bacterial culture and 70 μ L of DMSO and storing at -80°C. The rest of the bacterial culture was harvested by centrifugation at 6000 x g for 40 min at 4 °C. Microgram quantities of plasmid DNA were purified using a Qiagen plasmid DNA Hi-speed midi kit (Qiagen) according to manufacturer's instructions. This kit utilises the alkaline lysis procedure. The supernatant was removed from the pellet which was then re-suspended using 6 mL of chilled P1 buffer. We added 6 mL of P2 buffer and mixed vigorously for 30 seconds to lyse the bacterial cells before they were incubated at room temperature for 5 min. We added 6 mL of P3 buffer to neutralise the lysing effect of the P2 buffer, and solution

was mixed vigorously again for 30 seconds. The cell lysate was then poured into the barrel of a QIA midi-cartridge and incubated at room temperature for 10 min to allow cell debris settle. Using the QIA filter the cell lysate was filtered into a previously equilibrated hi speed midi-prep tip where the DNA was allowed bind to the resin column. Bacterial cell proteins were removed by washing the column with 20 mL of QC buffer and then precipitated with 3.5 mL room temperature Isopropanol which was gently mixed by inversion. The DNA was then allowed to precipitate by incubation at room temperature for 5 min. The Isopropanol mixture was then added to the QIA-precipitator and filtered through. Plasmid bound to the precipitator was then washed with 2 mL 70% (v/v) ethanol, air dried and eluted into a 1.5 mL micro- centrifuge tube using 700 µl sterile TE buffer. Lastly, the eluted DNA was flushed through the precipitator once again to remove any unbound DNA. The DNA was quantified using a NanoDrop® ND-1000. The purity of the DNA was determined by measuring the ratio of absorbance at 260 nm and 280 nm. Pure DNA which has no bound protein impurities should have an A260/A280 ratio of 1.8-1.9. Stocks were aliquoted and stored in the -20°C freezer and used for transfection. A 500 mL culture typically yielded 1-2 µg/mL of plasmid DNA.

2.2.11 Transient Transfection of Cells

Hek-293 or Hek TLR4/MD2/CD14 cells were cultured (**see Section 2.2.4**) and counted (**see Section 2.2.2**) before they were seeded at 0.2×10^6 cells/mL in 200 µL DMEM media per well in a 96 well plate. Cells were allowed to adhere for 18 hours to approximately 60% confluency. Cells were transfected using Lipofectamine 2000 which is a cationic liposome that functions by complexing with nucleic acid molecules, allowing them to overcome the electrostatic repulsion of the cell membrane and to be taken up by the cell (Dalby, 2004). For each well to be transfected, 25 µl of OptiMEM was mixed with DNA. DNA mixes were made up for the appropriate construct (**see Sections 2.2.11.1 – 2.2.11.3**). Lipofectamine 2000 (0.4 µL) was diluted in OptiMEM and made up to 25 µl per sample. The reaction was mixed gently and left at room temperature for 5 min. After incubation, the Lipofectamine/OptiMEM solution was added to the DNA/OptiMEM mix for a total volume of 50 µl per well to be transfected. The combined reaction was mixed gently and incubated at room temperature for 20 min.

The transfection mixture was then added to each well and mixed gently by tapping the side of the plate. Cells were placed back in the incubator at 37°C 5% CO₂ for 18-24 hours depending on the experiment.

2.2.11.1 NF-κB assays

To measure activation of the NF-κB pathway, cells were transfected with NF-κB regulated firefly luciferase reporter plasmid (80 ng) and constitutively expressed *Renilla* luciferase reporter construct phRL-TK (20 ng). An empty vector control reaction was set up in parallel using the same concentrations of NF-κB and IRF3 constructs with the additions of pcDNA3.1 empty vector (50 ng). Firefly luminescence readings were corrected for *Renilla* activity and expressed as fold stimulation over empty vector control.

2.2.11.2 IRF3 assays

To measure the activation of IRF3, cells were transfected with pFR-Luc (60 ng), the trans-activator plasmid pFA-IRF3 (IRF3 fused downstream of the yeast Gal4 DNA binding domain, (30 ng) and phRL-TK (20 ng). An empty vector control reaction was set up in parallel using the same concentrations of pFR, IRF3 and TK constructs with the additions of pcDNA3.1 empty vector (50 ng). Firefly luminescence readings were corrected for *Renilla* activity and expressed as fold stimulation over empty vector control.

2.2.11.3 MiRNA mimics

MiRNA mimics are small chemically modified double-stranded RNAs that mimic endogenous miRNAs and enable miRNA functional analysis as they can up-regulate miRNA activity. We examined the effect of over-expressing miRNAs on NF-κB and IRF3 gene expression. 0-100 nM of individual miRNA mimics/ miRNA controls (**see Appendix A**) were added to DNA/OptiMEM mix of NF-κB (**see Section 2.2.11.1**) and IRF3 (**see Section 2.2.11.2**). The volume of OptiMEM was adjusted to give a 50 µl total volume at the time of transfection (**see Section 2.2.11**).

2.2.12 Luciferase Assays

Firefly luciferase is a 61 kDa monomeric protein that does not require post-translational processing for enzymatic activity. Firefly luciferase catalyzes an oxidative reaction involving ATP, firefly Luciferin and molecular oxygen, yielding an electronically excited oxyluciferin species and this excited species emits visible light (Baldwin, 1996). Thus it functions as a genetic reporter immediately upon translation when expressed under an experimental promoter, in this case NF- κ B or IRF3. This assay enabled us to examine NF- κ B and IRF3 signalling induced by the SLPs from differing ribotypes of *C. difficile* using the luciferase assay. Both sets of plasmid DNA were co-transfected with constitutively expressed TK renilla luciferase construct. Renilla luciferase is a 36 kDa monomeric protein where post-translational modification is not required for its activity and the enzyme may function as a genetic reporter immediately following translation however it is expressed under the control of a constitutive promoter (Matthews, Hori, & Cormier, 1975; Shifera & Hardin, 2010). The utility of an internal control plasmid is dependent on the fact that the encoded protein is expressed in a constitutive manner without being influenced by experimental factors and can therefore be used to normalise the transfection efficiency (Shifera & Hardin, 2010).

Hek-293 or Hek TLR4/MD2/CD14 cells were cultured (see Section 2.2.4) and counted (see Section 2.2.2.2) before being seeded at 0.2×10^6 cells/mL in 200 μ L DMEM media per well in a 96 well plate and allowed to adhere for 18 hours to approximately 60% confluency. Cells were transiently transfected (see Section 2.2.11) with NF- κ B (see Section 2.2.11.1), IRF3 (see Section 2.2.11.2) and in some cases combined with miRNA mimics (see Section 2.2.11.3). 18-24 hours post transfection (depending on the experiment) cells were stimulated with LPS and SLPs (see Section 2.2.4) for 18-24 hours (depending on the experiment). Media was aspirated from each well and 100 μ L 1X luciferase lysis buffer (see Appendix A) was added. The plates were covered in foil and placed on a rocker for 20 min at room temperature. The plates were then placed in the -80°C freezer for a minimum of 1 hour. Samples were then thawed at room temperature, for a maximum of 2 hours, to release the contents of the cell. Lysed cells were transferred to white plates. Firefly luciferase activity was assayed by the addition of 40 μ L of luciferase assay mix (see Appendix A) to each sample. *Renilla* luciferase

was made by diluting Coelenterazine in PBS to give a 1:1000 dilution. 40 μ l *Renilla* luciferase was also added to duplicated samples on each plate. The luminescence was read using a GloMax® Microplate Luminometer (Promega). Firefly luminescence readings were corrected for *Renilla* activity and expressed as fold stimulation over empty vector control.

2.2.13 RNA Isolation

A dedicated RNase-free environment specific for RNA work was established with specific gloves and pipettes used with filter tips, to ensure the quality of RNA starting product. Prior to any RNA work, surfaces and equipment were cleaned down with DNA Zap (Invitrogen). DNA Zap is a potent nucleic acid degrading solution which can degrade any contaminating genomic DNA

2.2.13.1 Total Isolation from Cell Lines

Hek TLR4/MD2/CD 14 cells (see Section 2.2.4) and JAWS II cells (see Section 2.2.5) were cultured and counted (see Section 2.2.2.2) before they were seeded at 2×10^6 cells/mL in 2 mL media. Cells were stimulated with LPS and SLPs (see Section 2.2.2.6). Cells were harvested after 8 hours and total RNA was isolated using the mirVana™ miRNA Isolation Kit (Ambion) as per manufacturer's instructions, **Figure 2.2.2** shows a summary of this procedure. The cells were scraped in media and transferred to 15 mL falcons, the tubes were centrifuged at $250 \times g$ for 5 min. The supernatants were removed and the pellets washed with 5 mL sterile PBS. The samples were diluted in lysis solution and vortexed for 1 min to obtain a homogenous lysate. The volume was recorded and used to calculate the volume of miRNA homogenate additive to add in (1/10). The solution was mixed by vortexing for 30-60 seconds and incubated on ice for ten min. The volume prior to addition of the miRNA homogenate additive was used to calculate the volume of acid-phenol chloroform to add in, making sure to take the bottom phase. The lysate solution was again vortexed for 30-60 seconds before being centrifuged for 5 min at $10,000 \times g$ at room temperature to separate the aqueous and organic phases. Following centrifugation, the lysate solution was checked for a compact interphase and if this was not evident the centrifugation step was repeated. The upper aqueous phase was transferred to a fresh tube taking care not to

disturb or carryover any of the bottom organic phase. The volume of upper aqueous phase recovered was noted and 1.25 X of this volume of room temperature 100% high grade ethanol was added to the fresh tube. A maximum of 700 μ l of this lysate/ethanol mixture was pipetted onto a glass-fibre filter cartridge, which was placed in a fresh tube. This was centrifuged at 10,000 x g for 15 seconds to pass the mixture through the filter. This step was repeated until all of the lysate/ethanol had been passed through making sure to discard the flow through each time. 700 μ l of wash buffer 1 was then added to the filter column and passed through by centrifugation at 10,000 x g for 15 seconds. This was repeated using 500 μ l of wash buffer 2/3 again with the flow through being discarded each time. After the third wash the filter column was centrifuged at 10,000 x g for 1 min to dry off the filter column and prevent ethanol carry over to the new tube in which filter column was placed. The total RNA was then eluted into a fresh collection tube by centrifugation at 10,000 x g for 30 seconds using 100 μ l elution solution which was pre-heated to 95°C. The RNA was quantified and qualified on the NanoDrop® ND-1000 Spectrophotometer. The purity of the RNA was analysed by measuring the 260nm and 280 nm absorption wavelengths, where RNA with an A260/A280 ratio between 1.8- 2.1 is considered pure. The RNA samples were then run on a 1% agarose gel where the 28S and 18S ribosomal RNA bands were assessed for integrity (see Section 2.2.14).

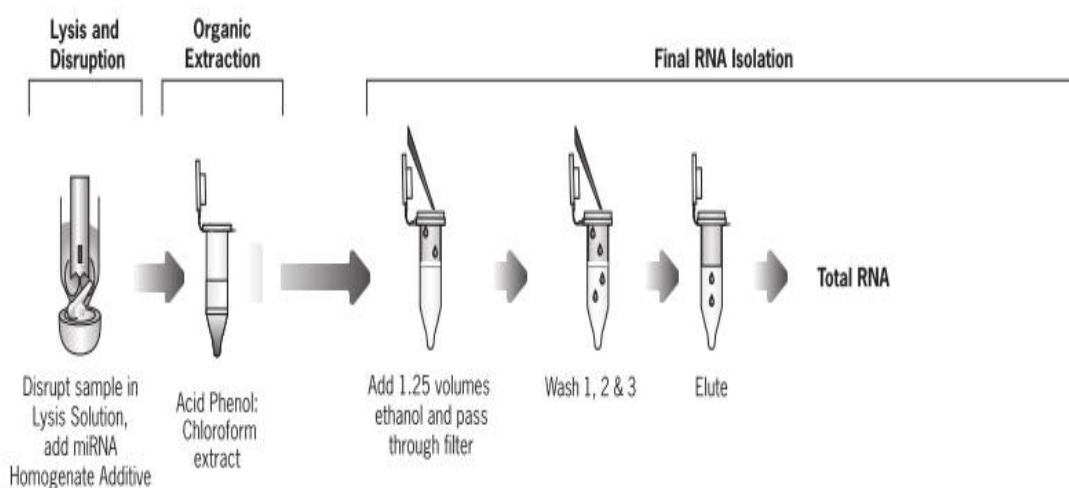


Figure 2.2.2 Summary of the RNA Isolation procedure. Image modified from mirVana™ miRNA Isolation Kit protocol (Life Technologies, 2011)

2.2.13.2 Enrichment of Total RNA Derived from *C. difficile* Infection model

All procedures were carried out in accordance with the Health Products Regulatory Authority. The *in vivo* *C. difficile* infection model was carried out in collaboration with Pat Casey and Professor Colin Hill in the Alimentary Pharmabiotic Centre, University College Cork. Isolation of colonic samples were carried out by Dr Maja Kristek, Dr Mark Lynch and Dr Joseph deCoursey. Total RNA samples were generated by Dr. Mark Lynch, a member of the Immunomodulation Research group (DCU), as part of his PhD research project. C57BL/6J mice were infected with *C. difficile* using an antibiotic-induced model of mouse infection (Chen et al., 2008). Mice were treated for three days with an antibiotic mixture of Kanamycin (400 µg/mL), Gentamicin (35 µg/mL), Colistin (850 U/mL), Metronidazole (215 µg/mL) and Vancomycin (45 µg/mL) in the drinking water. Mice were subsequently given autoclaved water. On day 5, mice were injected intraperitoneally with Clindamycin (10 mg/kg). Mice were infected with 10^3 *C. difficile* spores on day six by oral gavage. Initial studies determined infection with 10^3 spores of *C. difficile* R13537 caused mild transient weight loss and diarrhoea in wild-type C57BL/6J strain mice. Animals were weighed daily and monitored for overt disease, including diarrhoea. Moribund animals with >15% loss in body weight were humanely culled. The colon was harvested from uninfected and infected mice at days three and seven of infection. Squares of tissue from the distal colon roughly 5 mm³ were cut for the preparation of RNA. This tissue was stored in RA1 buffer until required, it was homogenised using a rotor-stator homogeniser. RNA was isolated using the NucleoSpin® RNA II Total RNA Isolation Kit (Macherey-Nagel) as per manufacturer's instructions. The RNA was quantified using a NanoDrop Spectrophotometer and then stored in the -80°C freezer until ready for use (Lynch 2014, unpublished).

For this study small RNAs were enriched from 50 µg Total RNA samples from the *C. difficile* infection model using the mirVana™ miRNA Isolation Kit (Ambion) as per manufacturer's instructions. Total RNA samples were mixed with 5 volumes of lysis/binding buffer and 1/10 volume of miRNA homogenate additive before being placed on ice for 10 min. 1/3 volume of 100% ethanol was added to each sample and pipetted onto a filter cartridge. The filter cartridge was placed in a collection tube and spun at 5000 x g for 1 min. The filtrate was collected and 2/3 volume of 100% ethanol

was added to each sample. The filtrate/ethanol mixture was pipetted onto a new filter cartridge and spun at 5000 x g for 1 min. The flow through was discarded and the filter was washed sequentially with 700 µl miRNA Wash solution 1, followed by two 500 µl Wash solution 2/3 using the centrifugation method where the filter cartridge was spun at 5000 x g for 1 min in between washes. Following the last wash the filter cartridge was placed in a fresh collection tube and 50 µl Elution solution (which had been heated to 95°C) was added to the centre of the filter and incubated at room temperature for 2 min. The filter cartridge and collection tube were then spun at 10,000 x g for 1 min. The flow through contained the RNA enriched for the small RNA fraction. RNA was quantified using a NanoDrop Spectrophotometer and RNA integrity was assessed by analysing the A260/A280 ratio. RNA with a ratio between 1.8- 2.1 was considered of good quality.

2.2.14 Agarose Gel Electrophoresis to Assess RNA Integrity

To assess the integrity of the RNA, 1 µg of total RNA from each sample was used for visualisation. Briefly, 1% agarose gel was prepared in 100 ml of 1X TAE buffer made from 50X TAE (**see Appendix A**). To visualise the RNA, 10 µl of SYBR Safe was added to cooled agarose solution and poured into a sealed gel cassette with the comb set in place. The gel was left to set for 30 min covered in tin foil to prevent photo bleaching. Samples were prepared by in 5X loading buffer and heated to 65°C for 10 min. The apparatus consisted of a horizontal rig which housed the gel cassette and comb. The rig was then filled with 1X TAE buffer. Samples along with 1 kb ladder were loaded into the wells created by the comb. The gel was electrophoresised at 150 V for approximately 30 min or until the loading dye ran three quarters of the way down the rig. The gel was then visualised using the G-Box Gel Imagine System. Intact total RNA has two clear bands, corresponding to 28S and 18S subunits. The ratio of intensity of 28S to 18S should be 2:1.

2.2.15 cDNA Synthesis

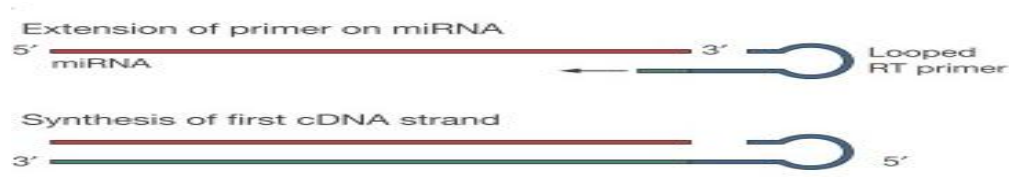


Figure 2.2.3 Image depicting RNA-specific stem-looped reverse transcription primers (Life Technologies, 2013)

Reverse transcription is used to convert single stranded RNA into complementary DNA (cDNA). Standard and quantitative Polymerase Chain Reaction (PCR) methods require a template that is at least two times the length of either of the specific forward or reverse primers, each typically 20 nucleotides (nt) in length. Thus, the target minimum length is ≥ 40 nts, making miRNAs too short for standard reverse transcription qPCR methods. They require primers that contain a highly stable stem-loop structure see **Figure 2.2.3**, that lengthen the target cDNA. The forward PCR primer adds additional length with nt that optimise its melting temperature ($T(m)$). Assay specificity is further optimised by placement of the probe over much of the original miRNA sequence, and the probe $T(m)$ is optimised by addition of a minor groove binding (MGB) moiety (Kramer, 2011).

2.2.15.1 cDNA Synthesis for Pool A and B TLDA Cards

Single stranded cDNA was synthesised using TaqMan® microRNA Reverse Transcription Kit (Applied Biosystems™) which utilises stem-loop technology and creates cDNA from mature miRNAs only and not precursors. For a full miRNA profile two reverse transcription reactions were needed incorporating RNA-specific stem-looped primers for both pool A and pool B miRNA panels. Total RNA from Hek TLR4/MD2/CD14 cells stimulated with LPS and SLPs for 8 hours were isolated (see **Section 2.2.13.1**). The final volume for each reaction was 7.5 μL where either 350 ng or 500 ng in 3 μL total volume was added to 4.5 μL master mix see **Table 2.2.2**. For the no template control (NTC) 3 μl of nuclease water was added instead of total RNA. The samples were then run on the bench top thermocycler (PTC-200 DNA Engine cycler, Biorad) see **Table 2.2.3** for the conditions.

Table 2.2.2 Recipe for cDNA synthesis for pool A and pool B TLDA cards

Mix Components	Volume for 1 sample (μL)	Volume for 10 samples (μL) *
Megaplex RT Primers (10 \times)	0.8	9.0
dNTPs with dTTP (100 mM)	0.2	2.3
MultiScribe Reverse Transcriptase (50 U/ μl)	1.5	17.0
10 \times RT Buffer	0.8	9.0
MgCl ₂ (25 mM) RNase	0.9	10.1
RNase Inhibitor (20 U/ μl)	0.1	1.1
Nuclease-free water	0.2	2.3
Total	4.5	50.8

*Includes 12.5% excess for volume loss from pipetting.

Table 2.2.3 Thermocycler conditions for cDNA synthesis for pool A and B TLDA cards

Stage	Temperature	Time
Cycle (40 Cycles)	16 °C	2 min
	42 °C	1 min
	50 °C	1 sec
Hold	85 °C	5 min
Hold	4 °C	∞

2.2.15.2 cDNA Synthesis for Custom TLDA Cards and Individual miRNA assays

Custom pools of 5X RT primers were made in 1X TE buffer. Total RNA from Hek TLR4/MD2/CD14 cells and JAWS II cells (see Section 2.2.13.1) and RNA enriched for miRNAs from the *C. difficile* model (see Section 2.2.13.2) was taken out of the -80°C freezer and thawed on ice. The final volume for each reaction was 15 μL where 350 ng total RNA in 3 μL (total volume) was added to 12.0 μL master mix see Table 2.2.4. For the NTC 3 μL of nuclease water was added instead of total RNA. The samples were then run on the bench top thermocycler (PTC-200 DNA Engine cycler, Biorad) see Table 2.2.5 for the conditions.

Table 2.2.4 Recipe for cDNA synthesis for custom TLDA cards and individual miRNA assays

Mix Components	Volume for 1 sample (μL)
RT Primers ‡	6.0
dNTPs with dTTP (100 mM)	0.3
MultiScribe Reverse Transcriptase (50 U/ μl)	3.0
10 \times RT Buffer	1.5
RNase Inhibitor (20 U/ μl)	0.2
Nuclease-free water	1.0
Total	12.0

‡ 10 μl of each 5X RT primer added to 1X TE for a final volume of 1 mL to give final 0.05X concentration in each reaction tube.

Table 2.2.5 Thermocycler conditions for cDNA synthesis for custom TLDA cards and individual miRNA assays

Stage	Temperature	Time
Hold	16 °C	30 min
Hold	42 °C	30 min
Hold	85 °C	5 min
Hold	4 °C	∞

2.2.16 Pre-amplification of cDNA

Pre-amplification of cDNA was used to uniformly amplify desired cDNA by increasing the amount on starting template (Noutsias et al., 2008). This increases sensitivity of the miRNAs detected without biasing the estimation of miRNA expression ratio (Chen, Gelfond, McManus, & Shireman, 2009)

2.2.16.1 Pre-amplification Reaction for Pool A and pool B TLDA Cards

The pre-amplification reaction had a final volume of 25 μl containing 2.5 μL cDNA product originally isolated from Hek TLR4/MD2/CD14 cells (see Section 2.2.15.1) and

22.5 μ L PreAmp reaction mix see **Table 2.2.6**. The samples were then run on the bench top thermocycler (PTC-200 DNA Engine cycler, Biorad) see **Table 2.2.7** for the conditions. Following this the reaction samples were diluted with 0.1X TE pH 8.0.

Table 2.2.6 Recipe for pre-amplification master mix for pool A and B TLDA cards

	Volume for 1 Sample (μl)	Volume for 10 Samples (μl)*
TaqMan PreAmp Master Mix (2X)	12.5	140.62
Megaplex PreAmp Primers (10X)	2.5	28.13
Nuclease-free water	7.5	84.37
Total	22.5	253.12

*Includes 12.5% excess for volume loss from pipetting.

Table 2.2.7 Thermocycler conditions for pre-amplification

Stage	Temperature	Time
Hold	95 °C	10min
Hold	55 °C	2 min
Hold	72 °C	2 min
Cycle (12 Cycles)	95°C	15 sec
	60°C	4 min
Hold	99.9 °C	10 min
Hold	4°C	∞

2.2.16.2 Pre-amplification for Custom TLDA Cards and Individual miRNA Assays

The pre-amplification reaction had a final volume of 25 μ l containing 2.5 μ L cDNA product originally isolated from Hek TLR4/MD2/CD14 cells, JAWS II cells and miRNAs enriched from the *C. difficile* model (see **Section 2.2.15.2**). The cDNA products were mixed with 22.5 μ L PreAmp reaction mix see **Table 2.2.8**. The samples were then run on the bench top thermocycler (PTC-200 DNA Engine cycler, Biorad) see **Table 2.2.7** for the conditions. Following this the reaction samples were diluted with 0.1X TE pH 8.0.

Table 2.2.8 Recipe for pre-amplification master mix for custom TLDA cards and individual miRNA assays

	Volume for 1 sample (μl)
TaqMan PreAmp Master Mix (2X)	12.5
PreAmp Primer Pool [‡]	3.75
Nuclease-free water	6.25
Total	22.5

[‡] 10 μ l of each 20X individual Taqman miRNA assay was added to 1X TE for a final volume of 1 mL to give final 0.2X concentration in each reaction tube.

2.2.17 Running Taqman® Low Density Arrays (TLDA) cards

DNA polymerase from the TaqMan® Universal PCR Master Mix amplifies the target cDNA using sequence specific primers and a probe on the TaqMan microRNA array. The presence of the target is detected in real time through cleavage of the TaqMan probe by the polymerase 5'-3' activity. Pre-amplified cDNA (see **Section 2.2.16.1**) was added to the following master mix see **Table 2.2.9**. During optimisation, cDNA product (see **Section 2.2.15.1**) originating from 350 ng and 500 ng starting RNA was investigated, therefore cDNA product was added to the following master mix see **Table 2.2.10**. Pool A and B TLDA cards were allowed to come to room temperature before 100 μ l of the mix was dispensed into each port on the cards. The cards were centrifuged twice in specialised Sorvall/Heraeus buckets at 200 x g for 1 min to fill each of the 384 wells on the array card. The card was then sealed using the Micro Fluidic Card Sealer which uses a precision stylus assembly to isolate and seal the channels of the micro fluidic card. The loading chambers were cut off and the card was run on the Applied Biosystems 7900HT Fast Real-Time PCR System using the default parameters contained within the SDS setup file on the supplied CD specific for either pool A or pool B as shown in **Table 2.2.11**.

Table 2.2.9 Recipe for cDNA with pre-amplification for running on pool A and B TLDA cards

Component	Volume for one array
TaqMan® Universal PCR Master Mix No AmpErase® UNG, 2x	450
Diluted PreAmp product	9
Nuclease-free water	441
Total	900

Table 2.2.10 Recipe for cDNA without pre-amplification for running on pool A and B TLDA cards

Component	Volume for one array
TaqMan® Universal PCR Master Mix No AmpErase® UNG, 2x	450
Megaplex™ RT product	6
Nuclease-free water	444
Total	900

Table 2.2.11 Default thermocycler parameters for running pool A and B TLDA cards

Stage	Temperature	Time
Cycle	16 °C	2min
	42 °C	1 min
	50 °C	1 sec
(40 Cycles)		
Hold	85°C	5 min
Hold	4°C	∞

2.2.18 Running Custom TLDA cards

Following the profiling study with pool A and B TLDA cards, a list of 31 miRNAs of interest were generated. We commissioned custom 384 well microRNA cards to be made by Applied Biosystems™ containing our 31 miRNAs of interest and an endogenous control U6 snRNA (see **Appendix E**). Pre-amplified cDNA originally from Hek TLR4/MD2/CD14 cells (see **Section 2.2.16.2**) were added to the master mix for 96 reactions for 4 replicates see **Table 2.2.12**. Each custom card was allowed to come to room temperature before 513 µl of the mix was dispensed into each port on the array.

The card was centrifuged twice for 1 min at 200 x g to fill each of the 384 wells on the array card. It was then sealed using the Micro Fluidic Card Sealer and the loading chambers were cut off. The cards were run on the Applied Biosystems 7900HT Fast Real-Time PCR System using the parameters shown in **Table 2.2.13**

Table 2.2.12 Recipe for reaction mix for Custom TLDA cards

	Volume for 1 sample (µl)	Volume for 96 reactions x 4 replicates (µl)*
20X Taqman microRNA Assays Mix	0.5	Pre-loaded on array
Diluted PreAmp Product	0.08	34.60
TaqMan® Universal PCR Master Mix No AmpErase® UNG, 2x	5.0	2160.0
Nuclease-free water	4.42	1900.80
Total	10.0	4104.0

*Includes 12.5% excess for volume loss from pipetting.

Table 2.2.13 Thermocycler conditions for custom TLDA cards

Stage	Temperature	Time
Hold	95 °C	10 min
Cycle (12 Cycles)	95°C	15 sec
	60°C	1 min
Hold	4°C	∞

2.2.19 Running Individual Taqman miRNA Assays

In order to validate the results generated in the miRNA custom TLDA cards, individual Taqman assays were carried out for human and murine miRNAs. Pre-amplified cDNA from Hek TLR4/MD2/CD14 cells, JAWS II cells and miRNAs enriched from the *C. difficile* model (see **Section 2.2.15.2**) were added to the master mix see **Table 2.2.14**. 19 µl of master mix was added to each well on a 96 well PCR plate before 1 µl of either human or murine 20X TaqMan® MicroRNA Assays was added (see **Appendix E**). snRNA U6 was used as the endogenous control for the human Hek TLR4/MD2/CD14

cells, while snoRNA202 was used as the endogenous control for the murine JAWS II cells and samples from the murine *C. difficile* model. The plates were run on the Applied Biosystems 7900HT Fast Real-Time PCR System using the parameters shown in **Table 2.2.15**.

Table 2.2.14 Recipe for reaction mix for individual TaqMan® microRNA Assays

	Volume for 1 sample (µl)
Diluted PreAmp Product	0.20
TaqMan® Universal PCR Master Mix No	10.0
AmpErase® UNG, 2x	
Nuclease-free water	8.80
Total	19.00

Table 2.2.15 Thermocycler conditions for Individual TaqMan® microRNA Assays

Stage	Temperature	Time
Hold	95 °C	10 min
Cycle (12 Cycles)	95°C	15 sec
	60°C	1 min
Hold	4°C	∞

2.2.20 MiRNA Data Analysis following qPCR

Following the completion of each run the SDS files were exported from the Applied Biosystems 7900HT Fast Real-Time PCR System and opened in ExpressionSuite Software v1.0.3. Quantitative real time PCR (qPCR) data was analysed. The max Ct was set to 37.0 and a manual threshold of 0.1 was set to ensure Ct determination consistency across each miRNA target. Each assay was pre-designed from Applied Biosystems™ therefore the efficiency (100%) and limit of detection (10 copies) are guaranteed by the manufacturer. We implemented a number of quality control measures outlined in **Figure 2.2.4**. Samples that did not meet these criteria were omitted from the study. We then went through each amplification curve to ensure the curves were sigmoidal in shape and ones which were found not to be were also omitted from the study. The reference group was set to the control samples.

Flag	Icon	Description	Attribute	Condition	Value
AMPNC		Amplification in negative control	Ct	<	35
AMPSCORE		Low signal in linear phase	Amplification Score	<	1
BADROX		Bad passive reference signal	Bad passive reference algorithm result	>	0.6
BLFAIL		Baseline algorithm failed			
CQCONF		Low Cq confidence	Cq Confidence	<	0.8
CTFAIL		Ct algorithm failed			
EXPFAIL		Exponential algorithm failed			
HIGHSD		High standard deviation in replicate group	Ct standard deviation	>	0.5
MAXCT		Ct above maximum			37
MPOUTLIER		ΔCt outlier in multiplex replicate group	ΔCt	<	1
NOAMP		No amplification	Amplification algorithm result	<	0.1
NOISE		Noise higher than others in plate	Relative noise	>	4
NOSAMPLE		Wells with no sample information			
NOSIGNAL		No signal in well			
OFFSCALE		Fluorescence is offscale			
OUTLIERRG		Outlier in replicate group			
SPIKE		Noise spikes	Spike algorithm result	>	1
THOLDFAIL		Thresholding algorithm failed			

Figure 2.2.4 Screen shot from ExpressionSuite software of quality control criteria for TLDA card data

2.2.20.1 MiRNA Data Analysis of Targets from Pool A and B TLDA Cards

Data from pool A and pool B was combined in the one study file and sample groups were assigned. Global normalisation was carried out where the median Ct of common assays were used as the normaliser on a per sample basis (Mestdagh *et al.*, 2009). The normalised reporter ‘Rn’ value for each target was integrated into the calculations for global normalisation. The Rn value was calculated by dividing the fluorescence of the passive ROX dye by the fluorescence of the FAM reporter dye to normalise the reaction. Relative gene expression values were calculated using Expression Suite Software. The Benjamini-Hochberg false discovery rate (FDR) was used to adjust *p*-values to account for the number of tests being performed. To ensure data was normally distributed box plots for each sample were then constructed using the ExpressionSuite software where the box for each sample contained the middle 50% of the data, the black horizontal line indicated the median Ct value and the black dot denoted the mean Ct. The end of the vertical lines indicated the minimum and maximum Ct values and the outliers were the points outside the ends of the whiskers. Following this a student’s *t*-test was applied and values of $p \leq 0.05$ were considered statistically significant compared with the control group. Ct scatter plots were constructed to see if there were differences between groups. However to determine differences in individual miRNA targets a volcano plot was made where the log of the fold change was plotted on the x-

axis and the negative \log_{10} of p-values was plotted on the y-axis. The fold change boundary was set to 1.0 and the p-value boundary was set to $p \leq 0.05$.

2.2.20.2 MiRNA Data Analysis of Targets from Custom TLDA Cards

The endogenous control U6 snRNA was used to correct for variation of RNA input and relative gene expression values were calculated using the ExpressionSuite software. To ensure data was normally distributed box plots for each sample were then constructed using the ExpressionSuite software where the box for each sample contained the middle 50% of the data, the black horizontal line indicated the median Ct value and the black dot denoted the mean Ct. The end of the vertical lines indicated the minimum and maximum Ct values and the outliers were the points outside the ends of the whiskers. Following this a student's t-test was applied and values of $p \leq 0.05$ were considered statistically significant compared with the control group. Ct scatter plots were constructed to see if there were differences between groups. However to determine differences in individual miRNA targets a volcano plot was made where the log of the fold change was plotted on the x-axis and the negative \log_{10} of p-values was plotted on the y-axis. The fold change boundary was set to 1.0 and the p-value boundary was set to $p \leq 0.05$. A heat map was also generated incorporating Pearson's product moment Correlation Coefficient (PCC) using average linkage as a clustering method of miRNA profiles between pairs of samples analysed in this study. The heat map shows the corresponding relative miRNA expression levels rendered in a green-red colour scale, red represents high expression level, green represents low expression level and black being absence of detection. Each row represents a single miRNA and each column represents an individual sample. Dendograms indicate the correlation between groups of samples and miRNAs.

2.2.20.3 MiRNA Analysis of Targets from Individual miRNA Assays

U6 snRNA was used as the endogenous control for the human Hek TLR4/MD2/CD14 cells, while snoRNA202 was used as the endogenous control for the murine JAWS II cells and samples from the murine *C. difficile* model to correct for variation of RNA input (see **Appendix F**). Relative gene expression values were calculated using the ExpressionSuite software. A Mann Whitney U-test was applied in experiments

comparing miRNA expression in the Hek TLR4/MD2/CD14 and JAWS II cells. However a student's t-test was used to compare miRNA expression derived from tissue from differing mice. Values of $p \leq 0.05$ were considered statistically significant. Error bars were presented in all graphs as standard error of the mean (SEM).

2.2.21 MiRNA Gene/Target/Pathway Predictions using Bioinformatics

In the literature it is suggested that to select consensus targets, they must be identified by different prediction tools (Sun, Julie Li, Huang, Shyy, & Chien, 2010). We choose DIANA miRPath (Vlachos et al., 2012) to carry out our searches as this prediction tool highlights targets that are also predicted by miRanda and TargetScan, two well-known prediction tools or targets which are verified experimentally in TarBase v6.0 (Paraskevopoulou et al., 2013). See **Appendix G** for Web links to the databases used in this study.

The list of 24 miRNA targets induced by SLPs from ribotype 001 and 027 were inputted into miRConvertor on the miRSystem database (Lu et al., 2012). This was to ensure we had an up to date name for each of the miRNAs according to the version of miRBASE used by DIANA miRPath which is version 18 (see **Appendix G**). DIANA miRPath v2.0 is a free web-server which utilises miRNA targets in coding regions and 3'-UTR regions provided by the DIANA-microT-CDS algorithm (Vlachos et al., 2012). The lists of 24 miRNAs of interest were inputted into the prediction tool where a posteriori analysis was performed where the significance levels between all possible miRNA pathway pairs were calculated using enrichment analysis. The previously calculated significance levels were combined with this to provide a merged p-value for each pathway by applying Fisher's combined probability method (Vlachos *et al.*, 2012).

DIANA-miRPath enables the analysis of gene targets in the Kyoto Encyclopaedia of Genes and Genomes (KEGG) (Kanehisa & Goto, 2000) which generates graphical representations of pathways interactions. The web server also allows the generation of heat maps, the heat map is based on significance levels where the darker colours represent lower significance values and the adjacent dendrograms depict hierarchical clustering results for miRNAs and the pathways respectively. Gene lists that were targeted in the KEGG pathways were analysed and the 3'UTR region of gene was

crossed check in TargetScan (see **Appendix G**). TargetScan predicts biological targets of miRNAs by searching for the presence of 8mer, 7mer, and 6mer sites that match the seed region of each miRNA see **Figure 2.2.5**. Predictions are ranked by their probability of conserved targeting (P_{CT}) (Friedman & Jones, 2009) and considers matches to human 3' UTRs and their orthologs, as defined by UCSC whole genome alignments.

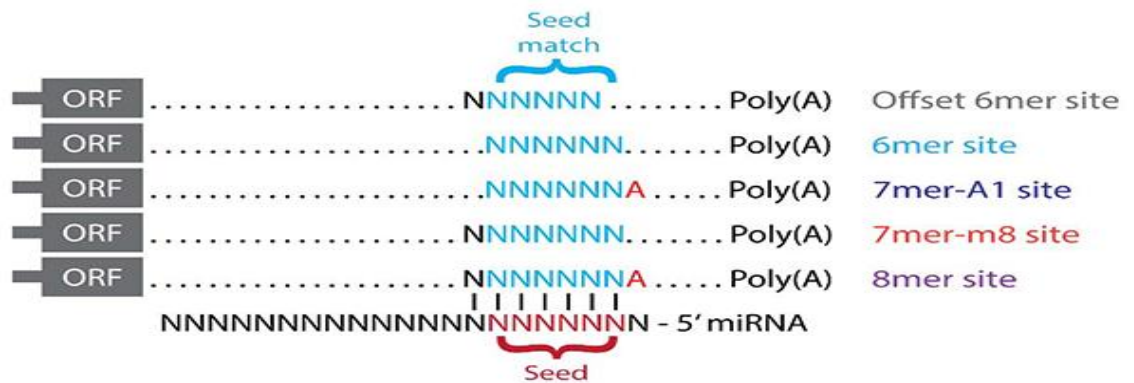


Figure 2.2.5 Diagrammatic representation of the types of miRNA matches predicted in TargetScan (Lewis, Burge, & Bartel, 2005)

**Chapter 3: Characterising the Immune
Response of SLPs from *C. difficile* in
BMDCs**

3.1 Introduction

C. difficile is the leading cause of antibiotic-associated diarrhoea worldwide, called *Clostridium difficile* infection (CDI) (Dawson et al., 2009; Dubberke, 2012). It can only colonise the gut if the normal intestinal microbiota is disturbed or absent- which, in most cases is achieved by the administration of antibiotics (Calabi et al., 2002; Denève et al., 2009; Rupnik et al., 2009). The bacterium's ability to grow in the presence of antibiotics in recent years has enabled its rapid spread among patients (Rupnik et al., 2009). Antibiotic treatment diminishes commensal micro-organisms in the gut and their ability to mediate innate immune responses, which enables the proliferation of the often antibiotic resistant *C. difficile* (Buffie & Pamer, 2013). The bacterium can then dominate the mucosal surfaces and destroy cellular barriers through toxin mediated destruction of the epithelial cells leading to apoptosis and cell death (Buffie & Pamer, 2013; Denève et al., 2009). CDI is potentially a very serious condition frequently effecting hospitalised patients and in particular the elderly (Ausiello et al., 2006). The severity of CDI may be dependent on the strain of *C. difficile* present (Goorhuis et al., 2007; Rupnik et al., 2009) which is illustrated in **Figure 3.1.1**. Ribotype 001 is associated with a milder CDI and efficient bacterial clearance compared with ribotype 027 which is known to be a 'hypervirulent strain'. Infection with ribotype 027 has been associated with more severe diarrhoea, higher mortality and more recurrences (Clements et al., 2010; Dawson et al., 2009; Goorhuis et al., 2007; Loo et al., 2005).

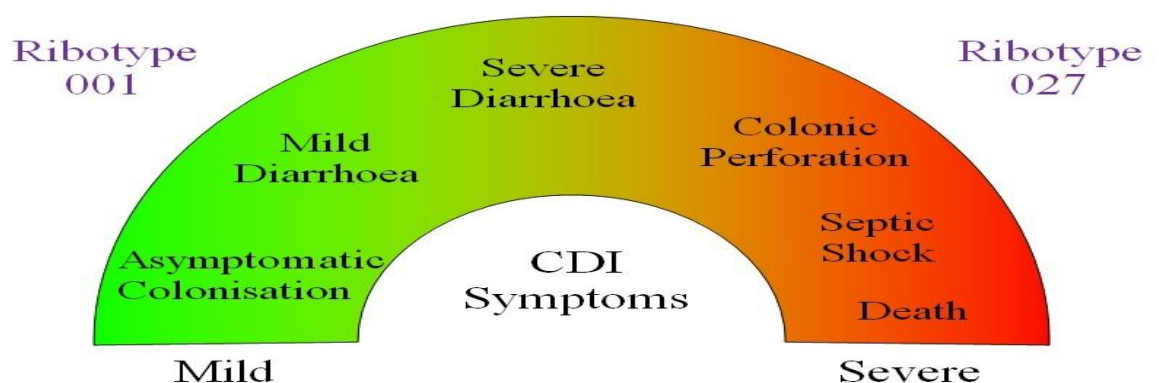


Figure 3.1.1 Illustration of the range of clinical symptoms associated with CDI, comparing ribotype 001 with ribotype 027

Calabi *et al.* (2002) found that S-layer proteins are considered to play the biggest role in the binding of *C. difficile* to the hosts gastrointestinal (GI) tract allowing bacterial adherence to the mucosa and the delivery of toxins (Calabi *et al.*, 2002). S-layer proteins have been detected in all *C. difficile* strains examined so far (Drudy *et al.*, 2004). *C. difficile* express a crystalline S-layer encoded by the *slpA* gene, the product of which is cleaved to give two mature peptides which associate to form layers (Ausiello *et al.*, 2006; Ní Eidhin *et al.*, 2006). These layers are commonly known as Surface layer proteins (SLPs) which are predominantly found in outer surface proteins in *C. difficile*. SLPs contain a HMW protein derived from the C-terminal portion of the precursor and a LMW partner protein derived from the N-terminal portion of the precursor, which form a tightly associated non-covalent complex (Fagan *et al.*, 2009; Ní Eidhin *et al.*, 2006). The HMW protein (42 kDa) is highly conserved between strains of *C. difficile*, while the LMW protein (32–38 kDa) demonstrates considerable sequence diversity and is a dominant antigen of the precursor (Drudy *et al.*, 2004; Ní Eidhin *et al.*, 2006; Sharp & Poxton, 1988).

SLPs have been shown to activate immune cells (Bianco *et al.*, 2011; Calabi *et al.*, 2002; Madan & Petri Jr, 2012; Vohra & Poxton, 2012). Previous research from our laboratory has shown that SLPs activate macrophages and induce bacterial clearance responses. SLPs from ribotype 001 activate pro-inflammatory cytokines and chemokines in a murine macrophage cell line. Furthermore SLPs increase co-stimulatory cell surface marker expression on macrophage and they display enhanced phagocytosis and migration (Collins *et al.*, 2014). In addition, other studies have shown that SLPs induce the maturation of DCs by inducing the expression of co-stimulatory cell surface markers which leads to the induction of pro-inflammatory cytokines (Ausiello *et al.*, 2006). Research from our group also have shown that intact SLPs from ribotype 001 containing both HMW and LMW proteins were required for DC activation and subsequently generated T helper cells required for bacterial clearance *via* TLR4 (Ryan *et al.*, 2011). Consequently SLPs isolated from ribotype 001 can activate innate and adaptive immunity. This would suggest, an important role for SLPs in the recognition of *C. difficile* by the immune system (Collins *et al.*, 2014; Ryan *et al.*, 2011).

SLPs from ribotype 001 evoke a similar response to that of LPS through TLR4 signalling. Ryan *et al.* (2011) showed that these SLPs induce MyD88-dependent signalling which leads to the activation of NF- κ B and Collins *et al.*, (2014), demonstrated that the SLPs induced downstream activation of p38 (Collins *et al.*, 2014; Ryan *et al.*, 2011). NF- κ B regulates the expression of a range of proteins including pro-inflammatory cytokines such as IL-1 β , IL-8, IL-6 and TNF α which mediate the innate immune response to the invading pathogen (Hayden & Ghosh, 2004; Pahl, 1999). It is well known that severe complications of infection result from excessive immune activation and there is an essential role for immunoregulatory components of the immune response in limiting pathology. Consequently nearly all major TLR signalling pathways are implicated as targets for suppression by anti-inflammatory cytokines (Williams, Ricchetti, Sarma, Smallie, & Foxwell, 2004). IL-10 is an anti-inflammatory cytokine that inhibits MHC class II and co-stimulatory molecules on monocytes and macrophages. IL-10 limits the production of pro-inflammatory cytokines including IL-1 β , IL-6, IL-12, TNF α and chemokines such as MCP-1, RANTES, IL-8 and MIP-2 (Lee & Kim, 2007; Williams *et al.*, 2004). During infection IL-10 inhibits the activity of Th1 cells, NK cells and macrophages (Couper, Blount, & Riley, 2008), all which are required for optimal pathogen clearance (Andoh *et al.*, 2007). During infections, the absence of IL-10 can be accompanied with immunopathological tissue damage that is potentially harmful to the host, whereas excessive IL-10 always results in chronic infectious diseases caused by less clearance of pathogens (Lin *et al.*, 2013).

Both MyD88-dependent and independent mechanisms are required for the development of full host response to bacterial challenge (Carrigan *et al.*, 2010). SLPs isolated from ribotype 001 did not induce the MyD88-independent signalling pathway *via* IRF3 (Ryan *et al.*, 2011). IRF3 is central for the induction of IFN- β and the balance between IL-12, IL-23 and IL-27 production is strongly dependent on IRF3. The production of IL-12 and IL-23 cytokines directly influence the development of Th1 and Th17 cells respectively and the ensuing immune response is therefore affected by the subset of T cell induced. This may be favourable in the context of auto-immune inflammation but deleterious for the host in the context of bacterial infection (Ysebrant de Lendonck *et al.*, 2014; Zhu *et al.*, 2010). Studies have shown the importance of IRF3 and type I IFNs in the modulation of host defence and bacterial clearance (O'Connell *et al.*, 2004).

Additionally, the production and signalling of type I IFN is required for LPS induced IL-10 up-regulation (Chang, Guo, Doyle, & Cheng, 2007).

Given the differences in clinical symptoms between strains of *C. difficile*, the aim of this chapter is to investigate the immune response to SLPs from various ribotypes of *C. difficile*. Firstly we will examine the ability of a variety of *C. difficile* ribotypes to induce the maturation of DCs. Secondly, we will measure co-stimulatory cell surface marker expression using flow cytometry and quantify the production of key cytokines using ELISA. It has been previously shown that SLPs from ribotype 001 activate TLR4 signalling; therefore we will examine downstream signalling of SLPs in Hek TLR4/MD2/CD14 cells, as they possess intracellular mechanisms necessary for TLR4 signalling. Finally, we will examine MyD88-dependent signalling by measuring NF- κ B activation and MyD88-independent signalling by measuring IRF3 activation- using the luciferase gene reporter assay to measure gene expression.

3.2 Results

3.2.1 Characterisation of SLPs from *C. difficile*

SLPs were purified from cultures grown anaerobically at 37°C in BHI/0.05% thioglycolate broth. Cultures were harvested and crude extracts of the SLPs were dialysed and applied to an anion exchange column attached to an AKTA FPLC. The pure SLPs were eluted with a linear gradient of 0-0.3 mol/L NaCl at a flow rate of 4 mL/min. Crude fractions of SLPs and peak fractions corresponding to pure SLPs were run on 12% SDS-PAGE gels, which were then stained with Coomassie blue see **Figure 3.2.1**. The gels were imaged and protein bands were examined. Two distinct bands were seen on the gel, the first HMW band was seen at 44 kDa and the second LMW band was seen at approximately 35-37 kDa. The HMW proteins were the same size for each of the five ribotypes. However the LMW protein differed between ribotypes (RT), for example SLPs from RT 005 and RT 001 had a larger LMW protein compared to the purified SLPs from RT 031, RT 027 and RT 078. Once we confirmed that pure SLPs were extracted we determined the total protein concentration using a BCA assay, (see **Appendix B**). Previous research in our laboratory established that 20 µg/mL was the concentration of SLPs required to evoke an optimum immune response (Ryan et al., 2011), therefore we used this concentration in experiments thereafter. In order to confirm that activity by SLPs was attributed to the SLPs alone and not an endotoxin contaminant from another bacterial source, a LAL assay was carried out (see **Appendix B**). There was no endotoxin activity detected in samples containing SLPs compared to LPS which was used as a positive control.

3.2.2 SLPs Modulate Cell Surface Marker Expression on BMDCs.

BMDC maturation is characterised by increased expression of cell surface markers such as CD40, CD80 and CD86 (Higgins et al., 2003; Lavelle et al., 2003). Flow cytometry was used to examine the cell surface marker expression on BMDCs which were stimulated with LPS and SLPs. BMDCs isolated from the bone marrow of BALB/c mice were differentiated in the presence of GM-CSF for 7 days and plated at 1×10^6 cells/mL. Cells were stimulated with either 100 ng/mL LPS or 20 µg/mL SLPs from RT 001 for 18 hours. BMDCs from each treatment group were counted and separated into

different staining groups. These staining groups consisted of PI and fluorescently labelled antibodies; Group 1) FITC rat anti-mouse CD14, PE rat anti-mouse CD40 and APC hamster anti-mouse CD11c, and Group 2) FITC rat anti-mouse CD86, PE rat anti-mouse CD80 and APC hamster anti-mouse CD11c.

Firstly, we assessed the viability of cells stimulated with LPS or SLPs from RT 001. Cells were stained with PI and analysed within 30 minutes on the BD FACs Aria I. Viable (PI negative) cells were identified by assessing the dot plot of forward scatter (FSC) against PI stained BMDCs see **Figure 3.2.2**. We gated on the PI negative cells and found that un-stimulated control BMDCs were 75.5% viable, BMDCs stimulated with LPS were 69.3% viable and cells stimulated with SLPs from RT 001 were 66.8% viable. Viability was not notably affected by the treatment with LPS or SLPs from RT 001. We also wanted to make sure that we were getting pure BMDC populations, the integrin CD11c is expressed on the cell surface of BMDCs and is an established phenotypic marker for pure BMDC populations. **Figure 3.2.3** shows dot plots of FSC and APC hamster anti-mouse CD11c stained BMDCs. We gated on CD11c⁺ cells and obtained 70-73.3% pure populations of BMDCs, this is in line with the average for our laboratory.

We then examined the expression of CD14 and CD40 cell surface markers as shown in **Figure 3.2.4**. Cell surface marker expression was examined by measuring the mean fluorescence intensity (MFI) of treated cells and comparing them to stained control cells. As expected the expression of CD14 (MFI 1851 V 1098) and CD40 (MFI 989 V 303) were up regulated in BMDCs stimulated with LPS as seen by increased fluorescence compared to the control cells. The expression of CD14 (MFI 1469 V 1098) and CD40 (MFI 588 V 303) were also up regulated in BMDCs stimulated with SLPs from RT 001. We then examined the expression of CD80 and CD86 cell surface markers, as shown in **Figure 3.2.5**. As expected the expression of CD80 (MFI 6832 V 1310) and CD86 (MFI 1394 V 428) were up regulated in BMDCs stimulated with LPS compared to the control cells. The expression of CD80 (MFI 2808 V 1310) and CD86 (MFI 465 V 428) were also up regulated in BMDCs stimulated with SLPs from RT 001 as seen by increased fluorescence compared to the controls cells.

We then went on to examine these parameters in response to SLPs from other ribotypes. Firstly, we gated on CD11c⁺ cells and obtained 70-75% pure populations of BMDCs see **Figure 3.2.6**. The expression of CD14 was up regulated in BMDCs stimulated with LPS (MFI 2275 V 2066) and SLPs from RT 005 (MFI 2664 V 2066) and RT 031 (MFI 2431 V 2066) as seen by increased fluorescence compared to the control cells. However, the expression of CD14 was slightly down regulated in BMDCs stimulated with SLPs from RT 027 (MFI 1916 V 2066) see **Figure 3.2.7**. In addition the expression of CD40 was up regulated in BMDCs stimulated with LPS (MFI 860 V 262) and SLPs from RT 005 (MFI 752 V 262), RT 031 (MFI 868 V 262) and RT 027 (MFI 630 V 262) as seen by an increase in fluorescence compared to the control cells in **Figure 3.2.8**. Furthermore the expression of CD80 was up regulated in BMDCs stimulated with LPS (MFI 9186 V 3306) and SLPs from RT 005 (MFI 6516 V 3306), RT 031 (MFI 7585 V 3306), and RT 027 (MFI 8146 V 3306) as seen by increased fluorescence compared to the control cells in **Figure 3.2.9**. We then examined the expression of CD86 and found it was also up regulated in BMDCs stimulated with LPS (MFI 2246 V 1322) and SLPs from RT 005 (MFI 1460 V 1322), RT 031 (MFI 1708 V 1322) and RT 027 (MFI 1838 V 1322) seen by increased fluorescence compared to the control cells in **Figure 3.2.10**.

3.2.3 SLPs Induce Cytokine Production in BMDCs

When BMDCs are activated they mature and produce inflammatory cytokines. We used ELISA to measure cytokines secreted in the supernatant of BMDCs stimulated with LPS and SLPs. BMDCs isolated from the bone marrow of BALB/c mice were differentiated in the presence of GM-CSF for 7 days and plated at 1×10^6 cells/mL and stimulated with either 100 ng/mL LPS or 20 μ g/mL SLPs from RT 001, RT 005, RT 031 and RT 027. After 18 hours the supernatants were collected and cytokines including IL-1 β , IL-6, IL-12p40, IL-10, IL-12p70, IL-23 and TNF α were measured using ELISA, see **Figure 3.2.11**. IL-1 β was produced at low levels in control BMDCs. However IL-1 β was produced at higher levels in cells stimulated with LPS and SLPs from RT 001, RT 005, RT 031 ($p \leq 0.001$) and RT 027 ($p \leq 0.001$) compared to the control cells. SLPs from RT 027 produced the most IL-1 β . IL-6 was not produced in control BMDCs. IL-6 was produced in BMDCs stimulated with LPS ($p \leq 0.001$) and SLPs from RT 001 ($p \leq$

0.001), RT 005 ($p \leq 0.001$), RT 031 ($p \leq 0.001$) and RT 027 ($p \leq 0.001$). It would appear that SLPs from RT 031 and RT 027 produced more IL-6 than cells stimulated with LPS. IL-10 was not produced in control BMDCs. IL-10 was produced in BMDCs stimulated with LPS ($p \leq 0.01$) and SLPs from RT 001 ($p \leq 0.001$), RT 005 ($p \leq 0.001$), RT 031 ($p \leq 0.001$) and RT 027 ($p \leq 0.001$), compared to the control cells. BMDCs stimulated with SLPs from RT 031 and RT 027 appeared to produce more IL-10 compared to cell stimulated with SLPs from RT 001, RT 005 and LPS. IL-12p40 was produced at low levels in control BMDCs however levels of IL-12p40 was increased in BMDCs stimulated with LPS ($p \leq 0.001$) and SLPs from RT 001 ($p \leq 0.001$), RT 005 ($p \leq 0.001$), RT 031 ($p \leq 0.001$) and RT 027 ($p \leq 0.001$), compared to the control cells. The level of IL-12p40 induced by SLPs from the various ribotypes was comparable to the response induced by LPS. IL-23 was not produced in control BMDCs. IL-23 was produced in BMDCs stimulated with LPS ($p \leq 0.001$) and SLPs from RT 001 ($p \leq 0.001$), RT 005 ($p \leq 0.001$), RT 031 ($p \leq 0.001$) and RT 027 ($p \leq 0.001$), compared to the control cells. The level of IL-23 induced by SLPs from the various ribotypes was comparable to the response induced by LPS. TNF α was produced at low levels in control BMDCs. However levels of TNF α were increased when BMDCs were stimulated with LPS ($p \leq 0.01$) and SLPs from RT 001 ($p \leq 0.01$), RT 005 ($p \leq 0.001$), RT 031 ($p \leq 0.001$) and RT 027 ($p \leq 0.001$), compared to the control cells. Cytokine production induced by SLPs from the various ribotypes was also comparable to the response induced by LPS. IL-12p70 was not produced in control BMDCs. IL-12p70 was produced in BMDCs stimulated with LPS ($p \leq 0.001$) and SLPs from RT 001, RT 005 ($p \leq 0.001$), RT 031 ($p \leq 0.001$) and RT 027 ($p \leq 0.001$), compared to the control cells. BMDCs stimulated with SLPs from RT 031 appeared to produce more IL-12p70 than cells stimulated with LPS and SLPs from the various ribotypes.

3.2.4 SLPs from RT 027 Activate NF- κ B and IRF3

It was previously shown in our laboratory that SLPs from RT 001 activate immune cells through TLR4 and induce NF- κ B signalling downstream of this, however it fails to induce IRF3 signalling (Ryan *et al.*, 2011). Given the difference observed in the immune response to SLPs from different ribotypes, we wanted to determine if there were any differences in the activation of transcription factors. Hek TLR4/MD2/CD14

cells were used to assess the activation of NF- κ B and IRF3 *via* TLR4 by measuring gene expression *via* firefly and renilla luciferase activity. Hek-293 cells do not express TLR4 and they were used in this study as an internal control. Firstly, we carried out a time course experiment on Hek TLR4/MD2/CD14 cells stimulated with LPS over multiple time points during an 18 hour period to identify the optimal time point to examine NF- κ B and IRF3 signalling, see **Figure 3.2.12**. The Hek TLR4/MD2/CD14 cells were transfected with either NF- κ B (80 ng) or IRF3 fused downstream of yeast GAL4 DNA binding domain known as pFA-IRF3 (30 ng) with pFR-regulated firefly luciferase (60 ng). Both sets of plasmid DNA were co-transfected with constitutively expressed TK renilla luciferase (20 ng). Post transfection cells were stimulated with 100 ng/mL LPS. Lysates were generated and assayed for firefly and renilla luciferase activity, where the TK renilla luciferase plasmid was used to normalise for transfection efficiency in all experiments. We show that the expression of NF- κ B increased 2.0 fold after 4 hours; expression increased steadily over time and reached 8.5 fold at 12 hours which was maintained at 18 hours. The expression of IRF3 followed a similar pattern, where expression increased 2.0 fold after 4 hours; this steadily increased over time and reached 8.1 fold after 18 hours. IL-8 and RANTES also known as Chemokine (C-C motif) ligand (CCL5) are indicative of NF- κ B and IRF3 signalling respectively (Lin et al., 1999; Mukaida, Okamoto, Ishikawa, & Matsushima, 1994). Therefore, we measured human IL-8 and RANTES expression from the cell supernatants using ELISA see **Figure 3.2.13**. IL-8 was secreted after 4 hours and steadily increased over time until 12 hours where it reached 7700 pg/mL which was maintained after 18 hours. RANTES secretion was low between 4-8 hours, it increased slightly at 12 hours however 50 pg/mL was reached at 18 hours. The 18 hour time point was chosen for experiments thereafter.

We first examined the expression of NF- κ B and IRF3 in Hek TLR4/MD2/CD14 and Hek-293 cells stimulated with 100 ng/mL LPS and 20 ng/mL SLPs from RT 001 see **Figure 3.2.14**. Cells stimulated with LPS induced the expression of NF- κ B 6.0 fold ($p \leq 0.001$) in Hek TLR4/MD2/CD14 cells compared to the control cells. Cells stimulated with SLPs from RT 001 induced the expression of NF- κ B 3.0 fold ($p \leq 0.01$) in Hek TLR4/MD2/CD14 cells compared to control cells. Cells stimulated with LPS induced the expression of IRF3 6.0 fold ($p \leq 0.001$) in Hek TLR4/MD2/CD14 cells compared to

control cells. SLPs from RT 001 did not induce the expression of IRF3 in Hek TLR4/MD2/CD14 cells. There was no expression of NF- κ B or IRF3 in Hek-293 cells when stimulated with either LPS or SLPs as expected since they do not contain the machinery for TLR4 signalling. The profile at gene level was also reflected in cytokine production. We measured human IL-8 and RANTES using ELISA see **Figure 3.2.15**. There were low levels of IL-8 produced by the control Hek TLR4/MD2/CD14 cells, however IL-8 production was increased when cells were stimulated with LPS ($p \leq 0.001$) and SLPs from RT 001 ($p \leq 0.01$) compared to control cells. There were low levels of RANTES produced in Hek TLR4/MD2/CD14 cells however RANTES production was increased in cells stimulated with LPS ($p \leq 0.001$) compared to the control cells. There was no significant increase in RANTES in Hek TLR4/MD2/CD14 cells stimulated with SLPs from RT 001. IL-8 and RANTES was not produced in Hek-293 cells when stimulated with either LPS or SLPs from RT 001 as expected.

To this end, it was decided to investigate the expression of NF- κ B and IRF3 in response to stimulation with SLPs from the other ribotypes, see **Figure 3.2.16**. It was shown that LPS ($p \leq 0.01$) and SLPs from RT 001 ($p \leq 0.05$), RT 014 ($p \leq 0.01$), RT 027 ($p \leq 0.01$) and RT 078 ($p \leq 0.01$) induced the expression of NF- κ B in Hek TLR4/MD2/CD14 cells compared to control cells. Cells stimulated by SLPs from RT 027 appeared to induce higher levels of NF- κ B than the cells stimulated with LPS. However SLPs from RT 001, RT 014 and RT 078 did not induce the expression of IRF3 in Hek TLR4/MD2/CD14. IRF3 expression was induced by Hek TLR4/MD2/CD14 cells stimulated with LPS ($p \leq 0.001$) and interestingly SLPs from RT 027 ($p \leq 0.01$) compared to the control cells. There was no expression of NF- κ B or IRF3 in Hek-293 cells when stimulated with either LPS or SLPs as expected. The profile at gene level was also reflected in cytokine production when we measured human IL-8 and RANTES using ELISA from cell supernatants see **Figure 3.2.17**. There were low levels of IL-8 produced by the control Hek TLR4/MD2/CD14 cells, however, IL-8 production was increased when cells were stimulated with LPS ($p \leq 0.001$), SLPs from RT 001 ($p \leq 0.001$), RT 014 ($p \leq 0.001$) and RT 027 ($p \leq 0.001$). There was an increase in IL-8 when cells were stimulated with SLPs from RT 078 but it was not statistically significant. There were low levels of RANTES produced in Hek TLR4/MD2/CD14 cells however RANTES production was increased when cells were stimulated with LPS ($p \leq 0.001$)

and SLPs from RT 027 ($p \leq 0.05$). There was no significant increase in RANTES when cells were stimulated with SLPs from RT 001, RT 014 and RT 078. RANTES was not produced, while minute levels of IL-8 was produced in Hek-293 cells when stimulated with either LPS or SLPs as expected.

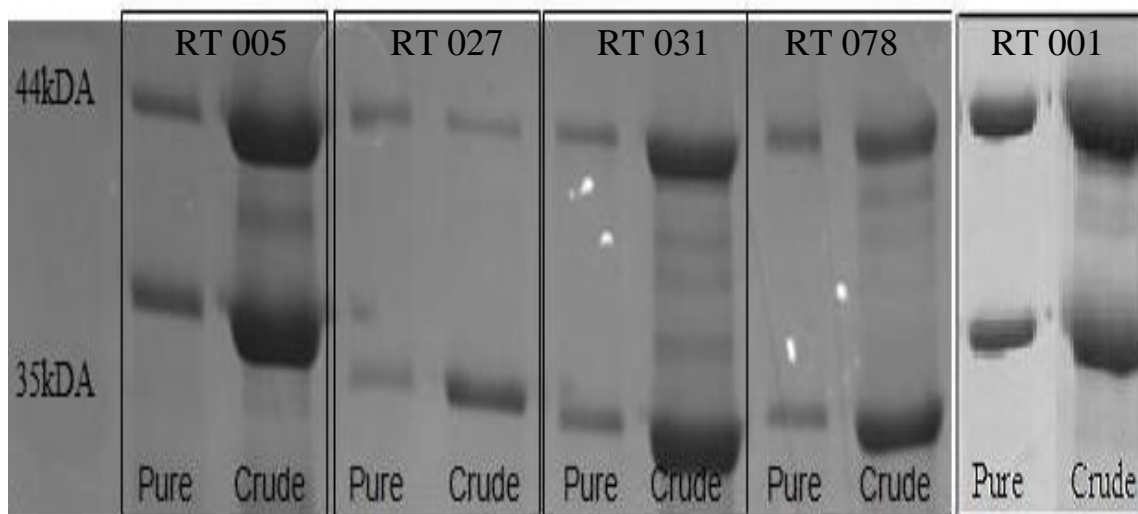


Figure 3.2.1 SLPs from RT 005, RT 027, RT 031, RT 078 and RT 001 contain a conserved HMW protein at 44kDA and variable LMW band ranging from 35-37 kDA. SLPs were purified from cultures grown anaerobically at 37°C in BHI/0.05% thioglycolate broth. Cultures were harvested and crude extracts of SLPs were dialysed and applied to an anion exchange column attached to an AKTA fast protein liquid chromatography (FPLC). Pure SLPs were eluted with a linear gradient of 0-0.3 mol/L NaCl at a flow rate of 4 mL/min. Crude fractions of SLPs and peak fractions corresponding to pure SLPs were run on 12% SDS-PAGE gels, which were then stained with Coomassie blue stain. The gels were imaged and protein bands were examined. Bands at 44 kDa represent the HMW protein and the bands at approximately 35-37 kDa represent LMW proteins respectively.

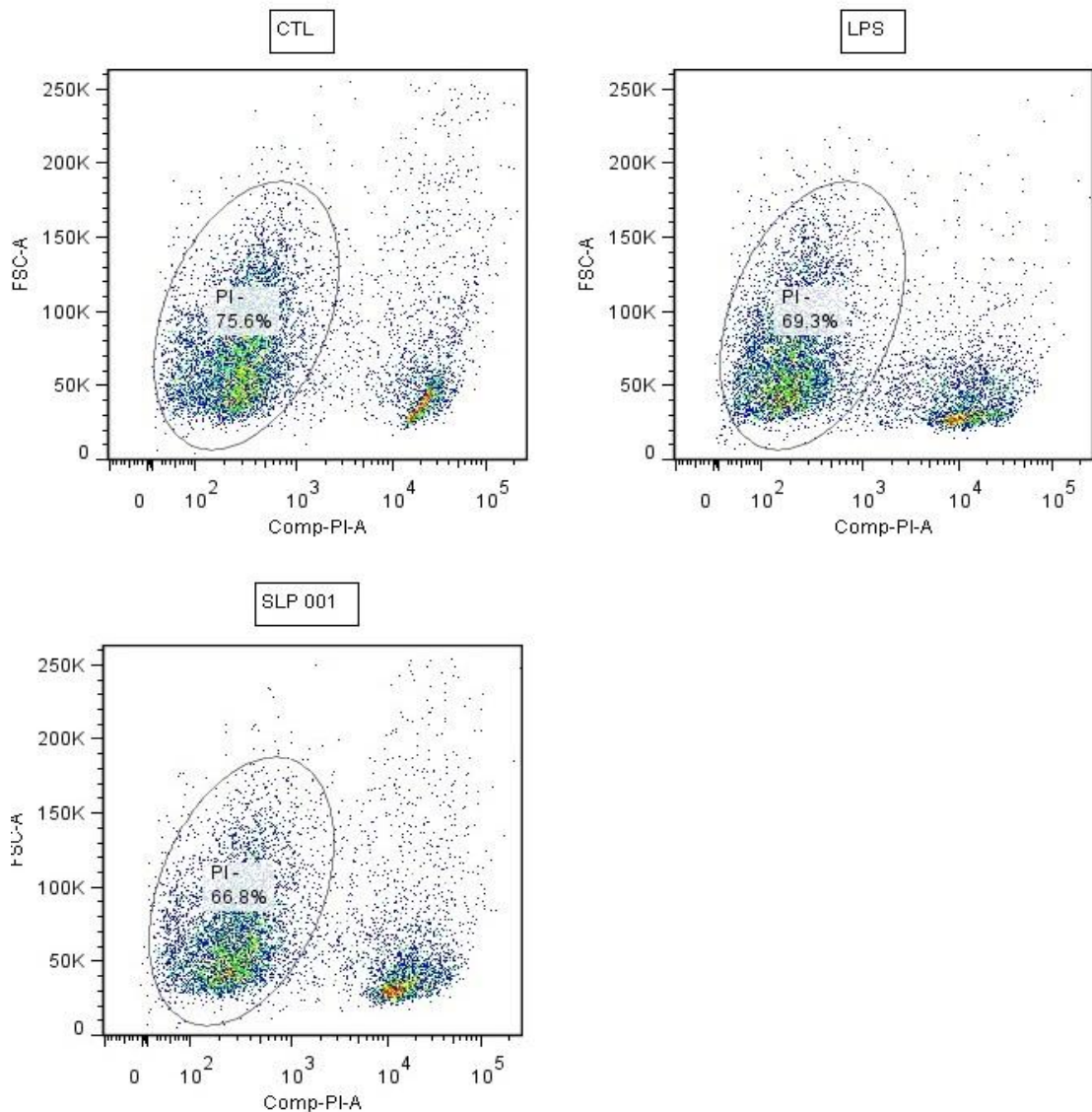


Figure 3.2.2 BMDCs stimulated with LPS and SLPs from RT 001 do not notably affect cell viability. Bone marrow from BALB/c mice was isolated and BMDCs differentiated in the presence of GM-CSF for 7 days. Cells were plated at 1×10^6 cells/mL and stimulated with 100 ng/mL of LPS or 20 μ g/mL SLPs from RT 001. After 18 hours, cells were stained with Propidium Iodide (PI) and cells were analysed within 30 minutes on the BD FACs Aria I. Data was analysed using Flowjo software. Dot plot showing forward scatter (FSC) and PI stained BMDC's. Data shows the percentage PI negative viable cells. Profiles are shown for a single experiment however are representative of three independent experiments.

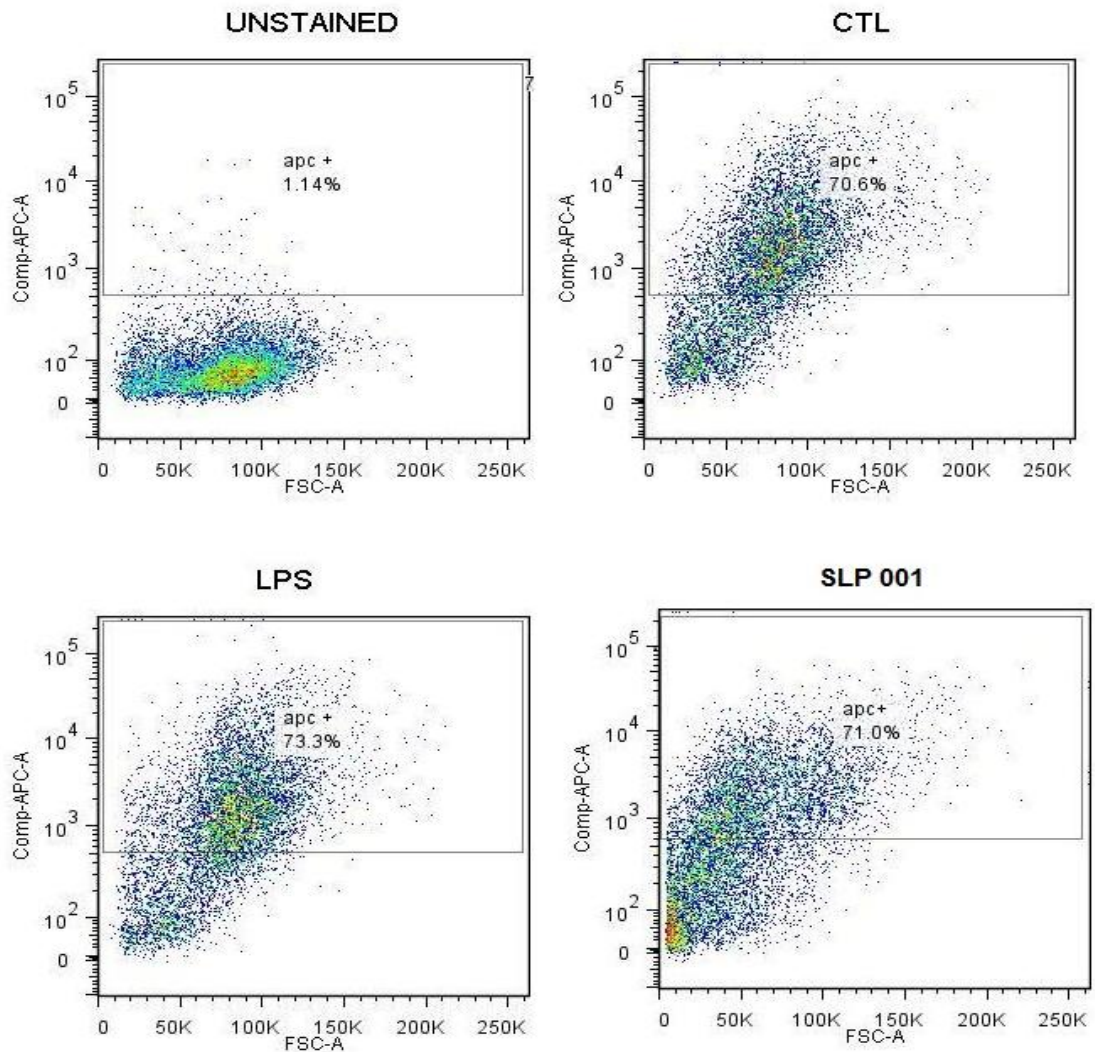


Figure 3.2.3 CD11c⁺ population of BMDCs range from 70-73% when stimulated with LPS and SLPs from RT 001. Bone marrow from BALB/c mice was isolated and BMDCs differentiated in the presence of GM-CSF for 7 days. Cells were plated at 1x10⁶ cells/mL and stimulated with 100 ng/mL of LPS or 20 µg/mL SLPs from RT 001. After 18 hours, cells were stained with fluorescently labelled APC hamster anti-mouse CD11c. Cells were analysed on the BD FACs Aria I and data was analysed using Flowjo software. Dot plot showing forward scatter (FSC) and APC hamster anti-mouse CD11c. Data represents the percentage of BMDCs stained for CD11c. Profiles are shown for a single experiment however are representative of three independent experiments.

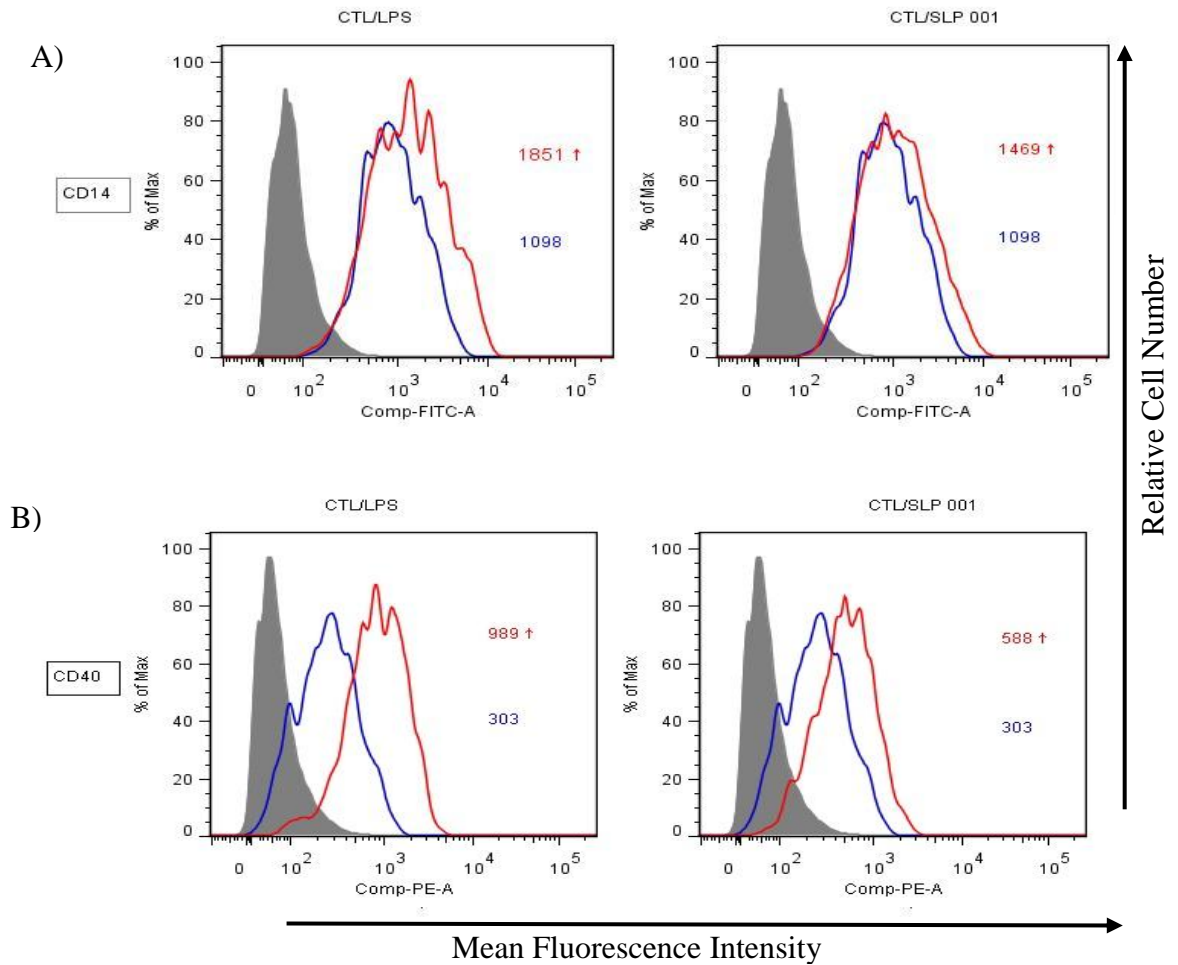


Figure 3.2.4 SLPs from RT 001 modulate the expression of CD40 and CD14 on BMDCs. Bone marrow from BALB/c mice was isolated and BMDCs differentiated in the presence of GM-CSF for 7 days. Cells were plated at 1×10^6 cells/mL and stimulated with 100 ng/mL of LPS or 20 μ g/mL SLPs from RT 001. After 18 hours, cells were stained with fluorescently labelled antibodies FITC rat anti-mouse CD14, PE rat anti-mouse CD40 and APC hamster anti-mouse CD11c. Cells were analysed on the BD FACs Aria I and data was analysed using Flowjo software. Cells were gated on the CD11c⁺ BMDC population. Histograms represent the mean fluorescent intensity (MFI) of conjugated **A)** CD14 and **B)** CD40, with unstained cells (grey) overlaid with control cells (blue line) and stimulated cells (red line). MFI values on the histogram show the stimulated cells (red) and the control cells (blue). Profiles are shown for a single experiment however are representative of three independent experiments.

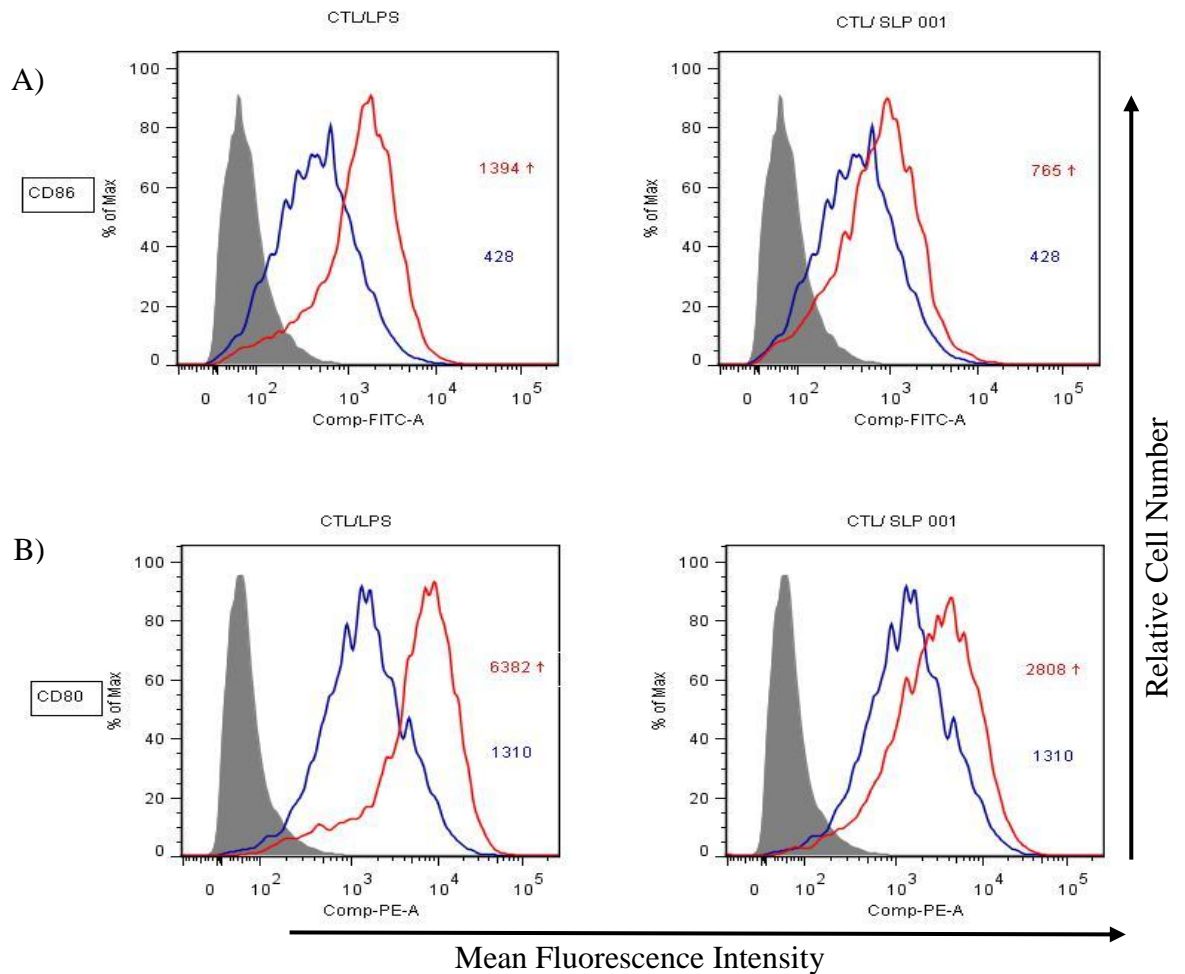


Figure 3.2.5 SLPs from RT 001 modulate the expression of CD80 and CD86 on BMDCs. Bone marrow from BALB/c mice was isolated and BMDCs differentiated in the presence of GM-CSF for 7 days. Cells were plated at 1×10^6 cells/mL and stimulated with 100 ng/mL of LPS or 20 μ g/mL SLPs from RT 001. After 18 hours, cells were stained with fluorescently labelled antibodies FITC rat anti-mouse CD86, PE rat anti-mouse CD80 and APC hamster anti-mouse CD11c. Cells were analysed on the BD FACs Aria I and data was analysed using Flowjo software. Cells were gated on the CD11c⁺ BMDC population. Histograms represent the mean fluorescent intensity (MFI) of conjugated **A)** CD86 and **B)** CD80, with unstained cells (grey) overlaid with control cells (blue line) and stimulated cells (red line). MFI values on the histogram show the stimulated cells (red) and the control cells (blue). Profiles are shown for a single experiment however are representative of three independent experiments.

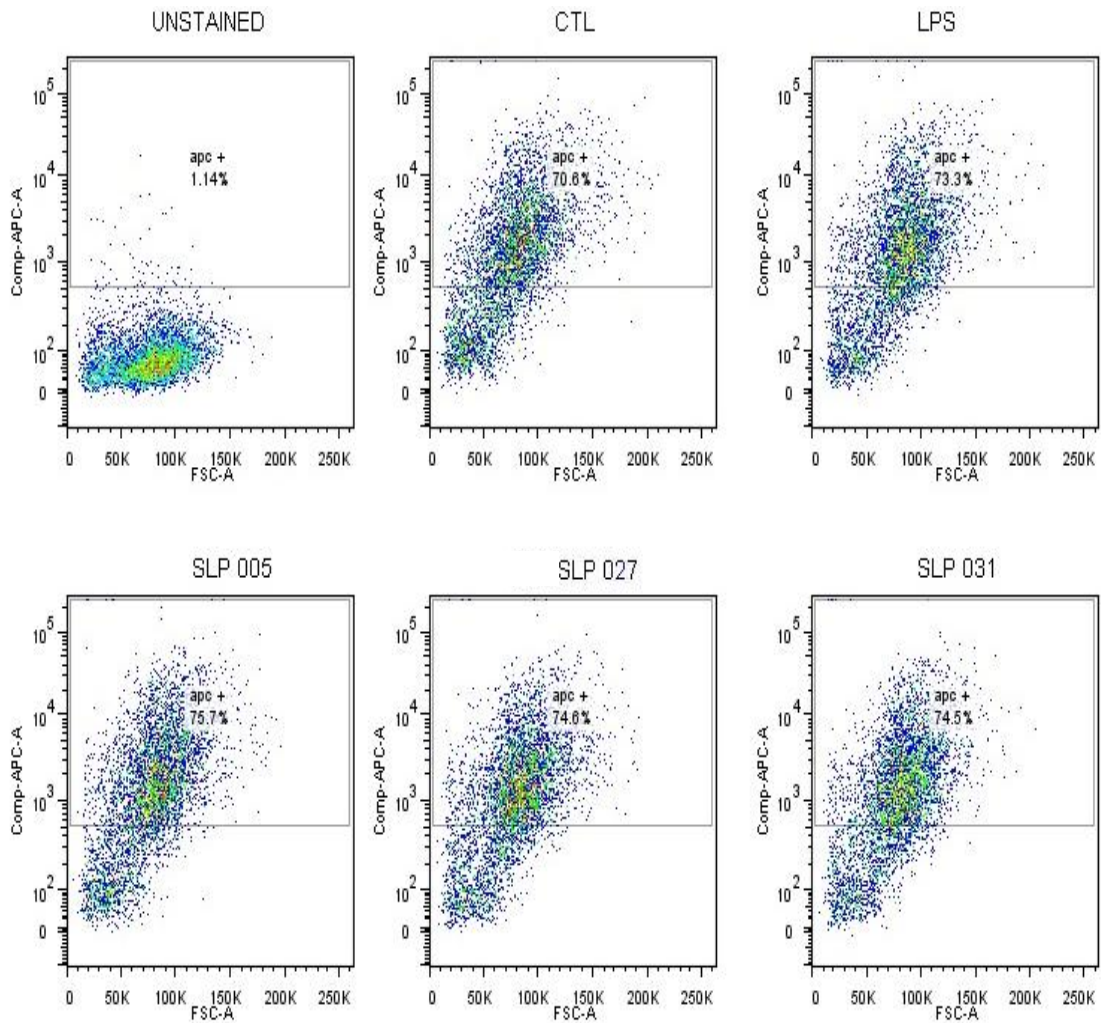


Figure 3.2.6 CD11c⁺ population of BMDCs range from 70-75% when stimulated with LPS and SLPs from RT 005, RT 027 and RT 031. Bone marrow from BALB/c mice was isolated and BMDCs differentiated in the presence of GM-CSF for 7 days. Cells were plated at 1×10^6 cells/mL and stimulated with 100 ng/mL of LPS or 20 μ g/mL SLPs from RT 005, RT 031 and RT 027. After 18 hours, cells were stained with fluorescently labelled APC hamster anti-mouse CD11c. Cells were analysed on the BD FACs Aria I and data was analysed using Flowjo software. Dot plot showing forward scatter (FSC) and APC hamster anti-mouse CD11c. Data represents the percentage of BMDCs stained for CD11c. Profiles are shown for a single experiment however are representative of three independent experiments.

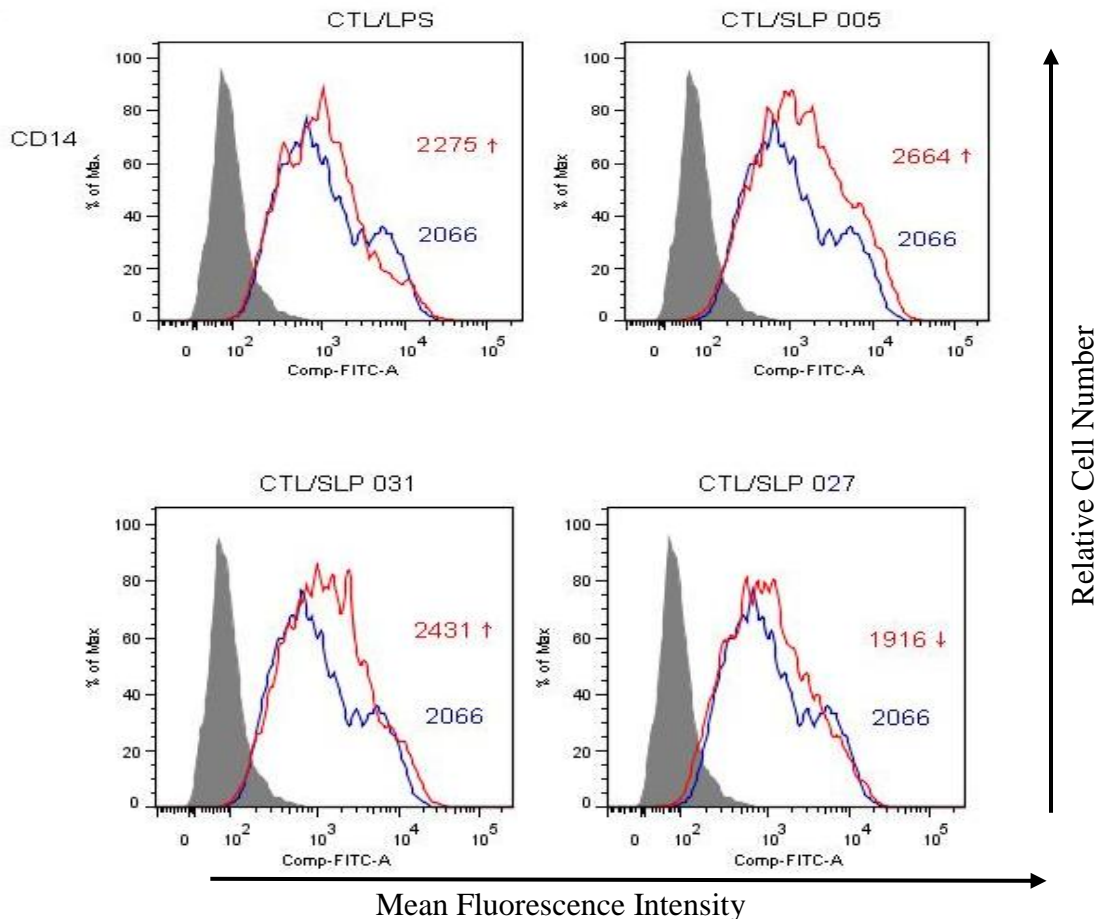


Figure 3.2.7 SLPs from RT 005, RT 031 and RT 027 modulate the expression of CD14 on BMDCs. Bone marrow from BALB/c mice was isolated and BMDCs differentiated in the presence of GM-CSF for 7 days. Cells were plated at 1×10^6 cells/mL and stimulated with 100 ng/mL of LPS or 20 μ g/mL SLPs from RT 005, RT 031 and RT 027. After 18 hours, cells were stained with fluorescently labelled antibodies FITC rat anti-mouse CD14 and APC hamster anti-mouse CD11c. Cells were analysed on the BD FACs Aria I and data was analysed using Flowjo software. Cells were gated on the CD11c⁺ BMDC population. Histograms represent the mean fluorescent intensity (MFI) of conjugated CD14 with unstained cells (grey) overlaid with control cells (blue line) and stimulated cells (red line). MFI values on the histogram show the stimulated cells (red) and the control cells (blue). Profiles are shown for a single experiment however are representative of three independent experiments.

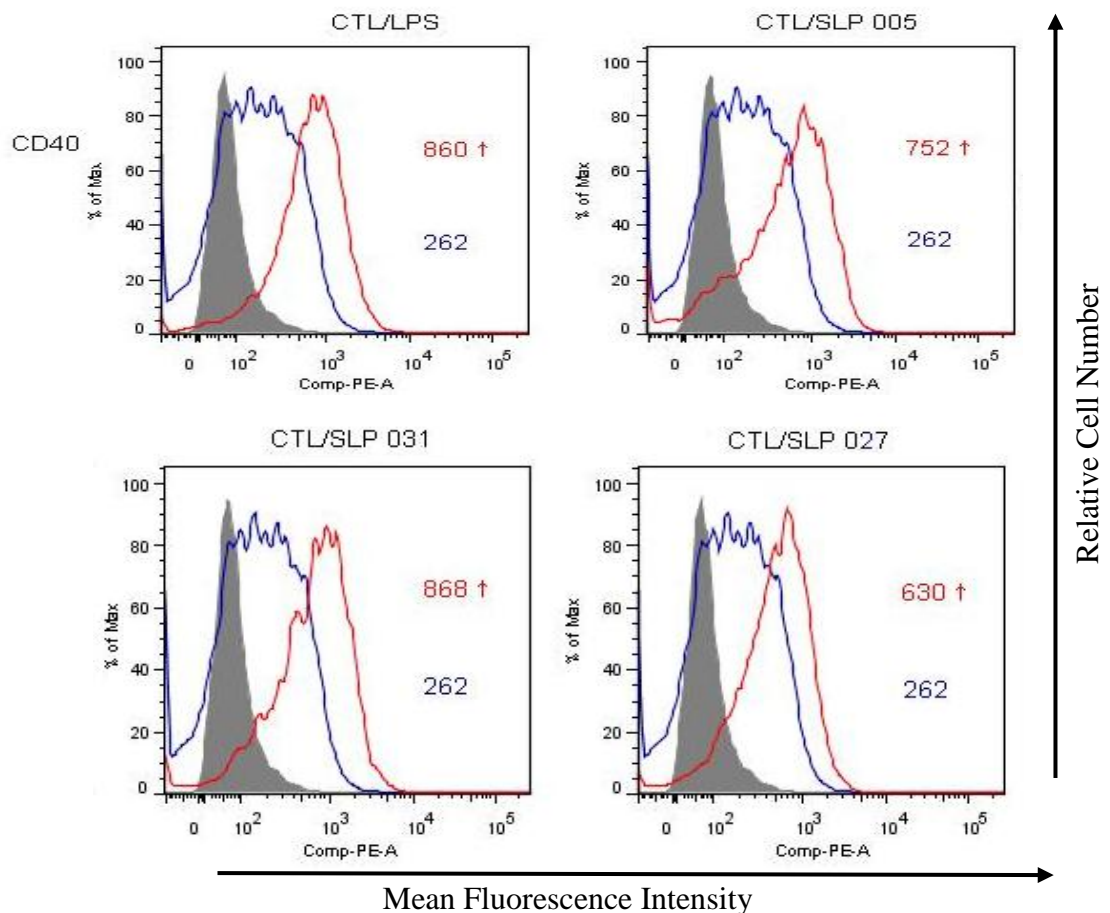


Figure 3.2.8 SLPs from RT 005, RT 031 and RT 027 modulate the expression of CD40 on BMDCs. Bone marrow from BALB/c mice was isolated and BMDCs differentiated in the presence of GM-CSF for 7 days. Cells were plated at 1×10^6 cells/mL and stimulated with 100 ng/mL of LPS or 20 μ g/mL SLPs from RT 005, RT 031 and RT 027. After 18 hours, cells were stained with fluorescently labelled antibodies PE rat anti-mouse CD40 and APC hamster anti-mouse CD11c. Cells were analysed on the BD FACs Aria I and data was analysed using Flowjo software. Cells were gated on the CD11c⁺ BMDC population. Histograms represent the mean fluorescent intensity (MFI) of conjugated CD40 with unstained cells (grey) overlaid with control cells (blue line) and stimulated cells (red line). MFI values on the histogram show the stimulated cells (red) and the control cells (blue). Profiles are shown for a single experiment however are representative of three independent experiments.

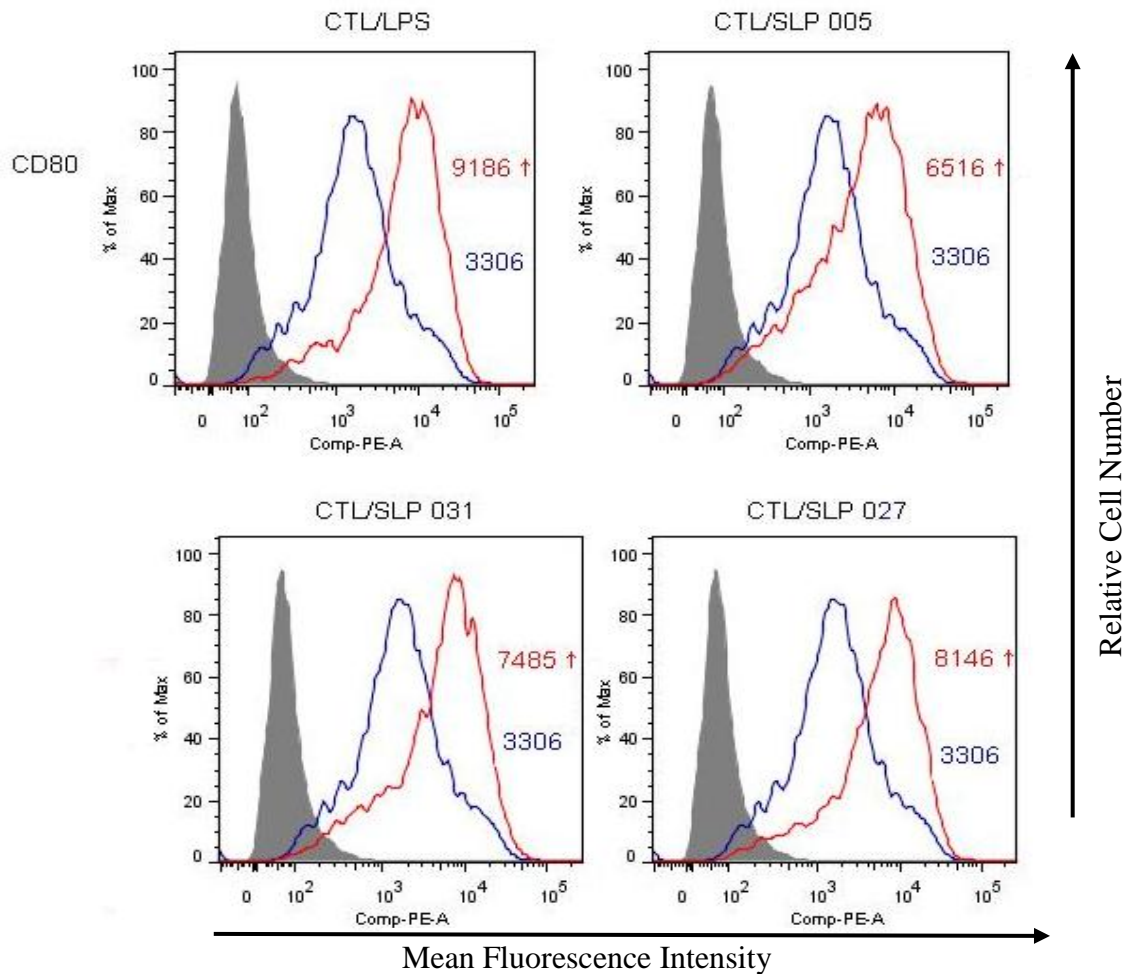


Figure 3.2.9 SLPs from RT 005, RT 031 and RT 027 modulate the expression of CD80 on BMDCs. Bone marrow from BALB/c mice was isolated and BMDCs differentiated in the presence of GM-CSF for 7 days. Cells were plated at 1×10^6 cells/mL and stimulated with 100 ng/mL of LPS or 20 $\mu\text{g/mL}$ SLPs from RT 005, RT 031 and RT 027. After 18 hours, cells were stained with fluorescently labelled antibodies PE rat anti-mouse CD80 and APC hamster anti-mouse CD11c. Cells were analysed on the BD FACs Aria I and data was analysed using Flowjo software. Cells were gated on the CD11c^+ BMDC population. Histograms represent the mean fluorescent intensity (MFI) of conjugated CD80 with unstained cells (grey) overlaid with control cells (blue line) and stimulated cells (red line). MFI values on the histogram show the stimulated cells (red) and to the control cells (blue). Profiles are shown for a single experiment however are representative of three independent experiments.

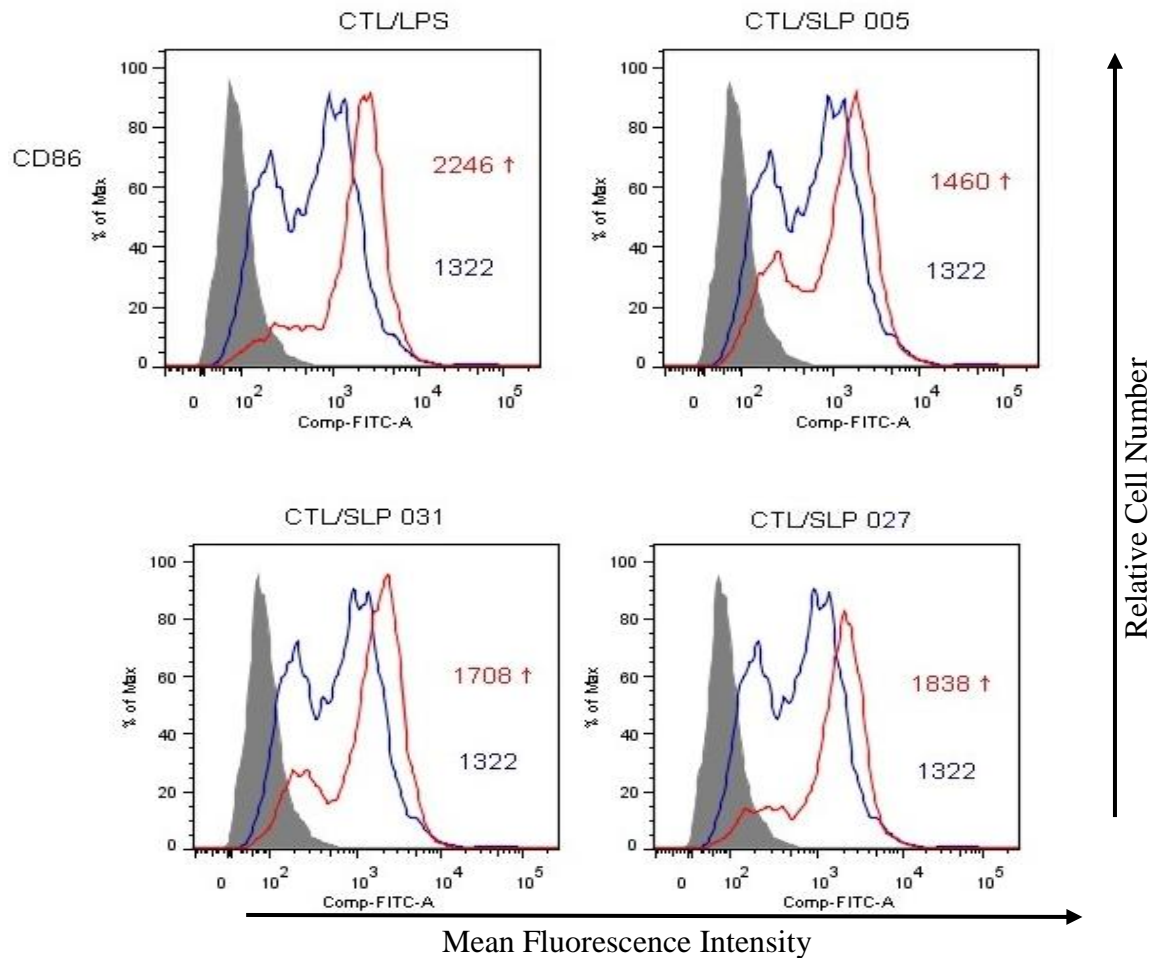


Figure 3.2.10 SLPs from RT 005, RT 031 and RT 027 modulate the expression of CD86 on BMDCs. Bone marrow from BALB/c mice was isolated and BMDCs differentiated in the presence of GM-CSF for 7 days. Cells were plated at 1×10^6 cells/mL and stimulated with 100 ng/mL of LPS or 20 μ g/mL SLP from RT 005, RT 031 and RT 027. After 18 hours, cells were stained with fluorescently labelled antibodies FITC rat anti-mouse CD86 and APC hamster anti-mouse CD11c. Cells were analysed on the BD FACS Aria I and data was analysed using Flowjo software. Cells were gated on the CD11c⁺ BMDC population. Histograms represent the mean fluorescent intensity (MFI) of conjugated CD86 with unstained cells (grey) overlaid with control cells (blue line) and stimulated cells (red line). MFI values on the histogram show the stimulated cells (red) and the control cells (blue). Profiles are shown for a single experiment however are representative of three independent experiments.

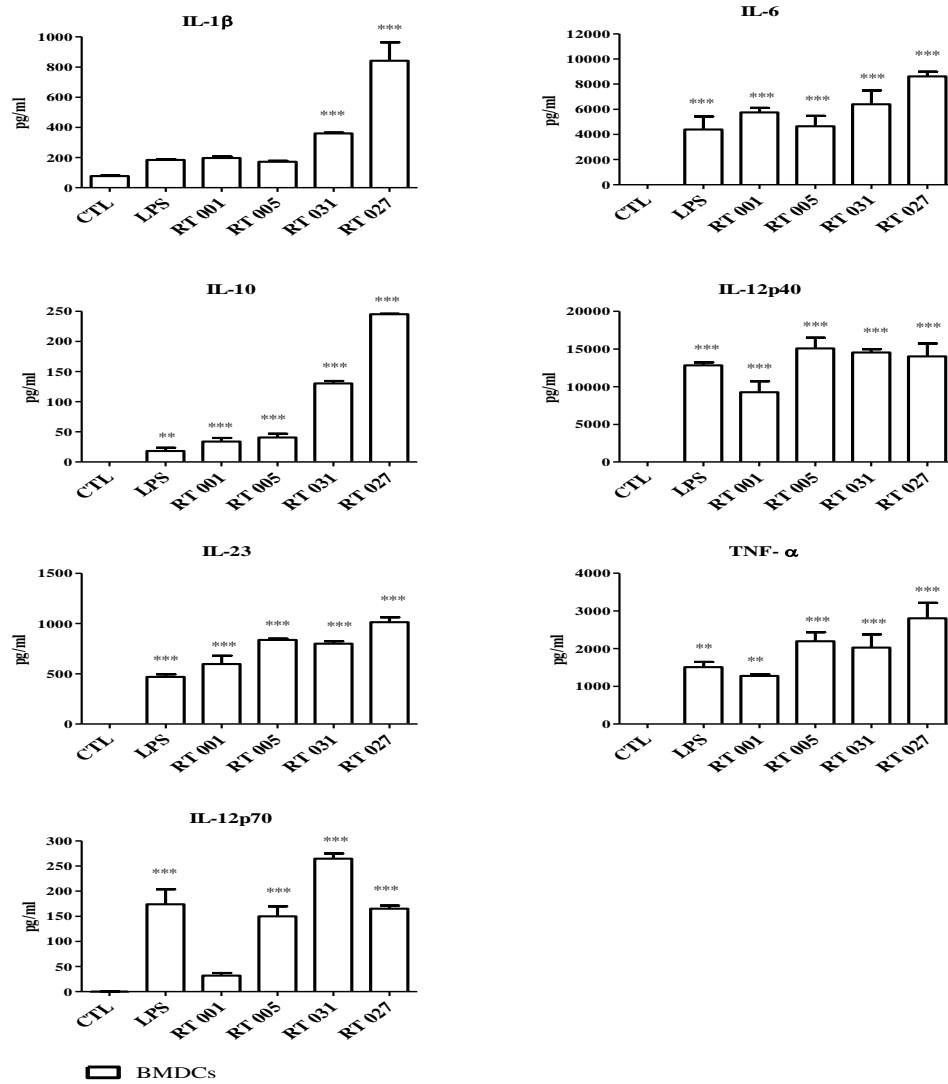


Figure 3.2.11 SLPs from RT 001, RT 005, RT 031 and RT 027 induce the production of murine IL-1 β, IL-6, IL-12p40, IL-10, IL-23, TNFα and IL-12p70 in BMDCs. Bone marrow from BALB/c mice was isolated and BMDCs differentiated in the presence of GM-CSF for 7 days. Cells were plated at 1×10^6 cells/mL and stimulated with 100 ng/ml of LPS or 20 μg/mL SLPs from RT 001, RT 005, RT 031 and RT 027. Supernatants were recovered after 18 hours and assessed for levels of cytokines using ELISA. The results show the mean (\pm SEM) measured in triplicate, one-way ANOVA followed by Newman-Keuls analysis was used to determine if differences between treatment groups were significantly different compared to the control, where * $p \leq 0.05$, ** $p \leq 0.01$ and *** $p \leq 0.001$. The results are indicative of three independent experiments.

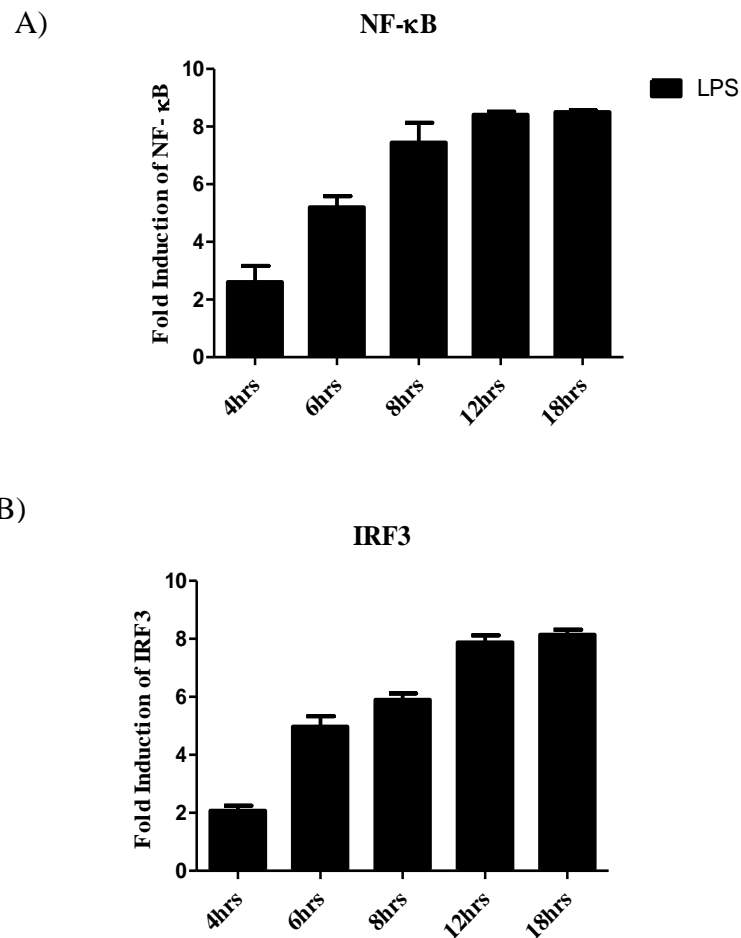


Figure 3.2.12 Time course analysis shows that the optimal time point is after 12 hours for examining the expression of NF-κB and IRF3 expression in Hek TLR4/MD2/CD14 cells stimulated with LPS. Hek TLR4/MD2/CD14 cells were plated at 1×10^6 cells/mL and allowed to adhere for 18 hours to approximately 60% confluency. The cells were then transfected with **A)** NF-κB (80 ng) **B)** pFA-IRF3 (30ng) and pFR-regulated firefly luciferase (60 ng). Both sets of plasmid DNA were co-transfected with constitutively expressed TK renilla luciferase (20 ng). 12-18 hours post transfection cells were stimulated with 100 ng/mL of LPS for 4, 6, 8, 12 and 18 hours. Lysates were generated and assayed for firefly and renilla luciferase activity. The TK Renilla luciferase plasmid was used to normalize for transfection efficiency in all experiments. The results show the mean (\pm SEM) measured in triplicate and the results are indicative of three independent experiments.

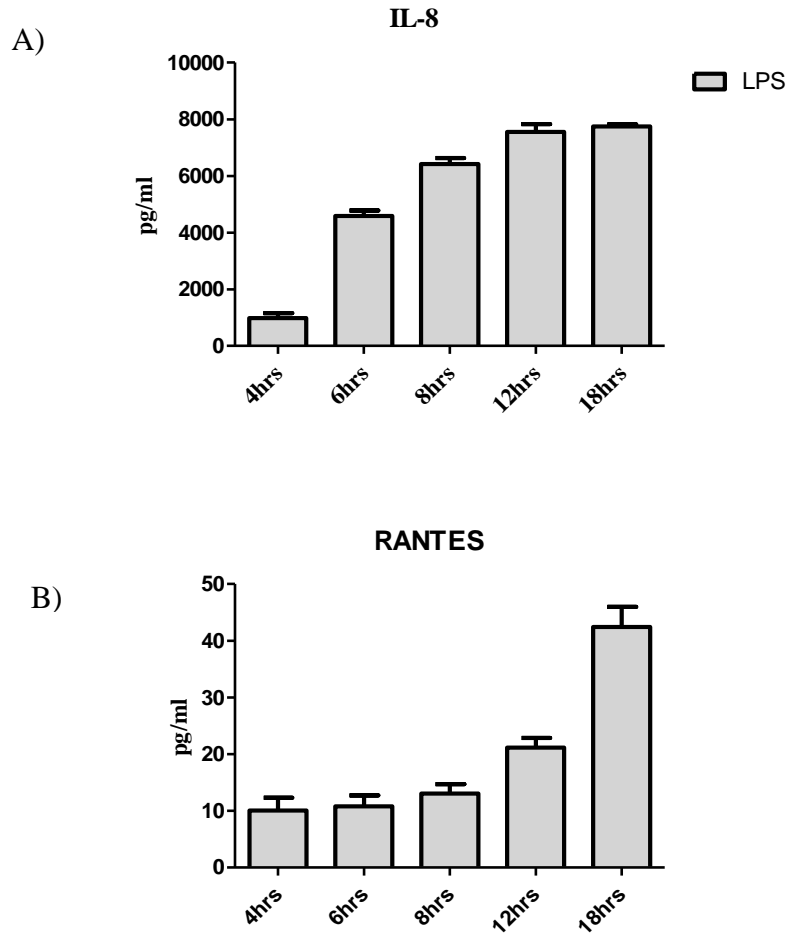


Figure 3.2.13 Time course analysis shows 18 hours is the optimal time for examining the expression of human IL-8 and RANTES expression in Hek TLR4/MD2/CD14 cells stimulated with LPS. Hek TLR4/MD2/CD14 cells were plated at 1×10^6 cells/ml and allowed to adhere for 18 hours to approximately 60% confluency. The cells were then transfected with NF- κ B (80 ng) or pFA-IRF3 (30 ng) and pFR-regulated firefly luciferase (60 ng). Both sets of plasmid DNA were co-transfected with constitutively expressed TK renilla luciferase (20 ng). 12-18 hours post transfection cells were stimulated with 100 ng/mL of LPS for 4, 6, 8, 12 and 18 hours. Supernatants were recovered and levels of **A)** IL-8 and **B)** RANTES were measured using ELISA. The results show the mean (\pm SEM) measured in triplicate. The results are indicative of three independent experiments.

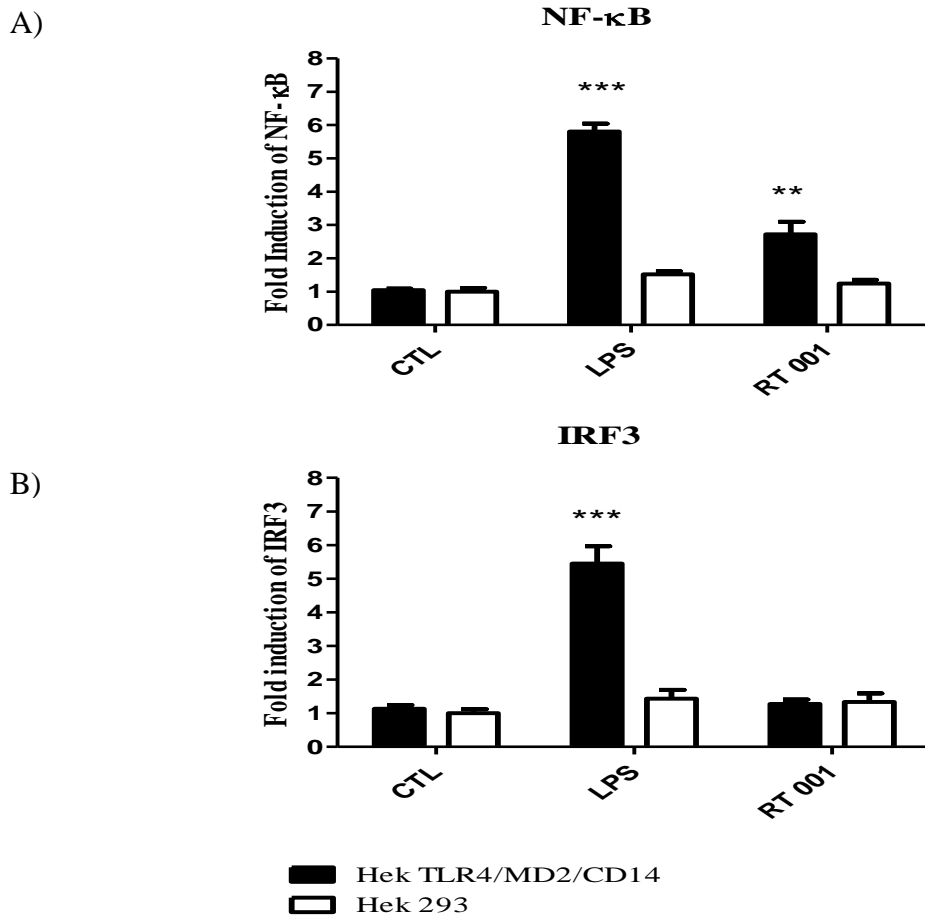


Figure 3.2.14 SLPs from RT 001 activates NF- κ B but it does not activate IRF3 downstream of TLR4. Hek TLR4/MD2/CD14 cells or Hek-293 cells were plated at 1×10^6 cells/mL and allowed to adhere for 18 hours to approximately 60% confluency. The cells were then transfected with **A)** NF- κ B (80 ng) **B)** pFA-IRF3 (30 ng) and pFR-regulated firefly luciferase (60 ng). Both sets of plasmid DNA were co-transfected with constitutively expressed TK renilla luciferase (20 ng). 12-18 hours post transfection cells were stimulated with 100 ng/mL of LPS or 20 μ g/mL SLPs from RT 001 for 18 hr. Lysates were generated and assayed for firefly and renilla luciferase activity. The TK Renilla luciferase plasmid was used to normalise for transfection efficiency in all experiments. The results show the mean (\pm SEM) measured in triplicate, one-way ANOVA followed by Newman-Keuls analysis was used to determine if differences between groups were significantly different compared to the control, where * $p \leq 0.05$, ** $p \leq 0.01$ and *** $p \leq 0.001$. The results are indicative of three independent experiments.

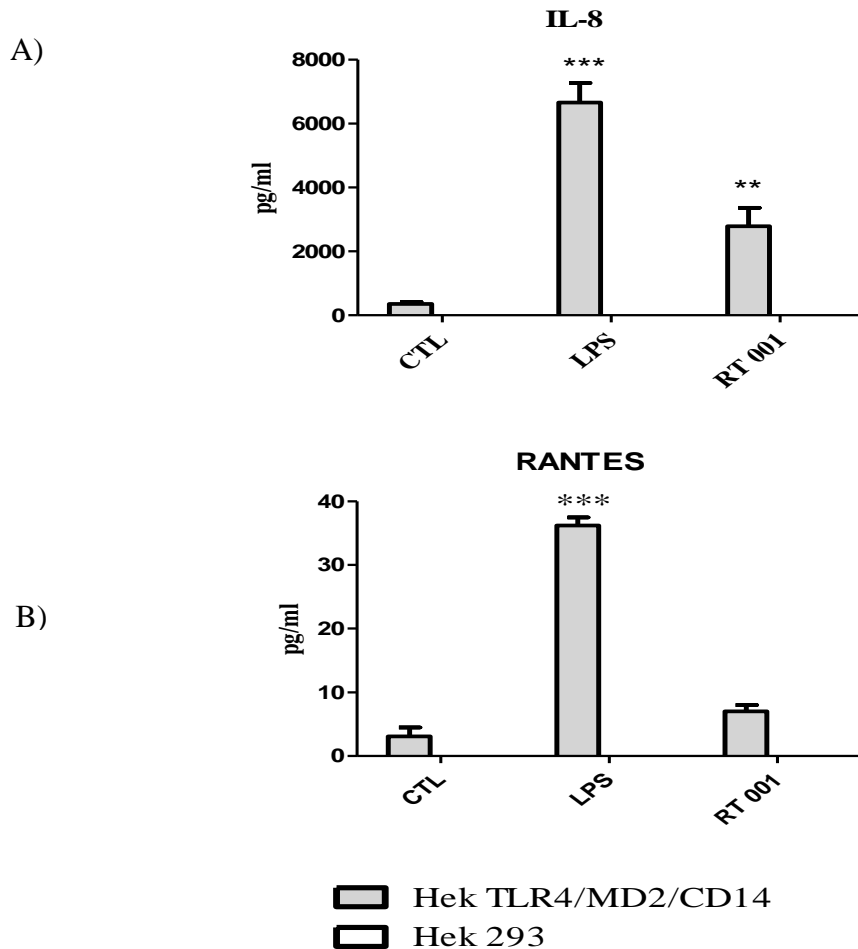


Figure 3.2.15 SLP from RT 001 activates NF- κ B but do not activate IRF3 downstream of TLR4. Hek TLR4/MD2/CD14 or Hek-293 cells were plated at 1×10^6 cells/mL and allowed to adhere for 18 hours to approximately 60% confluency. The cells were then transfected with NF- κ B (80 ng) or pFA-IRF3 (30 ng) and pFR-regulated firefly luciferase (60 ng). Both sets of plasmid DNA were co-transfected with constitutively expressed TK renilla luciferase (20 ng). 12-18 hours post transfection cells were stimulated with 100 ng/mL of LPS or 20 μ g/mL SLPs from RT 001 for 18 hours. Supernatants were recovered and levels of human **A)** IL-8 and **B)** RANTES were measured using ELISA. The results show the mean (\pm SEM) measured in triplicate, one-way ANOVA followed by Newman-Keuls analysis was used to determine if differences between groups were significantly different compared to the control, where * $p \leq 0.05$, ** $p \leq 0.01$ and *** $p \leq 0.001$. The results are indicative of three independent experiments.

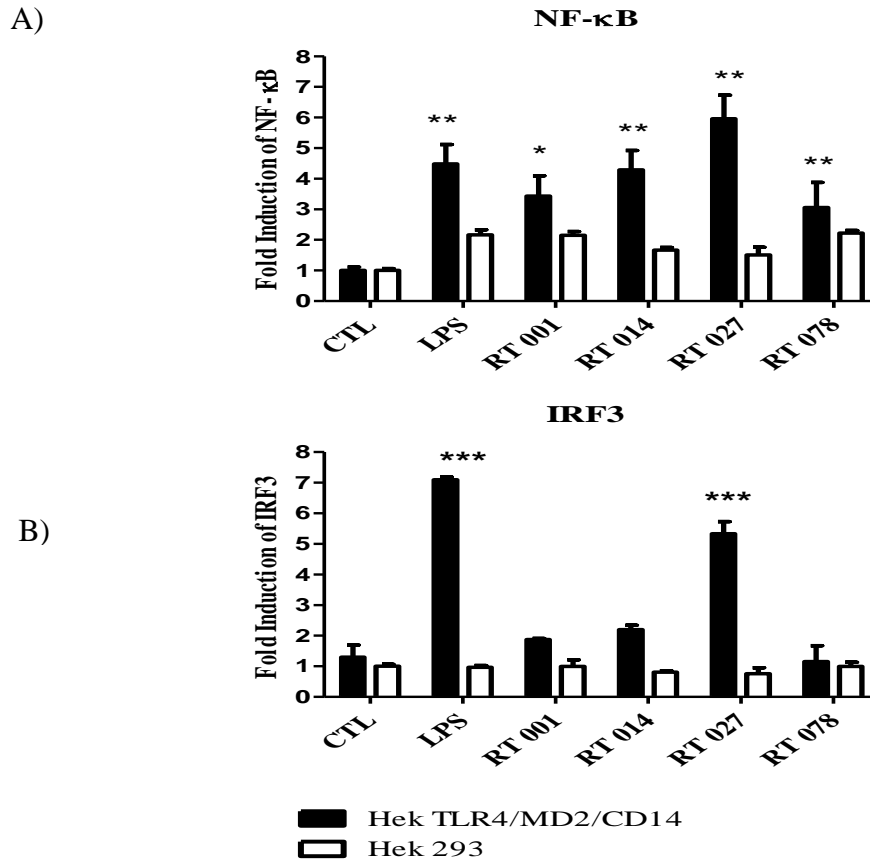


Figure 3.2.16 SLPs from RT 001, RT 014, RT 027 and RT 078 activate NF- κ B. SLPs do not activate IRF3 with the exception of SLPs from RT 027. Hek TLR4/MD2/CD14 cells or Hek-293 cells were plated at 1×10^6 cells/mL and allowed to adhere for 18 hours to approximately 60% confluency. The cells were then transfected with **A)** NF- κ B (80 ng) **B)** pFA-IRF3 (30 ng) and pFR-regulated firefly luciferase (60 ng). Both sets of plasmid DNA were co-transfected with constitutively expressed TK renilla luciferase (20 ng). 12-18 hours post transfection cells were stimulated with 100 ng/mL of LPS or 20 μ g/mL SLPs from RT 001, RT 014, RT 078 and RT 027 for 18 hours. Lysates were generated and assayed for firefly and renilla luciferase activity. The Renilla luciferase plasmid was used to normalise for transfection efficiency in all experiments. The results show the mean (\pm SEM) measured in triplicate, one-way ANOVA followed by Newman-Keuls analysis was used to determine if differences between groups were significantly different compared to the control, where * $p \leq 0.05$, ** $p \leq 0.01$ and *** $p \leq 0.001$. The results are indicative of three independent experiments.

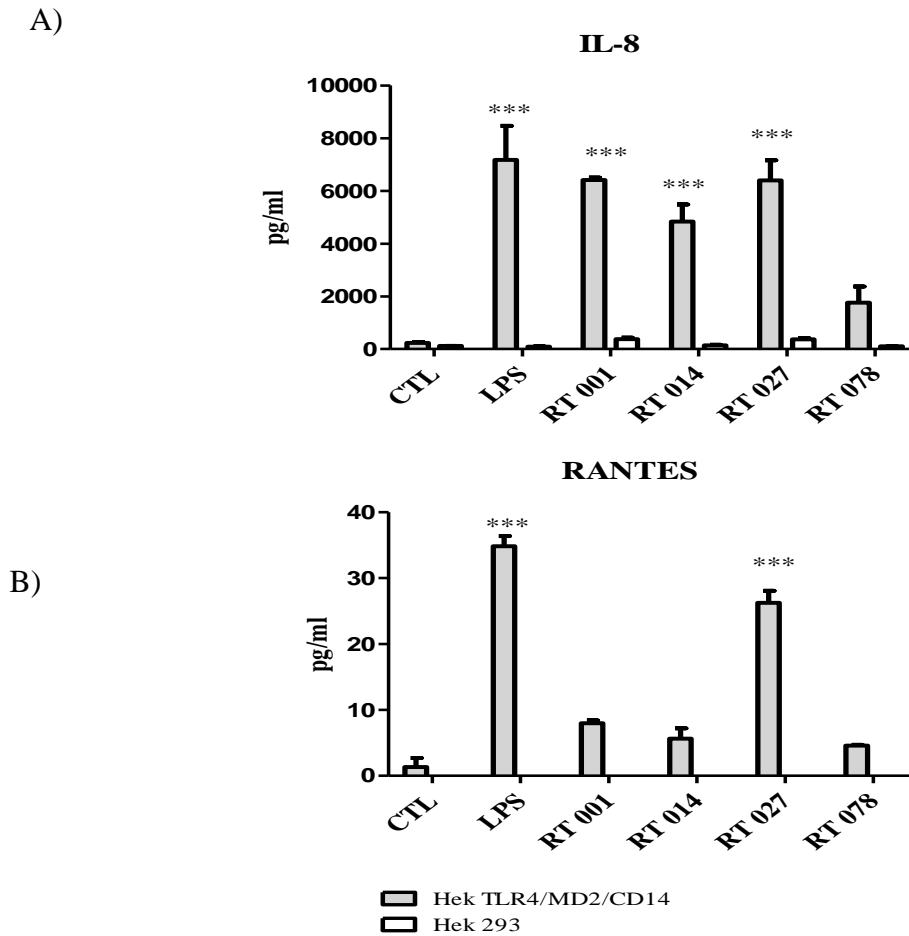


Figure 3.2.17 SLPs from RT 001, RT 014, RT 027 and RT 078 activate NF- κ B downstream of TLR4. SLPs do not activate IRF3 downstream of TLR4 with the exception of RT 027. Hek TLR4/MD2/CD14 cells or Hek-293 cells plated at 1×10^6 cells/mL and allowed to adhere for 18 hours to approximately 60% confluency. The cells were then transfected with NF- κ B (80 ng) or pFA-IRF3 (30 ng) and pFR-regulated firefly luciferase (60 ng). Both sets of plasmid DNA were co-transfected with constitutively expressed TK renilla luciferase (20 ng). 12-18 hours post transfection cells were stimulated with 100 ng/mL of LPS or 20 μ g/mL SLPs from RT 001, RT 014, RT 027 and RT 078 for 18 hours. Supernatants were recovered and levels of human **A)** IL-8 and **B)** RANTES were measured using ELISA. The results show the mean (\pm SEM) measured in triplicate, one-way ANOVA followed by Newman-Keuls analysis was used to determine if the difference between groups were significantly different compared to the control, where * $p \leq 0.05$, ** $p \leq 0.01$ and *** $p \leq 0.001$. The results are indicative of three independent experiments.

3.3 Discussion

C. difficile is a gram-positive, spore-forming, rod shaped anaerobic bacterium, that causes a range of gastrointestinal diseases known as CDI (Bartlett, 1994; Fagan et al., 2009; Kachrimanidou & Malisiovas, 2011). CDI is characterised by tissue injury and an acute intestinal inflammatory response where both pathogen and host play a major role in disease pathogenesis. *C. difficile* toxins cause direct injury to the intestinal epithelium leading to a robust host inflammatory response (El Feghaly et al., 2013). Approximately 15-25% of all cases of antibiotic-associated colitis are caused by *C. difficile* and patients with severe disease have elevated faecal IL-1 β , and IL-8 (Solomon, 2013; Steiner, Flores, Pizarro, & Guerrant, 1997). *C. difficile* has been one of the most intensively typed pathogens and to date there are more than 100 distinguishable ribotypes (Dawson et al., 2009; Stubbs et al., 1999). A study carried out by Ní Eidhin et al. (2006) sequenced the *slpA* gene and flanking DNA from *C. difficile* isolated from patients in St James's Hospital, Dublin Ireland over a 16-month period. The most frequently occurring ribotypes found in this study were 001, 012 and 017 (Ní Eidhin et al., 2006). There is evidence in the literature which suggests that *C. difficile* is evolving to occupy niche hospital populations and there has been rapid worldwide spread of ribotypes 027 and 078 (Dawson et al., 2009).

We had access to ribotypes 001, 005, 027, 031, 078 and 014 in this study. Evidence from the literature suggests that Ribotype 031 does not produce toxins and cause less severe infection, clinical outcomes range from asymptomatic colonisation to mild diarrhoea. In comparison ribotype 014 and 005 produce both toxins and are considered toxigenic, clinical symptoms range from mild to severe diarrhoea (Yakob et al., 2015). Some ribotypes are more 'hypervirulent' than others, ribotype 027 and 078 have been associated with more severe diarrhoea, higher mortality and more reoccurrences, compared to ribotype 001 which is associated with a milder infection (Clements et al., 2010; Dawson et al., 2009; Goorhuis et al., 2007; Loo et al., 2005). Evidence from the literature has shown that ribotype 027 induces more severe colitis and tissue injury than any other ribotype examined so far (Yakob et al., 2015). Increased virulence might be due to genetic mutations in *tcdC* a toxin regulator gene, leading to hyper production of toxins A and B (Barbut et al., 2007). Ribotype 027 also produces a binary toxin

associated with severe diarrhoea and isolates from recent epidemics have shown this ribotype acquired a resistance to fluoroquinolones, common antibiotics used to treat CDI (Cartman, Heap, Kuehne, Cockayne, & Minton, 2010). Studies carried out in a human gut model found that ribotype 027 germinates more readily, remains in a vegetative form and produced cytotoxin for substantially longer than ribotype 001 (Freeman, Baines, Saxton, & Wilcox, 2007). A Canadian study showed that the 30 day mortality rate for patients with ribotype 027 CDI was twice that for those infected with ribotype 001 (Labbé et al., 2008).

C. difficile expresses a crystalline S-layer encoded by the *slpA* gene, the product of which is cleaved to give two mature peptides which associate to form layers (Ausiello et al., 2006; Ní Eidhin et al., 2006). These layers are commonly known as SLPs and are found on the outer surface of *C. difficile*, facilitating interaction with the host enteric cells (Fagan et al., 2009). HMW proteins are highly conserved across strains, while the LMW proteins demonstrates considerable sequence diversity, and the latter have also been shown to be the dominant antigen (Drudy et al., 2004; Ní Eidhin et al., 2006; Sharp & Poxton, 1988). Research from our laboratory has shown that SLPs from ribotype 001 can induce the maturation of BMDCs and the response this elicits is comparable to that of LPS (Ryan et al., 2011). LPS is a well-known TLR4 agonist that activates both NF- κ B and IRF3 signalling (Akashi et al., 2003; Taro Kawai & Akira, 2007; Laird et al., 2009). However, while SLPs from ribotype 001 activate NF- κ B through TLR4 signalling, they fail to induce IRF3 signalling. SLPs from ribotype 001 can activate pro-inflammatory cytokines and chemokines in a murine macrophage cell line with an increase in cell surface marker expression, enhanced phagocytosis and migration (Collins *et al.*, 2014). Therefore, SLPs from ribotype 001 can activate innate and adaptive immunity, suggesting an important role for SLPs in the recognition of *C. difficile* by the immune system and possible bacterial clearance (Collins et al., 2014; Ryan et al., 2011). The goal of this chapter was to investigate the immune response of SLPs from various ribotypes of *C. difficile* and to examine NF- κ B and IRF3 signalling particularly, to see if there were any differences in signalling that could account for the differences in clinical symptoms between differing ribotypes.

BMDCs are known as the sentinels of the immune system and play an essential role in deciding when to mount the appropriate immune response, by sampling their local environment for antigens to present to T lymphocytes (Banchereau & Steinman, 1998), which require MyD88-dependent signals during infection (Chieppa, Rescigno, Huang, & Germain, 2006; Niess et al., 2005). BMDCs have traditionally been defined by phenotypic markers, such as the expression of the integrin CD11c on the cell surface, as well as other functional characteristics (Helft et al., 2015). BMDCs are relatively short lived and they are continuously replenished from bone marrow, blood or tissue derived precursors (Laar, Coffey, & Woltman, 2012). The first part of this study was to isolate and grow BMDCs from bone marrow in the presence of GM-CSF, a well-known stimulus for driving murine BMDC formation *in vitro* (Inaba et al., 1992). Before each experiment we assessed the cell surface of the BMDCs for the presence of the integrin CD11c using flow cytometry. Flow cytometry allows cells in solution to be individually analysed by focusing a stream of cells through a laser, one cell at a time. Specific cell surface markers can be targeted and analysed using monoclonal antibodies conjugated to fluorochemicals, which absorb and emit light at specific wavelengths (Herzenberg et al., 2002). Our data shows we isolated pure BMDC populations as they expressed CD11c on the surface and we were able to gate on these cell populations to look at other cell surface markers when we stimulated BMDCs with SLPs from the various ribotypes of *C. difficile*.

BMDC maturation is characterised by increased expression of cell surface markers such as CD40, CD80 and CD86 (Higgins et al., 2003; Lavelle et al., 2003). Co-receptors are molecules on the surface of T-cells that send signals to drive cell activation, without these signals they may become unreactive or die by programmed cell death. The main co-receptors for T-cell activation are CD80, CD86 and CD40 which bind to CD28, Cytotoxic T-lymphocyte Associated protein 4 (CTLA-4), and CD40 ligands respectively on the T-cell. Activated BMDCs are the most potent stimulators of naive T-cells (Janeway, Travers, Walport, & Schlomchik, 2001; Parkin & Cohen, 2001; Sharpe & Freeman, 2002). CD14 was the first identified PRR that bound directly to LPS (Wright et al., 1990) and is known to chaperone LPS molecules to the TLR4-MD2 signalling complex (da Silva Correia, Soldau, Christen, Tobias, & Ulevitch, 2001; Giannini et al., 2004; Moore et al., 2000). Our flow cytometry data shows that SLPs

from ribotypes 001, 005, 031, 027 induce CD80, CD86 and CD40 expression on the surface of BMDCs. The expression of CD14 was induced by LPS and SLPs from ribotypes 001, 005 and 031, however, BMDCs stimulated with SLPs from ribotype 027 exhibited slightly lower CD14 expression compared to the control cells. CD14 sits at the apex of all cellular responses and functions to induce an innate immune trafficking cascade that involves the transport of both TLR4 and its ligand (Zanoni et al., 2011). It is possible that ribotype 027 utilises the slight down regulation of CD14 to delay the innate immune trafficking cascade in order to evade the host immune response. Our data confirms the results previously seen with SLPs from ribotype 001 and we show that SLPs from ribotypes 005, 031, 027 induce BMDC maturation in a similar manner, the response seen is also comparable to the response by LPS.

Maturation of BMDCs are also characterised by the production of cytokines such as IL-12p70, TNF α , IL-23 and IL-6. Cytokines play a central role in the modulation of the immune system and they can have pro-inflammatory or anti-inflammatory functions (Gerhard & Andus, 1998). Our data demonstrates that SLPs from ribotypes 005, 031 and 027 induce the production of IL-12p40, IL-23 TNF α and IL-6 in BMDCs to a similar level to that of LPS and in a similar way to SLPs from ribotype 001. The IL-12 family of cytokines which include IL-23 and IL-12p40 play a major role in the inflammatory response (Parkin & Cohen, 2001). TNF α also acts on BMDCs, promoting migration to the lymph nodes where an adaptive immune response can be initiated and it has also been shown to induce bacterial clearance (Bekker *et al.*, 2000). IL-6 plays a crucial role in the differentiation of BMDCs and is an important modulator to maintain the balance between Th1 and Th2 effector functions (Jego et al., 2003; Yao et al., 2014). Both IL-6 and IL-23 are required to drive Th17 responses and Th17 cells have a role in the clearance of bacteria from the gut (Khader, Gaffen, & Kolls, 2009; Zhang, Clarke, & Weiser, 2009). It has been shown previously that SLPs can induce the production of pro-inflammatory cytokines in immune cells such as BMDCs, monocytes and macrophage (Ausiello et al., 2006; Bianco et al., 2011; Calabi et al., 2002; Collins et al., 2014; Madan & Petri Jr, 2012; Ryan et al., 2011; Vohra & Poxton, 2012) and the data presented in this chapter supports these claims.

However, our findings show differences in the potency of the immune response between ribotypes, with regard to the induction of IL-1 β , IL-12p70 and IL-10 in BMDCs which has not yet been reported in the literature. Our data shows that BMDCs stimulated with ribotype 027 and 031 appeared to produce more IL-1 β than BMDCs stimulated with LPS and SLPs from the other ribotypes examined in this study. IL-1 β is an important pro-inflammatory mediator that is generated at sites of injury or immunological challenge (Schroder & Tschopp, 2010). IL-1 β has also been shown to be critical in bacterial infection and clearance *in vivo* (Miller et al., 2014). Our data also demonstrates that BMDCs stimulated with SLPs from ribotypes 005, 031 and 027 produced IL-12p70 to a similar level as the response induced by LPS. However BMDCs stimulated with SLPs from ribotype 001 appeared to produce much less IL-12p70 than BMDCs stimulated with LPS and the other SLPs examined in this study. IL-12p70 part of the IL-23 family helps induce T-cells to differentiate into Th1 cells thus aiding the inflammatory response (Parkin & Cohen, 2001). Our data also shows that SLPs from ribotype 031 and 027 appeared to produce more IL-10 in BMDCs, compared to BMDCs stimulated with LPS and SLPs from the other ribotypes in this study. IL-10 is an anti-inflammatory cytokine that inhibits MHC class II and co-stimulatory molecules on monocytes and macrophages. IL-10 limits the production of pro-inflammatory cytokines including IL-1 β , IL-6, IL-12, TNF α and chemokines such as MCP-1, RANTES, IL-8 and MIP-2 (Lee & Kim, 2007; Williams et al., 2004). The production of and signalling by type I IFN is required for LPS induced IL-10 up regulation (Chang et al., 2007). STAT3 is an important player mediating the anti-inflammatory effect of IL-10, studies have shown that IL-10 production is abolished in STAT3 $-/-$ mice (Takeda et al., 1999). STAT3 is activated by the IL-23 family of cytokines, we know from the literature that the production of the IL-23 family of cytokines is strongly dependent on IRF3 (Goriely et al., 2008; Molle et al., 2007).

During infection IL-10 inhibits the activity of Th1 cells, NK cells and macrophages (Couper, Blount, & Riley, 2008), all which are required for optimal pathogen clearance (Andoh et al., 2007). The absence of IL-10 can be accompanied with immunopathological tissue damage that is potentially harmful to the host, whereas excessive IL-10 production always results in chronic infectious diseases caused by less clearance of pathogens (Lin et al., 2013). Furthermore other organisms such as *Brucella*

abortus and *Mycobacterium tuberculosis* have been shown to utilise IL-10 to avoid clearance in host cells and mediate long term infection (Redford, Murray, & O'Garra, 2011; Xavier et al., 2013). It is possible that the ability of ribotype 027 to induce pro-inflammatory tissue damaging responses and anti-inflammatory responses is beneficial for the pathogen. Ribotype 027 could increase tissue damage to potentially invade deeper into the gut resulting in a more persistent disease while switching off powerful immune cell responses. Ribotype 001 on the other hand induces a less potent inflammatory response. The ability of SLPs from certain ribotypes to induce anti-inflammatory responses and others to induce more potent pro-inflammatory responses may account for the variability of symptoms and severity of disease experienced by patients who contract *C. difficile*.

We have previously shown that SLPs from ribotype 001 activate TLR4 (Ryan et al., 2011). TLR4 initiates downstream signalling which in turn activates NF- κ B and IRF3 via MyD88-dependent and -independent pathways (Akira & Takeda, 2004). Activation of the MyD88 dependant pathway is mainly an event initiated at the plasma membrane, while induction of IRF3 via the MyD88- independent pathway is dependent on the endocytosis of TLR4 and requires the presence of CD14 and subsequently TRIF (Jiang et al., 2005; Kagan et al., 2008). IRF3 induce type I IFNs which have an important role in bridging innate and adaptive immunity by mediating the induction of co-stimulatory molecules on antigen presenting cells in response to pathogen associated molecules (Hoebe & Beutler, 2004). Both MyD88-dependent and independent mechanisms are required for the development of full host response to bacterial challenge and LPS can activate both NF- κ B and IRF3 signalling pathway (Carrigan et al., 2010). Given the similarity of the response of SLPs from ribotype 001 with LPS and the induction of DC maturation, it was not surprising to us that the response activated TLR4 signalling with downstream activation of p38 and NF- κ B signalling (Collins et al., 2014; Ryan et al., 2011). What was surprising was SLPs from ribotype 001 did not induce IRF3 signalling (Ryan et al., 2011).

The next part of this study was to investigate if there were differences between SLPs from the different ribotypes in signalling downstream of TLR4. We used HEK-293 cells which were stably transfected with TLR4, MD2 and CD14 receptors on the surface as

these cells have the machinery necessary for TLR4 signalling. The luciferase gene reporter assay enabled us to examine NF- κ B and IRF3 signalling induced by the SLPs from differing ribotypes of *C. difficile*. Both sets of plasmid DNA were co-transfected with constitutively expressed TK renilla luciferase construct. The utility of an internal control plasmid is dependent on the fact that the encoded protein is expressed in a constitutive manner without being influenced by experimental factors and can therefore be used to normalise the transfection efficiency (Shifera & Hardin, 2010). Our data shows that SLPs from ribotypes 001, 014, 078 and 027 activate NF- κ B signalling downstream of TLR4 and with subsequent production of IL-8. We also show that SLPs from ribotypes 001, 014 and 078 do not induce IRF3 activation, whereas SLPs from ribotype 027 induced IRF3 signalling with independent production of RANTES by the cells. Therefore, there are key signalling differences between SLPs from ribotype 027 which is known to be hypervirulent and other ribotypes of *C. difficile* such as ribotype 001. SLPs from ribotype 027 can induce both NF- κ B and IRF3 signalling and we know from the literature that activation of both arms of the TLR4 signalling pathway is required for full bacterial clearance. Yet clearance of ribotype 027 appears more difficult given the clinical symptoms of CDI, even though both arms of the TLR4 pathway are activated. It is possible that there is another level of regulation influencing bacterial clearance induced by the SLPs from ribotype 027. SLPs from ribotype 001 did not induce IRF3 signalling, this could account for the reduced IL-12p70 and IL-10 production in BMDCs as there is a link between IL-10 production, IL-12p70 a member of the IL-23 family and IRF3 expression and thus warrants further investigation.

The differences between SLPs isolated from differing *C. difficile* ribotypes is the amino acid sequence changes in the LMW protein (Lynch 2014, unpublished). Consequently, this variability in SLPs sequence may be an important mechanism in *C. difficile* escaping the host's response (Fagan, et al. 2009, Ryan, et al. 2011). Sequence differences could affect the recognition of SLPs by the immune system and therefore may explain why some strains of *C. difficile* cause severe infection and have a higher frequency of reoccurrence and yet others are associated with minimum clinical symptoms and varying pathology (Ryan, et al. 2011). Given the continuing challenge that *C. difficile* poses, understanding how it activates the immune response by either switching on or off certain arms of the pathway may ultimately provide insights for

novel therapies to improve clearance in patients and prevent reoccurrence of infection (Collins et al., 2014; Ryan et al., 2011). It has now emerged that TLR pathways are tightly regulated by miRNAs (He et al., 2014; O'Neill et al., 2011). In the next chapter we hope to elucidate further differences between miRNA profiles of cells stimulated with LPS and SLPs *via* the TLR4 signalling pathway.

**Chapter 4: Profiling the MiRNAs
Induced by SLPs from *C. difficile***

4.1 Introduction

The inflammatory response to infection involves the induction of several hundred genes, a process that must be tightly regulated to achieve pathogen clearance and at the same time avoid consequences of deregulated gene expression such as uncontrolled inflammation or cancer (Sonkoly, Stähle, & Pivarcsi, 2008). The innate immune response is the first line of defence against pathogens (Janeway, 1989). It is initiated by the binding of microbial ligands to membrane-associated pathogen recognition receptor proteins known as TLRs as previously described in the general introduction (Mogensen, 2009). Mature microRNAs (miRNAs) are short double stranded RNA molecules approximately 19-23 nt in length that pair to protein coding genes. They can block mRNA translation, reduce mRNA stability or induce mRNA cleavage after imperfect binding to the miRNA recognition elements within the 3' and 5' untranslated region (UTR) of target mRNA genes (Bartel, 2004). MiRNAs have been shown to be involved in innate immunity by regulating TLR signalling and ensuing cytokine response by targeting a variety of signalling proteins, regulatory molecules and transcription factors (Dalal & Kwon, 2010; He et al., 2014; Sonkoly et al., 2008). They can also regulate central elements of the adaptive immune response such as antigen presentation, T cell receptor signalling and the interferon system (Cullen, 2006; Sonkoly et al., 2008).

In recent times, unique miRNA expression profiles have been described in epithelial cells of patients with active ulcerative colitis, Crohn's ileitis, and Crohn's colitis, as well as in the peripheral blood of patients with active ulcerative colitis and Crohn's disease (Dalal & Kwon, 2010). There is also mounting evidence that miRNAs orchestrate immune regulation and host responses to pathogens during infection. Bacterial pathogens manipulate cellular functions and modulate signal transduction pathways and pro-inflammatory responses through the delivery of effectors into host cells. Each pathogen can use different molecular strategies to subvert the complex pathways that regulate the host immune response (Staedel & Darfeuille, 2013). *C. difficile* are no different and key effector molecules have been identified that can drive towards a protective anti-inflammatory response or a damaging pro-inflammatory response (Solomon, 2013). To date no one has examined miRNAs profiles induced in response to SLPs from *C. difficile*.

The severity of *C. difficile* infection may be dependent on the strain present (Goorhuis et al., 2007; Rupnik et al., 2009). Some ribotypes are more ‘hypervirulent’ than others, this is the case with ribotype 027 which has been associated with more severe diarrhoea, higher mortality and more recurrences (Clements et al., 2010; Dawson et al., 2009; Goorhuis et al., 2007; Loo et al., 2005). In comparison infection with ribotype 001 is associated with a milder infection and a more efficient clearance of the bacteria (Clements et al., 2010; Dawson et al., 2009; Goorhuis et al., 2007; Loo et al., 2005). In the previous chapter we determined that SLPs from ribotype 001 and 027 activate NF- κ B signalling. SLPs from ribotype 027 activate IRF3 signalling downstream of TLR4, while SLPs from ribotype 001 fail to induce this response. Given the role of miRNAs in the regulation of TLR4 signalling and during infection, we hypothesise that SLPs induce miRNAs and that profiles differ between ribotypes, which may explain the differences we see in signalling downstream of TLR4 signalling and ultimately the immune response to *C. difficile*.

Quantitative Real-Time PCR (qPCR) is the gold standard for detecting miRNAs (Schmittgen et al., 2009). However, many properties that are unique to miRNA pose challenges for their accurate detection and quantification using this method (Wark, Lee, & Corn, 2008). Their short length makes it difficult for traditional primers to anneal for reverse transcription. Unlike mRNA, miRNA lack a common structure/ sequence, such as a poly adenylated (poly-A) tail which is typically used for enrichment or as a binding site for primers. The poly-A tail is cleaved by the Drosha/DGCR8 microprocessor complex during biogenesis (Gromak et al., 2013). MiRNAs within a seed family also pose difficulties for qPCR as they may only differ from one another by as little as one nucleotide making specificity of the primer particularly crucial. Stem loop primers differentiate between mature and pre/pri miRNA as well as miRNA which differ by only a single nucleotide. This method has shown to have a high specificity and dynamic range of at least 7 logs and is capable of detecting as few as 7 copies of product in a qPCR reaction (Chen et al., 2005; Kramer, 2011).

Taqman chemistry utilises an oligonucleotide probe constructed from a fluorogenic labelled reporter fluorescent dye and a quencher dye see **Figure 4.1.1**. While the probe is intact, the proximity of the quencher dye greatly reduces the fluorescence emitted by

the reporter dye by fluorescence resonance energy transfer (FRET). If the target sequence is present, the probe anneals downstream from one of the primer sites and is cleaved by the 5' nuclease activity of Taq DNA polymerase as this primer is extended. Cleavage of the probe separates the reporter dye from the quencher dye, increasing the reporter dye signal. Removing the probe from the target strand, allows primer extension to continue to the end of the template strand. Additional reporter dye molecules are cleaved from their respective probes with each cycle, resulting in an increase in fluorescence intensity proportional to the amount of PCR product produced. The development of this mature TaqMan technology has led to an innovative design of Taqman Low Density Arrays (TLDA), a medium throughput method for qPCR that uses 384 well microfluidic cards pre-loaded with miRNA primer probes. Applied Biosystems™ have developed TLDA cards containing different pools of known human miRNAs found in pool A and lesser characterised miRNAs found in pool B, thus enabling the screening of over 756 miRNA targets found in miRBase.

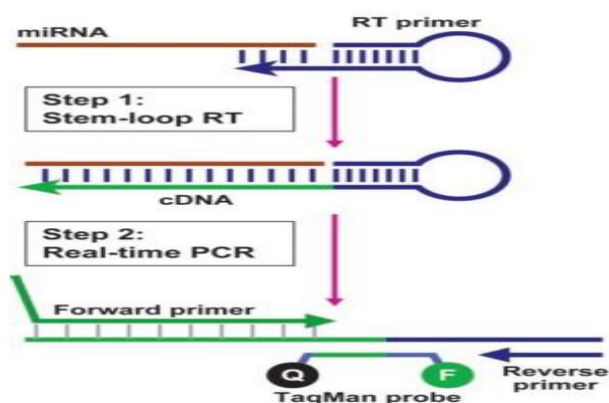


Figure 4.1.1 Stem loop primers for miRNA detection and PCR using TaqMan chemistry (Chen et al., 2005)

The aim of this chapter is to profile and compare miRNA expression induced by SLPs from ribotypes 001 and 027. Initially miRNAs induced in response to LPS and SLPs from ribotype 001 will be screened using TLDA cards to validate our method and narrow down the target list. This target list will be further validated using custom made to order TLDA cards. The differences in miRNA profiles between ribotype 001 and 027 will then be examined and validated in individual Taqman PCR assays in both human and murine cell lines.

4.2 Results

4.2.1 Optimising a Method for Profiling MiRNAs Induced by SLPs from *C. difficile*

MiRNAs are known to regulate immune signalling by targeting a variety of signalling proteins, regulatory molecules, cytokines, transcription factors and TLR receptors post immune stimulation (He et al., 2014). We hypothesise that SLPs from RT 001 and RT 027 induce miRNAs and these profiles differ, which may explain the differences we see in TLR4 signalling. To test this hypothesis we had to first establish a protocol for detecting miRNAs. qPCR is the gold standard for examining miRNA expression and this technology is utilised in TLDA cards. TLDA cards are 384 well microfluidic cards preloaded with probes for different pools of known human miRNAs found in pool A and lesser characterised miRNAs found in pool B. Three endogenous small RNA controls are included on each of the pool A and B cards, thus enabling the screening of 756 miRNAs from each sample. SLPs modulate TLR4 signalling therefore we wanted to examine miRNA profiles induced by SLPs *via* TLR4 signalling specifically, for that reason Hek TLR4/MD2/CD14 cells were used throughout the initial profiling studies. We also incorporated cells stimulated with LPS in our study as it is a well-known TLR4 agonist that can activate both NF- κ B & IRF3 signalling and miRNA activation by LPS has also been reported (Akashi et al., 2003; Taro Kawai & Akira, 2007; Laird et al., 2009). Evidence from the literature shows that LPS induces miRNAs; miR-155, miR-125, miR-9, the let-7 family, miR-145, miR-146a and miR-187 as little as eight hours post stimulation and they have been shown to modulate the immune response and target key molecules in the TLR4 signalling pathway (Curtale et al., 2013; Rossato et al., 2012; Tili et al., 2007).

We first needed to establish the time point we could assess miRNAs activation seeing as LPS can induce miRNAs that modulate the immune response as little as 8 hours post stimulation. We first had to establish if SLPs from RT 001 & RT 027 could activate NF- κ B and if SLPs from RT 027 could activate IRF3 signalling at this time point. We measured IL-8 and RANTES production in Hek TLR4/MD2/CD14 cells stimulated with LPS and SLPs from RT 001 and RT 027 for 8 hours. IL-8 and RANTES are indicative of NF- κ B and IRF3 signalling respectively (Lin et al., 1999; Mukaida et al., 1994). We measured human IL-8 and RANTES expression from the cell supernatants

using ELISA see **Figure 4.2.1**. There were low levels of IL-8 produced by the control Hek TLR4/MD2/CD14 cells, however IL-8 production was increased when cells were stimulated with LPS ($p \leq 0.001$) and SLPs from RT 001 ($p \leq 0.001$) and RT 027 ($p \leq 0.001$) compared to the control cells. There were low levels of RANTES produced in Hek TLR4/MD2/CD14 cells, however production was increased in cells stimulated with LPS ($p \leq 0.001$) and SLPs from RT 027 ($p \leq 0.01$) compared to the control cells. There was no significant increase in RANTES produced in Hek TLR4/MD2/CD14 cells stimulated with SLPs from RT 001 compared to the control cells. In summary SLPs from RT 001 and RT 027 activated NF- κ B and SLPs from RT 027 activated IRF3 signalling at 8 hours, therefore we decided to profile miRNAs at this time point thereafter.

Total RNA was extracted from cells using the using miRVana™ miRNA isolation kit and we did so according to manufacturer's instructions. This method preserves the small RNA fraction containing miRNAs and includes the slightly longer endogenous small RNA control sequences. The RNA was quantified following isolation using the NanoDrop® ND-1000 Spectrophotometer. The purity of the RNA was also examined by measuring the 260 nm and 280 nm absorption wavelengths, where RNA with an A260/A280 ratio between 1.8- 2.1 was considered pure. RNA samples were subsequently run on 1% agarose gels where the 28S and 18S ribosomal RNA (rRNA) bands were assessed to confirm integrity. Two bands were seen on the gel, the first band was located between the 1500-2000 bp molecular markers indicative of the 18S rRNA band. A second band twice the intensity of the other was located between the 4000-5000 bp molecular markers indicative of 28S rRNA band (**see Appendix D**). Total RNA of good quality was used exclusively throughout the studies.

cDNA synthesis with and without downstream pre-amplification supports the analysis of miRNA with 1 to 1000 ng starting total RNA, however the manufacturer recommends downstream pre-amplification if the starting product is below 350 ng. Pre-amplification PCR uniformly amplifies desired cDNA by increasing the amount of starting template (Noutsias et al., 2008). The increased amount of starting material boosts the sensitivity of miRNAs detected without biasing the estimation of miRNA expression ratio (Chen et al., 2009). We established the optimal quantity of input total

RNA for our study. A pre-amplification reaction with 350 ng total RNA increased the quantity of starting template seen by the detection of miRNAs at earlier cycle numbers see **Figure 4.2.2**. Once we optimised these conditions we ran Megaplex reverse transcription reactions (pool A and B), two pre-amplification reactions (pool A and B) and two TLDA cards (A and B) per sample from three biological replicates. Initially we screened control samples, samples stimulated with LPS and SLPs from RT 001.

4.2.2 TLDA Card Analysis Parameters

Following each run SDS files were exported from the Applied Biosystems 7900HT Fast Real time PCR machine and the qPCR data from pool A and B TLDA cards was analysed using ExpressionSuite software. The fluorescence threshold was set to 0.1 so that the experimental conditions lay within the exponential phase of the PCR reaction. When fluorescence crosses this value, the cycle is termed the "Threshold cycle" (Ct) and the higher the Ct, the smaller the initial amount of DNA. The max Ct for analysis was set to 37.0, anything beyond this Ct was deemed outside the limit of detection for this study. Each assay was pre-designed from Applied Biosystems™ and assay efficiency is guaranteed at 100%. A proper normalisation strategy is crucial for any qPCR data analysis, it minimises the effects of systematic technical variations and is a prerequisite for getting meaningful biological changes (Meyer, Kaiser, Wagner, Thirion, & Pfaffl, 2012). For large scale miRNA expression profiling studies, global normalisation out performs the normalisation strategies using endogenous controls (Mestdagh et al., 2009). Seeing as we generated a large data set global normalisation was carried out, the median Ct of common assays was used as the normaliser on a per sample basis. The normalised reporter 'Rn' value for each target was also integrated into these calculations. Relative gene expression was calculated and Benjamini-Hochberg False Discovery Rate (FDR) was used to adjust p-values. Increasing the number of tests increases the probability of finding a significant p-value by chance and to avoid this effect the FDR adjusts the p-values according to the number of total tests. The statistics used in a t-test are defined as the difference of the arithmetic mean of two groups divided by the estimated standard deviation of that difference. The t-test statistic runs under the assumption that the given variable follow normal distribution (Goni, García, & Foissac, 2009; Li, 2012). Therefore we examined the overall Ct value

distribution for each sample from the data generated from the pool A and B TLDA cards see **Figure 4.2.3**. The box plot shows the Ct distribution for each treatment group with three biological replicates per group. The box contains the middle 50% of the data, the black horizontal line indicates the median Ct value and the black dot denotes the mean Ct. The end of the vertical lines indicates the minimum and maximum Ct values and the outliers are the points outside the ends of the whiskers. The overall Ct values follow normal distribution therefore we applied a student's t-test where values of $p \leq 0.05$ were considered statistically significant compared with the control cell group.

4.2.3 Profiling Studies Using TLDA Cards Revealed 16 MiRNAs were Differentially Regulated in Response to LPS and SLPs from RT 001

qPCR data analysis revealed 248 miRNAs were detected out of the 756 miRNAs analysed using pool A and B TLDA cards see **Table 4.2.1**, the other miRNAs were not expressed. There was also no expression in the NTC reactions on both A and B arrays (data not shown). Ct scatter plots showed there were differences in miRNA profiles between cells stimulated with LPS and SLPs from RT 001. We compared Ct values between each group and found they fell outside of the regression line- indicating they are not entirely linear see **Figure 4.2.4**. However in order to fully elucidate the difference between individual miRNA targets with statistically significant fold changes, the data was analysed using a volcano plot. According to the literature, there is a relationship between fold change and t-statistics with logarithm transformation (Li, 2012). Therefore $-\log_{10}$ p-value was plotted against \log_2 fold change. For our study the fold change boundary was set to 1.0 and the p-value boundary was set to $p \leq 0.05$. miRNA targets above the central horizontal line had statistically relevant high magnitude fold changes. The top left quadrant displayed down regulated miRNAs, while the top right quadrant displayed miRNA targets that were up regulated.

Four miRNAs were differentially regulated in response to LPS. The volcano plot showed that one miRNA was down regulated miR-586 ($p \leq 0.05$) while three miRNAs were upregulated miR-302c ($p \leq 0.05$), miR-374 ($p \leq 0.05$) and miR-543 ($p \leq 0.01$) see **Figure 4.2.5**. Twelve miRNAs were differentially regulated in response to SLPs from RT 001. The volcano plot showed three miRNAs were down regulated miR-1293 ($p \leq$

0.001), miR-422a ($p \leq 0.01$) and miR-874 ($p \leq 0.05$). Nine miRNAs were up regulated miR-1292 ($p \leq 0.05$), miR-148b ($p \leq 0.001$), miR-152 ($p \leq 0.05$), miR-24 ($p \leq 0.05$), miR-215 ($p \leq 0.05$), miR-339-5p ($p \leq 0.001$), miR-432# ($p \leq 0.05$), miR550 ($p \leq 0.05$) and miR-590 ($p \leq 0.05$) see **Figure 4.2.6**. In total 16 miRNAs had significantly significant high magnitude fold changes in response to LPS and SLPs from RT 001, a summary of these results are shown in **Table 4.2.2**.

4.2.4 Additional MiRNAs of Interest were Chosen for Further Validation Following a Review of the Literature and Re-examination of the Profiling Study

We reviewed the literature for miRNAs known to regulate key elements of TLR4 signalling including; signalling proteins, transcription factors, cytokines and regulatory molecules, to create a short list of potential miRNAs of interest. We also included miRNAs that are known to be induced by LPS and miRNAs induced during an immune response to infection. The short list comprised of let-7b, let-7c, let-7d, let-7e, let-7e#, miR-125a-5p, miR-132, miR-145, miR-146a miR-155, miR-187, miR-221, miR-221#, miR-9 and miR-9#. We then re-examined the profiling study to see if the short list of miRNAs were present in the initial experimental profiling study see **Table 4.2.3**. The miRNAs identified from the literature were in fact present but were over the significance value set in this experiment. MiR-155, miR-9, the let-7 family, miR-145, miR-146a and miR-187 have all been shown to be induced by LPS in the literature (Curtale et al., 2013; Rossato et al., 2012; Tili et al., 2007). Although not significantly expressed these miRNAs were shown to be induced by LPS in our study, thus validating our experimental method. We also found that there were differences in the expression of miRNAs between LPS and SLPs from RT 001, therefore we decided to include the short list of miRNAs from the literature for further analysis. The lists of 16 miRNAs identified from the experimental profiling study and the short list of 15 miRNAs from the literature were combined and custom TLDA cards containing the now 31 miRNAs of interest were commissioned. The endogenous control U6 snRNA was selected as it out performed the two other human small RNA endogenous controls RNU44 and RNU48 (see **Appendix F**). Therefore U6 snRNA was included as the endogenous control on the custom TLDA cards.

4.2.5 Custom TLDA Card Analysis Parameters

New RNA samples were generated and included Hek TLR4/MD2/CD14 cells stimulated with LPS, SLPs from RT 001 and RT 027. qPCR data from the custom cards was analysed using ExpressionSuite software, where the threshold was set to 0.1 and the max Ct set to 37.0 as previously determined. There was also no miRNA expression detected in cards with NTC (data not shown). Due to the reduction in the number of total targets, U6 snRNA was used as the endogenous control instead of global normalisation and relative gene expression was calculated. We also examined the overall Ct value distribution for each sample from the custom cards see **Figure 4.2.7**. The box plot shows the Ct distribution for each treatment group from three biological replicates per group which also included 4 technical replicates. The overall Ct values followed normal distribution therefore we could apply a student's t-test where values of $p \leq 0.05$ were considered statistically significant compared with the control cell group.

4.2.6 Twenty-Four MiRNAs were Differentially Regulated by SLPs from RT 001 and RT 027

qPCR data analysis revealed 28 miRNAs were detected out of the 31 miRNAs analysed using the custom TLDA cards see **Table 4.2.4**. Ct scatter plots analysis showed there were differences in miRNA profiles between cells stimulated with LPS, SLPs from RT 001 and RT 027 see **Figure 4.2.8** and **Figure 4.2.9**. When we compared Ct values between each group we found they fell outside of the regression line- indicating they were not entirely linear. The data was then visualised using a supervised heat map incorporating average linkage and Pearson's correlation **Figure 4.2.10**. The heat map shows the corresponding relative miRNA expression levels and renders them in a green-red scale. Green represents low expression levels while red represents high expression levels and black indicates an absence of detection. Each row represents a single miRNA and each column represents an individual sample. Cells stimulated with SLPs from RT 027 had low expression for most of the miRNAs analysed and this was consistent between each of the biological replicates as shown by the green colour on the heat map.

A dendrogram is a tree diagram frequently used to illustrate the arrangement of the clusters produced by hierarchical clustering. According to the dendrogram on the y-axis shown with the heat map, miRNAs were clustered in one main clade with another smaller clade containing 2 branches. The first branch in the smaller clade contained branch tips for let-7e* and miR-1293, while the second branch contained tips for miR-221* and miR-543. The larger main clade contained 7 distinct branches. The first, second and third branches contained a single branch tip for miR-586, miR550 and miR-146a respectively. The fourth branch contained branch tips for miR-221, let-7c, let-7d, miR-9*, miR-9, miR-152, miR-432*, miR-148b and miR-339-5p. The fifth branch contained branch tips for miR-125a-5p, let-7e, let-7b and miR874. The sixth branch contained branch tips for miR-187, miR-215 and miR-24. The seventh branch contained branch tips for miR-1292, miR-145, miR-155, miR-422a, miR-132, miR-302c, miR-374 and miR-590-5p. MiRNAs included within each clade and subsequent branch group, are more likely to be expressed together based on the experimental data in this study.

In order to fully elucidate the difference between individual miRNA targets between treatment groups with statistically significant fold changes, the data was analysed using a volcano plot. Consequently $-\log_{10}$ p-value was plotted against \log_2 fold change, for our study the fold change boundary was set to 1.0 and the p-value boundary was set to $p \leq 0.05$. Targets above the central horizontal line had statistically relevant high magnitude fold changes. The top left quadrant displayed down regulated miRNAs, while the top right quadrant displayed miRNA targets that were up regulated. Analysis showed 24 miRNAs were differentially regulated in response to SLPs from RT 001 and RT 027. Two miRNAs, miR-145 ($p \leq 0.05$) and miR-146a ($p \leq 0.001$) were up regulated in response to SLPs from RT 001 see **Figure 4.2.11**. Twenty three miRNAs were down regulated in response to SLPs from RT 027 let-7b ($p \leq 0.05$), let-7c ($p \leq 0.001$), let-7d ($p \leq 0.001$), let-7e ($p \leq 0.001$), miR-125a-5p ($p \leq 0.001$), miR-1292 ($p \leq 0.001$), miR-132 ($p \leq 0.001$), miR-145 ($p \leq 0.001$), miR-148b ($p \leq 0.01$), miR-152 ($p \leq 0.05$), miR-155 ($p \leq 0.05$), miR-221 ($p \leq 0.05$), miR-24 ($p \leq 0.05$), miR339-5p ($p \leq 0.001$), miR-374 ($p \leq 0.05$), miR-422a ($p \leq 0.05$), miR-432* ($p \leq 0.01$), miR-543 ($p \leq 0.01$), miR-586 ($p \leq 0.05$), miR-590 ($p \leq 0.05$), miR-9 ($p \leq 0.05$), miR-9* ($p \leq 0.001$) and miR-221 ($p \leq 0.05$) see **Figure 4.2.12**. miR-145 was differentially regulated by both SLPs from RT 001 and RT 027.

4.2.7 Further Validation Confirmed let-7e, miR-155, miR-145 and miR-146a were Differentially Regulated in Response to SLPs from RT 001 and RT 027

We choose four miRNAs let-7e, miR-155, miR-146a and miR-145 for further validation based on the differences observed between SLPs from RT 001 and RT 027 see **Table 4.2.5**. Let-7e appeared to be down regulated in response to SLPs from RT 001, however it appeared to be even more down regulated when we compared the response to SLPs from RT 027. MiR-155 in response to SLPs from RT 001 remained at levels seen with control cells but appeared to be down regulated when we compared the response to SLPs from RT 027. MiR-146a and miR-145 were both up regulated in response to SLPs from RT 001 and appeared to be down regulated in response to SLPs from RT 027. New RNA samples were generated and included Hek TLR4/MD2/CD14 cells stimulated with LPS, SLPs from RT 001 and RT 027 from three biological replicates. Individual Taqman miRNA assays with three technical replicates per group were run for each miRNA examined and the qPCR data was analysed using ExpressionSuite software. The threshold was set to 0.1 and the max Ct set to 37.0, as previously determined. There was also no miRNA expression detected in assays containing NTC (data not shown). U6 snRNA was used as the endogenous control as previously determined and relative gene expression was calculated. The Mann Whitney U-test was used to test for significance between SLPs from RT 001 and RT 027. This statistical test was chosen because of the uncertainty of normal distribution due to the low number of miRNA targets in this experimental study (Goni et al., 2009).

qPCR data from the individual miRNA assays confirmed the results seen with the custom TLDA cards, let-7e, miR-155, miR-145 and miR-146a were differentially regulated in response to SLPs from RT 001 and RT 027 see **Figure 4.2.14**. Stimulation with LPS did not significantly increase or decrease miR-145, it increased miR-146a to 1.6 fold and it decreased let-7e and miR-155 to 0.6 and 0.7 fold respectively. Stimulation with SLPs from RT 001 did not significantly increase or decrease miR-155, it decreased let-7e and increased miR-146a and miR145 to 1.6 and 1.2 fold respectively. In all cases miRNAs were down regulated in response to SLPs from RT 027 compared to SLPs from RT 001, let-7e, miR-155, miR-146a and miR-145 were decreased to 0.1 ($p \leq 0.001$), 0.03 ($p \leq 0.001$), 0.6 ($p \leq 0.001$) and 0.2 ($p \leq 0.001$) fold respectively.

4.2.8 Let-7e, miR-155, miR-145 and miR-146a were Differentially Regulated in JAWS II Cells

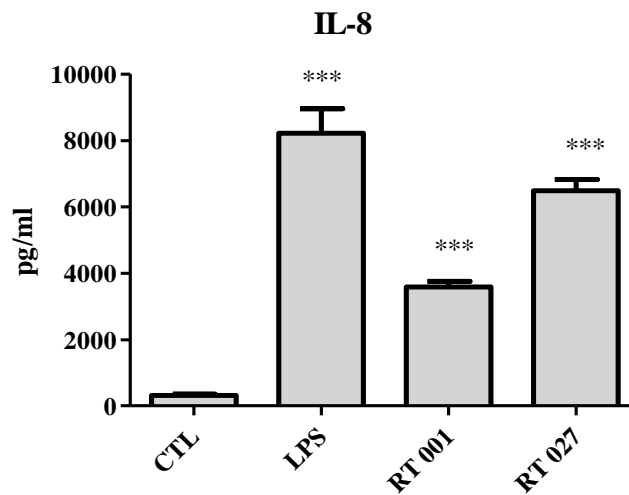
In order to validate our results further we examined miRNA expression of let-7e, miR-155, miR-146a and miR-145 in another cell line, we choose the murine dendritic cell line JAWS II as they behave in a similar way to BMDCs. JAWS II cells differ from BMDCs in that they fail to release the IL-12 cytokine family which include IL-12, IL-23 and IL-27 and IL-35 (Collins, 2014; Jørgensen, Haase, & Michelsen, 2002; Zapala et al., 2011). To begin we had to determine if LPS, SLPs from RT 001 and RT 027 could induce an immune response in JAWS II cells. We measured murine IL-1 β , TNF- α , IL-27p28, MCP, IL-6, RANTES, MIP-2 and IL-12p70 in supernatants upon stimulation for 8 hours using ELISA see **Figure 4.2.14**. IL-1 β was not produced in control JAWS II cells. IL-1 β was produced in JAWS II stimulated with LPS ($p \leq 0.001$), SLPs from RT 001 ($p \leq 0.001$) and RT 027 ($p \leq 0.001$). TNF- α was not produced in JAWS II cells. TNF- α was produced in JAWS II stimulated with LPS ($p \leq 0.001$), SLPs from RT 001 ($p \leq 0.001$) and RT 027 ($p \leq 0.001$). IL-27p28 was produced at negligible levels in control JAWS II cells, it did not increase when stimulated with LPS, SLPs from RT 001 and from RT 027 as expected. MCP was produced at low levels in control JAWS II cells. MCP was produced in JAWS II cells stimulated with LPS ($p \leq 0.001$), SLPs from RT 001 (ns) and RT 027 ($p \leq 0.001$). IL-6 was not produced in control JAWS II cells. IL-6 was produced in JAWS II cells stimulated with LPS ($p \leq 0.001$), SLPs from RT 001 ($p \leq 0.001$) and RT 027 ($p \leq 0.001$). RANTES was produced at low levels JAWS II cells. RANTES was produced in JAWS II cells stimulated with LPS ($p \leq 0.001$), SLPs from RT 001 ($p \leq 0.001$) and RT 027 ($p \leq 0.001$). MIP-2 was produced at low levels in control JAWS II cells. MIP-2 was produced in JAWS II cells stimulated with LPS ($p \leq 0.001$), SLPs from RT 001 ($p \leq 0.001$) and RT 027 ($p \leq 0.001$). IL-12p70 was produced at negligible levels in JAWS II cells and did not increase when stimulated with LPS, SLPs from RT 001 and RT 027 as expected.

Once we established that SLPs from RT 001 and RT 027 could induce an immune response in JAWS II cells and there was a difference in the potency of this response. Total RNA was extracted using the mirVana isolation kit at the 8 hour time point previously determined. RNA samples were generated from three biological replicates.

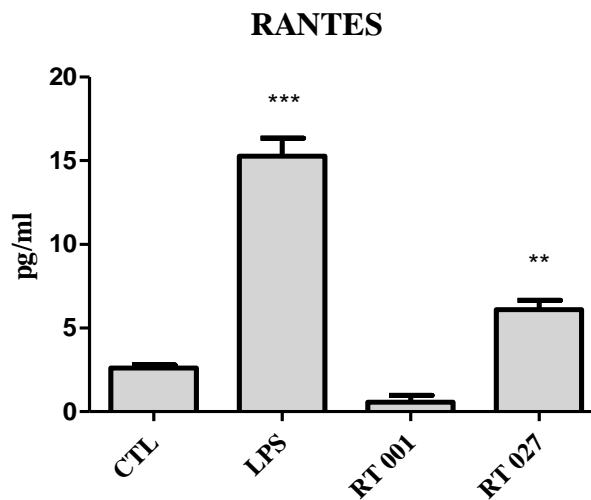
Individual murine miRNA assays with three technical replicates per group from the biological replicates were run for each miRNA examined and the qPCR data was analysed using ExpressionSuite software. The threshold was set to 0.1 and the max Ct set to 37.0, as previously determined. There was also no miRNA expression detected in assays containing NTC (data not shown). The endogenous control snoRNA202 outperformed the two other murine small RNA endogenous controls snoRNA234 and mammU6 (see **Appendix F**). snoRNA202 was used as the endogenous control and relative gene expression was calculated. The Mann Whitney U-test was used to test for significance between SLPs from RT 001 and RT 027. Stimulation with LPS did not significantly increase or decrease miR-146a, it increased miR-145, miR155 and let-7e to 2.5, 60.0 and 1.7 fold respectively. Stimulation with SLPs from RT 001 did not significantly increase or decrease let-7e, however it increased miR-146a, miR-145 and miR-155 to 2.5, 25.0 and 1.2 fold respectively. In all cases miRNAs were down regulated in response to SLPs from RT 027 compared to SLPs from RT 001. Let-7e, miR-155, miR-146a and miR-145 were decreased to 0.5 ($p \leq 0.05$), 5.0 ($p \leq 0.001$), 0.2 ($p \leq 0.001$) and 0.5 ($p \leq 0.001$) fold respectively see **Figure 4.2.15**.

When we compared the expression of miR-146a, miR-145, miR-155 and let-7e we found they were significantly decreased in response to SLPs from RT 027 in both Hek TLR4/MD2/CD14 and JAWS II cells see **Table 4.2.6**. There were slight differences in the response to LPS and SLPs from RT 001 between cell types. MiR-146a expression was increased in response to LPS in Hek TLR4/MD2/CD14 cells, it was not increased or decreased in JAWS II cells, yet miR-146a was increased in response to SLPs from RT 001 in both cell types. MiR-145 was not increased or decreased in response to LPS in Hek TLR4/MD2/CD14 cells but it was increased in JAWS II cells. MiR-145 was increased in response to SLPs from RT 001 in Hek TLR4/MD2/CD14 cells yet it was not increased or decreased in JAWS II cells. MiR-155 was decreased in response to LPS in Hek TLR4/MD2/CD14 cells, in JAWS II cells it was significantly increased. MiR-155 was not decreased nor increased in response to SLPs from RT 001 in Hek TLR4/MD2/CD14 cells, in JAWS II cells however it was increased. Let-7e was decreased in response to LPS in Hek TLR4/MD2/CD14 cells, in JAWS II cells it was increased. Let-7e was decreased in response to SLPs from RT 001 in Hek TL4/MD2/CD14 cells, in JAWS II cells it was increased.

A)



B)



█ Hek TLR4/MD2/CD14

Figure 4.2.1 SLPs from RT 001 and RT 027 induce IL-8 after 8 hours in Hek TLR4/MD2/CD14 cells, however SLPs from RT 001 fail to induce RANTES. Hek TLR4/MD2/CD14 cells were plated at 2×10^6 cells/mL and allowed to adhere for 18 hours to approximately 60% confluency. Cells were then stimulated with 100 ng/mL of LPS or 20 μ g/mL SLPs from RT 001 and RT 027 for 8 hours. Supernatants were recovered and levels of human **A) IL-8** and **B) RANTES** were measured using ELISA. The results show the mean (\pm SEM) measured in triplicate, one-way ANOVA followed by Newman-Keuls analysis was used to determine if differences were significantly different compared to the control, where * $p \leq 0.05$, ** $p \leq 0.01$ and *** $p \leq 0.001$. The results are indicative of three independent experiments.

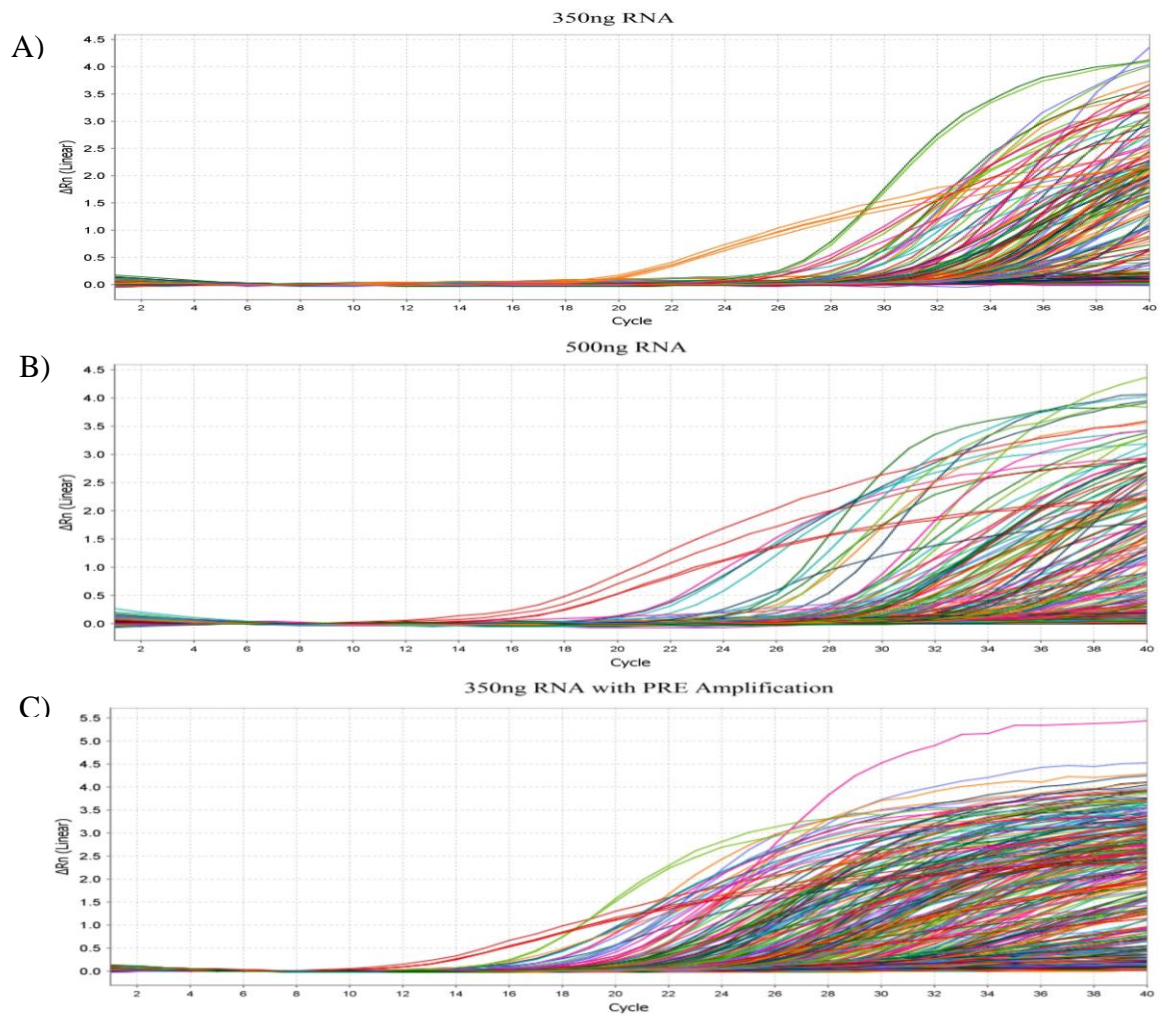


Figure 4.2.2 Starting RNA of 350 ng and a pre-amplification step are required for the detection of miRNA for use in this study. Hek TLR4/MD2/CD14 cells were plated at 2×10^6 cells/mL and allowed to adhere for 18 hours to approximately 60% confluency. Cells were harvested and total RNA was extracted using miRVana™ miRNA isolation kit. 350 ng or 500 ng starting total RNA was converted to first strand cDNA using specific stem loop primers. The products were either added to PCR reaction mixes for the TLDA cards or used in a pre-amplification PCR reaction. Samples were added to each port on Applied Biosystems® Taqman® Low Density Array (TLDA) Human miRNA cards, pool A and pool B. The cards were sealed and ran on the Applied Biosystems 7900HT Fast Real Time PCR Machine. Amplification graph showing the ΔRn V's cycle **A)** 350 ng starting total RNA without pre-amplification **B)** 500 ng starting total RNA without pre-amplification **C)** 350 ng starting total RNA with pre-amplification.

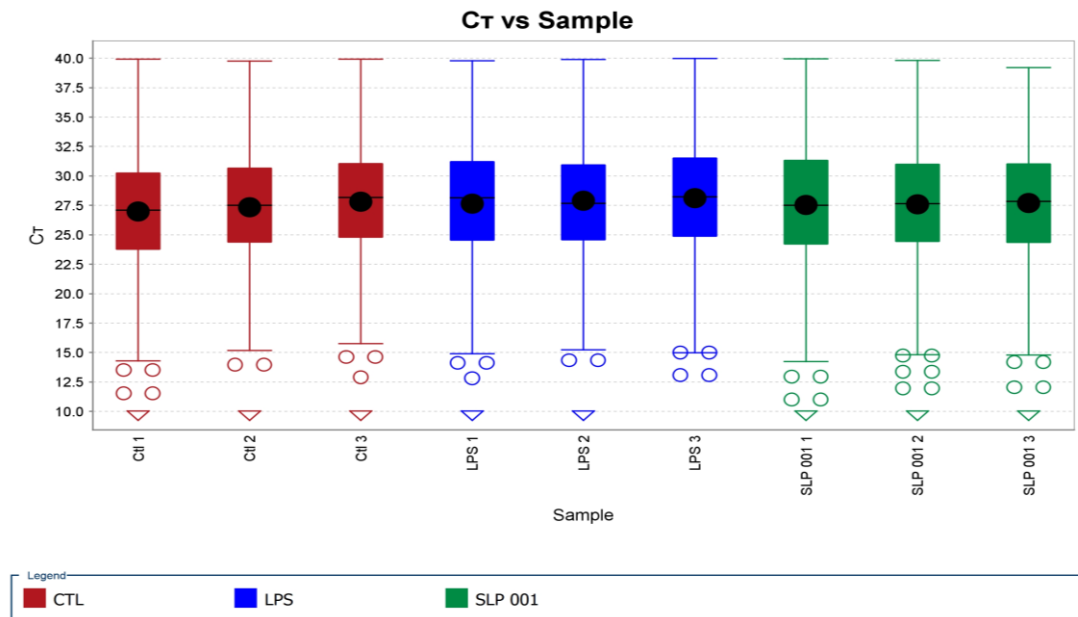


Figure 4.2.3. Overall Ct values follow normal distribution in miRNA profiling study with pool A & B TLDA cards. Hek TLR4/MD2/CD14 cells from three biological replicates were plated at 2×10^6 cells/mL and allowed to adhere for 18 hours to approximately 60% confluency. Cells were stimulated with 100 ng/mL LPS or 20 μ g/mL SLPs from RT 001 for 8 hours. Cells were harvested and total RNA was extracted using miRVana™ miRNA isolation kit. 350 ng starting total RNA was converted to first strand cDNA using specific stem loop primers. The products were used in a pre-amplification PCR reaction. Samples were added to PCR reaction mixes and added to each well on Applied Biosystems® Taqman® Low Density Array (TLDA) Human miRNA cards, pool A and pool B. The cards were sealed and ran on the Applied Biosystems 7900HT Fast Real Time PCR Machine. The SDS files were exported and data from pool A and pool B cards were analysed using ExpressionSuite software v1.0.3. Box plot showing Ct distribution for each treated group from three biological replicates per group. The box contains the middle 50% of the data, the black horizontal line indicates the median Ct value and the black dot denotes the mean Ct. The ends of the vertical lines indicate the minimum and maximum Ct values and outliers are the points outside the ends of the whiskers.

Table 4.2.1 qPCR analysis detected 254 miRNAs in Hek TLR4/MD2/CD14 cells from the 756 miRNAs analysed using the TLDA pool A & B cards. Hek TLR4/MD2/CD14 cells from three biological replicates were plated at 2×10^6 cells/mL and allowed to adhere for 18 hours to approximately 60% confluency. Cells were stimulated with 100 ng/mL LPS or 20 μ g/mL SLPs from RT 001 for 8 hours. Cells were harvested and total RNA was extracted using miRVana™ miRNA isolation kit. 350 ng starting total RNA was converted to first strand cDNA, the products of which were used in a pre-amplification PCR reaction. Samples were added to PCR reaction mixes and added to each well on Applied Biosystems® Taqman® Low Density Array (TLDA) Human miRNA cards, pool A and pool B. The cards were sealed and ran on the Applied Biosystems 7900HT Fast Real Time PCR Machine. The SDS files were exported and data from pool A and pool B cards analysed using ExpressionSuite software v1.0.3. The max Ct was set to 37.0 with a threshold of 0.1 and the reference group was set to the control cell group. Global normalisation was carried and relative gene expression values were calculated. The Benjamini-Hochberg false discovery rate was used to adjust p-values and a student's t-test was applied where values of $p \leq 0.05$ were considered statistically significant compared with the control group.

Group Name	Target Name	RQ	P-Value
CTL	dme-miR-7	1.0	1
LPS	dme-miR-7	0.7	0.586
RT 001	dme-miR-7	0.8	0.62
CTL	hsa-let-7a	1.0	1
LPS	hsa-let-7a	0.7	0.321
RT 001	hsa-let-7a	0.6	0.186
CTL	hsa-let-7b	1.0	1
LPS	hsa-let-7b	1.2	0.051
RT 001	hsa-let-7b	0.9	0.732
CTL	hsa-let-7c	1.0	1
LPS	hsa-let-7c	0.6	0.142
RT 001	hsa-let-7c	1.3	0.303
CTL	hsa-let-7d	1.0	1
LPS	hsa-let-7d	1.1	0.956

RT 001	hsa-let-7d	1.1	0.799
CTL	hsa-let-7e	1.0	1
LPS	hsa-let-7e	0.7	0.279
RT 001	hsa-let-7e	0.7	0.432
CTL	hsa-let-7e#	1.0	1
LPS	hsa-let-7e#	1.2	0.533
RT 001	hsa-let-7e#	0.9	0.895
CTL	hsa-miR-100	1.0	1
LPS	hsa-miR-100	0.8	0.621
RT 001	hsa-miR-100	0.5	0.161
CTL	hsa-miR-103	1.0	1
LPS	hsa-miR-103	0.7	0.309
RT 001	hsa-miR-103	0.6	0.254
CTL	hsa-miR-106a	1.0	1
LPS	hsa-miR-106a	0.9	0.516
RT 001	hsa-miR-106a	1.2	0.634
CTL	hsa-miR-106b	1.0	1
LPS	hsa-miR-106b	0.7	0.306
RT 001	hsa-miR-106b	1.0	0.713
CTL	hsa-miR-107	1.0	1
LPS	hsa-miR-107	0.4	0.167
RT 001	hsa-miR-107	1.0	0.765
CTL	hsa-miR-10a	1.0	1
LPS	hsa-miR-10a	0.8	0.457
RT 001	hsa-miR-10a	0.4	0.405
CTL	hsa-miR-10a#	1.0	1
LPS	hsa-miR-10a#	0.8	0.306
RT 001	hsa-miR-10a#	1.1	0.689
CTL	hsa-miR-10b	1.0	1
LPS	hsa-miR-10b	0.5	0.153
RT 001	hsa-miR-10b	0.8	0.468
CTL	hsa-miR-10b#	1.0	1
LPS	hsa-miR-10b#	1.9	0.263
RT 001	hsa-miR-10b#	1.5	0.237

CTL	hsa-miR-1180	1.0	1
LPS	hsa-miR-1180	0.9	0.311
RT 001	hsa-miR-1180	1.0	0.824
CTL	hsa-miR-1201	1.0	1
LPS	hsa-miR-1201	0.8	0.685
RT 001	hsa-miR-1201	1.1	0.453
CTL	hsa-miR-1208	1.0	1
LPS	hsa-miR-1208	0.6	0.091
RT 001	hsa-miR-1208	0.6	0.098
CTL	hsa-miR-1225-3p	1.0	1
LPS	hsa-miR-1225-3p	0.3	0.133
RT 001	hsa-miR-1225-3p	0.3	0.199
CTL	hsa-miR-1226#	1.0	1
LPS	hsa-miR-1226#	1.1	0.782
RT 001	hsa-miR-1226#	1.2	0.443
CTL	hsa-miR-1227	1.0	1
LPS	hsa-miR-1227	0.7	0.308
RT 001	hsa-miR-1227	1.0	0.784
CTL	hsa-miR-1233	1.0	1
LPS	hsa-miR-1233	0.7	0.741
RT 001	hsa-miR-1233	1.3	0.282
CTL	hsa-miR-1243	1.0	1
LPS	hsa-miR-1243	1.0	0.93
RT 001	hsa-miR-1243	0.4	0.144
CTL	hsa-miR-1248	1.0	1
LPS	hsa-miR-1248	1.1	0.703
RT 001	hsa-miR-1248	1.3	0.315
CTL	hsa-miR-1254	1.0	1
LPS	hsa-miR-1254	0.9	0.624
RT 001	hsa-miR-1254	1.0	0.912
CTL	hsa-miR-1255a	1.0	1
LPS	hsa-miR-1255a	1.2	0.968
RT 001	hsa-miR-1255a	0.9	0.621
CTL	hsa-miR-1255b	1.0	1

LPS	hsa-miR-1255b	0.7	0.357
RT 001	hsa-miR-1255b	0.5	0.225
CTL	hsa-miR-125a-3p	1.0	1
LPS	hsa-miR-125a-3p	0.5	0.385
RT 001	hsa-miR-125a-3p	1.1	0.89
CTL	hsa-miR-125b	1.0	1
LPS	hsa-miR-125b	0.5	0.233
RT 001	hsa-miR-125b	0.6	0.439
CTL	hsa-miR-126	1.0	1
LPS	hsa-miR-126	0.7	0.49
RT 001	hsa-miR-126	0.8	0.421
CTL	hsa-miR-126#	1.0	1
LPS	hsa-miR-126#	0.7	0.367
RT 001	hsa-miR-126#	1.5	0.3
CTL	hsa-miR-1260	1.0	1
LPS	hsa-miR-1260	1.2	0.449
RT 001	hsa-miR-1260	0.8	0.266
CTL	hsa-miR-1262	1.0	1
LPS	hsa-miR-1262	1.2	0.913
RT 001	hsa-miR-1262	1.1	0.891
CTL	hsa-miR-1269	1.0	1
LPS	hsa-miR-1269	0.7	0.314
RT 001	hsa-miR-1269	1.0	0.976
CTL	hsa-miR-1271	1.0	1
LPS	hsa-miR-1271	0.3	0.169
RT 001	hsa-miR-1271	1.0	0.877
CTL	hsa-miR-1274a	1.0	1
LPS	hsa-miR-1274a	1.2	0.191
RT 001	hsa-miR-1274a	1.1	0.338
CTL	hsa-miR-1274b	1.0	1
LPS	hsa-miR-1274b	1.2	0.714
RT 001	hsa-miR-1274b	1.1	0.997
CTL	hsa-miR-1275	1.0	1
LPS	hsa-miR-1275	0.6	0.197

RT 001	hsa-miR-1275	0.6	0.157
CTL	hsa-miR-1276	1.0	1
LPS	hsa-miR-1276	1.2	0.69
RT 001	hsa-miR-1276	2.0	0.149
CTL	hsa-miR-1282	1.0	1
LPS	hsa-miR-1282	0.9	0.599
RT 001	hsa-miR-1282	1.1	0.997
CTL	hsa-miR-1285	1.0	1
LPS	hsa-miR-1285	0.2	0.065
RT 001	hsa-miR-1285	0.9	0.887
CTL	hsa-miR-128a	1.0	1
LPS	hsa-miR-128a	0.6	0.084
RT 001	hsa-miR-128a	0.9	0.788
CTL	hsa-miR-1290	1.0	1
LPS	hsa-miR-1290	1.1	0.64
RT 001	hsa-miR-1290	0.9	0.832
CTL	hsa-miR-1291	1.0	1
LPS	hsa-miR-1291	1.3	0.305
RT 001	hsa-miR-1291	0.7	0.258
CTL	hsa-miR-1292	1.0	1
LPS	hsa-miR-1292	1.13	0.330
RT 001	hsa-miR-1292	1.4	0.03
CTL	hsa-miR-1293	1.0	1
LPS	hsa-miR-1293	1.17	0.413
RT 001	hsa-miR-1293	0.20	0.002
CTL	hsa-miR-1296	1.0	1
LPS	hsa-miR-1296	1.1	0.866
RT 001	hsa-miR-1296	1.1	0.68
CTL	hsa-miR-1303	1.0	1
LPS	hsa-miR-1303	0.7	0.343
RT 001	hsa-miR-1303	1.0	0.793
CTL	hsa-miR-130b	1.0	1
LPS	hsa-miR-130b	0.8	0.531
RT 001	hsa-miR-130b	1.1	0.735

CTL	hsa-miR-130b#	1.0	1
LPS	hsa-miR-130b#	0.8	0.51
RT 001	hsa-miR-130b#	0.7	0.31
CTL	hsa-miR-132	1.0	1
LPS	hsa-miR-132	1.0	0.902
RT 001	hsa-miR-132	0.9	0.673
CTL	hsa-miR-132#	1.0	1
LPS	hsa-miR-132#	1.2	0.848
RT 001	hsa-miR-132#	1.0	0.896
CTL	hsa-miR-144#	1.0	1
LPS	hsa-miR-144#	0.8	0.522
RT 001	hsa-miR-144#	1.0	0.672
CTL	hsa-miR-145	1.0	1
LPS	hsa-miR-145	1.3	0.182
RT 001	hsa-miR-145	0.5	0.268
CTL	hsa-miR-146b	1.0	1
LPS	hsa-miR-146b	0.6	0.34
RT 001	hsa-miR-146b	0.2	0.092
CTL	hsa-miR-148a	1.0	1
LPS	hsa-miR-148a	1.6	0.54
RT 001	hsa-miR-148a	0.9	0.709
CTL	hsa-miR-148a#	1.0	1
LPS	hsa-miR-148a#	0.5	0.065
RT 001	hsa-miR-148a#	0.7	0.176
CTL	hsa-miR-148b	1.0	1
LPS	hsa-miR-148b	1.61	0.416
RT 001	hsa-miR-148b	4.0	0.009
CTL	hsa-miR-148b#	1.0	1
LPS	hsa-miR-148b#	1.4	0.212
RT 001	hsa-miR-148b#	1.0	0.935
CTL	hsa-miR-149	1.0	1
LPS	hsa-miR-149	1.1	0.61
RT 001	hsa-miR-149	1.3	0.282
CTL	hsa-miR-151-3p	1.0	1

LPS	hsa-miR-151-3p	1.5	0.716
RT 001	hsa-miR-151-3p	0.3	0.214
CTL	hsa-miR-151-5p	1.0	1
LPS	hsa-miR-151-5p	0.9	0.948
RT 001	hsa-miR-151-5p	1.7	0.794
CTL	hsa-miR-152	1.0	1
LPS	hsa-miR-152	1.53	0.818
RT 001	hsa-miR-152	2.46	0.05
CTL	hsa-miR-155	1.0	1
LPS	hsa-miR-155	1.0	0.133
RT 001	hsa-miR-155	1.0	0.202
CTL	hsa-miR-15a	1.0	1
LPS	hsa-miR-15a#	1.0	0.876
RT 001	hsa-miR-15a#	0.8	0.333
CTL	hsa-miR-15b	1.0	1
LPS	hsa-miR-15b	0.7	0.075
RT 001	hsa-miR-15b	0.9	0.496
CTL	hsa-miR-16	1.0	1
LPS	hsa-miR-16	0.7	0.353
RT 001	hsa-miR-16	0.8	0.527
CTL	hsa-miR-16-1#	1.0	1
LPS	hsa-miR-16-1#	1.1	0.564
RT 001	hsa-miR-16-1#	0.9	0.614
CTL	hsa-miR-17	1.0	1
LPS	hsa-miR-17	0.6	0.282
RT 001	hsa-miR-17	0.7	0.368
CTL	hsa-miR-17#	1.0	1
LPS	hsa-miR-17#	1.2	0.747
RT 001	hsa-miR-17#	1.5	0.308
CTL	hsa-miR-181a	1.0	1
LPS	hsa-miR-181a	1.1	0.308
RT 001	hsa-miR-181a	0.6	0.096
CTL	hsa-miR-181a-2#	1.0	1
LPS	hsa-miR-181a-2#	0.8	0.795

RT 001	hsa-miR-181a-2#	0.9	0.775
CTL	hsa-miR-182	1.0	1
LPS	hsa-miR-182	0.9	0.42
RT 001	hsa-miR-182	1.2	0.852
CTL	hsa-miR-1825	1.0	1
LPS	hsa-miR-1825	3.1	0.419
RT 001	hsa-miR-1825	0.9	0.992
CTL	hsa-miR-183	1.0	1
LPS	hsa-miR-183	1.7	0.85
RT 001	hsa-miR-183	0.7	0.193
CTL	hsa-miR-183#	1.0	1
LPS	hsa-miR-183#	1.0	0.82
RT 001	hsa-miR-183#	1.1	0.651
CTL	hsa-miR-186	1.0	1
LPS	hsa-miR-186	0.9	0.413
RT 001	hsa-miR-186	1.4	0.153
CTL	hsa-miR-18a	1.0	1
LPS	hsa-miR-18a	0.6	0.23
RT 001	hsa-miR-18a	0.9	0.812
CTL	hsa-miR-18a#	1.0	1
LPS	hsa-miR-18a#	0.9	0.47
RT 001	hsa-miR-18a#	1.3	0.237
CTL	hsa-miR-18b	1.0	1
LPS	hsa-miR-18b	0.3	0.08
RT 001	hsa-miR-18b	1.5	0.263
CTL	hsa-miR-190b	1.0	1
LPS	hsa-miR-190b	1.2	0.563
RT 001	hsa-miR-190b	2.2	0.210
CTL	hsa-miR-191	1.0	1
LPS	hsa-miR-191	0.7	0.736
RT 001	hsa-miR-191	0.6	0.105
CTL	hsa-miR-191#	1.0	1
LPS	hsa-miR-191#	0.9	0.897
RT 001	hsa-miR-191#	1.2	0.838

CTL	hsa-miR-192	1.0	1
LPS	hsa-miR-192	1.0	0.745
RT 001	hsa-miR-192	0.7	0.22
CTL	hsa-miR-192#	1.0	1
LPS	hsa-miR-192#	0.8	0.347
RT 001	hsa-miR-192#	1.2	0.377
CTL	hsa-miR-193a-3p	1.0	1
LPS	hsa-miR-193a-3p	0.2	0.613
RT 001	hsa-miR-193a-3p	0.6	0.13
CTL	hsa-miR-193a-5p	1.0	1
LPS	hsa-miR-193a-5p	1.2	0.832
RT 001	hsa-miR-193a-5p	0.7	0.413
CTL	hsa-miR-193b	1.0	1
LPS	hsa-miR-193b	0.7	0.287
RT 001	hsa-miR-193b	0.6	0.217
CTL	hsa-miR-193b#	1.0	1
LPS	hsa-miR-193b#	1.0	0.818
RT 001	hsa-miR-193b#	1.6	0.292
CTL	hsa-miR-194	1.0	1
LPS	hsa-miR-194	0.6	0.645
RT 001	hsa-miR-194	1.4	0.332
CTL	hsa-miR-196b	1.0	1
LPS	hsa-miR-196b	0.4	0.055
RT 001	hsa-miR-196b	1.0	0.843
CTL	hsa-miR-197	1.0	1
LPS	hsa-miR-197	0.7	0.097
RT 001	hsa-miR-197	0.7	0.141
CTL	hsa-miR-199a	1.0	1
LPS	hsa-miR-199a	1.3	0.417
RT 001	hsa-miR-199a	2.6	0.177
CTL	hsa-miR-19a	1.0	1
LPS	hsa-miR-19a	1.9	0.596
RT 001	hsa-miR-19a	1.1	0.692
CTL	hsa-miR-19a#	1.0	1

LPS	hsa-miR-19a#	6.0	0.114
RT 001	hsa-miR-19a#	2.1	0.253
CTL	hsa-miR-19b	1.0	1
LPS	hsa-miR-19b	1.0	0.927
RT 001	hsa-miR-19b	0.7	0.281
CTL	hsa-miR-19b-1#	1.0	1
LPS	hsa-miR-19b-1#	0.1	0.266
RT 001	hsa-miR-19b-1#	0.8	0.511
CTL	hsa-miR-200c	1.0	1
LPS	hsa-miR-200c	1.1	0.785
RT 001	hsa-miR-200c	0.9	0.813
CTL	hsa-miR-20a	1.0	1
LPS	hsa-miR-20a	0.6	0.716
RT 001	hsa-miR-20a	2.0	0.423
CTL	hsa-miR-20a#	1.0	1
LPS	hsa-miR-20a#	0.7	0.305
RT 001	hsa-miR-20a#	0.8	0.337
CTL	hsa-miR-20b	1.0	1
LPS	hsa-miR-20b	0.8	0.713
RT 001	hsa-miR-20b	0.9	0.816
CTL	hsa-miR-21	1.0	1
LPS	hsa-miR-21	0.3	0.205
RT 001	hsa-miR-21	0.5	0.259
CTL	hsa-miR-21#	1.0	1
LPS	hsa-miR-21#	0.3	0.504
RT 001	hsa-miR-21#	0.9	0.521
CTL	hsa-miR-210	1.0	1
LPS	hsa-miR-210	0.3	0.104
RT 001	hsa-miR-210	0.7	0.157
CTL	hsa-miR-213	1.0	1
LPS	hsa-miR-213	0.8	0.456
RT 001	hsa-miR-213	0.8	0.306
CTL	hsa-miR-215	1.0	1
LPS	hsa-miR-215	1.7	0.923

RT 001	hsa-miR-215	2.0	0.048
CTL	hsa-miR-218	1.0	1
LPS	hsa-miR-218	0.9	0.3
RT 001	hsa-miR-218	1.1	0.657
CTL	hsa-miR-22#	1.0	1
LPS	hsa-miR-22#	0.7	0.468
RT 001	hsa-miR-22#	1.0	0.976
CTL	hsa-miR-221	1.0	1
LPS	hsa-miR-221	0.7	0.285
RT 001	hsa-miR-221	0.8	0.553
CTL	hsa-miR-222	1.0	1
LPS	hsa-miR-222	1.0	0.834
RT 001	hsa-miR-222	0.9	0.913
CTL	hsa-miR-222#	1.0	1
LPS	hsa-miR-222#	0.9	0.737
RT 001	hsa-miR-222#	1.4	0.67
CTL	hsa-miR-23b	1.0	1
LPS	hsa-miR-23b	0.5	0.589
RT 001	hsa-miR-23b	0.8	0.503
CTL	hsa-miR-24	1.0	1
LPS	hsa-miR-24	1.53	0.876
RT 001	hsa-miR-24	1.4	0.023
CTL	hsa-miR-24-2#	1.0	1
LPS	hsa-miR-24-2#	1.0	0.861
RT 001	hsa-miR-24-2#	2.3	0.199
CTL	hsa-miR-25	1.0	1
LPS	hsa-miR-25	0.5	0.072
RT 001	hsa-miR-25	0.6	0.12
CTL	hsa-miR-25#	1.0	1
LPS	hsa-miR-25#	0.9	0.696
RT 001	hsa-miR-25#	1.0	0.813
CTL	hsa-miR-26a	1.0	1
LPS	hsa-miR-26a	1.1	0.3
RT 001	hsa-miR-26a	1.2	0.521

CTL	hsa-miR-26a-1#	1.0	1
LPS	hsa-miR-26a-1#	1.2	0.521
RT 001	hsa-miR-26a-1#	0.8	0.313
CTL	hsa-miR-26a-2#	1.0	1
LPS	hsa-miR-26a-2#	0.7	0.685
RT 001	hsa-miR-26a-2#	1.2	0.811
CTL	hsa-miR-26b	1.0	1
LPS	hsa-miR-26b	0.7	0.305
RT 001	hsa-miR-26b	0.6	0.19
CTL	hsa-miR-26b#	1.0	1
LPS	hsa-miR-26b#	1.2	0.552
RT 001	hsa-miR-26b#	0.9	0.786
CTL	hsa-miR-27a	1.0	1
LPS	hsa-miR-27a	0.5	0.226
RT 001	hsa-miR-27a	0.9	0.725
CTL	hsa-miR-27a#	1.0	1
LPS	hsa-miR-27a#	1.3	0.151
RT 001	hsa-miR-27a#	1.1	0.823
CTL	hsa-miR-27b	1.0	1
LPS	hsa-miR-27b	0.6	0.052
RT 001	hsa-miR-27b	0.9	0.636
CTL	hsa-miR-27b#	1.0	1
LPS	hsa-miR-27b#	1.7	0.3
RT 001	hsa-miR-27b#	0.9	0.647
CTL	hsa-miR-28	1.0	1
LPS	hsa-miR-28	0.5	0.055
RT 001	hsa-miR-28	0.5	0.059
CTL	hsa-miR-28-3p	1.0	1
LPS	hsa-miR-28-3p	1.1	0.868
RT 001	hsa-miR-28-3p	0.9	0.73
CTL	hsa-miR-29a	1.0	1
LPS	hsa-miR-29a	0.8	0.979
RT 001	hsa-miR-29a	0.7	0.285
CTL	hsa-miR-29a#	1.0	1

LPS	hsa-miR-29a#	0.6	0.346
RT 001	hsa-miR-29a#	0.9	0.746
CTL	hsa-miR-29b	1.0	1
LPS	hsa-miR-29b	1.3	0.3
RT 001	hsa-miR-29b	2.2	0.49
CTL	hsa-miR-29b-1#	1.0	1
LPS	hsa-miR-29b-1#	0.3	0.218
RT 001	hsa-miR-29b-1#	0.8	0.3
CTL	hsa-miR-29b-2#	1.0	1
LPS	hsa-miR-29b-2#	1.2	0.547
RT 001	hsa-miR-29b-2#	1.4	0.451
CTL	hsa-miR-29c	1.0	1
LPS	hsa-miR-29c	0.4	0.3
RT 001	hsa-miR-29c	2.1	0.145
CTL	hsa-miR-301	1.0	1
LPS	hsa-miR-301	1.4	0.926
RT 001	hsa-miR-301	0.4	0.129
CTL	hsa-miR-301b	1.0	1
LPS	hsa-miR-301b	0.4	0.138
RT 001	hsa-miR-301b	0.6	0.297
CTL	hsa-miR-302a	1.0	1
LPS	hsa-miR-302a	0.1	0.207
RT 001	hsa-miR-302a	0.0	0.191
CTL	hsa-miR-302c	1.0	1
LPS	hsa-miR-302c	2.68	0.028
RT 001	hsa-miR-302c	1.53	0.139
CTL	hsa-miR-30a-3p	1.0	1
LPS	hsa-miR-30a-3p	0.8	0.3
RT 001	hsa-miR-30a-3p	1.2	0.488
CTL	hsa-miR-30a-5p	1.0	1
LPS	hsa-miR-30a-5p	0.7	0.321
RT 001	hsa-miR-30a-5p	0.9	0.817
CTL	hsa-miR-30b	1.0	1
LPS	hsa-miR-30b	1.0	0.926

RT 001	hsa-miR-30b	0.8	0.25
CTL	hsa-miR-30c	1.0	1
LPS	hsa-miR-30c	0.6	0.082
RT 001	hsa-miR-30c	0.7	0.188
CTL	hsa-miR-30d	1.0	1
LPS	hsa-miR-30d	1.3	0.926
RT 001	hsa-miR-30d	1.3	0.323
CTL	hsa-miR-30d#	1.0	1
LPS	hsa-miR-30d#	0.6	0.319
RT 001	hsa-miR-30d#	0.9	0.727
CTL	hsa-miR-30e-3p	1.0	1
LPS	hsa-miR-30e-3p	0.8	0.236
RT 001	hsa-miR-30e-3p	1.2	0.216
CTL	hsa-miR-31	1.0	1
LPS	hsa-miR-31	0.8	0.926
RT 001	hsa-miR-31	0.8	0.161
CTL	hsa-miR-31#	1.0	1
LPS	hsa-miR-31#	0.8	0.405
RT 001	hsa-miR-31#	0.8	0.321
CTL	hsa-miR-320	1.0	1
LPS	hsa-miR-320	0.8	0.245
RT 001	hsa-miR-320	1.1	0.626
CTL	hsa-miR-320b	1.0	1
LPS	hsa-miR-320b	0.6	0.254
RT 001	hsa-miR-320b	0.6	0.301
CTL	hsa-miR-324-3p	1.0	1
LPS	hsa-miR-324-3p	0.9	0.913
RT 001	hsa-miR-324-3p	1.1	0.71
CTL	hsa-miR-324-5p	1.0	1
LPS	hsa-miR-324-5p	0.6	0.137
RT 001	hsa-miR-324-5p	0.9	0.713
CTL	hsa-miR-328	1.0	1
LPS	hsa-miR-328	0.7	0.243
RT 001	hsa-miR-328	0.8	0.16

CTL	hsa-miR-335#	1.0	1
LPS	hsa-miR-335#	4.1	0.241
RT 001	hsa-miR-335#	7.8	0.103
CTL	hsa-miR-338-5p	1.0	1
LPS	hsa-miR-338-5p	1.0	0.783
RT 001	hsa-miR-338-5p	1.8	0.26
CTL	hsa-miR-339-3p	1.0	1
LPS	hsa-miR-339-3p	0.9	0.962
RT 001	hsa-miR-339-3p	1.0	0.996
CTL	hsa-miR-339-5p	1.0	1
LPS	hsa-miR-339-5p	3.3	0.86
RT 001	hsa-miR-339-5p	5.0	0.006
CTL	hsa-miR-33a	1.0	1
LPS	hsa-miR-33a	10.7	0.310
RT 001	hsa-miR-33a	0.2	0.248
CTL	hsa-miR-340	1.0	1
LPS	hsa-miR-340	0.3	0.180
RT 001	hsa-miR-340	0.4	0.052
CTL	hsa-miR-340#	1.0	1
LPS	hsa-miR-340#	1.3	0.252
RT 001	hsa-miR-340#	1.2	0.328
CTL	hsa-miR-342-3p	1.0	1
LPS	hsa-miR-342-3p	0.7	0.091
RT 001	hsa-miR-342-3p	0.8	0.203
CTL	hsa-miR-345	1.0	1
LPS	hsa-miR-345	1.2	0.585
RT 001	hsa-miR-345	1.1	0.795
CTL	hsa-miR-34a	1.0	1
LPS	hsa-miR-34a	0.4	0.12
RT 001	hsa-miR-34a	0.6	0.193
CTL	hsa-miR-34a#	1.0	1
LPS	hsa-miR-34a#	1.2	0.595
RT 001	hsa-miR-34a#	0.8	0.571
CTL	hsa-miR-34b	1.0	1

LPS	hsa-miR-34b	0.2	0.178
RT 001	hsa-miR-34b	0.5	0.388
CTL	hsa-miR-34c	1.0	1
LPS	hsa-miR-34c	1.2	0.938
RT 001	hsa-miR-34c	1.5	0.851
CTL	hsa-miR-365	1.0	1
LPS	hsa-miR-365	0.5	0.073
RT 001	hsa-miR-365	0.8	0.526
CTL	hsa-miR-374	1.0	1
LPS	hsa-miR-374	2.0	0.03
RT 001	hsa-miR-374	2.9	0.05
CTL	hsa-miR-374b#	1.0	1
LPS	hsa-miR-374b#	1.7	0.545
RT 001	hsa-miR-374b#	0.9	0.656
CTL	hsa-miR-375	1.0	1
LPS	hsa-miR-375	0.6	0.173
RT 001	hsa-miR-375	0.5	0.213
CTL	hsa-miR-378	1.0	1
LPS	hsa-miR-378	3.0	0.938
RT 001	hsa-miR-378	0.5	0.353
CTL	hsa-miR-383	1.0	1
LPS	hsa-miR-383	0.8	0.355
RT 001	hsa-miR-383	0.9	0.638
CTL	hsa-miR-409-3p	1.0	1
LPS	hsa-miR-409-3p	1.8	0.208
RT 001	hsa-miR-409-3p	4.6	0.938
CTL	hsa-miR-422a	1.0	1
LPS	hsa-miR-422a	0.69	0.08
RT 001	hsa-miR-422a	0.2	0.010
CTL	hsa-miR-423-5p	1.0	1
LPS	hsa-miR-423-5p	0.8	0.406
RT 001	hsa-miR-423-5p	0.7	0.201
CTL	hsa-miR-424#	1.0	1
LPS	hsa-miR-424#	1.0	0.895

RT 001	hsa-miR-424#	1.1	0.651
CTL	hsa-miR-425#	1.0	1
LPS	hsa-miR-425#	0.8	0.338
RT 001	hsa-miR-425#	1.0	0.904
CTL	hsa-miR-425-5p	1.0	1
LPS	hsa-miR-425-5p	0.8	0.571
RT 001	hsa-miR-425-5p	0.8	0.341
CTL	hsa-miR-432#	1.0	1
LPS	hsa-miR-432#	0.95	0.818
RT 001	hsa-miR-432#	2.27	0.043
CTL	hsa-miR-454	1.0	1
LPS	hsa-miR-454	1.2	0.975
RT 001	hsa-miR-454	0.2	0.092
CTL	hsa-miR-454#	1.0	1
LPS	hsa-miR-454#	1.2	0.588
RT 001	hsa-miR-454#	1.1	0.68
CTL	hsa-miR-484	1.0	1
LPS	hsa-miR-484	0.8	0.248
RT 001	hsa-miR-484	0.8	0.395
CTL	hsa-miR-497	1.0	1
LPS	hsa-miR-497	0.8	0.975
RT 001	hsa-miR-497	0.8	0.445
CTL	hsa-miR-500	1.0	1
LPS	hsa-miR-500	0.9	0.697
RT 001	hsa-miR-500	0.7	0.454
CTL	hsa-miR-501	1.0	1
LPS	hsa-miR-501	1.2	0.937
RT 001	hsa-miR-501	0.9	0.645
CTL	hsa-miR-502-3p	1.0	1
LPS	hsa-miR-502-3p	0.6	0.502
RT 001	hsa-miR-502-3p	0.5	0.394
CTL	hsa-miR-505#	1.0	1
LPS	hsa-miR-505#	0.9	0.531
RT 001	hsa-miR-505#	1.0	0.977

CTL	hsa-miR-516-3p	1.0	1
LPS	hsa-miR-516-3p	32.4	0.937
RT 001	hsa-miR-516-3p	1.0	0.773
CTL	hsa-miR-517b	1.0	1
LPS	hsa-miR-517b	0.4	0.937
RT 001	hsa-miR-517b	0.5	0.056
CTL	hsa-miR-518f	1.0	1
LPS	hsa-miR-518f	3.9	0.937
RT 001	hsa-miR-518f	1.3	0.807
CTL	hsa-miR-520c-3p	1.0	1
LPS	hsa-miR-520c-3p	0.9	0.902
RT 001	hsa-miR-520c-3p	1.0	0.75
CTL	hsa-miR-520d-3p	1.0	1
LPS	hsa-miR-520d-3p	4.6	0.937
RT 001	hsa-miR-520d-3p	1.2	0.61
CTL	hsa-miR-532	1.0	1
LPS	hsa-miR-532	0.8	0.734
RT 001	hsa-miR-532	0.9	0.497
CTL	hsa-miR-532-3p	1.0	1
LPS	hsa-miR-532-3p	0.5	0.288
RT 001	hsa-miR-532-3p	0.6	0.338
CTL	hsa-miR-543	1.0	1
LPS	hsa-miR-543	2.6	0.010
RT 001	hsa-miR-543	2.1	0.937
CTL	hsa-miR-545#	1.0	1
LPS	hsa-miR-545#	3.5	0.231
RT 001	hsa-miR-545#	0.8	0.532
CTL	hsa-miR-548H	1.0	1
LPS	hsa-miR-548H	1.2	0.426
RT 001	hsa-miR-548H	0.8	0.691
CTL	hsa-miR-548J	1.0	1
LPS	hsa-miR-548J	1.4	0.937
RT 001	hsa-miR-548J	2.6	0.077
CTL	hsa-miR-548K	1.0	1

LPS	hsa-miR-548K	0.9	0.937
RT 001	hsa-miR-548K	1.5	0.418
CTL	hsa-miR-548L	1.0	1
LPS	hsa-miR-548L	1.2	0.937
RT 001	hsa-miR-548L	0.4	0.056
CTL	hsa-miR-550	1.0	1
LPS	hsa-miR-550	0.9	0.912
RT 001	hsa-miR-550	1.4	0.021
CTL	hsa-miR-551b#	1.0	1
LPS	hsa-miR-551b#	0.8	0.295
RT 001	hsa-miR-551b#	1.0	0.811
CTL	hsa-miR-572	1.0	1
LPS	hsa-miR-572	2.3	0.190
RT 001	hsa-miR-572	2.1	0.141
CTL	hsa-miR-574-3p	1.0	1
LPS	hsa-miR-574-3p	0.8	0.937
RT 001	hsa-miR-574-3p	0.8	0.114
CTL	hsa-miR-577	1.0	1
LPS	hsa-miR-577	0.7	0.235
RT 001	hsa-miR-577	0.9	0.657
CTL	hsa-miR-580	1.0	1
LPS	hsa-miR-580	0.7	0.156
RT 001	hsa-miR-580	0.6	0.168
CTL	hsa-miR-586	1.0	1
LPS	hsa-miR-586	0.6	0.037
RT 001	hsa-miR-586	0.6	0.143
CTL	hsa-miR-589	1.0	1
LPS	hsa-miR-589	1.9	0.255
RT 001	hsa-miR-589	1.0	0.845
CTL	hsa-miR-590-3p	1.0	1
LPS	hsa-miR-590-3p	0.6	0.128
RT 001	hsa-miR-590-3p	1.2	0.545
CTL	hsa-miR-590-5p	1.0	1
LPS	hsa-miR-590-5p	2.5	0.937

RT 001	hsa-miR-590-5p	2.0	0.015
CTL	hsa-miR-592	1.0	1
LPS	hsa-miR-592	0.9	0.798
RT 001	hsa-miR-592	0.9	0.8
CTL	hsa-miR-597	1.0	1
LPS	hsa-miR-597	0.7	0.179
RT 001	hsa-miR-597	0.9	0.876
CTL	hsa-miR-598	1.0	1
LPS	hsa-miR-598	0.7	0.057
RT 001	hsa-miR-598	0.7	0.056
CTL	hsa-miR-605	1.0	1
LPS	hsa-miR-605	0.7	0.937
RT 001	hsa-miR-605	0.5	0.078
CTL	hsa-miR-616	1.0	1
LPS	hsa-miR-616	0.8	0.391
RT 001	hsa-miR-616	1.1	0.452
CTL	hsa-miR-624	1.0	1
LPS	hsa-miR-624	0.7	0.291
RT 001	hsa-miR-624	0.4	0.178
CTL	hsa-miR-625#	1.0	1
LPS	hsa-miR-625#	0.8	0.294
RT 001	hsa-miR-625#	1.1	0.766
CTL	hsa-miR-628-3p	1.0	1
LPS	hsa-miR-628-3p	3.4	0.075
RT 001	hsa-miR-628-3p	0.7	0.515
CTL	hsa-miR-629	1.0	1
LPS	hsa-miR-629	0.6	0.578
RT 001	hsa-miR-629	1.2	0.488
CTL	hsa-miR-638	1.0	1
LPS	hsa-miR-638	0.5	0.098
RT 001	hsa-miR-638	1.0	0.775
CTL	hsa-miR-641	1.0	1
LPS	hsa-miR-641	0.9	0.685
RT 001	hsa-miR-641	1.2	0.613

CTL	hsa-miR-652	1.0	1
LPS	hsa-miR-652	0.8	0.937
RT 001	hsa-miR-652	1.1	0.917
CTL	hsa-miR-660	1.0	1
LPS	hsa-miR-660	0.9	0.937
RT 001	hsa-miR-660	0.9	0.956
CTL	hsa-miR-664	1.0	1
LPS	hsa-miR-664	1.2	0.513
RT 001	hsa-miR-664	1.1	0.348
CTL	hsa-miR-708	1.0	1
LPS	hsa-miR-708	0.4	0.937
RT 001	hsa-miR-708	0.8	0.394
CTL	hsa-miR-720	1.0	1
LPS	hsa-miR-720	1.3	0.214
RT 001	hsa-miR-720	1.1	0.591
CTL	hsa-miR-744	1.0	1
LPS	hsa-miR-744	0.8	0.937
RT 001	hsa-miR-744	0.8	0.187
CTL	hsa-miR-744#	1.0	1
LPS	hsa-miR-744#	0.7	0.188
RT 001	hsa-miR-744#	0.8	0.449
CTL	hsa-miR-766	1.0	1
LPS	hsa-miR-766	0.8	0.428
RT 001	hsa-miR-766	0.9	0.608
CTL	hsa-miR-769-3p	1.0	1
LPS	hsa-miR-769-3p	0.9	0.796
RT 001	hsa-miR-769-3p	1.0	0.826
CTL	hsa-miR-769-5p	1.0	1
LPS	hsa-miR-769-5p	0.8	0.307
RT 001	hsa-miR-769-5p	0.9	0.614
CTL	hsa-miR-872	1.0	1
LPS	hsa-miR-872	0.3	0.457
RT 001	hsa-miR-872	0.7	0.487
CTL	hsa-miR-874	1.0	1

LPS	hsa-miR-874	0.71	0.432
RT 001	hsa-miR-874	0.58	0.032
CTL	hsa-miR-886-5p	1.0	1
LPS	hsa-miR-886-5p	0.9	0.937
RT 001	hsa-miR-886-5p	0.8	0.19
CTL	hsa-miR-891a	1.0	1
LPS	hsa-miR-891a	1.4	0.937
RT 001	hsa-miR-891a	0.7	0.451
CTL	hsa-miR-9#	1.0	1
LPS	hsa-miR-9#	0.8	0.455
RT 001	hsa-miR-9#	0.9	0.795
CTL	hsa-miR-92a	1.0	1
LPS	hsa-miR-92a	0.6	0.937
RT 001	hsa-miR-92a	0.6	0.119
CTL	hsa-miR-92a-1#	1.0	1
LPS	hsa-miR-92a-1#	1.3	0.165
RT 001	hsa-miR-92a-1#	1.1	0.424
CTL	hsa-miR-93#	1.0	1
LPS	hsa-miR-93#	1.3	0.416
RT 001	hsa-miR-93#	1.2	0.147
CTL	hsa-miR-935	1.0	1
LPS	hsa-miR-935	1.0	0.858
RT 001	hsa-miR-935	1.0	0.945
CTL	hsa-miR-938	1.0	1
LPS	hsa-miR-938	1.2	0.487
RT 001	hsa-miR-938	1.5	0.192
CTL	hsa-miR-942	1.0	1
LPS	hsa-miR-942	0.8	0.284
RT 001	hsa-miR-942	1.2	0.389
CTL	hsa-miR-99a	1.0	1
LPS	hsa-miR-99a	0.7	0.180
RT 001	hsa-miR-99a	1.5	0.053
CTL	hsa-miR-99b	1.0	1
LPS	hsa-miR-99b	0.3	0.351

RT 001	hsa-miR-99b	1.1	0.764
CTL	mmu-miR-129-3p	1.0	1
LPS	mmu-miR-129-3p	0.7	0.553
RT 001	mmu-miR-129-3p	0.3	0.302
CTL	mmu-miR-140	1.0	1
LPS	mmu-miR-140	1.0	0.937
RT 001	mmu-miR-140	0.8	0.497
CTL	rno-miR-29c#	1.0	1
LPS	rno-miR-29c#	1.0	0.883
RT 001	rno-miR-29c#	1.1	0.937
CTL	rno-miR-7#	1.0	1
LPS	rno-miR-7#	1.6	0.180
RT 001	rno-miR-7#	1.2	0.169
CTL	hsa-miR-1	1.0	1
LPS	hsa-miR-1	1.5	0.587
RT 001	hsa-miR-1	1.2	0.436

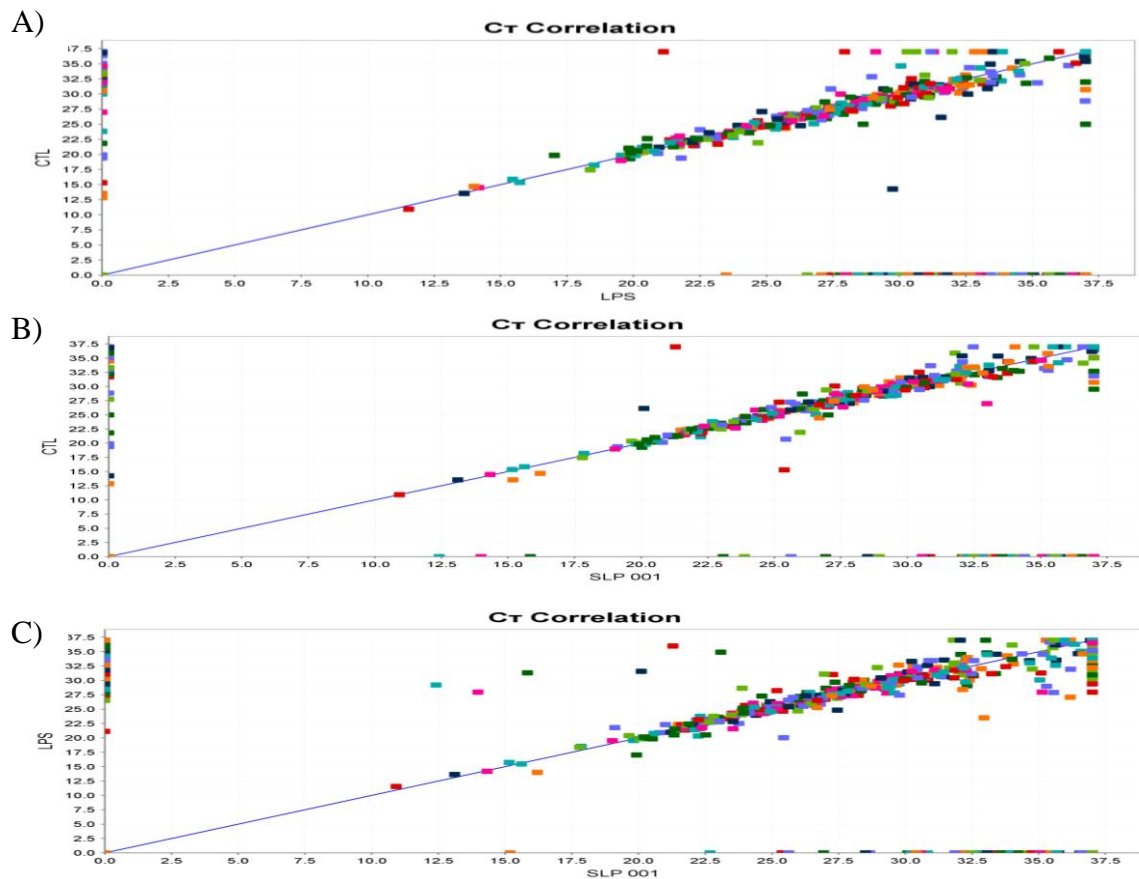


Figure 4.2.4. Ct Scatter plot shows there are differences in miRNA profiles between Hek TLR4/MD2/CD14 cells stimulated with LPS and SLPs from RT 001. Hek TLR4/MD2/CD14 cells from three biological replicates were plated at 2×10^6 cells/mL and allowed to adhere for 18 hours to approximately 60% confluency. Cells were stimulated with 100 ng/mL LPS or 20 μ g/mL SLPs from RT 001 for 8 hours. Cells were harvested and total RNA was extracted using miRVana™ miRNA isolation kit. 350 ng starting total RNA was converted to first strand cDNA using specific stem loop primers, the products of which were used in a pre-amplification PCR reaction. Samples were added to PCR reaction mixes and added to each well on Applied Biosystems® Taqman® Low Density Array (TLDA) Human miRNA cards, pool A and pool B. The cards were sealed and ran on the Applied Biosystems 7900HT Fast Real Time PCR Machine. The SDS files were exported and data from pool A and pool B cards analysed using ExpressionSuite software. The Ct scatter plot shows the relationship between **A)** CTL V's LPS **B)** CTL V's SLPs from RT 001 and **C)** LPS V's SLPs from RT 001 for all miRNAs in the profiling study.

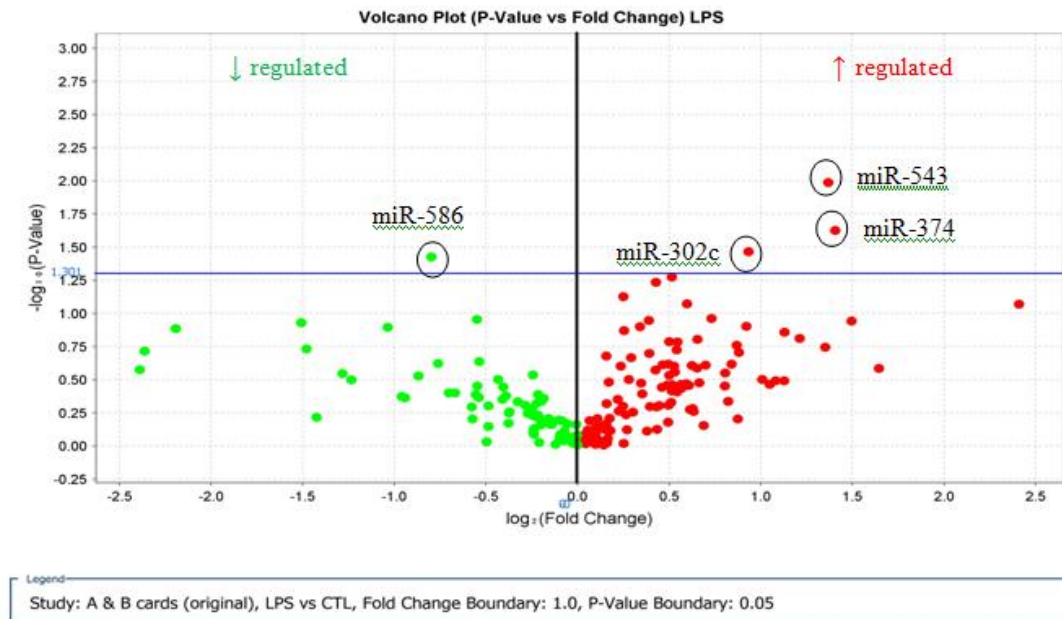


Figure 4.2.5. Volcano plot showing four miRNAs are significantly differentially regulated when Hek TLR4/MD2/CD14 cells were stimulated with LPS. Hek TLR4/MD2/CD14 cells from three biological replicates were plated at 2×10^6 cells/mL and allowed to adhere for 18 hours to approximately 60% confluency. Cells were stimulated with 100 ng/mL LPS for 8 hours. Cells were harvested and total RNA was extracted using miRvana™ miRNA isolation kit. 350 ng starting total RNA was converted to first strand cDNA, the products of which were used in a pre-amplification PCR reaction. Samples were added to PCR reaction mixes and added to each well on pool A and pool B TLDA human miRNA cards. The cards were sealed and ran on the Applied Biosystems 7900HT Fast Real Time PCR Machine. The SDS files were exported and data from pool A and pool B cards analysed using ExpressionSuite software v1.0.3. The max Ct was set to 37.0 with a threshold of 0.1 and the reference group was set to the control cell group. Global normalisation was carried and relative gene expression calculated. The Benjamini-Hochberg false discovery rate was used to adjust p-values and a student's t-test applied, values of $p \leq 0.05$ were considered statistically significant compared with the control group. The volcano plot displays $-\log_{10}$ p-value Vs \log_2 fold change. The p-value and fold change boundaries were set at 0.05 & 1.0. Targets above the horizontal line have statistically significant fold changes. The top left quadrant shows miRNAs targets that are down regulated while the top right quadrant shows miRNA targets that are up regulated.

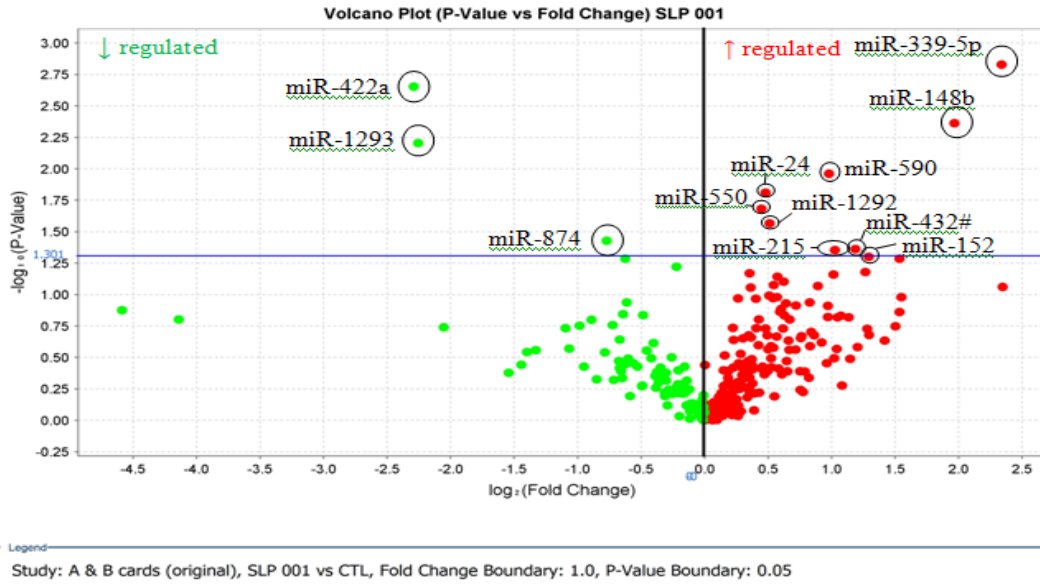


Figure 4.2.6. Volcano plot showing 12 miRNAs were significantly differentially regulated when Hek TLR4/MD2/CD14 cells were stimulated with SLPs from RT 001. Hek TLR4/MD2/CD14 cells from three biological replicates were plated at 2×10^6 cells/mL and allowed to adhere for 18 hours to approximately 60% confluency. Cells were stimulated with 20 $\mu\text{g}/\text{mL}$ SLPs from RT 001 for 8 hours. Cells were harvested and total RNA was extracted using miRVana™ miRNA isolation kit. 350 ng starting total RNA was converted to first strand cDNA, the products of which were used in a pre-amp PCR reaction. Samples were added to PCR reaction mixes and added to each well on pool A and pool B TLDA human miRNA cards. The cards were sealed and ran on the Applied Biosystems 7900HT Fast Real Time PCR Machine. The SDS files were exported and data from pool A and pool B cards analysed using ExpressionSuite software v1.0.3. The max Ct was set to 37.0 with a threshold of 0.1 and the reference group was set to the control cell group. Global normalisation was carried and relative gene expression calculated. The Benjamini-Hochberg false discovery rate was used to adjust p-values and a student's t-test applied, values of $p \leq 0.05$ were considered statistically significant compared with the control group. The volcano plot displays $-\log_{10}$ p-value Vs \log_2 fold change. The p-value and fold change boundaries were set at 0.05 & 1.0. Targets above the horizontal line have statistically significant fold changes. The top left quadrant shows miRNAs targets that are down regulated while the top right quadrant shows miRNA targets that are up regulated.

Table 4.2.2. Sixteen miRNAs have statistically significant fold changes when Hek TLR4/MD2/CD14 cells were stimulated with LPS and SLPs from RT 001.

Summary of statistically significant miRNAs from Hek TLR4/MD2/CD14 cells stimulated with either LPS or SLPs from RT 001, their relative gene expression and p-value. Data generated from pool A and pool B TLDA card analysis.

miRNA	RQ	p-value	Target
miR-1292	1.4	0.03	RT 001
miR-1293	0.2	0.002	RT 001
miR-148b	4.0	0.004	RT 001
miR-152	2.5	0.05	RT 001
miR-215	2.0	0.05	RT 001
miR-24	1.4	0.02	RT 001
miR-302c	2.7	0.03	LPS
miR-339	5.0	0.001	RT 001
miR-374a	1.9	0.03	LPS
miR-422	0.2	0.001	RT 001
miR-432#	2.3	0.04	RT 001
miR-543	2.6	0.01	LPS
miR-550	1.4	0.02	RT 001
miR-586	0.5	0.04	LPS
miR-590-5p	2.0	0.02	RT 001
miR-874	0.6	0.03	RT 001

Table 4.2.3. List of miRNAs to be included in custom TLDA cards based on a review of the literature and re-examination of the profiling study. We reviewed the literature and included miRNAs known to target; TLR receptors including TLR4, signalling proteins, transcription factors, cytokines and regulatory molecules. We also included miRNAs that are known to be induced by LPS and miRNAs induced during infections. We re-examined the profiling study to see if the miRNAs from the literature were present in the profiling study, most miRNAs were but just over the significance value.

MiRNA	Evidence from the literature	Present	Up or down regulation
let-7b	Barron, Sanchez, Kelly, & Clynes, 2011; Chen et al., 2005; Koh, Lee, Chang, & Nissom, 2009; Kumar, 2009; Oglesby, McElvaney, & Greene, 2010	Y	↑ LPS ↓ RT 001
let -7c	Kim, Gregersen, & Diamond, 2013; Li et al., 2009; Nelson et al., 2004	Y	↑ LPS ↑ RT 001
let-7d	Krichevsky, 2003; Li et al., 2009	Y	↑ RT 001
let-7e	Li et al., 2009; Virtue, Wang, & Yang, 2012; Wei et al., 2013	Y	↑ LPS ↑ RT 001
let-7e#	Li et al., 2009; Virtue, Wang, & Yang, 2012; Wei et al., 2013	Y	↑ LPS ↑ RT 001
miR-125a-5p	Roderburg et al., 2011	Y	↓ LPS ↑ RT 001
miR-132	Krichevsky, 2003; Nahid, Satoh, & Chan, 2011; O'Connell et al., 2007; Quinn & O'Neill, 2011; Taganov, Boldin, Chang, & Baltimore, 2006	Y	↑ LPS ↑ RT 001
miR-145	Bandrés et al., 2006; Quinn & O'Neill, 2011; Starczynowski et al., 2010	Y	↓ LPS ↑ RT 001
miR-146a	Nahid et al., 2011; Starczynowski et al., 2010; Taganov et al., 2006; Xie et al., 2013	N	N/A

miR-155	Ceppi et al., 2009; Dai et al., 2011; Kohlhaas et al., 2009; O'Connell, Taganov, Boldin, Cheng, & Baltimore, 2007; Quinn & O'Neill, 2011	Y	↑ LPS ↑ 001
miR-187	Rossato et al., 2012	N	N/A
miR-221	Wu et al., 2007	Y	↑ LPS ↓ RT 001
miR-221#	Wu et al., 2007	Y	↑ LPS ↑ RT 001
miR-9/#	Bazzoni et al., 2009	Y	↑ LPS ↑ RT 001

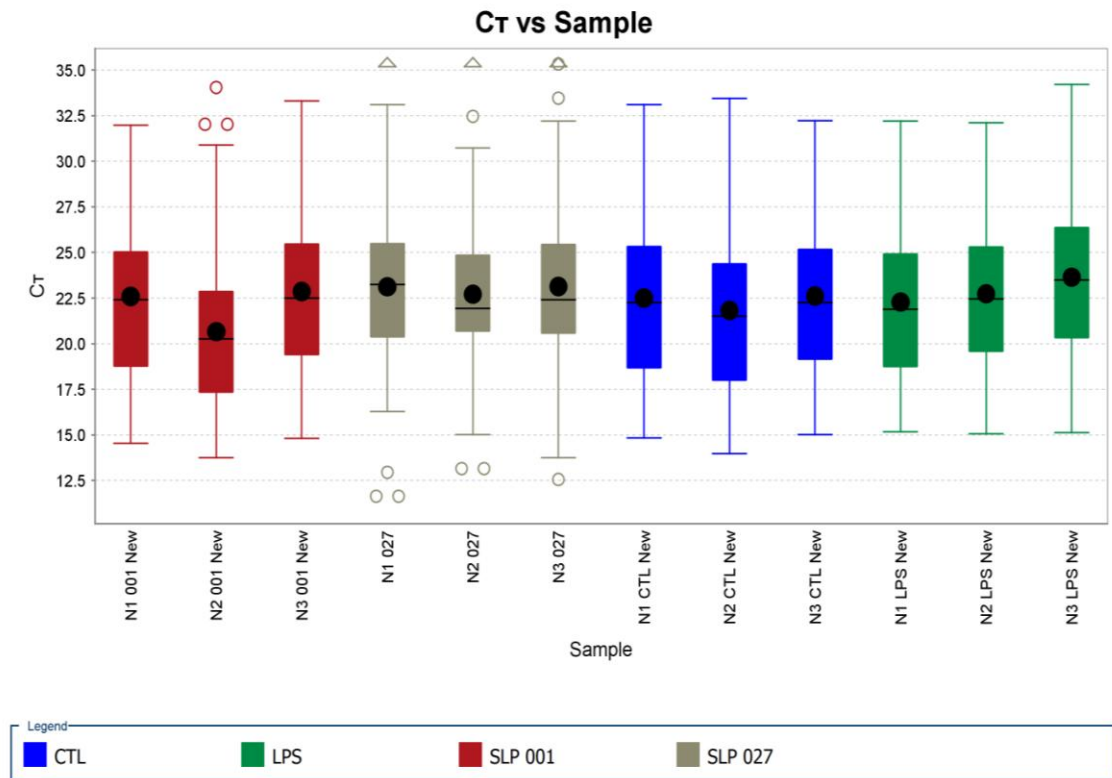


Figure 4.2.7 Overall Ct values follow normal distribution in miRNAs detected in custom TLDA cards. Hek TLR4/MD2/CD14 cells from three biological replicates were plated at 2×10^6 cells/mL and allowed to adhere for 18 hours to approximately 60% confluency. Cells were stimulated with 100 ng/mL LPS or 20 μ g/mL SLPs from RT 001 and RT 027 for 8 hours. Cells were harvested and total RNA was extracted using miRVana™ miRNA isolation kit. 350 ng starting total RNA was converted to first strand cDNA, the products of which were used in a pre-amplification PCR reaction. Samples were added to PCR reaction mixes and added to each well on custom made TLDA cards. The cards were sealed and ran on the Applied Biosystems 7900HT Fast Real Time PCR Machine. The SDS files were exported and data the cards analysed using ExpressionSuite software v1.0.3. Box plot showing Ct distribution for each treated group from three biological replicates per group. The box contains the middle 50% of the data, the black horizontal line indicates the median Ct value and the black dot denotes the mean Ct. The ends of the vertical lines indicate the minimum and maximum Ct values and outliers are the points outside the ends of the whiskers.

Table 4.2.4 qPCR data analysis detected 28 miRNAs in Hek TLR4/MD2/CD14 cells stimulated with LPS, SLPs from RT 001 and RT 027 from the 31 miRNAs analysed on custom TLDA cards. Hek TLR4/MD2/CD14 cells from three biological replicates were plated at 2×10^6 cells/mL and allowed to adhere for 18 hours to approximately 60% confluency. Cells were stimulated with 100 ng/mL LPS or 20 μ g/mL SLPs from RT 001 and RT 027 for 8 hours. Cells were harvested and total RNA was extracted using miRVana™ miRNA isolation kit. 350 ng starting total RNA was converted to first strand cDNA, the products of which were used in a pre-amplification PCR reaction. Samples were added to PCR reaction mixes and added to each well on the custom TLDA cards. The cards were sealed and ran on the Applied Biosystems 7900HT Fast Real Time PCR Machine. The SDS files were exported and data from the custom cards were analysed using ExpressionSuite software v1.0.3. The max Ct was set to 37.0 with a threshold of 0.1 and the reference group was set to the control cell group. U6 snRNA was used to correct for variation of RNA input and relative gene expression was calculated. A Student's t-test was applied and values of $p \leq 0.05$ were considered statistically significant compared to the control group.

Group	Target	RQ	p-value
CTL	hsa-let-7b	1.0	1.000
LPS	hsa-let-7b	0.9	0.646
RT 001	hsa-let-7b	0.8	0.299
RT 027	hsa-let-7b	0.05	0.030
CTL	hsa-let-7c	1.0	1.000
LPS	hsa-let-7c	0.8	0.621
RT 001	hsa-let-7c	1.0	0.997
RT 027	hsa-let-7c	0.1	0.007
CTL	hsa-let-7d	1.0	1.000
LPS	hsa-let-7d	0.7	0.359
RT 001	hsa-let-7d	0.9	0.280
RT 027	hsa-let-7d	0.1	0.001
CTL	hsa-let-7e	1.0	1.000
LPS	hsa-let-7e	0.6	0.088
RT 001	hsa-let-7e	0.7	0.070
RT 027	hsa-let-7e	0.1	0.0001

CTL	hsa-miR-125a-5p	1.0	1.000
LPS	hsa-miR-125a-5p	0.8	0.271
RT 001	hsa-miR-125a-5p	0.8	0.176
RT 027	hsa-miR-125a-5p	0.4	0.007
CTL	hsa-miR-1292	1.0	1.000
LPS	hsa-miR-1292	0.7	0.564
RT 001	hsa-miR-1292	0.8	0.451
RT 027	hsa-miR-1292	0.2	0.007
CTL	hsa-miR-132	1.0	1.000
LPS	hsa-miR-132	1.0	0.722
RT 001	hsa-miR-132	0.8	0.220
RT 027	hsa-miR-132	0.1	0.001
CTL	hsa-miR-145	1.0	1.000
LPS	hsa-miR-145	1.0	0.956
RT 001	hsa-miR-145	1.2	0.035
RT 027	hsa-miR-145	0.2	0.001
CTL	hsa-miR-146a	1.0	1.000
LPS	hsa-miR-146a	1.6	0.227
RT 001	hsa-miR-146a	1.6	0.009
RT 027	hsa-miR-146a	0.6	0.068
CTL	hsa-miR-148b	1.0	1.000
LPS	hsa-miR-148b	0.9	0.803
RT 001	hsa-miR-148b	0.9	0.661
RT 027	hsa-miR-148b	0.1	0.010
CTL	hsa-miR-152	1.0	1.000
LPS	hsa-miR-152	0.8	0.652
RT 001	hsa-miR-152	0.9	0.700
RT 027	hsa-miR-152	0.1	0.012
CTL	hsa-miR-155	1.0	1.000
LPS	hsa-miR-155	0.7	0.375
RT 001	hsa-miR-155	1.0	0.698
RT 027	hsa-miR-155	0.03	0.0002
CTL	hsa-miR-215	1.0	1.000
LPS	hsa-miR-215	1.4	0.401
RT 001	hsa-miR-215	1.3	0.362

RT 027	hsa-miR-215	0.2	0.027
CTL	hsa-miR-221	1.0	1.000
LPS	hsa-miR-221	0.8	0.482
RT 001	hsa-miR-221	0.8	0.315
RT 027	hsa-miR-221	0.03	0.021
CTL	hsa-miR-24	1.0	1.000
LPS	hsa-miR-24	1.2	0.395
RT 001	hsa-miR-24	1.1	0.212
RT 027	hsa-miR-24	0.4	0.036
CTL	hsa-miR-339-5p	1.0	1.000
LPS	hsa-miR-339-5p	1.0	0.931
RT 001	hsa-miR-339-5p	0.9	0.744
RT 027	hsa-miR-339-5p	0.2	0.0003
CTL	hsa-miR-374	1.0	1.000
LPS	hsa-miR-374	0.7	0.282
RT 001	hsa-miR-374	0.7	0.264
RT 027	hsa-miR-374	0.2	0.019
CTL	hsa-miR-422a	1.0	1.000
LPS	hsa-miR-422a	0.5	0.320
RT 001	hsa-miR-422a	0.8	0.843
RT 027	hsa-miR-422a	0.1	0.013
CTL	hsa-miR-432*	1.0	1.000
LPS	hsa-miR-432*	1.1	0.646
RT 001	hsa-miR-432*	1.1	0.531
RT 027	hsa-miR-432*	0.1	0.010
CTL	hsa-miR-543	1.0	1.000
LPS	hsa-miR-543	1.2	0.557
RT 001	hsa-miR-543	0.7	0.360
RT 027	hsa-miR-543	0.1	0.003
CTL	hsa-miR-586	1.0	1.000
LPS	hsa-miR-586	0.6	0.198
RT 001	hsa-miR-586	0.6	0.070
RT 027	hsa-miR-586	0.05	0.015
CTL	hsa-miR-590-5p	1.0	1.000
LPS	hsa-miR-590-5p	0.9	0.823

RT 001	hsa-miR-590-5p	0.9	0.883
RT 027	hsa-miR-590-5p	0.2	0.015
CTL	hsa-miR-9	1.0	1.000
LPS	hsa-miR-9	0.8	0.747
RT 001	hsa-miR-9	0.8	0.405
RT 027	hsa-miR-9	0.1	0.019
CTL	hsa-miR-9*	1.0	1.000
LPS	hsa-miR-9*	0.9	0.871
RT 001	hsa-miR-9*	0.9	0.627
RT 027	hsa-miR-9*	0.2	0.001
CTL	hsa-miR-1293	1.0	1
LPS	hsa-miR-1293	1.3	0.491
RT 001	hsa-miR-1293	1.228	0.624
RT 027	hsa-miR-1293	0.179	0.08
CTL	hsa-miR-221*	1.0	1
LPS	hsa-miR-221*	1.4	0.412
RT 001	hsa-miR-221*	1.2	0.612
RT 027	hsa-miR-221*	0.04	0.06
CTL	hsa-miR-221	1.0	1
LPS	hsa-miR-221	0.8	0.482
RT 001	hsa-miR-221	0.8	0.315
RT 027	hsa-miR-221	0.03	0.021
CTL	hsa-miR-550	1.0	1
LPS	hsa-miR-550	1.2	0.379
RT 001	hsa-miR-550	1.0	0.792
RT 027	hsa-miR-550	0.05	0.02

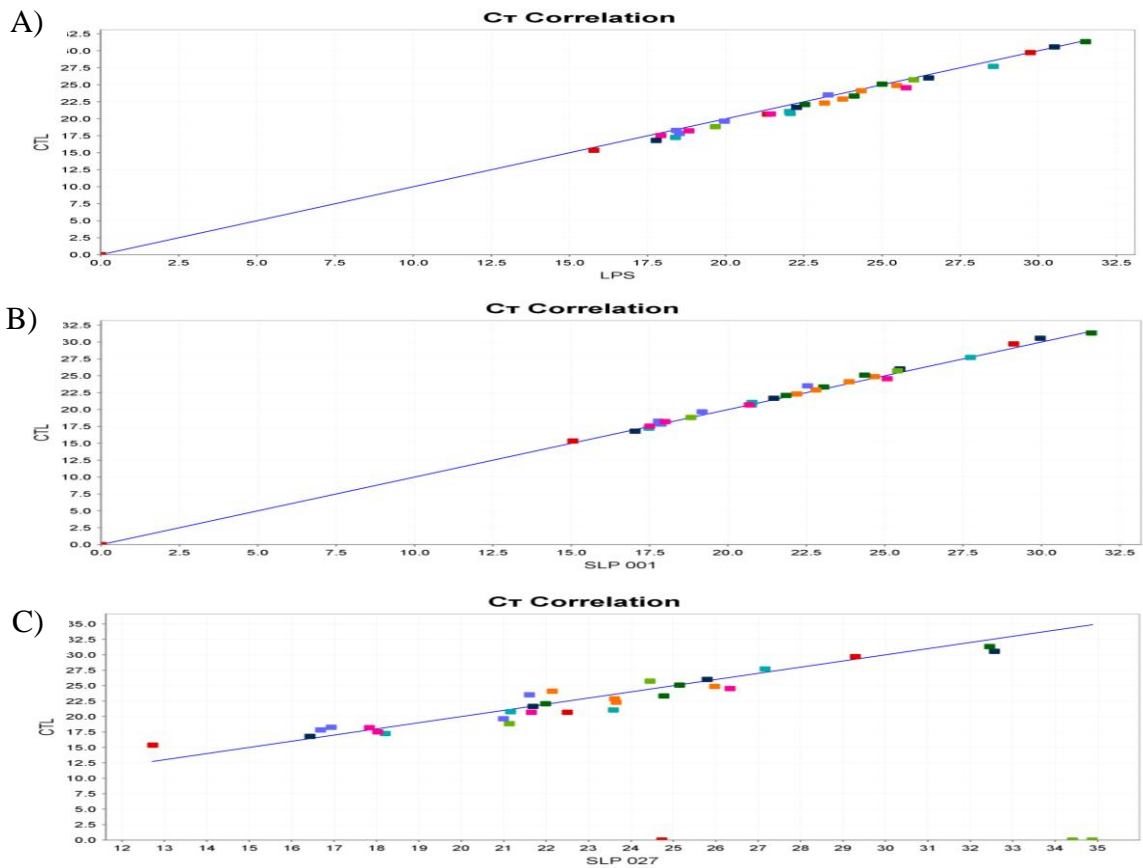


Figure 4.2.8 Ct Scatter plot shows there are differences in miRNA profiles between Hek TLR4/MD2/CD14 cells stimulated with LPS, SLPs from RT 001 and RT 027 compared to the control. Hek TLR4/MD2/CD14 cells from three biological replicates were plated at 2×10^6 cells/mL and allowed to adhere for 18 hours to approximately 60% confluency. Cells were stimulated with 100 ng/mL LPS or 20 μ g/mL SLPs from RT 001 and RT 027 for 8 hours. Cells were harvested and total RNA was extracted using miRVana™ miRNA isolation kit. 350 ng starting total RNA was converted to first strand cDNA, the product of which was used in a pre-amp PCR reaction. Samples were added to PCR reaction mixes and added to each well on custom made TLDA cards. The cards were sealed and ran on the Applied Biosystems 7900HT Fast Real Time PCR Machine. The SDS files were exported and data from the cards was analysed using ExpressionSuite software v1.0.3. The Ct scatter plot shows the relationship between **A)** CTL V's LPS **B)** CTL V's SLPs from RT 001 and **C)** CTL V's SLPs from RT 027 for all miRNAs in the profiling study with custom cards. Ct values are not entirely linear as they fall outside of the line.

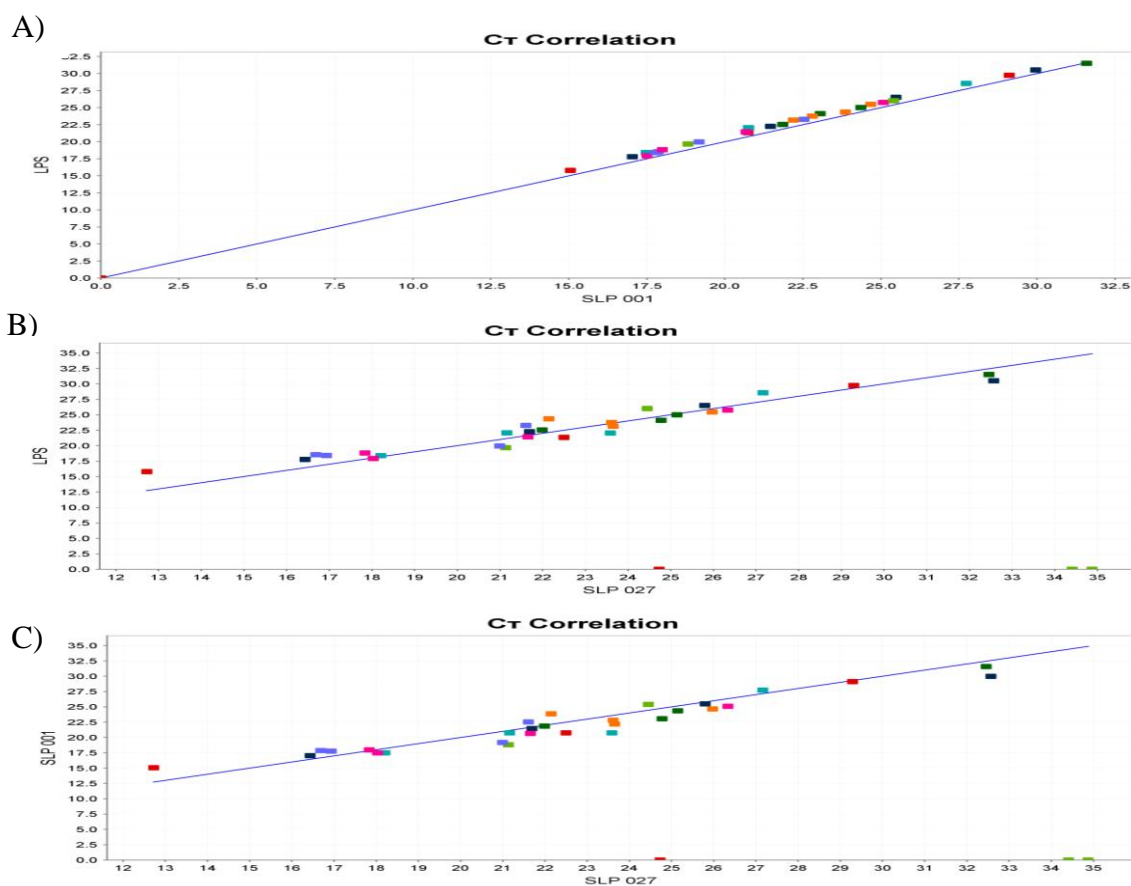


Figure 4.2.9 Ct Scatter plot shows there are differences in miRNA profiles between Hek TLR4/MD2/CD14 cells stimulated with LPS, SLPs from RT 001 and RT 027 compared to each other. Hek TLR4/MD2/CD14 cells from three biological replicates were plated at 2×10^6 cells/mL and allowed to adhere for 18 hours to approximately 60% confluency. Cells were stimulated with 100 ng/mL LPS or 20 μ g/mL SLPs from RT 001 and RT 027 for 8 hours. Cells were harvested and total RNA was extracted using miRVana™ miRNA isolation kit. 350 ng starting total RNA was converted to first strand cDNA, the product of which was used in a pre-amp PCR reaction. Samples were added to PCR reaction mixes and added to each well on custom made TLDA cards. The cards were sealed and ran on the Applied Biosystems 7900HT Fast Real Time PCR Machine. The SDS files were exported and data from the cards was analysed using ExpressionSuite software v1.0.3. The Ct scatter plot shows the relationship between **A)** LPS V's SLPs from RT 001 **B)** LPS V's SLPs from RT 027 and **C)** SLPs from RT 001 V's SLPs from RT 027 for all miRNAs in the profiling study with custom cards. Ct values are not entirely linear as they fall outside of the line.

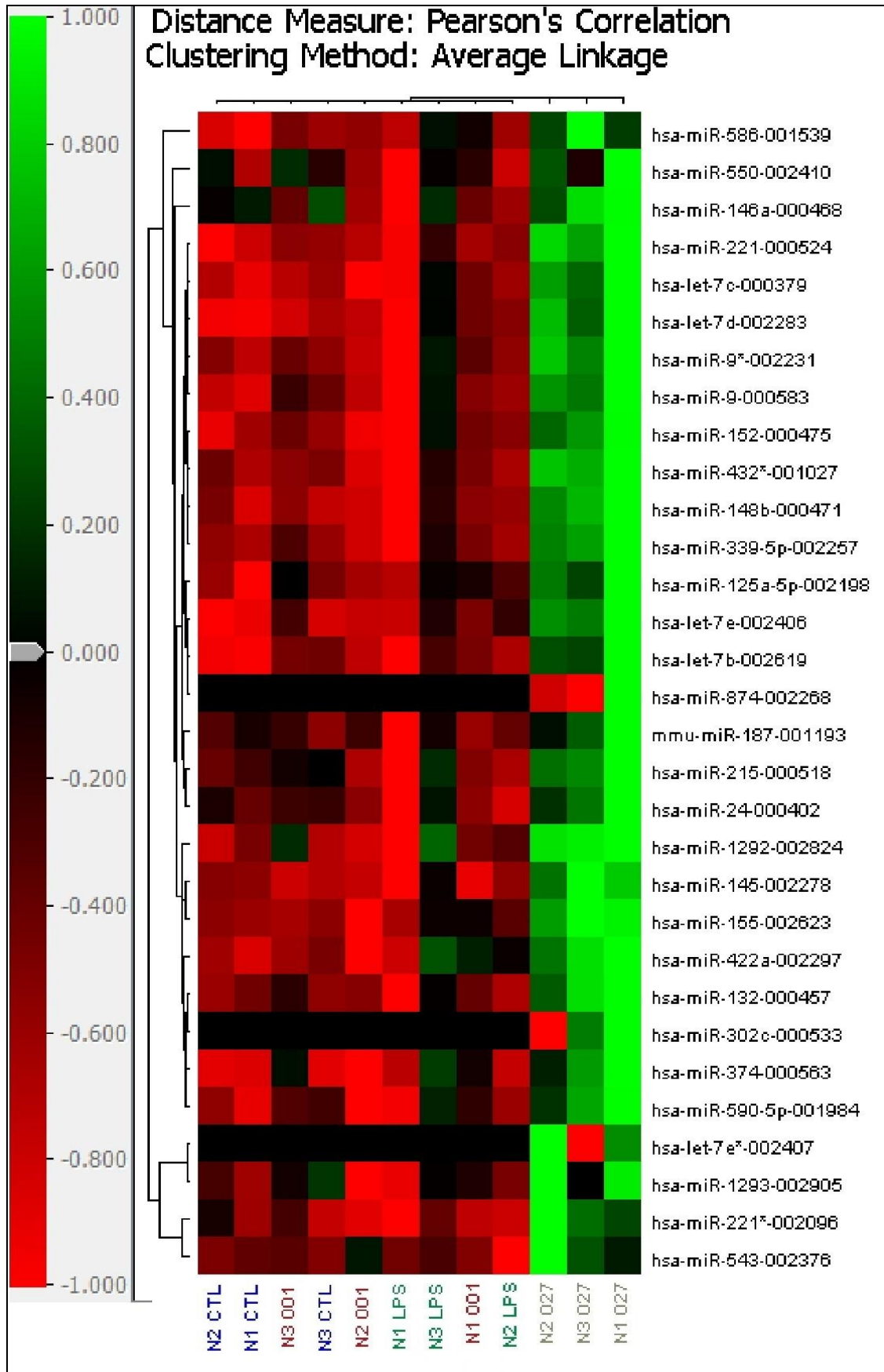


Figure 4.2.10 Visual representation of miRNAs differentially regulated when Hek TLR4/MD2/CD14 cells were stimulated with LPS and SLPs from RT 001 and RT 027. Hek TLR4/MD2/CD14 cells from three biological replicates were plated at 2×10^6 cells/mL and allowed to adhere for 18 hours to approximately 60% confluency. Cells were stimulated with 100 ng/mL LPS or 20 μ g/mL SLPs from RT 001 and RT 027 for 8 hours. Cells were harvested and total RNA was extracted using miRVana™ miRNA isolation kit. 350 ng starting total RNA was converted to first strand cDNA, the product of which was used in a pre-amp PCR reaction. Samples were added to PCR reaction mixes and added to each well on custom TLDA cards. The cards were sealed and ran on the Applied Biosystems 7900HT Fast Real Time PCR Machine. The SDS files were exported and data from the cards was analysed using ExpressionSuite software. The profiles of 31 miRNAs were visualised using a supervised heat map (average linkage and Pearson's correlation). The heat map shows the corresponding relative miRNA expression levels rendered in a green-red colour scale, red represents high expression level, green represents low expression level and black being absence of detection. Each row represents a single miRNA and each column represents an individual sample. Dendograms indicate the correlation between groups of samples and miRNAs.

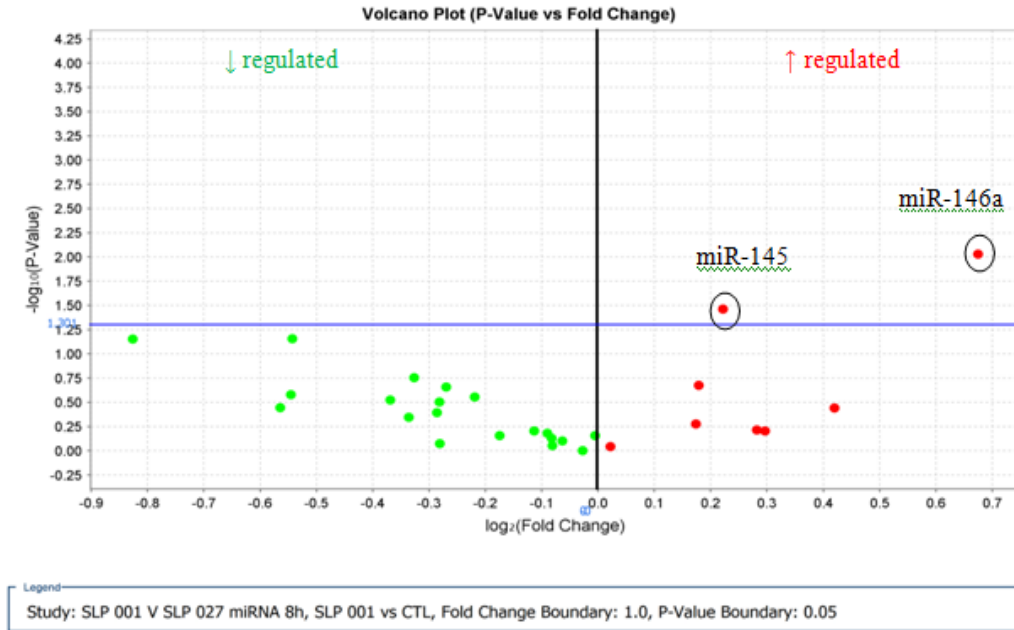


Figure 4.2.11 MiR-145 and miR-146a were significantly up regulated when Hek TLR4/MD2/CD14 cells were stimulated with SLPs from RT 001. Hek TLR4/MD2/CD14 cells from three biological replicates were plated at 2×10^6 cells/mL and allowed to adhere for 18 hours to approximately 60% confluency. Cells were stimulated with 20 μ h/mL SLPs from RT 001 for 8 hours. Cells were harvested and total RNA was extracted using miRVana™ miRNA isolation kit. 350 ng starting total RNA was converted to first strand cDNA, the products of which were used in a pre-amp PCR reaction. Samples were added to PCR reaction mixes and added to custom TLDA cards. The cards were sealed and ran on the Applied Biosystems 7900HT Fast Real Time PCR Machine. The SDS files were exported and data from the custom cards analysed using ExpressionSuite software. The max Ct was set to 37.0 with a threshold of 0.1 and the reference group was set to the control cell group. U6 snRNA was used to correct for variation of RNA input and relative gene expression was calculated. A student's t-test was applied and values of $p \leq 0.05$ were considered statistically significant compared to the control group. The volcano plot displays $-\log_{10}$ p-value Vs \log_2 fold change. The p-value and fold change boundaries were set at 0.05 & 1.0. Targets above the horizontal line have statistically significant fold changes. The top left quadrant shows miRNAs targets that are down regulated while the top right quadrant shows miRNA targets that are up regulated.

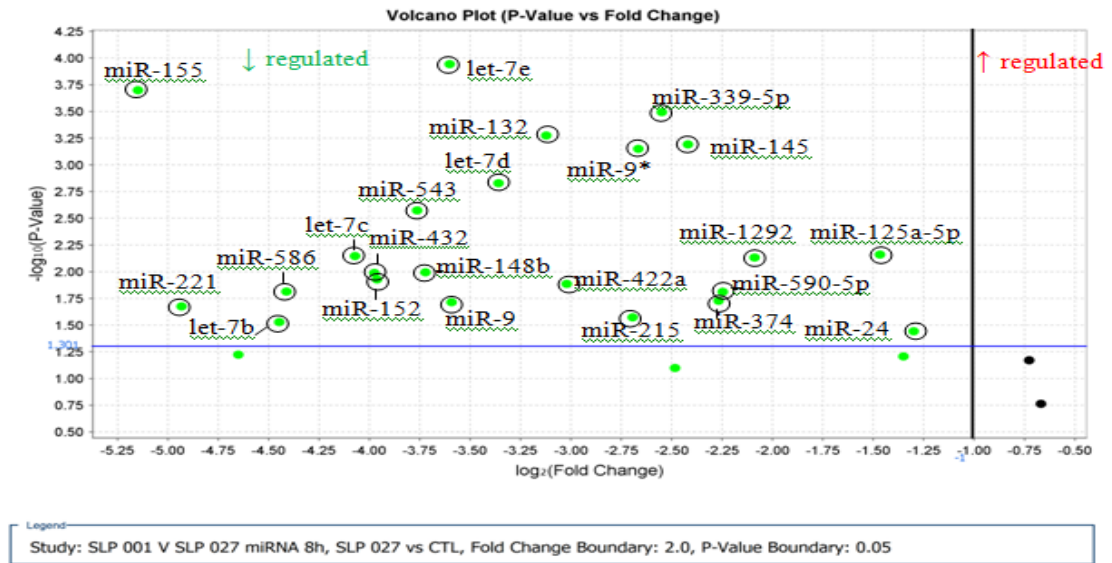


Figure 4.2.12 Twenty three miRNAs were significantly down regulated when Hek TLR4/MD2/CD14 cells were stimulated with SLPs from RT 027. Hek TLR4/MD2/CD14 cells from three biological replicates were plated at 2×10^6 cells/mL and allowed to adhere for 18 hours to approximately 60% confluency. Cells were stimulated with 20 μ g/mL SLPs from RT 027 for 8 hours. Cells were harvested and total RNA was extracted using miRVana™ miRNA isolation kit. 350 ng starting total RNA was converted to first strand cDNA, the products of which were used in a pre-amp PCR reaction. Samples were added to PCR reaction mixes and added to custom TLDA cards. The cards were sealed and ran on the Applied Biosystems 7900HT Fast Real Time PCR Machine. The SDS files were exported and data from the custom cards analysed using ExpressionSuite software. The max Ct was set to 37.0 with a threshold of 0.1 and the reference group was set to the control cell group. U6 snRNA was used to correct for variation of RNA input and relative gene expression was calculated. A student's t-test was applied and values of $p \leq 0.05$ were considered statistically significant compared to the control group. The volcano plot displays $-\log_{10}$ p-value Vs \log_2 fold change. The p-value and fold change boundaries were set at 0.05 & 2.0. Targets above the horizontal line have statistically significant fold changes. The top left quadrant shows miRNAs targets that are down regulated while the top right quadrant shows miRNA targets that are up regulated.

Table 4.2.5 Four miRNAs of interest were chosen for further validation based on the differences between expression in response to SLPs from RT 001 and RT 027.

23 miRNAs had statistically significant folds changes when Hek TLR4/MD2/CD14 cells were stimulated with SLPs from RT 001 and RT 027. The miRNAs highlighted in yellow are of most interest to us based on the possible differences between SLPs from RT 001 and RT 027 therefore let-7e, miR-155, miR-146a and miR-145 were chosen for further validation.

	RT 001	RT 027
let -7e	↓	↓↓
miR-155	↔	↓
miR-146a	↑	↓
miR-145	↑	↓
Let-7b	↓	↓↓
Let-7c	↔	↓
let-7d	↓	↓↓
miR-125a-5p	↓	↓↓
miR-1292	↓	↓↓
miR-132	↓	↓↓
miR-148b	↓	↓↓
miR-152	↓	↓↓
miR-215	↑	↓↓
miR-221	↓	↓↓
miR-24	↑	↓
miR-339-5p	↓	↓↓
miR-374	↓	↓↓
miR-422a	↓	↓↓
miR-432	↑	↓
miR-543	↑	↓
miR-586	↓	↓↓
miR-590-5p	↓	↓↓
miR-9	↓	↓↓

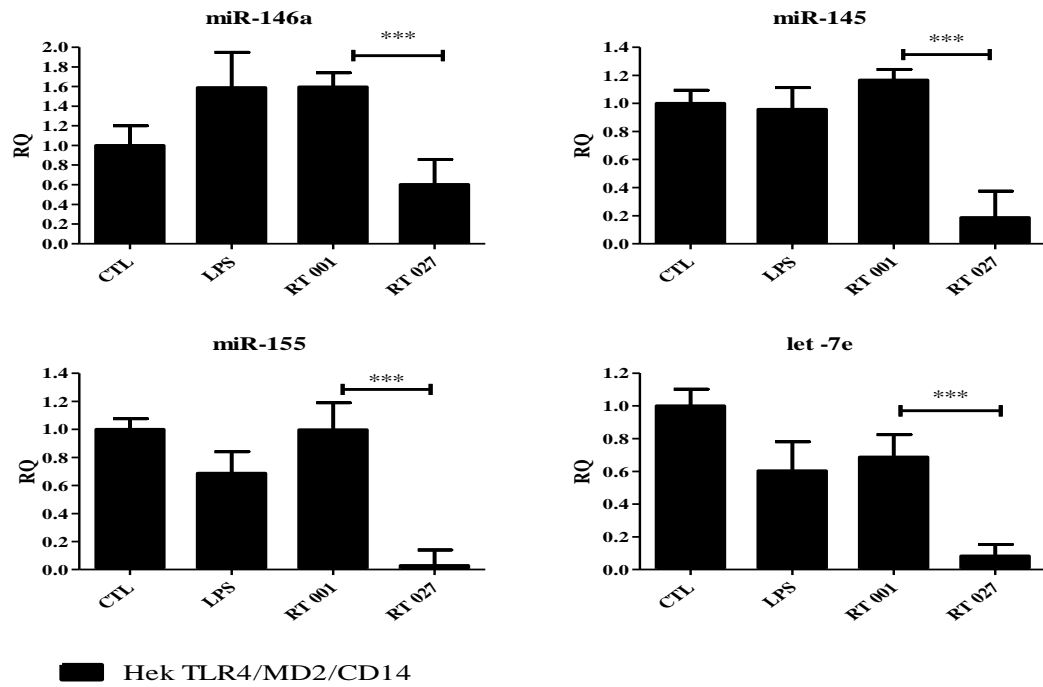


Figure 4.2.13 MiR-146a, miR-145, miR-155 and let-7e are differentially regulated in Hek TLR4/MD2/CD14 cells stimulated with SLPs from RT 001 and RT 027. Hek TLR4/MD2/CD14 cells from three biological replicates were plated at 2×10^6 cells/mL and allowed to adhere for 18 hours to approximately 60% confluency. Cells were stimulated with 100 ng/mL LPS, 20 μ g/mL SLPs from RT 001 and RT 027 for 8 hours. Cells were harvested and total RNA was extracted using miRVana™ miRNA isolation kit. 350 ng starting total RNA was converted to first strand cDNA, the products of which were used in a pre-amplification PCR reaction. Samples were added to PCR reaction mixes for individual Taqman miRNA assays and added to wells on a 96 well PCR plate. The plate was run on the Applied Biosystems 7900HT Fast Real Time PCR Machine. The SDS files were exported and data from the PCR plate analysed using ExpressionSuite software. The max Ct was set to 37.0 with a threshold of 0.1 and the reference group was set to the control cell group. U6 snRNA was used to correct for variation of RNA input and relative gene expression was calculated. Results show the mean (\pm SEM) from three biological replicates with 3 technical replicates each. The Mann Whitney U-test was used to test for significance comparing miRNAs induced by SLPs from RT 001 with SLPs from RT 027 where * $p \leq 0.05$, ** $p \leq 0.01$ and *** $p \leq 0.001$.

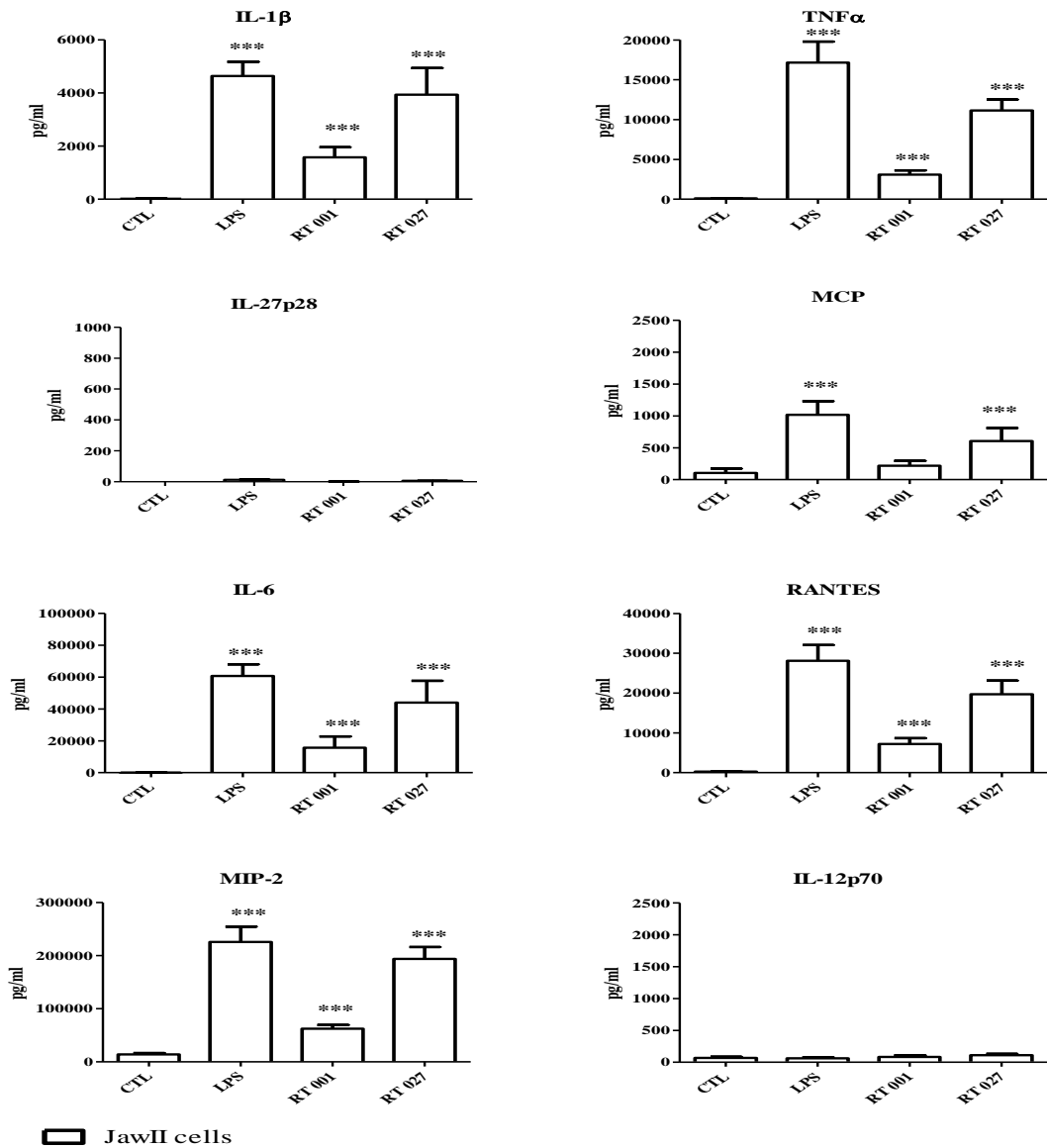


Figure 4.2.14 SLPs from RT 001 and RT 027 induce the production of murine IL-1 β , TNF α , MCP, IL-6, RANTES and MIP-2 in JAWS II cells. JAWS II Cells were plated at 1×10^6 cells/mL and stimulated with 100 ng/ml of LPS or 20 μ g/mL SLPs from RT 001 and RT 027. Supernatants were recovered after 18 hours and assessed for levels of cytokines and chemokines using ELISA. The results show the mean (\pm SEM) measured in triplicate, one-way ANOVA followed by Newman-Keuls analysis was used to determine if differences between treatment groups were significantly different compared to the control, where * $p \leq 0.05$, ** $p \leq 0.01$ and *** $p \leq 0.001$. The results are indicative of three independent experiments.

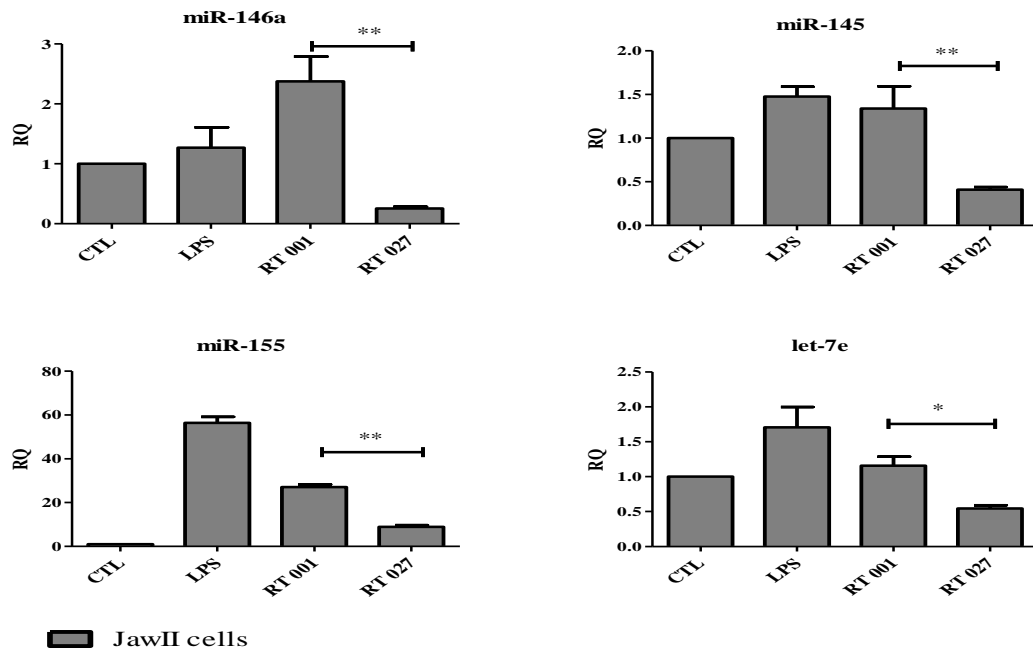


Figure 4.2.15 MiR-146a and miR-145, miR-155 and let-7e are differentially regulated in JAWS II cells stimulated with SLPs from RT 001 and RT 027. JAWS II cells from three biological replicates were plated at 2×10^6 cells/mL. Cells were stimulated with 100 ng/mL LPS, 20 μ g/mL SLPs from RT 001 and RT 027 for 8 hours. Cells were harvested and total RNA was extracted using miRVana™ miRNA isolation kit. 350 ng starting total RNA was converted to first strand cDNA, the products of which were used in a pre-amp PCR reaction. Samples were added to PCR reaction mixes for individual Taqman miRNA assays and added to wells on a 96 well PCR plate. The plate was run on the Applied Biosystems 7900HT Fast Real Time PCR Machine. The SDS files were exported and data from the PCR plate analysed using ExpressionSuite software. The max Ct was set to 37.0 with a threshold of 0.1 and the reference group was set to the control cell group. snoRNA202 was used to correct for variation of RNA input and relative gene expression was calculated. Results show the mean (\pm SEM) from three biological replicates with 3 technical replicates each. The Mann Whitney U-test was used to test for significance comparing miRNAs induced by SLPs from RT 001 with SLPs from RT 027 where * $p \leq 0.05$, ** $p \leq 0.01$ and *** $p \leq 0.001$. The results are indicative of three independent experiments.

Table 4.2.6 Expression of miR-146a, miR-145, miR-155 and let-7e in response to SLPs from RT 027 is similar in Hek TLR4/MD2/CD14 cells and JAWS II cells. Summary of qPCR data from Hek TLR4/MD2/CD14 cells and JAWS II cells stimulated with LPS, SLPs from RT 001 and RT 027.

	Hek TLR4/MD2/CD14			JAWS II		
	LPS	RT 001	RT 027	LPS	RT 001	RT 027
miR-146a	↑	↑	↓↓	↔	↑	↓↓
miR-145	↔	↑	↓	↑	↔	↓↓
miR-155	↓	↔	↓	↑↑	↑	↓
let-7e	↓	↓	↓↓	↑	↔	↓

4.3 Discussion

TLR signalling plays an important role in detecting pathogens and initiating the inflammatory response. It has now emerged that these TLR pathways are highly regulated by miRNAs and there is evidence to suggest they function as immunomodulators (Coll & O'Neill, 2010; He et al., 2014). Differences in miRNA expression profiles have been observed depending on the TLR stimulus used, treatment time, technology used and the cell type. MiRNAs have been shown to be involved in innate immunity by regulating TLR signalling and ensuing cytokine response by targeting a variety of signalling proteins, regulatory molecules and transcription factors (Dalal & Kwon, 2010; He et al., 2014; Sonkoly et al., 2008). MiRNAs also regulate central elements of the adaptive immune response such as antigen presentation, T cell receptor signalling and the interferon system (Cullen, 2006; Sonkoly et al., 2008). There is mounting evidence that miRNAs orchestrate immune regulation and host responses to pathogens during infection (Sonkoly et al., 2008).

Until recently little was known about the recognition of *C. difficile* by the immune system, however research from our laboratory showed that SLPs from *C. difficile* activate TLR4, with subsequent activation of downstream signalling pathways known to be important in the immune response to infection (Collins et al., 2014; Ryan et al., 2011). SLPs from ribotype 001 fail to fully activate all signalling pathways *via* TLR4 (Ryan et al., 2011). In the previous chapter we showed that SLPs isolated from ribotype 001 activate NF- κ B signalling and they do not activate IRF3 downstream of TLR4. On the other hand SLPs from ribotype 027 activate both NF- κ B and IRF3 signalling. The severity of *C. difficile* infection may be dependent on the strain present (Goorhuis et al., 2007; Rupnik et al., 2009). Some ribotypes are more 'hypervirulent' than others, ribotype 027 is associated with more severe diarrhoea, higher mortality and more recurrences. In comparison ribotype 001 is associated with milder infection and clearance of the bacteria (Clements et al., 2010; Dawson et al., 2009; Goorhuis et al., 2007; Loo et al., 2005). Given the role of miRNAs in the regulation of TLR4 signalling and during infection, we hypothesise that SLPs induce miRNAs and that profiles may differ between ribotypes. These miRNAs may modulate TLR4 signalling ultimately

leading to changes in the immune response to *C. difficile*, which may explain the differences in clinical symptoms between different ribotypes. The aim of this chapter was to profile and compare miRNA expression regulated by SLPs from ribotypes 001 and 027.

SLPs modulate TLR4 signalling therefore we wanted to examine miRNA profiles induced by SLPs *via* TLR4 signalling specifically, for that reason Hek TLR4/MD2/CD14 cells were used throughout the initial profiling studies. We also incorporated cells stimulated with LPS in our study as it is a known TLR4 agonist that activates NF- κ B and IRF3 signalling (Akashi et al., 2003; Taro Kawai & Akira, 2007; Laird et al., 2009). Evidence from the literature shows, LPS induces miRNAs such as miR-155, miR-125, miR-9, the let-7 family, miR-145, miR-146a and miR-187. These miRNAs have been shown to modulate the immune response including key molecules involved in the TLR4 signalling pathway 6-8 hours post immune stimulation *in vitro* (Curtale et al., 2013; Rossato et al., 2012; Tili et al., 2007). We wanted to ensure that samples generated reflected the correct signalling profile at this 8 hour time point as seen when stimulated at 18 hours in our previous chapter. As expected, SLPs from ribotype 001 and 027 activated NF- κ B signalling. SLPs from ribotype 027 activated IRF3 signalling but SLPs from ribotype 001 failed to induce this response. The profile at gene level was reflected in the production of human IL-8 and RANTES cytokines. Once we were confident we were generating the correct signalling profile, we went on to profile miRNAs at this 8 hour time point. Initially we profiled control untreated cells and compared them to cells stimulated with LPS and SLPs from ribotype 001.

Over the last number of years various strategies have been developed to identify and characterise miRNAs, quantitatively and qualitatively. Methods include cloning, hybridisation, deep sequencing, northern blotting, microarrays and qPCR (Lhakhang & Chaudhry, 2012). Each method has their advantages and disadvantages but the approach we choose for this study was qPCR, it is the gold standard for miRNA detection due to its sensitivity, specificity, and wide dynamic range. Also the less abundant miRNAs routinely escape detection with the other technologies (Chen et al., 2005; Lim, Glasner, Yekta, Burge, & Bartel, 2003). We used Taqman® Low Density Array (TLDA) cards with preloaded primers for pool A v2 and pool B v3 human miRNAs to look at mature

miRNA expression. Multiple stem-loop reverse transcription primers produce cDNA for multiple miRNAs therefore increasing the number of miRNAs being reverse transcribed within a single reverse transcription reaction (Fiedler, Carletti, & Christenson, 2010). This method allowed us to use a small amount of starting material and examine 756 miRNA targets between the two sets of cards. Pre-amplification uniformly amplifies desired cDNA by increasing the amount of starting template and this enhances the sensitivity of qPCR especially for low abundance genes (Noutsias et al., 2008). The substantially higher cDNA amounts expands the number of the target genes which can be analysed without biasing the estimation of miRNA expression ratio (Chen et al., 2009). We optimised the assay to see if pre-amplification was necessary for our study, we ran cards with and without pre-amplification product. We saw an increase in the amount of cDNA, so as not to lose any of the low abundance miRNAs we used the pre-amplification reaction for all samples thereafter.

We generated a large data set and how this data was managed was very important. We implemented strict quality control (QC) guidelines and thresholds to eliminate false positive/negative results. In this study we had three biological replicates so we had to compare samples between cards. The purpose of normalisation is to reduce variation within a dataset, enabling a better appreciation of the biological variation (Mestdagh et al., 2009). A proper normalisation strategy is crucial for any qPCR data analysis, it minimises the effects of systematic technical variations and is a prerequisite for getting meaningful biological changes (Meyer et al., 2012). For large scale miRNA expression profiling studies, global normalisation out performs the normalisation strategies using endogenous controls (Mestdagh et al., 2009). After careful consideration we thought this was the best approach under the circumstances due to the large data set, constraints with the number of technical and the biological replicates for this initial screen. Taqman assays are designed to include a passive internal reference dye and a reporter dye which are amplified simultaneously in the presence of a target sequence using a labelled fluorophore, which emits light at a different wavelength than the fluorophore used for the target sequence assay. The two fluorophores are detected in different channels by the real-time PCR instrument (Jothikumar, Hill, & Narayanan, 2009). The normalised reporter 'Rn' value is taken into account during analysis. The Rn value is calculated by dividing the fluorescence of the passive dye by the fluorescence of the reporter dye to

normalise the reaction. This improves the precision of the data and accounts for variability in the optics, uneven illumination and the amount of condensation present (Jothikumar et al., 2009). Once we had applied the QC checks and carried out the global normalisation, we set our reference group as the untreated control cell group.

The relative gene expression was calculated using the $\Delta\Delta\text{Ct}$ method to calculate fold change (RQ) (Livak & Schmittgen, 2001). Increasing the number of tests increases the probability of finding a significant p-value by chance and to avoid this effect the Benjamini-Hochberg False Discovery Rate (FDR) was used to adjust p-values according to the number of total tests. The statistics used in a t-test are defined as the difference of the arithmetic mean of two groups divided by the estimated standard deviation of that difference. The t-test statistic runs under the assumption that the given variable follow normal distribution (Goni et al., 2009; Li, 2012). Therefore we examined the overall Ct value distribution for each sample from the data generated from the TLDA cards. The overall Ct values followed normal distribution therefore we applied a student's t-test where values of $p \leq 0.05$ were considered statistically significant compared with the control cell group.

qPCR data analysis revealed 248 miRNAs were detected out of the 756 miRNAs analysed. In order to fully elucidate differences between individual miRNA targets with statistically significant fold changes we utilised volcano plots. MiR-155, miR-9, the let-7 family, miR-145, miR-146a and miR-187 have all been shown to be induced by LPS in the literature (Curtale et al., 2013; Rossato et al., 2012; Tili et al., 2007). Although not significantly expressed these miRNAs were shown to be regulated by LPS in our study, thus validating our experimental method. We cannot rely on RQ values alone to evaluate differential expression of our data. According to the literature RQ is a reasonable measure of effect size however, it is widely considered to be inadequate because as it does not incorporate variance and offers no associated level of confidence (Allison, Cui, Page, & Sabripour, 2006; Hsiao, Worrall, Olefsky, & Subramaniam, 2004; Miller, Galecki, & Shmookler-Reis, 2001). There is a relationship however between RQ and test statistics when both are transformed logarithmically (Li, 2012). We identified the miRNA targets for this study by examining the upper right and left quadrant of the volcano plot for statistically significant targets with large magnitude

fold changes. Three miRNAs miR-543, miR302 and miR-374a were up regulated in response to LPS and miR-586 was down regulated. None of these miRNAs have been shown before to be differentially expressed in response to LPS or *via* TLR4 signalling in human or murine cells before, therefore we have potentially uncovered novel miRNAs that regulate this signalling pathway. We also identified for the first time novel miRNAs that were up regulated in response to SLPs from ribotype 001; miR-339-5p, miR148b, miR590-5p, miR-24, miR-550a, miR-1292, miR-432#, miR-215 and miR152. On the other hand miR-422a, miR-874 and miR1293 were down regulated in response to SLPs from ribotype 001 compared to the control cells. In the literature miR-148a/b has been shown to inhibit the expression of calcium/calmodulin-dependent protein kinase II, and thus they can regulate TLR-signalling pathways (He et al., 2014). Some of the other miRNAs were found in other models of disease and present in epithelial cells in the gut, for instance miR-215 has been associated with colon cancer (Song et al., 2010). However the 16 miRNAs identified from the experimental profiling study needed to be validated further.

We began by reviewing the literature for miRNAs known to regulate key elements of TLR4 signalling including: signalling proteins, transcription factors, cytokines and regulatory molecules, to create a short list of potential miRNAs of interest. MiRNAs that were known to be induced by LPS and induced during an immune response to infection were also included. We re-examined the profiling study to see if the short list of miRNAs were present in the initial experimental profiling study. The miRNAs identified from the literature were in fact present but were over the significance value set in this experiment. Custom TLDA cards were commissioned and targets on these cards included the 16 miRNAs from the experimental profiling study and the 15 miRNAs from the review of the literature. The approach to data analysis had to be altered due to the decrease in the total number of tests from 756 to 31. We used the endogenous control U6 snRNA for data normalisation. New samples were generated and stimulated with LPS, SLPs from ribotype 001 and 027. We were also able to increase the number of technical replicates thus reducing potential variation. qPCR data analysis showed miR-145 and miR-146a were significantly up regulated in response to SLPs from ribotype 001. On the other hand there was a striking global down regulation of let-7b, let-7c, let-7d, let-7e, miR-125a-5p, miR-1292, miR-132, miR-145, miR-148b,

miR-152, miR-155, miR-221, miR-24, miR339-5p, miR-374, miR-422a, miR-432*, miR-543, miR-586, miR-590, miR-9, miR-9* and miR-221 in response to SLPs from ribotype 027. Hierarchical clustering analysis showed that miRNAs induced in response to SLPs from ribotype 001 and 027 were grouped together in distinctive clades. MiRNAs contained within these branches were more likely to be expressed together based on the experimental data in this study, this will have to be further validated in future work.

Four miRNAs; let-7e, miR-155, miR-146a and miR-145- were chosen for further validation based on the differences between expression in response to SLPs from ribotype 001 and 027. Again we used U6 snRNA for data analysis however we used the Mann Whitney U-test when testing for significance. This statistical test was chosen because of the uncertainty of normal distribution due to low number of miRNA targets in this experimental study (Goni et al., 2009). qPCR data using individual Taqman assays confirmed that each of the miRNAs were down regulated in response to SLPs from ribotype 027 and that miR-146a and miR-145 were up regulated in response to SLPs from ribotype 001. We then validated these results in another cell line. We choose the murine dendritic cell line JAWS II as they behave in a similar way to BMDCs. JAWS II cells differ from BMDCs in that they fail to release the IL-12 cytokine family which include IL-12, IL-23 and IL-27 and IL-35 (Collins et al., 2014; Jørgensen et al., 2002; Zapala et al., 2011). We observed that RANTES was produced in JAWS II cells when stimulated with SLPs from ribotype 001, however, the trend was the same in that ribotype 027 produced more RANTES compared to ribotype 001 as seen in the Hek TLR4/MD2/CD14 cells. JAWS II cells stimulated with SLPs from ribotype 001 and 027 induced the production of murine cytokine and chemokines indicating the SLPs induced an immune response in these cells. We used snoRNA202 to correct for variation in RNA input, this is a murine small RNA endogenous control and was used as it showed the least variation across samples. qPCR data analysis showed that miR-146a, miR-145, miR-155 and let-7e were down regulated in response to SLPs from ribotype 027 and this was comparable to the response seen in the human Hek TLR/MD2/CD14 cell line. There were slight differences in the levels at which these miRNAs were expressed between the cell lines. However we showed that there were distinct miRNA profiles

regulated by SLPs from ribotype 001 and 027, which differed between ribotypes at this 8 hour time point.

Our data shows that SLPs from ribotype 001 and 027 down regulate let-7e in both human and murine cells. Evidence from the literature shows, the mRNA encoding TLR4 is regulated by members of the let-7 miRNA family and can be targeted by other isoforms of the let-7 family, such as let-7i. Down regulation of let-7i expression was shown to increase TLR4 expression by human epithelial cells after *Cryptosporidium parvum* infection or LPS treatment (Chen, Splinter, O'Hara, & LaRusso, 2008). In mouse peritoneal macrophages, the induction of let-7e expression decreases cell surface expression of TLR4, furthermore the transfection of macrophages with antisense miRNA to let-7e leads to an increased LPS induced cytokine response (Androulidaki et al., 2009). It is possible that the SLPs from both ribotypes utilise let-7e to activate TLR4 signalling and increase cell surface marker expression leading to the production of cytokines. Our data also showed that miR-146a and miR-145 were up regulated in human and murine cells lines in response to SLPs from ribotype 001, in comparison these miRNAs were down regulated by SLPs from ribotype 027. MiRNA expression has been shown to contribute to disease. For example, loss of miR-145 and miR-146a transcripts within the 5q locus identified these miRNAs as key mediators of 5q syndrome, a haematopoietic malignancy that progresses to acute myeloid leukaemia (Starczynowski et al., 2010). Studies have shown that when miR-145 and miR-146a are absent their targets Mal, IRAK1 and TRAF6 are up regulated (Izar, Mannala, Mraheil, Chakraborty, & Hain, 2012; Taganov et al., 2006). It is possible that the down regulation of miR-145 and miR-146a induced in response to SLPs from ribotype 027 leads to up regulation of Mal, IRAK1 and TRAF6- all three are implicated in NF- κ B signalling pathways. This may account for the increased potency of the immune response to ribotype 027 compared to the immune response to ribotype 001.

Lastly our data showed that miR-155 was down regulated in both human and murine cell lines in response to SLPs from ribotype 027 compared to SLPs from ribotype 001. The role of miR-155 in the TLR response is more complex (O'Neill et al., 2011). Studies using inhibition or over expression of miR-155 has shown that miR-155 negatively regulates the expression of cytokines and chemokines such as IL-1 and

CXCL8 (Ceppi et al., 2009; Tang et al., 2010; Xiao et al., 2009). On the other hand, miR-155 is required for the expression of certain cytokines and type I IFNs (Androulidaki et al., 2009; O'Connell et al., 2007; Wang et al., 2010; Zhou et al., 2010). An effect that is probably mediated by the targeted suppression of suppressor of cytokine signalling 1 (SOCS1) and/or SHIP1, two negative regulators of cytokine-mediators and TLR signalling pathways (Androulidaki et al., 2009; Wang et al., 2010; Yoshimura, Naka, & Kubo, 2007). IL-10, which is an important regulator of both innate and adaptive immune responses, can inhibit LPS induced expression of miR-155 (McCoy et al., 2010; O'Connell, Rao, Chaudhuri, & Baltimore, 2010). IL-10 is known to dampen the innate immune response by down regulating TLR-induced pro-inflammatory gene expression in macrophages and DCs after pathogen infection and can inhibit the proliferation of and cytokine production by CD4⁺ T cells (O'Neill et al., 2011). In the previous chapter we showed that SLPs from ribotype 027 induced the production of IL-10 in BMDCs. It is possible that the IL-10 produced by SLPs from ribotype 027 inhibits the expression of miR-155 and this warrants further investigation. In the previous chapter we also showed that SLPs from ribotype 001 appeared to produce much less IL-10 and IL-1 β in BMDCs compared to SLPs from ribotype 027. Therefore it is possible that miR-155 expression was uninhibited by IL-10 and thus able to negatively regulate the expression of IL-1 β . Consequently we have potentially identified a novel mechanism in which SLPs modulate TLR4 signalling in response to *C. difficile* infection *in vitro*.

This profiling study and subsequent validation studies with the SLPs from ribotype 001 and 027 only give us a snapshot into the signalling occurring at this particular point in time *in vitro*. Evidence from the literature shows that these miRNAs play key roles in modulating TLR4 and they have roles orchestrating the immune response to infection. In the next chapter we hope to elucidate further the role miR-146a, miR-145, miR-155 and let-7e in NF- κ B and IRF3 signalling. We hope to validate these miRNAs targets *in vivo* in a *C. difficile* infection model and use bioinformatics tools to search for biologically relevant miRNA gene interactions induced when SLPs activate TLR4 signalling.

**Chapter 5: Validation of miRNA Targets
in a *C. difficile* Infection Model and
Analysis of miRNA Functionality**

5.1 Introduction

To date 28,645 miRNA hairpin precursors corresponding to 35,828 mature miRNAs in 223 species have been determined, 2588 mature miRNAs are currently annotated in the human genome (Eulalio & Mano, 2015). It has been estimated that up to 30% of all human genes are regulated by miRNAs in many cell types (Bartel, 2009; Fabian et al., 2010; Yates et al., 2013). MiRNAs have been shown to be involved in innate immunity by regulating TLR signalling and ensuing cytokine response by targeting a variety of signalling proteins, regulatory molecules and transcription factors (Dalal & Kwon, 2010; He et al., 2014; Sonkoly et al., 2008). They can also regulate central elements of the adaptive immune response such as antigen presentation, T cell receptor signalling and the interferon system (Cullen, 2006; Sonkoly et al., 2008). There is also mounting evidence that miRNAs orchestrate immune regulation and the host response to pathogens during infection. In chapter three we showed that SLPs from ribotype 001 and 027 activate NF- κ B and the potency of the response differed between ribotypes. SLPs from ribotype 027 activated IRF3 signalling but SLPs from ribotype 001 failed to induce this response. In chapter four we identified 24 miRNAs that were differentially regulated by SLPs from ribotype 001 and 027 using qPCR. We validated the expression of miR-146a, miR-145, miR-155 and let-7e in a human and murine cell line.

Despite their clear importance as a class of regulatory molecule, determining the biological relevance of individual miRNAs has proven challenging (Vidigal & Ventura, 2014). The implication of miRNAs in human diseases warrants a critical need to identify miRNA regulated genes in a biologically relevant context (Tarang & Weston, 2014). The function of specific miRNAs have been predominantly inferred from over expression studies in animals and cultured cells, or from studies that used antisense molecules as a means of disrupting their pairing to targets (Vidigal & Ventura, 2014). The aim of the first part of this chapter is to determine the functionality of miR-146a, miR-145, miR-155 and let-7e in NF- κ B and IRF3 signalling using chemically synthesised miRNA mimics. Nonetheless the most commonly used cellular assays are based on the principle of studying the functional consequences of artificially manipulating miRNAs levels. However, as the biological concentrations of these miRNAs *in vivo* may be several orders of magnitude different than *in vitro* conditions, it

is essential that the results of target recognition are recapitulated in appropriate animal models (Tarang & Weston, 2014). We had access to a bank of RNA samples derived from colonic tissue from a *C. difficile* infection model. Mice were treated with a cocktail of antibiotics before being infected with 10^3 *C. difficile* spores from ribotype 001 and 027. The colon was harvested at two time points during infection and RNA was extracted from the distal colon (Lynch 2014, unpublished). The aim of the next part of this chapter is to examine the expression of miR-146a, miR-145, miR-155 and let-7e from the colonic tissue generated in the *C. difficile* infection model.

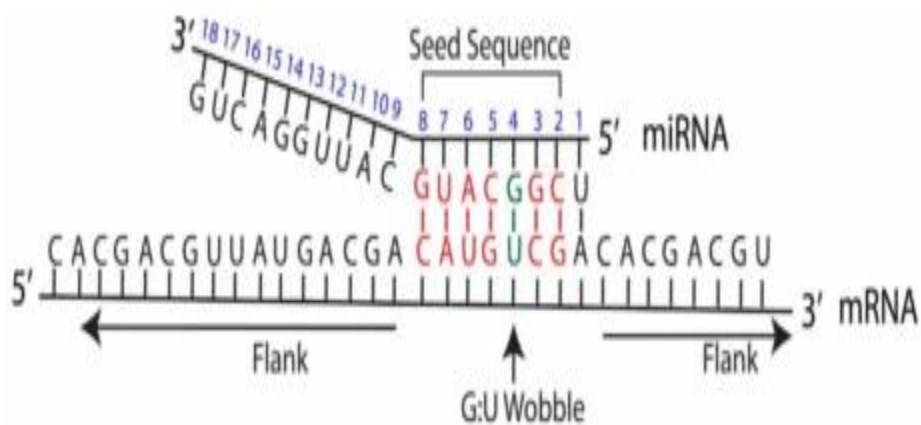


Figure 5.1.1 Diagram depicting seed match between miRNA and target mRNA (Peterson et al., 2014)

Experimental data is not enough to give a comprehensive view of miRNA biology. It is thought that to get a more complete view, experimental data must be combined with computational predications (Bentwich et al., 2005; Ghosh, Chakrabarti, & Mallick, 2007; Sachidanandam, 2005). MiRNA target prediction programs on the market today use algorithms to model how miRNAs target specific mRNAs based on four common features. A seed match occurs when adenosine pairs with uracil and guanine pairs with cytosine between a miRNA and its target sequence at the first two to eight nucleotides at the 5' end moving toward the 3' end of the sequence see **Figure 5.1.1** (Lewis et al., 2003; Peterson et al., 2014). Conservation refers to the maintenance of a sequence across species on regions in the 3' UTR, the 5' UTR, the miRNA, or any combination of the three (Peterson et al., 2014). The binding of a miRNA to a candidate target mRNA is considered more likely if it is stable. Stability can be estimated by calculating

ΔG or free energy, negative ΔG means there is less energy available to bind thus stability is deemed to be increased. Site accessibility is a measure of the ease with which a miRNA can locate and hybridise with an mRNA target. Following transcription, mRNA assumes a secondary structure which can interfere with a miRNA's ability to bind to a target site. To assess the likelihood that an mRNA is the target of a miRNA, the predicted amount of energy required to make a site accessible to a miRNA can be evaluated (Mahen, Watson, Cottrell, & Fedor, 2010).

An increasing collection of prediction tools are available, each with a distinct approach to miRNA target prediction (Peterson et al., 2014). It is thought that in order to find true miRNA targets they must be flagged in more than two prediction tools (Madden et al., 2010; Sun et al., 2010). Two recent reviews outlined the features of numerous miRNA prediction tools and DIANA stood out from other prediction tools due to its range of capabilities, ease of use, relatively current input data and maintenance of the software (Eulalio & Mano, 2015; Peterson et al., 2014). DIANA miRPath highlights targets that are also predicted by two well-known prediction tools and this database is capable of detecting pathways targeted by single or multiple miRNAs. DIANA miRPath utilises complex algorithms incorporating all four of the common features; seed match, conservation, free energy, and site accessibility. It can also select between *in silico* predicted miRNA gene targets and experimentally validated targets. MiRNA and pathway information are then related back to biologically relevant genes and pathways found in Kyoto Encyclopaedia of Genes and Genomes (KEGG) (Paraskevopoulou et al., 2013; Vlachos et al., 2012).

MiRNAs regulate many different targets, individual 3' UTRs also contain binding sites for multiple miRNAs, allowing for elaborate and complicated networks in which redundancy and cooperation between miRNAs determine the effect on gene expression (Bartel, 2009; Martinez & Walhout, 2009; Obermayer & Levine, 2014; van Rooij, 2011). The number and distribution of miRNA binding sites are particularly important. Studies have demonstrated that two sites in the same or different miRNAs can act synergistically and that the distance between neighbouring miRNA binding sites affects the strength of the targets down regulation (Koscianska, Witkos, Kozłowska, Wojciechowska, & Krzyzosiak, 2015). Specifically, optimal down regulation was

observed when the distance between the 3' end of the first miRNA site and the 5' end of the subsequent miRNA was > 7 and < 40 nt and when the 5' ends of both miRNA seeds were separated by between 13 and 35 nt. Therefore the target site's activity depends on its surrounding context (Grimson et al., 2007; Saetrom et al., 2007). TargetScan allows the user to input gene names and search for predicted miRNA binding sites in the 3'UTR of the gene of interest. The output screen shows the position of the predicted miRNA binding sites and ranks them by the probability of conserved targeting (P_{CT}). The conservation of the predicted binding site in the 3' UTR is determined following the analysis of possible subsequence's (Lewis et al., 2005). Since one 3' UTR can contain multiple target sites, an aggregate P_{CT} is provided, the closer the P_{CT} score is to 1.0 the more likely it is to be conserved (Friedman et al., 2009). Therefore the final aim of the last part of this chapter is to use bioinformatics to identify miRNA regulated genes in a biologically relevant context using DIANA miRPath and to see if these genes contain predicted miRNA binding sites in TargetScan for the 24 miRNAs that were identified experimentally, given that miRNAs work in complex networks.

5.2 Results

5.2.1 Optimising miRNA Mimics for Luciferase Gene Reporter Assays

At the beginning of chapter four we hypothesised that miRNAs may be induced in response to SLPs from *C. difficile* and that these miRNA profiles differed between ribotypes. Subsequently we confirmed this hypothesis and found that 24 miRNAs were differentially regulated in response to SLPs from RT 001 and RT 027. We choose four miRNAs for further validation and found miR-146a, miR-155, let-7e and miR-145 were differentially regulated in response to SLPs from RT 001 and RT 027 in both a human and murine cell line. We also hypothesised that the miRNAs induced by SLPs modulate TLR4 signalling, given that in Chapter 3 SLPs from RT 027 activated IRF3 signalling but SLPs from RT 001 failed to induce this response. A common method to determine miRNA functionality is to transfect cells with both luciferase reporter constructs and increasing the amounts of the miRNA of interest with chemically synthesised miRNA mimics (van Rooij, 2011). The advantage of introducing a miRNA is that if the miRNA actually targets the binding site in the 3'UTR region, there will be a dose-dependent decrease in gene expression and this can be determined from the luciferase read out. To accurately assess whether miRNA/mRNA regulation occurs, transfection experiments should be performed in the cell type of interest where all endogenously expressed cofactors are present (Bartel, 2009). In chapter 3 we established a luciferase reporter gene assay for NF- κ B and IRF3 using Hek TLR4/MD2/CD14 cells. These cells contain the machinery necessary for TLR4 signalling and they express all essential endogenous cofactors. We decided to utilise the already established luciferase gene reporter assay to assess if the miRNAs of interest modulate both arms of the TLR4 signalling pathway by transfecting miRNA mimics for these 4 miRNAs in Hek TLR4/MD2/CD14 cells along with plasmid DNA for NF- κ B and IRF3. Seeing as IL-8 and RANTES cytokine production was well aligned with NF- κ B and IRF3 signalling in chapter 3, we decided to include ELISA analysis in our study.

We began by optimising the concentration of each of the miRNA mimics to transfect into Hek TLR4/MD2/CD14 cells, initially we used cells stimulated with LPS as a model to study this. Hek TLR4/MD2/CD14 cells were transfected with plasmid DNA required for NF- κ B and IRF3 signalling. At the time of transfection increasing amounts of

miRNA mimics for miR-146a, miR-145, let-7e and miR-155 were added to the transfection mixes (0-100 nM). 24 hours post transfection cells were stimulated with LPS for 24 hours and IL-8 & RANTES were measured from cell supernatants using ELISA. We first examined the effect of miRNA mimics over expressing miR-146a. Hek TLR4/MD2/CD14 cells produced minimal levels of IL-8 however when stimulated with LPS, IL-8 production was increased to 2390 pg/mL. Transfection of 1 nM, 5 nM, 10 nM, 50 nM and 100 nM miR-146a mimic did not affect IL-8 production when cells were stimulated with LPS, levels remained at approximately 2400 pg/mL. In contrast miRNA mimics over expressing miR-146a decreased RANTES production in a dose dependent manner in response to LPS see **Figure 5.2.1**. Hek TLR4/MD2/CD14 cells produced minimal levels of RANTES which was increased to 100 pg/mL when cells were stimulated with LPS. Transfection of 1 nM, 5 nM, 10 nM, 50 nM and 100 nM miR-146a mimic decreased RANTES production to 55 pg/mL ($p \leq 0.001$), 45 pg/mL ($p \leq 0.001$), 40 pg/mL ($p \leq 0.001$) 30 pg/mL ($p \leq 0.001$) and 20 pg/mL ($p \leq 0.001$) respectively when cells were stimulated with LPS.

We then examined the effect of miRNA mimics over expressing miR-145. Hek TLR4/MD2/CD14 cells produced minimal levels of IL-8, however when stimulated with LPS, IL-8 production was increased to 1500 pg/mL. Transfection of 1 nM, 5 nM, 10 nM, 50 nM and 100 nM miR-146a mimic did not affect IL-8 production when cells were stimulated with LPS, levels remained at approximately 1300 pg/mL. In contrast miRNA mimics over expressing miR-145 decreased RANTES production in a dose dependent manner in response to LPS see **Figure 5.2.2**. Hek TLR4/MD2/CD14 cells produced minimal levels of RANTES, this was increased to 100 pg/mL when cells were stimulated with LPS. Transfection of 1 nM, 5 nM, 10 nM, 50 nM and 100 nM miR-145 mimic decreased RANTES production to 50 pg/mL ($p \leq 0.001$), 35 pg/mL ($p \leq 0.001$), 35 pg/mL ($p \leq 0.001$), 54 pg/mL ($p \leq 0.001$) and 20 pg/mL ($p \leq 0.001$) respectively when cells were stimulated with LPS.

We then studied the effect of miRNA mimics over expressing miR-155. Hek TLR4/MD2/CD14 cells produced minimal levels of IL-8 however when stimulated with LPS, IL-8 production was increased to 2600 pg/mL. Transfection of 1 nM, 5 nM, 10 nM, 50 nM and 100 nM miR-155 mimic did not affect IL-8 production when cells were

stimulated with LPS, levels remained at approximately 2400 pg/mL. In contrast miRNA mimics over expressing miR-155 decreased RANTES production in a dose dependent manner in response to LPS see **Figure 5.2.3**. Hek TLR4/MD2/CD14 cells produced minimal levels of RANTES, this was increased to 40 pg/mL RANTES. Transfection of 1 nM, 5 nM, 10 nM, 50 nM and 100 nM miR-155 mimic decreased RANTES production to 22 pg/mL ($p \leq 0.001$), 25 pg/mL ($p \leq 0.001$), 20 pg/mL ($p \leq 0.001$), 10 pg/mL ($p \leq 0.001$) and 8 pg/mL ($p \leq 0.001$) respectively when cells were stimulated with LPS.

Lastly we examined the effect of miRNA mimics over expressing let-7e. Hek TLR4/MD2/CD14 cells produced minimal levels of IL-8 however when stimulated with LPS, IL-8 production was increased to 2500 pg/mL. Transfection of 1 nM, 5 nM, 10 nM, 50 nM and 100 nM let-7e mimic did not affect IL-8 production when cells were stimulated with LPS, levels remained at approximately 2600 pg/mL. In contrast miRNA mimics over expressing let-7e decreased RANTES production in response to LPS see **Figure 5.2.4**. Hek TLR4/MD2/CD14 cells produced minimal levels of RANTES, this was increased to 140 pg/mL when cells were stimulated with LPS. Transfection of 1 nM, 50 nM and 100 nM let-7e mimic decreased RANTES production to 60 pg/mL ($p \leq 0.05$), 106 pg/mL (ns) and 80 pg/mL ($p \leq 0.05$) respectively when cells were stimulated with LPS. 10 nM let-7e mimic did not significantly decrease or increase RANTES production when cells were stimulated with LPS. On the other hand 5 nM let-7e mimic increased RANTES production to 195 pg/mL ($p \leq 0.05$) when cells were stimulated with LPS.

Given that 100 nM of each of the miRNA mimics affected RANTES production we choose this concentration for all further studies. Negative control miRNA mimics consist of random sequences of miRNA mimic molecules that do not produce identifiable effects on known miRNA functions. We incorporated 100 nM of the negative control miRNA mimic into our study to make sure results were specific and not due to the effects of transient transfection. In contrast the positive control miRNA mimic miR-1 is known to down regulate many genes at the mRNA level and has been used as a positive control miRNA mimic in previous studies (Wendlandt et al., 2012). We needed to establish if the miRNA mimics had the ability to bind to the 3'UTR

region of our NF- κ B and IRF3 constructs to see if they were suitable for our study. Therefore we incorporated this positive control miR-1 miRNA mimic into our study.

We also wanted to make sure that cellular viability of the Hek TLR4/MD2/CD14 cells would not be affected by transient transfection with plasmid DNA and the miRNA mimics followed by cell stimulation. We used an “MTS” cytotoxicity assay to measure cell viability. Hek TLR4/MD2/CD14 cells were transfected with plasmid DNA required for NF- κ B and IRF3. Both sets of plasmid DNA were co-transfected with constitutively expressed TK renilla luciferase and 100 nM of each of the miRNA mimics including the positive and negative control miRNA mimics. 24 hours post transfection cells were stimulated with LPS, SLPs from RT 001 and RT 027 for 24 hours. Cellular viability was then assessed using the Cell titer 96 Aqueous One solution containing MTS. Results were expressed as a percentage of untreated cells and cells treated with 10% DMSO were used as a positive control see **Figure 5.2.5**. Percentage viability did not fall below 75%, therefore transient transfection and stimulation did not have any significant cytotoxic effects on the Hek TLR4/MD2/CD14 cells.

Luciferase activity in Hek TLR4/MD2/CD14 cells transfected with NF- κ B and IRF3 were measured. Both sets of plasmid DNA were co-transfected with constitutively expressed TK renilla luciferase and 100 nM of the positive and negative control miRNA mimics. 24 hours post transfection cells were stimulated with LPS or SLPs from RT 001 and RT 027 for 24 hours. Lysates were generated and assayed for firefly and renilla activities see **Figure 5.2.6**. Transfection with each of the positive and negative control miRNA mimics did not affect NF- κ B signalling, fold change remained at 1.0. NF- κ B was increased in cells stimulated with LPS to 7.5 fold. Transfection of 100 nM positive control mimic decreased NF- κ B expression to 4.0 fold ($p \leq 0.001$), while NF- κ B expression remained at 7.5 fold with the addition of 100 nM negative control mimic. NF- κ B increased in cells stimulated with SLPs from RT 001 to 4.5 fold. Transfection of 100 nM positive control mimic decreased NF- κ B expression to 1.5 fold ($p \leq 0.05$), while NF- κ B expression remained at 4.5 fold with the transfection of 100 nM negative control mimic. NF- κ B expression was increased in cells stimulated with SLPs from RT 027 to 8.3 fold. Transfection of 100 nM positive control mimic decreased NF- κ B expression to

3.0 fold ($p \leq 0.001$), while NF- κ B expression remained at 8.3 fold with the transfection of 100 nM negative control miRNA mimic.

A similar pattern emerged when we examined IRF3 expression, transfection with each of the positive and negative control miRNA mimics did not affect IRF3 signalling alone, fold change remained at 1.0. IRF3 was increased in cells stimulated with LPS to 7.7 fold. Transfection of 100 nM positive control mimic decreased IRF3 expression to 1.4 fold ($p \leq 0.001$), while IRF3 expression remained at 7.7 fold with the transfection of 100 nM negative control mimic. There was minimal IRF3 expression in cells stimulated with SLPs from RT 001, however this was not significantly increased compared to the control cells. Transfection of 100 nM positive control mimic appeared to decrease IRF3 expression to 0.1 fold (ns), while IRF3 expression remained at the same levels as the control with the transfection of 100 nM negative control mimic. IRF3 expression was increased in cells stimulated with SLPs from RT 027 to 6.0 fold. Transfection of 100 nM positive control mimic decreased IRF3 expression to 0.5 fold ($p \leq 0.001$), while IRF3 expression remained at 6.0 fold with the transfection of 100 nM negative control miRNA mimic.

The profile at gene level was also reflected in IL-8 and RANTES production. Transfection with each of the positive and negative control miRNA mimics did not significantly affect IL-8 production. Control cells produced 640 pg/mL, which was decreased to 370 pg/mL (ns) with the addition of the positive control mimic and remained close to 640 pg/mL with the transfection of the negative control mimic. IL-8 was increased to 2500 pg/mL in response to LPS. Transfection of 100 nM positive control mimic decreased IL-8 production to 1000 pg/mL ($p \leq 0.001$), while IL-8 production remained at 2500 pg/mL with the transfection of 100 nM negative control mimic. IL-8 was increased to 1500 pg/mL in response to SLPs from RT 001. Transfection of 100 nM positive control mimic decreased IL-8 production to 930 pg/mL ($p \leq 0.05$), while IL-8 production remained at 1500 pg/mL with the transfection of 100 nM negative control mimic. IL-8 was increased to 2700 pg/mL in response to SLPs from RT 027. Transfection of 100 nM positive control mimic decreased IL-8 production to 1000 pg/mL ($p \leq 0.001$), while IL-8 production remained at 2500 pg/mL with the transfection of 100 nM negative control miRNA mimic. A similar pattern emerged

when we examined RANTES production. Transfection alone with each of the positive and negative control miRNA mimics did not significantly affect RANTES production. Control cells produced 70 pg/mL, which was decreased to 32 pg/mL (ns) with the transfection of the positive control mimic but remained close to 70 pg/mL with the transfection of the negative control mimic. RANTES production was increased to 350 pg/mL in response to LPS. Transfection of 100 nM positive control mimic decreased RANTES production to 50 pg/mL ($p \leq 0.001$), while RANTES production remained at 400 pg/mL with the transfection of 100 nM negative control mimic. There were low levels of RANTES detected in cells stimulated with SLPs from RT 001, however this was not significant compared to the control cells. Transfection of 100 nM positive control mimic decreased RANTES production to 50 pg/mL ($p \leq 0.05$), while RANTES production remained at similar levels with the transfection of 100 nM negative control mimic. RANTES production increased to 400 pg/mL in response to SLPs from RT 027. Transfection of 100 nM positive control mimic decreased RANTES production to 70 pg/mL ($p \leq 0.001$), while RANTES production remained at similar levels 350 pg/mL with the transfection of 100 nM negative control miRNA mimics.

The positive control miRNA mimic over expressing miR-1 bound to sites in the 3'UTR region of our NF- κ B and IRF3 constructs thus modulating signalling when cells were stimulated with LPS, SLPs from RT 001 and RT 027. The results were not due to the effects of transient transfection as this was confirmed by the use of the negative control. Therefore we could use this method to assess if the four miRNAs of interest modulated NF- κ B and IRF3 signalling in response to LPS, SLPs from RT 001 and RT 027. We over expressed each of the miRNAs of interest using specific mimics and measured luciferase activity and cytokine production.

5.2.2 Mimics Over Expressing miR-146a, miR-145, miR-155 and let-7e Individually Target IRF3 Signalling in Response to LPS but not in Response to SLPs from RT 001 and RT 027

Firstly the effect of over expressing miR-146a on NF- κ B and IRF3 signalling was examined see **Figure 5.2.8**. Transfection with the miRNA mimic over expressing miR-146a alone did not induce NF- κ B or IRF3 signalling, expression remained at 1.0 fold

consistent with the control Hek TLR4/MD2/CD14 cells. NF- κ B was increased to 7.2 fold in response to LPS and these levels remained the same with the transfection of 100 nM miR-146a mimic. NF- κ B was increased to 4.5 fold in response to SLPs from RT 001 and these levels remained the same with the transfection of 100 nM miR-146a mimic. NF- κ B was increased to 7.3 fold in response to SLPs from RT 027 and these levels remained the same with the transfection of 100 nM miR-146a mimic. Conversely IRF3 expression increased to 7.7 fold in response to LPS, however the transfection of miR-146a mimic decreased IRF3 expression to 4.5 fold ($p \leq 0.001$) in response to LPS. IRF3 expression was not significantly increased or decreased in response to SLPs from RT 001 and levels remained at 1.5 fold with the transfection of 100 nM miR-146a mimic. IRF3 expression increased to 6.0 fold in response to SLPs from RT 027 and levels remained the same with the transfection of 100 nM miR-146a mimic. The profile as gene level was also reflected in the production of IL-8 and RANTES see **Figure 5.2.9**. Transfection with the miR-146a mimic alone did not affect IL-8 and RANTES production, as they remained at levels consistent with the control Hek TLR4/MD2/CD14 cells. IL-8 production was increased to 2600 pg/mL in response to LPS and the levels remained around the same levels with the transfection of 100 nM miR-146a mimic. IL-8 production was increased to 1500 pg/mL in response to SLPs from RT 001 and the levels remained the same with the transfection of 100 nM miR-146a mimic. IL-8 production was increased to 2700 pg/mL in response to SLPs from RT 027 and levels decreased to 2500 pg/mL with the transfection of 100 nM miR-146a mimic, however this decrease was not significant. RANTES expression increased to 390 pg/mL in response to LPS, while production decreased to 55 pg/mL ($p \leq 0.001$) with the transfection of 100 nM miR-146a mimic. RANTES production did not either increase or decrease in response to SLPs from RT 001 and levels remained the same with the transfection of 100 nM miR-146a mimic. RANTES production increased to 450 pg/mL in response to SLPs from RT 027 and levels remained the same with the transfection of 100 nM miR-146a mimic.

Next, the effects of over expressing miR-145 on NF- κ B and IRF3 signalling were examined see **Figure 5.2.10**. Transfection with the miRNA mimic over expressing miR-145 alone did not induce NF- κ B or IRF3 signalling, expression remained at 1.0 fold consistent with the control Hek TLR4/MD2/CD14 cells. NF- κ B was increased to 6.8

fold in response to LPS and these levels remained the same with the transfection of 100 nM miR-145 mimic. NF- κ B was increased to 4.7 fold in response to SLPs from RT 001 and decreased to 3.9 fold with the transfection of 100 nM miR-145 mimic however this decrease was not significant. NF- κ B was increased to 7.3 fold in response to SLPs from RT 027 and these levels remained the same with the transfection of 100 nM miR-145 mimic. On the other hand IRF3 expression increased to 7.7 fold in response to LPS, however the transfection of miR-145 mimic decreased IRF3 expression to 4.5 fold ($p \leq 0.001$) in response to LPS. IRF3 expression did not increase or decrease in response to SLPs from RT 001 and levels remained at 1.5 fold with the transfection of 100 nM miR-145 mimic. IRF3 expression increased to 6.0 fold in response to SLPs from RT 027 and levels remained the same with the transfection of 100 nM miR-145 mimic. The profile as gene level were also reflected in the production of IL-8 and RANTES see **Figure 5.2.11**. Transfection with the miR-145 mimic did not affect IL-8 and RANTES production, as they remained at levels consistent with the control Hek TLR4/MD2/CD14 cells. IL-8 production was increased to 2500 pg/mL in response to LPS and the levels remained the same with the transfection of 100 nM miR-145 mimic. IL-8 production was increased to 1500 pg/mL in response to SLPs from RT 001 and the levels remained the same with the transfection of 100 nM miR-145 mimic. IL-8 production was increased to 2700 pg/mL in response to SLPs from RT 027 and levels remained the same with the transfection of 100 nM miR-145. RANTES expression increased to 390 pg/mL in response to LPS, while production decreased to 53 pg/mL ($p \leq 0.001$) with the transfection of the 100 nM miR-145 mimic. RANTES production did not increase or decrease in response to SLPs from RT 001 and levels remained the same with the transfection of the 100 nM miR-145 mimic. RANTES production increased to 450 pg/mL in response to SLPs from RT 027 and increased to 520 pg/mL with the transfection of 100 nM miR-145 mimic however this increase was not significant.

The effect of over expressing miR-155 on NF- κ B and IRF3 signalling was then studied see **Figure 5.2.12**. Transfection with the miRNA mimic over expressing miR-155 alone did not induce NF- κ B or IRF3 signalling, expression remained at 1.0 fold consistent with the control Hek TLR4/MD2/CD14 cells. NF- κ B was increased to 7.2 fold in response to LPS and these levels remained the same with the transfection of 100 nM

miR-155 mimic. NF- κ B was increased to 4.7 fold in response to SLPs from RT 001 and these levels remained the same with the transfection of 100 nM miR-155 mimic. NF- κ B was increased to 7.3 fold in response to SLPs from RT 027 and these levels remained the same with the transfection of 100 nM miR-155 mimic. On the other hand IRF3 expression increased to 7.7 fold in response to LPS, however the transfection of miR-155 mimic decreased IRF3 expression to 5.4 fold ($p \leq 0.001$) in response to LPS. IRF3 expression was not increased or decreased in response to SLPs from RT 001 and levels remained at 1.5 fold with the transfection of the 100 nM miR-155 mimic. IRF3 expression increased to 6.0 fold in response to SLPs from RT 027 and decreased to 5.5 fold with the transfection of the 100 nM miR-155 mimic however this decrease was not significant. The profile as gene level was also reflected in the production of IL-8 and RANTES see **Figure 5.2.13**. Transfection with the miR-155 mimic did not affect IL-8 and RANTES production, as they remained at levels consistent with the control Hek TLR4/MD2/CD14 cells. IL-8 production was increased to 2500 pg/mL in response to LPS and the levels remained the same with the transfection of 100 nM miR-155 mimic. IL-8 production was increased to 1500 pg/mL in response to SLPs from RT 001 and the levels remained the same with the transfection of 100 nM miR-155 mimic. IL-8 production was increased to 2700 pg/mL in response to SLPs from RT 027 and decreased to 2300 pg/mL with the transfection of 100 nM miR-155 mimic however this decrease was not significant. RANTES expression increased to 350 pg/mL in response to LPS, while production decreased to 40 pg/mL ($p \leq 0.001$) with the transfection of 100 nM miR-155 mimic. RANTES production did not increase or decrease in response to SLPs from RT 001 and levels remained the same with the transfection of 100 nM miR-155 mimic. RANTES production increased to 450 pg/mL in response to SLPs from RT 027 and levels remained the same with the transfection of 100 nM miR-155 mimic.

Lastly the effect of over expressing let-7e on NF- κ B and IRF3 signalling was studied see **Figure 5.2.14**. Transfection with miRNA mimic over expressing let-7e alone did not induce NF- κ B or IRF3 signalling, expression remained at 1.0 fold consistent with the control Hek TLR4/MD2/CD14 cells. NF- κ B was increased to 6.8 fold in response to LPS and these levels remained the same with the transfection of 100 nM let-7e mimic. NF- κ B was increased to 4.7 fold in response to SLPs from RT 001 and these levels remained the same with the transfection of the 100 nM let-7e mimic. NF- κ B was

increased to 7.3 fold in response to SLPs from RT 027 and these levels remained the same with the transfection of 100 nM let-7e mimic. On the other hand IRF3 expression increased to 7.7 fold in response to LPS, however the transfection of let-7e mimic decreased IRF3 expression to 6.0 fold ($p \leq 0.001$) in response to LPS. IRF3 expression was not increased or decreased in response to SLPs from RT 001 and levels remained at 1.5 fold with the transfection of 100 nM let-7e mimic. IRF3 expression increased to 6.0 fold in response to SLPs from RT 027 and levels remained the same with the transfection of 100 nM let-7e mimic. The profile as gene level was also reflected in the production of IL-8 and RANTES see **Figure 5.2.15**. Transfection with let-7e mimic did not affect IL-8 and RANTES production, as they remained at levels consistent with the control Hek TLR4/MD2/CD14 cells. IL-8 production was increased to 2500 pg/mL in response to LPS and the levels remained the same with the transfection of 100 nM let-7e mimic. IL-8 production was increased to 1500 pg/mL in response to SLPs from RT 001 and the levels remained the same with the transfection of 100 nM let-7e mimic. IL-8 production was increased to 2700 pg/mL in response to SLPs from RT 027 and levels remained the same with the transfection of 100 nM let-7e mimic. RANTES expression increased to 350 pg/mL in response to LPS, while production decreased to 160 pg/mL ($p \leq 0.001$) with the transfection of the 100 nM let-7e mimic. RANTES production did not increase or decrease in response to SLPs from RT 001 and levels remained the same with the addition of the 100 nM let-7e mimic. RANTES production increased to 420 pg/mL in response to SLPs from RT 027 and levels remained the same with the transfection of the 100 nM let-7e mimic.

Therefore miRNA mimics over expressing miR-146a, miR-145, miR-155 and let-7e reduced IRF3 signalling in response to LPS, this was also reflected in RANTES production. We could not relate miRNA function of the individual miRNAs to IRF3 signalling in response to SLPs from RT 001 and RT 027 in this experiment. LPS and SLPs from ribotype 027 signal through the same receptor and activate NF- κ B and IRF3 downstream of TLR4. However miR-146a, miR-145, miR-155 and let-7e appear to regulate IRF3 signalling differently in response to LPS compared with SLPs from ribotype 027.

5.2.3 MiRNAs were Enriched from RNA Derived from Colonic Tissue from an *in vivo C. difficile* Infection Model

Up until now we have exclusively looked at miRNAs regulated in response to SLPs from RT 001 and RT 027 in a human and murine cell line. We identified four miRNAs of interest miR-146a, miR-145, miR-155 and let-7e. The next part of this chapter was to examine these miRNAs in colonic tissue from an *in vivo C. difficile* infection model, where mice had been infected with *C. difficile* spores from RT 001 and RT 027. Total RNA samples derived from colonic tissue had already been generated by Dr. Mark Lynch, a member of the Immunomodulation Research group (DCU), as part of his PhD research project. C57BL/6J mice were infected with *C. difficile* using an antibiotic-induced model of mouse infection (Chen et al., 2008). There were four animals per treatment group: control group n=4, group treated with RT 001 n=4 and group treated with RT 027 n=4. Mice were treated for three days with an antibiotic mixture of Kanamycin (400 µg/mL), Gentamicin (35 µg/mL), Colistin (850 U/mL), Metronidazole (215 µg/mL) and Vancomycin (45 µg/mL) in the drinking water. Mice were subsequently given autoclaved water. On day 5, mice were injected intraperitoneally with Clindamycin (10 mg/kg). Mice were infected with 10^3 *C. difficile* spores on day six by oral gavage. The colon was harvested from uninfected and infected mice after day three and seven of infection. Squares of tissue from the distal colon roughly 5 mm³ were cut for the preparation of RNA. Total RNA was extracted using the NucleoSpin® RNA II Total RNA Isolation Kit (Macherey-Nagel) as per manufacturer's instructions. The RNA was quantified using a NanoDrop Spectrophotometer and then stored in the -80°C freezer until ready for use (Lynch 2014, unpublished). Firstly we had to determine if total RNA generated contained miRNAs and small RNA endogenous controls for our study.

Small RNAs were enriched from 50 µg total RNA from samples generated in the *C. difficile* infection model using the mirVana™ miRNA Isolation Kit (Ambion) as per manufacturer's instructions. The RNA was quantified following isolation using the NanoDrop® ND-1000 Spectrophotometer. The purity of the RNA was also examined by measuring the 260 nm and 280 nm absorption wavelengths, where RNA with an A260/A280 ratio between 1.8-2.1 was considered pure. RNA samples were

subsequently run on 1% agarose gels where the 28S and 18S rRNA bands were assessed to confirm integrity. Two bands were seen on the gel indicative of the 18S rRNA and 28S rRNA band (see **Appendix D**). 100 ng enriched RNA was converted to first strand cDNA from each of the four biological replicates per treatment group and the products of which were used in a pre amplification reaction. Individual murine TaqMan miRNA assays with three technical replicates per group were run for each miRNAs and endogenous controls examined. The qPCR data was analysed using ExpressionSuite software, the threshold was set to 0.1 and the max Ct set to 37.0, as previously determined. There was also no miRNA expression detected in assays containing NTC (data not shown). We found that the RNA samples contained each of the three small RNA endogenous controls. snoRNA202 was chosen as the endogenous control for this study as it out performed snoRNA234 and mammU6 in samples from day 3 and day 7 (see **Appendix F**). Relative gene expression was calculated and the student's t-test was used to test for significance between mice treated with RT 001 and RT 027. Murine miR-146a, miR-145, miR-155 and let-7e were present in samples derived from colonic tissue from the *in vivo C. difficile* infection model.

5.2.4 MiR-146a, miR-145, miR-155 and let-7e were Differentially Regulated in Colonic Tissue During *C. difficile* Infection with RT 001 and RT 027

MiR-146a was differentially regulated in colonic tissue from mice infected with RT 001 and RT 027, three and seven days post infection see **Figure 5.2.16**. Colonic tissue from control mice contained low levels of miR-146a. Three days post infection, colonic tissue from mice infected with RT 001 had a 1.4 fold increase in miR-146a compared to tissue from control mice. Colonic tissue from mice infected with RT 027 had a 0.7 fold decrease in miR-146a compared to tissue from control mice. MiR-146a was significantly decreased ($p \leq 0.05$) in colonic tissue from mice infected with RT 027 compared with colonic tissue from mice infected with RT 001, three days post infection. However miRNA profiles changed seven days post infection. Colonic tissue from mice infected with RT 001 had a 1.2 fold increase in miR-146a compared to tissue from control mice. Whereas colonic tissue from mice infected with RT 027 had a 9.4 fold increase in miR-146a compared to tissue from control mice. MiR-146a was significantly increased ($p \leq 0.001$) in colonic tissue from mice infected with RT 027

compared with colonic tissue from mice infected with RT 001, seven days post infection.

MiR-145 was differentially regulated in colonic tissue from mice infected with RT 001 and RT 027, three and seven days post infection see **Figure 5.2.17**. Colonic tissue from control mice contained low levels of miR-145. Three days post infection, miR-145 expression remained the same in colonic tissue from mice infected with RT 001 as in tissue from control mice. Colonic tissue from mice infected with RT 027 had a 0.2 fold decrease in miR-145 compared to tissue from control mice. MiR-145 was significantly decreased ($p \leq 0.01$) in colonic tissue from mice infected with RT 027 compared with colonic tissue from mice infected with RT 001, three days post infection. However miRNA profiles changed seven days post infection. Colonic tissue from mice infected with RT 001 had a 0.7 fold decrease in miR-145 compared to tissue from control mice. Whereas colonic tissue from mice infected with RT 027 had a 4.6 fold increase in miR-145 compared to tissue from control mice. MiR-145 was significantly increased ($p \leq 0.001$) in colonic tissue from mice infected with RT 027 compared with colonic tissue from mice infected with RT 001, seven days post infection.

MiR-155 was differentially regulated in colonic tissue from mice infected with RT 001 and RT 027, three days post infection see **Figure 5.2.18**. Colonic tissue from control mice contained low levels of miR-155. Three days post infection, colonic tissue from mice infected with RT 001 had a 25.6 fold increase in miR-155 compared to tissue from control mice. Colonic tissue from mice infected with RT 027 had a 1.7 fold increase in miR-155 compared to tissue from control mice. MiR-155 was significantly decreased ($p \leq 0.01$) in colonic tissue from mice infected with RT 027 compared with colonic tissue from mice infected with RT 001, three days post infection. However miRNA profiles changed seven days post infection. Colonic tissue from mice infected with RT 001 had a 1.3 fold increase in miR-155 compared to tissue from control mice. Colonic tissue from mice infected with RT 027 had a 1.5 fold increase in miR-155 compared to tissue from control mice. MiR-155 expression was not significantly different when we compared its expression in colonic tissue from mice infected with RT 027 with colonic tissue from mice infected with RT 001, seven days post infection.

Let-7e was differentially regulated in colonic tissue from mice infected with RT 001 and RT 027, three days post infection see **Figure 5.2.19**. Colonic tissue from control mice contained low levels of let-7e. Three days post infection, colonic tissue from mice infected with RT 001 had a 3.2 fold increase in let-7e compared to tissue from control mice. Colonic tissue from mice infected with RT 027 had a 1.2 fold increase in let-7e compared to tissue from control mice. Let -7e was significantly decreased ($p \leq 0.01$) in colonic tissue from mice infected with RT 027 compared with colonic tissue from mice infected with RT 001, three days post infection. However miRNA profiles changed seven days post infection. Colonic tissue from mice infected with RT 001 had a 1.3 fold increase in let-7e compared to tissue from control mice. Colonic tissue from mice infected with RT 027 had a 1.6 fold increase in let-7e compared to tissue from control mice. Let-7e expression was not significantly different when we compared its expression in colonic tissue from mice infected with RT 027 with colonic tissue from mice infected with RT 001, seven days post infection.

5.2.5 Bioinformatics Analysis Reveals miRNAs Induced by SLPs from RT 001 and RT 027 Target Genes Involved in Essential Cell Signalling Pathways

In chapter three we identified 24 miRNAs that were differentially regulated by SLPs from RT 001 and RT 027. We validated our results and showed miR-146a, miR-145, miR-155 and let-7e were differentially regulated in response to SLPs from RT 001 and RT 027 in a human and murine cell line. At the beginning of this chapter we were unable to link miR-146a, miR-145, miR-155 and let-7e individually to NF- κ B and IRF3 signalling downstream of TLR4 in response to SLPs from RT 001 and RT 027. However we confirmed that miR-146a, miR-145, miR-155 and let-7e were differentially regulated in colonic tissue during *C. difficile* infection with whole bacteria from RT 001 and RT 027. It is still possible that miRNA expression induced by SLPs modulate infection with RT 001 and RT 027. We know from the literature that miRNAs regulate many different targets, individual 3' UTRs also contain binding sites for multiple miRNAs, allowing for elaborate and complicated networks in which redundancy and cooperation between miRNAs determine the effect on gene expression (Bartel, 2009; Martinez & Walhout, 2009; Obermayer & Levine, 2014; van Rooij, 2011). We decided to utilise bioinformatics to identify possible miRNA/pathway/gene

interactions from the list of 24 miRNAs we showed were differentially regulated by SLPs from RT 001 and RT 027 experimentally.

In the literature it is suggested that to select consensus targets, they must be identified by different prediction tools (Sun et al., 2010). We choose DIANA miRPath to carry out our searches as this prediction tool highlights targets that are also predicted by miRanda and TargetScan, two well-known prediction tools and targets which have also been verified experimentally in TarBase v6.0 (Paraskevopoulou et al., 2013; Vlachos et al., 2012). DIANA miRPath uses miRNA names according to version 18 of miRBase, therefore we made sure we had the correct miRNA name for our targets according to this version. We inputted the list of miRNAs into miRConvertor on another database called miRSystem and crossed references the miRNA accession of each of our 24 miRNAs of interest (see **Appendix G**). DIANA miRPath v2.0 is a free web-server which utilises miRNA targets in coding regions and 3'UTR regions provided by the DIANA-microT-CDS algorithm. The lists of 24 miRNAs of interest were inputted into the prediction tool where a posteriori analysis was performed. The significance levels between all possible miRNA pathway pairs were calculated using enrichment analysis. The previously calculated significance levels were combined with this to provide a merged p-value for each pathway by applying Fisher's combined probability method. DIANA miRPath predicted that the 24 miRNAs of interest targeted 2551 genes in 146 different pathways found in KEGG pathway database, 54 of these pathways had p-values where $p \leq 0.05$ (see **Appendix G**). DIANA miRPath generated a heat map showing the 24 miRNAs versus 54 of the pathways where miRNA/gene/pathway interactions where $p \leq 0.05$. Darker colours represent lower significance values and the adjacent dendrograms depict hierarchical clustering. We identified miRNAs clustered together in two main clades exhibiting similar pathway targeting patterns see **Figure 5.2.20**. The first clade contained two branches which were further sub divided, group 1 contained branch tips for miR-221-3p, miR-1292, miR-215, miR-145-5p, miR-125a-5p, miR-432-3p, miR-146a-5p, miR-24-3p, miR-590-5p, let-7d-5p miR-422a, miR-339-5p and miR-586. Group 2 contained branch tips for let-7b-5p, let-7c, let-7e-5p and miR-374a-5p. The second clade contained two branches which were further sub divided, group 1 contained branch tips for miR-148b-3p, miR-152, miR-9-3p, miR-155, miR-132-3p, miR-543 while group 2 contained a single branch tip for miR-9-5p.

The top five KEGG pathways were selected for further analysis from the list of 54 pathways generated in DIANA miRPath where miRNA/gene/pathway interactions had p-values of $p \leq 0.05$ see **Table 5.2.1**. DIANA miRPath predicted 15 genes were targeted by 6 of the miRNAs in ECM receptor interactions ($p \leq 1E-16$), **Figure 5.2.21** shows an image generated in KEGG from this data. Genes highlighted in orange such as COL4A1, LAMA4, ITGA5, ITGA9, ITGA7 and ITGB6 present predicted targets for multiple miRNAs while genes highlighted in green were predicted not to be targeted by the miRNAs of interest. DIANA miRPath predicted 42 genes were targeted by 9 of the miRNAs in TGF- β signalling ($p \leq 1E-16$). **Figure 5.2.22** shows an image generated in KEGG from this data. Genes highlighted in yellow such as GDF5, BMPR1A, SMAD7, SMURF2, LTBP1, SMAD3, SMAD2, CREBP, ROCK2, PPP2CB, RPS6KB1, FST, ACVR2A and PITX2 represent predicted targets for an individual miRNA. Genes highlighted in orange such as NOG, SMAD5, ID4, MAPK4, SKP1, DCN, TGFB2, TGFB1, TGFB2, ZFYVE, E2F5, TFDPs, INHRA, ACVR2A and ACVR1C represent predicted targets for multiple miRNAs and genes highlighted in green were predicted not to be targeted by the miRNAs of interest. DIANA miRPath predicted 98 genes were targeted by 10 of the miRNAs in MAPK signalling ($p \leq 1E-16$). **Figure 5.2.23** shows an image generated in KEGG from this data. Genes highlighted in yellow such as CACNB4, CHUK, RELA, NTF3, NTRK2, RASGRP1, RPSKA1, FGFR1, PDGFRB, STMN1, PLA2G4E, RAF1, GNA12, MYC, DUSP5, PPP2R1, TRAF6, AKT1, MAPK1, MAX, MAP2K AND GADD4 represent predicted targets for an individual miRNA. Genes highlighted in orange such as NGF, BDNF, FGF7, SOS1, KRAS, RASA, RASGRP2, RAP1, MAPK1, ELK4, SRF, FOS, IL1A, FASLG, TGFBR, CASP3, PAK2, MAP4K, FLNA, CRK, NFATC, HSPA8, MAP2K and TAOK1 represent predicted targets for multiple miRNAs and genes highlighted in green were predicted not to be targeted by the miRNAs of interest.

DIANA miRPath predicted 121 genes were targeted by 11 of the miRNAs in PI3K-Akt signalling pathway ($p \leq 1E-16$). **Figure 5.2.24** shows an image generated in KEGG from this data. Genes highlighted in yellow such as EFNA1, PKN2, PRKCA, RAF2, IL2, ITGA8, PTK, AKT2, RELA, CHUK, CREB2, FASLG, PPP2CB and GSK3B represent predicted targets for an individual miRNA. Genes highlighted in orange such as LAMA4, TEK, IL6R, ITGB1, PTEN, PIK3CA, SOS1, KRAS, PRKA, TSC1, EIF4E,

RPS6KB1, SGK3, MAPK1, MYB, PIK2CA, CDKN1A and FOXO3 represent predicted targets for multiple miRNAs and genes highlighted in green were predicted not to be targeted by the miRNAs of interest. DIANA miRPath predicted 74 genes were targeted by 10 miRNAs in Focal adhesion ($p \leq 1.1E-16$). **Figure 5.2.25** shows an image generated in KEGG from this data. Genes highlighted in yellow such as ITGA6, ITGB1, RASGRF, ROCK2, SRC, VCL, MYLK, AKT3, PAK4, CTNNB1, SHC1 and RAF1 represent predicted targets for an individual miRNA. Genes highlighted in orange such as LAMA4, ARHGAP2, PPP1CB, ACTB, FLNA, CAV2, PTK2, PTEN, PIK3CA, VAV3, CCND2, CRK, RAP1B, MAPK8, IGF1, FLT1, MAPK4 and XIAP represent predicted targets for multiple miRNAs and genes highlighted in green were predicted not to be targeted by the miRNAs of interest.

5.2.6 Forty-nine Genes Crossed Two or More Pathways from the Top Five Analysed, Most Genes had Predicted Binding sites in the 3'UTR regions for the miRNAs of Interest according to TargetScan

DIANA miRPath analysis identified 350 genes in total from the top 5 KEGG pathways that were targeted by the miRNAs of interest. The number and distribution of miRNA binding sites is particularly important. Studies have demonstrated that two sites in the same or different miRNAs can act synergistically and that the distance between neighbouring miRNA binding sites affects the strength of the target down regulation (Koscianska et al., 2015). Specifically, optimal down-regulation was observed when the distance between the 3' end of the first miRNA site and the 5' end of the subsequent one was > 7 and < 40 nt and when the 5' ends of both miRNA seeds were separated by between 13 and 35 nt (Grimson et al., 2007; Saetrom et al., 2007). However, miRNA target interactions are not only bidirectional but rather form complex networks as previously mentioned, therefore the target site's activity will depend on its surrounding context (Saetrom et al., 2007). The online tool TargetScan searches for conserved seed regions of 7 and 8 nucleotides in length as well as for 3' compensated sites in 3'-UTRs. It ranks its predicted results based on further miRNA/mRNA binding properties including seed pairing, stability and target site abundance. Therefore we inputted each of the 350 genes into the TargetScan database to confirm if there were possible binding

sites in the 3'UTR regions of each gene for any of the 24 miRNAs which were expressed in response to SLPs from RT 001 and RT 027.

We identified the individual positions within the 3'UTR region, the type of seed match and the probability of conserved targeting P_{CT} (see **Appendix G**). Upon analysis of the gene lists we noticed that some genes came up as targets in more than one pathway. Therefore we cross referenced the gene lists from the 5 pathways and found 49 genes crossed two or more pathways see **Table 5.2.2**. MAPK1 was found in four of the five KEGG pathways; Focal adhesion, PI3K-AKT, TGF- β and MAPK signalling, however it did not contain any predicted miRNA binding sites for the miRNAs of interest according to TargetScan. The following genes; ITGA9, COL27A1, ITGB6, ITGA5, COL3A1, ITGA11, COL2A1, COL4A2, COL1A1, ITGA7, COL4A6, COL5A2, COL4A1 and LAMA4, were found in three of the five pathways; ECM-receptor interactions, PI3K-AKT signalling and focal adhesion. All genes except COL27A1, ITGB6 and ITGA7 contained possible binding sites for the miRNAs of interest.

AKT1 and SOS2 were found in three of the five pathways; Focal adhesion, PI3K-AKT and MAPK signalling. SOS1 contained possible binding sites for the miRNAs of interest however AKT1 did not. The following genes; FGF12, NFKB1, NRAS, CHUK, KRAS, SOS1, FGF9, FGF18, NGF, RASGRF1, RELA and FGFR1, were found in two of the five pathways; PI3K-AKT and MAPK signalling. All genes except NFKB1 and FGF18 contained possible binding sites for the miRNAs of interest. RAP1A and MAPK8 were found in two of the five pathways; focal adhesion and MAPK signalling, neither genes contained possible binding sites for the miRNAs of interest. ROCK1, ITGB8 and ROCK2 were found in two of the five pathways; Focal adhesion and TGF- β signalling. ROCK2 and ITGB8 contained possible binding sites for the miRNAs of interest, while ROCK1 did not. The following genes; COL4A5, RAF1, PIK3R3, PDK1, VEGFC, ITGA2, COL1A2, AKT3, COL11A1, PTEN and COL4A4, were found in two of the five pathways; focal adhesion and PI3K-AKT signalling. All genes except VEGFC, ITGA2, AKT3 and COL4A4 contained possible binding sites for the miRNAs of interest. The following genes; PPP2CB, RPS6KB1, PPP2CA and RPS6KB2, were found in two of the five pathways; PI3K-Akt and TGF- β signalling. All genes except PPP2CA and RPS6KB2 contained possible binding sites for the miRNAs of interest.

Analysis showed that some genes were found in the PI3K-Akt signalling pathway only and all genes except PRLR, PPP2R2C, HSP90AA1, IL17R, PPP2R5A, IL4, IL2, THEM4, PPP2R3C, CHRM2, ANGPT1 and FN1 contained possible binding sites for the miRNAs of interest see **Table 5.2.3**. Genes found in the TGF- β signalling pathway only are shown in **Table 5.2.4** and All genes except ID2, SMAD9, SMURF2, BMP5, INHBA, DCN, BMP2, TFDP1, BMPR1A and CREBBP contained possible binding sites for the miRNAs of interest. Genes found to be involved in focal adhesion included; ACTB, SHC1, COL24A1, PPP1CC, PAK7, VCL, CAV2, PPP1R12A, CTNNB1, DIAPH1, SRC, PAK4, MYLK3, BIRC3, VAV3, ARHGAP5, MYLK, XIAO and PPP1CB. All genes except PPP1CC, PAK7, CTNNB1, DIAPH1, MYLK3 and BIRC3 contained possible binding sites for the miRNAs of interest see **Table 5.2.5**. Analysis showed that some genes were found in the MAPK signalling pathway only. All genes except NTRK2, DUSP22, CACNA1G, PTPRQ, DUSP14, RASGRF2, LAMTOR3, RASGRP2, MAP2K6, NFATC2, MYC, HSPA8, MECOM, STMN1, MAP3K2, PPM1B, CACNA2D1, PLA2G4E, MAP3K7 and MAPKAPK2 contained possible binding sites for the miRNAs of interest see **Table 5.2.6**. All 15 genes that were identified as being targeted in the ECM receptor were found in two or more of the other five KEGG pathways.

5.2.7 Genes with Predicted Binding Sites for the miRNAs of Interest are found in Distinctive Groups, Examples from IL-6, NRAS, SMAD2, SOS1 and TRAF6

We selected 5 genes from each of the top 5 KEGG pathways for a more in depth look at the position of potential binding sites for the 24 miRNAs of interest in the 3'UTR region of each of the genes. The IL-6 receptor gene contained possible binding sites for several of the miRNAs which were differentially regulated by SLPs from RT 001 and RT 027 see **Figure 5.2.26**. MiR-125a-5p contained a predicted binding site at position 836-842 (5'-3') on the IL6R 3'UTR (P_{CT} 0.73). MiR-590-5p and miR-155-5p were predicted to be located further downstream on the IL6R gene to miR-125a-5p but in close proximity to each other. MiR-590-5p and miR-155-5p were predicted at position 2954-2961 (P_{CT} 0.78) and 3300-3307 (P_{CT} 0.45) respectively. The 3' end of miR-590-5p was 353 nt away from the 5' end of miR-155, while the 5' end of both miRNAs were 346 nt away. MiR-9-5p, let-7b-5p, let-7c-5p, let-7d-5p and let-7e-5p were predicted to

be located further downstream on the *IL6R* gene from miR-590-5p and miR-155-5p, but in close proximity to each other. MiR-9-5p was predicted at position 4164-4170 (P_{CT} 0.56) and let-7b/c/d/e-5p were all predicted to be at positions 4077-4083 (P_{CT} 0.94). The 3' end of miR-9-5p was 81 nt away from each of the 5' ends of let-7b/c/d/e-5p, while the 5' end of miR-9-5p was 87 nt away from the 5' ends of let-7b/c/d/e-5p. MiRNA binding sites were clustered in three distinct locations on the 3'UTR region of the IL-6 receptor gene.

The *NRAS* gene contained possible binding sites for eight miRNAs which were differentially regulated by SLPs from RT 001 and RT 027 see **Figure 5.2.27**. MiR-152-3p, miR-148b-3p, miR-146a-5p, let-7b-5p, let-7c-5p, let-7d-5p and let-7e-5p had predicted binding sites in close proximity to each other. MiR-152-3p and miR-148b-3p were predicted to be located at position 45-52 (5'-3') on *NRAS* (P_{CT} 0.88). MiR-146a-5p was predicted to be located at position 172-179 (P_{CT} <0.1). The 3' end of miR-152-3p and miR-148b-3p were 134 nt away from the 5' end of miR-146a-5p, while the 5' ends of miR-152-3p and miR-148b-3p were 127 nt away from miR-146a-5p. Let-7b/c/d/e-5p were predicted to be located at position 186-192 (P_{CT} > 0.99). The 3' end of miR-152-3p and miR-148b-3p were 147 nt away from let-7b/c/d/e-5p, while the 3' end of miR-146a-5p was 20 nt away from let-7b/c/d/e-5p. The 5' end of miR-152-3p and miR-148b were 140 nt away from let-7b/c/d/e-5p, while the 5' end of miR-146a-5p was 13 nt away from let-7b/c/d/e-5p. Second binding sites were predicted for let-7b/c/d/e-5p further downstream on the *NRAS* gene at positions 2592-2598 (P_{CT} 0.87). MiR-145-5p had predicted binding site further downstream on the *NRAS* gene at position 3599-3606 (P_{CT} 0.84). MiRNA binding sites were clustered in three distinct locations on the 3'UTR region of the *NRAS* gene and there may be synergy between miR-146a-5p and let-7b/c/d/e-5p between positions 172-192 on the *NRAS* gene.

The *SMAD2* gene contained possible binding sites for ten miRNAs which were differentially regulated by SLPs from RT 001 and RT 027 see **Figure 5.2.28**. MiR-132-3p and miR-125a-5p had predicted binding sites in close proximity to each other. MiR-132-3p was predicted to be located at position 77-83 (5'-3') on *SMAD2* (P_{CT} 0.46). MiR-125a-5p was predicted to be located at position 977-963 (P_{CT} 0.80). The 3' end of miR-132-3p was 851 nt away from the 5' end of miR-125a-5p, while the 5' end of miR-

132-3p was 900 nt away from the 5' end of miR-125a-5p. Predicted binding sites for let-7b-5p, let-7c-5p, let-7d-5p and let-7e-5p were located further downstream from miR-132-3p and miR-125a-5p on the SMAD2 gene. Let-7b/c/d/e-5p had predicted binding sites located at position 3772-3778 (P_{CT} 0.79). Predicted binding sites for miR-145-5p, miR-152-3p, miR-148b and miR-155-5p were located further downstream from 7b/c/d/e-5p on the SMAD2 gene. MiR-145-5p had predicted binding sites located at position 7056-7062 (P_{CT} 0.38). MiR-152-3p and miR-148b-3p had predicted binding sites at positions 8334-8340 (P_{CT} 0.65). The 3' end of miR-145-5p was 1284 nt away from the 5' end of miR-152-3p and miR-148b-3p, while the 5' end of miR-145-5p was 1278 nt away from the 5' end of miR-152-3p and miR-148b-3p. A predicted binding site for miR-155-5p was located at position 8694-8701 (P_{CT} 0.78). The 3' end of miR-145-5p was 1645 nt away from the 5' end of miR-155-5p, while the 3' ends of miR-152-3p and miR-148-3p were 364 nt away from the 5' end of miR-155-5p. The 5' end of miR-145-5p was 1639 nt away from the 5' end of miR-155-5p, while the 5' ends of miR-152-3p and miR-148-3p were 361 nt away from the 5' end of miR-155-5p. MiRNA binding sites were clustered in three distinct locations on the 3'UTR region of the SMAD2 gene.

The SOS1 gene contained possible binding sites for five miRNAs which were differentially regulated by SLPs from RT 001 and RT 027 see **Figure 5.2.29**. MiR-152-3p, miR-148b-3p, miR-9-5p and miR-132-3p had predicted binding sites in close proximity to each other. MiR-152-3p and miR-148b-3p were predicted to be located at position 58-65 (5'-3') on SOS1 (P_{CT} 0.59). MiR-9-5p had a predicted binding site located at position 597-604 (P_{CT} 0.87). The 3' ends of miR-152-3p and miR-148b-3p were 539 nt away from the 5' end of miR-9-5p, while the 5' ends of miR-152-3p and miR-148b-3p were 539 nt away from the 5' end of miR-9-5p. MiR-132-3p had a predicted binding site located at position 798-804 (P_{CT} 0.38). The 3' ends of miR-152-3p and miR-148b-3p were 739 nt away from the 5' end of miR-132-3p, while the 3' end of miR-9-5p was 207 nt away from the 5' end of miR-132-3p. The 5' ends of miR-152-3p and miR-148b-3p were 739 nt away from the 5' end of miR-132-3p, while the 5' end of miR-9-5p was 200 nt away from miR-132-3p. MiR-155-5p was located further downstream than miR-152-3p, miR-148b-3p, miR-9-5p and miR-132-3p on the SOS 1 gene. MiR-155-5p had a predicted binding site located at position 3666-3672 (P_{CT} 0.36).

miRNA binding sites were clustered in two distinct locations on the 3'UTR region of the SOS1 gene. The TRAF6 gene contained possible binding sites for two miRNAs which were differentially regulated by SLPs from RT 001 and RT 027 see **Figure 5.2.30**. Unlike the other genes the miRNAs were clustered in one group on the 3'UTR region. There were three predicted binding sites for miR-146a-5p located at positions 473-480 ($P_{CT} < 0.1$), 538-545 ($P_{CT} < 0.1$) and 1272-1279 ($P_{CT} < 0.1$) respectively. MiR-125a-5p had a predicted binding site located at position 1276-1283 ($P_{CT} 0.60$). The 3' ends of miR-146a-5p were 810, 745 and 11 nt away from the 5' end of miR-125a-5p, while the 5' ends of the miR-146a-5p were 803, 738 and 4 nt away from the 5' end of miR-125a-5p. There may be synergy between miR-146a-5p and miR-125a-5p between positions 1272-1283 on the 3' UTR region of TRAF6.

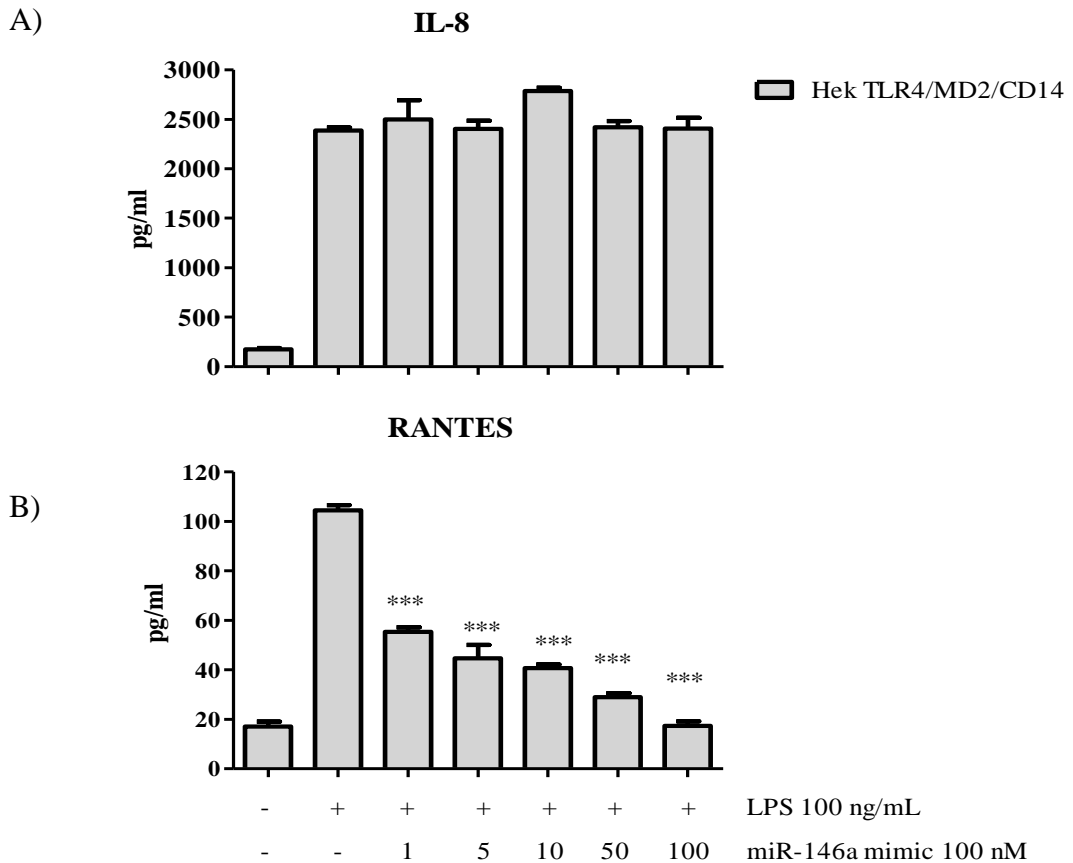


Figure 5.2.1 MiRNA mimic over expressing miR-146a decrease RANTES production in a dose dependent but do not effect IL-8 production in response to LPS. Hek TLR4/MD2/CD14 cells were plated at 1×10^6 cells/mL and allowed to adhere for 18 hours to approximately 60% confluency. The cells were then transfected with NF- κ B (80 ng) or pFA-IRF3 (30 ng) and pFR-regulated firefly luciferase (60 ng). Both sets of plasmid DNA were co-transfected with constitutively expressed TK renilla luciferase (20 ng) and +/- 0-100 nM miR-146a mimic. 24 hours post transfection cells were stimulated with 100 ng/mL for 18 hours. Cells supernatants were collected and human **A)** IL-8 and **B)** RANTES was measured by ELISA. The results show the mean (\pm SEM) measured in triplicate, one-way ANOVA followed by Newman-Keuls analysis was used to determine if differences between groups were significantly different compared to cells stimulated with LPS, where * $p \leq 0.05$, ** $p \leq 0.01$ and *** $p \leq 0.001$. The results are indicative of three independent experiments.

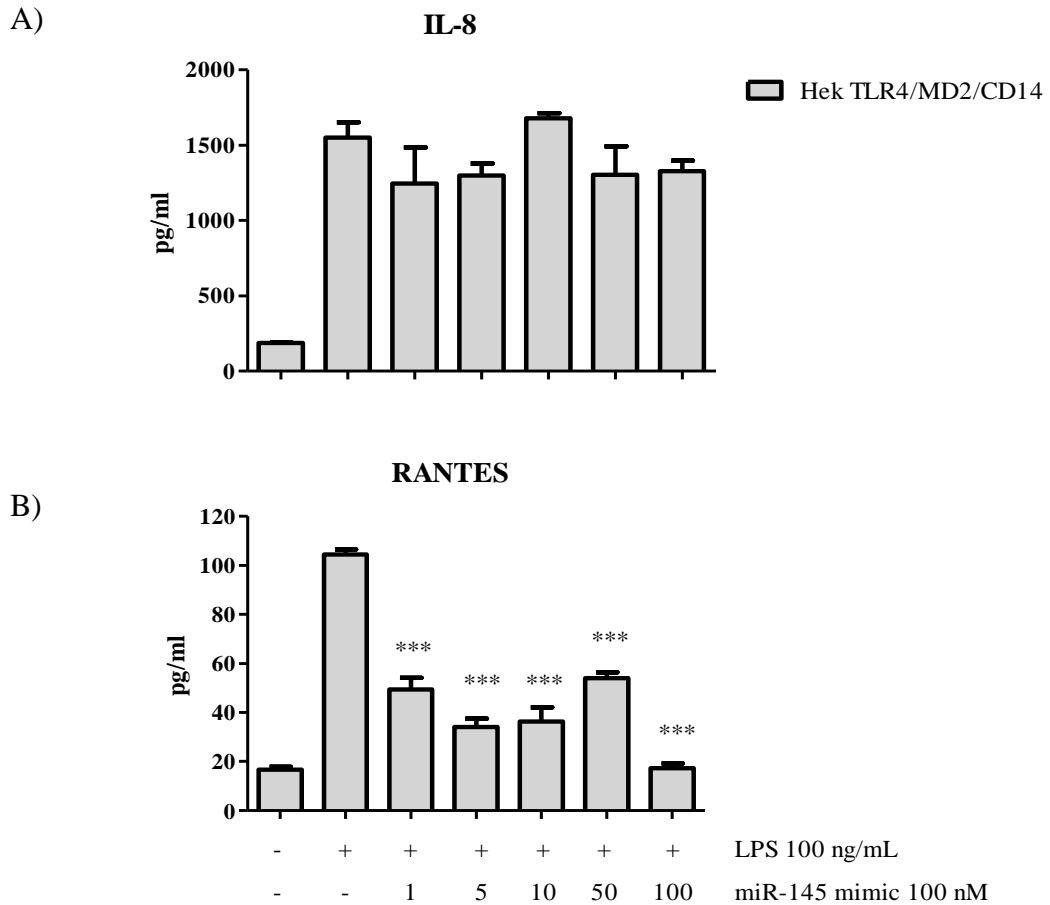


Figure 5.2.2 MiRNA mimic over expressing miR-145 decrease RANTES production in a dose dependent manner but do not significantly affect IL-8 production in response to LPS. Hek TLR4/MD2/CD14 cells were plated at 1×10^6 cells/mL and allowed to adhere for 18 hours to approximately 60% confluency. The cells were then transfected with NF- κ B (80 ng) or pFA-IRF3 (30 ng) and pFR-regulated firefly luciferase (60 ng). Both sets of plasmid DNA were co-transfected with constitutively expressed TK renilla luciferase (20 ng) and +/- 0-100 nM miR-145 mimic. 24 hours post transfection cells were stimulated with 100 ng/mL for 18 hours. Cells supernatants were collected and human **A) IL-8** and **B) RANTES** was measured by ELISA. The results show the mean (\pm SEM) measured in triplicate, one-way ANOVA followed by Newman-Keuls analysis was used to determine if differences between groups were significantly different compared to cells stimulated with LPS, where * $p \leq 0.05$, ** $p \leq 0.01$ and *** $p \leq 0.001$. The results are indicative of three independent experiments.

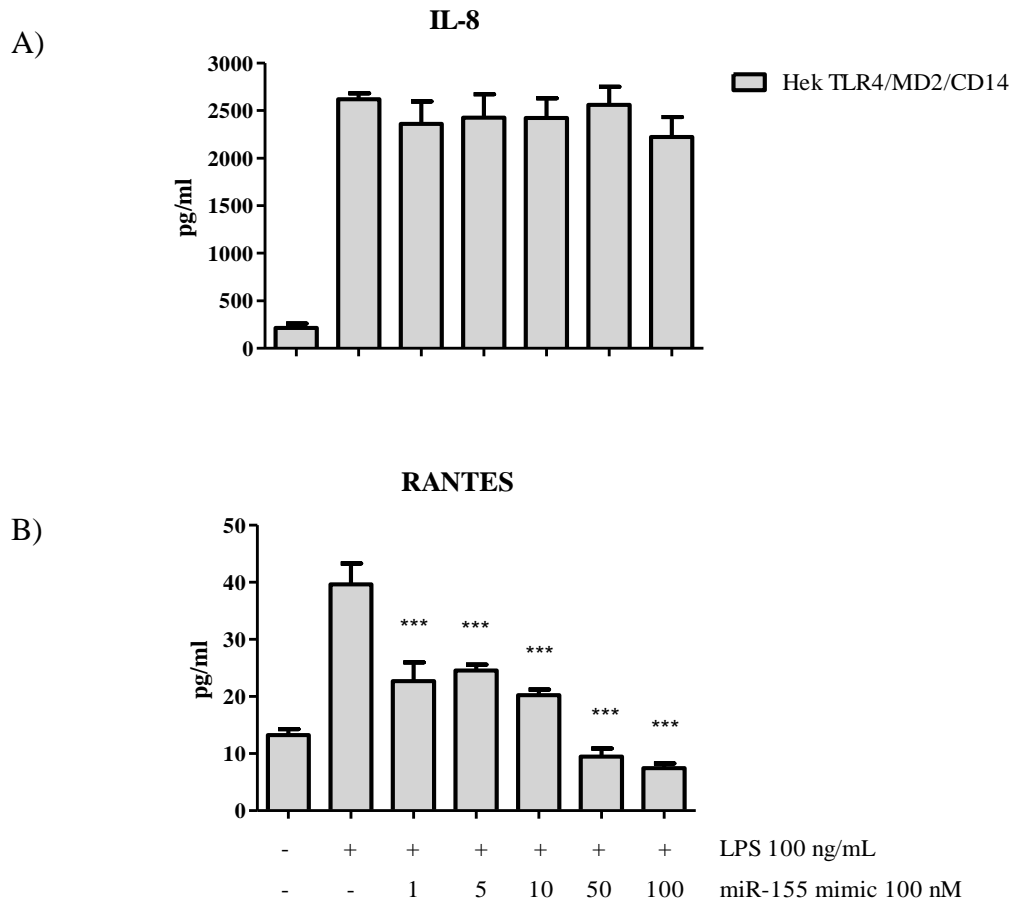


Figure 5.2.3 MiRNA mimic over expressing miR-155 decrease RANTES production in a dose dependent manner but does not affect IL-8 production in response to LPS. Hek TLR4/MD2/CD14 cells were plated at 1×10^6 cells/mL and allowed to adhere for 18 hours to approximately 60% confluency. The cells were then transfected with NF- κ B (80 ng) or pFA-IRF3 (30 ng) and pFR-regulated firefly luciferase (60 ng). Both sets of plasmid DNA were co-transfected with constitutively expressed TK renilla luciferase (20 ng) and +/- 0-100 nM miR-155 mimic. 24 hours post transfection cells were stimulated with 100 ng/mL for 18 hours. Cells supernatants were collected and human **A) IL-8** and **B) RANTES** was measured by ELISA. The results show the mean (\pm SEM) measured in triplicate, one-way ANOVA followed by Newman-Keuls analysis was used to determine if differences between groups were significantly different compared to cells stimulated with LPS, where * $p \leq 0.05$, ** $p \leq 0.01$ and *** $p \leq 0.001$. The results are indicative of three independent experiments.

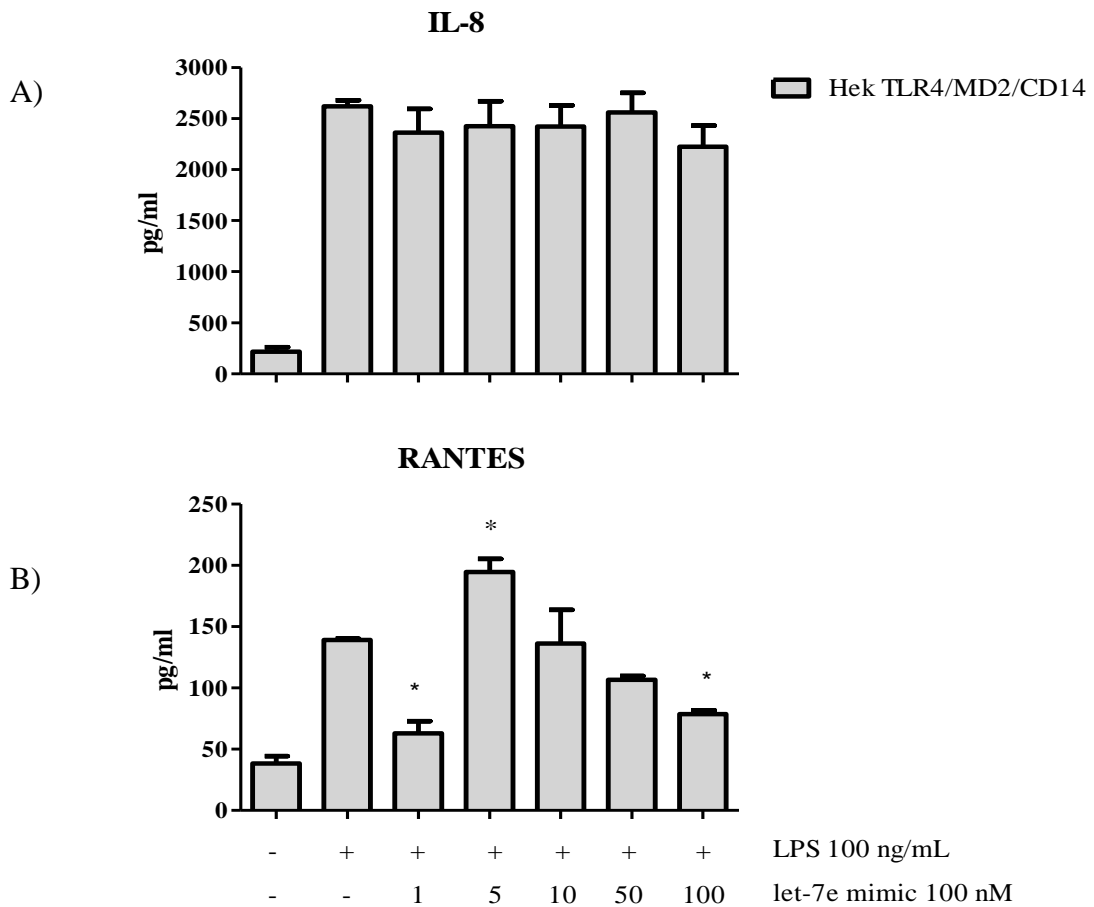


Figure 5.2.4 1nM and 100 nM miRNA mimic over expressing let-7e decreases RANTES production but do not effect IL-8 production when stimulated with LPS. Hek TLR4/MD2/CD14 cells were plated at 1×10^6 cells/mL and allowed to adhere for 18 hours to approximately 60% confluency. The cells were then transfected with NF- κ B (80 ng) or pFA-IRF3 (30 ng) and pFR-regulated firefly luciferase (60 ng). Both sets of plasmid DNA were co-transfected with constitutively expressed TK renilla luciferase (20 ng) and +/- 0-100 nM let-7e mimic. 24 hours post transfection cells were stimulated with 100 ng/mL LPS for 18 hours. Cells supernatants were collected and human **A)** IL-8 and **B)** RANTES was measured by ELISA. The results show the mean (\pm SEM) measured in triplicate, one-way ANOVA followed by Newman-Keuls analysis was used to determine if differences between groups were significantly different compared to cells stimulated with LPS, where * $p \leq 0.05$, ** $p \leq 0.01$ and *** $p \leq 0.001$. The results are indicative of three independent experiments.

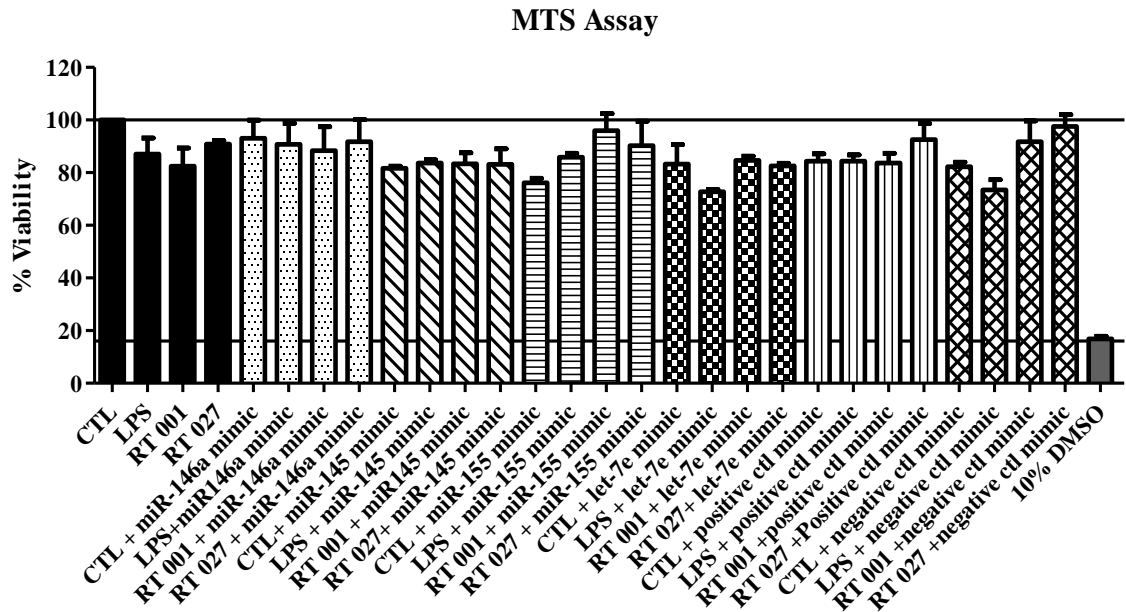


Figure 5.2.5 Transfection of plasmid DNA, miRNA mimics and stimulation with LPS and SLPs from RT 001 and RT 027 do not notably affect viability of the Hek TLR4/MD2/CD14 cells. Hek TLR4/MD2/CD14 cells were plated at 1×10^6 cells/mL and allowed to adhere for 18 hours to approximately 60% confluency. The cells were then transfected with NF- κ B (80 ng) or pFA-IRF3 (30 ng) and pFR-regulated firefly luciferase (60 ng). Both sets of plasmid DNA were co-transfected with constitutively expressed TK renilla luciferase (20 ng) and +/- 100 nM of each of the miRNA mimics. 24 hours post transfection cells were stimulated with 100 ng/mL LPS or SLPs from RT 001/ RT 027 for 18 hours. Cellular viability was then assessed using an MTS assay. Cells treated with 10% DMSO were used as a positive control. Results are expressed as a percentage of untreated cells with the mean \pm SEM of triplicate assays. Data represents three independent experiments.

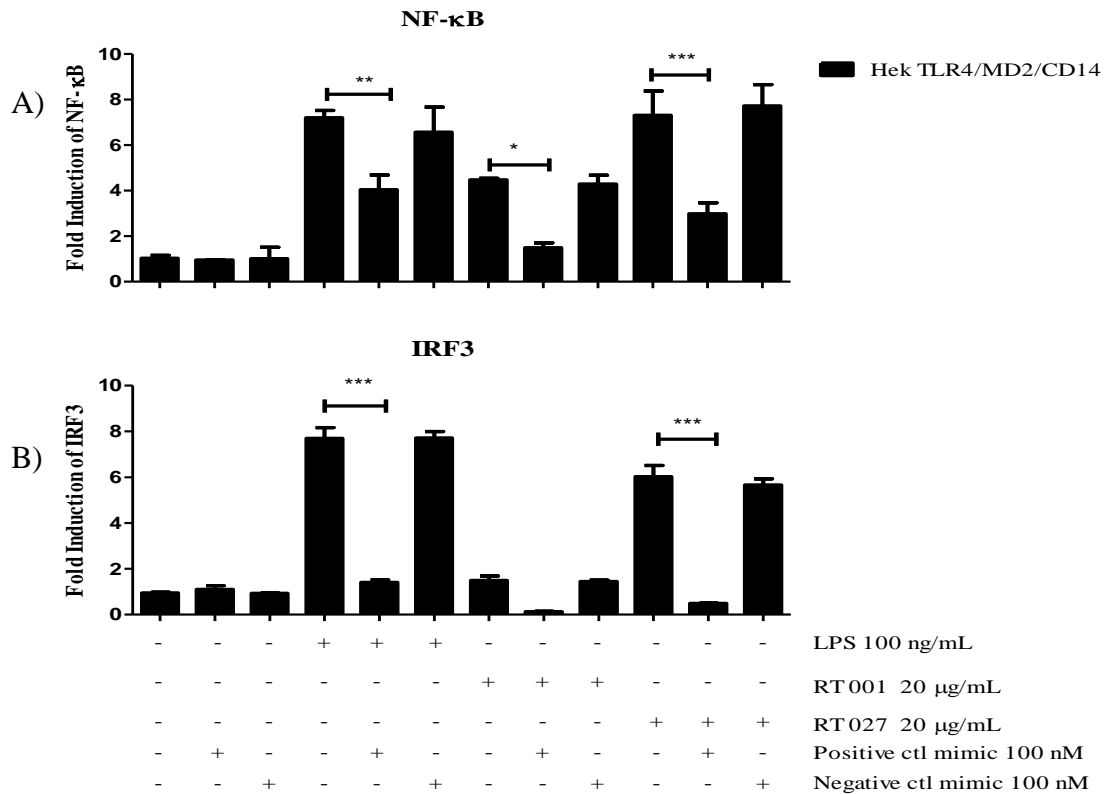


Figure 5.2.6 The positive control miRNA mimic decreased NF-κB and IRF3 gene expression in response to LPS and SLPs from RT 001 and 027. Hek TLR4/MD2/CD14 cells were plated at 1×10^6 cells/mL and allowed to adhere for 18 hours to approximately 60% confluency. The cells were transfected with **A)** NF-κB (80 ng) or **B)** pFA-IRF3 (30 ng) and pFR-regulated firefly luciferase (60 ng). Both sets of plasmid DNA were co-transfected with constitutively expressed TK renilla luciferase (20 ng) and +/- 100 nM positive or negative control miRNA mimic. 24 hours post transfection cells were stimulated with 100 ng/mL LPS or 20μg/mL SLPs from RT 001/RT 027 for 18 hours. Lysates were generated and assayed for firefly and renilla luciferase activity. The Renilla luciferase plasmid was used to normalise for transfection efficiency in all experiments. The results show the mean (\pm SEM) measured in triplicate, one-way ANOVA followed by Newman-Keuls analysis was used to determine if differences between groups were significantly different, where * $p \leq 0.05$, ** $p \leq 0.01$ and *** $p \leq 0.001$. The results are indicative of three independent experiments.

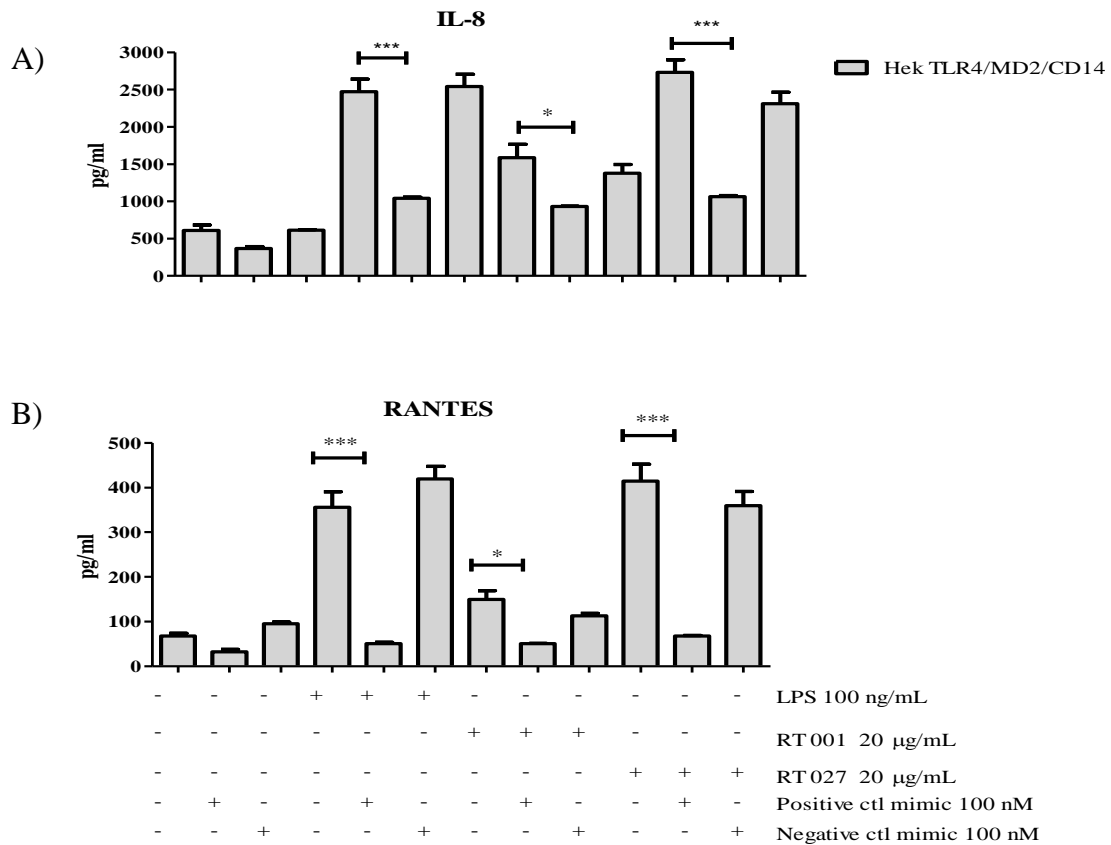


Figure 5.2.7 The positive control miRNA mimic decreased IL-8 and RANTES cytokine production in response to LPS and SLPs from RT 001 and 027. Hek TLR4/MD2/CD14 cells were plated at 1×10^6 cells/mL and allowed to adhere for 18 hours to approximately 60% confluency. The cells were then transfected with NF- κ B (80 ng) or pFA-IRF3 (30 ng) and pFR-regulated firefly luciferase (60 ng). Both sets of plasmid DNA were co-transfected with constitutively expressed TK renilla luciferase (20 ng) and +/- 100 nM positive/negative control miRNA mimics. 24 hours post transfection cells were stimulated with 100 ng/mL LPS or SLPs from RT 001/ RT 027 for 18 hours. Cells supernatants were collected and human **A)** IL-8 and **B)** RANTES was measured by ELISA. The results show the mean (\pm SEM) measured in triplicate, one-way ANOVA followed by Newman-Keuls analysis was used to determine if differences between groups were significantly different compared to cells stimulated with LPS, where * $p \leq 0.05$, ** $p \leq 0.01$ and *** $p \leq 0.001$. The results are indicative of three independent experiments.

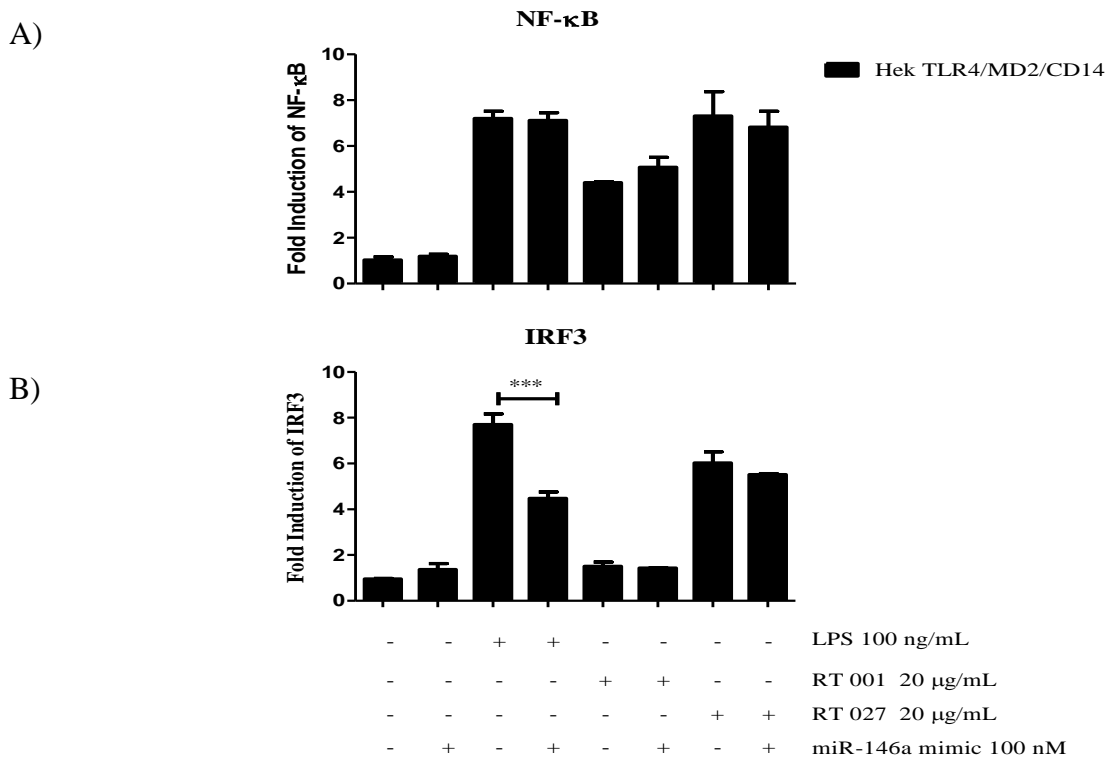
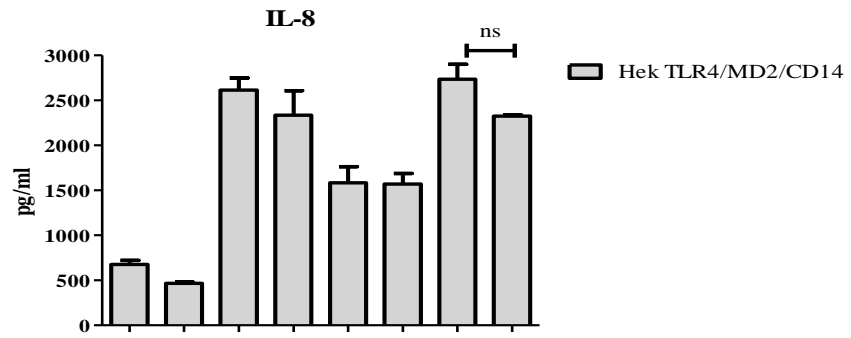


Figure 5.2.8 MiR-146a targets IRF3 signalling in response to LPS but not in response to SLPs from RT 001 and RT 027. Hek TLR4/MD2/CD14 cells were plated at 1×10^6 cells/mL and allowed to adhere for 18 hours to approximately 60% confluency. The cells were transfected with A) NF- κ B (80 ng) or B) pFA-IRF3 (30 ng) and pFR-regulated firefly luciferase (60 ng). Both sets of plasmid DNA were co-transfected with constitutively expressed TK renilla luciferase (20 ng) and +/- 100 nM miR-146a mimic. 24 hours post transfection cells were stimulated with 100 ng/mL LPS or 20 μ g/mL SLPs from RT 001/RT 027 for 18 hours. Lysates were generated and assayed for firefly and renilla luciferase activity. The Renilla luciferase plasmid was used to normalise for transfection efficiency in all experiments. The results show the mean (\pm SEM) measured in triplicate, one-way ANOVA followed by Newman-Keuls analysis was used to determine if differences between groups were significantly different, where * $p \leq 0.05$, ** $p \leq 0.01$ and *** $p \leq 0.001$. The results are indicative of three independent experiments.

A)



B)

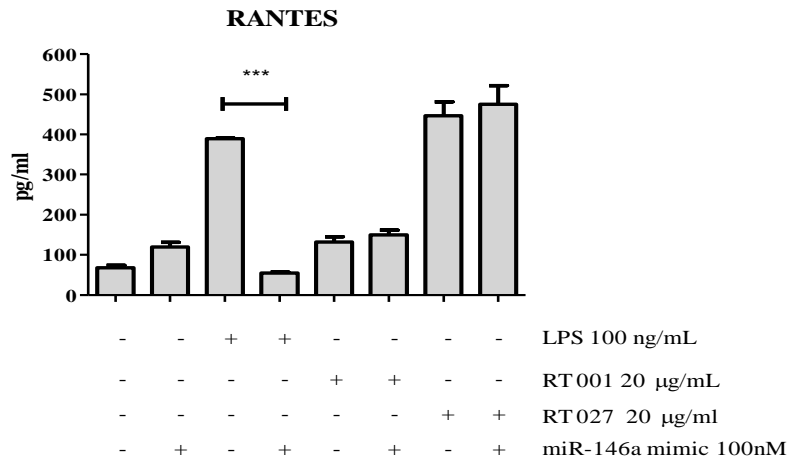


Figure 5.2.9 MiR-146a targets RANTES production in response to LPS but not in response to SLPs from RT 001 and RT 027. Hek TLR4/MD2/CD14 cells were plated at 1×10^6 cells/mL and allowed to adhere for 18 hours to approximately 60% confluency. The cells were then transfected with NF- κ B (80 ng) or pFA-IRF3 (30 ng) and pFR-regulated firefly luciferase (60 ng). Both sets of plasmid DNA were co-transfected with constitutively expressed TK renilla luciferase (20 ng) and +/- 100 nM miR146a mimic. 24 hours post transfection cells were stimulated with 100 ng/mL LPS or SLPs from RT 001/ RT 027 for 18 hours. Cells supernatants were collected and human **A)** IL-8 and **B)** RANTES was measured by ELISA. The results show the mean (\pm SEM) measured in triplicate, one-way ANOVA followed by Newman-Keuls analysis was used to determine if differences between groups were significantly different compared to cells stimulated with LPS, where * $p \leq 0.05$, ** $p \leq 0.01$ and *** $p \leq 0.001$. The results are indicative of three independent experiments.

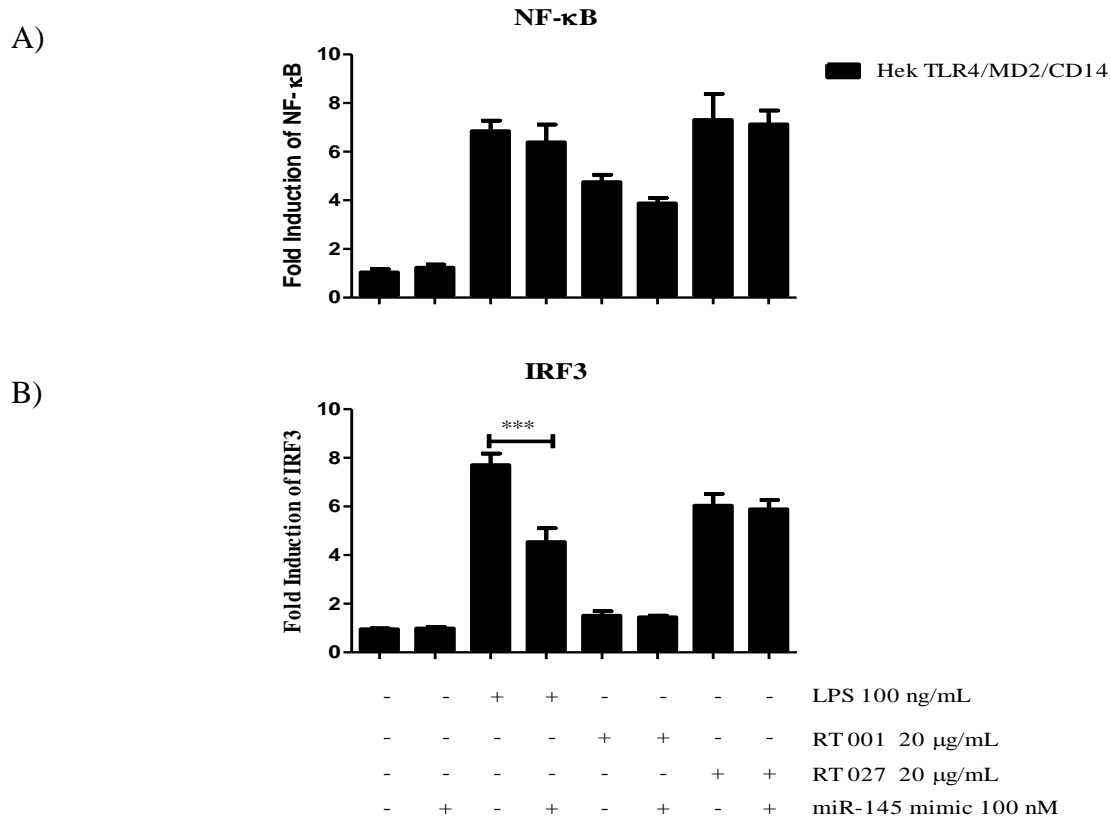


Figure 5.2.10 MiR-145 targets IRF3 signalling in response to LPS but not in response to SLPs from RT 001 and RT 027. Hek TLR4/MD2/CD14 cells were plated at 1×10^6 cells/mL and allowed to adhere for 18 hours to approximately 60% confluency. The cells were transfected with **A**) NF- κ B (80 ng) or **B**) pFA-IRF3 (30 ng) and pFR-regulated firefly luciferase (60 ng). Both sets of plasmid DNA were co-transfected with constitutively expressed TK renilla luciferase (20 ng) and 100 nM miR-146a mimic. 24 hours post transfection cells were stimulated with 100 ng/mL LPS or 20 μ g/mL SLPs from RT 001/RT 027 for 18 hours. Lysates were generated and assayed for firefly and renilla luciferase activity. The Renilla luciferase plasmid was used to normalise for transfection efficiency in all experiments. The results show the mean (\pm SEM) measured in triplicate, one-way ANOVA followed by Newman-Keuls analysis was used to determine if differences between groups were significantly different, where * $p \leq 0.05$, ** $p \leq 0.01$ and *** $p \leq 0.001$. The results are indicative of three independent experiments.

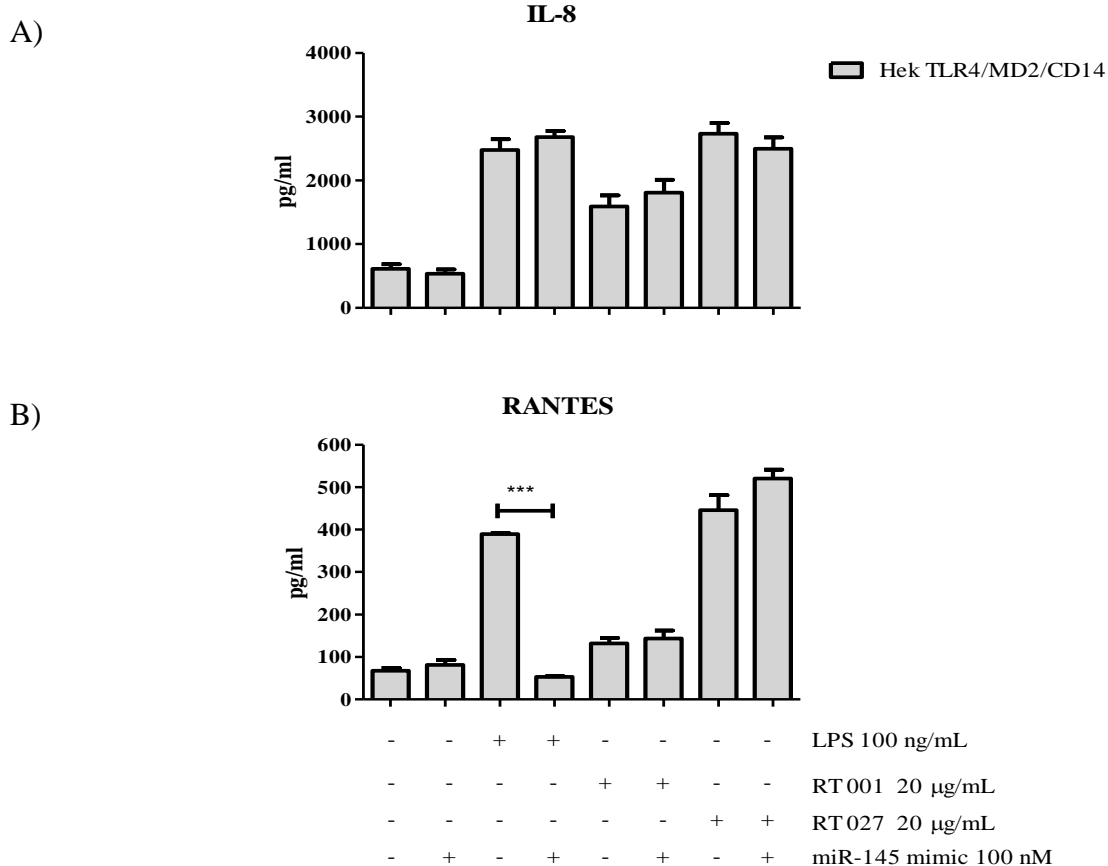


Figure 5.2.11 MiR-145 targets RANTES production in response to LPS but not in response to SLPs from RT 001 and RT 027. Hek TLR4/MD2/CD14 cells were plated at 1×10^6 cells/mL and allowed to adhere for 18 hours to approximately 60% confluency. The cells were then transfected with NF- κ B (80 ng) or pFA-IRF3 (30 ng) and pFR-regulated firefly luciferase (60 ng). Both sets of plasmid DNA were co-transfected with constitutively expressed TK renilla luciferase (20 ng) and +/- 100 nM miR145 mimic. 24 hours post transfection cells were stimulated with 100 ng/mL LPS or SLPs from RT 001/ RT 027 for 18 hours. Cells supernatants were collected and human **A)** IL-8 and **B)** RANTES was measured by ELISA. The results show the mean (\pm SEM) measured in triplicate, one-way ANOVA followed by Newman-Keuls analysis was used to determine if differences between groups were significantly different compared to cells stimulated with LPS, where * $p \leq 0.05$, ** $p \leq 0.01$ and *** $p \leq 0.001$. The results are indicative of three independent experiments.

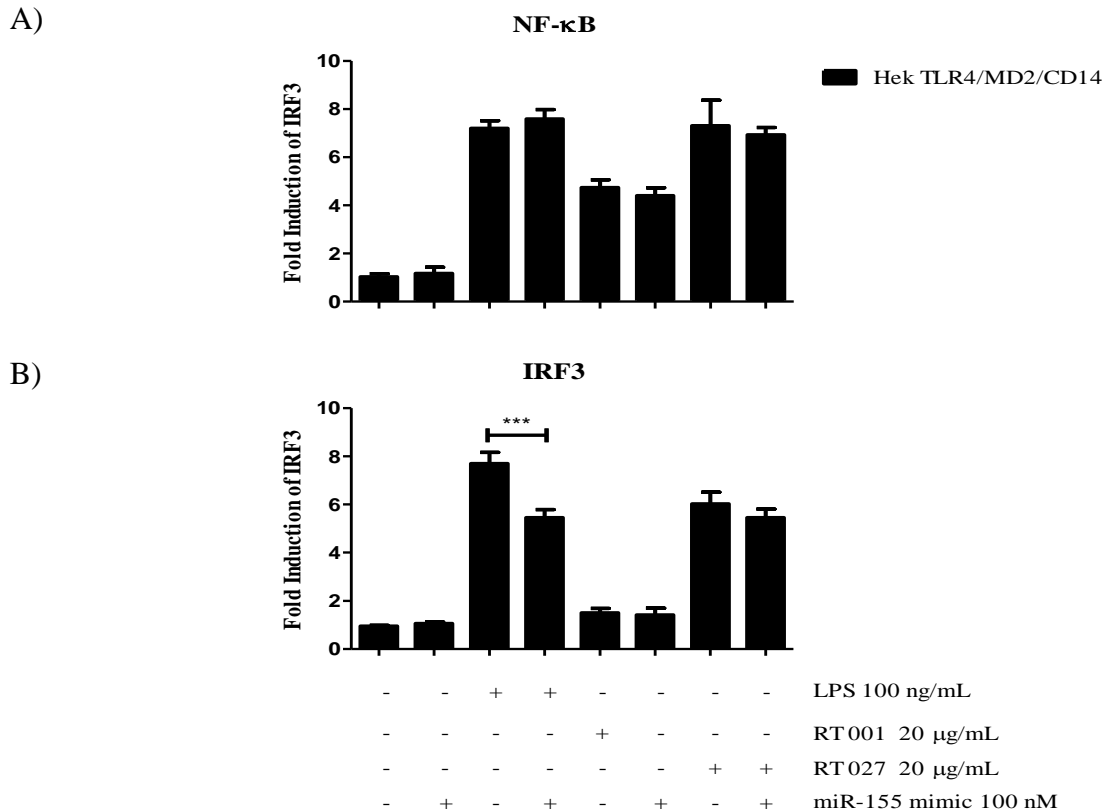


Figure 5.2.12 MiR-155 targets IRF3 signalling in response to LPS but not in response to SLPs from RT 001 and RT 027. Hek TLR4/MD2/CD14 cells were plated at 1×10^6 cells/mL and allowed to adhere for 18 hours to approximately 60% confluency. The cells were transfected with **A)** NF-κB (80 ng) or **B)** pFA-IRF3 (30 ng) and pFR-regulated firefly luciferase (60 ng). Both sets of plasmid DNA were co-transfected with constitutively expressed TK renilla luciferase (20 ng) and 100 nM miR-155 mimic. 24 hours post transfection cells were stimulated with 100 ng/mL LPS or 20 μg/mL SLPs from RT 001/RT 027 for 18 hours. Lysates were generated and assayed for firefly and renilla luciferase activity. The Renilla luciferase plasmid was used to normalise for transfection efficiency in all experiments. The results show the mean (\pm SEM) measured in triplicate, one-way ANOVA followed by Newman-Keuls analysis was used to determine if differences between groups were significantly different, where * $p \leq 0.05$, ** $p \leq 0.01$ and *** $p \leq 0.001$. The results are indicative of three independent experiments.

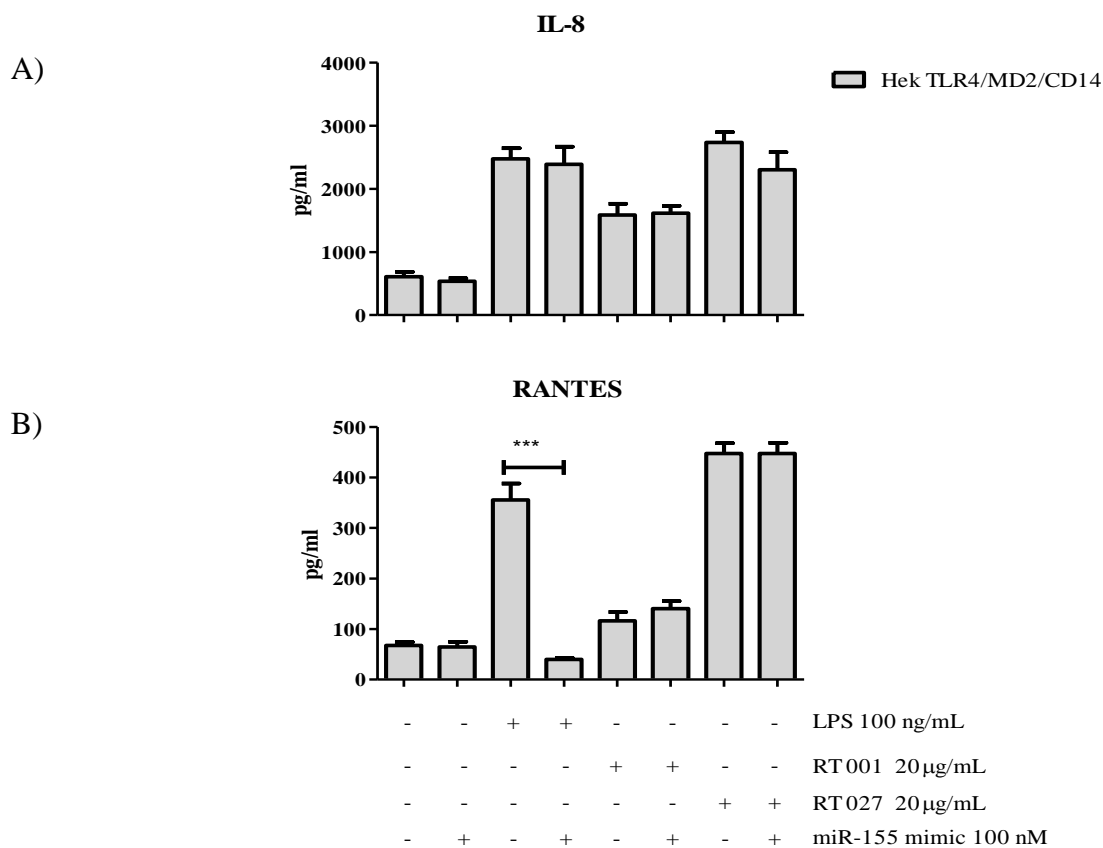


Figure 5.2.13 MiR-155 targets RANTES production in response to LPS but not in response to SLPs from RT 001 and RT 027. Hek TLR4/MD2/CD14 cells were plated at 1×10^6 cells/mL and allowed to adhere for 18 hours to approximately 60% confluency. The cells were then transfected with NF- κ B (80 ng) or pFA-IRF3 (30 ng) and pFR-regulated firefly luciferase (60 ng). Both sets of plasmid DNA were co-transfected with constitutively expressed TK renilla luciferase (20 ng) and +/- 100 nM miR-155 mimic. 24 hours post transfection cells were stimulated with 100 ng/mL LPS or SLPs from RT 001/ RT 027 for 18 hours. Cells supernatants were collected and human **A)** IL-8 and **B)** RANTES was measured by ELISA. The results show the mean (\pm SEM) measured in triplicate, one-way ANOVA followed by Newman-Keuls analysis was used to determine if differences between groups were significantly different compared to cells stimulated with LPS, where * $p \leq 0.05$, ** $p \leq 0.01$ and *** $p \leq 0.001$. The results are indicative of three independent experiments.

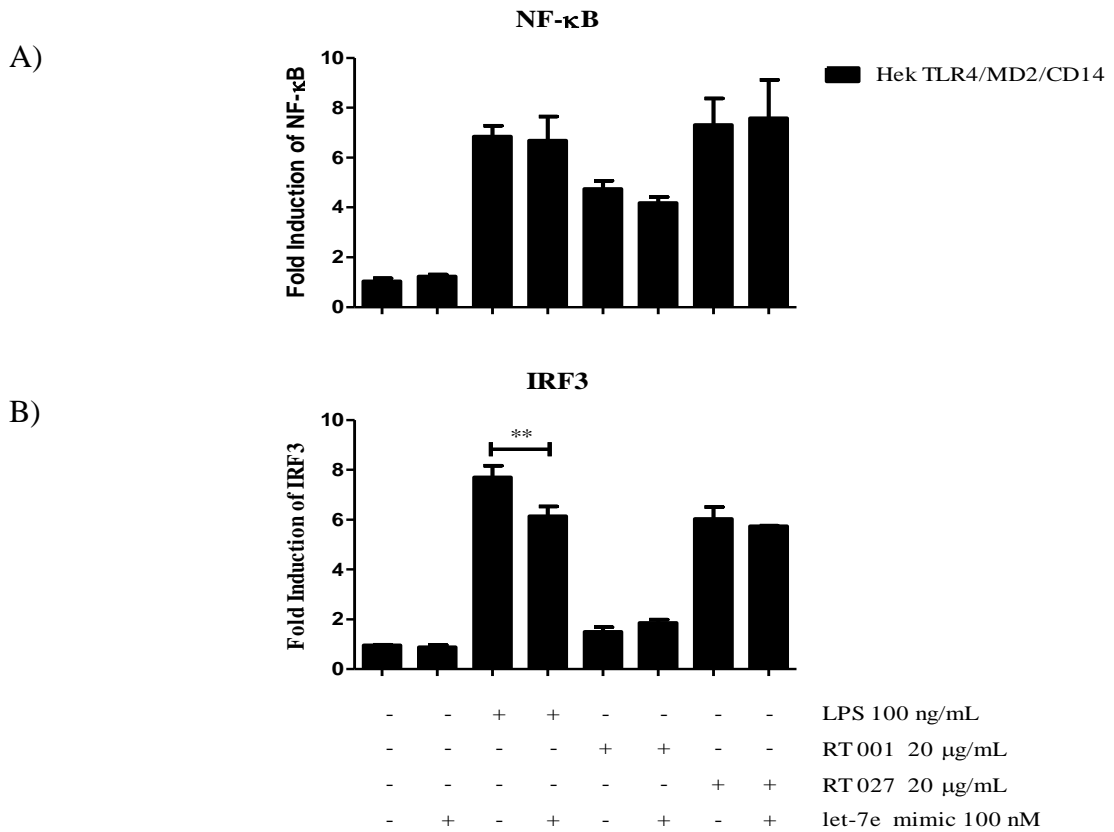


Figure 5.2.14 Let-7e targets IRF3 signalling in response to LPS but not in response to SLPs from RT 001 and RT 027. Hek TLR4/MD2/CD14 cells were plated at 1×10^6 cells/mL and allowed to adhere for 18 hours to approximately 60% confluency. The cells were transfected with **A)** NF- κ B (80 ng) or **B)** pFA-IRF3 (30 ng) and pFR-regulated firefly luciferase (60 ng). Both sets of plasmid DNA were co-transfected with constitutively expressed TK renilla luciferase (20 ng) and 100 nM let-7e mimic. 24 hours post transfection cells were stimulated with 100 ng/mL LPS or 20 μ g/mL SLPs from RT 001/RT 027 for 18 hours. Lysates were generated and assayed for firefly and renilla luciferase activity. The Renilla luciferase plasmid was used to normalise for transfection efficiency in all experiments. The results show the mean (\pm SEM) measured in triplicate, one-way ANOVA followed by Newman-Keuls analysis was used to determine if differences between groups were significantly different, where * $p \leq 0.05$, ** $p \leq 0.01$ and *** $p \leq 0.001$. The results are indicative of three independent experiments.

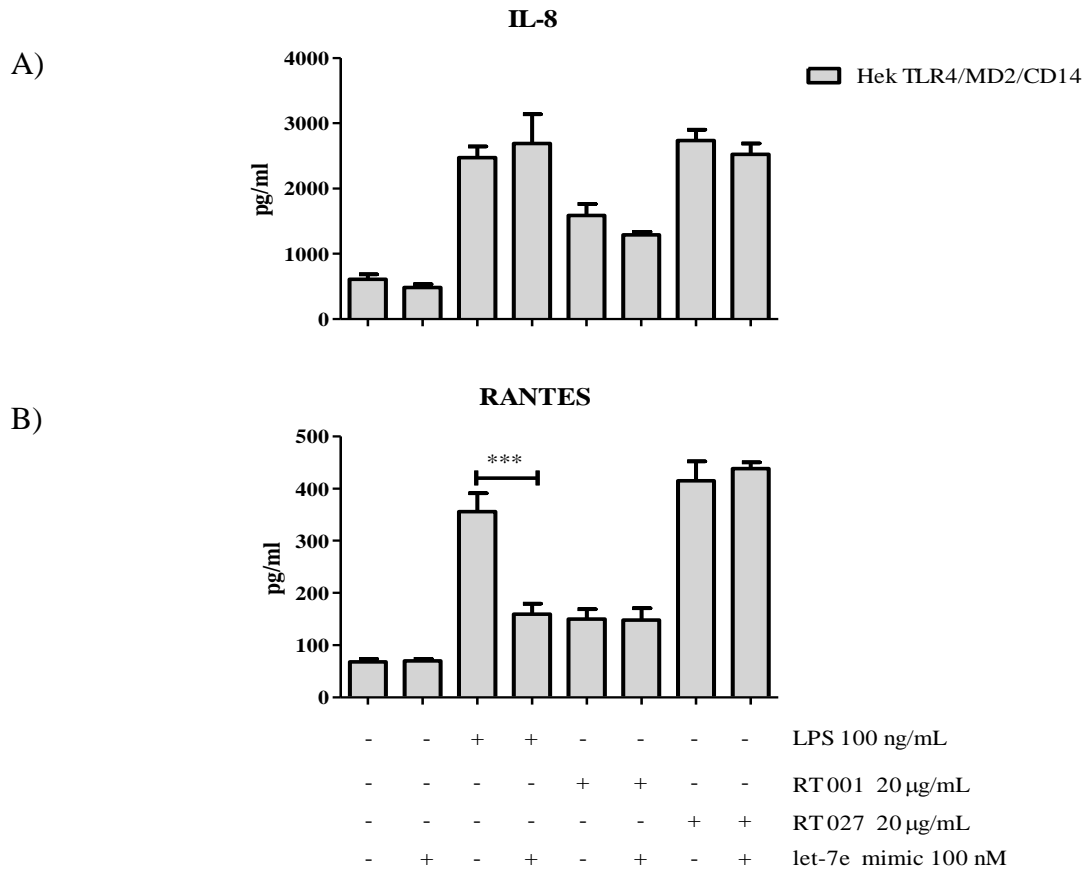


Figure 5.2.15 Let-7e targets RANTES production in response to LPS but not in response to SLPs from RT 001 and RT 027. Hek TLR4/MD2/CD14 cells were plated at 1×10^6 cells/mL and allowed to adhere for 18 hours to approximately 60% confluency. The cells were then transfected with NF- κ B (80 ng) or pFA-IRF3 (30 ng) and pFR-regulated firefly luciferase (60 ng). Both sets of plasmid DNA were co-transfected with constitutively expressed TK renilla luciferase (20 ng) and +/- 100 nM let-7e mimic. 24 hours post transfection cells were stimulated with 100 ng/mL LPS or SLPs from RT 001/ RT 027 for 18 hours. Cells supernatants were collected and human **A) IL-8** and **B) RANTES** was measured by ELISA. The results show the mean (\pm SEM) measured in triplicate, one-way ANOVA followed by Newman-Keuls analysis was used to determine if differences between groups were significantly different compared to cells stimulated with LPS, where * $p \leq 0.05$, ** $p \leq 0.01$ and *** $p \leq 0.001$. The results are indicative of three independent experiments.

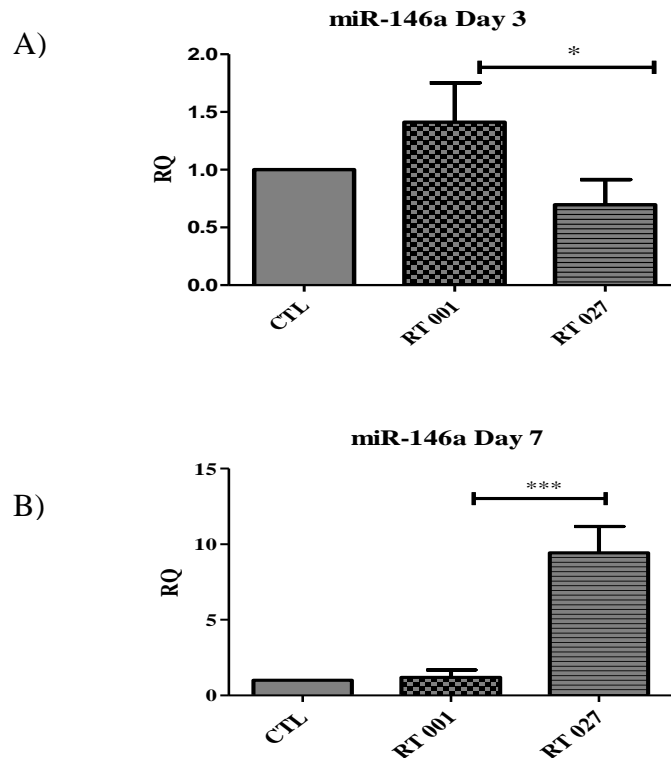


Figure 5.2.16 MiR-146a is differentially regulated in colonic tissue of mice treated with RT 027 at day 3 and day 7 of infection. Total RNA derived from colonic tissue from an *in vivo* model of *C. difficile* was enriched for miRNAs using the mirVana Isolation kit, there were 4 animals per treatment group: control group n=4, group treated with RT 001 n=4 and group treated with RT 027 n=4. 100 ng RNA enriched for miRNAs was converted to first strand cDNA, the products of which were used in a pre-amp PCR reaction. Samples were added to PCR reaction mixes for individual Taqman miRNA assays and added to wells on a 96 well PCR plate. The plate was run on the Applied Biosystems 7900HT Fast Real Time PCR Machine. The SDS files were exported and data from the PCR plate was analysed using ExpressionSuite software. The max Ct was set to 37.0 with a threshold of 0.1 and the reference group was set to the control group. snoRNA202 was used to correct for variation of RNA input and relative gene expression was calculated. The results show the mean (\pm SEM) measured in triplicate, a student's t-test was used to test for significance by comparing samples of colonic tissue of mice treated with RT 001 with RT 027 where * $p \leq 0.05$, ** $p \leq 0.01$ and *** $p \leq 0.001$.

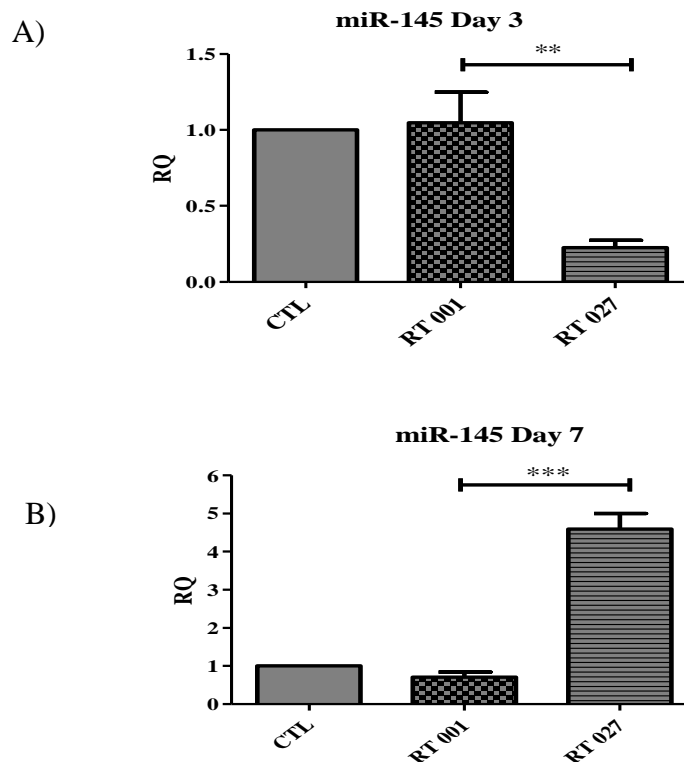


Figure 5.2.17 MiR-145 is differentially regulated in colonic tissue of mice treated with RT 027 at day 3 and day 7 of infection. Total RNA derived from colonic tissue from an in vivo model of *C. difficile* was enriched for miRNAs using the mirVana Isolation kit, there were 4 animals per treatment group: control group n=4, group treated with RT 001 n=4 and group treated with RT 027 n=4. 100 ng RNA enriched for miRNAs was converted to first strand cDNA, the products of which were used in a pre-amp PCR reaction. Samples were added to PCR reaction mixes for individual Taqman miRNA assays and added to wells on a 96 well PCR plate. The plate was run on the Applied Biosystems 7900HT Fast Real Time PCR Machine. The SDS files were exported and data from the PCR plate was analysed using ExpressionSuite software. The max Ct was set to 37.0 with a threshold of 0.1 and the reference group was set to the control group. snoRNA202 was used to correct for variation of RNA input and relative gene expression was calculated. The results show the mean (\pm SEM) measured in triplicate, a student's t-test was used to test for significance by comparing samples of colonic tissue of mice treated with RT 001 with RT 027 where * $p \leq 0.05$, ** $p \leq 0.01$ and *** $p \leq 0.001$.

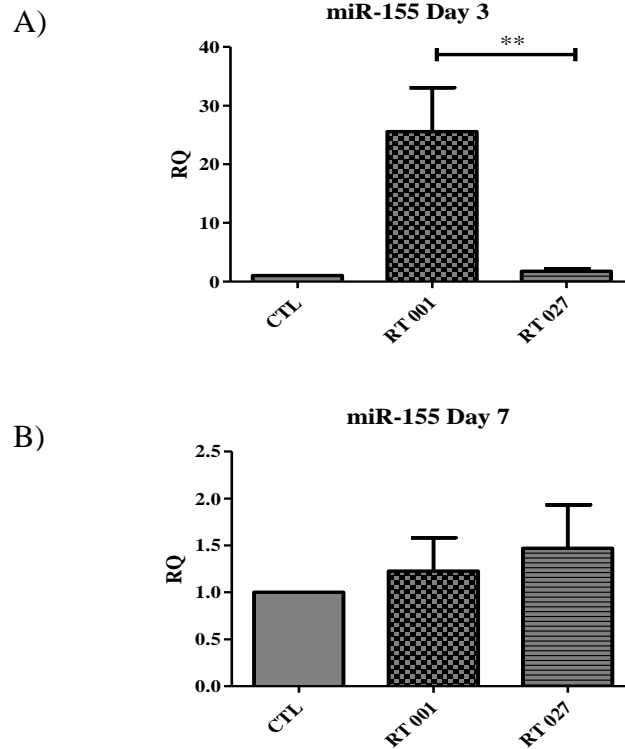


Figure 5.2.18 MiR-155 is differentially regulated in colonic tissue of mice treated with RT 001 at day 3 of infection. Total RNA derived from colonic tissue from an *in vivo* model of *C. difficile* was enriched for miRNAs using the mirVana Isolation kit, there were 4 animals per treatment group: control group n=4, group treated with RT 001 n=4 and group treated with RT 027 n=4. 100 ng RNA enriched for miRNAs was converted to first strand cDNA, the products of which were used in a pre-amp PCR reaction. Samples were added to PCR reaction mixes for individual Taqman miRNA assays and added to wells on a 96 well PCR plate. The plate was run on the Applied Biosystems 7900HT Fast Real Time PCR Machine. The SDS files were exported and data from the PCR plate was analysed using ExpressionSuite software. The max Ct was set to 37.0 with a threshold of 0.1 and the reference group was set to the control group. snoRNA202 was used to correct for variation of RNA input and relative gene expression was calculated. The results show the mean (\pm SEM) measured in triplicate, a student's t-test was used to test for significance by comparing samples of colonic tissue of mice treated with RT 001 with RT 027 where * $p \leq 0.05$, ** $p \leq 0.01$ and *** $p \leq 0.001$.

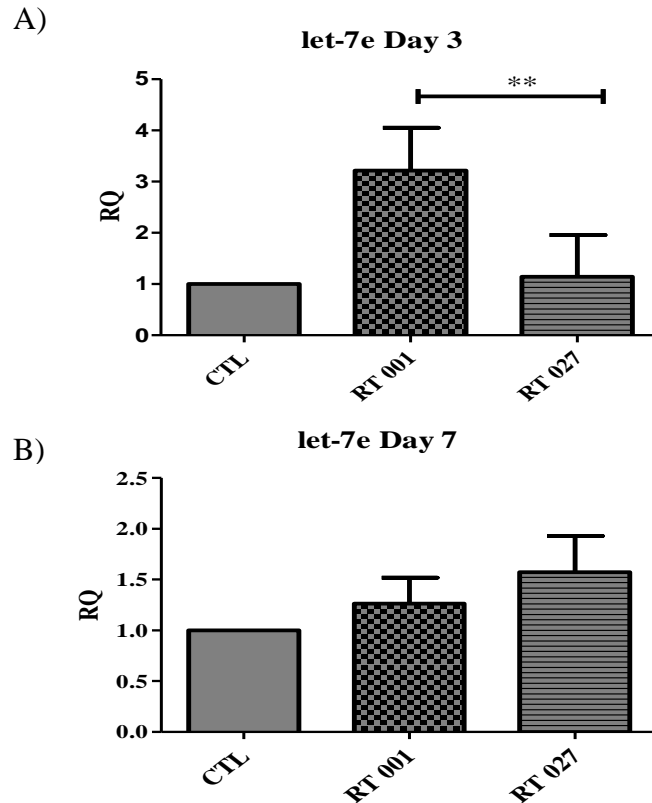


Figure 5.2.19 Let-7e is differentially regulated in colonic tissue of mice treated with RT 001 at day 3 of infection. Total RNA derived from colonic tissue from an in vivo model of *C. difficile* was enriched for miRNAs using the mirVana Isolation kit, there were 4 animals per treatment group: control group n=4, group treated with RT 001 n=4 and group treated with RT 027 n=4. 100 ng RNA enriched for miRNAs was converted to first strand cDNA, the products of which were used in a pre-amp PCR reaction. Samples were added to PCR reaction mixes for individual Taqman miRNA assays and added to wells on a 96 well PCR plate. The plate was run on the Applied Biosystems 7900HT Fast Real Time PCR Machine. The SDS files were exported and data from the PCR plate was analysed using ExpressionSuite software. The max Ct was set to 37.0 with a threshold of 0.1 and the reference group was set to the control group. snoRNA202 was used to correct for variation of RNA input and relative gene expression was calculated. The results show the mean (\pm SEM) measured in triplicate, a student's t-test was used to test for significance by comparing samples of colonic tissue of mice treated with RT 001 with RT 027 where * $p \leq 0.05$, ** $p \leq 0.01$ and *** $p \leq 0.001$.

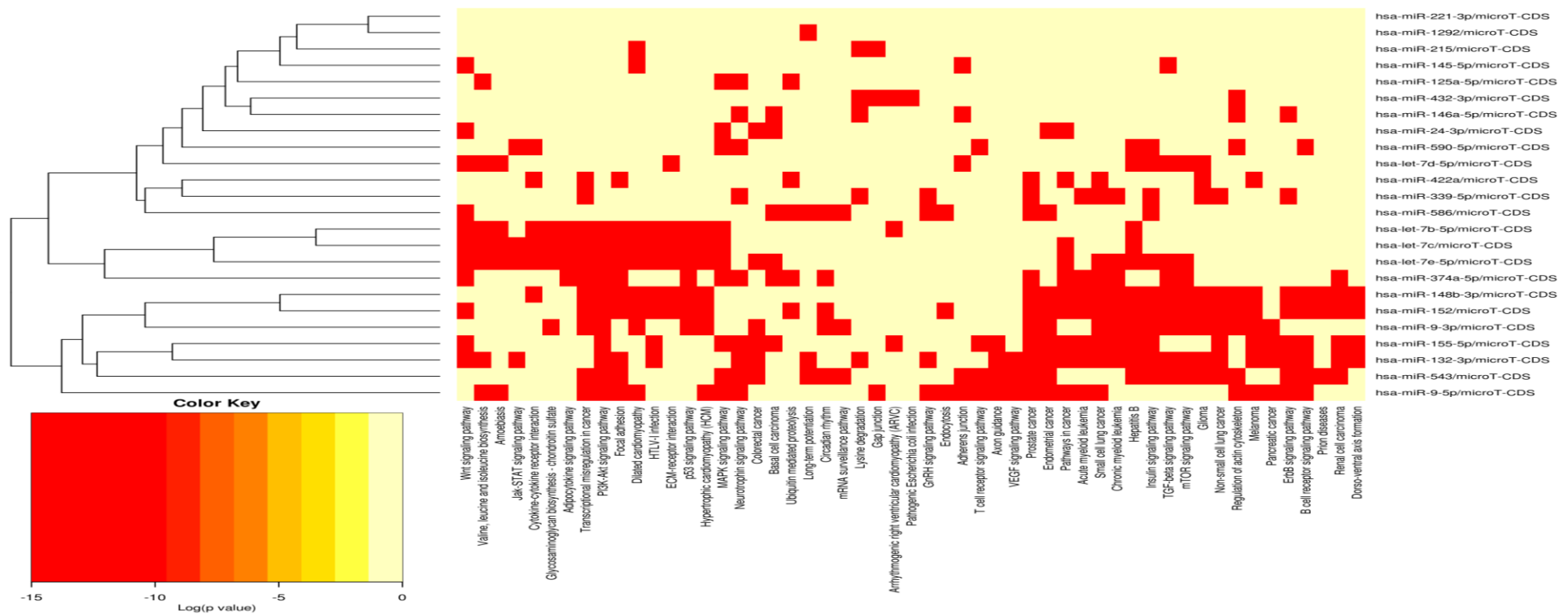


Figure 5.2.20. Heat map showing pathways interactions from miRNAs differentially regulated by SLPs from RT 001 and RT 027. The target list generated from experimental data of miRNAs differentially regulated by SLPs from RT 001 and RT 027 was inputted into DIANA-miRPath v2.0 database. A posteriori analysis was performed where the significance levels between all possible miRNA pathway pairs were calculated using enrichment analysis. The previously calculated significance levels were combined to provide a merged p-value for each pathway, by applying Fisher's combined probability method. The heat map shows miRNAs versus 54 of the pathways where miRNA gene interactions where $p \leq 0.05$. Darker colours represent lower significance values and the adjacent dendrograms depict hierarchical clustering. We can identify miRNAs clustered together by exhibiting similar pathway targeting patterns.

Table 5.2.1 MiRNAs differentially regulated by SLPs from RT 001 and RT 027 are involved in essential cell signalling pathways. Table showing the top 5 KEGG pathways where gene/miRNA/pathway interactions are likely to occur. The list of 24 miRNAs differentially regulated by SLPs from RT 001 and RT 027 were inputted into DIANA-miRPath v2.0 database where a posteriori analysis was performed. The significance levels between all possible miRNA pathways pairs were calculated using enrichment analysis. The previously calculated significance levels were combined to provide a merged p-value for each pathway, by applying Fisher's combined probability method.

KEGG pathway	p-value	#genes	#miRNAs
ECM- receptor Interaction	<1E-16	15	6
TGF-beta signalling pathway	<1E-16	42	9
MAPK signalling pathway	<1E-16	98	10
PI3K-Akt signalling pathway	<1E-16	121	11
Focal adhesion	1.1E-16	74	10

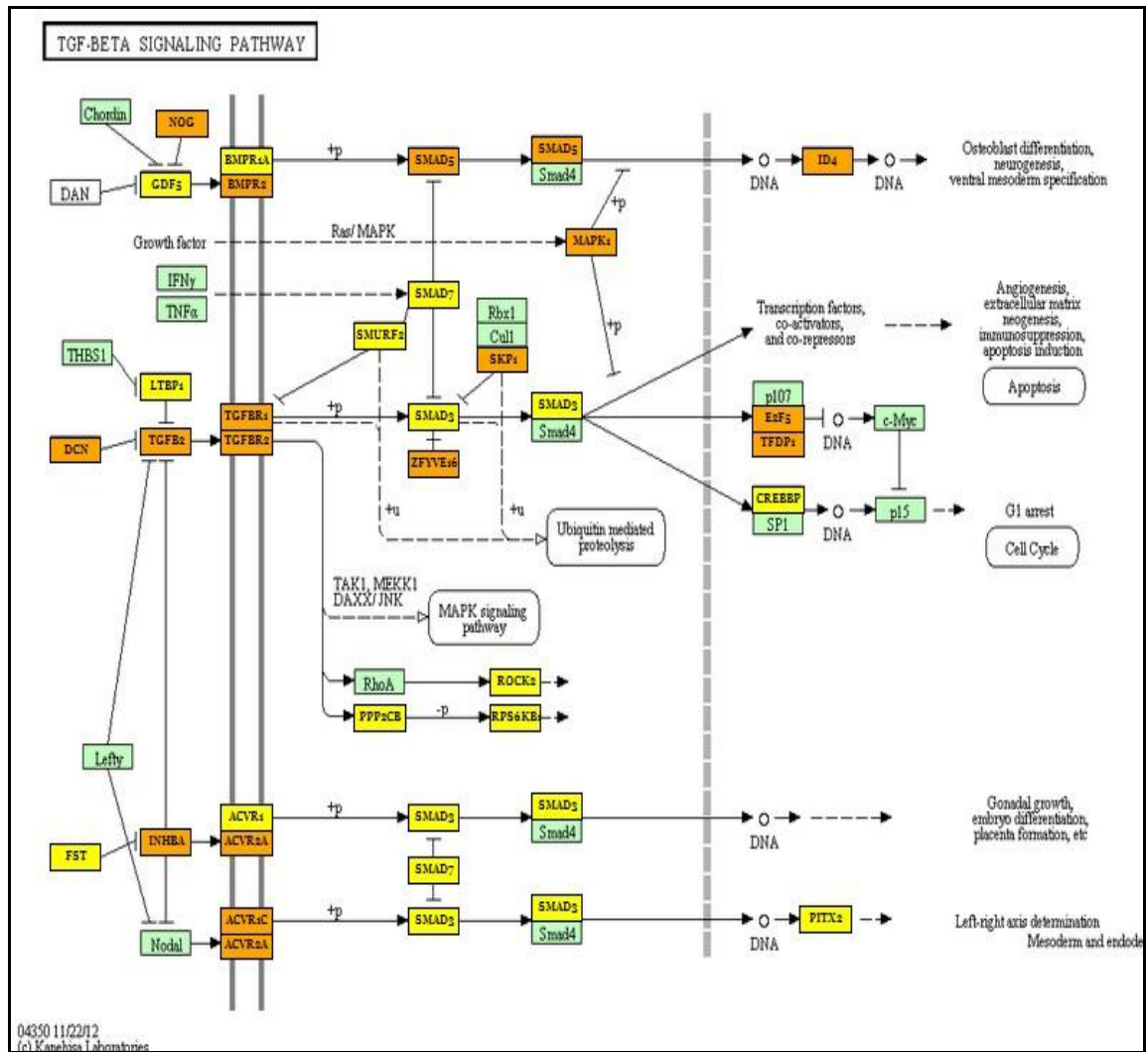


Figure 5.2.22. MiRNAs differentially regulated by SLPs from RT 001 and RT 027 may modulate genes involved in TGF- β signalling pathway. The target list generated from experimental data of miRNAs differentially regulated by SLPs from RT 001 and RT 027 was inputted into DIANA-miRPath. A posteriori analysis was performed where the significance levels between all possible miRNA pathway pairs were calculated using enrichment analysis. The previously calculated significance levels were combined to provide a merged p-value for each pathway, by applying Fisher's combined probability method. The resulting gene lists were converted into KEGG images. Genes highlighted in yellow represent predicted targets for an individual miRNA, genes highlighted in orange represent predicted targets for multiple miRNAs and genes highlighted in green are not targeted by the miRNAs of interest in this pathway.

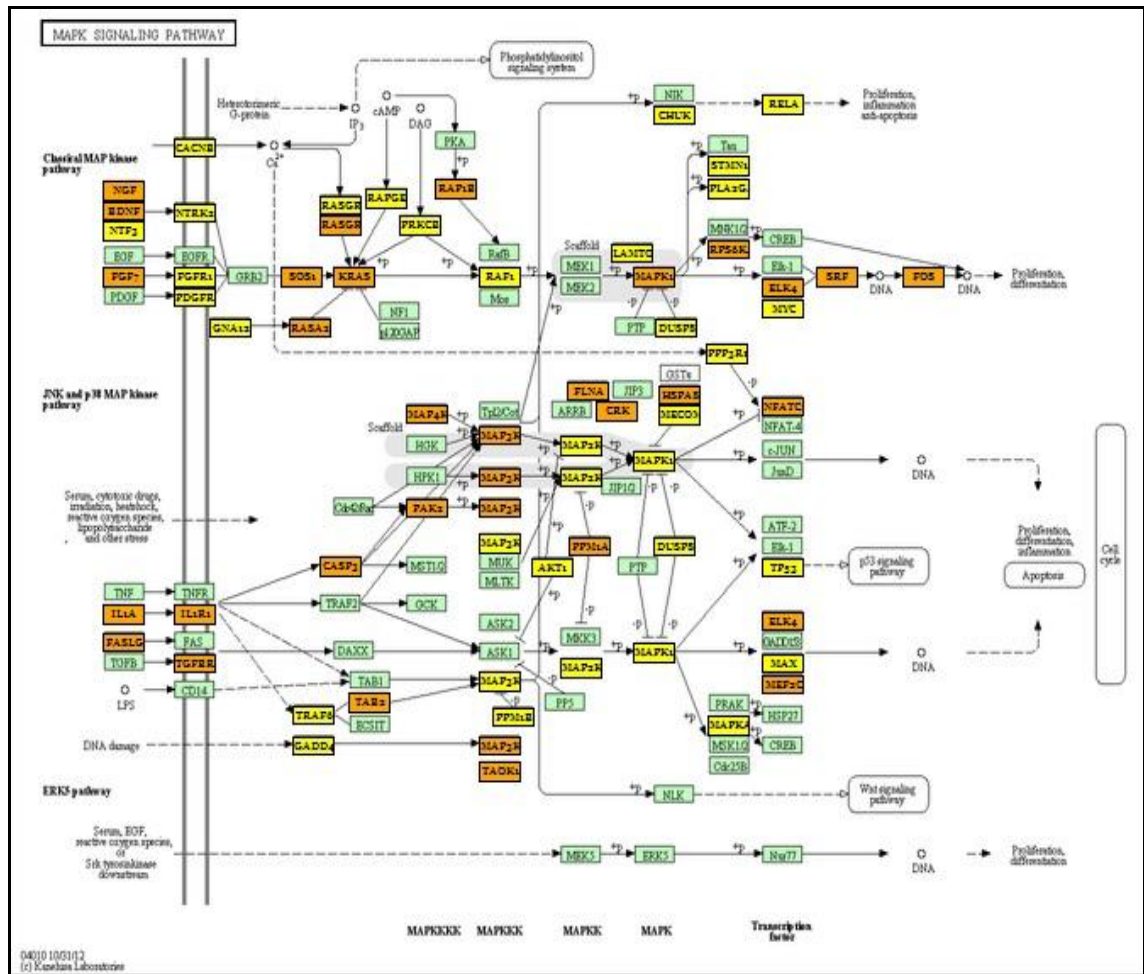


Figure 5.2.23 MiRNAs differentially regulated by SLPs from RT 001 and RT 027 may modulate genes involved in the MAPK signalling pathway. The target list generated from experimental data of miRNAs differentially regulated by SLPs from RT 001 and RT 027 was inputted into DIANA-miRPath. A posteriori analysis was performed where the significance levels between all possible miRNA pathway pairs were calculated using enrichment analysis. The previously calculated significance levels were combined to provide a merged p-value for each pathway, by applying Fisher's combined probability method. The resulting gene lists were converted into KEGG images. Genes highlighted in yellow represent predicted targets for an individual miRNA, genes highlighted in orange represent predicted targets for multiple miRNAs and genes highlighted in green are not targeted by the miRNAs of interest in this pathway.

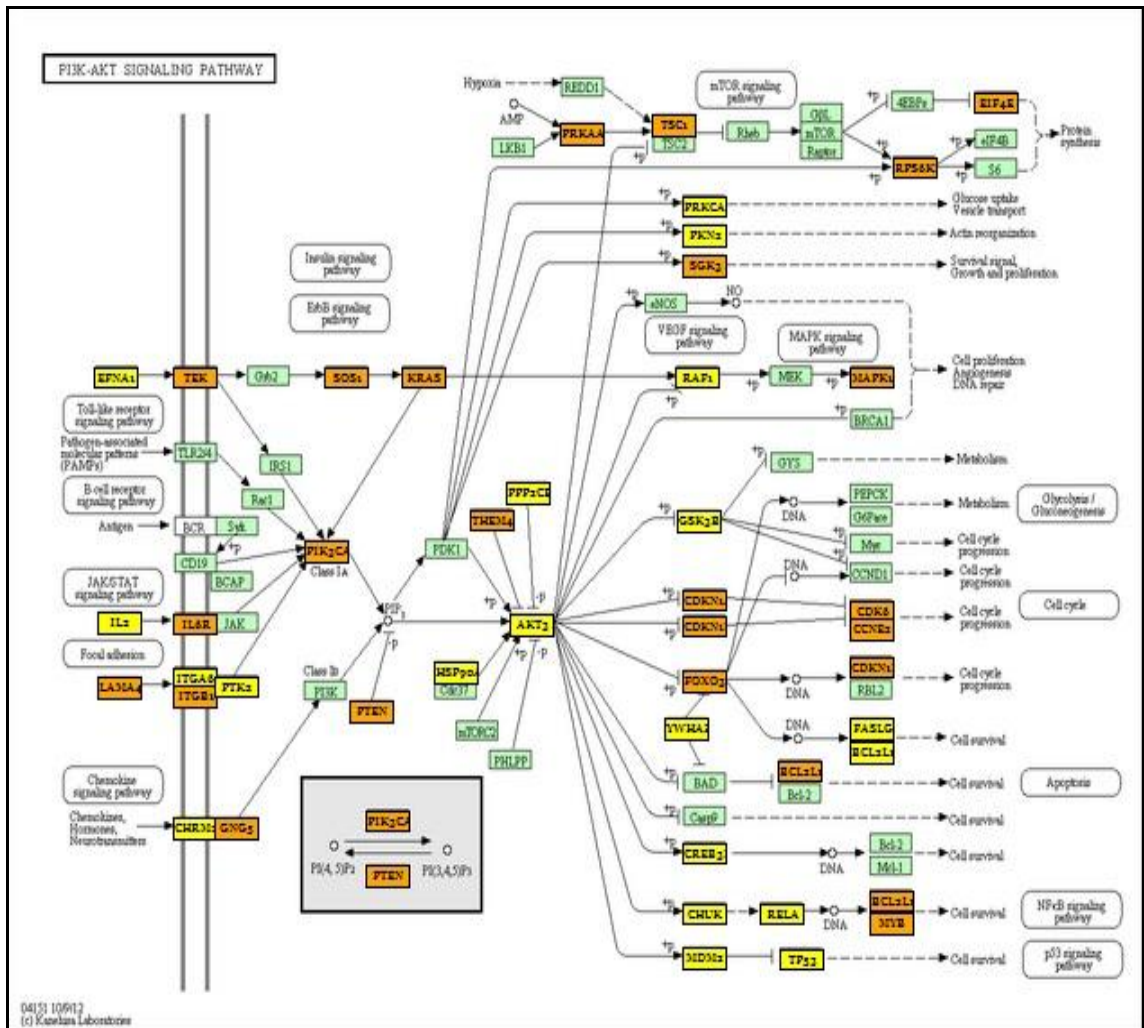


Figure 5.2.24 MiRNAs differentially regulated by SLPs from RT 001 and RT 027 may modulate genes involved in the PI3K-Akt signalling. The target list generated from experimental data of miRNAs differentially regulated by SLPs from RT 001 and RT 027 was inputted into DIANA-miRPath. A posteriori analysis was performed where the significance levels between all possible miRNA pathway pairs were calculated using enrichment analysis. The previously calculated significance levels were combined to provide a merged p-value for each pathway, by applying Fisher's combined probability method. The resulting gene lists were converted into KEGG images. Genes highlighted in yellow represent predicted targets for an individual miRNA, genes highlighted in orange represent predicted targets for multiple miRNAs and genes highlighted in green are not targeted by the miRNAs of interest in this pathway.

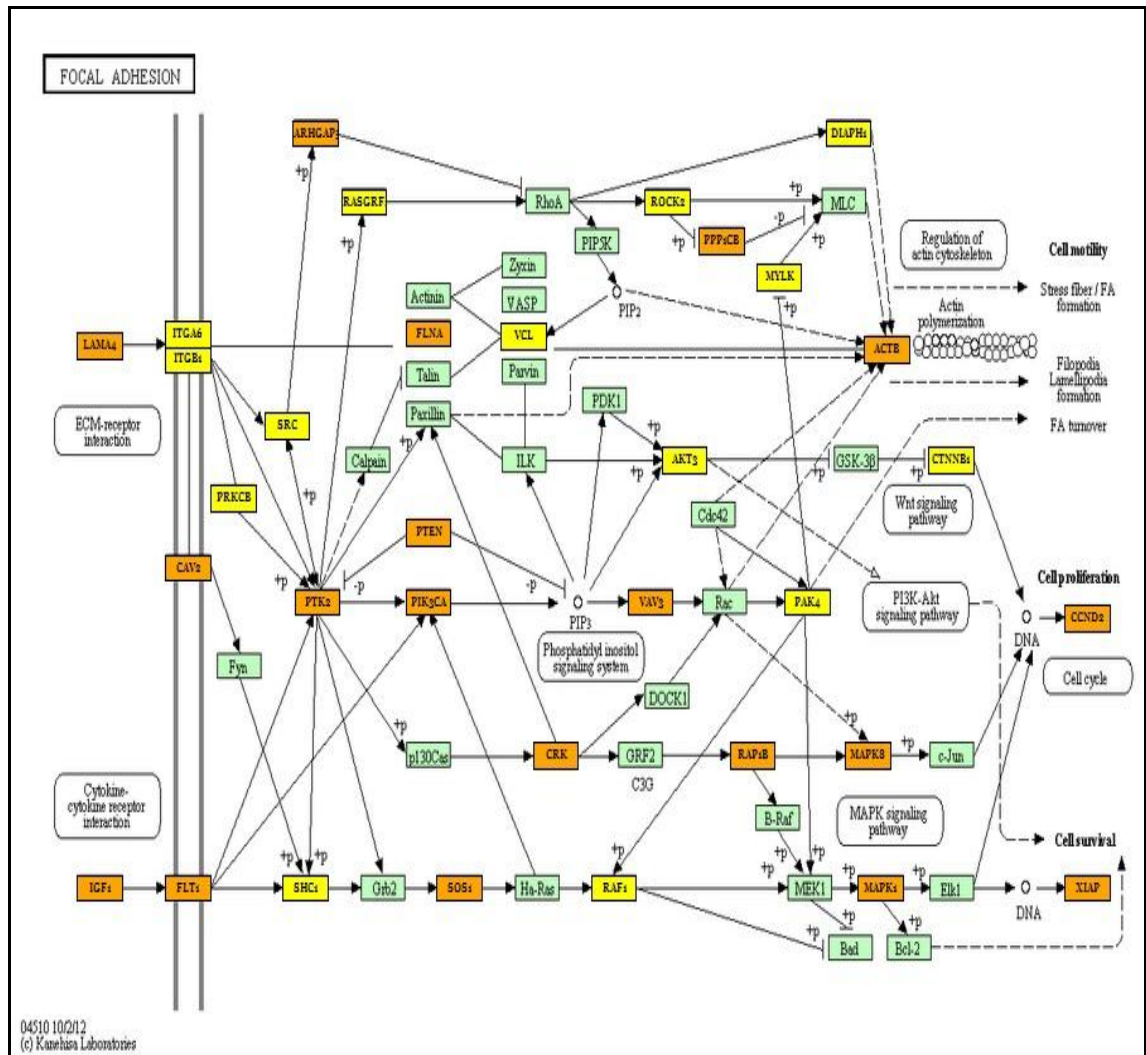


Figure 5.2.25 MiRNAs differentially regulated by SLPs from RT 001 and RT 027 may modulate genes involved in focal adhesion. The target list generated from experimental data of miRNAs differentially regulated by SLPs from RT 001 and RT 027 was inputted into DIANA-miRPath. A posteriori analysis was performed where the significance levels between all possible miRNA pathway pairs were calculated using enrichment analysis. The previously calculated significance levels were combined to provide a merged p-value for each pathway, by applying Fisher's combined probability method. The resulting gene lists were converted into KEGG images. Genes highlighted in yellow represent predicted targets for an individual miRNA, genes highlighted in orange represent predicted targets for multiple miRNAs and genes highlighted in green are not targeted by the miRNAs of interest in this pathway

Table 5.2.2 Forty-nine genes crossed two or more of the top 5 KEGG pathways and not all genes had predicted binding sites for the 24 miRNAs of interest. Gene lists generated in DIANA-miRPath, from the top 5 KEGG pathways were compared. Table showing the gene, the pathways it belongs to and if the gene contained a predicted binding site in its 3'UTR region according to TargetScan. TargetScan assesses miRNA seed complementarity and conservation.

Gene	ECM-receptor	PI3K	TGF-β	MAPK	Focal adhesion	miRNA seed regions in 3'UTR
MAPK1	-	√	√	√	√	-
ITGA9	√	√	-	-	√	miR-148b miR-152 miR-125a-5p
COL27A1	√	√	-	-	√	-
ITGB6	√	√	-	-	√	-
ITGA5	√	√	-	-	√	miR-148b miR-152
COL3A1	√	√	-	-	√	let-7 b/c/d/e
ITGA11	√	√	-	-	√	let-7 b/c/d/e miR-148b miR-152
COL2A1	√	√	-	-	√	miR-148b
COL4A2	√	√	-	-	√	let-7 b/c/d/e miR-9
COL1A1	√	√	-	-	√	let-7 b/c/d/e
ITGA7	√	√	-	-	√	-
COL4A6	√	√	-	-	√	let-7 b/c/d/e
COL5A2	√	√	-	-	√	let-7 b/c/d/e
COL4A1	√	√	-	-	√	miR-148b miR-152 miR-590-5p

						let-7 b/c/d/e
LAMA4	√	√	-	-	√	miR-148b miR-152
AKT1	-	√	-	√	√	-
SOS2	-	√	-	√	√	miR-148b miR-152
FGF12	-	√	-	√	-	miR-9
NFKB1	-	√	-	√	-	-
NRAS	-	√	-	√	-	miR-148b miR-145 miR-146a let-7 b/c/d/e
RAP1A	-	-	-	√	√	-
CHUK	-	√	-	√	-	let-7 b/c/d/e
KRAS	-	√	-	√	-	miR-155
MAPK8	-	-	-	√	√	-
SOS1	-	√	-	√	-	miR-9 miR148-b miR152 miR-155
FGF9	-	√	-	√	-	miR-155 miR-9
FGF18	-	√	-	√	-	-
NGF	-	√	-	√	-	let-7 b/c/d/e
RASGRF1	-	√	-	√	-	miR-125a-5p
RELA	-	√	-	√	-	miR-155
FGFR1	-	√	-	√	-	miR-125a-5p
ROCK1	-	-	√	-	√	miR148-b miR152 miR-145
ITGB8	-	-	√	-	√	miR-145 miR-221

						miR-152 miR-148b let-7 b/c/d/e
COL4A5	-	√	-	-	√	let-7 b/c/d/e
ROCK2	-	-	√	-	√	-
RAF1	-	√	-	-	√	miR-125a-5p
PIK3R3	-	√	-	-	√	miR-152 miR-148b miR-9 miR-24
PDK1	-	√	-	-	√	miR-155
VEGFC	-	√	-	-	√	-
ITGA2	-	√	-	-	√	-
COL1A2	-	√	-	-	√	let-7 b/c/d/e
PPP2CB	-	√	√	-	-	miR-132
AKT3	-	√	-	-	√	-
COL11A1	-	√	-	-	√	let-7 b/c/d/e
PTEN	-	√	-	-	√	miR-152 miR-148b
RPS6KB1	-	√	√	-	-	miR-145
PPP2CA	-	√	√	-	-	miR125a-5p
RPS6KB2	-	√	√	-	-	-
COL4A4	-	√	-	-	√	-

Table 5.2.3 Some genes in the PI3K-Akt signalling pathway had predicted binding sites for the 24 miRNAs of interest. Table showing the list of genes generated from DIANA miRPath and if the gene contained a predicted binding site in its 3'UTR region according to TargetScan, for the list of 24 miRNAs differentially regulated by SLPs from RT 001 and RT 027. TargetScan assesses miRNA seed complementarity and conservation, see Appendix G for the exact position of the predicted binding sites in the 3'UTR regions for each gene.

Gene	Conserved miRNA seed regions in 3'UTR
PRLR	-
GSK3B	miR-132 miR-9 miR-24
TSC1	let-7 b/c/d/e
PDGFRA	miR-24
PPP2R5E	miR-132 miR-148b miR-152
MYB	miR-155
PRKAA2	miR-125a-5p miR-146a let-7 b/c/d/e
PPP2R2C	-
CREB5	miR-9 miR-132 miR-145
YWHAG	miR-132 miR-125a-5p miR-221 miR-145
HSP90AA1	-
CREB1	miR-155

	miR-125a-5p
ANGPT2	miR-145
	miR-125a-5p
CDKN1B	miR-221
	miR-24
	miR-148b
	miR-152
YWHAB	miR-148b
	miR-152
GNB1	miR-145
PPP2R5C	miR-125a-5p
	miR-132
CDK6	miR-148b
	miR-152
	miR-145
	let-7 b/c/d/e
IL7R	-
PPP2R5A	-
GHR	let-7 b/c/d/e
IL4	-
IL2	-
THEM4	-
EIF4E	miR-9
CCNE2	miR-9
PPP2R2A	miR-9
	miR-221
	let-7 b/c/d/e
PIK3R1	miR-221
	miR-590-5p
	miR-155
YWHAZ	miR-155
PPP2R3C	-

KITLG	miR-132 miR-9
INSR	let-7 b/c/d/e
PRKAA1	miR-148b miR-152
FGF2	miR-148b miR-152
CHRM2	-
BCL2L1	let-7 b/c/d/e
CREB3L2	miR-9
ANGPT1	-
FOXO3	miR-132 miR-155 miR-9
FN1	-
PKN2	miR-145 miR-155 let-7 b/c/d/e
CDKN1A	let-7 b/c/d/e miR-132
SGK3	miR-132 miR-9 miR-155
CSF1R	miR-24 miR-155
OSMR	let-7 b/c/d/e
CSF1	miR-148b miR-152
GNG5	let-7 b/c/d/e
TEK	miR-148b miR-152
BCL2L11	miR-24

	miR-221
	miR-148b
	miR-152
	miR-9
IL6R	miR-590-5p
	miR-125a-5p
	miR-155
	miR-9
	let-7 b/c/d/e
EFNA1	miR-145
	miR-9

Table 5.2.4 Some genes in the TGF- β signalling pathway had predicted binding sites for the 24 miRNAs of interest. Table showing the list of genes generated from DIANA miRPath and if the gene contained a predicted binding site in its 3'UTR region according to TargetScan, for the list of 24 miRNAs differentially regulated by SLPs from RT 001 and RT 027. TargetScan assesses miRNA seed complementarity and conservation, see Appendix G for the exact position of the predicted binding sites in the 3'UTR regions for each gene.

Gene	Conserved miRNA seed regions in 3'UTR
ID2	-
SMAD2	miR-125a-5p let-7 b/c/d/e miR-145 miR-155 miR-148b miR-152
SMAD6	-
INHBB	miR-148b miR-152 miR-145 miR-9
SMAD9	-
SMURF2	-
BMPR1B	miR-125a-5p
BMP5	-
PITX2	miR-590-5p
SMAD3	miR-145
INHBA	-
ID4	miR-9
ACVR1	miR-148b miR-152

SKP1	miR-148b miR-152 miR-145 miR-221
ZFYVE16	miR-221
DCN	-
E2F5	miR-132 let-7 b/c/d/e miR-132
SMAD5	miR-145 miR-148b miR-152 miR-132 miR-24 miR-155
ACVR2A	miR-145 miR-155 let-7 b/c/d/e
GDF6	miR-148b miR-152 miR-155 let-7 b/c/d/e
BMP2	-
TFDP1	-
ACVR1C	let-7 b/c/d/e miR-125a-5p miR-9
GDF5	miR-132
TGFB2	miR-145 miR-590-5p miR-148b miR-152

EP300	miR-132
BMPR1A	-
LTBP1	miR-148b miR-152
SMAD7	miR-590-5p
NOG	miR-148b miR-152
CREBBP	-
BMPR2	miR-125a-5p miR-590-5p

Table 5.2.5 Some genes involved in Focal adhesion had predicted binding sites for the 24 miRNAs of interest. Table showing the list of gens generated from DIANA miRPath and if the gene contained a predicted biding site in its 3'UTR region according to TargetScan, for the list of 24 miRNAs differentially regulated by SLPs from RT 001 and RT 027. TargetScan assesses miRNA seed complementarity and conservation, see Appendix G for the exact position of the predicted binding sites in the 3'UTR regions for each gene.

Gene	Conserved miRNA seed regions in 3'UTR
ACTB	miR-145
SHC1	miR-9
COL24A1	let-7 b/c/d/e
PPP1CC	-
PAK7	-
VCL	miR-590-5p miR-9
CAV2	miR-148b miR-152 miR-145
PPP1R12A	miR-148b miR-152
CTNNB1	-
DIAPH1	-
SRC	miR-9
PAK4	miR-9 miR-145 miR-24
MYLK3	-
BIRC3	-
VAV3	miR-125a-5p miR-155

	let-7 b/c/d/e
	miR-9
MYLK	miR-155
	miR-9
	miR-24
XIAP	miR-146a
PPP1CB	miR-148b
	miR-152

Table 5.2.6 Some genes in the MAPK signalling pathway had predicted binding sites for the 24 miRNAs of interest. Table showing the list of genes generated from DIANA miRPath and if the gene contained a predicted binding site in its 3'UTR region according to TargetScan, for the list of 24 miRNAs differentially regulated by SLPs from RT 001 and RT 027. TargetScan assesses miRNA seed complementarity and conservation, see Appendix G for the exact position of the predicted binding sites in the 3'UTR regions for each gene.

Gene	Conserved miRNA seed regions in 3'UTR
FOS	miR-221 miR-155
NTRK2	-
NTF3	miR-221 miR-590-5p
DUSP22	-
CACNA1G	-
PTPRQ	-
GNA12	miR-132
IL1R1	miR-24
RASA2	miR-145 miR-9 miR-125a-5p miR-590-5p
ELK4	miR-145 let-7 b/c/d/e miR-221
MAP3K3	miR-9 miR-145 miR-125a-5p let-7 b/c/d/e miR-132

MAP2K7	miR-125a-5p miR-9
DUSP14	-
CACNB4	miR-221 miR-155 let-7b/c/d/e
DUSP6	miR-9 miR-145 miR-125a-5p
RASGRF2	-
LAMTOR3	-
MAP4K3	let-7 b/c/d/e
RPS6KA1	miR-125a-5p
RASGRP2	-
GADD45A	miR-148b miR-152
MAP3K4	miR-148b miR-152
MAP3K1	miR-9 let-7 b/c/d/e
MAP3K13	let-7 b/c/d/e
TAB2	let-7 b/c/d/e miR-155
BDNF	miR-155
MAP3K11	miR-145 miR-125a-5p
TAOK1	miR-155 miR-24 let-7 b/c/d/e miR-145 miR-221
MAP2K6	-

FGF11	miR-24 let-7 b/c/d/e
PPP3CA	miR-145 miR-590-5p let-7 b/c/d/e
NLK	miR-24 miR-221 miR-148b miR-152 let-7 b/c/d/e
CASP3	let-7 b/c/d/e
RASGRP1	let-7 b/c/d/e
RAPGEF2	miR-145 miR-155
NFATC2	-
TRAF6	miR-146a miR-125a-5p
MYC	-
PPM1A	miR-125a-5p
CACNB1	miR-125a-5p
CACNA1E	miR-24 let-7 b/c/d/e miR-9
DUSP8	miR-590-5p miR-9 miR-24 miR-148b miR-152
PPP3R1	miR-221
HSPA8	-
MAX	-
FAS	let-7 b/c/d/e

RPS6KA3	let-7 b/c/d/e miR-155 miR-590-5p miR-145
MAPK12	miR-125a-5p
MECOM	-
STMN1	-
MAP3K2	-
PPM1B	-
CACNA2D1	-
CACNB2	miR-125a-5p miR-145 miR-9
MEF2C	miR-590-5p miR-9 let-7 b/c/d/e
IL1A	miR-24
MAP2K4	miR-145
PLA2G4E	-
MAP3K7	-
SRF	miR-9 miR-125a-5p
MAPKAPK2	-
DUSP1	let-7 b/c/d/e
MAPK10	miR-590-5p miR-221
PDGFRB	miR-24 miR-9
CACNB3	miR-125a-5p

Human IL6R ENST00000344086.4 3' UTR length: 4285

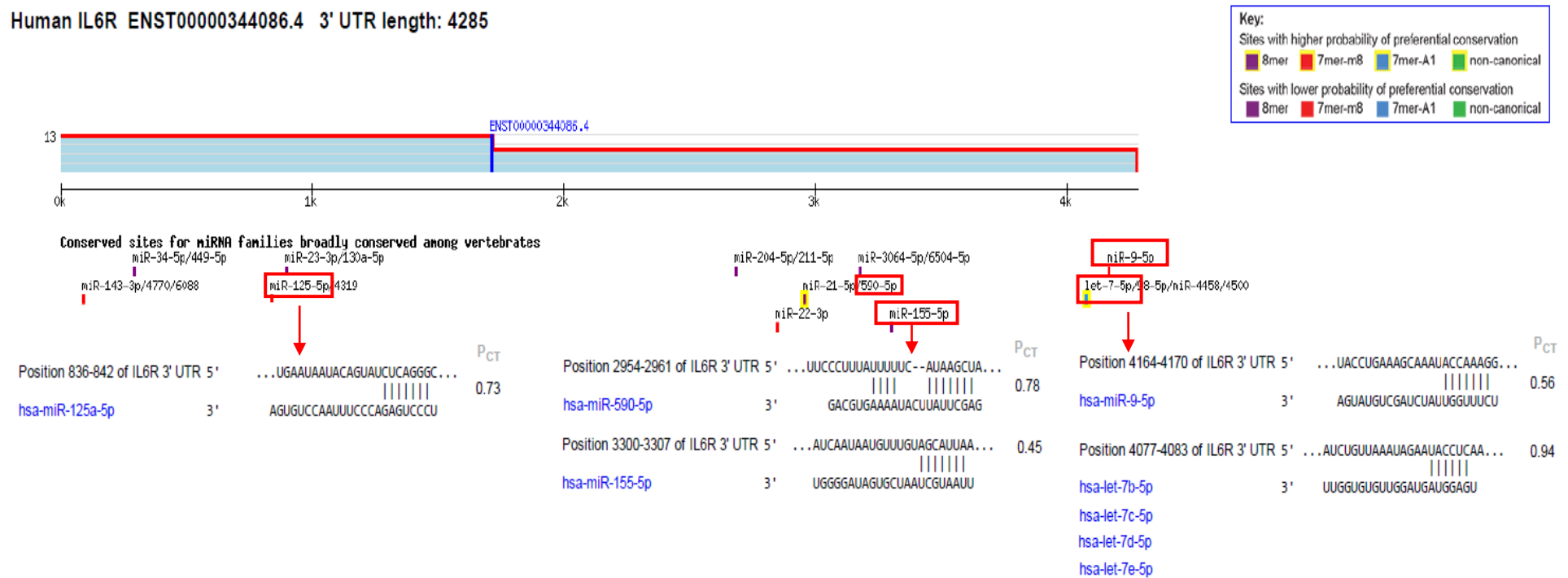


Figure 5.2.26 The IL-6 receptor gene contains possible 3'UTR binding sites for miR-125, miR-590, miR-155, miR-9 and let-7 b/c/d/e which were differentially regulated by SLPs from RT 001 and RT 027. These miRNAs were clustered in three distinct groups. The target list generated from experimental data of miRNAs differentially regulated by SLPs from RT 001 and RT 027 was inputted into DIANA-miRPath. A posteriori analysis was performed where the significance levels between all possible miRNA pathway pairs were calculated using enrichment analysis. The previously calculated significance levels were combined to provide a merged p-value for each pathway, by applying Fisher's combined probability method. Gene lists from the PI3K-Akt signalling pathway were inputted into TargetScan were seed match conservation and P_{CT} scores were determined.

Human NRAS ENST00000369535.4 3' UTR length: 3630

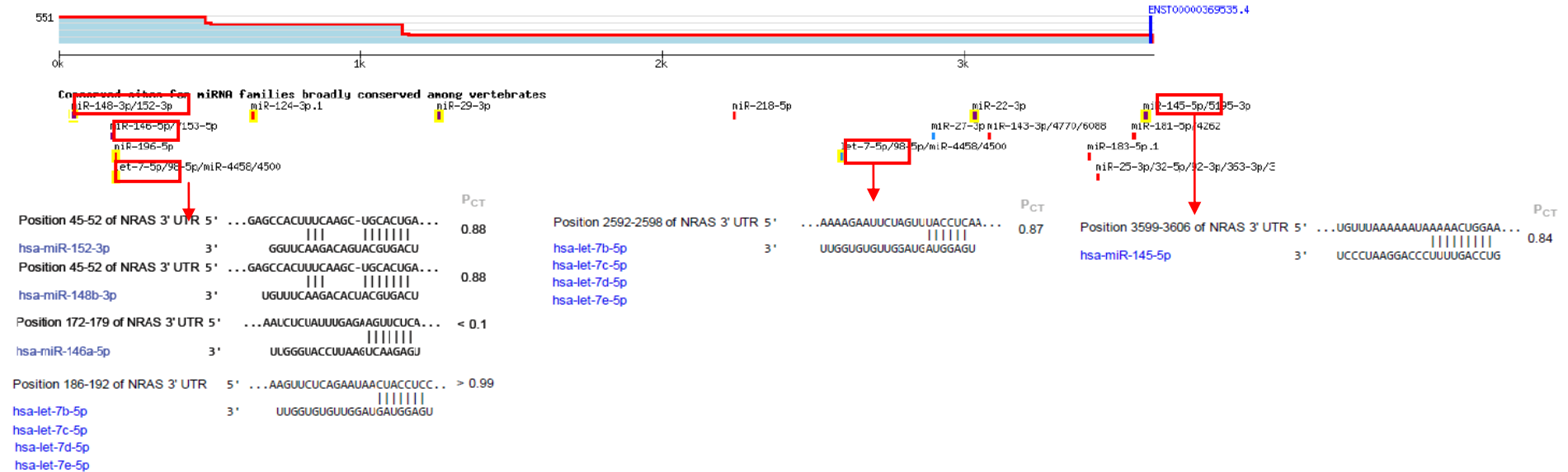
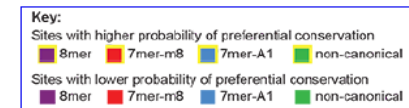


Figure 5.2.27 The NRAS gene contains possible 3'UTR binding sites for miR-152, miR-148b, miR-146a, let-7 b/c/d/e and miR-145 which are differentially regulated by SLPs from RT 001 and RT 027. These miRNAs were clustered in three distinct groups and let-7 b/c/d/e had 2 possible binding sites. The target list generated from experimental data of miRNAs differentially regulated by SLPs from RT 001 and RT 027 was inputted into DIANA-miRPath. A posteriori analysis was performed where the significance levels between all possible miRNA pathway pairs were calculated using enrichment analysis. The previously calculated significance levels were combined to provide a merged p-value for each pathway, by applying Fisher's combined probability method. Gene lists from the PI3K-Akt signalling pathway and MAPK signalling pathway were inputted into TargetScan were seed match conservation and P_{CT} scores were determined.

Human SMAD2 ENST00000262160.6 3' UTR length: 10276

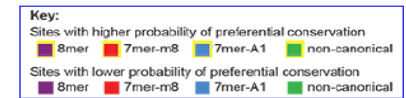


Figure 5.2.28 The SMAD2 gene contains possible 3'UTR binding sites for miR-132, miR-125a, let-7 b/c/d/e, miR-145, miR-152, miR-148b and miR-155 which are differentially regulated by SLPs from RT 001 and RT 027. These miRNAs were clustered in three distinct groups. The target list generated from experimental data of miRNAs differentially regulated by SLPs from RT 001 and RT 027 was inputted into DIANA-miRPath. A posteriori analysis was performed where the significance levels between all possible miRNA pathway pairs were calculated using enrichment analysis. The previously calculated significance levels were combined to provide a merged p-value for each pathway, by applying Fisher's combined probability method. Gene lists from the TGF- β signalling pathway were inputted into TargetScan were seed match conservation and P_{CT} scores were determined.

Human SOS1 ENST00000426016.1 3' UTR length: 4428

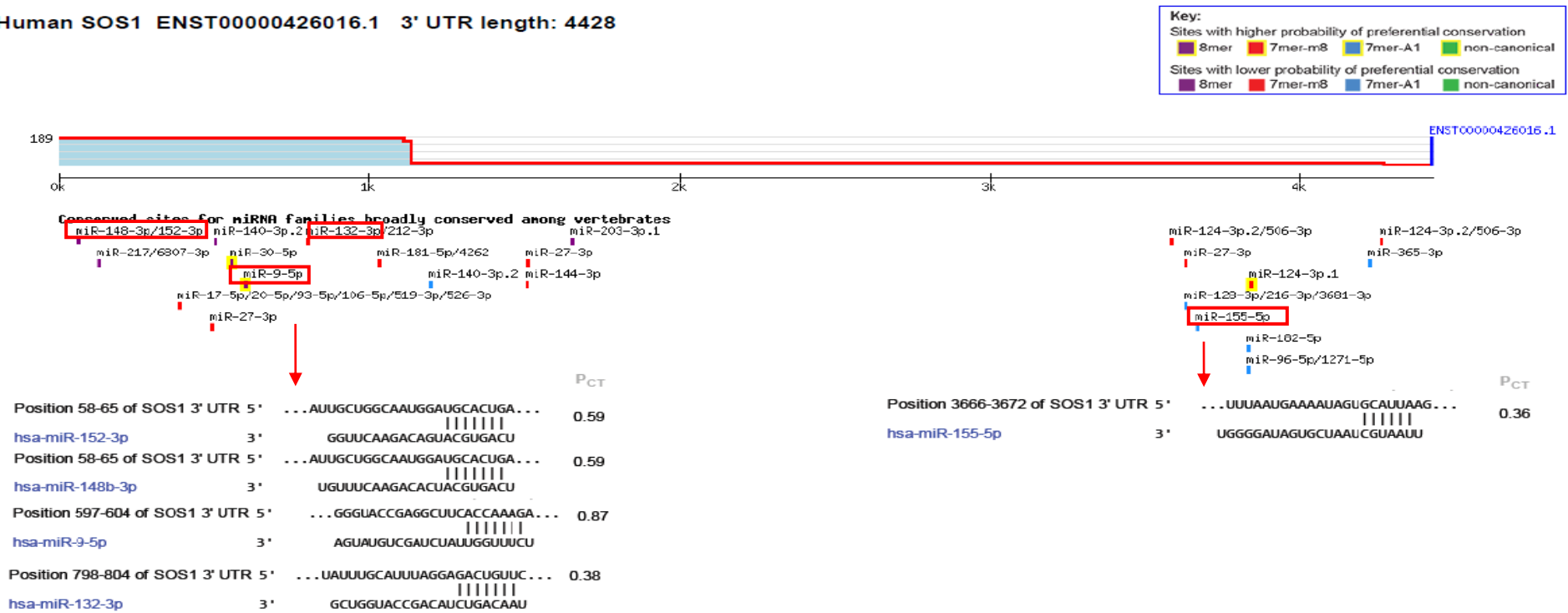


Figure 5.2.29 The SOS1 gene contains possible 3'UTR binding sites for miR-152, miR-148b, miR-9, miR-132 and miR-155 which are differentially regulated by SLPs from RT 001 and RT 027. These miRNAs were clustered in two distinct groups. The target list generated from experimental data of miRNAs differentially regulated by SLPs from RT 001 and RT 027 was inputted into DIANA-miRPath. A posteriori analysis was performed where the significance levels between all possible miRNA pathway pairs were calculated using enrichment analysis. The previously calculated significance levels were combined to provide a merged p-value for each pathway, by applying Fisher's combined probability method. Gene lists from the MAPK and PI3K-Akt signalling were inputted into TargetScan were seed match conservation and P_{CT} scores were determined.

Human TRAF6 ENST00000526995.1 3' UTR length: 6100

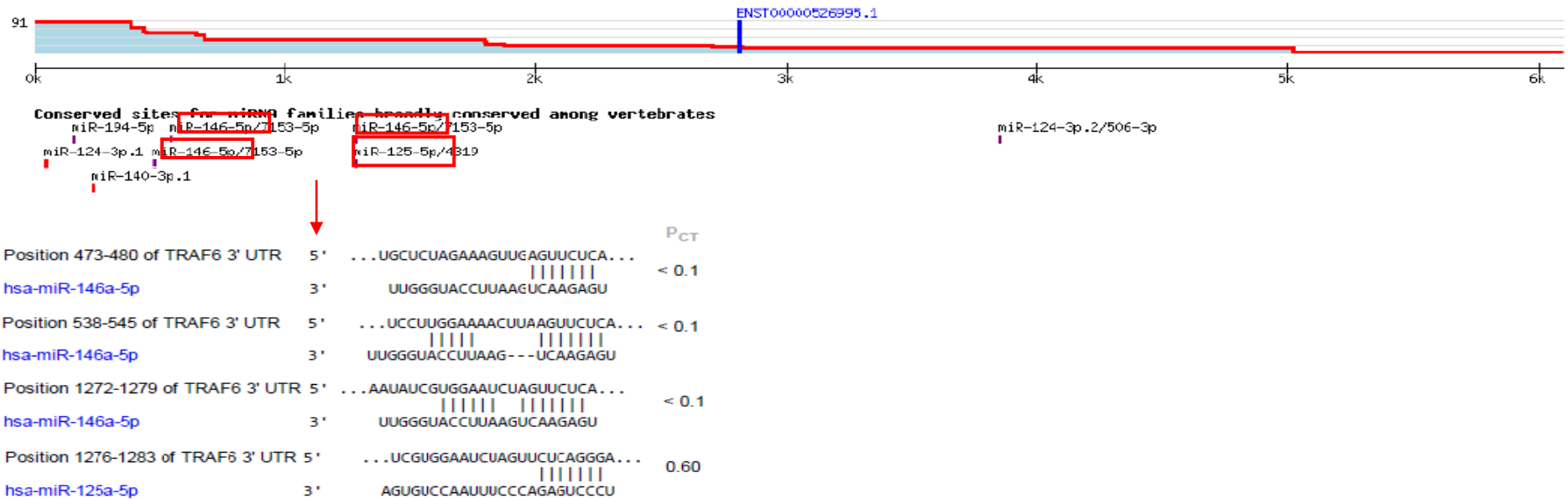
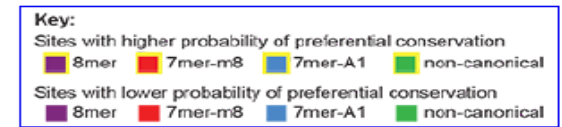


Figure 5.2.30 The TRAF6 gene contains possible 3'UTR binding sites for miR-146a and miR-125a which are differentially regulated by SLPs from RT 001 and RT 027. These miRNAs were clustered in one group and miR-146a has 3 possible binding sites. The target list generated from experimental data of miRNAs differentially regulated by SLPs from RT 001 and RT 027 was inputted into DIANA-miRPath. A posteriori analysis was performed where the significance levels between all possible miRNA pathway pairs were calculated using enrichment analysis. The previously calculated significance levels were combined to provide a merged p-value for each pathway, by applying Fisher's combined probability method. Gene lists from the MAPK signalling were inputted into TargetScan where seed match conservation and PCT scores were determined.

5.3 Discussion

A pathogen must successfully infiltrate the host's tissues by attaching to cells and suppressing the cell's natural functions for its own end, all while avoiding the host's immune system and other defences (Krachler, Woolery, & Orth, 2011). Some strains of *C. difficile* can do this more effectively than others and there are differences in the severity of infection between ribotypes 001 and 027, as previously outlined. In order to protect against invading pathogens, organ specific and systemic immunological host responses are activated by PAMPS *via* membrane associated TLRs and cytoplasmic Nod-like receptors (Staedel & Darfeuille, 2013). TLR4 was the first mammalian TLR to be discovered, it detects LPS which is one of the best studied components of bacteria that can activate an immune response (Ruslan Medzhitov et al., 1997). TLR4 is distinctive among TLRs in that it activates the MyD88-dependent and MyD88-independent signalling pathways (Akira & Takeda, 2004). Activation of both arms of the TLR4 signalling pathway is required for full bacterial clearance. Downstream signalling following activation of TLR4 with LPS ultimately leads to the activation of transcription factors such as AP-1, NF- κ B and IRF3 and the induction of pro-inflammatory cytokines, IFN and IFN-inducible genes (Mogensen, 2009). NF- κ B activates innate and adaptive immunity aimed at eliminating the detected pathogen and developing a long lasting protection against future infection (Staedel & Darfeuille, 2013). Other studies have shown the importance of IRF3 and type I IFNs in the modulation of host defence and bacterial clearance (O'Connell et al., 2004).

The inflammatory response to infection must be tightly regulated in order to achieve pathogen clearance and at the same time avoid detrimental consequences of deregulated gene expression (Staedel & Darfeuille, 2013). The discovery in eukaryotic cells of small non-coding RNAs known as miRNAs has greatly expanded our understanding of the mechanisms that regulate gene expression (Friedman, Farh, Burge, & Bartel, 2009). MiRNAs have been shown to be involved in innate immunity by regulating TLR signalling and ensuing cytokine response by targeting a variety of signalling proteins, regulatory molecules and transcription factors (Dalal & Kwon, 2010; He et al., 2014; Sonkoly et al., 2008). There is also mounting evidence that miRNAs orchestrate immune regulation and the host response to pathogens during infection. Despite their

clear importance as a class of regulatory molecule, determining the biological relevance of individual miRNAs has proven challenging (Vidigal & Ventura, 2014). The implication of miRNAs in human diseases warrants a critical need to identify miRNA regulated genes in a biologically relevant context (Tarang & Weston, 2014). It is currently estimated that the human genome encodes thousands of miRNAs, targeting approximately 60% of all protein coding genes (Friedman et al., 2009). MiRNAs, similar to mRNA, are expressed in a time and tissue specific manner, and are involved in many fundamental biological processes.

The function of specific miRNAs have been predominantly inferred from over expression studies in cultured cells or from studies that use antisense molecules as a means of disrupting their pairing to target mRNA (Vidigal & Ventura, 2014). A common method to determine miRNA functionality is to transfect cells with both luciferase reporter constructs and increasing the amounts of the miRNA of interest with chemically synthesised miRNA mimics (van Rooij, 2011). The advantage of introducing a miRNA is that if the miRNA actually targets the binding site in the 3'UTR region, there will be a dose dependent decrease in gene expression and this can be determined from a luciferase gene reporter assay read out. In chapter three we established a luciferase gene reporter assay to examine the expression of NF- κ B and IRF3 signalling in Hek TLR4/MD2/CD14 cells. We showed that SLPs from ribotype 001 and 027 activate NF- κ B and the potency of the response differed between ribotypes. SLPs from ribotype 027 activate IRF3 signalling but SLPs from ribotype 001 fail to induce this response. In chapter four we identified 24 miRNAs that were differentially regulated by SLPs from ribotype 001 and 027 using qPCR. We validated the expression of miR-146a, miR-145, miR-155 and let-7e in human and murine cell lines. The aim of the first part of this chapter was to determine the functionality of; miR-146a, miR-145, miR-155 and let-7e, in NF- κ B and IRF3 signalling in response to SLPs following TLR4 activation, using chemically synthesised miRNA mimics in the already established luciferase gene reporter assay.

Initial findings suggested that miR-146a, miR-145, miR-155 and let-7e individually targeted RANTES production in response to TLR4 activation with LPS. MiRNA mimics over expressing miR-146a, miR-145 and miR-155 decreased RANTES

production in a dose dependent manner, while miRNA mimics over expressing let-7e decreased RANTES production with 1 and 100 nM, in response to LPS. On the other hand IL-8 production was not affected by the individual miRNA mimics in response to TLR4 activation with LPS. Seeing as transfection with 100 nM of each miRNA mimic affected RANTES production we choose this concentration for all further studies. We incorporated positive and negative control miRNA mimics into our study and showed that miRNA mimics had the ability to bind to constructs leading to decreased NF- κ B/IRF3 gene expression as well as IL-8/RANTES cytokine production. We also showed that the outcome was not due to the effects of transient transfection alone and the combination of transient transfection with cell stimulation did not have any significant cytotoxic effects on the cells. Consequently we were unable to link the individual miRNAs to NF- κ B and IRF3 signalling. Over expressing miR-146a, miR-145, miR-155 and let-7e did not decrease IRF3 signalling or RANTES production in response to SLPs from ribotype 001 and 027. We confirmed however that miR-146a, miR-145, miR-155 and let-7e targeted IRF3 gene expression and RANTES production specifically in response to TLR4 activation with LPS. NF- κ B and IL-8 production was not affected when the miRNAs were over expressed in response to LPS, SLPs from ribotype 001 and 027.

Interestingly both LPS and SLPs from ribotype 027 activate the same TLR4 receptor and lead to downstream activation of NF- κ B and IRF3 signalling. Yet there are distinct differences in the miRNAs induced and how they target essential signalling molecules in regard to IRF3 signalling. This has not yet been reported in the literature to the best of our knowledge. These proteins seemingly activate the same signalling pathways however our study highlights that miRNAs regulate this further and thus warrants further investigation. It is possible that miRNAs that target IRF3 signalling in response to SLPs from ribotype 001 and 027 require the cooperation of other miRNAs to effectively target this signalling pathway. Evidence from the literature shows that miRNAs rarely act in isolation and they have been shown to be incorporated into various negative feedback and feed forward loops (Tsang, Zhu, & Oudenaarden, 2007). Recently studies have shown that transcriptional regulation by transcription factors and post-transcriptional regulation by miRNAs are often highly coordinated (Cai, Zhou, & Liu, 2013; Martinez & Walhout, 2009; Tsang et al., 2007). In negative feedback loops a

transcription factor suppresses a miRNA and the transcription factor itself is negatively regulated by the miRNA. Evidence from the literature has also shown that this type of feedback loop behaves like a switch, even without cooperative binding of the transcription factor (Cai et al., 2013). MiRNAs regulate many different targets, individual 3'UTRs also contain binding sites for multiple miRNAs, allowing for elaborate and complicated networks in which redundancy and cooperation between miRNAs determine the effect on gene expression (Bartel, 2009; Martinez-Sanchez & Murphy, 2013; Obermayer & Levine, 2014; van Rooij, 2011).

Nonetheless the most commonly used cellular assays are based on the principle of studying the functional consequences of artificially manipulating miRNA levels. However, as the biological concentrations of these miRNAs *in vivo* may be several orders of magnitude different than *in vitro* conditions, it is essential that the results of target recognition are recapitulated in appropriate animal models (Tarang & Weston, 2014). We had access to a bank of RNA samples derived from colonic tissue from a *C. difficile* infection model. Mice were treated with a cocktail of antibiotics before being infected with 10^3 *C. difficile* spores from ribotype 001 and 027. The colon was harvested at two time points post infection and RNA was extracted from the distal colon. Data previously generated in our laboratory from this infection model linked infection with ribotype 027 with more severe disease. Animals infected with this ribotype showed greater weight loss, more tissue damage, and higher bacterial load relative to control and mice infected with ribotype 001. Mice infected with ribotype 001 were able to effectively recover after seven days, with lowered CFU counts and weights comparable to control mice. Histology of colonic tissue supported this analysis, revealing mice infected with ribotype 001 had healthy gut morphology seven days after infection, while mice infected with ribotype 027 had more severe and persistent damage (Lynch 2014, unpublished). The aim of the next part of this chapter was to examine the expression of miR-146a, miR-145, miR-155 and let-7e from the colonic tissue generated in the *C. difficile* infection model, seeing as we validated these miRNAs in both a human and murine cell lines in the previous chapter.

We found that the total RNA derived from the *C. difficile* infection model contained each of the miRNAs and small RNA endogenous controls. Our results suggest a role for

miR-146a, miR-145, miR-155 and let-7e in *C. difficile* infection. Our data showed that miR-146a and miR-145 were differentially regulated in colonic tissue of mice infected with ribotype 001 and 027, three and seven days post infection. These miRNAs were down regulated in colonic tissue of mice infected with ribotype 027 three days post infection. This data aligned with *in vitro* results, however at day 7 these miRNAs were up regulated. Our data shows that miR-145 and miR-146a were down regulated at day 3 of infection in response to ribotype 027. In comparison miR-145 and miR-146a were up regulated in the tissue of mice infected with ribotype 001 at day 3 of infection. On the other hand miR-155 and let-7e were differentially regulated in colonic tissue from mice infected with ribotype 001 and 027 three days post infection. Both miRNAs were up regulated in colonic tissue of mice infected with ribotype 001 three days post infection, this was significantly different to the levels induced by mice infected with ribotype 027. These miRNA levels in mice infected with ribotype 001 and 027 appeared to return to levels comparable to levels seen in the control mice seven days post infection. The infection data does not align with *in vitro* data in that we do not see a down regulation of these miRNAs, therefore expression may not be linked to the SLPs alone. However we did see differential regulation of miR-155 and let-7e between both ribotypes suggesting they may have other important roles in regulating the host immune response to *C. difficile*. Research from our laboratory previously found that IL-10 was increased in mice infected with ribotype 027 at day 3 of infection in this model (Lynch 2014, unpublished). In contrast IL-10 was not produced in response to ribotype 001 at day 3 of infection possibly allowing the increase in miR-155 expression at this point in infection- this data also aligns with *in vitro* experiments. Therefore there may be a link between the induction of IL-10 and miR-155 expression in response to *C. difficile*.

The implication of miRNAs in human diseases warrants a critical need to identify miRNA regulated genes in a biologically relevant context (Tarang & Weston, 2014). Identification of miRNA target genes has been a great challenge and computational algorithms have been the major driving force in predicting miRNA targets (Bentwich et al., 2005; Jens & Rajewsky, 2014; Kuhn et al., 2008; Lewis et al., 2005). Experimental data is not enough to give a comprehensive view of miRNA biology, it is thought that to get a more complete view experimental data must be combined with computational predications (Bentwich et al., 2005; Ghosh et al., 2007; Sachidanandam, 2005). In

chapter four we identified 24 miRNAs that were differentially regulated by SLPs from ribotypes 001 and 027 experimentally using qPCR. Seeing as miRNAs may work in complex networks we decided to utilise bioinformatics to identify possible miRNA/pathway/gene interactions from the list of 24 miRNAs to identify biologically relevant miRNA target genes. DIANA miRPath is thought to stand out from other prediction tools due to its range of capabilities, ease of use, relatively current input data and maintenance of the software (Peterson et al., 2014). Our data shows that SLPs from ribotypes 001 and 027 may regulate miRNAs that target genes involved in these essential cell signalling processes. The bioinformatics search identified 54 pathways in which the 24 miRNAs of interest were predicted to target genes in pathways found in KEGG. The top 5 pathways; ECM, MAPK signalling, PI3K-AKT signalling, TGF- β signalling and focal adhesion- were predicted to be involved in essential cell signalling processes targeting 350 genes.

MAPKs are serine-threonine kinases that mediate intracellular signalling associated with a variety of cellular activities including; cell proliferation, differentiation, survival, death, and transformation (Kim & Choi, 2010). Our data shows that 98 genes were predicted to be targeted by 10 of the miRNAs of interest in the MAPK signalling pathway. The genes targeted consisted of key kinases that regulate this pathway and other genes that are known to modulate the immune response. We also show that 121 genes were predicted to be targeted by 11 of the miRNAs in the PI3K-Akt signalling pathway. This pathway plays an important role in a variety of cellular processes, including migration, survival and proliferation. For this reason, the pathway is targeted by many pathogens to reinforce or destroy focal adhesions, which play an integral role in phagocytosis (Krachler et al., 2011). Activation of PI3K can also activate small GTPases, such as Ras and Rac, which are linked to proliferation. Focal adhesions lie at the convergence of integrin adhesion, signalling and the actin cytoskeleton. Our data shows 74 genes were predicted to be targeted by 10 of the miRNAs in the focal adhesion pathway. Cells modify focal adhesions in response to changes in the molecular composition and physical forces present in their ECM thus modulation of focal adhesion can regulate cell proliferation, survival, migration and invasion (Wozniak, Modzelewska, Kwong, & Keely, 2004). MiRNAs regulated in response to ribotype 001 and 027 potentially alter cell fate. Evidence from the literature has shown that altering

cell fate may be vital in the fine tuning of the immune response against infection (Kim & Choi, 2010; Liu, Drescher, & Chen, 2009).

As well as nonspecific hydrophobic and electrostatic forces, bacteria use surface proteins with specific affinity for plasma proteins and components of the ECM to physically interact with host cells and mucins *via* a number of different adhesins. Our data also shows that 15 genes were predicted to be targeted by 6 of the miRNAs of interest in ECM receptor signalling pathway. The ECM is not generally exposed in the gut of healthy individuals and thus is not accessible for interaction with bacteria. However, these molecules become exposed after a tissue trauma following a mechanical or chemical injury or after an infection- thus aiding the adherence of the bacteria to epithelial cells (Dubreuil, Giudice, & Rappuoli, 2002). The genes targeted by the miRNAs of interest were integrins which are involved in cell surface adhesion and collagens which form structural elements in the ECM. It is possible that down regulation of miRNAs induced by ribotype 027 preserve the expression of ECM genes allowing the bacteria to adhere to epithelial cells. In contrast miRNAs regulated in response to ribotype 001 may bind to the 3'UTR of genes involved in the ECM preventing expression thus leading to reduced bacterial adherence. We also identified 42 genes that were predicted to be targeted by 9 miRNAs of interest in the TGF- β signalling pathway.

Members of the TGF- β family exert a wide range of biological effects on a large variety of cell types, for example they regulate cell growth, differentiation, matrix production and apoptosis. Many of them have important functions during embryonic development in pattern formation and tissue specification; in the adult they are involved in processes such as tissue repair and modulation of the immune system (Heldin, Miyazono, & ten Dijke, 1997). The genes targeted by the miRNAs of interest were SMAD proteins and other growth factors. SMAD3 inhibits activated macrophages and is essential in suppressing the inflammatory response by sequestering p300 an essential co-activator from the target promoter (Werner et al., 2000). SMAD3 contains a predicted binding site for miR-145 and in chapter four we showed that miR-145 was up regulated in response to SLPs from ribotype 001, however it is down regulated in response to SLPs from ribotype 027 in Hek TLR4/MD2/CD14 cells. It is possible that miR-145 induced

by SLPs from ribotype 001 bind to the 3'UTR region of SMAD3 preventing its expression, thus stopping SMAD3 from suppressing the inflammatory response leading to more efficient bacterial clearance. In contrast miR-145 is down regulated in response to SLPs from ribotype 027, therefore SMAD3 may be free to suppress the inflammatory response allowing for the persistence of infection seen with ribotype 027. Hence we have identified possible biologically relevant genes that are predicted to be targeted by the miRNAs induced in response to ribotype 001 and 027 and must therefore be validated experimentally in future work.

MiRNAs can be transcribed from intergenic regions, where an individual gene or cluster of miRNAs form an independent transcriptional unit, or from introns of coding genes. 38% of murine miRNAs fall within introns of mRNAs (Chiang et al., 2010). In most cases the miRNA is processed from the intron of the host transcript thus the miRNAs and host gene are co-ordinately expressed. Additionally, multiple miRNA hairpins are often encoded as clusters within a single primary transcript. These clusters can encode multiple miRNA seed families (Gurtan & Sharp, 2013). While expression between clustered miRNAs is strongly correlated, it is not absolute thus indicating regulation at the level of processing (Chiang et al., 2010). The clustered organisation of miRNAs suggests shared biological function among related miRNAs present in the same primary transcript (Gurtan & Sharp, 2013). MiRNAs regulate a plethora of target mRNAs, the simultaneous targeting of individual transcripts by multiple miRNAs and the redundancy of miRNA mediated control of gene expression- particularly for miRNAs sharing common seed sequences, are important factors that contribute to this complexity (Eulalio & Mano, 2015). The number and distribution of miRNA binding sites is particularly important. Studies have demonstrated that two sites in the same or different miRNAs can act synergistically and that the distance between neighbouring miRNA binding sites affects the strength of the targets down regulation (Koscianska, Witkos, Kozłowska, Wojciechowska, & Krzyzosiak, 2015). Specifically, optimal down regulation was observed when the distance between the 3' end of the first miRNA site and the 5' end of the subsequent one was > 7 and < 40 nt and when the 5' ends of both miRNA seeds were separated by between 13 and 35 nt. Therefore the target site's activity depends on its surrounding context (Grimson et al., 2007; Saetrom et al., 2007). We searched for the 24 miRNAs of interest in the 3'UTR gene in each of the 350 genes

identified by DIANA miRPath in TargetScan. Not all of the genes had predicted 3'UTR regions for the 24 miRNAs of interest according to TargetScan, however the majority did have possible predicted binding sites. We selected 5 genes IL-6R, NRAS, SMAD2, SOS1 and TRAF6 for further investigation.

Through IL-6R, IL-6 signalling activates tyrosine kinases JAK1, JAK2, and TYK2, which leads to the phosphorylation of STAT1 and STAT3. STAT3 is an important regulator for a number of anti-apoptotic genes (Yao et al., 2014). NRAS is from a family of GTPase that control basic cellular functions including control of proliferation, differentiation and apoptosis and there is increasing evidence that it plays a role in the induction of T cells (Mor, Keren, Kloog, & George, 2008). SMAD2 plays a critical role in TGF- β signalling (Ungefroren et al., 2011). Targeted SOS1 deletion reveals a critical role in early T-cell development (Kortum et al., 2013). While TRAF6 a signalling adapter molecule plays a significant role in MyD88-dependent signalling, it is also important for DC maturation, cytokine production and has a T cell stimulatory capacity (Kobayashi, Walsh, & Choi, 2004). Our data shows that the miRNAs of interest were predicted to be found in distinctive groups in the 3'UTR region of each of the 5 genes. There were possible binding sites for miR-148b and miR-152 in the same location in 3 out of the 5 genes. There were also possible binding sites for let-7b, let-7c, let-7d and let-7e in the same location in 4 out of 5 of the genes. There were also predicted cooperation between miR-146a and miR-125 in the TRAF6 gene, and the miRNAs were predicted to be separated by 11 nt possibly allowing for optimal down regulation. MiR-155 were is close proximity to miR-550 in the 3'UTR region of the IL6 receptor gene while miR-145 and miR-146a were in close proximity in the 3'UTR region of the SMAD2 gene. This computational data shows that the miRNAs induced by SLPs from ribotype 001 and 027 may work together in distinctive miRNA clusters which regulate genes involved in a variety of cellular functions that may regulate the immune response and T cell function.

In summary, LPS and SLPs from ribotype 027 activate the same TLR4 receptor and lead to downstream activation of NF- κ B and IRF3 signalling. Yet there are distinct differences in the miRNAs regulated and how they target essential signalling molecules in regard to IRF3 signalling. This has not yet been reported in the literature to the best

of our knowledge. These proteins seemingly activate the same signalling pathways however our study highlights that miRNAs regulate this further and thus warrants further investigation. We were unable to link the individual miRNAs to NF- κ B and IRF3 signalling- over expressing miR-146a, miR-145, miR-155 and let-7e did not decrease IRF3 signalling or RANTES production in response to SLPs from ribotype 001 and 027. However our data suggests a role these miRNAs in CDI. There may also be a link between the induction of IL-10 and miR-155 expression in response to *C. difficile* and this novel finding has yet to be reported in the literature, it also warrants further investigation. The impact of the modulation of the immune response by the miRNAs may lead to biologically relevant changes at the cell level in a variety of processes such as the regulation of cell growth, differentiation, matrix production, apoptosis, proliferation, cytoskeletal dynamics, cell surface adhesion and collagens which form structural elements. Further work is needed to validate these results experimentally, however we identified genes that could be used in future work. We know from the literature that miRNAs regulate many different targets, individual 3' UTRs also contain binding sites for multiple miRNAs, allowing for elaborate and complicated networks in which redundancy and cooperation between miRNAs determine the effect on gene expression (Bartel, 2009; Martinez-Sanchez & Murphy, 2013; Obermayer & Levine, 2014; van Rooij, 2011). We have identified 24 miRNAs of interest that are found in distinctive groups in the 3'UTR region of the predicted genes, more work is needed to fully elucidate the complexities of these miRNAs in relation to these networks they induce in response to *C. difficile*. However the data generated in this study could be potentially used to help target therapeutics for the clearance of persistent CDI.

Chapter 6: General Discussion

6.1 General Discussion

C. difficile like other bacterial pathogens may manipulate cellular functions, signal transduction pathways and pro-inflammatory responses through the delivery of effectors into host cells to drive towards a protective anti-inflammatory response or a damaging pro-inflammatory response (Solomon, 2013; Staedel & Darfeuille, 2013). *C. difficile* is highly transmissible between humans, which is key to its survival and persistence (Deakin et al., 2012). CDI is now the leading cause of antibiotic-associated diarrhoea worldwide (Solomon, 2013). The bacterium's ability to grow in the presence of antibiotics in recent years has enabled its rapid spread among patients (Rupnik et al., 2009). Advances in molecular methods and improved animal models have facilitated an understanding of how this organism survives in the environment, adapts to the GI tract and accomplishes its unique pathogenesis (Carroll & Bartlett, 2011). The combination of more aggressive strains, the expansion of the pool of individuals at risk of CDI and the difference in severity of infection between strains, has led to a renewed effort to understand the molecular mechanisms associated with the pathogenesis of this disease.

The severity of CDI can vary depending on the strain causing infection (Barbut et al., 2007; Dawson et al., 2009; Warny et al., 2005). Some strains including ribotype 001 may induce mild disease, while others such as ribotype 027 can induce severe colitis, leading to sepsis and in some cases even death. Many virulence factors have been examined over the years, with a particular interest in toxin production. Toxins mediate destruction of the epithelial cells leading to apoptosis and cell death, all of which have been studied in detail (Buffie & Pamer, 2013; Denève et al., 2009). Nonetheless the main mode of transmission of CDI is through the ingestion of *C. difficile* spores, although the timing and signals triggered to initiate germination following ingestion are not as well studied (Jump et al., 2007). Unlike most pathogens, *C. difficile* produce a metabolically dormant spore that is excreted by infected patients (Lawley, Croucher, et al., 2009). Infective spores persist in the environment because they are resistant to a wide range of physical and chemical stresses (Carlson et al., 2015; Paredes-Sabja et al., 2014). Spores represent the infectious stage of *C. difficile* and diversity in germination characteristics of particular strains may also contribute to the observed differences in disease severity. Another important factor to consider is the attachment of *C. difficile* to

the mucosa, as this is an important step in disease pathogenesis (Péchiné et al., 2005). CWPs are extremely important components of the S-layer that have an essential role in facilitating adherence. The S-layer of most bacterial species are composed of one major protein, which is modified by glycosylation (Sara & Sleytr, 2000). However, *C. difficile* is unique in that a single gene encodes two SLPs which are derived from post-translational cleavage of a single precursor *slpA* gene (Fagan et al., 2009). Mature SLPs contain a HMW protein which is highly conserved across strains of *C. difficile*, and a LMW protein which has been shown to be the dominant antigen (Drudy et al., 2004; Ní Eidhin et al., 2006; Sharp & Poxton, 1988).

Mutation is the primary source of variation in any organism. Without it, natural selection cannot operate and organisms cannot adapt to novel environments (Gordo, Perfeito, & Sousa, 2011). Evidence from the literature suggests that sequence differences in essential genes between strains of bacteria may affect virulence. *CagA* is noted for its amino acid sequence diversity and can determine the outcome of infection between different strains of *Helicobacter pylori* (*H. pylori*) (Evans & Evans, 2001). LMW SLPs exhibit vast sequence variability between strains (Calabi et al., 2001; Ní Eidhin et al., 2006). A change in structure or specific motifs in LMW proteins may result in the host immune cells no longer being able to recognise *C. difficile* as a pathogen (Ausiello et al., 2006). Bioinformatic analysis carried out in our laboratory on mutations in the *slpA* gene from 16 ribotypes of *C. difficile*, showed amino acid residues undergo positive selection giving a fitness advantage to particular ribotypes enabling their survival (Lynch 2014, unpublished). Previous research from our laboratory also showed that intact SLPs from ribotype 001 containing both HMW and LMW proteins were required for DC activation and subsequently generated T helper cells required for bacterial clearance *via* TLR4 (Ryan et al., 2011). SLPs isolated from ribotype 001 activate innate and adaptive immunity, suggesting an important role for SLPs in the recognition of *C. difficile* by the immune system (Collins et al., 2014; Ryan et al., 2011). Given the known sequence differences in LMW SLPs and differences in clinical symptoms between strains of *C. difficile*, the aim of the first part of this study was to investigate the immune response of SLPs from various ribotypes of *C. difficile*, following TLR4 activation and the induction of downstream signalling.

Analysis revealed there are differences in the potency of the immune response between ribotypes. SLPs from a variety of *C. difficile* ribotypes induced the maturation of BMDCs, key immune cells. DC maturation is characterised by increased expression of cell surface markers such as CD40, CD80 and CD86 (Higgins et al., 2003; Lavelle et al., 2003). SLPs from the various ribotypes induced the expression of these surface markers in BMDCs and the response was similar to that induced by LPS, a well-known TLR4 agonist (Akashi et al., 2003; Taro Kawai & Akira, 2007; Laird et al., 2009). DC maturation is also characterised by the production of cytokines such as IL-12p40, TNF α , IL-23 and IL-6. These cytokines play a central role in the modulation of the immune system and they can have pro-inflammatory or anti-inflammatory functions (Gerhard & Andus, 1998). It has been shown previously that SLPs can induce the production of pro-inflammatory cytokines in immune cells such as BMDCs, monocytes and macrophage (Ausiello et al., 2006; Bianco et al., 2011; Collins et al., 2014; Drudy et al., 2004; Madan & Petri Jr, 2012; Ryan et al., 2011; Vohra & Poxton, 2012) and our data agrees with what was been reported. However, our findings show differences in the potency of the immune response between ribotypes, with regard to the induction of IL-1 β , IL-12p70 and IL-10 in BMDCs, which has not yet been reported in the literature. The ability of SLPs from certain ribotypes to induce anti-inflammatory responses and others to induce more potent pro-inflammatory responses may account for the variability of symptoms and severity of disease experienced by patients who contract *C. difficile*.

We have previously shown in our laboratory that SLPs from ribotype 001 activate TLR4 (Ryan et al., 2011). TLR4 initiates downstream signalling which in turn activates NF- κ B and IRF3 via MyD88-dependant and -independent pathways (Akira & Takeda, 2004). IRF3 induce type I IFNs which have an important role in bridging innate and adaptive immunity by mediating the induction of co-stimulatory molecules on antigen presenting cells in response to pathogen associated molecules (Hoebe & Beutler, 2004). Given the similarity of the response of SLPs from ribotype 001 with LPS and the induction of DC maturation, it was not surprising to us that the response activated TLR4 signalling with downstream activation of p38 and NF- κ B signalling (Collins et al., 2014; Ryan et al., 2011). What was surprising was SLPs from ribotype 001 did not induce IRF3 signalling, which may have direct consequences for the immune response

elicited upon infection and subsequent clearance (Ryan et al., 2011). The aim of the next part of this study was to investigate if there were differences between SLPs from the different ribotypes in signalling downstream of TLR4. Analysis revealed that SLPs from ribotype 027 activate both NF- κ B and IRF3 signalling, leading to the production of IL-8 and RANTES cytokines. SLPs from the other ribotypes examined activated NF- κ B and IL-8 production only. Therefore there are key signalling differences between SLPs from ribotype 027, which is known to be hypervirulent and other ribotypes of *C. difficile* such as 001. For the first time we show evidence that SLPs from *C. difficile* can activate differing signalling pathways downstream of TLR4.

Both MyD88-dependent and independent mechanisms are required for the development of full host response to bacterial challenge and LPS can activate both signalling pathways (Carrigan et al., 2010). Yet clearance of ribotype 027 appears more difficult given the clinical symptoms of CDI, even though both arms of the TLR4 pathway are activated. MiRNAs are short double stranded RNA molecules approximately 19-23 nt in length that pair to protein coding genes. To date 28,645 miRNA hairpin precursors corresponding to 35,828 mature miRNAs in 223 species have been determined, 2588 mature miRNAs are currently annotated in the human genome (Eulalio & Mano, 2015). It has been estimated that up to 30% of all human genes are regulated by miRNAs in many cell types (Bartel, 2009; Fabian et al., 2010; Yates et al., 2013). MiRNAs block mRNA translation, reduce mRNA stability or induce mRNA cleavage after imperfect binding to the miRNA recognition elements within the 3' and 5' UTR of target mRNA genes (Bartel, 2004). MiRNAs have been shown to be involved in innate immunity by regulating TLR signalling and ensuing cytokine responses by targeting a variety of signalling proteins, regulatory molecules and transcription factors (Dalal & Kwon, 2010; He et al., 2014; Sonkoly et al., 2008). Until now, nobody has examined miRNAs regulated in response to SLPs. Given the role of miRNAs in the regulation of TLR4 signalling and during infection, our hypothesis states that SLPs regulate miRNAs and that profiles may differ between ribotypes. These miRNAs may modulate TLR4 signalling ultimately leading to changes in the immune response to *C. difficile*, which may explain the differences in clinical symptoms between different ribotypes.

We developed a protocol to examine miRNAs using qPCR and our initial profiling study examined miRNAs regulated in response to LPS and SLPs from ribotype 001. Our qPCR data analysis revealed 248 miRNAs were detected out of the 756 miRNAs analysed. MiR-155, miR-9, the let-7 family, miR-145, miR-146a and miR-187 have all been shown to be induced by LPS and shown to modulate the immune response, including key molecules involved in TLR4 *in vitro* (Curtale et al., 2013; Rossato et al., 2012; Tili et al., 2007). These miRNAs were present in our initial profiling study thus validating our method. We identified novel miRNAs; miR-543, miR302 and miR-374a, which were up regulated while miR-586 were down regulated in response to LPS. These miRNAs have never before been shown to be involved in TLR4 signalling upon activation with LPS *in vitro*. We also identified novel miRNAs; miR-339-5p, miR148b, miR590-5p, miR-24, miR-550a, miR-1292, miR-432#, miR-215 and miR152, which were up regulated in response to SLPs from ribotype 001. On the other hand miR-422a, miR-874 and miR1293 were down regulated in response to SLPs from ribotype 001 compared to the control cells. MiR-148b was the only miRNA from this list that was linked with regulating TLR signalling before (He et al., 2014; Liu et al., 2010). Some of the other miRNAs were found in other models of disease and present in epithelial cells in the gut. Given the limitations of the initial profiling study, we combined the experimental data with a list of miRNAs generated from the literature, for miRNAs known to regulate key elements of TLR4 signalling- as these miRNAs were present in the initial study but just over the significance value set in the experiment. The aim of the next part of this study was to examine the miRNA profiles regulated in response to SLPs from ribotype 001 and 027 using custom TLDA cards for the miRNAs of interest.

Analysis revealed that miRNAs were differentially regulated in response to SLPs from ribotype 001 compared to ribotype 027. There was a striking down regulation of the 24 miRNAs regulated in response to SLPs from ribotype 027 compared to ribotype 001. We chose 4 miRNAs; let-7e, miR-155, miR-146a and miR-145 for further validation based on the differences in expression of these miRNAs between ribotypes 001 and 027. These miRNAs have been shown to regulate a variety of signalling molecules that modulate immune function and have been shown to play a vital role in infection. We validated these miRNAs further using qPCR for individual miRNAs in a human and murine cell line. There were slight differences in the levels at which these miRNAs

were expressed between cell lines. However, we showed that there were distinct miRNA profiles regulated by SLPs from ribotype 001 and 027, which differed between ribotypes at this 8 hour time point. There are potential limitations to the use of cell lines such as Hek TLR4/MD2/CD14 and JAWS II cells. MiRNAs *in vivo* may be several orders of magnitude different than *in vitro* conditions, therefore it is essential that the results are recapitulated in appropriate animal models (Tarang & Weston, 2014). We had access to a bank of RNA samples derived from colonic tissue from a *C. difficile* infection model. Mice were treated with a cocktail of antibiotics prior to inoculation with 10^3 *C. difficile* spores from ribotype 001 and 027. The colon was harvested at two time points during infection (Lynch 2014, unpublished). The aim of the next part of this study was to validate miRNAs induced during early and late stage CDI from an *in vivo* model of *C. difficile*.

Analysis revealed that miR-146a and miR-145 were differentially regulated in colonic tissue of mice infected with ribotype 001 and 027 during early and late stage of CDI. These miRNAs were down regulated in colonic tissue of mice infected with ribotype 027 three days post infection. This data aligned with *in vitro* results, however at day 7 these miRNAs were up regulated. MiR-146a and miR-145 may be regulated by the SLPs from *C. difficile* to modulate the host immune response during infection. Evidence from the literature suggests that miR-145 is strongly up regulated during colonic inflammation and it has been recently shown that blocking miR-145 leads to a strong anti-inflammatory response (Izar et al., 2012; Starczynowski et al., 2010). Regulation of miR-145 has also been associated with inflammation in ulcerative colitis allowing for more persistent disease (Pekow et al., 2012). It was also shown that miR-146a expression negatively regulates severe inflammation during the innate immune response and inhibition of miRNA-146a was found to increase IL-8 and RANTES release (Perry et al., 2008). Our data shows that miR-145 and miR-146a were down regulated at day 3 of infection in response to ribotype 027. It is possible that ribotype 027 utilise miR-145 to elicit a strong anti-inflammatory response and miR-146a to diminish the host immune response, to facilitate survival of the pathogen at this early stage of infection leading to more persistent and severe infection. In comparison miR-145 and miR-146a were up regulated in the tissue of mice infected with ribotype 001 at day 3 of infection, possibly allowing the host to clear the infection more effectively leading to the healthy gut

morphology seen previously with this animal model. Damage to the colonic tissue was evident in the gut morphology of tissue from mice infected with ribotype 027 at day 7 of infection (Lynch 2014, unpublished). Tissue damage leads to increased inflammation which may account for the increase in miR-145 and miR-146a at this late stage of infection in our study. It was also noted that there was a decrease in miR-146a in response to ribotype 027 at day 3 which may possibly lead to increased IL-8 and RANTES production. This aligns with *in vitro* data, in which SLPs from ribotype 027 appeared to produce high levels of IL-8 and RANTES. Therefore ribotype 027 may utilise miR-146a to modulate IL-8 and RANTES production thus affecting the adaptive immune response and the polarisation of CD4⁺ T cells.

On the other hand, miR-155 and let-7e were differentially regulated in colonic tissue from mice infected with ribotype 001 and 027 only during early stage CDI. Both miRNAs were up regulated in colonic tissue of mice infected with ribotype 001 three days post infection. This was significantly different to the levels induced by mice infected with ribotype 027. These miRNA levels in mice infected with ribotype 001 and 027 appeared to return to levels comparable to levels seen in the control mice seven days post infection. The infection data does not align with *in vitro* data in that, we do not see a down regulation of these miRNAs, therefore expression may not be linked to the SLPs alone. However, we did see differential regulation of miR-155 and let-7e between both ribotypes suggesting they may have other important roles in regulating the host immune response to *C. difficile*. Evidence from the literature suggests that mRNA encoding TLR4 are regulated by members of the let-7 miRNA family (Androulidaki et al., 2009). It is possible that let-7e induced in response to ribotype 001 at early stage of infection modulates TLR4, leading to enhanced bacterial clearance. This may account for the less potent immune response seen *in vitro* and also in clinical outcomes during CDI.

Evidence from the literature shows that miR-155 functions as a novel negative regulator that helps to fine tune the inflammatory response of *H. pylori* infection (Xiao et al., 2009). Another study showed that IL-10 inhibits the expression of miR-155 in response to LPS, leading to an increase in the expression of SHIP1 and SOCS1, known negative regulators of TLR signalling (Androulidaki et al., 2009; McCoy et al., 2010). Research

from our laboratory previously found that in this *in vivo* model IL-10 was increased in mice infected with ribotype 027 at day 3 of infection in this *in vivo* model (Lynch 2014, unpublished). It is also possible that miR-155 is inhibited by the release of IL-10 in response to ribotype 027. Evidence from the literature shows that IL-10 increases SHIP1, which acts to switch off the pro-inflammatory response (McCoy et al., 2010). In contrast, IL-10 was not produced in response to ribotype 001 at day 3 of infection, possibly allowing the increase in miR-155 expression at this point early stage of infection. This data also aligns with *in vitro* experiments. Therefore there may be a link between the induction of IL-10 and miR-155 expression in response to *C. difficile*. This novel finding has yet to be reported in the literature and it also warrants further investigation. The absence of miRNAs induced in response to ribotype 027 in our experiment may correlate to less efficient clearance by the host's immune response and more persistent infection.

MiRNAs induced in response to *C. difficile* from ribotype 001 and 027, may work together in complex networks. Evidence from the literature suggests that miRNAs regulate many different targets, individual 3' UTRs also contain binding sites for multiple miRNAs, allowing for elaborate and complicated networks in which redundancy and cooperation between miRNAs determine the effect on gene expression (Bartel, 2009; Martinez-Sanchez & Murphy, 2013; Obermayer & Levine, 2014). We were unable to link the four individual miRNAs to NF- κ B and IRF3 signalling in response to SLPs from *C. difficile*. Over expressing miR-146a, miR-145, miR-155 and let-7e did not decrease IRF3 signalling or induce the production of RANTES in response to SLPs from ribotype 001 and 027. We confirmed however, that miR-146a, miR-145, miR-155 and let-7e targeted IRF3 gene expression and RANTES production specifically in response to TLR4 activation with LPS. Whilst NF- κ B and IL-8 production was not affected when the miRNAs were over expressed in response to LPS and SLPs from ribotype 001 and 027.

LPS and SLPs from ribotype 027 activate the same TLR4 receptor and lead to downstream activation of NF- κ B and IRF3 signalling. Yet, there are distinct differences in the miRNAs induced and how they target essential signalling molecules in regard to IRF3 signalling. This has not yet been reported in the literature, to the best of our

knowledge. These proteins seemingly activate the same signalling pathways however our study highlights that miRNAs may regulate this further. It is also possible that miRNAs that target IRF3 signalling, in response to SLPs from ribotype 001 and 027 require the cooperation of other miRNAs to effectively target IRF3 in this signalling pathway.

We found that the 24 miRNAs of interest, as a group were predicted to target 350 genes involved in essential cell processes including; ECM, MAPK signalling, PI3K-AKT signalling, TGF- β signalling and focal adhesion. MiRNAs induced in response to ribotype 001 and 027 potentially alter cell fate. Evidence from the literature has shown that altering cell fate may be vital in the fine tuning of the immune response against infection (Kim & Choi, 2010; Liu et al., 2009). It is possible that down regulation of miRNAs, induced by ribotype 027 preserve the expression of ECM genes allowing the bacteria to adhere to epithelial cells. In contrast, miRNAs induced in response to ribotype 001 may bind to the 3'UTR of genes involved in the ECM preventing expression, thus leading to reduced bacterial adherence. The impact of the modulation of the immune response by the miRNAs may lead to biologically relevant changes at the cell level in a variety of processes such as the regulation of cell growth, differentiation, matrix production, apoptosis, proliferation, cytoskeletal dynamics, cell surface adhesion and collagens which form structural elements. More work is needed to validate these results experimentally, however we identified genes that could be used in future work.

Furthermore, evidence from the literature suggests that miR-152 and miR-148b cooperatively target genes to impair the innate immune responses and antigen presentation, which was validated experimentally (Liu et al., 2010). MiR-152 and miR-148b are two of the miRNAs out of our list of 24 miRNAs of interest. They are predicted to be located together in the 3'UTR regions of predicted genes in our top 5 pathways during our bioinformatics search. Differing combinations of the 24 miRNAs of interest were found in distinct groups in the 3'UTR region of the predicted genes, which may account for our inability to link the miRNAs individually to NF- κ B and IRF3 in our experiment. We have identified 24 miRNAs of interest that are found in distinctive groups in the 3'UTR region of the predicted genes, more work is needed to

fully elucidate the complexities of these miRNAs in relation to the networks they induce in response to *C. difficile*.

Antibiotics are the classical way of dealing with fully symptomatic CDI, there are an increasing number of strains showing antibiotic resistant and a limited number of drugs that can be used to treat CDI. There is much evidence to suggest that *C. difficile* is evolving to occupy niche hospital populations and there has been rapid worldwide spread of ribotypes 027 and 078 (Dawson et al., 2009). Ribotypes 027 and 078 are known to be ‘hypervirulent’ and have been associated with more severe diarrhoea, higher mortality and more recurrences (Clements et al., 2010; Dawson et al., 2009; Goorhuis et al., 2007; Loo et al., 2005). The impact of CDI in healthcare settings throughout the developed world is considerable in terms of mortality, morbidity, and disease management (Cartman et al., 2010). The profile of patients presenting with CDI has also changed in the last decade. CDI affects populations previously considered at low risk, including patients without previous exposure to antibiotics, young individuals and pregnant women (Le Monnier, Zahar, & Barbut, 2014). Oral Metronidazole is often the antibiotic of choice in cases of mild-to-moderate CDI, and oral Vancomycin is often the choice for severe infections (Burke & Lamont, 2014). Unfortunately, the effectiveness of these antibiotic treatments is limited by a lack of response in some patients and high recurrence rates. A third antimicrobial agent, Fidaxomicin, was recently approved for the treatment of CDI (Mullane, 2014). A new drug, CRS3123 is currently in early stage clinical trials for the treatment of CDI. Initial results show it is a narrow spectrum agent resulting in a high concentration of drug in the GI tract. CRS3123 was demonstrated to have potent *in vitro* anti-bacterial activity against all *C. difficile* strains tested, including the hypervirulent ribotype 027 (Goldberg et al., 2015). The continued prevalence of antibiotic-resistant strains, along with the emergence of new hypervirulent strains, reveals the need for new alternative forms of treatment against CDI.

There are some emerging therapies to treat CDI currently in development. Monoclonal antibodies that have selectivity for toxins A and B are being developed. Monoclonal antibodies were reported to be superior in reducing rates of recurrent CDI in humans than current treatments in a Phase II randomised, double-blind, placebo- controlled trial

(Lowy, Molrine, & Ambrosino, 2010). Although the results reduced rates of reoccurring CDI this sort of therapy has its limitations in the delivery of therapy, effectiveness of the response in already very sick patients and the high costs associated with the production of monoclonal antibodies. There are several phase II clinical trials and one phase III clinical trial in the United States that are testing vaccines against *C. difficile* using monoclonal antibodies against toxins (Goldberg et al., 2015). More recently the use of microbe based treatment such as Faecal Microbiota Transplantation (FMT) from healthy donors has been developed for treatment of CDI (Ihunnah et al., 2013). The goals of this procedure are to restore the normal balance of the intestinal flora and to provide natural competition for *C. difficile*, thereby decreasing its overgrowth. FMT treatment has been successful in reducing reoccurring CDI however there is insufficient experience to guarantee that there are no long-term adverse effects or risks involved in this treatment, including the transmission of other life threatening bacteria (Bowman, Broussard, & Surawicz, 2015; Goldberg et al., 2015).

In recent times miRNAs are thought to be viable targets for therapeutics given that mature miRNA sequences are short and often completely conserved across multiple vertebrate species, making miRNAs easy targets for therapeutics (van Rooij, 2011; van Rooij & Kauppinen, 2014). MiRNAs typically have many targets within cellular networks, which, in turn, enable modulation of entire pathways in a disease state. MiRNAs may be utilised to restore the function of a miRNA using either synthetic double-stranded miRNAs or viral vector-based over expression. Two strategies have been used to deliver miRNA replacement therapies *in vivo* using formulated, synthetic, double-stranded miRNA mimics, and viral constructs over-expressing the lost or down-regulated miRNA (van Rooij & Kauppinen, 2014). Intravenously and intratumorally injected miRNA mimics complexed with liposome nanoparticles (Pramanik et al., 2011), polyethyleneimine (Ibrahim et al., 2011) or atelocollagen (Takeshita et al., 2010) have been used to restore the functions of various tumour-suppressive miRNAs in mouse cancer models. Notably, the first liposome-formulated mimic is currently being tested in a Phase I clinical trial in patients with primary liver cancer (van Rooij & Kauppinen, 2014). Other strategies have been utilised to enhance delivery of anti-miR oligonucleotides and have become a well validated experimental tool for *in vivo* inhibition of miRNAs (Krützfeldt et al., 2005).

This work is in its infancy, however given the results of our study this data could be used to develop a viable new method to treat CDI. It may be possible to target miRNAs which are down regulated during infection with persistent ribotypes such as 027 with miRNA mimics to allow bacterial clearance. Another option is to target miRNAs that are up regulated using antimiR oligonucleotides to inhibit miRNAs modulating important anti-inflammatory cytokines in less persistent ribotypes such as ribotype 001. Another option is to target the ECM, MAPK signalling, PI3K-Akt signalling, TGF- β signalling and focal adhesion which alter cell fate and adhesion of the bacteria in the gut.

In conclusion, our study showed that there are differences in the potency of the immune response between ribotypes. There were key signalling differences between SLPs from ribotype 027, which is known to be hypervirulent and other ribotypes of *C. difficile* such as 001. For the first time we show evidence that SLPs from *C. difficile* can activate differing signalling pathways downstream of TLR4. Until now nobody examined miRNA profiles regulated in response to SLPs from *C. difficile*. We identified novel miRNAs induced in response to LPS, SLPs from ribotype 001 and ribotype 027 *in vitro*. These miRNAs were differentially regulated between ribotypes, there was a global down regulation of miRNAs in response to SLPs from ribotype 027 compared with ribotype 001. LPS and SLPs from ribotype 027 activate the same TLR4 receptor and lead to downstream activation of NF- κ B and IRF3 signalling. Yet there are distinct differences in the miRNAs regulated and how they target essential signalling molecules in regard to IRF3 signalling. Our data suggests a role for miR-146a, miR-145, miR-155 and let-7e in regulating the host immune response to *C. difficile* infection from an *in vivo* animal model. The absence of miRNAs induced in response to ribotype 027 may correlate to less efficient clearance by the host's immune response and more persistent infection. The miRNAs regulated in response to *C. difficile* from ribotype 001 and 027 are predicted to target essential cell processes and the impact of the modulation of the immune response by the miRNAs may lead to biologically relevant changes at the cell level in a variety of processes. More work is needed to fully elucidate the complexities of these miRNAs in relation to the networks they regulate in response to *C. difficile*. The effectiveness of current treatments is limited by a lack of response in some patients and the high recurrence rates. Current and emerging therapies to treat CDI currently

focus on the neutralisation of toxins, the development of vaccines and FMT. MiRNAs are emerging as viable targets for therapeutics and the data generated in this study may be used to develop a miRNA based therapy for the treatment of persistent CDI, allowing bacterial clearance by the host's immune system without the need for antibiotics.

Chapter 7: Bibliography

7.1 Bibliography

- Adhikari, A., Xu, M., & Chen, Z. J. (2007). Ubiquitin-Mediated Activation of TAK1 and IKK. *Oncogene*, *26*(22), 3214–3226. <http://doi.org/10.1038/sj.onc.1210413>
- Agalioti, T., Lomvardas, S., Parekh, B., Yie, J., Maniatis, T., & Thanos, D. (2000). Ordered Recruitment of Chromatin Modifying and General Transcription Factors to the IFN-beta promoter. *Cell*, *103*(4), 667–678. [http://doi.org/10.1016/S0092-8674\(00\)00169-0](http://doi.org/10.1016/S0092-8674(00)00169-0)
- Akashi, S., Saitoh, S., Wakabayashi, Y., Kikuchi, T., Takamura, N., Nagai, Y., ... Miyake, K. (2003). Lipopolysaccharide Interaction with Cell Surface Toll-like Receptor 4-MD-2: Higher Affinity than that with MD-2 or CD14. *The Journal of Experimental Medicine*, *198*(7), 1035–1042. <http://doi.org/10.1084/jem.20031076>
- Akira, S., & Takeda, K. (2004). Toll-Like Receptor Signalling. *Nature Reviews. Immunology*, *4*(7), 499–511. <http://doi.org/10.1038/nri1391>
- Alexander, C., & Rietschel, E. T. (2001). Bacterial Lipopolysaccharides and Innate Immunity. *Journal of Endotoxin Research*, *7*(3), 167–202. <http://doi.org/10.1179/096805101101532675>
- Alexopoulou, L., Holt, A. C., Medzhitov, R., & Flavell, R. A. (2001). Recognition of Double-Stranded RNA and Activation of NF- κ B by Toll-like Receptor 3. *Nature*, *413*(6857), 732–738. <http://doi.org/10.1038/35099560>
- Allison, D. B., Cui, X., Page, G. P., & Sabripour, M. (2006). Microarray Data Analysis: from Disarray to Consolidation and Consensus. *Nature Reviews. Genetics*, *7*(1), 55–65. <http://doi.org/10.1038/nrg1749>
- Altschul, S. (1990). Basic Local Alignment Search Tool. *Journal of Molecular Biology*, *215*(3), 403–410. <http://doi.org/10.1006/jmbi.1990.9999>
- Andoh, M., Zhang, G., Russell-Lodrigue, K. E., Shive, H. R., Weeks, B. R., & Samuel, J. E. (2007). T cells are essential for bacterial clearance, and gamma interferon, tumor necrosis factor alpha, and B cells are crucial for disease development in *Coxiella burnetii* infection in mice. *Infection and Immunity*, *75*(7), 3245–55. <http://doi.org/10.1128/IAI.01767-06>
- Androulidaki, A., Iliopoulos, D., Arranz, A., Doxaki, C., Schworer, S., Zacharioudaki, V., ... Tsatsanis, C. (2009). The Kinase Akt1 Controls Macrophage Response to Lipopolysaccharide by Regulating microRNAs. *Immunity*, *31*(2), 220–31. <http://doi.org/10.1016/j.immuni.2009.06.024>
- Asirvatham, A. J., Gregorie, C. J., Hu, Z., Magner, W. J., & Tomasi, T. B. (2008). MicroRNA Targets in Immune Genes and the Dicer/Argonaute and ARE Machinery Components. *Molecular Immunology*, *45*(7), 1995–2006. <http://doi.org/10.1016/j.molimm.2007.10.035>
- Asirvatham, A. J., Magner, W. J., & Tomasi, T. B. (2009). miRNA Regulation of Cytokine Genes. *Cytokine*, *45*(2), 58–69. <http://doi.org/10.1016/j.cyto.2008.11.010>
- Au, W. C., Moore, P. A., Lowther, W., Juang, Y. T., & Pitha, P. M. (1995). Identification of a

- Member of the Interferon Regulatory Factor Family that Binds to the Interferon-Stimulated Response Element and Activates Expression of Interferon-Induced Genes. *Proceedings of the National Academy of Sciences of the United States of America*, 92(25), 11657–11661. <http://doi.org/10.1073/pnas.92.25.11657>
- Ausiello, C. M., Cerquetti, M., Fedele, G., Spensieri, F., Palazzo, R., Nasso, M., ... Mastrantonio, P. (2006). Surface Layer Proteins from *Clostridium difficile* Induce Inflammatory and Regulatory Cytokines in Human Monocytes and Dendritic Cells. *Microbes and Infection*, 8(11), 2640–6. <http://doi.org/10.1016/j.micinf.2006.07.009>
- Baeuerle, P. A., & Baltimore, D. (1988). Activation of DNA-Binding Activity in an Apparently Cytoplasmic Precursor of the NF- κ B Transcription Factor. *Cell*, 53(2), 211–217. [http://doi.org/10.1016/0092-8674\(88\)90382-0](http://doi.org/10.1016/0092-8674(88)90382-0)
- Bai, Y., Qian, C., Qian, L., Ma, F., Hou, J., Chen, Y., ... Cao, X. (2012). Integrin CD11b Negatively Regulates TLR9-Triggered Dendritic Cell Cross-Priming by Upregulating microRNA-146a. *Journal of Immunology*, 188(11), 5293–302. <http://doi.org/10.4049/jimmunol.1102371>
- Bain, C. C., Scott, C. L., Uronen-Hansson, H., Gudjonsson, S., Jansson, O., Grip, O., ... Mowat, A. M. (2013). Resident and Pro-Inflammatory Macrophages in the Colon Represent Alternative Context-Dependent Fates of the same Ly6Chi Monocyte Precursors. *Mucosal Immunology*, 6(3), 498–510. <http://doi.org/10.1038/mi.2012.89>
- Baldwin, T. O. (1996). Firefly Luciferase: the Structure is Known, but the Mystery Remains. *Structure*, 4(3), 223–228. [http://doi.org/10.1016/S0969-2126\(96\)00026-3](http://doi.org/10.1016/S0969-2126(96)00026-3)
- Banchereau, J., & Steinman, R. M. (1998). Dendritic Cells and the Control of Immunity. *Nature*, 392(6673), 245–252. <http://doi.org/10.1038/32588>
- Bandrés, E., Cubedo, E., Agirre, X., Malumbres, R., Zárata, R., Ramirez, N., ... García-Foncillas, J. (2006). Identification by Real-Time PCR of 13 Mature microRNAs Differentially Expressed in Colorectal Cancer and Non-Tumoral Tissues. *Molecular Cancer*, 5(29). <http://doi.org/10.1186/1476-4598-5-29>
- Barbut, F., Mastrantonio, P., Delmée, M., Brazier, J., Kuijper, E., Poxton, I., ... Rupnik, M. (2007). Prospective study of *clostridium difficile* infections in Europe with phenotypic and genotypic characterisation of the isolates. *Clinical Microbiology and Infection*, 13(11), 1048–1057. <http://doi.org/10.1111/j.1469-0691.2007.01824.x>
- Barron, N., Sanchez, N., Kelly, P., & Clynes, M. (2011). MicroRNAs: Tiny Targets for Engineering CHO Cell Phenotypes? *Biotechnology Letters*, 33(1), 11–21. <http://doi.org/10.1007/s10529-010-0415-5>
- Bartel, D. P. (2004). MicroRNAs: Genomics, Biogenesis, Mechanism, and Function. *Cell*, 116(2), 281–97. [http://doi.org/10.1016/S0092-8674\(04\)00045-5](http://doi.org/10.1016/S0092-8674(04)00045-5)
- Bartel, D. P. (2009). MicroRNAs: Target Recognition and Regulatory Functions. *Cell*, 136(2), 215–233. <http://doi.org/10.1016/j.cell.2009.01.002>
- Barth, H., Aktories, K., Popoff, M. R., & Stiles, B. G. (2004). Binary Bacterial Toxins: Biochemistry, Biology, and Applications of Common *Clostridium* and *Bacillus* proteins.

Microbiology and Molecular Biology Reviews: MMBR, 68(3), 373–402.
<http://doi.org/10.1128/MMBR.68.3.373-402.2004>

- Bartlett, J. G. (1994). Clostridium difficile : History of Its Role as an Enteric Pathogen and the Current About the Organism State of Knowledge. *Clinical Infectious Diseases*, 18(4), S265– S272.
- Bazzoni, F., Rossato, M., Fabbri, M., Gaudiosi, D., Mirolo, M., Mori, L., ... Locati, M. (2009). Induction and Regulatory Function of miR-9 in Human Monocytes and Neutrophils Exposed to Proinflammatory Signals. *Proceedings of the National Academy of Sciences of the United States of America*, 106(13), 5282–5287.
<http://doi.org/10.1073/pnas.0810909106>
- Bekker, L., Moreira, A. L., Bergtold, A., Ryffel, B., Kaplan, G., Bergtold, A. M. Y., & Freeman, S. (2000). Immunopathologic Effects of Tumor Necrosis Factor Alpha in Murine Mycobacterial Infection Are Dose Dependent Immunopathologic Effects of Tumor Necrosis Factor Alpha in Murine Mycobacterial Infection Are Dose Dependent. *Infection and Immunity*, 68(12), 6954–6961. <http://doi.org/10.1128/IAI.68.12.6954-6961.2000>.Updated
- Bentwich, I., Avniel, A., Karov, Y., Aharonov, R., Gilad, S., Barad, O., ... Bentwich, Z. (2005). Identification of Hundreds of Conserved and Nonconserved Human microRNAs. *Nature Genetics*, 37(7), 766–70. <http://doi.org/10.1038/ng1590>
- Bianco, M., Fedele, G., Quattrini, A., Spigaglia, P., Barbanti, F., Mastrantonio, P., & Ausiello, C. M. (2011). Immunomodulatory Activities of Surface Layer Proteins Obtained from Epidemic and Hypervirulent Clostridium difficile Strains. *Journal of Medical Microbiology*, 60, 1162–1167. <http://doi.org/10.1099/jmm.0.029694-0>
- Bowman, K., Broussard, E. K., & Surawicz, C. M. (2015). Fecal microbiota transplantation: current clinical efficacy and future prospects. *Clinical and Experimental Gastroenterology*, 8, 285–291. Retrieved from http://apps.webofknowledge.com.remote.library.dcu.ie/full_record.do?product=UA&search_mode=GeneralSearch&qid=5&SID=V2bJDJ1mhq8DlpOTEIx&page=1&doc=1
- Braun, V., Hundsberger, T., Leukel, P., Sauerborn, M., & Von Eichel-Streiber, C. (1996). Definition of the Single Integration Site of the Pathogenicity Locus in Clostridium difficile. *Gene*, 181(1-2), 29–38. [http://doi.org/10.1016/S0378-1119\(96\)00398-8](http://doi.org/10.1016/S0378-1119(96)00398-8)
- Broz, P., & Monack, D. M. (2013). Newly Described Pattern Recognition Receptors Team up Against Intracellular Pathogens. *Nature Reviews. Immunology*, 13(8), 551–565. <http://doi.org/10.1038/nri3479>
- Buffie, C. G., & Pamer, E. G. (2013). Microbiota-Mediated Colonization Resistance Against Intestinal Pathogens. *Nature Reviews. Immunology*, 13(11), 790–801. <http://doi.org/10.1038/nri3535>
- Burke, K. E., & Lamont, J. T. (2014). Clostridium difficile infection: A worldwide disease. *Gut and Liver*, 8(1), 1–6. <http://doi.org/10.5009/gnl.2014.8.1.1>
- Burns, D. A., Heap, J. T., & Minton, N. P. (2010a). Clostridium difficile Spore Germination: An Update. *Research in Microbiology*, 161(9), 730–734.

<http://doi.org/10.1016/j.resmic.2010.09.007>

- Burns, D. A., Heap, J. T., & Minton, N. P. (2010b). SleC is Essential for Germination of *Clostridium difficile* Spores in Nutrient-Rich Medium Supplemented with the Bile Salt Taurocholate. *Journal of Bacteriology*, *192*(3), 657–664. <http://doi.org/10.1128/JB.01209-09>
- Cai, S., Zhou, P., & Liu, Z. (2013). Functional Characteristics of a Double Negative Feedback Loop Mediated by microRNAs. *Cognitive Neurodynamics*, *7*, 417–429. <http://doi.org/10.1007/s11571-012-9236-7>
- Calabi, E., Calabi, F., Phillips, A. D., & Fairweather, N. F. (2002). Binding of *Clostridium difficile* Surface Layer Proteins to Gastrointestinal Tissues. *Infection and Immunity*, *70*(10), 5770–5778. <http://doi.org/10.1128/IAI.70.10.5770>
- Calabi, E., Ward, S., Wren, B., Paxton, T., Panico, M., Morris, H., ... Fairweather, N. (2001). Molecular Characterization of the Surface Layer Proteins from *Clostridium difficile*. *Molecular Microbiology*, *40*(5), 1187–1199.
- Carlson, P. E., Kaiser, A. M., McColm, S. A., Bauer, J. M., Young, V. B., Aronoff, D. M., & Hanna, P. C. (2015). Variation in Germination of *Clostridium difficile* Clinical Isolates Correlates to Disease Severity. *Anaerobe*, *33*, 64–70. <http://doi.org/10.1016/j.anaerobe.2015.02.003>
- Carrigan, S. O., Junkins, R., Yang, Y. J., Macneil, A., Richardson, C., Johnston, B., & Lin, T.-J. (2010). IFN Regulatory Factor 3 Contributes to the Host Response During *Pseudomonas aeruginosa* Lung Infection in Mice. *Journal of Immunology*, *185*(6), 3602–3609. <http://doi.org/10.4049/jimmunol.0903429>
- Carroll, K. C., & Bartlett, J. G. (2011). Biology of *Clostridium difficile*: Implications for Epidemiology and Diagnosis. *Annual Review of Microbiology*, *65*, 501–521. <http://doi.org/10.1146/annurev-micro-090110-102824>
- Cartman, S. T., Heap, J. T., Kuehne, S. a, Cockayne, A., & Minton, N. P. (2010). The Emergence of “Hypervirulence” in *Clostridium difficile*. *International Journal of Medical mMicrobiology*, *300*(6), 387–395. <http://doi.org/10.1016/j.ijmm.2010.04.008>
- Ceppi, M., Pereira, P. M., Dunand-Sauthier, I., Barras, E., Reith, W., Santos, M. A., & Pierre, P. (2009). MicroRNA-155 Modulates the Interleukin-1 Signaling Pathway in Activated Human Monocyte-Derived Dendritic Cells. *Proceedings of the National Academy of Sciences of the United States of America*, *106*(8), 2735–2740. <http://doi.org/10.1073/pnas.0811073106>
- Chang, E. Y., Guo, B., Doyle, S. E., & Cheng, G. (2007). Cutting edge: involvement of the type I IFN production and signaling pathway in lipopolysaccharide-induced IL-10 production. *Journal of Immunology*, *178*(11), 6705–6709. <http://doi.org/10.1172/jci30111> [pii]
- Chen, C., Ridzon, D. A., Broomer, A. J., Zhou, Z., Lee, D. H., Nguyen, J. T., ... Guegler, K. J. (2005). Real-time Quantification of microRNAs by Stem-Loop RT-PCR. *Nucleic Acids Research*, *33*(20), e179. <http://doi.org/10.1093/nar/gni178>
- Chen, F., Bhatia, D., Chang, Q., & Castranova, V. (2006). Finding NEMO by K63-Linked

Polyubiquitin Chain. *Cell Death and Differentiation*, 13(11), 1835–1838. <http://doi.org/10.1038/sj.cdd.4402014>

- Chen, Q., Wang, H., Liu, Y., Song, Y., Lai, L., Han, Q., ... Wang, Q. (2012). Inducible microRNA-223 down-Regulation Promotes TLR-Triggered IL-6 and IL-1 β Production in Macrophages by Targeting STAT3. *PLoS ONE*, 7(8), e42971. <http://doi.org/10.1371/journal.pone.0042971>
- Chen, X., Katchar, K., Goldsmith, J. D., Nanthakumar, N., Cheknis, A., Gerding, D. N., & Kelly, C. P. (2008). A Mouse Model of Clostridium difficile Associated Disease. *Gastroenterology*, 135(6), 1984–1992. <http://doi.org/10.1053/j.gastro.2008.09.002>
- Chen, X.-M., Splinter, P. L., O'Hara, S. P., & LaRusso, N. F. (2008). A Cellular Micro-RNA, let-7i, Regulates Toll-like Receptor 4 Expression and Contributes to Cholangiocyte Immune Responses against Cryptosporidium parvum Infection. *J Biol Chem*, 282(39), 28929–28938.
- Chen, Y., Gelfond, J. Al, McManus, L. M., & Shireman, P. K. (2009). Reproducibility of Quantitative RT-PCR Array in miRNA Expression Profiling and Comparison with Microarray Analysis. *BMC Genomics*, 10(1), 407–417. <http://doi.org/10.1186/1471-2164-10-407>
- Chiang, H. R., Schoenfeld, L. W., Ruby, J. G., Auyeung, V. C., Spies, N., Baek, D., ... Bartel, D. P. (2010). Mammalian microRNAs: Experimental Evaluation of Novel and Previously Annotated Genes. *Genes and Development*, 24(10), 992–1009. <http://doi.org/10.1101/gad.1884710>
- Chieppa, M., Rescigno, M., Huang, A. Y. C., & Germain, R. N. (2006). Dynamic Imaging of Dendritic Cell Extension Into the Small Bowel Lumen in Response to Epithelial Cell TLR Engagement. *The Journal of Experimental Medicine*, 203(13), 2841–2852. <http://doi.org/10.1084/jem.20061884>
- Clark, M. A., & Jepson, M. A. (2003). Intestinal M Cells and their Role in Bacterial infection. *International Journal of Medical Microbiology*, 293(1), 17–39. <http://doi.org/10.1078/1438-4221-00242>
- Clements, A. C., Magalhães, R. J. S., Tatem, A. J., Paterson, D. L., & Riley, T. V. (2010). Clostridium difficile PCR ribotype 027: assessing the risks of further worldwide spread. *The Lancet Infectious Diseases*, 10(6), 395–404. [http://doi.org/10.1016/S1473-3099\(10\)70080-3](http://doi.org/10.1016/S1473-3099(10)70080-3)
- Coll, R. C., & O'Neill, L. A. J. (2010). New insights into the regulation of signalling by toll-like receptors and nod-like receptors. *Journal of Innate Immunity*, 2(5), 406–21. <http://doi.org/10.1159/000315469>
- Collins, L. E. (2014). *Defining a Role for SNARE Proteins in Dendritic Cell Secretion*. Dublin City University.
- Collins, L. E., Lynch, M., Marszalowska, I., Kristek, M., Rochfort, K., O'Connell, M. J., ... Loscher, C. E. (2014). Surface Layer Proteins Isolated from Clostridium difficile Induce Clearance Responses in Macrophages. *Microbes and Infection*, 1–10. <http://doi.org/10.1016/j.micinf.2014.02.001>

- Coombes, J. L., & Powrie, F. (2008). Dendritic cells in intestinal immune regulation. *Nature Reviews. Immunology*, 8(6), 435–46. <http://doi.org/10.1038/nri2335>
- Costinean, S., Sandhu, S. K., Pedersen, I. M., Tili, E., Trotta, R., Perrotti, D., ... Croce, C. M. (2009). Src Homology 2 Domain-Containing Inositol-5 Phosphatase and CCAAT Enhancer-Binding Protein β are Targeted by miR-155 in B Cells E μ -MiR-155 Transgenic Mice. *Comparative and General Pharmacology*, 114(7), 1374–1382. <http://doi.org/10.1182/blood-2009-05-220814>.
- Couper, K., Blount, D., & Riley, E. (2008). IL-10: the master regulator of immunity to infection. *Journal of Immunology*, 180(9), 5771–5777. <http://doi.org/10.4049/jimmunol.180.9.5771>
- Cremer, T. J., Ravneberg, D. H., Clay, C. D., Piper-Hunter, M. G., Marsh, C. B., Elton, T. S., ... Tridandapani, S. (2009). MiR-155 induction by *F. novicida* but not the virulent *F. tularensis* results in SHIP down-regulation and enhanced pro-inflammatory cytokine response. *PLoS One*, 4(12), e8508. <http://doi.org/10.1371/journal.pone.0008508>
- Cullen, B. R. (2006). Viruses and microRNAs. *Nature Genetics*, 38(6s), S25–S30. <http://doi.org/10.1038/ng1793>
- Curtale, G., Mirolo, M., Renzi, T. A., Rossato, M., Bazzoni, F., & Locati, M. (2013). Negative Regulation of Toll-Like Receptor 4 Signaling by IL-10-Dependent microRNA-146b. *Proceedings of the National Academy of Sciences of the United States of America*, 110(28), 11499–11504. <http://doi.org/10.1073/pnas.1219852110>
- da Silva Correia, J., Soldau, K., Christen, U., Tobias, P. S., & Ulevitch, R. J. (2001). Lipopolysaccharide is in close proximity to each of the proteins in its membrane receptor complex. transfer from CD14 to TLR4 and MD-2. *The Journal of Biological Chemistry*, 276(24), 21129–35. <http://doi.org/10.1074/jbc.M009164200>
- Dai, Y., Diao, Z., Sun, H., Li, R., Qiu, Z., & Hu, Y. (2011). MicroRNA-155 is Involved in the Remodelling of Human-Trophoblast-Derived HTR-8/SVneo Cells Induced by Lipopolysaccharides. *Human Reproduction*, 26(7), 1882–1891. <http://doi.org/10.1093/humrep/der118>
- Dalal, S. R., & Kwon, J. H. (2010). The Role of MicroRNA in Inflammatory Bowel Disease. *Gastroenterology and Hepatology*, 6(11), 714–722.
- Dalby, B. (2004). Advanced transfection with Lipofectamine 2000 reagent: primary neurons, siRNA, and high-throughput applications. *Methods*, 33(2), 95–103. <http://doi.org/10.1016/j.ymeth.2003.11.023>
- Dang, T. H. T., De La Riva, L., Fagan, R. P., Storck, E. M., Heal, W. P., Janoir, C., ... Tate, E. W. (2010). Chemical probes of surface layer biogenesis in *Clostridium difficile*. *ACS Chemical Biology*, 5(3), 279–285. <http://doi.org/10.1021/cb9002859>
- Dawson, L. F., Valiente, E., & Wren, B. W. (2009). *Clostridium difficile*- A Continually Evolving and Problematic Pathogen. *Infection, Genetics and Evolution*, 9(6), 1410–1417. <http://doi.org/10.1016/j.meegid.2009.06.005>
- de la Riva, L., Willing, S. E., Tate, E. W., & Fairweather, N. F. (2011). Roles of cysteine

- proteases Cwp84 and Cwp13 in biogenesis of the cell wall of *Clostridium difficile*. *Journal of Bacteriology*, *193*(13), 3276–3285. <http://doi.org/10.1128/JB.00248-11>
- Deakin, L. J., Clare, S., Fagan, R. P., Dawson, L. F., Pickard, D. J., West, M. R., ... Lawley, T. D. (2012). The *Clostridium difficile* spo0A gene is a persistence and transmission factor. *Infection and Immunity*, *80*(8), 2704–2711. <http://doi.org/10.1128/IAI.00147-12>
- Denève, C., Janoir, C., Poilane, I., Fantinato, C., & Collignon, A. (2009). New Trends in *Clostridium difficile* Virulence and Pathogenesis. *International Journal of Antimicrobial Agents*, *33*(S1), S24–S28. [http://doi.org/10.1016/S0924-8579\(09\)70012-3](http://doi.org/10.1016/S0924-8579(09)70012-3)
- Denli, A. M., Tops, B. B. J., Plasterk, R. H. A., Ketting, R. F., & Hannon, G. J. (2004). Processing of primary microRNAs by the Microprocessor complex. *Nature*, *432*(7014), 231–5. <http://doi.org/10.1038/nature03049>
- Dingle, K. E., Didelot, X., Ansari, M. A., Eyre, D. W., Vaughan, A., Griffiths, D., ... Crook, D. W. (2013). Recombinational switching of the *Clostridium difficile* S-layer and a novel glycosylation gene cluster revealed by large-scale whole-genome sequencing. *The Journal of Infectious Diseases*, *207*(4), 675–686. <http://doi.org/10.1093/infdis/jis734>
- Doe, W. F. (1989). The intestinal immune system. *Gut*, *30*(12), 1679–1685. <http://doi.org/10.1136/gut.30.12.1679>
- Doench, J. G., & Sharp, P. A. (2004). Specificity of microRNA target selection in translational repression. *Genes & Development*, *18*(5), 504–11. <http://doi.org/10.1101/gad.1184404>
- Doyle, S. E., Vaidya, S. a., O'Connell, R., Dadgostar, H., Dempsey, P. W., Wu, T. T., ... Cheng, G. (2002). IRF3 Mediates a TLR3/TLR4-Specific Antiviral Gene Program. *Immunity*, *17*(3), 251–263. [http://doi.org/10.1016/S1074-7613\(02\)00390-4](http://doi.org/10.1016/S1074-7613(02)00390-4)
- Drudy, D., Calabi, E., Kyne, L., Sougioultzis, S., Kelly, E., Fairweather, N., & Kelly, C. P. (2004). Human Antibody Response to Surface Layer Proteins in *Clostridium difficile* Infection. *FEMS Immunology and Medical Microbiology*, *41*(3), 237–242. <http://doi.org/10.1016/j.femsim.2004.03.007>
- Dubberke, E. (2012). *Clostridium difficile* infection: the scope of the problem. *Journal of Hospital Medicine*, *7 Suppl 3*, S1–4. <http://doi.org/10.1002/jhm.1916>
- Dubreuil, J. D., Giudice, G. Del, & Rappuoli, R. (2002). *Helicobacter pylori* Interactions with Host Serum and Extracellular Matrix Proteins : Potential Role in the Infectious Process. *Microbiology and Molecular Biology Reviews*, *66*(4), 617–629. <http://doi.org/10.1128/MMBR.66.4.617>
- Dupuy, B., Govind, R., Antunes, A., & Matamouros, S. (2008). *Clostridium difficile* toxin synthesis is negatively regulated by TcdC. *Journal of Medical Microbiology*, *57*(6), 685–689. <http://doi.org/10.1099/jmm.0.47775-0>
- Eichel-streiber, C. V. O. N., Sauerborn, M., & Kuramitsu, H. K. (1992). Toxins and *Streptococcus mutans* Glucosyltransferases. *Journal of Bacteriology*, *174*(20), 6707–6710.
- El Feghaly, R. E., Stauber, J. L., Deych, E., Gonzalez, C., Tarr, P. I., & Haslam, D. B. (2013).

Markers of Intestinal Inflammation, not Bacterial Burden, Correlate with Clinical Outcomes in *Clostridium difficile* infection. *Clinical Infectious Diseases*, 56(12), 1713–1721. <http://doi.org/10.1093/cid/cit147>

Emerson, J. E., Reynolds, C. B., Fagan, R. P., Shaw, H. A., Goulding, D., & Fairweather, N. F. (2009). A novel genetic switch controls phase variable expression of CwpV, a *Clostridium difficile* cell wall protein. *Molecular Microbiology*, 74(3), 541–556. <http://doi.org/10.1111/j.1365-2958.2009.06812.x>

Emerson, J., & Fairweather, N. F. (2009). Surface Structures of *C. difficile* and Other Clostridia: Implications for Pathogenesis and Immunity. In H. Bruggemann & G. Gottschalk (Eds.), *Clostridia : Molecular Biology in the Post-Genomic Era* (pp. 157–167). WYMONDHAM , UK: CAISTER ACADEMIC PRESS.

Eulalio, A., & Mano, M. (2015). MicroRNA Screening and the Quest for Biologically Relevant Targets. *Journal of Biomolecular Screening*, 20(8), 1003–1017. <http://doi.org/10.1177/1087057115578837>

Evans, D. J., & Evans, D. G. (2001). Helicobacter pylori CagA: analysis of sequence diversity in relation to phosphorylation motifs and implications for the role of CagA as a virulence factor. *Helicobacter*, 6(3), 187–98. <http://doi.org/10.1046/j.1523-5378.2001.00028.x>

Fabian, M. R., Sonenberg, N., & Filipowicz, W. (2010). Regulation of mRNA translation and stability by microRNAs. *Annual Review of Biochemistry*, 79, 351–379. <http://doi.org/10.1146/annurev-biochem-060308-103103>

Fagan, R. P., Albesa-Jové, D., Qazi, O., Svergun, D. I., Brown, K. A., & Fairweather, N. F. (2009). Structural Insights into the Molecular Organization of the S-Layer from *Clostridium difficile*. *Molecular Microbiology*, 71(5), 1308–1322. <http://doi.org/10.1111/j.1365-2958.2009.06603.x>

Fiedler, S. D., Carletti, M. Z., & Christenson, L. K. (2010). Quantitative RT-PCR methods for mature microRNA expression analysis. *Methods in Molecular Biology (Clifton, N.J.)*, 630, 49–64. http://doi.org/10.1007/978-1-60761-629-0_4

Filipowicz, W., Bhattacharyya, S. N., & Sonenberg, N. (2008). Mechanisms of post-transcriptional regulation by microRNAs: are the answers in sight? *Nature Reviews. Genetics*, 9(2), 102–114. <http://doi.org/10.1038/nrg2290>

Flannery, S., & Bowie, A. G. (2010). The interleukin-1 receptor-associated kinases: Critical regulators of innate immune signalling. *Biochemical Pharmacology*, 80(12), 1981–1991. <http://doi.org/10.1016/j.bcp.2010.06.020>

Freeman, J., Baines, S. D., Saxton, K., & Wilcox, M. H. (2007). Effect of Metronidazole on Growth and Toxin Production by Epidemic *Clostridium difficile* PCR Ribotypes 001 and 027 in a Human Gut Model. *The Journal of Antimicrobial Chemotherapy*, 60(1), 83–91. <http://doi.org/10.1093/jac/dkm113>

Friedman, J. M., & Jones, P. a. (2009). MicroRNAs: critical mediators of differentiation, development and disease. *Swiss Medical Weekly*, 139(33-34), 466–72. <http://doi.org/smw-12794>

- Friedman, R. C., Farh, K. K.-H., Burge, C. B., & Bartel, D. P. (2009). Most Mammalian mRNAs are Conserved Targets of microRNAs. *Genome Research*, *19*(1), 92–105. <http://doi.org/10.1101/gr.082701.108>
- Gabhann, J. N., Higgs, R., Brennan, K., Thomas, W., Damen, J. E., Ben Larbi, N., ... Jefferies, C. a. (2010). Absence of SHIP-1 results in constitutive phosphorylation of tank-binding kinase 1 and enhanced TLR3-dependent IFN-beta production. *Journal of Immunology*, *184*(5), 2314–2320. <http://doi.org/10.4049/jimmunol.0902589>
- Garg, M., Potter, J. A., & Abrahams, V. M. (2013). Identification of microRNAs That Regulate TLR2-Mediated Trophoblast Apoptosis and Inhibition of IL-6 mRNA. *PLoS ONE*, *8*(10), 4–15. <http://doi.org/10.1371/journal.pone.0077249>
- Gauzzi, C. M., Del Cornò, M., & Gessani, S. (2010). Dissecting TLR3 signalling in dendritic cells. *Immunobiology*, *215*(9-10), 713–723. <http://doi.org/10.1016/j.imbio.2010.05.008>
- Gerhard, R., & Andus, T. (1998). Cytokines in Inflammatory Bowel Disease. *World Journal of Surgery*, *(22)*, 382–389.
- Gerondakis, S., Grumont, R. J., & Banerjee, A. (2007). Regulating B-cell activation and survival in response to TLR signals. *Immunology and Cell Biology*, *85*(6), 471–475. <http://doi.org/10.1038/sj.icb.7100097>
- Ghosh, Z., Chakrabarti, J., & Mallick, B. (2007). miRNomics-The bioinformatics of microRNA genes. *Biochemical and Biophysical Research Communications*, *363*(1), 6–11. <http://doi.org/10.1016/j.bbrc.2007.08.030>
- Gill, S. R., Pop, M., Deboy, R. T., Eckburg, P. B., Turnbaugh, P. J., Samuel, B. S., ... Nelson, K. E. (2006). Metagenomic analysis of the human distal gut microbiome. *Science*, *312*(5778), 1355–1359.
- Gilmore, T. D. (1990). NF-κB, KBF1, dorsal, and related matters. *Cell*, *62*(5), 841–843. [http://doi.org/10.1016/0092-8674\(90\)90257-F](http://doi.org/10.1016/0092-8674(90)90257-F)
- Gilmore, T. D. (2006). Introduction to NF-kappaB: players, pathways, perspectives. *Oncogene*, *25*(51), 6680–6684. <http://doi.org/10.1038/sj.onc.1209954>
- Gilmore, T. D., & Temin, H. M. (1986). Different localization of the product of the v-rel oncogene in chicken fibroblasts and spleen cells correlates with transformation by REV-T. *Cell*, *44*(5), 791–800. [http://doi.org/10.1016/0092-8674\(86\)90845-7](http://doi.org/10.1016/0092-8674(86)90845-7)
- Gioannini, T. L., Teghanemt, A., Zhang, D., Coussens, N. P., Dockstader, W., Ramaswamy, S., & Weiss, J. P. (2004). Isolation of an endotoxin-MD-2 complex that produces Toll-like receptor 4-dependent cell activation at picomolar concentrations. *Proceedings of the National Academy of Sciences of the United States of America*, *101*(12), 4186–91. <http://doi.org/10.1073/pnas.0306906101>
- Goldberg, E. J., Bhalodia, S., Jacob, S., Patel, H., Trinh, K. V., Varghese, B., ... Raffa, R. B. (2015). Clostridium difficile infection: A brief update on emerging therapies. *American Journal of Health-System Pharmacy*, *72*(12), 1007–1012. <http://doi.org/10.2146/ajhp140645>

- Goni, R., García, P., & Foissac, S. (2009). The qPCR Data Statistical Analysis. *Integromics White Paper*, (September), 1–9.
- Goorhuis, A., Van der Kooi, T., Vaessen, N., Dekker, F. W., Van den Berg, R., Harmanus, C., ... Kuijper, E. J. (2007). Spread and epidemiology of *Clostridium difficile* polymerase chain reaction ribotype 027/toxinotype III in The Netherlands. *Clinical Infectious Diseases*, 45(6), 695–703. <http://doi.org/10.1086/520984>
- Gordo, I., Perfeito, L., & Sousa, A. (2011). Fitness effects of mutations in bacteria. *Journal of Molecular Microbiology and Biotechnology*, 21(1-2), 20–35. <http://doi.org/10.1159/000332747>
- Goriely, S., Molle, C., Nguyen, M., Albarani, V., Haddou, N. O., Lin, R., ... Goldman, M. (2008). Interferon regulatory factor 3 is involved in Toll-like receptor 4 (TLR4) and TLR3-induced IL-12p35 gene activation. *Blood*, 107(3), 1078–1084. <http://doi.org/10.1182/blood-2005-06-2416>
- Griffiths-Jones, S. (2004). The microRNA Registry. *Nucleic Acids Research*, 32(Database issue), D109–D111. <http://doi.org/10.1093/nar/gkh023>
- Griffiths-Jones, S. (2010). miRBase: microRNA sequences and annotation. In A. D. Baxevanis (Ed.), *Current protocols in bioinformatics* (p. Unit 12.9.1–10). Retrieved from http://apps.webofknowledge.com.remote.library.dcu.ie/full_record.do?product=UA&search_mode=GeneralSearch&qid=5&SID=N1j8EqyQJbYIZwh56MW&page=1&doc=1
- Griffiths-Jones, S., Grocock, R. J., van Dongen, S., Bateman, A., & Enright, A. J. (2006). miRBase: microRNA sequences, targets and gene nomenclature. *Nucleic Acids Research*, 34(Database issue), D140–D144. <http://doi.org/10.1093/nar/gkj112>
- Griffiths-Jones, S., Saini, H. K., Van Dongen, S., & Enright, A. J. (2008). miRBase: Tools for microRNA genomics. *Nucleic Acids Research*, 36(SUPPL. 1), 154–158. <http://doi.org/10.1093/nar/gkm952>
- Grimson, A., Farh, K. K.-H., Johnston, W. K., Garrett-Engle, P., Lim, L. P., & Bartel, D. P. (2007). MicroRNA Targeting Specificity in Mammals: Determinants Beyond Seed Pairing. *Molecular Cell*, 27(1), 91–105. <http://doi.org/10.1016/j.molcel.2007.06.017>
- Grogono-Thomas, R., Dworkin, J., Blaser, M. J., & Newell, D. G. (2000). Roles of the surface layer proteins of *Campylobacter fetus* subsp. *fetus* in ovine abortion. *Infection and Immunity*, 68(3), 1687–1691. <http://doi.org/10.1128/IAI.68.3.1687-1691.2000>
- Gromak, N., Dienstbier, M., Macias, S., Plass, M., Eyraes, E., Cáceres, J. F., & Proudfoot, N. J. (2013). Droscha Regulates Gene Expression Independently of RNA Cleavage Function. *Cell Reports*, 5(6), 1499–1510. <http://doi.org/10.1016/j.celrep.2013.11.032>
- Gurtan, A. M., & Sharp, P. a. (2013). The role of miRNAs in regulating gene expression networks. *Journal of Molecular Biology*, 425(19), 3582–600. <http://doi.org/10.1016/j.jmb.2013.03.007>
- Hammond, G. A., & Johnson, J. L. (1995). The toxigenic element of *Clostridium difficile* strain VPI 10463. *Microbial Pathogenesis*, 19(4), 203–213. [http://doi.org/10.1016/S0882-4010\(95\)90263-5](http://doi.org/10.1016/S0882-4010(95)90263-5)

- Hayashi, F., Smith, K. D., Ozinsky, A., Hawn, T. R., Yi, E. C., Goodlett, D. R., ... Aderem, A. (2001). The innate immune response to bacterial flagellin is mediated by Toll-like receptor 5. *Nature*, *410*(6832), 1099–1103. <http://doi.org/10.1038/35074106>
- Hayden, M. S., & Ghosh, S. (2004). Signaling to NF-kappaB. *Genes & Development*, *18*(18), 2195–224. <http://doi.org/10.1101/gad.1228704>
- Haziot, A., Chen, S., Ferrero, E., Low, M., Silber, R., & Goyert, S. (1988). The Monocyte Differentiation Antigen, CD14, is Anchored to the Cell Membrane by a Phosphatidylinositol Linkage. *Journal of Immunology*, *141*(2), 547–552. Retrieved from http://apps.webofknowledge.com.remote.library.dcu.ie/full_record.do?product=UA&search_mode=GeneralSearch&qid=7&SID=U15UtGJ9VwflgapWl5Z&page=1&doc=1
- He, X., Jia, H., Jing, Z., & Liu, D. (2013). Recognition of pathogen-associated nucleic acids by endosomal nucleic acid-sensing toll-like receptors. *Acta Biochimica et Biophysica Sinica*, *45*(4), 241–258. <http://doi.org/10.1093/abbs/gms122>
- He, X., Jing, Z., & Cheng, G. (2014). MicroRNAs: new regulators of Toll-like receptor signalling pathways. *BioMed Research International*, *2014*, 945169. <http://doi.org/10.1155/2014/945169>
- Heldin, C. H., Miyazono, K., & ten Dijke, P. (1997). TGF-beta signalling from cell membrane to nucleus through SMAD proteins. *Nature*, *390*(6659), 465–71. <http://doi.org/10.1038/37284>
- Helft, J., Böttcher, J., Chakravarty, P., Zelenay, S., Huotari, J., Schraml, B. U., ... Reis e Sousa, C. (2015). GM-CSF Mouse Bone Marrow Cultures Comprise a Heterogeneous Population of CD11c+MHCII+ Macrophages and Dendritic Cells. *Immunity*, *42*(6), 1197–1211. <http://doi.org/10.1016/j.immuni.2015.05.018>
- Hemmi, H., Takeuchi, O., Kawai, T., Kaisho, T., Sato, S., Sanjo, H., ... Akira, S. (2000). A Toll-like receptor recognizes bacterial DNA. *Nature*, *408*(6813), 740–745. <http://doi.org/10.1038/35047123>
- Hennequin, C. (2003). Identification and Characterization of a Fibronectin-Binding Protein from *Clostridium difficile*. *Microbiology*, *149*(10), 2779–2787. <http://doi.org/10.1099/mic.0.26145-0>
- Herzenberg, L. A., Parks, D. R., Sahaf, B., Perez, O., Roederer, M., & Herzenberg, L. A. (2002). The History and Future of the Fluorescence Activated Cell Sorter and Flow Cytometry: A view from Stanford. *Clinical Chemistry*, *48*(10), 1819–1827.
- Higgins, D., & Dworkin, J. (2012). Recent progress in *Bacillus subtilis* sporulation. *FEMS Microbiology Reviews*, *36*(1), 131–48. <http://doi.org/10.1111/j.1574-6976.2011.00310.x>
- Higgins, S. C., Lavelle, E. C., Mccann, C., Mcneela, E., Byrne, P., Gorman, B. O., ... Keogh, B. (2003). Toll-Like Receptor 4-Mediated Innate IL-10 Activates Antigen-Specific Regulatory T Cells and Confers Resistance to *Bordetella pertussis* by Inhibiting Inflammatory Pathology. *The Journal of Immunology*, *171*(6), 3119–3127.
- Hoebe, K., & Beutler, B. (2004). LPS, dsRNA and the interferon bridge to adaptive immune responses: Trif, Tram, and other TIR adaptor proteins. *Journal of Endotoxin Research*,

- Hofmann, F., Busch, C., Just, I., Aktories, K., & Prepens, U. (1997). Cell Biology and Metabolism: Localization of the Glucosyltransferase Activity of Clostridium difficile Toxin B to the N-terminal Part of the Holotoxin Localization of the Glucosyltransferase Activity of Clostridium difficile Toxin B to the N-terminal Par. *The Journal of Biological Chemistry*, 272(17), 11074–11078.
- Honda, K., Takaoka, A., & Taniguchi, T. (2006). Type I Inteferon Gene Induction by the Interferon Regulatory Factor Family of Transcription Factors. *Immunity*, 25(3), 349–360. <http://doi.org/10.1016/j.immuni.2006.08.009>
- Honda, K., & Taniguchi, T. (2006). IRFs: master regulators of signalling by Toll-like receptors and cytosolic pattern-recognition receptors. *Nature Reviews. Immunology*, 6(9), 644–658. <http://doi.org/10.1038/nri1900>
- Hou, J., Wang, P., Lin, L., Liu, X., Ma, F., An, H., ... Cao, X. (2009). MicroRNA-146a feedback inhibits RIG-I-dependent Type I IFN production in macrophages by targeting TRAF6, IRAK1, and IRAK2. *Journal of Immunology*, 183(3), 2150–8. <http://doi.org/10.4049/jimmunol.0900707>
- Hsiao, A., Worrall, D. S., Olefsky, J. M., & Subramaniam, S. (2004). Variance-Modeled Posterior Inference of Microarray Data: Detecting Gene-Expression Changes in 3T3-L1 Adipocytes. *Bioinformatics*, 20(17), 3108–27. <http://doi.org/10.1093/bioinformatics/bth371>
- Huang, R., Hu, G., Lin, B., Lin, Z., & Sun, C. (2010). MicroRNA-155 silencing enhances inflammatory response and lipid uptake in oxidized low-density lipoprotein-stimulated human THP-1 macrophages. *Journal of Investigative Medicine: The Official Publication of the American Federation for Clinical Research*, 58(8), 961–7. <http://doi.org/10.231/JIM.0b013e3181ff46d7>
- Hundsberger, T., Braun, V., Weidmann, M., Leukel, P., Sauerborn, M., & Von Eichel-Streiber, C. (1997). Transcription analysis of the genes tcA-E of the pathogenicity locus of Clostridium difficile. *European Journal of Biochemistry*, 244, 735–742.
- Husebye, H., Halaas, Ø., Stenmark, H., Tunheim, G., Sandanger, Ø., Bogen, B., ... Espevik, T. (2006). Endocytic pathways regulate Toll-like receptor 4 signaling and link innate and adaptive immunity. *The EMBO Journal*, 25(4), 683–692. <http://doi.org/10.1038/sj.emboj.7600991>
- Hutvágner, G., McLachlan, J., Pasquinelli, A. E., Bálint, E., Tuschl, T., & Zamore, P. D. (2001). A Cellular Function for the RNA-Interference Enzyme Dicer in the Maturation of the let-7 Small Temporal RNA. *Science*, 293(5531), 834–838. <http://doi.org/10.1126/science.1062961>
- Ibrahim, A. F., Weirauch, U., Thomas, M., Grunweller, A., Hartmann, R. K., & Aigner, A. (2011). MicroRNA Replacement Therapy for miR-145 and miR-33a Is Efficacious in a Model of Colon Carcinoma. *Cancer Research*, 71(15), 5214–5224. <http://doi.org/10.1158/0008-5472.CAN-10-4645>
- Ihunnah, C., Khoruts, A., Fischer, M., Afzali, A., Aroniadis, O., Barto, A., ... Kelly, C. (2013).

- Fecal Microbiota Transplantation (FMT) for Treatment of Clostridium difficile Infection (CDI) in Immunocompromised Patients. *AMERICAN JOURNAL OF GASTROENTEROLOGY*, 108, S179–S180. Retrieved from http://apps.webofknowledge.com.remote.library.dcu.ie/full_record.do?product=UA&search_mode=GeneralSearch&qid=5&SID=V2bJDJ1mhq8DlpOTEIx&page=1&doc=4
- Inaba, K., Steinman, R. M., Pack, M. W., Aya, H., Inaba, M., Sudo, T., ... Schuler, G. (1992). Identification of proliferating dendritic cell precursors in mouse blood. *The Journal of Experimental Medicine*, 175(5), 1157–1167. <http://doi.org/10.1084/jem.175.5.1157>
- Iwasaki, A. (2007). Mucosal dendritic cells. *Annual Review of Immunology*, 25, 381–418. <http://doi.org/10.1146/annurev.immunol.25.022106.141634>
- Izar, B., Mannala, G. K., Mraheil, M. A., Chakraborty, T., & Hain, T. (2012). microRNA response to Listeria monocytogenes infection in epithelial cells. *International Journal of Molecular Sciences*, 13(1), 1173–85. <http://doi.org/10.3390/ijms13011173>
- Janeway, C. A. (1989). Approaching the Asymptote? Evolution and Revolution in Immunology. *Cold Spring Harbor Symposia on Quantitative Biology*, 54(0), 1–13. <http://doi.org/10.1101/SQB.1989.054.01.003>
- Janeway, C., Travers, P., Walport, M., & Schlomchik, M. (2001). *Immunobiology: The immune system in health & Disease*. New York: Garland Science.
- Jank, T., Giesemann, T., & Aktories, K. (2007). Rho-glucosylating Clostridium difficile Toxins A and B: New Insights into Structure and Function. *Glycobiology*, 17(4), 15R–22R. <http://doi.org/10.1093/glycob/cwm004>
- Jego, G., Palucka, K. A., Blanck, J., Chalouni, C., Pascual, V., & Banchereau, J. (2003). Plasma Cell Differentiation through Type I Interferon and Interleukin 6. *Immunity*, 19(2), 225–234.
- Jennewein, C., von Knethen, A., Schmid, T., & Brüne, B. (2010). MicroRNA-27b Contributes to Lipopolysaccharide-Mediated Peroxisome Proliferator-Activated Receptor γ (PPAR γ) mRNA Destabilization. *The Journal of Biological Chemistry*, 285(16), 11846–11853. <http://doi.org/10.1074/jbc.M109.066399>
- Jens, M., & Rajewsky, N. (2014). Competition between target sites of regulators shapes post-transcriptional gene regulation. *Nature Reviews Genetics*, 16(2), 113–126. <http://doi.org/10.1038/nrg3853>
- Jiang, Z., Georgel, P., Du, X., Shamel, L., Sovath, S., Mudd, S., ... Beutler, B. (2005). CD14 is Required for MyD88-Independent LPS Signaling. *Nature Immunology*, 6(6), 565–570. <http://doi.org/10.1038/ni1207>
- Jing, Q., Huang, S., Guth, S., Zarubin, T., Motoyama, A., Chen, J., ... Han, J. (2005). Involvement of microRNA in AU-rich element-mediated mRNA instability. *Cell*, 120(5), 623–34. <http://doi.org/10.1016/j.cell.2004.12.038>
- Johnnidis, J. B., Harris, M. H., Wheeler, R. T., Stehling-Sun, S., Lam, M. H., Kirak, O., ... Camargo, F. D. (2008). Regulation of progenitor cell proliferation and granulocyte function by microRNA-223. *Nature*, 451(7182), 1125–1129.

<http://doi.org/10.1038/nature06607>

- Jørgensen, T. N., Haase, C., & Michelsen, B. K. (2002). Treatment of an Ommortalized APC Cell Line with Both Cytokines and LPS Ensures Effective T-cell Activation In Vitro. *Scandinavian Journal of Immunology*, 56(5), 492–503. <http://doi.org/10.1046/j.1365-3083.2002.01166.x>
- Joshi, L. T., Phillips, D. S., Williams, C. F., Alyousef, A., & Baillie, L. (2012). Contribution of spores to the ability of clostridium difficile to adhere to surfaces. *Applied and Environmental Microbiology*, 78(21), 7671–7679. <http://doi.org/10.1128/AEM.01862-12>
- Jothikumar, P., Hill, V., & Narayanan, J. (2009). Design of FRET-TaqMan probes for multiplex real-time PCR using an internal positive control. *BioTechniques*, 46(7), 519–24. <http://doi.org/10.2144/000113127>
- Jump, R. L. P., Pultz, M. J., & Donskey, C. J. (2007). Vegetative Clostridium difficile survives in room air on moist surfaces and in gastric contents with reduced acidity: A potential mechanism to explain the association between proton pump inhibitors and C. difficile-associated diarrhea? *Antimicrobial Agents and Chemotherapy*, 51(8), 2883–2887. <http://doi.org/10.1128/AAC.01443-06>
- Jung, C., Hugot, J. P., & Barreau, F. (2010). Peyer's Patches: The Immune Sensors of the Intestine. *International Journal of Inflammation*, 2010, 823710. Retrieved from http://apps.webofknowledge.com.remote.library.dcu.ie/full_record.do?product=UA&search_mode=GeneralSearch&qid=4&SID=R2AW8PJzUKv9qw6X7KV&page=1&doc=3
- Just, I., & Gerhard, R. (2004). Large clostridial cytotoxins. *Reviews of Physiology, Biochemistry and Pharmacology*, 152, 23–47. <http://doi.org/10.1007/s10254-004-0033-5>
- Kachrimanidou, M., & Malisiovas, N. (2011). Clostridium difficile Infection: A Comprehensive Review. *Critical Reviews in Microbiology*, 37(3), 178–187. <http://doi.org/10.3109/1040841X.2011.556598>
- Kagan, J. C., Su, T., Horng, T., Chow, A., Akira, S., & Medzhitov, R. (2008). TRAM Couples Endocytosis of Toll-Like Receptor 4 to the Induction of interferon- β . *Nature Immunology*, 9, 361–368.
- Kanehisa, M., & Goto, S. (2000). KEGG: kyoto encyclopedia of genes and genomes. *Nucleic Acids Research*, 28(1), 27–30. Retrieved from <http://www.pubmedcentral.nih.gov/articlerender.fcgi?artid=102409&tool=pmcentrez&rendertype=abstract>
- Karjalainen, T., Cerquetti, M., Spigaglia, P., Maggioni, A., Mauri, P., & Mastrantonio, P. (2001). Molecular and Genomic Analysis of Genes Encoding Surface- Anchored Proteins from Clostridium difficile. *Infection and Immunity*, 69(5), 3442–3446. <http://doi.org/10.1128/IAI.69.5.3442>
- Kawai, T., & Akira, S. (2006). TLR Signaling. *Cell Death and Differentiation*, 13(5), 816–825. <http://doi.org/10.1038/sj.cdd.4401850>
- Kawai, T., & Akira, S. (2007). Signaling to NF-kappaB by Toll-like receptors. *Trends in Molecular Medicine*, 13(11), 460–9. <http://doi.org/10.1016/j.molmed.2007.09.002>

- Kawai, T., Takeuchi, O., Fujita, T., Inoue, J., Mührladt, P. F., Sato, S., ... Akira, S. (2001). Lipopolysaccharide stimulates the MyD88-independent pathway and results in activation of IFN-regulatory factor 3 and the expression of a subset of lipopolysaccharide-inducible genes. *Journal of Immunology*, 167(10), 5887–5894. <http://doi.org/10.4049/jimmunol.167.10.5887>
- Khader, S., Gaffen, S. L., & Kolls, J. K. (2009). Th17 cells at the cross roads of innate and adaptive immunity against infectious diseases at the mucosa. *Mucosal Immunology*, 2(5), 403–411. <http://doi.org/10.1038/mi.2009.100.Th17>
- Kim, E. K., & Choi, E.-J. (2010). Pathological roles of MAPK Signaling Pathways in Human Diseases. *Biochimica et Biophysica Acta (BBA) - Molecular Basis of Disease*, 1802(4), 396–405. <http://doi.org/10.1016/j.bbadis.2009.12.009>
- Kim, K. H., Fekety, R., Batts, D. H., Brown, D., Cudmore, M., Silva, J., & Waters, D. (1981). Isolation of *Clostridium difficile* from the environment and contacts of patients with antibiotic-associated colitis. *The Journal of Infectious Diseases*, 143(1), 42–50. <http://doi.org/10.1093/infdis/143.1.42>
- Kim, S. J., Gregersen, P. K., & Diamond, B. (2013). Regulation of Dendritic Cell Activation by microRNA let-7c and BLIMP1. *The Journal of Clinical Investigation*, 123(2), 823–833. <http://doi.org/10.1172/JCI64712DS1>
- Klement, J. F., Rice, N. R., Car, B. D., Abbondanzo, S. J., Powers, G. D., Bhatt, P. H., ... Stewart, C. L. (1996). IkappaBalpha deficiency results in a sustained NF-kappaB response and severe widespread dermatitis in mice. *Molecular and Cellular Biology*, 16(5), 2341–2349.
- Kobayashi, T., Walsh, M. C., & Choi, Y. (2004). The role of TRAF6 in signal transduction and the immune response. *Microbes Infect*, 6(14), 1333–1338. <http://doi.org/10.1016/j.micinf.2004.09.001>
- Koh, T.-C., Lee, Y.-Y., Chang, S.-Q., & Nissom, P. M. (2009). Identification and Expression Analysis of miRNAs During Batch Culture of HEK-293 cells. *Journal of Biotechnology*, 140(3-4), 149–155. <http://doi.org/10.1016/j.jbiotec.2009.01.021>
- Kohlhaas, S., Garden, O. A., Scudamore, C., Turner, M., Okkenhaug, K., & Vigorito, E. (2009). Cutting edge: the Foxp3 target miR-155 contributes to the development of regulatory T cells. *Journal of Immunology*, 182(5), 2578–82. <http://doi.org/10.4049/jimmunol.0803162>
- Kondo, T., Kawai, T., & Akira, S. (2012). Dissecting negative regulation of Toll-like receptor signaling. *Trends in Immunology*, 33(9), 449–458. <http://doi.org/10.1016/j.it.2012.05.002>
- Kortum, R. L., Sommers, C. L., Alexander, C. P., Pinski, J. M., Li, W., Grinberg, A., ... Samelson, L. E. (2013). Targeted *Sosl* deletion reveals its critical role in early T-cell development. *Proceedings of the National Academy of Sciences of the United States of America*, 108(30), 12407–12412. <http://doi.org/10.1073/pnas.1>
- Koscianska, E., Witkos, T. M., Kozłowska, E., Wojciechowska, M., & Krzyzosiak, W. J. (2015). Cooperation Meets Competition in microRNA-Mediated DMPK Transcript Regulation. *Nucleic Acids Research*, 43(19), 9500–9518. <http://doi.org/10.1093/nar/gkv849>

- Krachler, A. M., Woolery, A. R., & Orth, K. (2011). Manipulation of kinase signaling by bacterial pathogens. *The Journal of Cell Biology*, *195*(7), 1083–92. <http://doi.org/10.1083/jcb.201107132>
- Kramer, M. F. (2011). Stem-loop RT-qPCR for miRNAs. In F. Ausubel (Ed.), *Current protocols in molecular biology* (p. Unit 15.10). <http://doi.org/10.1002/0471142727.mb1510s95>
- Krichevsky, A. M. (2003). A microRNA Array Reveals Extensive Regulation of microRNAs During Brain Development. *RNA*, *9*(10), 1274–1281. <http://doi.org/10.1261/rna.5980303>
- Krützfeldt, J., Rajewsky, N., Braich, R., Rajeev, K. G., Tuschl, T., Manoharan, M., & Stoffel, M. (2005). Silencing of microRNAs in vivo with “antagomirs.” *Nature*, *438*(7068), 685–689. <http://doi.org/10.1038/nature04303>
- Kuhn, D. E., Martin, M. M., Feldman, D. S., Terry, A. V., Nuovo, G. J., & Elton, T. S. (2008). Experimental Validation of miRNA Targets. *Methods*, *44*(1), 47–54. <http://doi.org/10.1016/j.ymeth.2007.09.005>
- Kumar, K. P., McBride, K. M., Weaver, B. K., Dingwall, C., & Reich, N. C. (2000). Regulated nuclear-cytoplasmic localization of interferon regulatory factor 3, a subunit of double-stranded RNA-activated factor 1. *Molecular and Cellular Biology*, *20*(11), 4159–4168. <http://doi.org/10.1128/MCB.20.11.4159-4168.2000>
- Kumar, N. (2009). *Investigation of the Molecular Mechanisms Regulating Growth and Recombinant Protein Productivity in Suspension Adapted CHI-K1 Cells*. Dublin City University.
- Kunsch, C., Ruben, S. M., & Rosen, C. A. (1992). Selection of optimal kappa B/Rel DNA-binding motifs: interaction of both subunits of NF-kappa B with DNA is required for transcriptional activation. *Molecular and Cellular Biology*, *12*(10), 4412–4421. <http://doi.org/10.1128/MCB.12.10.4412.Updated>
- Laar, L. Van De, Coffey, P. J., & Woltman, A. M. (2012). Review article Regulation of dendritic cell development by GM-CSF : molecular control and implications for immune homeostasis and therapy. *Development*, *119*(15), 3383–3393. <http://doi.org/10.1182/blood-2011-11-370130.The>
- Labbé, A. C., Poirier, L., MacCannell, D., Louie, T., Savoie, M., Béliveau, C., ... Pépin, J. (2008). Clostridium difficile infections in a Canadian Tertiary Care Hospital before and during a regional epidemic associated with the BI/NAP1/027 strain. *Antimicrobial Agents and Chemotherapy*, *52*(9), 3180–3187. <http://doi.org/10.1128/AAC.00146-08>
- Lagos-Quintana, M., Rauhut, R., Lendeckel, W., & Tuschl, T. (2001). Identification of novel genes coding for small expressed RNAs. *Science*, *294*(5543), 853–858. <http://doi.org/10.1126/science.1064921>
- Laird, M. H. W., Rhee, S. H., Perkins, D. J., Medvedev, A. E., Piao, W., Fenton, M. J., & Vogel, S. N. (2009). TLR4/MyD88/PI3K interactions regulate TLR4 signaling. *Journal of Leukocyte Biology*, *85*(6), 966–77. <http://doi.org/10.1189/jlb.1208763>
- Larson, H. E. (1978). Clostridium difficile and the aetiology of pseudomembranous colitis. *The*

Lancet, 1(8073), 1096–1066.

- Lau, N. C., Lim, L. P., Weinstein, E. G., & Bartel, D. P. (2001). An abundant class of tiny RNAs with probable regulatory roles in *Caenorhabditis elegans*. *Science*, 294(5543), 858–862. <http://doi.org/10.1126/science.1065062>
- Lavelle, E. C., McNeela, E., Armstrong, M. E., Leavy, O., Higgins, S. C., & Mills, K. H. G. (2003). Cholera Toxin Promotes the Induction of Regulatory T cells Specific for Bystander Antigens by Modulating Dendritic Cell Activation. *Journal of Immunology*, 171(5), 2384–2392.
- Lawley, T. D., Clare, S., Walker, A. W., Goulding, D., Stabler, R. A., Croucher, N., ... Dougan, G. (2009). Antibiotic treatment of *Clostridium difficile* carrier mice triggers a supershedder state, spore-mediated transmission, and severe disease in immunocompromised hosts. *Infection and Immunity*, 77(9), 3661–3669. <http://doi.org/10.1128/IAI.00558-09>
- Lawley, T. D., Croucher, N. J., Yu, L., Clare, S., Sebahia, M., Goulding, D., ... Dougan, G. (2009). Proteomic and genomic characterization of highly infectious *Clostridium difficile* 630 spores. *Journal of Bacteriology*, 191(17), 5377–5386. <http://doi.org/10.1128/JB.00597-09>
- Le Monnier, A., Zahar, J. R., & Barbut, F. (2014). Update on *Clostridium difficile* infections. *Medecine et Maladies Infectieuses*, 44(8), 354–365. <http://doi.org/10.1016/j.medmal.2014.04.002>
- Lee, M. S., & Kim, Y.-J. (2007). Signaling Pathways Downstream of Pattern-Recognition Receptors and Their Cross Talk. *Annual Review of Biochemistry*, 76(1), 447–480. <http://doi.org/10.1146/annurev.biochem.76.060605.122847>
- Lee, R. C., & Ambros, V. (2001). An extensive class of small RNAs in *Caenorhabditis elegans*. *Science*, 294(5543), 862–864. <http://doi.org/10.1126/science.1065329>
- Lee, R. C., Feinbaum, R. L., & Ambros, V. (1993). The *C. elegans* heterochronic gene *lin-4* encodes small RNAs with antisense complementarity to *lin-14*. *Cell*, 75(5), 843–854. [http://doi.org/10.1016/0092-8674\(93\)90529-Y](http://doi.org/10.1016/0092-8674(93)90529-Y)
- Lee, S. H., Starkey, P. M., & Gordon, S. (1985). Quantitative analysis of total macrophage content in adult mouse tissues. Immunochemical studies with monoclonal antibody F4/80. *The Journal of Experimental Medicine*, 161(3), 475–489. <http://doi.org/10.1084/jem.161.3.475>
- Lee, Y., Ahn, C., Han, J., Choi, H., Kim, J., Yim, J., ... Kim, V. N. (2003). The nuclear RNase III Drosha initiates microRNA processing. *Nature*, 425(6956), 415–9. <http://doi.org/10.1038/nature01957>
- Lewis, B. P., Burge, C. B., & Bartel, D. P. (2005). Conserved seed pairing, often flanked by adenosines, indicates that thousands of human genes are microRNA targets. *Cell*, 120(1), 15–20. <http://doi.org/10.1016/j.cell.2004.12.035>
- Lewis, B. P., Shih, I., Jones-Rhoades, M. W., Bartel, D. P., & Burge, C. B. (2003). Prediction of mammalian microRNA targets. *Cell*, 115(7), 787–98. Retrieved from

<http://www.ncbi.nlm.nih.gov/pubmed/14697198>

- Ley, R. E., Peterson, D. A., & Gordon, J. I. (2006). Ecological and evolutionary forces shaping microbial diversity in the human intestine. *Cell*, *124*(4), 837–848. <http://doi.org/10.1016/j.cell.2006.02.017>
- Lhakhang, T. W., & Chaudhry, M. A. (2012). Current approaches to micro-RNA analysis and target gene prediction. *Journal of Applied Genetics*, *53*(2), 149–58. <http://doi.org/10.1007/s13353-011-0060-2>
- Li, S., Strelow, A., Fontana, E. J., & Wesche, H. (2009). IRAK-4: A novel member of the IRAK family with the properties of an IRAK-kinase. *Proceedings of the National Academy of Sciences*, *99*(8), 5567–5572.
- Li, S., Yue, Y., Xu, W., & Xiong, S. (2013). MicroRNA-146a represses mycobacteria-induced inflammatory response and facilitates bacterial replication via targeting IRAK-1 and TRAF-6. *PloS One*, *8*(12), e81438. <http://doi.org/10.1371/journal.pone.0081438>
- Li, W. (2012). Volcano plots in analyzing differential expressions with mRNA microarrays. *Journal of Bioinformatics and Computational Biology*, *10*(6), 1231003. <http://doi.org/10.1142/S0219720012310038>
- Li, Y., & Shi, X. (2013). MicroRNAs in the regulation of TLR and RIG-I pathways. *Cellular & Molecular Immunology*, *10*(1), 65–71. <http://doi.org/10.1038/cmi.2012.55>
- Li, Y., VandenBoom II, T. G., Kong, D., Wang, Z., Ali, S., Philip, P. A., & Sarkar, F. H. (2009). Up-regulation of miR-200 and let-7 by Natural Agents Leads to the Reversal of Epithelial-to-Mesenchymal Transition in Gemcitabine-Resistant Pancreatic Cancer Cells. *Cancer Research*, *69*(16), 6704–6712. <http://doi.org/10.1158/0008-5472.CAN-09-1298>
- Lim, L. P., Glasner, M. E., Yekta, S., Burge, C. B., & Bartel, D. P. (2003). Vertebrate microRNA genes. *Science*, *299*(5612), 1540. <http://doi.org/10.1126/science.1080372>
- Lin, L., Hou, J., Ma, F., Wang, P., Liu, X., Li, N., ... Cao, X. (2013). Type I IFN inhibits innate IL-10 production in macrophages through histone deacetylase 11 by downregulating microRNA-145. *Journal of Immunology*, *191*(7), 3896–904. <http://doi.org/10.4049/jimmunol.1203450>
- Lin, R., Heylbroeck, C., Genin, P., Pitha, P. M., & Hiscott, J. (1999). Essential Role of Interferon Regulatory Factor 3 in Direct Activation of RANTES Chemokine Transcription. *Molecular and Cellular Biology*, *19*(2), 959–966.
- Lindsay, M. A. (2008). microRNAs and the Immune Response. *Trends in Immunology*, *29*(7), 343–351. <http://doi.org/10.1016/j.it.2008.04.004>
- Littman, D. R., & Pamer, E. G. (2011). Role of the commensal microbiota in normal and pathogenic host immune responses. *Cell Host and Microbe*, *10*(4), 311–323. <http://doi.org/10.1016/j.chom.2011.10.004>
- Liu, J., Carmell, M. A., Rivas, F. V., Marsden, C. G., Thomson, J. M., Song, J.-J., ... Hannon,

- G. J. (2004). Argonaute2 is the catalytic engine of mammalian RNAi. *Science*, 305(5689), 1437–41. <http://doi.org/10.1126/science.1102513>
- Liu, J., Drescher, K. M., & Chen, X.-M. (2009). MicroRNAs and Epithelial Immunity. *International Reviews of Immunology*, 28(3-4), 139–154. <http://doi.org/10.1016/j.biotechadv.2011.08.021>. Secreted
- Liu, X., & Rennard, S. I. (2011). MicroRNA and Cytokines. *Molecular and Cellular Pharmacology*, 3(3), 143–151. Retrieved from <https://doaj.org/article/7a254fd79df449509068847be2de0f9b>
- Liu, X., Zhan, Z., Xu, L., Ma, F., Li, D., Guo, Z., ... Cao, X. (2010). MicroRNA-148/152 impair innate response and antigen presentation of TLR-triggered dendritic cells by targeting CaMKII α . *Journal of Immunology*, 185(12), 7244–7251. <http://doi.org/10.4049/jimmunol.1001573>
- Liu, Z., Xiao, B., Tang, B., Li, B., Li, N., Zhu, E., ... Zou, Q. (2010). Up-regulated microRNA-146a negatively modulate Helicobacter pylori-induced inflammatory response in human gastric epithelial cells. *Microbes and Infection / Institut Pasteur*, 12(11), 854–63. <http://doi.org/10.1016/j.micinf.2010.06.002>
- Livak, K. J., & Schmittgen, T. D. (2001). Analysis of Relative Gene Expression Data Using Real-Time Quantitative PCR and the 2- $\Delta\Delta$ CT Method. *Methods*, 25(4), 402–408. <http://doi.org/10.1006/meth.2001.1262>
- Loh, P. G., Yang, H.-S., Walsh, M. a, Wang, Q., Wang, X., Cheng, Z., ... Song, H. (2009). Structural basis for translational inhibition by the tumour suppressor Pcd4. *The EMBO Journal*, 28(3), 274–285. <http://doi.org/10.1038/emboj.2008.278>
- Loo, V. G., Poirier, L., Miller, M. A., Oughton, M., Libman, M. D., Michaud, S., ... Dascal, A. (2005). A predominantly clonal multi-institutional outbreak of Clostridium difficile-associated diarrhea with high morbidity and mortality. *The New England Journal of Medicine*, 353(23), 2442–9. <http://doi.org/10.1056/NEJMoa051639>
- Lowy, I., Molrine, D. C., & Ambrosino, D. M. (2010). Treatment with Monoclonal Antibodies against Clostridium difficile Toxins REPLY. *NEW ENGLAND JOURNAL OF MEDICINE*, 362(15), 1445–1446. Retrieved from http://apps.webofknowledge.com.remote.library.dcu.ie/full_record.do?product=UA&search_mode=GeneralSearch&qid=3&SID=V2bJDJ1mhq8DlpOTEIx&page=1&doc=4
- Lu, T. X., Munitz, A., & Rothenberg, M. E. (2009). MicroRNA-21 is up-regulated in allergic airway inflammation and regulates IL-12p35 expression. *Journal of Immunology*, 182(8), 4994–5002. <http://doi.org/10.4049/jimmunol.0803560>
- Lu, T.-P., Lee, C.-Y., Tsai, M.-H., Chiu, Y.-C., Hsiao, C. K., Lai, L.-C., & Chuang, E. Y. (2012). miRSystem: an integrated system for characterizing enriched functions and pathways of microRNA targets. *PloS One*, 7(8), e42390. <http://doi.org/10.1371/journal.pone.0042390>
- Lutz, M. B., Kukutsch, N., Ogilvie, A. L., Rössner, S., Koch, F., Romani, N., & Schuler, G. (1999). An Advanced Culture Method for Generating Large Quantities of Highly Pure Dendritic Cells from Mouse Bone Marrow. *Journal of Immunological Methods*, 223(1),

77–92. [http://doi.org/10.1016/S0022-1759\(98\)00204-X](http://doi.org/10.1016/S0022-1759(98)00204-X)

- Lynch, M. (2014). *Surface Layer Proteins as Virulence Factors in Clostridium Difficile Infection*. Dublin City University.
- Ma, F., Xu, S., Liu, X., Zhang, Q., Xu, X., Liu, M., ... Cao, X. (2011). The microRNA miR-29 controls innate and adaptive immune responses to intracellular bacterial infection by targeting interferon- γ . *Nature Immunology*, *12*(9), 861–869. <http://doi.org/10.1038/ni.2073>
- Ma, X., Buscaglia, L. E. B., Barker, J. R., & Li, Y. (2011). MicroRNAs in NF- κ B signaling. *Journal of Molecular Cell Biology*, *3*, 159–166. <http://doi.org/doi:10.1093/jmcb/mjr007>
- MacKay, V. ., & Moore, E. . (1997). Immortalized dendritic cells. *Official Gazette of the United States Patent and Trademark Office Patents*. USA. Retrieved from http://apps.whoofknowledge.com.remote.library.dcu.ie/full_record.do?product=UA&search_mode=GeneralSearch&qid=2&SID=Z2xeuvndx8Ch7uUGrah&page=1&doc=1
- Madan, R., & Petri Jr, W. A. (2012). Immune Responses to Clostridium difficile Infection. *Trends in Molecular Medicine*, *18*(11), 658–666. <http://doi.org/10.1016/j.molmed.2012.09.005>
- Madden, S. F., Carpenter, S. B., Jeffery, I. B., Björkbacka, H., Fitzgerald, K. A., O'Neill, L. A. J., & Higgins, D. G. (2010). Detecting microRNA Activity from Gene Expression Data. *BMC Bioinformatics*, *11*(257).
- Mahen, E. M., Watson, P. Y., Cottrell, J. W., & Fedor, M. J. (2010). mRNA secondary structures fold sequentially but exchange rapidly in vivo. *PLoS Biology*, *8*(2), e1000307. <http://doi.org/10.1371/journal.pbio.1000307>
- Marszalowska, I. (2015). *Unravelling the Role of Glycosylation in Clostridium Difficile Infection*. Dublin City University.
- Martinez, N. J., & Walhout, A. J. M. (2009). The Interplay Between Transcription Factors and microRNAs in Genome-Scale Regulatory Networks. *BioEssays*, *31*(4), 435–445. <http://doi.org/10.1002/bies.200800212>
- Martinez-Sanchez, A., & Murphy, C. (2013). MicroRNA Target Identification-Experimental Approaches. *Biology*, *2*(1), 189–205. <http://doi.org/10.3390/biology2010189>
- Matthews, J. C., Hori, K., & Cormier, M. J. (1975). Purification and properties. *Life Sciences*, *16*(1970), 85–91. Retrieved from <http://www.sciencedirect.com/science/article/pii/0024320575902726>
- McCoy, C. E., Sheedy, F. J., Qualls, J. E., Doyle, S. L., Quinn, S. R., Murray, P. J., & O'Neill, L. a J. (2010). IL-10 inhibits miR-155 induction by toll-like receptors. *The Journal of Biological Chemistry*, *285*(27), 20492–8. <http://doi.org/10.1074/jbc.M110.102111>
- Medzhitov, R., & Janeway, C. A. J. (1997). Innate immunity: Minireview the virtues of a nonclonal system of recognition. *Cell*, *91*, 295–298. <http://doi.org/10.1016/j.immuni.2007.05.022>

- Medzhitov, R., Preston-hurlburt, P., & Janeway, C. A. J. (1997). A Human Homologue of the Drosophila Toll protein Signals Activation of Adaptive Immunity. *Letters to Nature*, 388(July), 6–9.
- Meister, G., Landthaler, M., Patkaniowska, A., Dorsett, Y., Teng, G., & Tuschl, T. (2004). Human Argonaute2 mediates RNA cleavage targeted by miRNAs and siRNAs. *Molecular Cell*, 15(2), 185–97. <http://doi.org/10.1016/j.molcel.2004.07.007>
- Merrigan, M. M., Venugopal, A., Roxas, J. L., Anwar, F., Mallozzi, M. J., Roxas, B. A. P., ... Vedantam, G. (2013). Surface-Layer Protein A (SlpA) is a major contributor to host-cell adherence of clostridium difficile. *PLoS ONE*, 8(11), e78404. <http://doi.org/10.1371/journal.pone.0078404>
- Mestdagh, P., Van Vlierberghe, P., De Weer, A., Muth, D., Westermann, F., Speleman, F., & Vandesompele, J. (2009). A novel and universal method for microRNA RT-qPCR data normalization. *Genome Biology*, 10(6), R64. <http://doi.org/10.1186/gb-2009-10-6-r64>
- Meyer, S. U., Kaiser, S., Wagner, C., Thirion, C., & Pfaffl, M. W. (2012). Profound Effect of Profiling Platform and Normalization Strategy on Detection of Differentially Expressed microRNAs- A Comparative Study. *PloS One*, 7(6), e38946. <http://doi.org/10.1371/journal.pone.0038946>
- Meylan, E., Burns, K., Hofmann, K., Blancheteau, V., Martinon, F., Kelliher, M., & Tschopp, J. (2004). RIP1 is an essential mediator of Toll-like receptor 3-induced NF-kappa B activation. *Nature Immunology*, 5(5), 503–507. <http://doi.org/10.1038/ni1061>
- Miller, H., Zhang, J., KuoLee, R., Patel, G. B., & Chen, W. (2007). Intestinal M cells: The fallible sentinels? *World Journal of Gastroenterology*, 13(10), 1477–1486.
- Miller, L. S., Pietras, E. M., Uricchio, L. H., Hirano, K., Rao, S., Lin, H., ... Modlin, R. L. (2014). Neutrophil Recruitment against Staphylococcus aureus In Vivo 1. *The Journal of Immunology*, 179, 6933–6944. <http://doi.org/10.4049/jimmunol.179.10.6933>
- Miller, R. A., Galecki, A., & Shmookler-Reis, R. J. (2001). Interpretation, design, and analysis of gene array expression experiments. *The Journals of Gerontology. Series A, Biological Sciences and Medical Sciences*, 56(8), B327–30. Retrieved from <http://www.ncbi.nlm.nih.gov/pubmed/11487590>
- Mogensen, T. H. (2009). Pathogen recognition and inflammatory signaling in innate immune defenses. *Clinical Microbiology Reviews*, 22(2), 240–273. <http://doi.org/10.1128/CMR.00046-08>
- Molle, C., Nguyen, M., Flamand, V., Renneson, J., Trottein, F., De Wit, D., ... Goriely, S. (2007). IL-27 synthesis induced by TLR ligation critically depends on IFN regulatory factor 3. *Journal of Immunology*, 178(12), 7607–7615. <http://doi.org/10.4049/jimmunol.178.12.7607>
- Moore, K. J., Andersson, L. P., Ingalls, R. R., Monks, B. G., Li, R., Arnaout, A. M., ... Freeman, M. W. (2000). Divergent Response to LPS and Bacteria in CD14-Deficient Murine Macrophages. *The Journal of Immunology*, 165(8), 4272–4280. <http://doi.org/10.4049/jimmunol.165.8.4272>

- Mor, A., Keren, G., Kloog, Y., & George, J. (2008). N-Ras or K-Ras inhibition increases the number and enhances the function of Foxp3 regulatory T cells. *European Journal of Immunology*, 38(6), 1493–502. <http://doi.org/10.1002/eji.200838292>
- Moriguchi, T., Kuroyanagis, N., Yamaguchi, K., Gotoh, Y., Iriel, K., Kano, T., ... Hagiwara, M. (1996). A Novel Kinase Cascade Mediated by Mitogen-activated Protein Kinase Kinase 6 and MKK3. *Journal of Biological Chemistry*, 271(23), 13675–13679. <http://doi.org/10.1074/jbc.271.23.13675>
- Mukaida, N., Okamoto, S., Ishikawa, Y., & Matsushima, K. (1994). Molecular mechanism of interleukin-8 gene expression. *Journal of Leukocyte Biology*, 56(November), 554–558.
- Mullane, K. (2014). Fidaxomicin in *Clostridium difficile* infection: latest evidence and clinical guidance. *Therapeutic Advances in Chronic Disease*, 5(2), 69–84. <http://doi.org/10.1177/2040622313511285>
- Nahid, M. A., Satoh, M., & Chan, E. K. L. (2011). Mechanistic Role of microRNA-146a in Endotoxin-Induced Differential Cross-Regulation of TLR Signaling. *Journal of Immunology*, 186(3), 1723–34. <http://doi.org/10.4049/jimmunol.1002311>
- Nahid, M. A., Yao, B., Dominguez-Gutierrez, P. R., Kesavalu, L., Satoh, M., & Chan, E. K. L. (2013). Regulation of TLR2-mediated tolerance and cross-tolerance through IRAK4 modulation by miR-132 and miR-212. *Journal of Immunology*, 190(3), 1250–63. <http://doi.org/10.4049/jimmunol.1103060>
- Nelson, P. T., Baldwin, D. A., Scarce, M. L., Oberholtzer, C. J., Tobias, J. W., & Mourelatos, Z. (2004). Microarray-Based, High-Throughput Gene Expression Profiling of microRNAs. *Nature Methods*, 1(2), 1–8. <http://doi.org/10.1038/NMETH717>
- Neutra, M. R., Mantis, N. J., & Kraehenbuhl, J. P. (2001). Collaboration of epithelial cells with organized mucosal lymphoid tissues. *Nature Immunology*, 2(11), 1004–1009. <http://doi.org/10.1038/ni1101-1004>
- Newton, K., & Dixit, V. M. (2012). Signaling in innate immunity and inflammation. *Cold Spring Harbor Perspectives in Biology*, 4(3), a006049. <http://doi.org/10.1101/cshperspect.a006049>
- Ní Eidhin, D., Ryan, A. W., Doyle, R. M., Walsh, J. B., & Kelleher, D. (2006). Sequence and Phylogenetic Analysis of the Gene for Surface Layer Protein, slpA, from 14 PCR Ribotypes of *Clostridium difficile*. *Journal of Medical Microbiology*, 55(Pt 1), 69–83. <http://doi.org/10.1099/jmm.0.46204-0>
- Niess, J. H., Brand, S., Gu, X., Landsman, L., Jung, S., McCormick, B. A., ... Reinecker, H.-C. (2005). CX3CR1-mediated dendritic cell access to the intestinal lumen and bacterial clearance. *Science*, 307(5707), 254–258. <http://doi.org/10.1126/science.1102901>
- Noutsias, M., Rohde, M., Block, A., Klippert, K., Lettau, O., Blunert, K., ... Kotsch, K. (2008). Pre-amplification techniques for real-time RT-PCR analyses of endomyocardial biopsies. *BMC Molecular Biology*, 9(DCM), 3. <http://doi.org/10.1186/1471-2199-9-3>
- O’Connell, R. M., Rao, D. S., Chaudhuri, A. a, & Baltimore, D. (2010). Physiological and pathological roles for microRNAs in the immune system. *Nature Reviews. Immunology*,

10(2), 111–122. <http://doi.org/10.1038/nri2708>

- O’Connell, R. M., Saha, S. K., Vaidya, S. A., Bruhn, K. W., Miranda, G. A., Zarnegar, B., ... Cheng, G. (2004). Type I Interferon Production Enhances Susceptibility to *Listeria monocytogenes* Infection. *The Journal of Experimental Medicine*, 200(0022-1007), 437–445. <http://doi.org/10.1084/jem.20040712>
- O’Connell, R. M., Taganov, K. D., Boldin, M. P., Cheng, G., & Baltimore, D. (2007). MicroRNA-155 is Induced During the Macrophage Inflammatory Response. *Proceedings of the National Academy of Sciences of the United States of America*, 104(5), 1604–1609. <http://doi.org/10.1073/pnas.0610731104>
- O’Neill, L. A. J. (2008). When Signaling Pathways Collide: Positive and Negative Regulation of Toll-like Receptor Signal Transduction. *Immunity*, 29(1), 12–20. <http://doi.org/10.1016/j.immuni.2008.06.004>
- O’Neill, L. A. J., & Bowie, A. G. (2007). The Family of five: TIR-Domain-Containing Adaptors in Toll-Like Receptor Signalling. *Nature Reviews. Immunology*, 7(May), 353–364. <http://doi.org/10.1038/nri2079>
- O’Neill, L. A. J., Sheedy, F. J., & McCoy, C. E. (2011). MicroRNAs: the Fine-Tuners of Toll-like Receptor Signalling. *Nature Reviews. Immunology*, 11(3), 163–175. <http://doi.org/10.1038/nri2957>
- Obermayer, B., & Levine, E. (2014). Exploring the miRNA Regulatory Network Using Evolutionary Correlations. *PLoS Computational Biology*, 10(10), e1003860. <http://doi.org/10.1371/journal.pcbi.1003860>
- Oeckinghaus, A., & Ghosh, S. (2009). The NF-kappaB family of transcription factors and its regulation. *Cold Spring Harbor Perspectives in Biology*, 1(4), 1–14. <http://doi.org/10.1101/cshperspect.a000034>
- Oglesby, I. K., McElvaney, N. G., & Greene, C. M. (2010). MicroRNAs in Inflammatory Lung Disease- Master Regulators or Target Practice? *Respiratory Research*, 11(1), 148. <http://doi.org/10.1186/1465-9921-11-148>
- Olivieri, F., Ripponi, M. R., Prattichizzo, F., Babini, L., Graciotti, L., Recchioni, R., & Procopio, A. D. (2013). Toll like receptor signaling in “inflammaging”: microRNA as new players. *Immunity & Ageing: I & A*, 10(1), 11. <http://doi.org/10.1186/1742-4933-10-11>
- Oshiumi, H., Sasai, M., Shida, K., Fujita, T., Matsumoto, M., & Seya, T. (2003). TIR-containing Adapter Molecule (TICAM)-2, a Bridging Adapter Recruiting to Toll-like Receptor 4 TICAM-1 That Induces Interferon- β . *Journal of Biological Chemistry*, 278(50), 49751–49762. <http://doi.org/10.1074/jbc.M305820200>
- Otte, J. M., Cario, E., & Podolsky, D. K. (2004). Mechanisms of Cross Hyporesponsiveness to Toll-Like Receptor Bacterial Ligands in Intestinal Epithelial Cells. *Gastroenterology*, 126(4), 1054–1070. <http://doi.org/10.1053/j.gastro.2004.01.007>
- Pahl, H. L. (1999). Activators and target genes of Rel/NF-kappaB transcription factors. *Oncogene*, 18(49), 6853–6866. <http://doi.org/10.1038/sj.onc.1203239>

- Paraskevopoulou, M. D., Georgakilas, G., Kostoulas, N., Vlachos, I. S., Vergoulis, T., Reczko, M., ... Hatzigeorgiou, A. G. (2013). DIANA-MicroT Web Server v5.0: Service Integration into miRNA Functional Analysis Workflows. *Nucleic Acids Research*, *41*(Web Server issue), W169–73. <http://doi.org/10.1093/nar/gkt393>
- Paredes-Sabja, D., Cofre-Araneda, G., Brito-Silva, C., Pizarro-Guajardo, M., & Sarker, M. R. (2012). *Clostridium difficile* spore-macrophage interactions: Spore survival. *PLoS ONE*, *7*(8). <http://doi.org/10.1371/journal.pone.0043635>
- Paredes-Sabja, D., Shen, A., & Sorg, J. A. (2014). *Clostridium difficile* spore biology: sporulation, germination, and spore structural proteins. *Trends in Microbiology*, *22*(7), 406–416. <http://doi.org/10.1016/j.tim.2014.04.003>
- Parkin, J., & Cohen, B. (2001). An overview of the immune system. *Lancet*, *357*(9270), 1777–89. [http://doi.org/10.1016/S0140-6736\(00\)04904-7](http://doi.org/10.1016/S0140-6736(00)04904-7)
- Pasquinelli, A. E., Reinhart, B. J., Slack, F., Martindale, M. Q., Kuroda, M. I., Maller, B., ... Ruvkun, G. (2000). Conservation of the Sequence and Temporal Expression of let-7 Heterochronic Regulatory RNA. *Nature*, *408*(6808), 86–89. <http://doi.org/10.1038/35040556>
- Péchiné, S., Janoir, C., & Collignon, A. (2005). Variability of *Clostridium difficile* surface proteins and specific serum antibody response in patients with *Clostridium difficile*-associated disease. *Journal of Clinical Microbiology*, *43*(10), 5018–25. <http://doi.org/10.1128/JCM.43.10.5018-5025.2005>
- Pekow, J. R., Dougherty, U., Mustafi, R., Zhu, H., Kocherginsky, M., Rubin, D. T., ... Bissonnette, M. (2012). miR-143 and miR-145 are Down-Regulated in Ulcerative Colitis: Putative Regulators of Inflammation and Protooncogenes. *Inflammatory Bowel Diseases*, *18*(1), 94–100. <http://doi.org/10.1002/ibd.21742>
- Perry, M. M., Moschos, S. A., Williams, A. E., Shepherd, N. J., Larner-Svensson, H. M., & Lindsay, M. A. (2008). Rapid Changes in MicroRNA-146a Expression Negatively Regulate the IL-1 -Induced Inflammatory Response in Human Lung Alveolar Epithelial Cells. *The Journal of Immunology*, *180*(8), 5689–5698. <http://doi.org/10.4049/jimmunol.180.8.5689>
- Peterson, L. W., & Artis, D. (2014). Intestinal epithelial cells: regulators of barrier function and immune homeostasis. *Nature Reviews. Immunology*, *14*(3), 141–53. <http://doi.org/10.1038/nri3608>
- Peterson, S. M., Thompson, J. A., Ufkin, M. L., Sathyanarayana, P., Liaw, L., & Congdon, C. B. (2014). Common features of microRNA target prediction tools. *Frontiers in Genetics*, *5*(February), 23. <http://doi.org/10.3389/fgene.2014.00023>
- Pfeifer, G., Schirmer, J., Leemhuis, J., Busch, C., Meyer, D. K., Aktories, K., & Barth, H. (2003). Cellular uptake of *Clostridium difficile* toxin B. Translocation of the N-terminal catalytic domain into the cytosol of eukaryotic cells. *Journal of Biological Chemistry*, *278*(45), 44535–44541. <http://doi.org/10.1074/jbc.M307540200>
- Pizarro-Guajardo, M., Olgún-Araneda, V., Barra-Carrasco, J., Brito-Silva, C., Sarker, M. R., & Paredes-Sabja, D. (2014). Characterization of the collagen-like exosporium protein,

- BclA1, of *Clostridium difficile* spores. *Anaerobe*, 25, 18–30. <http://doi.org/10.1016/j.anaerobe.2013.11.003>
- Pramanik, D., Campbell, N. R., Karikari, C., Chivukula, R., Kent, O. A., Mendell, J. T., & Maitra, A. (2011). Restitution of tumor suppressor microRNAs using a systemic nanovector inhibits pancreatic cancer growth in mice. *Molecular Cancer Therapeutics*, 10(8), 1470–80. <http://doi.org/10.1158/1535-7163.MCT-11-0152>
- Qi, J., Qiao, Y., Wang, P., Li, S., Zhao, W., & Gao, C. (2012). MicroRNA-210 negatively regulates LPS-induced production of proinflammatory cytokines by targeting NF- κ B1 in murine macrophages. *FEBS Letters*, 586(8), 1201–1207. <http://doi.org/10.1016/j.febslet.2012.03.011>
- Qualls, J. E., Kaplan, A. M., Rooijen, N. Van, & Cohen, D. A. (2006). Suppression of experimental colitis by intestinal mononuclear phagocytes Abstract: The contribution of innate immunity to inflammatory bowel disease (IBD) remains an area. *Journal of Leukocyte Biology*, 80, 802–815. <http://doi.org/10.1189/jlb.1205734.0741-5400/06/0080-802>
- Quinn, S. R., Mangan, N. E., Caffrey, B. E., Gantier, M. P., Williams, B. R. G., Hertzog, P. J., ... O'Neill, L. A. J. (2014). The role of Ets2 transcription factor in the induction of microrna-155 (miR-155) by lipopolysaccharide and its targeting by interleukin-10. *Journal of Biological Chemistry*, 289(7), 4316–4325. <http://doi.org/10.1074/jbc.M113.522730>
- Quinn, S. R., & O'Neill, L. A. J. (2011). A Trio of microRNAs that Control Toll-Like Receptor Signalling. *International Immunology*, 23(7), 421–5. <http://doi.org/10.1093/intimm/dxr034>
- Ramirez-Carrozzi, V. R., Braas, D., Bhatt, D. M., Cheng, C. S., Hong, C., Doty, K. R., ... Smale, S. T. (2009). A Unifying Model for the Selective Regulation of Inducible Transcription by CpG Islands and Nucleosome Remodeling. *Cell*, 138(1), 114–128. <http://doi.org/10.1016/j.cell.2009.04.020>
- Redford, P. S., Murray, P. J., & O'Garra, A. (2011). The role of IL-10 in immune regulation during M. tuberculosis infection. *Mucosal Immunology*, 4(3), 261–270. <http://doi.org/10.1038/mi.2011.7>
- Reineke, J., Tenzer, S., Rupnik, M., Koschinski, A., Hasselmayer, O., Schratzenholz, A., ... von Eichel-Streiber, C. (2007). Autocatalytic Cleavage of *Clostridium difficile* Toxin B. *Nature*, 446(7134), 415–419. <http://doi.org/10.1038/nature05622>
- Reinhart, B. J., Slack, F. J., Basson, M., Pasquinelli, A. E., Bettinger, J. C., Rougvie, A. E., ... Ruvkun, G. (2000). The 21-nucleotide let-7 RNA regulates developmental timing in *Caenorhabditis elegans*. *Nature*, 403(6772), 901–906. <http://doi.org/10.1038/35002607>
- Rescigno, M., Urbano, M., Valzasina, B., Francolini, M., Rotta, G., Bonasio, R., ... Ricciardi-Castagnoli, P. (2001). Dendritic cells express tight junction proteins and penetrate gut epithelial monolayers to sample bacteria. *Nature Immunology*, 2(4), 361–367. <http://doi.org/10.1038/86373>
- Roderburg, C., Urban, G.-W., Bettermann, K., Vucur, M., Zimmermann, H., Schmidt, S., ... Luedde, T. (2011). MicroRNA Profiling Reveals a Role for miR-29 in Human and Murine Liver fibrosis. *Hepatology*, 53(1), 209–218. <http://doi.org/10.1002/hep.23922>

- Rogler, G., Hausmann, M., Vogl, D., Aschenbrenner, E., Andus, T., Falk, W., ... Gross, V. (1998). Isolation and phenotypic characterization of colonic macrophages. *Clinical and Experimental Immunology*, 112(2), 205–215. <http://doi.org/10.1046/j.1365-2249.1998.00557.x>
- Rossato, M., Curtale, G., Tamassia, N., Castellucci, M., Mori, L., Gasperini, S., ... Bazzoni, F. (2012). IL-10-Induced microRNA-187 Negatively Regulates TNF- α , IL-6, and IL-12p40 Production in TLR4-Stimulated Monocytes. *Proceedings of the National Academy of Sciences of the United States of America*, 109(45), E3101–10. <http://doi.org/10.1073/pnas.1209100109>
- Rothwarf, D. M., Zandi, E., Natoli, G., & Karin, M. (1998). IKK-gamma is an essential regulatory subunit of the I κ B kinase complex. *Nature*, 395(6699), 297–300. <http://doi.org/10.1038/26261>
- Rupnik, M., Wilcox, M. H., & Gerding, D. N. (2009). Clostridium difficile Infection: New Developments in Epidemiology and Pathogenesis. *Nature Reviews. Microbiology*, 7, 526–536. <http://doi.org/10.1038/nrmicro2164>
- Ryan, A., Lynch, M., Smith, S. M., Amu, S., Nel, H. J., McCoy, C. E., ... Loscher, C. E. (2011). A Role for TLR4 in Clostridium difficile Infection and the Recognition of Surface Layer Proteins. *PLoS Pathogens*, 7(6), e1002076. <http://doi.org/10.1371/journal.ppat.1002076>
- Sachidanandam, R. (2005). RNAi as a bioinformatics consumer. *Briefings in Bioinformatics*, 6(2), 146–62. Retrieved from <http://www.ncbi.nlm.nih.gov/pubmed/15975224>
- Saetrom, P., Heale, B. S. E., Snove, O., Aagaard, L., Alluin, J., & Rossi, J. J. (2007). Distance Constraints Between microRNA Target Sites Dictate Efficacy and Cooperativity. *Nucleic Acids Research*, 35(7), 2333–2342. <http://doi.org/10.1093/nar/gkm133>
- Sara, M., & Sleytr, U. B. (2000). S-Layer Proteins. *Journal of Bacteriology*, 182(4), 859–868.
- Sasai, M., Oshiumi, H., Matsumoto, M., Inoue, N., Fujita, F., Nakanishi, M., & Seya, T. (2005). Cutting Edge: NF-kappaB-activating kinase-associated protein 1 participates in TLR3/Toll-IL-1 homology domain-containing adapter molecule-1-mediated IFN regulatory factor 3 activation. *Journal of Immunology*, 174(1), 27–30. <http://doi.org/10.4049/jimmunol.174.1.27>
- Sato, A., & Iwasaki, A. (2005). Peyer's patch dendritic cells as regulators of mucosal adaptive immunity. *Cellular and Molecular Life Sciences: CMLS*, 62(12), 1333–8. <http://doi.org/10.1007/s00018-005-5037-z>
- Schmittgen, T. D., Lee, E. J., Jiang, J., Sarker, A., Yang, L., Eltan, T. S., & Chen, C. (2009). Real-Time PCR Quantification of Precursor and Mature microRNA. *Methods*, 44(1), 31–38. <http://doi.org/10.1016/j.ymeth.2007.09.006>.Real-time
- Schneitz, C., Nuotio, L., & Lounatma, K. (1993). Adhesion of Lactobacillus acidophilus to avian intestinal epithelial cells mediated by the crystalline bacterial cell surface layer (S-layer). *Journal of Applied Bacteriology*, 74(3), 290–294. <http://doi.org/10.1111/j.1365-2672.1993.tb03028.x>

- Schroder, K., & Tschopp, J. (2010). The Inflammasomes. *Cell*, *140*(6), 821–832. <http://doi.org/10.1016/j.cell.2010.01.040>
- Sen, R., & Baltimore, D. (1986). Inducibility of κ immunoglobulin enhancer-binding protein NF- κ B by a posttranslational mechanism. *Cell*, *47*(6), 921–928. [http://doi.org/10.1016/0092-8674\(86\)90807-X](http://doi.org/10.1016/0092-8674(86)90807-X)
- Setoguchi, M., Nasu, N., Yoshida, S., Higuchi, Y., Akizuki, S., & Yamamoto, S. (1989). Mouse and human CD14 (myeloid cell-specific leucine-rich glycoprotein) primary structure deduced from cDNA clones. *Biochimica et Biophysica Acta (BBA) - Gene Structure and Expression*, *1008*(2), 213–222. [http://doi.org/10.1016/0167-4781\(80\)90012-3](http://doi.org/10.1016/0167-4781(80)90012-3)
- Shaked, I., Meerson, A., Wolf, Y., Avni, R., Greenberg, D., Gilboa-Geffen, A., & Soreq, H. (2009). MicroRNA-132 Potentiates Cholinergic Anti-Inflammatory Signaling by Targeting Acetylcholinesterase. *Immunity*, *31*(6), 965–973. <http://doi.org/10.1016/j.immuni.2009.09.019>
- Sharma, S., TenOever, B. R., Grandvaux, N., Zhou, G.-P., Lin, R., & Hiscott, J. (2003). Triggering the interferon antiviral response through an IKK-related pathway. *Science*, *300*(5622), 1148–1151. <http://doi.org/10.1126/science.1081315>
- Sharp, J., & Poxton, I. R. (1988). Cell Wall Proteins of Clostridium Difficile. *FEMS Microbiology Letters*, *55*(1), 99–103. <http://doi.org/10.1111/j.1574-6968.1988.tb02805.x>
- Sharpe, A. H., & Freeman, G. J. (2002). The B7-CD28 superfamily. *Nature Reviews Immunology*, *2*(2), 116–26. <http://doi.org/10.1038/nri727>
- Sheedy, F. J., Palsson-McDermott, E., Hennessy, E. J., Martin, C., O’Leary, J. J., Ruan, Q., ... O’Neill, L. A. J. (2010). Negative regulation of TLR4 via targeting of the proinflammatory tumor suppressor PDCD4 by the microRNA miR-21. *Nature Immunology*, *11*(2), 141–147. <http://doi.org/10.1038/ni.1828>
- Shifera, A. S., & Hardin, J. A. (2010). Factors modulating expression of Renilla luciferase from control plasmids used in luciferase reporter gene assays. *Analytical Biochemistry*, *396*(2), 167–172. <http://doi.org/10.1016/j.ab.2009.09.043>
- Shimazu, R., Akashi, S., Ogata, H., Nagai, Y., Fukudome, K., Miyake, K., & Kimoto, M. (1999). MD-2, a molecule that confers lipopolysaccharide responsiveness on Toll-like receptor 4. *The Journal of Experimental Medicine*, *189*(11), 1777–1782. <http://doi.org/10.1084/jem.189.11.1777>
- Smith, P. D., Smythies, L. E., Shen, R., Greenwell-Wild, T., Gliozzi, M., & Wahl, S. M. (2011). Intestinal macrophages and response to microbial encroachment. *Mucosal Immunology*, *4*(1), 31–42. <http://doi.org/10.1038/mi.2010.66>
- Solomon, K. (2013). The Host Immune Response to Clostridium difficile Infection. *Therapeutic Advances in Infectious Disease*, *1*(1), 19–35. <http://doi.org/10.1177/2049936112472173>
- Song, B., Wang, Y., Titmus, M. A., Botchkina, G., Formentini, A., Kornmann, M., & Ju, J. (2010). Molecular Mechanism of Chemoresistance by miR-215 in Osteosarcoma and Colon Cancer Cells. *Molecular Cancer*, *9*(1), 96. <http://doi.org/10.1186/1476-4598-9-96>

- Sonkoly, E., Stähle, M., & Pivarcsi, A. (2008). MicroRNAs and Immunity: Novel Players in the Regulation of Normal Immune function and Inflammation. *Seminars in Cancer Biology*, 18(2), 131–140. <http://doi.org/10.1016/j.semcancer.2008.01.005>
- Sorg, J. A., & Sonenshein, A. L. (2008). Bile salts and glycine as cogerminants for *Clostridium difficile* spores. *Journal of Bacteriology*, 190(7), 2505–2512. <http://doi.org/10.1128/JB.01765-07>
- Spigaglia, P., & Mastrantonio, P. (2002). Molecular Analysis of the Pathogenicity Locus and Polymorphism in the Putative Negative Regulator of Toxin Production (TcdC) among *Clostridium difficile* Clinical Isolates Molecular Analysis of the Pathogenicity Locus and Polymorphism in the Putative Neg. *Journal of Clinical Microbiology*, 40(9), 3470–3475. <http://doi.org/10.1128/JCM.40.9.3470>
- Staedel, C., & Darfeuille, F. (2013). MicroRNAs and bacterial infection. *Cellular Microbiology*, 15(July), 1496–1507. <http://doi.org/10.1111/cmi.12159>
- Starczynowski, D. T., Kuchenbauer, F., Argiropoulos, B., Sung, S., Morin, R., Muranyi, A., ... Karsan, A. (2010). Identification of miR-145 and miR-146a as Mediators of the 5q-Syndrome Phenotype. *Nature Medicine*, 16(1), 49–58. <http://doi.org/10.1038/nm.2054>
- Steiner, T. S., Flores, C. A., Pizarro, T. T., & Guerrant, R. L. (1997). Fecal lactoferrin, interleukin-1beta, and interleukin-8 are elevated in patients with severe *Clostridium difficile* colitis. *Clinical and Diagnostic Laboratory Immunology*, 4(6), 719–22. Retrieved from <http://www.pubmedcentral.nih.gov/articlerender.fcgi?artid=170647&tool=pmcentrez&rendertype=abstract>
- Steward, R., Zusman, S. B., Huang, L. H., & Schedl, P. (1988). The dorsal protein is distributed in a gradient in early drosophila embryos. *Cell*, 55(3), 487–495. [http://doi.org/10.1016/0092-8674\(88\)90035-9](http://doi.org/10.1016/0092-8674(88)90035-9)
- Stubbs, S. L. J., Brazier, J. S., O'Neill, G. L., & Duerden, B. I. (1999). PCR targeted to the 16S-23S rRNA gene intergenic spacer region of *Clostridium difficile* and construction of a library consisting of 116 different PCR ribotypes. *Journal of Clinical Microbiology*, 37(2), 461–463.
- Sun, W., Li, Y.-S. J., Huang, H.-D., Shyy, J. Y.-J., & Chien, S. (2010). microRNA: a master regulator of cellular processes for bioengineering systems. *Annual Review of Biomedical Engineering*, 12, 1–27. <http://doi.org/10.1146/annurev-bioeng-070909-105314>
- Sun, Y., Varambally, S., Maher, C. A., Cao, Q., Chockley, P., Toubai, T., ... Reddy, P. (2015). Targeting of microRNA-142-3p in dendritic cells regulates endotoxin induced mortality. *Blood*, 117(23), 6172–6183. <http://doi.org/10.1182/blood-2010-12-325647>
- Taganov, K. D., Boldin, M. P., Chang, K.-J., & Baltimore, D. (2006). NF-κB-Dependent Induction of microRNA miR-146, an Inhibitor Targeted to Signaling Proteins of Innate Immune Responses. *PNAS*, 103(33), 12481–12486. <http://doi.org/10.1073/pnas.0605298103>
- Takeda, K., Clausen, B. E., Kaisho, T., Tsujimura, T., Terada, N., Förster, I., & Akira, S. (1999). Enhanced Th1 activity and development of chronic enterocolitis in mice devoid of

stat3 in macrophages and neutrophils. *Immunity*, 10(1), 39–49. [http://doi.org/10.1016/S1074-7613\(00\)80005-9](http://doi.org/10.1016/S1074-7613(00)80005-9)

- Takeshita, F., Patrawala, L., Osaki, M., Takahashi, R. U., Yamamoto, Y., Kosaka, N., ... Ochiya, T. (2010). Systemic delivery of synthetic microRNA-16 inhibits the growth of metastatic prostate tumors via downregulation of multiple cell-cycle genes. *Mol Ther*, 18(1), 181–187. <http://doi.org/10.1038/mt.2009.207>
- Takeuchi, O., Hoshino, K., Kawai, T., Sanjo, H., Takada, H., Ogawa, T., ... Akira, S. (1999). Differential roles of TLR2 and TLR4 in recognition of gram-negative and gram-positive bacterial cell wall components. *Immunity*, 11(4), 443–451. [http://doi.org/10.1016/S1074-7613\(00\)80119-3](http://doi.org/10.1016/S1074-7613(00)80119-3)
- Tang, B., Xiao, B., Liu, Z., Li, N., Zhu, E.-D., Li, B.-S., ... Mao, X.-H. (2010). Identification of MyD88 as a novel target of miR-155, involved in negative regulation of Helicobacter pylori-induced inflammation. *FEBS Letters*, 584(8), 1481–6. <http://doi.org/10.1016/j.febslet.2010.02.063>
- Tarang, S., & Weston, M. D. (2014). Macros in microRNA Target Identification: A comparative Analysis of in silico, in vitro, and in vivo Approaches to microRNA Target Identification. *RNA Biology*, 11(4), 324–333. <http://doi.org/10.4161/rna.28649>
- Tasteyre, A., Barc, M. C., Collignon, A., Boureau, H., & Karjalainen, T. (2001). Role of FliC and FliD flagellar proteins of Clostridium difficile in adherence and gut colonization. *Infection and Immunity*, 69(12), 7937–7940. <http://doi.org/10.1128/IAI.69.12.7937-7940.2001>
- Technologies, L. (2011). *mirVana™ miRNA Isolation Kit* (1560M Rev.). California, USA.: Life Technologies.
- Technologies, L. (2013). *Protocol for Running Custom RT and Preamplification Pools on Custom TaqMan® Array MicroRNA Cards* (Vol. 2013).
- Tili, E., Michaille, J.-J., Cimino, A., Costinean, S., Dumitru, C. D., Adair, B., ... Croce, C. M. (2007). Modulation of miR-155 and miR-125b Levels following Lipopolysaccharide/TNF-Stimulation and Their Possible Roles in Regulating the Response to Endotoxin Shock. *The Journal of Immunology*, 179(8), 5082–5089. <http://doi.org/10.4049/jimmunol.179.8.5082>
- Tsang, J., Zhu, J., & Oudenaarden, A. Van. (2007). MicroRNA-Mediated Feedback and Feedforward Loops Are Recurrent Network Motifs in Mammals. *Molecular Cell*, (26), 753–767. <http://doi.org/10.1016/j.molcel.2007.05.018>
- Tserel, L., Runnel, T., Kisand, K., Pihlap, M., Bakhoff, L., Kolde, R., ... Rebane, A. (2011). MicroRNA expression profiles of human blood monocyte-derived dendritic cells and macrophages reveal miR-511 as putative positive regulator of Toll-like receptor 4. *The Journal of Biological Chemistry*, 286(30), 26487–95. <http://doi.org/10.1074/jbc.M110.213561>
- Underdown, B. J., & Schiff, J. M. (1986). Immunoglobulin A: Strategic Defense Initiative at the Mucosal Surface. *Annual Review of Immunology*, 4(1), 389–417. <http://doi.org/10.1146/annurev.immunol.4.1.389>

- Ungefroren, H., Groth, S., Sebens, S., Lehnert, H., Gieseler, F., & Fändrich, F. (2011). Differential roles of Smad2 and Smad3 in the regulation of TGF- β 1-mediated growth inhibition and cell migration in pancreatic ductal adenocarcinoma cells: control by Rac1. *Molecular Cancer*, *10*(1), 67. <http://doi.org/10.1186/1476-4598-10-67>
- van Rooij, E. (2011). The Art of MicroRNA Research. *Circulation Research*, *108*(2), 219–234. <http://doi.org/10.1161/CIRCRESAHA.110.227496>
- van Rooij, E., & Kauppinen, S. (2014a). Development of microRNA therapeutics is coming of age. *EMBO Molecular Medicine*, *6*(7), 851–64. <http://doi.org/10.15252/emmm.201100899>
- van Rooij, E., & Kauppinen, S. (2014b). Development of microRNA therapeutics is coming of age. *EMBO Molecular Medicine*, *6*(7), 851–64. <http://doi.org/10.15252/emmm.201100899>
- Vidigal, J. a., & Ventura, A. (2014). The biological functions of miRNAs: lessons from in vivo studies. *Trends in Cell Biology*, *25*(3), 137–147. <http://doi.org/10.1016/j.tcb.2014.11.004>
- Virtue, A., Wang, H., & Yang, X. (2012). MicroRNAs and Toll-Like Receptor/Interleukin-1 Receptor Signaling. *Journal of Hematology & Oncology*, *5*(1), 66. <http://doi.org/10.1186/1756-8722-5-66>
- Viswanathan, V. K., Sharma, R., & Hecht, G. (2004). Microbes and their Products- Physiological Effects upon Mammalian Mucosa. *Advanced Drug Delivery Reviews*, *56*(6), 727–762. <http://doi.org/10.1016/j.addr.2003.09.005>
- Vlachos, I. S., Kostoulas, N., Vergoulis, T., Georgakilas, G., Reczko, M., Maragkakis, M., ... Hatzigeorgiou, A. G. (2012). DIANA miRPath v.2.0: investigating the combinatorial effect of microRNAs in pathways. *Nucleic Acids Research*, *40*(Web Server issue), W498–504. <http://doi.org/10.1093/nar/gks494>
- Vohra, P., & Poxton, I. R. (2012). Induction of Cytokines in a Macrophage Cell Line by Proteins of *Clostridium difficile*. *FEMS Immunology and Medical Microbiology*, *65*(1), 96–104. <http://doi.org/10.1111/j.1574-695X.2012.00952.x>
- von Eichel-Streiber, C., Boquet, P., Sauerborn, M., & Thelestam, M. (1996). Large clostridial cytotoxins--a family of glycosyltransferases modifying small GTP-binding proteins. *Trends in Microbiology*, *4*(10), 375–82. [http://doi.org/10.1016/0966-842X\(96\)10061-5](http://doi.org/10.1016/0966-842X(96)10061-5)
- Voth, D., & Ballard, J. (2005). *Clostridium difficile* toxins: mechanism of action and role in disease. *Clinical Microbiology Reviews*, *18*(2), 247–263. <http://doi.org/10.1128/CMR.18.2.247>
- Waligora, A. J., Hennequin, C., Mullany, P., & Bourlioux, P. (2001). Characterization of a Cell Surface Protein of *Clostridium difficile* with Adhesive Properties. *Infection and Immunity*, *69*(4), 2144–2153. <http://doi.org/10.1128/IAI.69.4.2144>
- Wang, C., Deng, L., Hong, M., Akkaraju, G. R., Inoue, J., & Chen, Z. J. (2001). TAK1 is a ubiquitin-dependent kinase of MKK and IKK. *Nature*, *412*(6844), 346–51. <http://doi.org/10.1038/35085597>
- Wang, P., Gu, Y., Zhang, Q., Han, Y., Hou, J., Lin, L., ... Cao, X. (2012). Identification of

- resting and type I IFN-activated human NK cell miRNomes reveals microRNA-378 and microRNA-30e as negative regulators of NK cell cytotoxicity. *Journal of Immunology*, 189(1), 211–21. <http://doi.org/10.4049/jimmunol.1200609>
- Wang, P., Hou, J., Lin, L., Wang, C., Liu, X., Li, D., ... Cao, X. (2010). Inducible microRNA-155 Feedback Promotes Type I IFN Signaling in Antiviral Innate Immunity by Targeting Suppressor of Cytokine Signaling 1. *The Journal of Immunology*, 185(10), 6226–6233. <http://doi.org/10.4049/jimmunol.1000491>
- Wark, A. W., Lee, H. J., & Corn, R. M. (2008). Multiplexed Detection Methods for Profiling MicroRNA Expression in Biological Samples. *Angewandte Chemie International Edition*, 47(4), 644–652. <http://doi.org/10.1002/anie.200702450>
- Warny, M., Pepin, J., Fang, A., Killgore, G., Thompson, A., Brazier, J., ... McDonald, L. C. (2005). Toxin Production by an Emerging Strain of *Clostridium difficile* Associated with Outbreaks of Severe Disease in North America and Europe. *Lancet*, 366, 1079–1084. [http://doi.org/10.1016/S0140-6736\(05\)67420-X](http://doi.org/10.1016/S0140-6736(05)67420-X)
- Wei, J., Huang, X., Zhang, Z., Jia, W., Zhao, Z., Zhang, Y., ... Xu, G. (2013). MyD88 as a Target of microRNA-203 in Regulation of Lipopolysaccharide or Bacille Calmette-Guerin Induced Inflammatory Response of Macrophage RAW264.7 cells. *Molecular Immunology*, 55(3-4), 303–309. <http://doi.org/10.1016/j.molimm.2013.03.004>
- Wendlandt, E. B., Graff, J. W., Gioannini, T. L., McCaffrey, A. P., & Wilson, M. E. (2012). The Role of MicroRNAs miR-200b and miR-200c in TLR4 Signaling and NF- κ B Activation. *Innate Immunity*, 18(6), 846–855. <http://doi.org/10.1177/1753425912443903>
- Werner, F., Jain, M. K., Feinberg, M. W., Sibinga, N. E. S., Pellacani, A., Wiesel, P., ... Lee, M. (2000). Transforming growth factor(TGF)-Beta1 inhibition of macrophage activation is mediated via Smad3. *J. Biol. Chem.*, 275(47), M004536200. <http://doi.org/10.1074/jbc.M004536200>
- Wesche, H., Henzel, W. J., Shillinglaw, W., Li, S., & Cao, Z. (1997). MyD88: An adapter that recruits IRAK to the IL-1 receptor complex. *Immunity*, 7(6), 837–847. [http://doi.org/10.1016/S1074-7613\(00\)80402-1](http://doi.org/10.1016/S1074-7613(00)80402-1)
- Wheeldon, L. J., Worthington, T., & Lambert, P. A. (2011). Histidine acts as a co-germinant with glycine and taurocholate for *Clostridium difficile* spores. *Journal of Applied Microbiology*, 110(4), 987–994. <http://doi.org/10.1111/j.1365-2672.2011.04953.x>
- Whiteside, S. T., & Israel, A. (1997). I κ B proteins : structure , function and regulation. *Seminars in Cancer Biology*, 8, 75–82.
- Wightman, B., Ha, I., & Ruvkun, G. (1993). Posttranscriptional regulation of the heterochronic gene lin-14 by lin-4 mediates temporal pattern formation in *C. elegans*. *Cell*, 75(5), 855–862. [http://doi.org/10.1016/0092-8674\(93\)90530-4](http://doi.org/10.1016/0092-8674(93)90530-4)
- Williams, L. M., Ricchetti, G., Sarma, U., Smallie, T., & Foxwell, B. M. J. (2004). Interleukin-10 suppression of myeloid cell activation - A continuing puzzle. *Immunology*, 113(3), 281–292. <http://doi.org/10.1111/j.1365-2567.2004.01988.x>
- Witwer, K. W., Sisk, J. M., Gama, L., & Clements, J. E. (2010). MicroRNA regulation of IFN-

beta protein expression: rapid and sensitive modulation of the innate immune response. *Journal of Immunology*, 184(5), 2369–76. <http://doi.org/10.4049/jimmunol.0902712>

- Worm, J., Stenvang, J., Petri, A., Frederiksen, K. S., Obad, S., Elmén, J., ... Kauppinen, S. (2009). Silencing of microRNA-155 in mice during acute inflammatory response leads to derepression of c/ebp Beta and down-regulation of G-CSF. *Nucleic Acids Research*, 37(17), 5784–5792. <http://doi.org/10.1093/nar/gkp577>
- Wozniak, M. A., Modzelewska, K., Kwong, L., & Keely, P. J. (2004). Focal Adhesion Regulation of Cell Behavior. *Biochimica et Biophysica Acta*, 1692(2-3), 103–119. <http://doi.org/10.1016/j.bbamcr.2004.04.007>
- Wright, S. D., Ramos, R. A., Tobias, P. S., Ulevitch, R. J., & Mathison, J. C. (1990). CD14, a receptor for complexes of lipopolysaccharide (LPS) and LPS binding protein. *Science*, 249(4975), 1431–3. <http://doi.org/10.1126/science.1698311>
- Wu, H., Neilson, J. R., Kumar, P., Manocha, M., Shankar, P., Sharp, P. A., & Manjunath, N. (2007). miRNA Profiling of Naïve, Effector and Memory CD8 T Cells. *PLoS One*, 2(10), e1020. <http://doi.org/10.1371/journal.pone.0001020>
- Xavier, M. N., Winter, M. G., Spees, A. M., Nguyen, K., Atluri, V. L., Silva, T. M. A., ... Tsolis, R. M. (2013). CD4+ T Cell-derived IL-10 Promotes *Brucella abortus* Persistence via Modulation of Macrophage Function. *PLoS Pathogens*, 9(6). <http://doi.org/10.1371/journal.ppat.1003454>
- Xiao, B., Liu, Z., Li, B.-S., Tang, B., Li, W., Guo, G., ... Zou, Q. (2009). Induction of microRNA-155 during *Helicobacter pylori* infection and its negative regulatory role in the inflammatory response. *The Journal of Infectious Diseases*, 200(6), 916–25. <http://doi.org/10.1086/605443>
- Xie, Y.-F., Shu, R., Jiang, S.-Y., Liu, D.-L., Ni, J., & Zhang, X.-L. (2013). MicroRNA-146 Inhibits Pro-inflammatory Cytokine Secretion Through IL-1 Receptor-Associated Kinase 1 in Human Gingival Fibroblasts. *Journal of Inflammation*, 10(1), 20. <http://doi.org/10.1186/1476-9255-10-20>
- Xu, G., Zhang, Z., Xing, Y., Wei, J., Ge, Z., Liu, X., ... Huang, X. (2014). MicroRNA-149 negatively regulates TLR-triggered inflammatory response in macrophages by targeting MyD88. *Journal of Cellular Biochemistry*, 115(5), 919–27. <http://doi.org/10.1002/jcb.24734>
- Xu, Z., Xiao, S. B., Xu, P., Xie, Q., Cao, L., Wang, D., ... Fang, L. R. (2011). miR-365, a novel negative regulator of interleukin-6 gene expression, is cooperatively regulated by Sp1 and NF- κ B. *Journal of Biological Chemistry*, 286(24), 21401–21412. <http://doi.org/10.1074/jbc.M110.198630>
- Yakob, L., Riley, T. V, Paterson, D. L., Marquess, J., Magalhaes, R. J. S., Furuya-Kanamori, L., & Clements, A. C. A. (2015). Mechanisms of hypervirulent *Clostridium difficile* ribotype 027 displacement of endemic strains: an epidemiological model. *Scientific Reports*, 5(November 2014), 1–9. <http://doi.org/10.1038/srep12666>
- Yamamoto, M., Sato, S., Hemmi, H., Hoshino, K., Kaisho, T., Sanjo, H., ... Akira, S. (2003). Role of Adaptor TRIF in the MyD88-Independent Toll-Like Receptor Signaling Pathway.

Science, 301, 640–642.

- Yamamoto, M., Sato, S., Hemmi, H., Sanjo, H., Uematsu, S., Tsuneyasu, K., ... Shizuo, A. (2002). Essential Role for TIRAP in Activation of the Signalling Cascade Shared by TLR2 and TLR4. *Letters to Nature*, 420(November), 324–328. <http://doi.org/10.1038/nature01190.1>.
- Yang, H., Jansen, A. P., Komar, A. a, Zheng, X., Merrick, W. C., Costes, S., ... Lockett, S. J. (2003). The Transformation Suppressor Pdc4 Is a Novel Eukaryotic Translation Initiation Factor 4A Binding Protein That Inhibits Translation The Transformation Suppressor Pdc4 Is a Novel Eukaryotic Translation Initiation Factor 4A Binding Protein That Inhibits T. *Society*, 23(1), 26–37. <http://doi.org/10.1128/MCB.23.1.26>
- Yang, K., He, Y. S., Wang, X. Q., Lu, L., Chen, Q. J., Liu, J., ... Shen, W. F. (2011). MiR-146a inhibits oxidized low-density lipoprotein-induced lipid accumulation and inflammatory response via targeting toll-like receptor 4. *FEBS Letters*, 585(6), 854–60. <http://doi.org/10.1016/j.febslet.2011.02.009>
- Yao, X., Huang, J., Zhong, H., Shen, N., Faggioni, R., Fung, M., & Yao, Y. (2014). Targeting interleukin-6 in inflammatory autoimmune diseases and cancers. *Pharmacology & Therapeutics*, 141(2), 125–39. <http://doi.org/10.1016/j.pharmthera.2013.09.004>
- Yates, L. A., Norbury, C. J., & Gilbert, R. J. C. (2013). The long and short of microRNA. *Cell*, 153(3), 516–519. <http://doi.org/10.1016/j.cell.2013.04.003>
- Yi, R., Qin, Y., Macara, I. G., & Cullen, B. R. (2003). Exportin-5 mediates the nuclear export of pre-microRNAs and short hairpin RNAs. *Genes & Development*, 17(24), 3011–6. <http://doi.org/10.1101/gad.1158803>
- Yoshimura, A., Naka, T., & Kubo, M. (2007). SOCS Proteins, Cytokine Signalling and Immune Regulation. *Nature Reviews. Immunology*, 7(6), 454–465. <http://doi.org/10.1038/nri2093>
- Ysebrant de Lendonck, L., Martinet, V., & Goriely, S. (2014). Interferon regulatory factor 3 in adaptive immune responses. *Cellular and Molecular Life Sciences : CMLS, (Imi)*, 3873–3883. <http://doi.org/10.1007/s00018-014-1653-9>
- Zanoni, I., Ostuni, R., Marek, L. R., Barresi, S., Barbalat, R., Barton, G. M., ... Kagan, J. C. (2011). CD14 Controls the LPS-Induced Endocytosis of Toll-like Receptor 4. *Cell*, 147, 868–880. <http://doi.org/10.1016/j.cell.2011.09.051>
- Zapala, L., Drela, N., Bil, J., Nowis, D., Basak, G. W., & Lasek, W. (2011). Optimization of Activation Requirements of Immature Mouse Dendritic JAWSII cells for in vivo Application. *Oncology Reports*, 25(3), 831–840. <http://doi.org/10.3892/or.2010.1128>
- Zhang, H., Kolb, F. A., Jaskiewicz, L., Westhof, E., & Filipowicz, W. (2004). Single processing center models for human Dicer and bacterial RNase III. *Cell*, 118(1), 57–68. <http://doi.org/10.1016/j.cell.2004.06.017>
- Zhang, M., Liu, Q., Mi, S., Liang, X., Zhang, Z., Su, X., ... Yang, R. (2011). Both miR-17-5p and miR-20a alleviate suppressive potential of myeloid-derived suppressor cells by modulating STAT3 expression. *Journal of Immunology*, 186(8), 4716–4724. <http://doi.org/10.4049/jimmunol.1002989>

- Zhang, Z., Clarke, T. B., & Weiser, J. N. (2009). Cellular effectors mediating Th17-dependent clearance of pneumococcal colonization in mice. *Journal of Clinical Investigation*, *119*(7), 1899–1909. <http://doi.org/10.1172/JCI36731>
- Zhou, H., Huang, X., Cui, H., Luo, X., Tang, Y., Chen, S., ... Shen, N. (2010). miR-155 and its Star-Form Partner miR-155* Cooperatively Regulate Type I Interferon Production by Human Plasmacytoid Dendritic Cells. *Blood*, *116*(26), 5885–5894. <http://doi.org/10.1182/blood-2010-04-280156>
- Zhou, R., O'Hara, S. P., & Chen, X.-M. (2011). MicroRNA regulation of innate immune responses in epithelial cells. *Cellular & Molecular Immunology*, *8*(5), 371–379. <http://doi.org/10.1038/cmi.2011.19>
- Zhu, J., Yamane, H., & Paul, W. E. (2010). Differentiation of effector CD4 T cell populations. *Annual Review of Immunology*, *28*, 445–489. <http://doi.org/10.1146/annurev-immunol-030409-101212>

Appendices

Appendix A- Buffers and Solutions

5X Loading Buffer

Bromophenol Blue	0.05% (w/v)
DTT	0.25 M
SDS	2%
Glycerol	10%
Trizma Base	125 mM

The solution was dissolved in dH₂O to the required volume. 250 µl 1 M DTT was added per 1 mL 5X loading buffer just before use. 3µl was added to 12 µl of each sample for SDS PAGE analysis.

Separating Gel (12% (w/v))

Acrylamide/ Bisacrylamide (30% stock)	12.5%
Tris HCL pH 6.8	1.5 M
SDS	1%
Ammonium persulphate	0.5% (w/v)
TEMED	0.1% (v/v)

The solution was dissolved in dH₂O to the required volume. Ammonium persulphate and TEMED were added last. The gel was covered with Isopropanol to exclude air and aid polymerisation.

Stacking Gel (5% (w/v))

Acrylamide/ Bisacrylamide (30% stock)	5%
Tris HCL pH 8.8	0.5 M
SDS	1%
Ammonium persulphate	0.5% (w/v)
TEMED	0.1% (v/v)

The solution was dissolved in dH₂O to the required volume. Ammonium persulphate and TEMED were added last.

Electrode Running Buffer

Trizma Base	25 mM
Glycine	200 nM
SDS	17 mM

The solution was dissolved in dH₂O to the required volume.

Coomassie Stain

Brilliant Blue	0.2%
Methanol	45%
Acetic Acid	10%

The solution was dissolved in dH₂O to the required volume.

Destain solution

Methanol	25%
Acetic Acid	10%

The solution was dissolved in dH₂O to the required volume.

Complete RPMI Culture Media

Heat inactivated FBS	10%
Penicillin/Streptomycin/L-glutamine	100 µg/mL/ 100 µg/mL/ 2 nM

Complete DMEM Culture Media

Heat inactivated FBS	10%
Penicillin/Streptomycin/L-glutamine	100 µg/mL/ 100 µg/mL/ 2 nM

10 µg/mL Blasticidin was added to maintain the hTLR4a and 50 µg/mL HygroGold were added to maintain the plasmid coding for MD2 and CD14 during Hek TLR4/MD2/CD14 cell culture.

Complete α -MEM Culture Media

Non-heat inactivated FBS	10%
Penicillin/Streptomycin/L-glutamine	100 μ g/mL/ 100 μ g/mL/ 2 nM
Gentamycin	50 μ g/mL
rGMCSF	5 ng/mL

DuoSet ELISA Kits

hIL-8	DY208
hRANTES	DY278
IL-12p28	DY1834
MCP-1	DY479
mIL-10	DY417
mIL-12p40	DY404
mIL-12p70	DY419
mIL-1 β	DY401
mIL-23	DY1887
mIL-6	DY406
MIP-2	DY452
mRANTES	DY478
mTNF α	DY410

10X Phosphate Buffered Saline (PBS)

Na ₂ HPO ₄ .2H ₂ O	8 mM
KH ₂ PO ₄	1.5 mM
NaCL	137 mM
KCL	2.7 mM

The solution was dissolved in dH₂O to the required volume and the pH was adjusted to pH 7.4.

10X Tris buffered Saline (TBS)

NaCL	1.5 M
Trizma Base	0.2 M

The solution was dissolved in dH₂O to the required volume and the pH was adjusted to pH 7.6.

FACS Buffer

FBS	2%
NaN ₃	0.05%
EDTA	0.5 M

The solution was dissolved in PBS and filtered through a 0.2 µM filter before use.

MiRNA mimics

MC12601	mirVana™ miRNA mimic hsa-miR-155
MC10722	mirVana™ miRNA mimic hsa-miR-146a
MC12304	mirVana™ miRNA mimic hsa-let-7e
MC11480	mirVana™ miRNA mimic hsa-miR-145
4464058	mirVana™ miRNA mimic Negative Control #1
4465062	mirVana™ miRNA mimic miR-1 Positive Control

1X Luciferase Lysis buffer

Luciferase cell culture lysis reagent	20%
Sigma water	80%

100 µl 1X solution was added to each well to lyse the cells for luciferase assay analysis.

50X TAE Buffer

Trizma Base	40 mM
Glacial Acetic Acid	20 mM

EDTA 1 mM

The solution was dissolved in dH₂O to the required volume and the pH was adjusted to pH 8.5.

Luciferase Assay Mixture

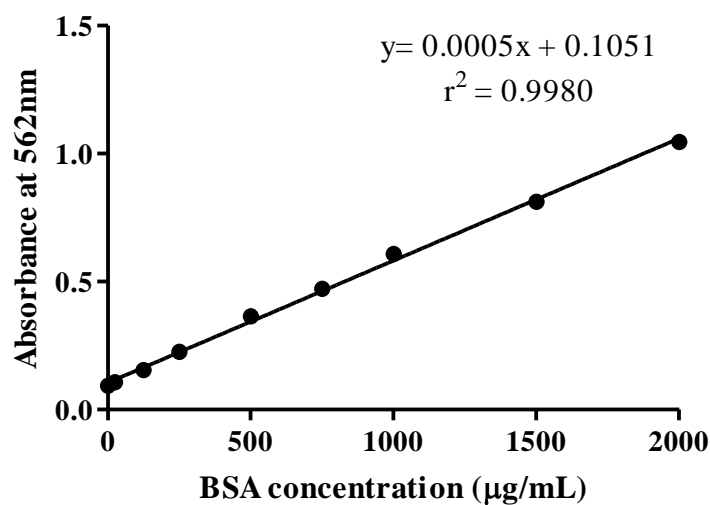
Tricine	0.2 M
MgSO ₄ .7H ₂ O	2.67 mM
EDTA	0.1 mM
DTT	33.3 mM
ATP	530 μM
Acetyl Co Enzyme A	270 μM
D-Luciferin	30 mg
NaOH	2 M
((MgCO ₃) ₄ Mg(OH) ₂ .5H ₂ O	50 mM

The solution was dissolved in dH₂O to the required volume. The NaOH and Magnesium Carbonate Hydroxide pentahydrate were added last and kept in the dark thereafter. The solution was aliquoted and kept in the -20°C. The solution was thawed to room temperature before use and 40 μl was added per well to measure luciferase activity.

Appendix B- SLP Characterisation

A)

BCA Standard curve



B)

<u>C. difficile</u> Ribotype	<u>SLP Concentration</u> µg/mL
RT 001	3335
RT 005	883.2
RT 014	2456
RT 027	2100
RT 031	848
RT 078	7234

Figure B.1 The protein concentration of each of the SLPs was measured using the **BCA assay**. A Bicinchoninic acid (BCA) assay was performed to determine protein concentrations for each of the SLPs used in this project. **A)** Standard curve were the standard concentration was plotted against absorbance at 562 nm. Graph includes the equation of the line and the r^2 value **B)** Protein concentration of each of the SLPs in µg/mL. 20 µg/mL was used to stimulate cells for each experiment.

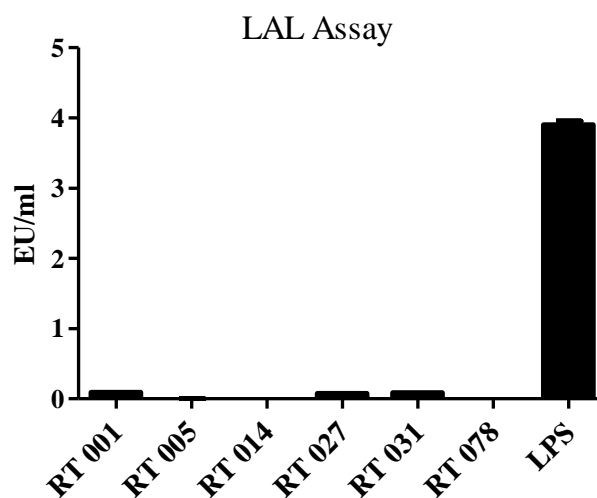


Figure B.2. Endotoxin activity was not detected in samples of purified SLPs. Endotoxin activity was measured in purified SLPs and LPS using the ToxinSensor™ ChromogeniLAL Endotoxin Assay Kit according to manufacturer's specifications. Endotoxin activity was detected in LPS which was used as a positive control. Therefore any immune response was due to the SLPs and not due to contamination from other bacterial sources.

Appendix C- Plasmid DNA Constructs

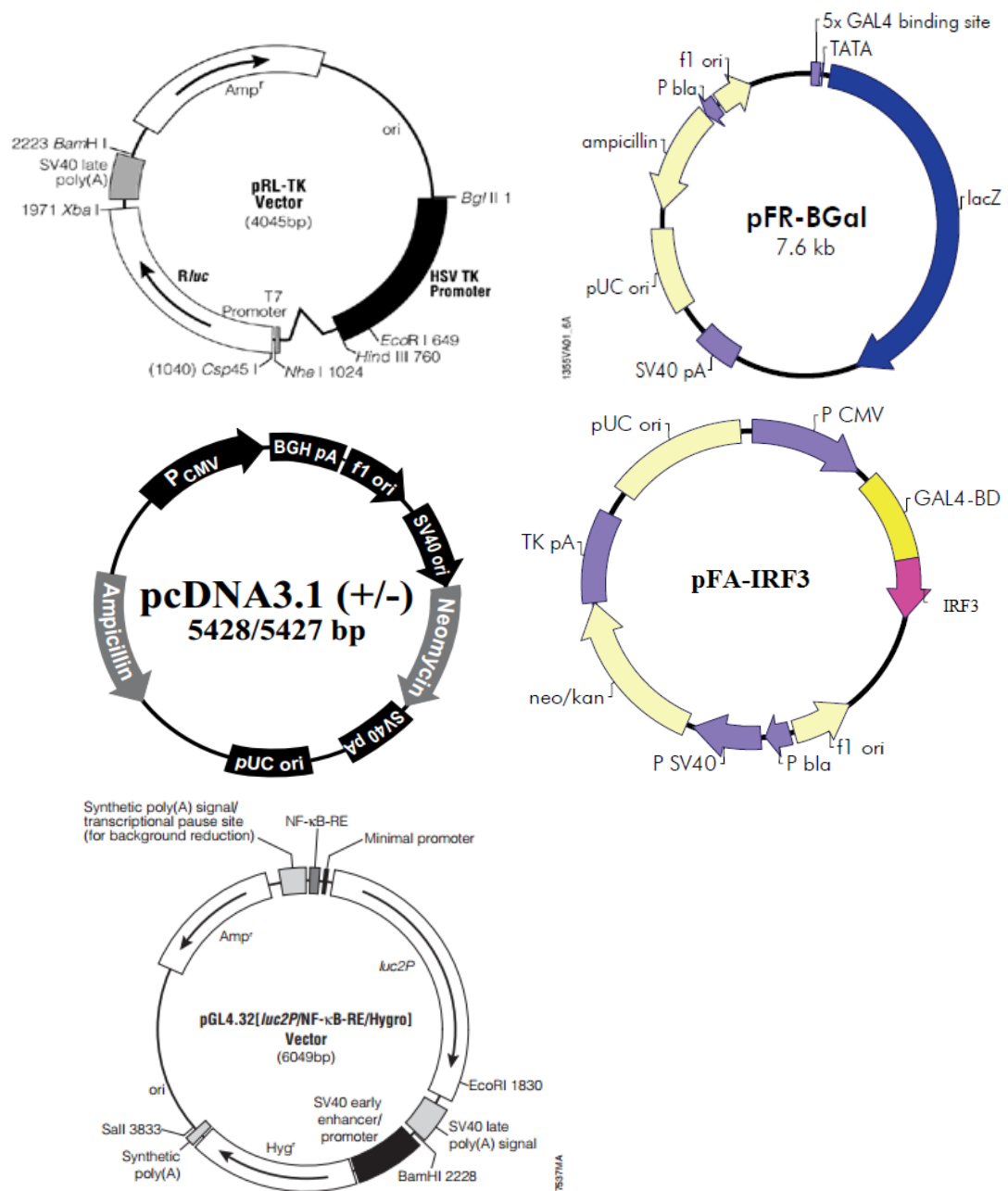


Figure C.1 pRL-TK, pFR, pcDNA3.1, pFA-IRF3 and NF-κB construct maps. Expression vectors used in the generation of plasmid DNA for transient transfections. Chemically competent DH5α *E. coli* transformed with NF-κB, pFA-IRF3, pFR and pRL-TK renilla ligated DNA were a gift from Prof. Paul Moynagh, The Institute of Immunology, National University of Ireland Maynooth, Maynooth, Co. Kildare.

Appendix D- RNA Quality Assurance

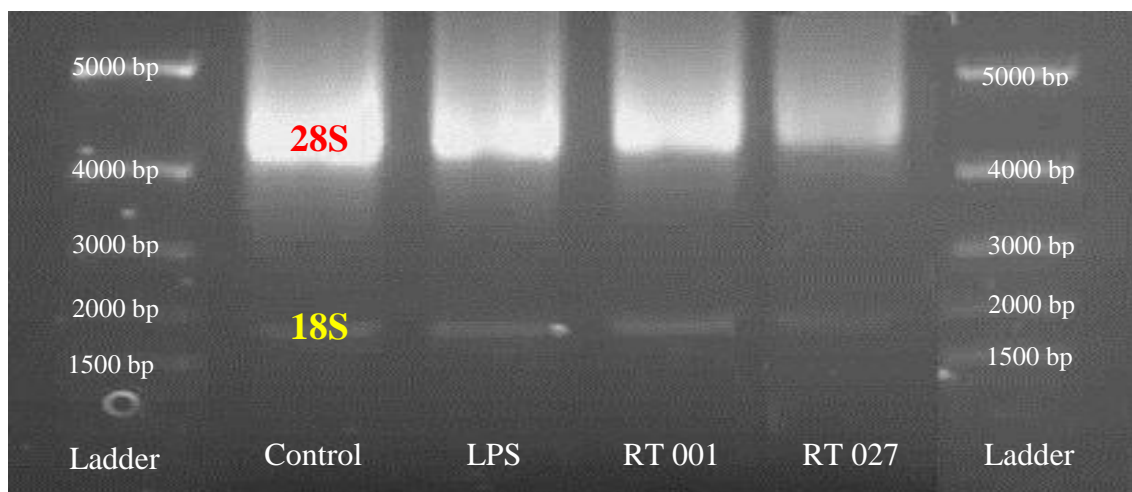


Figure D.1 RNA Isolation product analysis by gel Electrophoresis. After each RNA isolation, 1 μ g RNA from each sample was mixed with RNA loading buffer and loaded on 1% agarose gel along with GeneRuler 1 kb plus ladder. The gel was run for 45 minutes at 150 volts and visualised using the G-box imaging system. The 28S:18S ribosomal RNA (rRNA) bands were assessed for integrity.

Appendix E- Taqman Assays

	1	2	3	4	5	6	7	8	9	10	11	12	13	14	15	16	17	18	19	20	21	22	23	24	
A	hsa-let-7a	hsa-let-7c	hsa-let-7d	hsa-let-7e	hsa-let-7f	hsa-let-7g	hsa-miR-1	hsa-miR-9	hsa-miR-10a	hsa-miR-10b	U6 snRNA	U6 snRNA	hsa-miR-15a	hsa-miR-15b	hsa-miR-16	hsa-miR-17	hsa-miR-18a	hsa-miR-18b	hsa-miR-19a	hsa-miR-19b	hsa-miR-20a	hsa-miR-20b	hsa-miR-21	hsa-miR-22	
B	hsa-miR-23a	hsa-miR-23b	hsa-miR-24	hsa-miR-25	hsa-miR-26a	hsa-miR-26b	hsa-miR-27a	hsa-miR-27b	hsa-miR-28-3p	hsa-miR-28	U6 snRNA	U6 snRNA	hsa-miR-29a	hsa-miR-29b	hsa-miR-29c	hsa-miR-30b	hsa-miR-30c	hsa-miR-31	hsa-miR-32	hsa-miR-33b	hsa-miR-34a	hsa-miR-34c	hsa-miR-92a	mmu-miR-93	
C	hsa-miR-95	mmu-miR-95	hsa-miR-95	hsa-miR-99a	hsa-miR-99b	hsa-miR-100	hsa-miR-101	hsa-miR-103	hsa-miR-105	hsa-miR-106a	RNU 44	hsa-miR-106b	hsa-miR-107	hsa-miR-122	hsa-miR-124a	hsa-miR-125a	hsa-miR-125b	hsa-miR-125b	hsa-miR-126	hsa-miR-127	hsa-miR-127-5p	hsa-miR-128a	mmu-miR-129-3p	hsa-miR-129	
D	hsa-miR-130a	hsa-miR-130b	hsa-miR-132	hsa-miR-133a	hsa-miR-133b	mmu-miR-134	hsa-miR-135a	hsa-miR-135b	hsa-miR-136	mmu-miR-137	hsa-miR-138	hsa-miR-139-3p	hsa-miR-139-5p	hsa-miR-140-3p	hsa-miR-141	hsa-miR-142-3p	hsa-miR-142-5p	hsa-miR-143	hsa-miR-144	hsa-miR-145	hsa-miR-146a	hsa-miR-146b-3p	hsa-miR-146b	hsa-miR-147b	
E	hsa-miR-148a	hsa-miR-148b	hsa-miR-149	hsa-miR-150	hsa-miR-152	hsa-miR-153	hsa-miR-154	hsa-miR-181a	hsa-miR-181c	hsa-miR-182	RNU 48	hsa-miR-183	hsa-miR-184	hsa-miR-185	hsa-miR-186	hsa-miR-187	hsa-miR-188-3p	hsa-miR-190	hsa-miR-191	hsa-miR-192	hsa-miR-193a-3p	hsa-miR-193a	hsa-miR-193b	hsa-miR-194	
F	hsa-miR-195	hsa-miR-195b	hsa-miR-197	hsa-miR-198	hsa-miR-199a	hsa-miR-199a-3p	hsa-miR-199b	hsa-miR-200a	hsa-miR-200b	hsa-miR-200c	hsa-miR-202	hsa-miR-203	hsa-miR-204	hsa-miR-205	hsa-miR-208b	hsa-miR-210	hsa-miR-214	hsa-miR-215	hsa-miR-216a	hsa-miR-216b	hsa-miR-217	hsa-miR-218	hsa-miR-219	hsa-miR-221	
G	hsa-miR-222	hsa-miR-223	hsa-miR-224	hsa-miR-296-3p	hsa-miR-296	hsa-miR-299-3p	hsa-miR-299-5p	hsa-miR-301	hsa-miR-301b	hsa-miR-302a	ath-miR159a	hsa-miR-302b	hsa-miR-302c	hsa-miR-320	hsa-miR-323-3p	hsa-miR-324-3p	hsa-miR-324-5p	hsa-miR-326	hsa-miR-328	hsa-miR-328	hsa-miR-329	hsa-miR-330	hsa-miR-330-5p	hsa-miR-331	hsa-miR-331-5p
H	hsa-miR-335	hsa-miR-337-5p	hsa-miR-338-3p	hsa-miR-339-3p	hsa-miR-339-5p	hsa-miR-340	hsa-miR-342-5p	hsa-miR-342-3p	hsa-miR-342-5p	hsa-miR-345	hsa-miR-361	hsa-miR-362-3p	hsa-miR-362	hsa-miR-363	hsa-miR-365	hsa-miR-367	hsa-miR-369-3p	hsa-miR-369-5p	hsa-miR-370	hsa-miR-371-3p	hsa-miR-372	hsa-miR-373	hsa-miR-374	hsa-miR-450b	hsa-miR-450a-3p
I	mmu-miR-374-5p	hsa-miR-375	hsa-miR-376a	hsa-miR-376b	hsa-miR-377	mmu-miR-379	hsa-miR-380-3p	hsa-miR-381	hsa-miR-382	hsa-miR-383	hsa-miR-409-5p	hsa-miR-410	hsa-miR-411	hsa-miR-422a	hsa-miR-423-5p	hsa-miR-424	hsa-miR-425-5p	hsa-miR-429	hsa-miR-431	hsa-miR-433	hsa-miR-449	hsa-miR-449b	hsa-miR-450a	hsa-miR-450a-3p	
J	hsa-miR-450b-5p	mmu-miR-451	hsa-miR-452	hsa-miR-453	hsa-miR-454	hsa-miR-455-3p	hsa-miR-455-5p	hsa-miR-483-5p	hsa-miR-484	hsa-miR-485-3p	hsa-miR-485-5p	hsa-miR-486-3p	hsa-miR-486	hsa-miR-487a	hsa-miR-487b	hsa-miR-488	hsa-miR-489	hsa-miR-490	hsa-miR-491-3p	mmu-miR-491	hsa-miR-493	hsa-miR-494	hsa-miR-495	mmu-miR-496	
K	hsa-miR-499-3p	mmu-miR-499	hsa-miR-500	hsa-miR-501-3p	hsa-miR-501	hsa-miR-502-3p	hsa-miR-502	hsa-miR-603	hsa-miR-504	hsa-miR-505	hsa-miR-507	hsa-miR-508	hsa-miR-508-5p	hsa-miR-509-5p	hsa-miR-510	hsa-miR-512-3p	hsa-miR-512-5p	hsa-miR-513-5p	hsa-miR-515-3p	hsa-miR-515-5p	hsa-miR-516a-5p	hsa-miR-516a	hsa-miR-516b	hsa-miR-517a	hsa-miR-517c
L	hsa-miR-518a	hsa-miR-518a-5p	hsa-miR-518b	hsa-miR-518c	hsa-miR-518d	hsa-miR-518d-5p	hsa-miR-518e	hsa-miR-518f	hsa-miR-519a	hsa-miR-519d	hsa-miR-519e	hsa-miR-520a	hsa-miR-520a	hsa-miR-520d-5p	hsa-miR-520g	hsa-miR-521	hsa-miR-522	hsa-miR-523	hsa-miR-524-5p	hsa-miR-525-3p	hsa-miR-525	hsa-miR-526b	hsa-miR-532-3p	hsa-miR-532	
M	hsa-miR-539	hsa-miR-541	hsa-miR-542-3p	hsa-miR-542-5p	hsa-miR-544	hsa-miR-545	hsa-miR-548a	hsa-miR-548a-5p	hsa-miR-548b	hsa-miR-548c-5p	hsa-miR-548c	hsa-miR-548d	hsa-miR-548d-5p	hsa-miR-551b	hsa-miR-556-3p	hsa-miR-556-5p	hsa-miR-561	hsa-miR-570	hsa-miR-574-3p	hsa-miR-574-5p	hsa-miR-576-3p	hsa-miR-576-5p	hsa-miR-579	hsa-miR-582-3p	
N	hsa-miR-582-5p	hsa-miR-589	hsa-miR-590-5p	hsa-miR-597	hsa-miR-598	mmu-miR-615	hsa-miR-615-5p	hsa-miR-616	hsa-miR-618	hsa-miR-624	hsa-miR-625	hsa-miR-627	hsa-miR-628-5p	hsa-miR-629	hsa-miR-636	hsa-miR-642	hsa-miR-651	hsa-miR-652	hsa-miR-653	hsa-miR-654-3p	hsa-miR-654	hsa-miR-655	hsa-miR-660	hsa-miR-671-3p	
O	hsa-miR-672	hsa-miR-674	hsa-miR-708	hsa-miR-744	hsa-miR-758	hsa-miR-871	hsa-miR-872	hsa-miR-873	hsa-miR-874	hsa-miR-875-3p	hsa-miR-876-3p	hsa-miR-876-5p	hsa-miR-885-3p	hsa-miR-885-5p	hsa-miR-886-3p	hsa-miR-886-5p	hsa-miR-887	hsa-miR-888	hsa-miR-889	hsa-miR-890	hsa-miR-891a	hsa-miR-891b	hsa-miR-892a	hsa-miR-147	
P	hsa-miR-208	hsa-miR-211	hsa-miR-212	hsa-miR-219-1-3p	hsa-miR-219-2-3p	hsa-miR-220	hsa-miR-220b	hsa-miR-220c	hsa-miR-298	hsa-miR-325	hsa-miR-346	hsa-miR-376c	hsa-miR-384	hsa-miR-412	hsa-miR-448	hsa-miR-492	hsa-miR-506	hsa-miR-509-3-5p	hsa-miR-511	hsa-miR-517b	hsa-miR-519c	hsa-miR-520b	hsa-miR-520e	hsa-miR-520f	

Figure E.1 Map of miRNA assays on TLDA Pool A v2 cards. Location of the 384 miRNA assays on TLDA pool A v2 cards. Each card was pre loaded with 0.5 µl 20X Taqman microRNA Assays.

Table E.1 miRNA target sequence and assay position on pool A TLDA cards.

Location, assay ID, assay name and target sequence of each of the 20X Taqman microRNA assays on the pool A v2 TLDA cards used in this study

Well location	Assay ID	Assay Name	Target Sequence 5' → 3'
A1	000377	hsa-let-7a	UGAGGUAGUAGGUUGUAUAGUU
A2	000379	hsa-let-7c	UGAGGUAGUAGGUUGUAUGGUU
A3	002283	hsa-let-7d	AGAGGUAGUAGGUUGCAUAGUU
A4	002406	hsa-let-7e	UGAGGUAGGAGGUUGUAUAGUU
A5	000382	hsa-let-7f	UGAGGUAGUAGAUUGUAUAGUU
A6	002282	hsa-let-7g	UGAGGUAGUAGUUUGUACAGUU
A7	002222	hsa-miR-1	UGGAAUGUAAAGAAGUAUGUAU
A8	000583	hsa-miR-9	UCUUUGGUUAUCUAGCUGUAUGA
A9	000387	hsa-miR-10a	UACCCUGUAGAUCCGAAUUUGUG
A10	002218	hsa-miR-10b	UACCCUGUAGAACCGAAUUUGUG
A11	001973	U6 snRNA	GTGCTCGCTTCGGCAGCACATATAC TAAAATTGGAACGATACAGAGAAGA TTAGCATGGCCCCTGCGCAAGGATG ACACGCAAATTCGTGAAGCGTTCCA TATTTT
A12	001973	U6 snRNA	GTGCTCGCTTCGGCAGCACATATAC TAAAATTGGAACGATACAGAGAAGA TTAGCATGGCCCCTGCGCAAGGATG ACACGCAAATTCGTGAAGCGTTCCA TATTTT
A13	000389	hsa-miR-15a	UAGCAGCACAUAAUGGUUUGUG
A14	000390	hsa-miR-15b	UAGCAGCACAUCAUGGUUACA
A15	000391	hsa-miR-16	UAGCAGCACGUAAAUAUUGGCG
A16	002308	hsa-miR-17	CAAAGUGCUUACAGUGCAGGUAG
A17	002422	hsa-miR-18a	UAAGGUGCAUCUAGUGCAGAUAG
A18	002217	hsa-miR-18b	UAAGGUGCAUCUAGUGCAGUUAG
A19	000395	hsa-miR-19a	UGUGCAAUUCUAUGCAAACUGA
A20	000396	hsa-miR-19b	UGUGCAAUCCAUGCAAACUGA
A21	000580	hsa-miR-20a	UAAAGUGCUUAUAGUGCAGGUAG
A22	001014	hsa-miR-20b	CAAAGUGCUCAUAGUGCAGGUAG
A23	000397	hsa-miR-21	UAGCUUAUCAGACUGAUGUUGA
A24	000398	hsa-miR-22	AAGCUGCCAGUUGAAGAACUGU
B1	000399	hsa-miR-23a	AUCACAUUGCCAGGGAUUUC
B2	000400	hsa-miR-23b	AUCACAUUGCCAGGGAUUACC
B3	000402	hsa-miR-24	UGGCUCAGUUCAGCAGGAACAG
B4	000403	hsa-miR-25	CAUUGCACUUGUCUCGGUCUGA
B5	000405	hsa-miR-26a	UUCAAGUAAUCCAGGAUAGGCU
B6	000407	hsa-miR-26b	UUCAAGUAAUCCAGGAUAGGU
B7	000408	hsa-miR-27a	UUCACAGUGGCUAAGUCCGC
B8	000409	hsa-miR-27b	UUCACAGUGGCUAAGUUCUGC
B9	002446	hsa-miR-28-3p	CACUAGAUUGUGAGCUCCUGGA
B10	000411	hsa-miR-28	AAGGAGCUCACAGUCUAUUGAG
B11	001973	U6 snRNA	GTGCTCGCTTCGGCAGCACATATAC TAAAATTGGAACGATACAGAGAAGA

			TTAGCATGGCCCCTGCGCAAGGATG ACACGCAAATTCGTGAAGCGTTCCA TATTTT
B12	001973	U6 snRNA	GTGCTCGCTTCGGCAGCACATATAC TAAAATTGGAACGATACAGAGAAGA TTAGCATGGCCCCTGCGCAAGGATG ACACGCAAATTCGTGAAGCGTTCCA TATTTT
B13	002112	hsa-miR-29a	UAGCACCAUCUGAAAUCGGUUA
B14	000413	hsa-miR-29b	UAGCACCAUUUGAAAUCAGUGUU
B15	000587	hsa-miR-29c	UAGCACCAUUUGAAAUCGGUUA
B16	000602	hsa-miR-30b	UGUAAACAUCUACACUCAGCU
B17	000419	hsa-miR-30c	UGUAAACAUCUACACUCUCAGC
B18	002279	hsa-miR-31	AGGCAAGAUGCUGGCAUAGCU
B19	002109	hsa-miR-32	UAUUGCACAUUACUAAGUUGCA
B20	002085	hsa-miR-33b	GUGCAUUGCUGUUGCAUUGC
B21	000426	hsa-miR-34a	UGGCAGUGUCUAGCUGGUUGU
B22	000428	hsa-miR-34c	AGGCAGUGUAGUUAGCUGAUUGC
B23	000431	hsa-miR-92a	UAUUGCACUUGUCCCGGCCUGU
B24	001090	mmu-miR-93	CAAAGUGCUGUUCGUGCAGGUAG
C1	000433	hsa-miR-95	UUCAACGGGUUUUUUAGGCA
C2	000186	mmu-miR-96	UUUGGCACUAGCACAUUUUUGCU
C3	000577	hsa-miR-98	UGAGGUAGUAAGUUGUAUUGUU
C4	000435	hsa-miR-99a	AACCCGUAGAUCCGAUCUUGUG
C5	000436	hsa-miR-99b	CACCCGUAGAACCGACCUUGCG
C6	000437	hsa-miR-100	AACCCGUAGAUCCGAACUUGUG
C7	002253	hsa-miR-101	UACAGUACUGUGAUACUGAA
C8	000439	hsa-miR-103	AGCAGCAUUGUACAGGGCUAUGA
C9	002167	hsa-miR-105	UCAAUUGCUCAGACUCCUGUGGU
C10	002169	hsa-miR-106a	AAAAGUGCUCUACAGUGCAGGUAG
C11	001094	RNU44	CCUGGAUGAUGAUAGCAAUUGCUG ACUGAACAUAGAAGGUCUAAUUG CUCUAACUGACU
C12	000442	hsa-miR-106b	UAAAGUGCUGACAGUGCAGAU
C13	000443	hsa-miR-107	AGCAGCAUUGUACAGGGCUAUGA
C14	002245	hsa-miR-122	UGGAGUGUGACAAUGGUGUUUG
C15	001182	mmu-miR-124a	UAAGGCACGCGGUGAAUGCC
C16	002199	hsa-miR-125a-3p	ACAGGUGAGGUUCUUGGGAGCC
C17	002198	hsa-miR-125a-5p	UCCCUGAGACCCUUUAACCUGUGA
C18	000449	hsa-miR-125b	UCCCUGAGACCCUAACUUGUGA
C19	002228	hsa-miR-126	UCGUACCGUGAGUAAUAAUGCG
C20	000452	hsa-miR-127	UCGGAUCCGUCUGAGCUUGGCU
C21	002229	hsa-miR-127-5p	CUGAAGCUCAGAGGGCUCUGAU
C22	002216	hsa-miR-128a	UCACAGUGAACCGGUCUCUUU
C23	001184	mmu-miR-129-3p	AAGCCCUUACCCCAAAAAGCAU
C24	000590	hsa-miR-129	CUUUUUGCGGUCUGGGCUUGC
D1	000454	hsa-miR-130a	CAGUGCAAUGUAAAAGGGCAU
D2	000456	hsa-miR-130b	CAGUGCAAUGAUGAAAGGGCAU
D3	000457	hsa-miR-132	UACAGUCUACAGCCAUGGUCG
D4	002246	hsa-miR-133a	UUUGGUCCCUUCAACCAGCUG
D5	002247	hsa-miR-133b	UUUGGUCCCUUCAACCAGCUA
D6	001186	mmu-miR-134	UGUGACUGGUUGACCAGAGGGG

D7	000460	hsa-miR-135a	UAUGGCUUUUUAUUCCUAUGUGA
D8	002261	hsa-miR-135b	UAUGGCUUUUCAUUCCUAUGUGA
D9	000592	hsa-miR-136	ACUCCAUUUGUUUUGAUGAUGGA
D10	001129	mmu-miR-137	UUAUUGCUUAAGAAUACGCGUAG
D11	002284	hsa-miR-138	AGCUGGUGUUGUGAAUCAGGCCG
D12	002313	hsa-miR-139-3p	GGAGACGCGGCCUGUUGGAGU
D13	002289	hsa-miR-139-5p	UCUACAGUGCACGUGUCUCCAG
D14	002234	hsa-miR-140-3p	UACCACAGGGUAGAACCACGG
D15	001187	mmu-miR-140	CAGUGGUUUUACCCUAUGGUAG
D16	000463	hsa-miR-141	UACACUGUCUGGUAAGAUGG
D17	000464	hsa-miR-142-3p	UGUAGUGUUCCUACUUUAUGGA
D18	002248	hsa-miR-142-5p	CAUAAAGUAGAAAGCACUACU
D19	002249	hsa-miR-143	UGAGAUGAAGCACUGUAGCUC
D20	002278	hsa-miR-145	GUCCAGUUUCCAGGAAUCCCU
D21	000468	hsa-miR-146a	UGAGAACUGAAUCCAUGGGUU
D22	002361	hsa-miR-146b-3p	UGCCUGUGGACUCAGUUCUGG
D23	001097	hsa-miR-146b	UGAGAACUGAAUCCAUGGGCU
D24	002262	hsa-miR-147b	GUGUGCGGAAUUGCUUCUGCUA
E1	000470	hsa-miR-148a	UCAGUGCACUACAGAACUUUGU
E2	000471	hsa-miR-148b	UCAGUGCAUCACAGAACUUUGU
E3	002255	hsa-miR-149	UCUGGCUCCGUGUCUUCACUCCC
E4	000473	hsa-miR-150	UCUCCCAACCCUUGUACCAGUG
E5	000475	hsa-miR-152	UCAGUGCAUGACAGAACUUGG
E6	001191	mmu-miR-153	UUGCAUAGUCACAAAAGUGAUC
E7	000477	hsa-miR-154	UAGGUUAUCCGUGUUGCCUUCG
E8	000480	hsa-miR-181a	AACAUUCAACGCUGUCGGUGAGU
E9	000482	hsa-miR-181c	AACAUUCAACCGUCGGUGAGU
E10	002334	hsa-miR-182	UUUGGCAAUGGUAGAACUCACACU
E11	001006	RNU48	GAUGACCCCAGGUAACUCUGAGUG UGUCGCUGAUGCCAUCACCGCAGC GCUCUGACC
E12	002269	hsa-miR-183	UAUGGCACUGGUAGAAUUCACU
E13	000485	hsa-miR-184	UGGACGGAGAACUGAUAAAGGGU
E14	002271	hsa-miR-185	UGGAGAGAAAGGCAGUUCUGA
E15	002285	hsa-miR-186	CAAAGAAUUCUCCUUUUGGGCU
E16	001193	mmu-miR-187	UCGUGUCUUGUGUUGCAGCCGG
E17	002106	hsa-miR-188-3p	CUCCACAUGCAGGGUUUGCA
E18	000489	hsa-miR-190	UGAU AUGUUUGAUUAUUAGGU
E19	002299	hsa-miR-191	CAACGGAAUCCCAAAGCAGCUG
E20	000491	hsa-miR-192	CUGACCUAUGAAUUGACAGCC
E21	002250	hsa-miR-193a-3p	AACUGGCCUACAAAGUCCCAGU
E22	002281	hsa-miR-193a-5p	UGGGUCUUUGCGGGCGAGAUGA
E23	002367	hsa-miR-193b	AACUGGCCUCAAAGUCCCGCU
E24	000493	hsa-miR-194	UGU AACAGCAACUCCAUGUGGA
F1	000494	hsa-miR-195	UAGCAGCACAGAAUAUUGGC
F2	002215	hsa-miR-196b	UAGGUAGUUCCUGUUGUUGGG
F3	000497	hsa-miR-197	UUCACCACCUUCUCCACCCAGC
F4	002273	hsa-miR-198	GGUCCAGAGGGGAGAUAGGUUC
F5	000498	hsa-miR-199a	CCCAGUGUUCAGACUACCUGUUC
F6	002304	hsa-miR-199a-3p	ACAGUAGUCUGCACAUUGGUUA
F7	000500	hsa-miR-199b	CCCAGUGUUUAGACUAUCUGUUC
F8	000502	hsa-miR-200a	UACACUGUCUGGUAACGAUGU

F9	002251	hsa-miR-200b	UAAUACUGCCUGGUAUAUGAUGA
F10	002300	hsa-miR-200c	UAAUACUGCCGGGUAUAUGAUGGA
F11	002363	hsa-miR-202	AGAGGUAUAGGGCAUGGGAA
F12	000507	hsa-miR-203	GUGAAAUGUUUAGGACCACUAG
F13	000508	hsa-miR-204	UUCCCUUUGUCAUCCUAUGCCU
F14	000509	hsa-miR-205	UCCUUCAUUCCACCGGAGUCUG
F15	002290	hsa-miR-208b	AUAAGACGAACAAAAGGUUUGU
F16	000512	hsa-miR-210	CUGUGCGUGUGACAGCGGCUGA
F17	002306	hsa-miR-214	ACAGCAGGCACAGACAGGCAGU
F18	000518	hsa-miR-215	AUGACCUAUGAAUUGACAGAC
F19	002220	hsa-miR-216a	UAAUCUCAGCUGGCAACUGUGA
F20	002326	hsa-miR-216b	AAAUCUCUGCAGGCAAUGUGA
F21	002337	hsa-miR-217	UACUGCAUCAGGAACUGAUUGGA
F22	000521	hsa-miR-218	UUGUGCUUGAUCUAACCAUGU
F23	000522	hsa-miR-219	UGAUUGUCCAAACGCAAUUCU
F24	000524	hsa-miR-221	AGCUACAUUGUCUGCUGGGUUC
G1	002276	hsa-miR-222	AGCUACAUCUGGCUACUGGGU
G2	002295	hsa-miR-223	UGUCAGUUUGUCAAAUACCCCA
G3	002099	hsa-miR-224	CAAGUCACUAGUGGUUCCGUU
G4	002101	hsa-miR-296-3p	GAGGGUUGGGUGGAGGCUCUCC
G5	000527	hsa-miR-296	AGGGCCCCCCCUCAAUCCUGU
G6	001015	hsa-miR-299-3p	UAUGUGGGAUGGUAACCGCUU
G7	000600	hsa-miR-299-5p	UGGUUUACCGUCCACAUAACA
G8	000528	hsa-miR-301	CAGUGCAAUAGUAUUGUCAAAGC
G9	002392	hsa-miR-301b	CAGUGCAAUGAUUUGUCAAAGC
G10	000529	hsa-miR-302a	UAAGUGCUCCAUGUUUUGGUGA
G11	000338	ath-miR159a	UUUGGAUUGAAGGGAGCUCUA
G12	000531	hsa-miR-302b	UAAGUGCUCCAUGUUUAGUAG
G13	000533	hsa-miR-302c	UAAGUGCUCCAUGUUUCAGUGG
G14	002277	hsa-miR-320	AAAAGCUGGGUUGAGAGGGCGA
G15	002227	hsa-miR-323-3p	CACAUACACGGUCGACCUCU
G16	002161	hsa-miR-324-3p	ACUGCCCCAGGUGCUGCUGG
G17	000539	hsa-miR-324-5p	CGCAUCCCCUAGGGCAUUGGGUGU
G18	000542	hsa-miR-326	CCUCUGGGCCCUUCCUCCAG
G19	000543	hsa-miR-328	CUGGCCUCUCUGCCUUCGGU
G20	001101	hsa-miR-329	AACACACCGGUUAACCUCUUU
G21	000544	hsa-miR-330	GCAAAGCACACGGCCUGCAGAGA
G22	002230	hsa-miR-330-5p	UCUCUGGGCCUGUGUCUUAGGC
G23	000545	hsa-miR-331	GCCCCUGGGCCUAUCCUAGAA
G24	002233	hsa-miR-331-5p	CUAGGUAUGGUCCAGGGAUCC
H1	000546	hsa-miR-335	UCAAGAGCAAUAACGAAAAAUGU
H2	002156	hsa-miR-337-5p	GAACGGCUUCAUACAGGAGUU
H3	002252	hsa-miR-338-3p	UCCAGCAUCAGUGAUUUUGUUG
H4	002184	hsa-miR-339-3p	UGAGCGCCUCGACGACAGAGCCG
H5	002257	hsa-miR-339-5p	UCCUGUCCUCCAGGAGCUCACG
H6	002258	hsa-miR-340	UUAUAAAGCAAUGAGACUGAUU
H7	002623	hsa-miR-155	UAAUAGCUAAUCGUGAUAGGGGU
H8	002619	hsa-let-7b	UGAGGUAGUAGGUUGUGUGGUU
H9	002260	hsa-miR-342-3p	UCUCACACAGAAAUCGCACCCGU
H10	002147	hsa-miR-342-5p	AGGGGUGCUAUCUGUGAUUGA
H11	002186	hsa-miR-345	GCUGACUCCUAGUCCAGGGCUC
H12	000554	hsa-miR-361	UUAUCAGAAUCUCCAGGGGUAC

H13	002117	hsa-miR-362-3p	AACACACCUAUUCAAGGAUUCA
H14	001273	hsa-miR-362	AAUCCUUGGAACCUAGGUGUGAGU
H15	001271	hsa-miR-363	AAUUGCACGGUAUCCAUCUGUA
H16	001020	hsa-miR-365	UAAUGCCCCUAAAAUCCUUAU
H17	000555	hsa-miR-367	AAUUGCACUUUAGCAAUGGUGA
H18	000557	hsa-miR-369-3p	AAUAAUACAUGGUUGAUCUUU
H19	001021	hsa-miR-369-5p	AGAUCGACCGUGUUUAUUAUCGC
H20	002275	hsa-miR-370	GCCUGCUGGGGUGGAACCUUGU
H21	002124	hsa-miR-371-3p	AAGUGCCGCCAUCUUUUGAGUGU
H22	000560	hsa-miR-372	AAAGUGCUGCGACAUUUGAGCGU
H23	000561	hsa-miR-373	GAAGUGCUCGAUUUUGGGGUGU
H24	000563	hsa-miR-374	UUAUAAUACAACCUGAUAAAGUG
I1	001319	mmu-miR-374-5p	AUAUAAUACAACCUGCUAAGUG
I2	000564	hsa-miR-375	UUUGUUCGUUCGGCUCGCGUGA
I3	000565	hsa-miR-376a	AUCAUAGAGGAAAAUCCACGU
I4	001102	hsa-miR-376b	AUCAUAGAGGAAAAUCCAUGUU
I5	000566	hsa-miR-377	AUCACACAAAGGCAACUUUUGU
I6	001138	mmu-miR-379	UGGUAGACUAUGGAACGUAGG
I7	000569	hsa-miR-380-3p	UAUGUAAU AUGGUCCACAUCUU
I8	000571	hsa-miR-381	UAUACAAGGGCAAGCUCUCUGU
I9	000572	hsa-miR-382	GAAGUUGUUCGUGGUGGAUUCG
I10	000573	hsa-miR-383	AGAUCAGAAGGUGAUUGUGGCU
I11	002331	hsa-miR-409-5p	AGGUUACCCGAGCAACUUUGCAU
I12	001274	hsa-miR-410	AAUAUAACACAGAUGGCCUGU
I13	001610	hsa-miR-411	UAGUAGACCGUAUAGCGUACG
I14	002297	hsa-miR-422a	ACUGGACUUAGGGUCAGAAGGC
I15	002340	hsa-miR-423-5p	UGAGGGGCAGAGAGCGAGACUUU
I16	000604	hsa-miR-424	CAGCAGCAAUUCAUGUUUUGAA
I17	001516	hsa-miR-425-5p	AAUGACACGAUCACUCCCGUUGA
I18	001024	hsa-miR-429	UAAUACUGUCUGGUAAAACCGU
I19	001979	hsa-miR-431	UGUCUUGCAGGCCGUAUGCA
I20	001028	hsa-miR-433	AUCAUGAUGGGCUCUCCUGGUGU
I21	001030	hsa-miR-449	UGGCAGUGUAUUGUUAGCUGGU
I22	001608	hsa-miR-449b	AGGCAGUGUAUUGUUAGCUGGC
I23	002303	hsa-miR-450a	UUUUGCGAUGUGUCCUAAUAU
I24	002208	hsa-miR-450b-3p	UUGGGAUCAUUUUGCAUCCAUA
J1	002207	hsa-miR-450b-5p	UUUUGCAAUAUGUCCUGAAUA
J2	001141	mmu-miR-451	AAACCGUUACCAUACUGAGUU
J3	002329	hsa-miR-452	AACUGUUUGCAGAGGAAACUGA
J4	002318	hsa-miR-453	AGGUUGUCCGUGGUGAGUUCGCA
J5	002323	hsa-miR-454	UAGUGCAAUAUUGCUUAUAGGGU
J6	002244	hsa-miR-455-3p	GCAGUCCAUGGGCAUAUACAC
J7	001280	hsa-miR-455	UAUGUGCCUUUGGACUACAUCG
J8	002338	hsa-miR-483-5p	AAGACGGGAGGAAAGAAGGGAG
J9	001821	hsa-miR-484	UCAGGCUCAGUCCCUCCCGAU
J10	001277	hsa-miR-485-3p	GUCAUACACGGCUCUCCUCUCU
J11	001036	hsa-miR-485-5p	AGAGGCUGGCCGUGAUGAAUUC
J12	002093	hsa-miR-486-3p	CGGGGCAGCUCAGUACAGGAU
J13	001278	hsa-miR-486	UCCUGUACUGAGCUGCCCCGAG
J14	001279	hsa-miR-487a	AAUCAUACAGGGACAUCAGUU
J15	001285	hsa-miR-487b	AAUCGUACAGGGUCAUCCACUU
J16	002357	hsa-miR-488	UUGAAAGGCUAUUUCUUGGUC

J17	002358	hsa-miR-489	GUGACAUCACAUAUACGGCAGC
J18	001037	hsa-miR-490	CAACCUGGAGGACUCCAUGCUG
J19	002360	hsa-miR-491-3p	CUUAUGCAAGAUUCCCUUCUAC
J20	001630	mmu-miR-491	AGUGGGGAACCCUCCAUGAGG
J21	002364	hsa-miR-493	UGAAGGUCUACUGUGGCCAGG
J22	002365	hsa-miR-494	UGAAACAUAACACGGGAAACCUC
J23	001663	mmu-miR-495	AAACAAACAUGGUGCACUUCUU
J24	001953	mmu-miR-496	UGAGUAUUACAUGGCCAAUCUC
K1	002427	hsa-miR-499-3p	AACAUCACAGCAAGUCUGUGCU
K2	001352	mmu-miR-499	UUAAGACUUGCAGUGAUGUUU
K3	002428	hsa-miR-500	UAAUCCUUGCACCUGGGUGAGA
K4	002435	hsa-miR-501-3p	AAUGCACCCGGGCAAGGAUUCU
K5	001047	hsa-miR-501	AAUCCUUUGUCCUGGGUGAGA
K6	002083	hsa-miR-502-3p	AAUGCACCUGGGCAAGGAUUCA
K7	001109	hsa-miR-502	AUCCUUGCUAUCUGGGUGCUA
K8	001048	hsa-miR-503	UAGCAGCGGGAACAGUUCUGCAG
K9	002084	hsa-miR-504	AGACCCUGGUCUGCACUCUAUC
K10	002089	hsa-miR-505	CGUCAACACUUGCUGGUUCCU
K11	001051	hsa-miR-507	UUUUGCACCUUUUGGAGUGAA
K12	001052	hsa-miR-508	UGAUUGUAGCCUUUUGGAGUAGA
K13	002092	hsa-miR-508-5p	UACUCCAGAGGGCGUCACUCAUG
K14	002235	hsa-miR-509-5p	UACUGCAGACAGUGGCAAUCA
K15	002241	hsa-miR-510	UACUCAGGAGAGUGGCAAUCAC
K16	001823	hsa-miR-512-3p	AAGUGCUGUCAUAGCUGAGGUC
K17	001145	hsa-miR-512-5p	CACUCAGCCUUGAGGGCACUUUC
K18	002090	hsa-miR-513-5p	UUCACAGGGAGGUGUCAU
K19	002369	hsa-miR-515-3p	GAGUGCCUUCUUUUGGAGCGUU
K20	001112	hsa-miR-515-5p	UUCUCCAAAAGAAAGCACUUUCUG
K21	002416	hsa-miR-516a-5p	UUCUCGAGGAAAGAAGCACUUUC
K22	001150	hsa-miR-516b	AUCUGGAGGUAAGAAGCACUUU
K23	002402	hsa-miR-517a	AUCGUGCAUCCCUUUAGAGUGU
K24	001153	hsa-miR-517c	AUCGUGCAUCCUUUUAGAGUGU
L1	002397	hsa-miR-518a-3p	GAAAGCGCUUCCCUUUGCUGGA
L2	002396	hsa-miR-518a-5p	CUGCAAAGGGAAGCCCUUUC
L3	001156	hsa-miR-518b	CAAAGCGCUCCCCUUUAGAGGU
L4	002401	hsa-miR-518c	CAAAGCGCUUCUCUUUAGAGUGU
L5	001159	hsa-miR-518d	CAAAGCGCUUCCCUUUGGAGC
L6	002389	hsa-miR-518d-5p	CUCUAGAGGGAAGCACUUUCUG
L7	002395	hsa-miR-518e	AAAGCGCUUCCCUUCAGAGUG
L8	002388	hsa-miR-518f	GAAAGCGCUUCUCUUUAGAGG
L9	002415	hsa-miR-519a	AAAGUGCAUCCUUUUAGAGUGU
L10	002403	hsa-miR-519d	CAAAGUGCCUCCCUUUAGAGUG
L11	002370	hsa-miR-519e	AAGUGCCUCCUUUUAGAGUGUU
L12	001167	hsa-miR-520a	AAAGUGCUUCCCUUUGGACUGU
L13	001168	hsa-miR-520a#	CUCCAGAGGGAAGUACUUUCU
L14	002393	hsa-miR-520d-5p	CUACAAAGGGAAGCCCUUUC
L15	001121	hsa-miR-520g	ACAAAGUGCUUCCCUUUAGAGUGU
L16	001122	hsa-miR-521	AACGCACUUCCCUUUAGAGUGU
L17	002413	hsa-miR-522	AAA AUGGUUCCCUUUAGAGUGU
L18	002386	hsa-miR-523	GAACGCGCUUCCCUAUAGAGGGU
L19	001982	hsa-miR-524-5p	CUACAAAGGGAAGCACUUUCUC
L20	002385	hsa-miR-525-3p	GAAGGCGCUUCCCUUUAGAGCG

L21	001174	hsa-miR-525	CUCCAGAGGGAUGCACUUUCU
L22	002382	hsa-miR-526b	CUCUUGAGGGAAGCACUUUCUGU
L23	002355	hsa-miR-532-3p	CCUCCCACACCCAAGGCUUGCA
L24	001518	hsa-miR-532	CAUGCCUUGAGUGUAGGACCGU
M1	001286	hsa-miR-539	GGAGAAAUAUCCUUGGUGUGU
M2	002201	hsa-miR-541	UGGUGGGCACAGAAUCUGGACU
M3	001284	hsa-miR-542-3p	UGUGACAGAUUGAUAACUGAAA
M4	002240	hsa-miR-542-5p	UCGGGGAUCAUCAUGUCACGAGA
M5	002265	hsa-miR-544	AUUCUGCAUUUUUAGCAAGUUC
M6	002267	hsa-miR-545	UCAGCAAACAUAUAUUGUGUGC
M7	001538	hsa-miR-548a	CAAACUGGGCAAUACUUUUGC
M8	002412	hsa-miR-548a-5p	AAAAGUAAUUGCGAGUUUACC
M9	001541	hsa-miR-548b	CAAGAACCUCAGUUGCUUUUGU
M10	002408	hsa-miR-548b-5p	AAAAGUAAUUGUGGUUUUGGCC
M11	001590	hsa-miR-548c	CAAAAUCUCAAUUACUUUUGC
M12	002429	hsa-miR-548c-5p	AAAAGUAAUUGCGGUUUUUGCC
M13	001605	hsa-miR-548d	CAAAAACCACAGUUUCUUUUGC
M14	002237	hsa-miR-548d-5p	AAAAGUAAUUGUGGUUUUUGCC
M15	001535	hsa-miR-551b	GCGACCCAUAUCUUGGUUUCAG
M16	002345	hsa-miR-556-3p	AUAUUACCAUAGCUCAUCUUU
M17	002344	hsa-miR-556-5p	GAUGAGCUCAUUGUAAUAUGAG
M18	001528	hsa-miR-561	CAAAGUUUAAGAUCUUGAAGU
M19	002347	hsa-miR-570	CGAAAACAGCAAUUACCUUUGC
M20	002349	hsa-miR-574-3p	CACGCUCAUGCACACACCCACA
M21	002351	hsa-miR-576-3p	AAGAUGUGGAAAAAUUGGAAUC
M22	002350	hsa-miR-576-5p	AUUCUAAUUCUCCACGUCUUU
M23	002398	hsa-miR-579	UUCAUUUGGUAUAAACCGCGAUU
M24	002399	hsa-miR-582-3p	U AACUGGUUGAACACUGAACC
N1	001983	hsa-miR-582-5p	UUACAGUUGUUAACCAGUUACU
N2	002409	hsa-miR-589	UGAGAACCACGUCUGCUCUGAG
N3	001984	hsa-miR-590-5p	GAGCUUAUUCAUAAAAGUGCAG
N4	001551	hsa-miR-597	UGUGUCACUCGAUGACCACUGU
N5	001988	hsa-miR-598	UACGUCAUCGUUGUCAUCGUCA
N6	001960	mmu-miR-615	UCCGAGCCUGGGUCUCCCUCUU
N7	002353	hsa-miR-615-5p	GGGGGUCCCCGGUGCUCGGAUC
N8	002414	hsa-miR-616	AGUCAUUGGAGGGUUUGAGCAG
N9	001593	hsa-miR-618	AAACUCUACUUGUCCUUCUGAGU
N10	002430	hsa-miR-624	CACAAGGUAAUUGGUAAUACCU
N11	002431	hsa-miR-625	AGGGGGAAAGUUCUAUAGUCC
N12	001560	hsa-miR-627	GUGAGUCUCUAAGAAAAGAGGA
N13	002433	hsa-miR-628-5p	AUGCUGACAUAUUUACUAGAGG
N14	002436	hsa-miR-629	UGGGUUUACGUUGGGAGAACU
N15	002088	hsa-miR-636	UGUGCUUGCUCGUCCCGCCCGCA
N16	001592	hsa-miR-642	GUCCUCUCCAAAUGUGUCUUU
N17	001604	hsa-miR-651	UUUAGGAUAAGCUUGACUUUUG
N18	002352	hsa-miR-652	AAUGGCGCCACUAGGGUUGUG
N19	002292	hsa-miR-653	GUGUUGAAACAAUCUCUACUG
N20	002239	hsa-miR-654-3p	UAUGUCUGCUGACCAUCACCUU
N21	001611	hsa-miR-654	UGGUGGGCCGCAGAACAUUGUC
N22	001612	hsa-miR-655	AUAAUACAUGGUUAACCUCUUU
N23	001515	hsa-miR-660	UACCAUUGCAUAUCGGAGUUG
N24	002322	hsa-miR-671-3p	UCCGGUUCUCAGGGCUCCACC

O1	002327	hsa-miR-672	UGAGGUUGGUGUACUGUGUGUGA
O2	002021	hsa-miR-674	GCACUGAGAUGGGAGUGGUGUA
O3	002341	hsa-miR-708	AAGGAGCUUACAAUCUAGCUGGG
O4	002324	hsa-miR-744	UGC GGGGCUAGGGCUAACAGCA
O5	001990	hsa-miR-758	UUUGUGACCUGGUCCACUAACC
O6	002354	hsa-miR-871	UAUUCAGAUUAGUGCCAGUCAUG
O7	002264	hsa-miR-872	AAGGUUACUUGUUAGUUCAGG
O8	002356	hsa-miR-873	GCAGGAACUUGUGAGUCUCCU
O9	002268	hsa-miR-874	CUGCCCUGGCCCGAGGGACCGA
O10	002204	hsa-miR-875-3p	CCUGGAAACACUGAGGUUGUG
O11	002225	hsa-miR-876-3p	UGGUGGUUUACAAAGUAAUUCA
O12	002205	hsa-miR-876-5p	UGGAUUUCUUUGUGAAUCACCA
O13	002372	hsa-miR-885-3p	AGGCAGCGGGGUGUAGUGGAUA
O14	002296	hsa-miR-885-5p	UCCAUAACACUACCCUGCCUCU
O15	002194	hsa-miR-886-3p	CGCGGGUGCUUACUGACCCUU
O16	002193	hsa-miR-886-5p	CGGGUCGGAGUUAGCUCAAGCGG
O17	002374	hsa-miR-887	GUGAACGGGCGCCAUCCCGAGG
O18	002212	hsa-miR-888	UACUCAAAAAGCUGUCAGUCA
O19	002202	hsa-miR-889	UUAUAUCGGACAACCAUUGU
O20	002209	hsa-miR-890	UACUUGGAAAGGCAUCAGUUG
O21	002191	hsa-miR-891a	UGCAACGAACCUGAGCCACUGA
O22	002210	hsa-miR-891b	UGCAACUUACCUGAGUCAUUGA
O23	002195	hsa-miR-892a	CACUGUGUCCUUUCUGCGUAG
O24	000469	hsa-miR-147	GUGUGUGGAAAUGCUUCUGC
P1	000511	hsa-miR-208	AUAAGACGAGCAAAAAGCUUGU
P2	000514	hsa-miR-211	UUCCCUUUGUCAUCCUUCGCCU
P3	000515	hsa-miR-212	UACAGUCUCCAGUCACGGCC
P4	002095	hsa-miR-219-1-3p	AGAGUUGAGUCUGGACGUCCCG
P5	002390	hsa-miR-219-2-3p	AGAAUUGUGGCUGGACAUCUGU
P6	000523	hsa-miR-220	CCACACCGUAUCUGACACUUU
P7	002206	hsa-miR-220b	CCACCACCGUGUCUGACACUU
P8	002211	hsa-miR-220c	ACACAGGGCUGUUGUGAAGACU
P9	002190	hsa-miR-298	AGCAGAAGCAGGGAGGUUCUCCA
P10	000540	hsa-miR-325	CCUAGUAGGUGUCCAGUAAGUGU
P11	000553	hsa-miR-346	UGUCUGCCC GCAUGCCUGCCUCU
P12	002122	hsa-miR-376c	AACAUAGAGGAAAUCCACGU
P13	000574	hsa-miR-384	AUCCUAGAAA UUGUUCAUA
P14	001023	hsa-miR-412	ACUUCACCUGGUCCACUAGCCGU
P15	001029	hsa-miR-448	UUGCAUAUGUAGGAUGUCCCAU
P16	001039	hsa-miR-492	AGGACCUGCGGGACAAGAUUCUU
P17	001050	hsa-miR-506	UAAGGCACCCUUCUGAGUAGA
P18	002155	hsa-miR-509-3-5p	UACUGCAGACGUGGCAAUCAUG
P19	001111	hsa-miR-511	GUGUCUUUUGCUCUGCAGUCA
P20	001152	hsa-miR-517b	UCGUGCAUCCCUUAGAGUGUU
P21	001163	hsa-miR-519c	AAAGUGCAUCUUUUUAGAGGAU
P22	001116	hsa-miR-520b	AAAGUGCUCCUUUUUAGAGGG
P23	001119	hsa-miR-520e	AAAGUGCUCCUUUUUAGAGGG
P24	001120	hsa-miR-520f	AAGUGCUCCUUUUUAGAGGGUU

	1	2	3	4	5	6	7	8	9	10	11	12	13	14	15	16	17	18	19	20	21	22	23	24
A	dme-miR-7	hsa-miR-548I	hsa-miR-30a-3p	hsa-miR-30a-5p	hsa-miR-30d	hsa-miR-30e-3p	hsa-miR-34b	hsa-miR-126#	hsa-miR-154#	hsa-miR-182#	U6 snRNA	U6 snRNA	hsa-miR-206	hsa-miR-213	hsa-miR-302c	hsa-miR-302d	hsa-miR-378	hsa-miR-380-5p	hsa-miR-1257	hsa-miR-200a	hsa-miR-432	hsa-miR-432#	hsa-miR-497	hsa-miR-500
B	hsa-miR-1238	hsa-miR-488	hsa-miR-517#	hsa-miR-516-3p	hsa-miR-518c	hsa-miR-519e	hsa-miR-520h	hsa-miR-524	mmu-let-7d#	hsa-miR-363#	U6 snRNA	U6 snRNA	rn-miR-7#	hsa-miR-666	hsa-miR-549	hsa-miR-657	hsa-miR-658	hsa-miR-659	hsa-miR-561a	hsa-miR-562	hsa-miR-563	hsa-miR-554	hsa-miR-555	hsa-miR-557
C	hsa-miR-568	hsa-miR-569	hsa-miR-562	hsa-miR-563	hsa-miR-564	hsa-miR-566	hsa-miR-567	hsa-miR-569	hsa-miR-586	hsa-miR-587	RNU 44	hsa-miR-588	hsa-miR-589	hsa-miR-560	hsa-miR-591	hsa-miR-592	hsa-miR-593	hsa-miR-596	hsa-miR-622	hsa-miR-599	hsa-miR-623	hsa-miR-600	hsa-miR-624	hsa-miR-601
D	hsa-miR-626	hsa-miR-629	hsa-miR-630	hsa-miR-631	hsa-miR-603	hsa-miR-604	hsa-miR-605	hsa-miR-606	hsa-miR-607	hsa-miR-608	hsa-miR-609	hsa-miR-633	hsa-miR-634	hsa-miR-635	hsa-miR-637	hsa-miR-638	hsa-miR-639	hsa-miR-640	hsa-miR-641	hsa-miR-613	hsa-miR-614	hsa-miR-616	hsa-miR-617	hsa-miR-643
E	hsa-miR-644	hsa-miR-645	hsa-miR-621	hsa-miR-646	hsa-miR-647	hsa-miR-648	hsa-miR-649	hsa-miR-650	hsa-miR-661	hsa-miR-662	RNU 48	hsa-miR-571	hsa-miR-572	hsa-miR-573	hsa-miR-575	hsa-miR-578	hsa-miR-580	hsa-miR-581	hsa-miR-583	hsa-miR-584	hsa-miR-585	hsa-miR-29c#	hsa-miR-766	hsa-miR-595
F	hsa-miR-668	hsa-miR-767-5p	hsa-miR-767-3p	hsa-miR-454#	hsa-miR-769-5p	hsa-miR-770-5p	hsa-miR-769-3p	hsa-miR-802	hsa-miR-675	hsa-miR-505#	hsa-miR-218-1#	hsa-miR-221#	hsa-miR-222#	hsa-miR-223#	hsa-miR-136#	hsa-miR-34b	hsa-miR-186#	hsa-miR-186#	hsa-miR-195#	hsa-miR-30c-1#	hsa-miR-30c-2#	hsa-miR-32#	hsa-miR-31#	hsa-miR-130b
G	hsa-miR-26a-2#	hsa-miR-361-3p	hsa-let-7g#	hsa-miR-302b	hsa-miR-302d	hsa-miR-367#	hsa-miR-374a	hsa-miR-23b#	hsa-miR-376a	hsa-miR-377#	ath-miR159a	hsa-miR-300#	hsa-miR-122#	hsa-miR-130a	hsa-miR-132#	hsa-miR-148a	hsa-miR-33a	hsa-miR-33a#	hsa-miR-92a-1#	hsa-miR-92a-2#	hsa-miR-93#	hsa-miR-96#	hsa-miR-96#	hsa-miR-100#
H	hsa-miR-101#	hsa-miR-138-2#	hsa-miR-141#	hsa-miR-143#	hsa-miR-144#	hsa-miR-145#	hsa-miR-920	hsa-miR-921	hsa-miR-922	hsa-miR-924	hsa-miR-337-3p	hsa-miR-125b	hsa-miR-136b	hsa-miR-148b	hsa-miR-146a	hsa-miR-149#	hsa-miR-29b-1#	hsa-miR-29b-2#	hsa-miR-106#	hsa-miR-106a	hsa-miR-16-2#	hsa-let-7f#	hsa-miR-15c#	hsa-miR-27#
I	hsa-miR-933	hsa-miR-934	hsa-miR-935	hsa-miR-936	hsa-miR-937	hsa-miR-938	hsa-miR-939	hsa-miR-941	hsa-miR-335#	hsa-miR-942	hsa-miR-943	hsa-miR-944	hsa-miR-99#	hsa-miR-124#	hsa-miR-541#	hsa-miR-875-5p	hsa-miR-888#	hsa-miR-892b	hsa-miR-9#	hsa-miR-411#	hsa-miR-378	hsa-miR-151-3p	hsa-miR-340#	hsa-miR-190b
J	hsa-miR-545#	hsa-miR-183#	hsa-miR-192#	hsa-miR-200b	hsa-miR-200c	hsa-miR-155#	hsa-miR-10a#	hsa-miR-214#	hsa-miR-218-2#	hsa-miR-129#	hsa-miR-22#	hsa-miR-42#	hsa-miR-30#	hsa-miR-7a#	hsa-let-424#	hsa-miR-181#	hsa-miR-201#	hsa-miR-431#	hsa-miR-7-2#	hsa-miR-101#	hsa-miR-34a#	hsa-miR-181a-2#	hsa-miR-74#	hsa-miR-452#
K	hsa-miR-409-3p	hsa-miR-181c	hsa-miR-196a	hsa-miR-483-3p	hsa-miR-708#	hsa-miR-92b#	hsa-miR-551b	hsa-miR-202#	hsa-miR-193b	hsa-miR-518e	hsa-miR-497#	hsa-miR-543	hsa-miR-125b-1#	hsa-miR-194#	hsa-miR-106b	hsa-miR-302a	hsa-miR-519b	hsa-miR-193b	hsa-miR-374b	hsa-miR-520c-3p	hsa-let-7b#	hsa-let-7c#	hsa-let-7e#	hsa-miR-550
L	hsa-miR-593	hsa-let-7f-1#	hsa-let-7f-2#	hsa-miR-15a#	hsa-miR-16-1#	hsa-miR-17#	hsa-miR-18a#	hsa-miR-19a#	hsa-miR-19b-1#	hsa-miR-625#	hsa-miR-628-3p	hsa-miR-20a#	hsa-miR-21#	hsa-miR-23a#	hsa-miR-24-1#	hsa-miR-24-2#	hsa-miR-26a	hsa-miR-26a-1#	hsa-miR-26b#	hsa-miR-27a#	hsa-miR-29a#	hsa-miR-151-5p	hsa-miR-765	hsa-miR-338-5p
M	hsa-miR-620	hsa-miR-577	hsa-miR-144	hsa-miR-590-3p	hsa-miR-191#	hsa-miR-665	hsa-miR-520D	hsa-miR-1224-3P	hsa-miR-1224-3P	hsa-miR-1306	hsa-miR-513C	hsa-miR-513B	hsa-miR-1226	hsa-miR-1228	hsa-miR-1225	hsa-miR-1227	hsa-miR-1227	hsa-miR-1227	hsa-miR-1286	hsa-miR-548M	hsa-miR-1179	hsa-miR-1178	hsa-miR-1205	hsa-miR-1201
N	hsa-miR-548J	hsa-miR-1263	hsa-miR-1294	hsa-miR-1269	hsa-miR-1265	hsa-miR-1244	hsa-miR-1303	hsa-miR-1259	hsa-miR-548P	hsa-miR-1264	hsa-miR-1255	hsa-miR-1282	hsa-miR-1255	hsa-miR-1270	hsa-miR-1197	hsa-miR-1324	hsa-miR-548H	hsa-miR-1254	hsa-miR-548K	hsa-miR-1251	hsa-miR-1285	hsa-miR-1245	hsa-miR-1292	hsa-miR-1301
O	hsa-miR-1200	hsa-miR-1182	hsa-miR-1288	hsa-miR-1291	hsa-miR-1275	hsa-miR-1183	hsa-miR-1184	hsa-miR-1276	hsa-miR-320B	hsa-miR-1272	hsa-miR-1180	hsa-miR-1256	hsa-miR-1278	hsa-miR-1262	hsa-miR-1243	hsa-miR-663B	hsa-miR-1252	hsa-miR-1298	hsa-miR-1290	hsa-miR-1249	hsa-miR-1248	hsa-miR-1289	hsa-miR-1204	hsa-miR-1826
P	hsa-miR-1304	hsa-miR-1203	hsa-miR-1206	hsa-miR-548G	hsa-miR-1208	hsa-miR-548E	hsa-miR-1274	hsa-miR-1274	hsa-miR-1267	hsa-miR-1250	hsa-miR-548N	hsa-miR-1283	hsa-miR-1247	hsa-miR-1253	hsa-miR-720	hsa-miR-1260	hsa-miR-664	hsa-miR-1302	hsa-miR-1300	hsa-miR-1284	hsa-miR-548L	hsa-miR-1293	hsa-miR-1825	hsa-miR-1296

Figure E.2 Map of miRNA assays on TLDA Pool B v3 cards. Location of the 384 miRNA assays on TLDA pool B v3 cards. Each card was pre loaded with 0.5 µl 20X Taqman microRNA Assays.

Table E.2 miRNA target sequence and assay position on pool B TLDA cards.

Location, assay ID, assay name and target sequence of each of the 20X Taqman microRNA assays on the pool B v3 TLDA cards used in this study

Well location	Assay ID	Assay Name	Target Sequence 5' → 3'
A1	000268	dme-miR-7	UGGAAGACUAGUGAUUUUGUUGU
A2	002909	hsa-miR-548I	AAAAGUAAUUGCGGAUUUUGCC
A3	000416	hsa-miR-30a-3p	CUUUCAGUCGGAUGUUUGCAGC
A4	000417	hsa-miR-30a-5p	UGUAAACAUCCUCGACUGGAAG
A5	000420	hsa-miR-30d	UGUAAACAUCCCCGACUGGAAG
A6	000422	hsa-miR-30e-3p	CUUUCAGUCGGAUGUUUACAGC
A7	000427	hsa-miR-34b	UAGGCAGUGUCAUUAGCUGAUUG
A8	000451	hsa-miR-126#	CAUUAUUACUUUUGGUACGCG
A9	000478	hsa-miR-154#	AAUCAUACACGGUUGACCUAUU
A10	000483	hsa-miR-182#	UGGUUCUAGACUUGCCAACUA
A11	001973	U6 snRNA	GTGCTCGCTTCGGCAGCACATATACTAA AATTGGAACGATACAGAGAAGATTAGC ATGGCCCCTGCGCAAGGATGACACGCA AATTCGTGAAGCGTTCATATTTT
A12	001973	U6 snRNA	GTGCTCGCTTCGGCAGCACATATACTAA AATTGGAACGATACAGAGAAGATTAGC ATGGCCCCTGCGCAAGGATGACACGCA AATTCGTGAAGCGTTCATATTTT
A13	000510	hsa-miR-206	UGGAAUGUAAGGAAGUGUGUGG
A14	000516	hsa-miR-213	ACCAUCGACCGUUGAUUGUACC
A15	000534	hsa-miR-302c#	UUUAAUAUGGGGGUACCUGCUG
A16	000535	hsa-miR-302d	UAAGUGCUUCCAUGUUUGAGUGU
A17	000567	hsa-miR-378	CUCCUGACUCCAGGUCCUGUGU
A18	000570	hsa-miR-380-5p	UGGUUGACCAUAGAACAUGCGC
A19	002910	hsa-miR-1257	AGUGAAUGAUGGGUUCUGACC
A20	001011	hsa-miR-200a#	CAUCUUACCGGACAGUGCUGGA
A21	001026	hsa-miR-432	UCUUGGAGUAGGUCAUUGGGUGG
A22	001027	hsa-miR-432#	CUGGAUGGCUCCUCCAUGUCU
A23	001043	hsa-miR-497	CAGCAGCACACUGUGGUUUGU
A24	001046	hsa-miR-500	AUGCACCUGGGCAAGGAUUCUG
B1	002927	hsa-miR-1238	CUUCCUCGUCUGUCUGCCCC
B2	001106	hsa-miR-488	CCCAGAUAAUGGCACUCUCA
B3	001113	hsa-miR-517#	CCUCUAGAUGGAAGCACUGUCU
B4	001149	hsa-miR-516-3p	UGCUCUUCUUCAGAGGGU
B5	001158	hsa-miR-518c#	UCUCUGGAGGGAAGCACUUUCUG
B6	001166	hsa-miR-519e#	UUCUCCAAAAGGGAGCACUUUC
B7	001170	hsa-miR-520h	ACAAAGUGCUUCCCUUAGAGU
B8	001173	hsa-miR-524	GAAGGCGCUUCCCUUUGGAGU
B9	001178	mmu-let-7d#	CUAUACGACCUGCUGCCUUUCU
B10	001283	hsa-miR-363#	CGGGUGGAUCACGAUGCAAUUU
B11	001973	U6 snRNA	GTGCTCGCTTCGGCAGCACATATACTAA AAATTGGAACGATACAGAGAAGATTAG CATGGCCCCTGCGCAAGGATGACACGC AAATTCGTGAAGCGTTCATATTTT

B12	001973	U6 snRNA	GTGCTCGCTTCGGCAGCACATATACTAA AATTGGAACGATACAGAGAAGATTAGC ATGGCCCCTGCGCAAGGATGACACGCA AATTCGTGAAGCGTTCATATTTT
B13	001338	rno-miR-7#	CAACAAAUCACAGUCUGCCAUA
B14	001510	hsa-miR-656	AAUAUUAUACAGUCAACCUCU
B15	001511	hsa-miR-549	UGACAACUAUGGAUGAGCUCU
B16	001512	hsa-miR-657	GGCAGGUUCUCACCCUCUCUAGG
B17	001513	hsa-miR-658	GGCGGAGGGAAGUAGGUCCGUUGGU
B18	001514	hsa-miR-659	CUUGGUUCAGGGAGGGUCCCCA
B19	001519	hsa-miR-551a	GCGACCCACUCUUGGUUUCCA
B20	001520	hsa-miR-552	AACAGGUGACUGGUUAGACAA
B21	001521	hsa-miR-553	AAAACGGUGAGAUUUUGUUUU
B22	001522	hsa-miR-554	GCUAGUCCUGACUCAGCCAGU
B23	001523	hsa-miR-555	AGGGUAAGCUGAACCCUCUGAU
B24	001525	hsa-miR-557	GUUUGCACGGGUGGGCCUUGUCU
C1	001526	hsa-miR-558	UGAGCUGCUGUACCAAAAUA
C2	001527	hsa-miR-559	UAAAGUAAAUAUGCACCAAAA
C3	001529	hsa-miR-562	AAAGUAGCUGUACCAUUUGC
C4	001530	hsa-miR-563	AGGUUGACAUACGUUUC
C5	001531	hsa-miR-564	AGGCACGGUGUCAGCAGGC
C6	001533	hsa-miR-566	GGGCGCCUGUGAUCCCAAC
C7	001534	hsa-miR-567	AGUAUGUUCUCCAGGACAGAAC
C8	001536	hsa-miR-569	AGUAAAUGAAUCCUGGAAAGU
C9	001539	hsa-miR-586	UAUGCAUUGUAUUUUUAGGUCC
C10	001540	hsa-miR-587	UUUCCAUAGGUGAUGAGUCAC
C11	001094	RNU44	CCUGGAUGAUGAUAGCAAAUGCUGAC UGAACAUAGAAGGUCUAAAUAGCUCU AACUGACU
C12	001542	hsa-miR-588	UUGGCCACAAUGGGUUAGAAC
C13	001543	hsa-miR-589	UCAGAACAAAUGCCGGUUC
C14	001544	hsa-miR-550	UGUCUUACUCCCUCAGGCACAU
C15	001545	hsa-miR-591	AGACCAUGGGUUCUCAUUGU
C16	001546	hsa-miR-592	UUGUGUCAUAUGCGAUGAUGU
C17	001547	hsa-miR-593	AGGCACCAGCCAGGCAUUGCUCAGC
C18	001550	hsa-miR-596	AAGCCUGCCCGGCUCUCGGG
C19	001553	hsa-miR-622	ACAGUCUGCUGAGGUUGGAGC
C20	001554	hsa-miR-599	GUUGUGUCAGUUUAUCAAAC
C21	001555	hsa-miR-623	AUCCCUUGCAGGGGCUGUUGGGU
C22	001556	hsa-miR-600	ACUUACAGACAAGAGCCUUGCUC
C23	001557	hsa-miR-624	UAGUACCAGUACCUUGUGUUA
C24	001558	hsa-miR-601	UGGUCUAGGAUUGUUGGAGGAG
D1	001559	hsa-miR-626	AGCUGUCUGAAAAUGUCUU
D2	001562	hsa-miR-629	GUUCUCCAACGUAAGCCCAGC
D3	001563	hsa-miR-630	AGUAUUCUGUACCAGGGAAGGU
D4	001564	hsa-miR-631	AGACCUGGCCAGACCUCAGC
D5	001566	hsa-miR-603	CACACACUGCAAUUACUUUUGC
D6	001567	hsa-miR-604	AGGCUGCGGAAUUCAGGAC
D7	001568	hsa-miR-605	UAAAUCCCAUGGUGCCUUCUCCU
D8	001569	hsa-miR-606	AAACUACUGAAAAUCAAGAU
D9	001570	hsa-miR-607	GUUCAAAUCCAGAUCUAUAAC
D10	001571	hsa-miR-608	AGGGGUGGUGUUGGGACAGCUCCGU

D11	001573	hsa-miR-609	AGGGUGUUUCUCUCAUCUCU
D12	001574	hsa-miR-633	CUAAUAGUAUCUACCACAAUAAA
D13	001576	hsa-miR-634	AACCAGCACCCCAACUUUGGAC
D14	001578	hsa-miR-635	ACUUGGGCACUGAAACAAUGUCC
D15	001581	hsa-miR-637	ACUGGGGGCUUUCGGGCUCUGCGU
D16	001582	hsa-miR-638	AGGGAUCGCGGGCGGGUGGCGGCCU
D17	001583	hsa-miR-639	AUCGCUCGCGGUUGCGAGCGCUGU
D18	001584	hsa-miR-640	AUGAUCCAGGAACCUGCCUCU
D19	001585	hsa-miR-641	AAAGACAUAGGAUAGAGUCACCUC
D20	001586	hsa-miR-613	AGGAAUGUCCUUCUUUGCC
D21	001587	hsa-miR-614	GAACGCCUGUUCUUGCCAGGUGG
D22	001589	hsa-miR-616	ACUCAAAACCCUUCAGUGACUU
D23	001591	hsa-miR-617	AGACUUCCEAUUUGAAGGUGGC
D24	001594	hsa-miR-643	ACUUGUAUGCUAGCUCAGGUAG
E1	001596	hsa-miR-644	AGUGUGGCUUUCUUAGAGC
E2	001597	hsa-miR-645	UCUAGGCUGGUACUGCUGA
E3	001598	hsa-miR-621	GGCUAGCAACAGCGCUUACCU
E4	001599	hsa-miR-646	AAGCAGCUGCCUCUGAGGC
E5	001600	hsa-miR-647	GUGGCUGCACUCACUUCUUC
E6	001601	hsa-miR-648	AAGUGUGCAGGGCACUGGU
E7	001602	hsa-miR-649	AAACCUGUGUUGUUCAAGAGUC
E8	001603	hsa-miR-650	AGGAGGCAGCGCUCUCAGGAC
E9	001606	hsa-miR-661	UGCCUGGGUCUCUGGCCUGCGCGU
E10	001607	hsa-miR-662	UCCACGUUGUGGCCCCAGCAG
E11	001006	RNU48	GAUGACCCCAGGUAACUCUGAGUGUGU CGCUGAUGCCAUCACCCGACGCUCUG ACC
E12	001613	hsa-miR-571	UGAGUUGGCCAUCUGAGUGAG
E13	001614	hsa-miR-572	GUCCGCUCGGCGGUGGCCCA
E14	001615	hsa-miR-573	CUGAAGUGAUGUGUAACUGAUCAG
E15	001617	hsa-miR-575	GAGCCAGUUGGACAGGAGC
E16	001619	hsa-miR-578	CUUCUUGUGCUCUAGGAUUGU
E17	001621	hsa-miR-580	UUGAGAAUGAUGAAUCAUAGG
E18	001622	hsa-miR-581	UCUUGUGUUCUCUAGAUCAGU
E19	001623	hsa-miR-583	CAAAGAGGAAGGUCCAUUAC
E20	001624	hsa-miR-584	UUAUGGUUUGCCUGGGACUGAG
E21	001625	hsa-miR-585	UGGGCGUAUCUGUAUGCUA
E22	001818	rno-miR-29c#	UGACCGAUUUCUCCUGGUGUUC
E23	001986	hsa-miR-766	ACUCCAGCCCCACAGCCUCAGC
E24	001987	hsa-miR-595	GAAGUGUGCCGUGGUGUGUCU
F1	001992	hsa-miR-668	UGUCACUCGGCUCGGCCCACUAC
F2	001993	hsa-miR-767-5p	UGCACCAUGGUUGUCUGAGCAUG
F3	001995	hsa-miR-767-3p	UCUGCUCAUACCCCAUGGUUUCU
F4	001996	hsa-miR-454#	ACCCUAUCAUAUUGUCUCUGC
F5	001998	hsa-miR-769-5p	UGAGACCUCUGGGUUCUGAGCU
F6	002002	hsa-miR-770-5p	UCCAGUACCACGUGUCAGGGCCA
F7	002003	hsa-miR-769-3p	CUGGGAUCUCCGGGGUCUUGGUU
F8	002004	hsa-miR-802	CAGUAACAAAGAUUCAUCCUUGU
F9	002005	hsa-miR-675	UGGUGCGGAGAGGGCCCACAGUG
F10	002087	hsa-miR-505#	GGGAGCCAGGAAGUAUUGAUGU
F11	002094	hsa-miR-218-1#	AUGGUUCCGUCAAGCACCAUGG
F12	002096	hsa-miR-221#	ACCUGGCAUACAAUGUAGAUUU

F13	002097	hsa-miR-222#	CUCAGUAGCCAGUGUAGAUCU
F14	002098	hsa-miR-223#	CGUGUAUUUGACAAGCUGAGUU
F15	002100	hsa-miR-136#	CAUCAUCGUCUCAAAUGAGUCU
F16	002102	hsa-miR-34b	CAAUCACU AACUCCACUGCCAU
F17	002104	hsa-miR-185#	AGGGGCUGGCCUUUCCUCUGGUC
F18	002105	hsa-miR-186#	GCCCAAAGGUGAAUUUUUUGGG
F19	002107	hsa-miR-195#	CCAAUAUUGGCUGUGCUGCUCC
F20	002108	hsa-miR-30c-1#	CUGGGAGAGGGUUGUUUACUCC
F21	002110	hsa-miR-30c-2#	CUGGGAGAAGGCUGUUUACUCU
F22	002111	hsa-miR-32#	CAAUUUAGUGUGUGUGAUUUU
F23	002113	hsa-miR-31#	UGCUAUGCCAACAUAUUGCCAU
F24	002114	hsa-miR-130b#	ACUCUUUCCCGUUGCACUAC
G1	002115	hsa-miR-26a-2#	CCUAUUCUUGAUUACUUGUUUC
G2	002116	hsa-miR-361-3p	UCCCCCAGGUGUGAUUCUGAUUU
G3	002118	hsa-let-7g#	CUGUACAGGCCACUGCCUUGC
G4	002119	hsa-miR-302b#	ACUUUAACAUGGAAGUGCUUUC
G5	002120	hsa-miR-302d#	ACUUUAACAUGGAGGCACUUGC
G6	002121	hsa-miR-367#	ACUGUUGC UAAUAUGCAACUCU
G7	002125	hsa-miR-374a#	CUUAUCAGAUUGUAUUGUAAUU
G8	002126	hsa-miR-23b#	UGGGUUCUGGCAUGCUGAUUU
G9	002127	hsa-miR-376a#	GUAGAUUCUCCUUCUAUGAGUA
G10	002128	hsa-miR-377#	AGAGGUUGCCCUUGGUGAAUUC
G11	000338	ath-miR159a	UUUGGAUUGAAGGGAGCUCUA
G12	002129	hsa-miR-30b#	CUGGGAGGUGGAUGUUUACUUC
G13	002130	hsa-miR-122#	AACGCCAUUAUCACACUAAAUA
G14	002131	hsa-miR-130a#	UUCACAUUGUGCUACUGUCUGC
G15	002132	hsa-miR-132#	ACCGUGGCUUUCGAUUGUUACU
G16	002134	hsa-miR-148a#	AAAGUUCUGAGACACUCCGACU
G17	002135	hsa-miR-33a	GUGCAUUGUAGUUGCAUUGCA
G18	002136	hsa-miR-33a#	CAAUGUUUCCACAGUGCAUCAC
G19	002137	hsa-miR-92a-1#	AGGUUGGGAUCGGUUGCAAUGCU
G20	002138	hsa-miR-92a-2#	GGGUGGGGAUUUGUUGCAUUAC
G21	002139	hsa-miR-93#	ACUGCUGAGCUAGCACUCCCCG
G22	002140	hsa-miR-96#	AAUCAUGUGCAGUGCCAAUAUG
G23	002141	hsa-miR-99a#	CAAGCUCGCUUCUAUGGGUCUG
G24	002142	hsa-miR-100#	CAAGCUUGUAUCUAUAGGUAUG
H1	002143	hsa-miR-101#	CAGUUAUCACAGUGCUGAUGCU
H2	002144	hsa-miR-138-2#	GCUAUUUCACGACACCAGGGUU
H3	002145	hsa-miR-141#	CAUCUUCAGUACAGUGUUGGA
H4	002146	hsa-miR-143#	GGUGCAGUGCUGCAUCUCUGGU
H5	002148	hsa-miR-144#	GGUAUCAUCAUAUACUGUAAG
H6	002149	hsa-miR-145#	GGAUUCCUGGAAAUACUGUUCU
H7	002150	hsa-miR-920	GGGGAGCUGUGGAAGCAGUA
H8	002151	hsa-miR-921	CUAGUGAGGGACAGAACCAGGAUUC
H9	002152	hsa-miR-922	GCAGCAGAGAAUAGGACUACGUC
H10	002154	hsa-miR-924	AGAGUCUUGUGAUGUCUUGC
H11	002157	hsa-miR-337-3p	CUCCUAUAUGAUGCCUUUCUUC
H12	002158	hsa-miR-125b-2#	UCACAAGUCAGGCUCUUGGGAC
H13	002159	hsa-miR-135b#	AUGUAGGGCUAAAAGCCAUGGG
H14	002160	hsa-miR-148b#	AAGUUCUGUUAUACACUCAGGC
H15	002163	hsa-miR-146a#	CCUCUGAAAUCAGUUCUUCAG
H16	002164	hsa-miR-149#	AGGGAGGGACGGGGCUGUGC

H17	002165	hsa-miR-29b-1#	GCUGGUUUCAUAUGGUGGUUUAGA
H18	002166	hsa-miR-29b-2#	CUGGUUUCACAUGGUGGCCUAG
H19	002168	hsa-miR-105#	ACGGAUGUUUGAGCAUGUGCUA
H20	002170	hsa-miR-106a#	CUGCAAUGUAAGCACUUCUAC
H21	002171	hsa-miR-16-2#	CCAAUAUUACUGUGCUGCUUUA
H22	002172	hsa-let-7i#	CUGCGCAAGCUACUGCCUUGCU
H23	002173	hsa-miR-15b#	CGAAUCAUUUUUGCUGCUCUA
H24	002174	hsa-miR-27b#	AGAGCUUAGCUGAUUGGUGAAC
I1	002176	hsa-miR-933	UGUGCGCAGGGAGACCUCUCCC
I2	002177	hsa-miR-934	UGUCUACUACUGGAGACACUGG
I3	002178	hsa-miR-935	CCAGUUACCGCUUCCGCUACCGC
I4	002179	hsa-miR-936	ACAGUAGAGGGAGGAAUCGCAG
I5	002180	hsa-miR-937	AUCCGCGCUCUGACUCUCUGCC
I6	002181	hsa-miR-938	UGCCCUUAAAGGUGAACCCAGU
I7	002182	hsa-miR-939	UGGGGAGCUGAGGCUCUGGGGGUG
I8	002183	hsa-miR-941	CACCCGGCUGUGUGCACAUGUGC
I9	002185	hsa-miR-335#	UUUUUCAUUUUGCUCUCCUGACC
I10	002187	hsa-miR-942	UCUUCUCUGUUUUGGCCAUGUG
I11	002188	hsa-miR-943	CUGACUGUUGCCGUCCUCCAG
I12	002189	hsa-miR-944	AAAUUAUUGUACAUCGGAUGAG
I13	002196	hsa-miR-99b#	CAAGCUCGUGUCUGUGGGUCCG
I14	002197	hsa-miR-124#	CGUGUUCACAGCGGACCUUGAU
I15	002200	hsa-miR-541#	AAAGGAUUCUGCUGUCGGUCCACU
I16	002203	hsa-miR-875-5p	UAUACCUCAGUUUUAUCAGGUG
I17	002213	hsa-miR-888#	GACUGACACCUCUUUGGGUGAA
I18	002214	hsa-miR-892b	CACUGGCUCUUUCUGGGUAGA
I19	002231	hsa-miR-9#	AUAAAGCUAGAUAAACCGAAAGU
I20	002238	hsa-miR-411#	UAUGUAACACGGUCCACUAACC
I21	002243	hsa-miR-378	ACUGGACUUGGAGUCAGAAGG
I22	002254	hsa-miR-151-3p	CUAGACUGAAGCUCCUUGAGG
I23	002259	hsa-miR-340#	UCCGUCUCAGUUACUUUAUAGC
I24	002263	hsa-miR-190b	UGAU AUGUUUGAU AUUGGGUU
J1	002266	hsa-miR-545#	UCAGUAAAUGUUUAUUAUGAUGA
J2	002270	hsa-miR-183#	GUGAAUUACCGAAGGGCCAUA
J3	002272	hsa-miR-192#	CUGCCAAUUCUUAUAGGUCACAG
J4	002274	hsa-miR-200b#	CAUCUACUGGGCAGCAUUGGA
J5	002286	hsa-miR-200c#	CGUCUACCCAGCAGUGUUUGG
J6	002287	hsa-miR-155#	CUCCUACAUAUUAGCAUUAACA
J7	002288	hsa-miR-10a#	CAAUUCGUAUCUAGGGGAAUA
J8	002293	hsa-miR-214#	UGCCUGUCUACACUUGCUGUGC
J9	002294	hsa-miR-218-2#	CAUGGUUCUGUCAAGCACCGCG
J10	002298	hsa-miR-129#	AAGCCCUUACCCCAAAAAGUAU
J11	002301	hsa-miR-22#	AGUUCUUCAGUGGCAAGCUUUA
J12	002302	hsa-miR-425#	AUCGGGAAUGUCGUGUCCGCC
J13	002305	hsa-miR-30d#	CUUUCAGUCAGAUGUUUGCUCG
J14	002307	hsa-let-7a#	CUAUACAAUCUACUGUCUUUC
J15	002309	hsa-miR-424#	CAAACGUGAGGGCGCUGCUAU
J16	002310	hsa-miR-18b#	UGCCCUAAAUGCCCUUCUGGC
J17	002311	hsa-miR-20b#	ACUGUAGUAUGGGCACUUCAG
J18	002312	hsa-miR-431#	CAGGUCGUCUUGCAGGGCUUCU
J19	002314	hsa-miR-7-2#	CAACAAAUCCAGUCUACCUA
J20	002315	hsa-miR-10b#	ACAGAUUCGAUUCUAGGGGAAU

J21	002316	hsa-miR-34a#	CAAUCAGCAAGUAUACUGCCCU
J22	002317	hsa-miR-181a-2#	ACCACUGACCGUUGACUGUACC
J23	002325	hsa-miR-744#	CUGUUGCCACUAACCUCAACCU
J24	002330	hsa-miR-452#	CUCAUCUGCAAAGAAGUAAGUG
K1	002332	hsa-miR-409-3p	GAAUGUUGCUCGGUGAACCCCU
K2	002333	hsa-miR-181c#	AACCAUCGACCGUUGAGUGGAC
K3	002336	hsa-miR-196a#	CGGCAACAAGAAACUGCCUGAG
K4	002339	hsa-miR-483-3p	UCACUCCUCUCCUCCCGUCUU
K5	002342	hsa-miR-708#	CAACUAGACUGUGAGCUUCUAG
K6	002343	hsa-miR-92b#	AGGGACGGGACGCGGUGCAGUG
K7	002346	hsa-miR-551b#	GAAAUCAAGCGUGGGUGAGACC
K8	002362	hsa-miR-202#	UCCUAUGCAUAUACUUCUUUG
K9	002366	hsa-miR-193b#	CGGGGUUUUGAGGGCGAGAUGA
K10	002368	hsa-miR-497#	CAAACCACACUGUGGUGUUAGA
K11	002371	hsa-miR-518e#	CUCUAGAGGGAAGCGCUUUCUG
K12	002376	hsa-miR-543	AAACAUUCGCGGUGCACUUCUU
K13	002378	hsa-miR-125b-1#	ACGGGUUAGGCUCUUGGGAGCU
K14	002379	hsa-miR-194#	CCAGUGGGGCUGCUGUUAUCUG
K15	002380	hsa-miR-106b#	CCGCACUGUGGGUACUUGCUGC
K16	002381	hsa-miR-302a#	ACUAAAACGUGGAUGUACUUGCU
K17	002384	hsa-miR-519b-3p	AAAGUGCAUCCUUUUAGAGGUU
K18	002387	hsa-miR-518f#	CUCUAGAGGGAAGCACUUUCUC
K19	002391	hsa-miR-374b#	CUUAGCAGGUUGUAUUAUCAUU
K20	002400	hsa-miR-520c-3p	AAAGUGCUUCCUUUUAGAGGGU
K21	002404	hsa-let-7b#	CUAUACAACCUACUGCCUUCCC
K22	002405	hsa-let-7c#	UAGAGUUACACCCUGGGAGUUA
K23	002407	hsa-let-7e#	CUAUACGGCCUCCUAGCUUUC
K24	002410	hsa-miR-550	AGUGCCUGAGGGAGUAAGAGCCC
L1	002411	hsa-miR-593	UGUCUCUGCUGGGGUUUCU
L2	002417	hsa-let-7f-1#	CUAUACAAUCUAUUGCCUUCCC
L3	002418	hsa-let-7f-2#	CUAUACAGUCUACUGUCUUUCC
L4	002419	hsa-miR-15a#	CAGGCCAUAUUGUGCUGCCUCA
L5	002420	hsa-miR-16-1#	CCAGUAUUAACUGUGCUGCUGA
L6	002421	hsa-miR-17#	ACUGCAGUGAAGGCACUUGUAG
L7	002423	hsa-miR-18a#	ACUGCCCUAAGUGCUCUUCUGG
L8	002424	hsa-miR-19a#	AGUUUUGCAUAGUUGCACUACA
L9	002425	hsa-miR-19b-1#	AGUUUUGCAGGUUUGCAUCCAGC
L10	002432	hsa-miR-625#	GACUAUAGAACUUUCCCCCUCA
L11	002434	hsa-miR-628-3p	UCUAGUAAGAGUGGCAGUCGA
L12	002437	hsa-miR-20a#	ACUGCAUUAUGAGCACUUAAG
L13	002438	hsa-miR-21#	CAACACCAGUCGAUGGGCUGU
L14	002439	hsa-miR-23a#	GGGGUCCUGGGGAUGGGAUUU
L15	002440	hsa-miR-24-1#	UGCCUACUGAGCUGAUUACAGU
L16	002441	hsa-miR-24-2#	UGCCUACUGAGCUGAAACACAG
L17	002442	hsa-miR-25#	AGGCGGAGACUUGGGCAAUUG
L18	002443	hsa-miR-26a-1#	CCUAUUCUUGGUUACUUGCACG
L19	002444	hsa-miR-26b#	CCUGUUCUCCAUAUACUUGGCUC
L20	002445	hsa-miR-27a#	AGGGCUUAGCUGCUUGUGAGCA
L21	002447	hsa-miR-29a#	ACUGAUUUCUUUUGGUGUUCAG
L22	002642	hsa-miR-151-5P	UCGAGGAGCUCACAGUCUAGU
L23	002643	hsa-miR-765	UGGAGGAGAAGGAAGGUGAUG
L24	002658	hsa-miR-338-5P	AACAAUAUCCUGGUGCUGAGUG

M1	002672	hsa-miR-620	AUGGAGAUAGAUAUAGAAAU
M2	002675	hsa-miR-577	UAGAUAAAAUUAUUGGUACCUG
M3	002676	hsa-miR-144	UACAGUAUAGAUGAUGUACU
M4	002677	hsa-miR-590-3P	UAAUUUUUAUGUAUAAGCUAGU
M5	002678	hsa-miR-191#	GCUGCUCUUGGAUUUCGUCCCC
M6	002681	hsa-miR-665	ACCAGGAGGCUGAGGCCCCU
M7	002743	hsa-miR-520D-3P	AAAGUGCUUCUCUUUGGUGGGU
M8	002752	hsa-miR-1224-3P	CCCCACCUCUCUCUCCUCAG
M9	002867	hsa-miR-1305	UUUUCAACUCUAAUGGGAGAGA
M10	002756	hsa-miR-513C	UUCUCAAGGAGGUGUCGUUUUAU
M11	002757	hsa-miR-513B	UUCACAAGGAGGUGUCAUUUAU
M12	002758	hsa-miR-1226#	GUGAGGGCAUGCAGGCCUGGAUGGGG
M13	002761	hsa-miR-1236	CCUCUCCCCUUGUCUCUCCAG
M14	002763	hsa-miR-1228#	GUGGGCGGGGCAGGUGUGUG
M15	002766	hsa-miR-1225-3P	UGAGCCCCUGUGCCGCCCCAG
M16	002768	hsa-miR-1233	UGAGCCUGUCCUCCCGCAG
M17	002769	hsa-miR-1227	CGUGCCACCCUUUCCCCAG
M18	002773	hsa-miR-1286	UGCAGGACCAAGAUGAGCCCU
M19	002775	hsa-miR-548M	CAAAGGUAAUUUGUGGUUUUUG
M20	002776	hsa-miR-1179	AAGCAUUCUUUCAUUGGUUGG
M21	002777	hsa-miR-1178	UUGCUCACUGUUCUCCCCUAG
M22	002778	hsa-miR-1205	UCUGCAGGGUUUGCUUUGAG
M23	002779	hsa-miR-1271	CUUGGCACCUAGCAAGCACUCA
M24	002781	hsa-miR-1201	AGCCUGAUUAAACACAUGCUCUGA
N1	002783	hsa-miR-548J	AAAAGUAAUUGCGGUCUUUGGU
N2	002784	hsa-miR-1263	AUGGUACCCUGGCAUACUGAGU
N3	002785	hsa-miR-1294	UGUGAGGUUGGCAUUGUUGUCU
N4	002789	hsa-miR-1269	CUGGACUGAGCCGUGCUACUGG
N5	002790	hsa-miR-1265	CAGGAUGUGGUCAAGUGUUGUU
N6	002791	hsa-miR-1244	AAGUAGUUGGUUUUGUAUGAGAUGGUU
N7	002792	hsa-miR-1303	UUUAGAGACGGGGUCUUGCUCU
N8	002796	hsa-miR-1259	AUAUAUGAUGACUUAGCUUUU
N9	002798	hsa-miR-548P	UAGCAAAAACUGCAGUUACUUU
N10	002799	hsa-miR-1264	CAAGUCUUAAUUUGAGCACCUGUU
N11	002801	hsa-miR-1255B	CGGAUGAGCAAAGAAAGUGGUU
N12	002803	hsa-miR-1282	UCGUUUGCCUUUUUCUGCUU
N13	002805	hsa-miR-1255A	AGGAUGAGCAAAGAAAGUAGAUU
N14	002807	hsa-miR-1270	CUGGAGAUUAUGGAAGAGCUGUGU
N15	002810	hsa-miR-1197	UAGGACACAUGGUCUACUUCU
N16	002815	hsa-miR-1324	CCAGACAGAAUUCUAUGCACUUUC
N17	002816	hsa-miR-548H	AAAAGUAAUCGCGGUUUUUGUC
N18	002818	hsa-miR-1254	AGCCUGGAAGCUGGAGCCUGCAGU
N19	002819	hsa-miR-548K	AAAAGUACUUGCGGAUUUUGCU
N20	002820	hsa-miR-1251	ACUCUAGCUGCCAAAGGCGCU
N21	002822	hsa-miR-1285	UCUGGGCAACAAAGUGAGACCU
N22	002823	hsa-miR-1245	AAGUGAUCUAAAGGCCUACAU
N23	002824	hsa-miR-1292	UGGGAACGGGUUCCGGCAGACGCUG
N24	002827	hsa-miR-1301	UUGCAGCUGCCUGGGAGUGACUUC
O1	002829	hsa-miR-1200	CUCCUGAGCCAUUCUGAGCCUC
O2	002830	hsa-miR-1182	GAGGGUCUUGGGAGGGAUGUGAC
O3	002832	hsa-miR-1288	UGGACUGCCUGAUCUGGAGA

O4	002838	hsa-miR-1291	UGGCCUGACUGAAGACCAGCAGU
O5	002840	hsa-miR-1275	GUGGGGGAGAGGCUGUC
O6	002841	hsa-miR-1183	CACUGUAGGUGAUGGUGAGAGUGGGC A
O7	002842	hsa-miR-1184	CCUGCAGCGACUUGAUGGCUUCC
O8	002843	hsa-miR-1276	UAAAGAGCCUGUGGAGACA
O9	002844	hsa-miR-320B	AAAAGCUGGGUUGAGAGGGCAA
O10	002845	hsa-miR-1272	GAUGAUGAUGGCAGCAAUUCUGAAA
O11	002847	hsa-miR-1180	UUUCCGGCUCGCGUGGGUGUGU
O12	002850	hsa-miR-1256	AGGCAUUGACUUCUCACUAGCU
O13	002851	hsa-miR-1278	UAGUACUGUGCAUAUCAUCUAU
O14	002852	hsa-miR-1262	AUGGGUGAAUUUGUAGAAGGAU
O15	002854	hsa-miR-1243	AACUGGAUCAAUUAUAGGAGUG
O16	002857	hsa-miR-663B	GGUGGCCCGGCCGUGCCUGAGG
O17	002860	hsa-miR-1252	AGAAGGAAAUUGAAUUCAUUUA
O18	002861	hsa-miR-1298	UUCAUUCGGCUGUCCAGAUGUA
O19	002863	hsa-miR-1290	UGGAUUUUUGGAUCAGGGA
O20	002868	hsa-miR-1249	ACGCCCUUCCCCCCUUCUUCA
O21	002870	hsa-miR-1248	ACCUUCUUGUAUAAGCACUGUGC AAA
O22	002871	hsa-miR-1289	UGGAGUCCAGGAAUCUGCAUUUU
O23	002872	hsa-miR-1204	UCGUGGCCUGGUCUCCAUAU
O24	002873	hsa-miR-1826	AUUGAUCAUCGACACUUCGAACGCAAU
P1	002874	hsa-miR-1304	UUUGAGGCUACAGUGAGAUGUG
P2	002877	hsa-miR-1203	CCCGGAGCCAGGAUGCAGCUC
P3	002878	hsa-miR-1206	UGUUCAUGUAGAUGUUUAAGC
P4	002879	hsa-miR-548G	AAAACUGUAAUACUUUUGUAC
P5	002880	hsa-miR-1208	UCACUGUUCAGACAGGCGGA
P6	002881	hsa-miR-548E	AAAAACUGAGACUACUUUUGCA
P7	002883	hsa-miR-1274A	GUCCUGUUCAGGCGCCA
P8	002884	hsa-miR-1274B	UCCUGUUCGGGCGCCA
P9	002885	hsa-miR-1267	CCUGUUGAAGUGUAAUCCCA
P10	002887	hsa-miR-1250	ACGGUGCUGGAUGUGGCCUUU
P11	002888	hsa-miR-548N	CAAAGUAAUUGUGGAUUUUGU
P12	002890	hsa-miR-1283	UCUACAAAGGAAAGCGCUUUCU
P13	002893	hsa-miR-1247	ACCCGUCCCGUUCGUCCCCGGA
P14	002894	hsa-miR-1253	AGAGAAGAAGAUCAGCCUGCA
P15	002895	hsa-miR-720	UCUCGCUGGGGCCUCCA
P16	002896	hsa-miR-1260	AUCCACCUCUGCCACCA
P17	002897	hsa-miR-664	UAUUCAUUUAUCCCCAGCCUACA
P18	002901	hsa-miR-1302	UUGGGACAUACUUAUGC UAAA
P19	002902	hsa-miR-1300	UUGAGAAGGAGGCUGCUG
P20	002903	hsa-miR-1284	UCUAUACAGACCCUGGCUUUUC
P21	002904	hsa-miR-548L	AAAAGUAUUUGCGGGUUUUGUC
P22	002905	hsa-miR-1293	UGGGUGGUCUGGAGAUUUGUGC
P23	002907	hsa-miR-1825	UCCAGUGCCCUCUCUCC
P24	002908	hsa-miR-1296	UUAGGGCCCUGGCUCCAUCUCC

Replicates																										Port	
1	1	1	1	2	2	2	3	3	3	CTL	CTL	CTL	4	4	4	5	5	5	6	6	6	7	7	7	A	1	
	8	8	8	9	9	9	10	10	10	11	11	11	12	12	12	13	13	13	14	14	14	15	15	15	B		
	16	16	16	17	17	17	18	18	18	19	19	19	20	20	20	21	21	21	22	22	22	23	23	23	C	2	
	24	24	24	25	25	25	26	26	26	27	27	27	28	28	28	29	29	29	30	30	30	31	31	31	D		
2	1	1	1	2	2	2	3	3	3	CTL	CTL	CTL	4	4	4	5	5	5	6	6	6	7	7	7	E	3	
	8	8	8	9	9	9	10	10	10	11	11	11	12	12	12	13	13	13	14	14	14	15	15	15	F		
	16	16	16	17	17	17	18	18	18	19	19	19	20	20	20	21	21	21	22	22	22	23	23	23	G	4	
	24	24	24	25	25	25	26	26	26	27	27	27	28	28	28	29	29	29	30	30	30	31	31	31	H		
3	1	1	1	2	2	2	3	3	3	CTL	CTL	CTL	4	4	4	5	5	5	6	6	6	7	7	7	I	5	
	8	8	8	9	9	9	10	10	10	11	11	11	12	12	12	13	13	13	14	14	14	15	15	15	J		
	16	16	16	17	17	17	18	18	18	19	19	19	20	20	20	21	21	21	22	22	22	23	23	23	K	6	
	24	24	24	25	25	25	26	26	26	27	27	27	28	28	28	29	29	29	30	30	30	31	31	31	L		
4	1	1	1	2	2	2	3	3	3	CTL	CTL	CTL	4	4	4	5	5	5	6	6	6	7	7	7	M	7	
	8	8	8	9	9	9	10	10	10	11	11	11	12	12	12	13	13	13	14	14	14	15	15	15	N		
	16	16	16	17	17	17	18	18	18	19	19	19	20	20	20	21	21	21	22	22	22	23	23	23	O	8	
	24	24	24	25	25	25	26	26	26	27	27	27	28	28	28	29	29	29	30	30	30	31	31	31	P		
		1	2	3	4	5	6	7	8	9	10	11	12	13	14	15	16	17	18	19	20	21	22	23	24		

Figure E.3 Position of miRNA assays on Custom TLDA cards. Format for the custom made 384 well microRNA arrays made by Applied Biosystems™, containing our 31 miRNAs of interest and endogenous control U6 snRNA.

Table E.3 miRNA target sequences for custom TLDA cards. The assay position, assay ID, assay name and target sequence for each of the 20X Taqman microRNA assays pre loaded on the custom made TLDA cards.

Position	Assay ID	Assay Name	Target Sequence 5' → 3'
1	002257	hsa-miR-339-5p	UCCCUGUCCUCCAGGAGCUCACG
2	000471	hsa-miR-148b	UCAGUGCAUCACAGAACUUUGU
3	002297	hsa-miR-422a	ACUGGACUUAGGGUCAGAAGGC
CTL	001973	U6 snRNA	GTGCTCGCTTCGGCAGCATATACT AAAATTGGAACGATACAGAGAAGATT AGCATGGCCCCTGCGCAAGGATGACA CGCAAATTCGTGAAGCGTTCATATTT T
4	001984	hsa-miR-590-5p	GAGCUUAUUCAUAAAAGUGCAG
5	000402	hsa-miR-24	UGGCUCAGUUCAGCAGGAACAG
6	000533	hsa-miR-302c	UAAGUGCUCUCCAUGUUUCAGUGG
7	000563	hsa-miR-374	UUAUAAUACAACCUGAUAAAGUG
8	002268	hsa-miR-874	CUGCCCUGGCCCGAGGGACCGA
9	000518	hsa-miR-215	AUGACCUAUGAAUUGACAGAC
10	000475	hsa-miR-152	UCAGUGCAUGACAGAACUUGG
11	002623	hsa-miR-155	UUA AUGCUAAUCGUGAUAGGGGU
12	000457	hsa-miR-132	UAACAGUCUACAGCCAUGGUCG
13	000468	hsa-miR-146a	UGAGAACUGAAUCCAUGGGUU
14	001193	mmu-miR-187	UCGUGUCUUGUGUUGCAGCCGG
15	002278	hsa-miR-145	GUCCAGUUUCCCAGGAAUCCCU
16	002619	hsa-miR-let7b	UGAGGUAGUAGGUUGUGUGGUU
17	000379	hsa-miR- let 7c	UGAGGUAGUAGGUUGUAUGGUU
18	002283	hsa-miR- let 7d	AGAGGUAGUAGGUUGCAUAGUU
19	002406	hsa-miR- let 7e	UGAGGUAGGAGGUUGUAUAGUU
20	000583	hsa-miR-9	UCUUUGGUUAUCUAGCUGUAUGA
21	002198	hsa-miR-125a-5p	UCCCUGAGACCCUUUAACCUGUGA
22	000524	hsa-miR-221	AGCUACAUUGUCUGCUGGGUUUC
23	002096	hsa-miR-221#	ACCUGGCAUACAAUGUAGAUUU
24	002905	hsa-miR-1293	UGGGUGGUCUGGAGAUUUGUGC
25	002376	hsa-miR-543	AAACAUCGCGGUGCACUUCUU
26	002410	hsa-miR-550	AGUGCCUGAGGGAGUAAGAGCCC
27	002824	hsa-miR-1292	UGGGAACGGGUUCCGGCAGACGCUG
28	001539	hsa-miR-586	UAUGCAUUGUAUUUUUAGGUCC
29	001027	hsa-miR-432#	CUGGAUGGCUCCUCCAUGUCU
30	002407	hsa-miR- let 7e#	CUAUACGGCCUCCUAGCUUUC
31	002231	hsa-miR-9#	AUAAAGCUAGAUAAACCGAAAGU

Table E.4. Human miRNA target sequences. Assay name, stem loop sequence and target sequence for each of the individual human 20X Taqman microRNA assays.

Assay ID	Assay Name	Stem loop sequence for RT	miRNA Target Sequence 5' → 3'
000468	hsa-miR-146a-5p	CCGAUGUGUAUCCUCAGCU UUGAGAACUGAAUCCAUG GGUUGUGUCAGUGUCAGAC CUCUGAAAUUCAGUUCUUC AGCUGGGGAUAUCUCUGUCA UCGU	UGAGAACUGAAUU CCAUGGGUU
002623	hsa-miR-155-5p	CUGUUA AUGCUAAUCGUGA UAGGGGUUUUGCCUCAA CUGACUCCUACAUAUUAGC AUUAACAG	UUA AUGCUAAUCG UGAUAGGGGU
002406	hsa-let-7e-5p	CCCGGGCUGAGGUAGGAGG UUGUAUAGUUGAGGAGGAC ACCAAGGAGAUCACUAUA CGGCCUCCUAGCUUCCCC AGG	UGAGGUAGGAGGU UGUAUAGUU
002278	hsa-miR-145a-5p	CACCUUGUCCUCACGGUCC AGUUUCCCAGGAAUCCCU UAGAUGCUAAGAUGGGGAU UCCUGGAAAUACUGUUCUU GAGGUCAUGGUU	GUCCAGUUUCCCA GGAAUCCCU

Table E.5 Murine miRNA target sequences. Assay name, stem loop sequence and target sequence for each of the individual murine 20X Taqman microRNA assays.

Assay ID	Assay Name	Stem loop sequence for RT	miRNA Target Sequence 5' → 3'
000468	mmu-miR-146a	AGCUCUGAGAACUGAAUU CCAUGGGUUUAUCAAUG UCAGACCUGUGAAAUUCA GUUCUUCAGCU	UGAGAACUGAAU UCCAUGGGUU
002571	mmu-miR-155	CUGUUA AUGCUAAUUGUG AUAGGGGUUUUGGCCUCU GACUGACUCCUACCUGUU AGCAUUAACAG	UUA AUGCUAAU GUGAUAGGGGU
002406	mmu-let-7e-5p	CGCGCCCCCGGGCUGAG GUAGGAGGUUGUAUAGUU GAGGAAGACACCCGAGGA GAUCACUAUACGGCCUCC UAGCUUCCCCAGGCUGC GCC	UGAGGUAGGAGG UUGUAUAGUU
002278	mmu-miR-145a-5p	CUCACGGUCCAGUUUCC CAGGAAUCCCUUGGAUGC UAAGAUGGGGAUCCUGG AAUACUGUUCUUGAG	GUCCAGUUUCCC AGGAAUCCCU

Table E.6 Endogenous control sequences. Assay ID, assay name and target sequence of endogenous controls for individual Taqman assays

Assay ID	Assay Name	Target Sequence 5' → 3'
001973	U6 snRNA	GTGCTCGCTTCGGCAGCACATATACTAAAATTGGAAC GATACAGAGAAGATTAGCATGGCCCCTGCGCAAGGA TGACACGCAAATTCGTGAAGCGTTCATATTT
001094	RNU44	CCUGGAUGAUGAUAGCAAUUGCUGACUGAACAUAGA AGGUCUUAUUAGCUCUAACUGACU
001006	RNU48	GAUGACCCCAGGUAACUCUGAGUGUGUCGUGAUG CCAUCACCGCAGCGCUCUGACC
001232	snoRNA202	GCTGTACTGACTTGATGAAAGTACTTTTGAACCCTTT TCCATCTGATG
001234	snoRNA234	CTTTTGGAAGTGAATCTAAGTGATTTAACAAAAATTC GTCACTACCACTGAGA
001973	MammuU6	GTGCTCGCTTCGGCAGCACATATACTAAAATTGGAAC GATACAGAGAAGATTAGCATGGCCCCTGCGCAAGGA TGACACGCAAATTCGTGAAGCGTTCATATTT

Appendix F- Endogenous Controls for qPCR

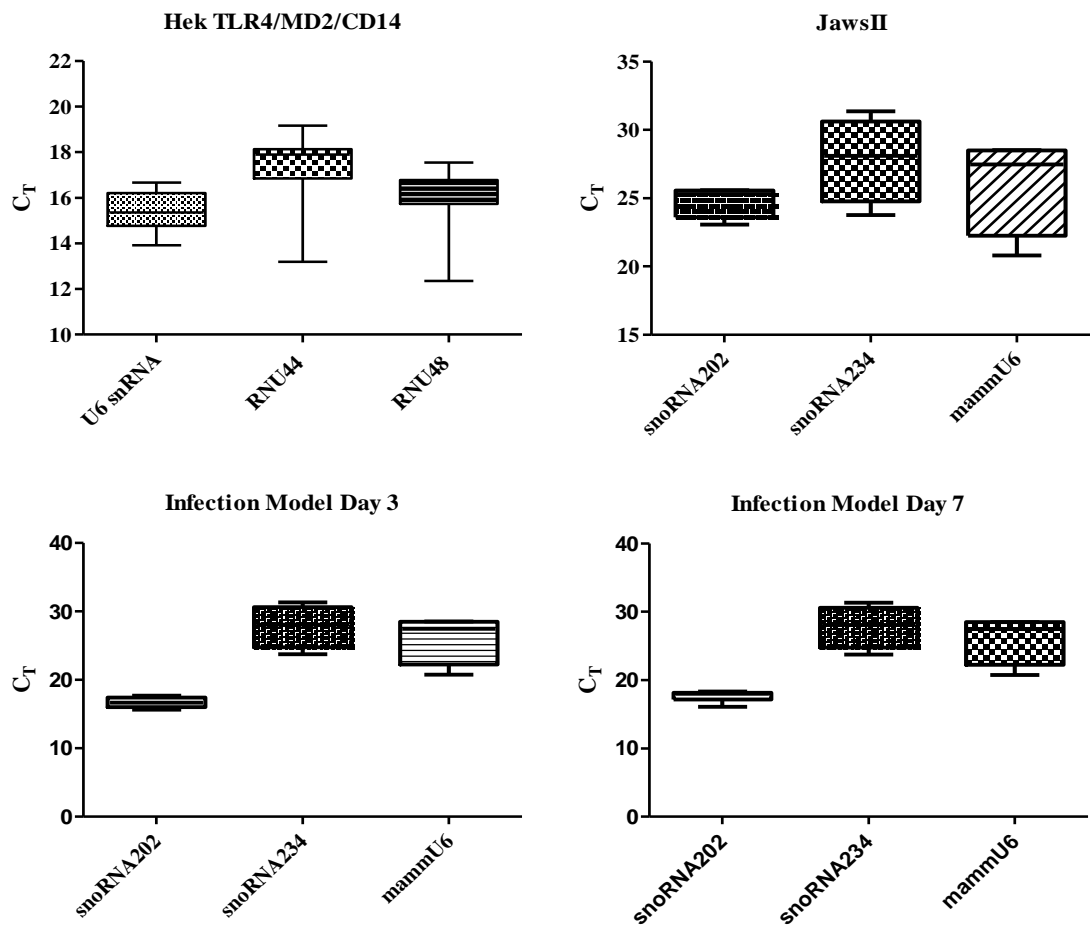


Figure F.1 Endogenous controls for microRNA individual Taqman assays. U6 snRNA was identified as an endogenous control for sample generate from human Hek TLR4/MD2/CD14 cells. snoRNA202 was identified as an endogenous control for samples generated from murine JAWS II cells and murine samples from the infection model at day 3 and day 7.

Appendix G- Bioinformatics

Table G.1 Database and Web links for bioinformatics tools used in this study

Database	Web link
DIANA miRPath	http://diana.imis.athena-innovation.gr/DianaTools/index.php?r=mirpath/index
TargetScan Human	http://www.targetscan.org/
miRNA Converter (miRSystem)	http://mirsystem.cgm.ntu.edu.tw/

Table G.2 miRNA names according to version 18 and 20 of miRBASE. The lists of miRNAs were inputted into miR Converter which is a feature of miRSystem to ensure we had up to date names for each of the miRNAs according to version 18 of miRBASE which is used by DIANA miRPath v2.0 for further analysis

INPUT_ID	ACCESSION	VER_20	VER_18
hsa-let-7b-5p	MIMAT0000063	hsa-let-7b-5p	hsa-let-7b-5p
hsa-let-7c-5p	MIMAT0000064	hsa-let-7c-5p	hsa-let-7c
hsa-let-7d-5p	MIMAT0000065	hsa-let-7d-5p	hsa-let-7d-5p
hsa-let-7e-5p	MIMAT0000066	hsa-let-7e-5p	hsa-let-7e-5p
hsa-miR-125a-5p	MIMAT0000443	hsa-miR-125a-5p	hsa-miR-125a-5p
hsa-miR-1292-5p	MIMAT0005943	hsa-miR-1292-5p	hsa-miR-1292
hsa-miR-132-3p	MIMAT0000426	hsa-miR-132-3p	hsa-miR-132-3p
hsa-miR-145-5p	MIMAT0000437	hsa-miR-145-5p	hsa-miR-145-5p
hsa-miR-146a-5p	MIMAT0000449	hsa-miR-146a-5p	hsa-miR-146a-5p
hsa-miR-148b-3p	MIMAT0000759	hsa-miR-148b-3p	hsa-miR-148b-3p
hsa-miR-152-3p	MIMAT0000438	hsa-miR-152-3p	hsa-miR-152
hsa-miR-155-5p	MIMAT0000646	hsa-miR-155-5p	hsa-miR-155-5p
hsa-miR-215-5p	MIMAT0000272	hsa-miR-215-5p	hsa-miR-215
hsa-miR-221-3p	MIMAT0000278	hsa-miR-221-3p	hsa-miR-221-3p
hsa-miR-24-3p	MIMAT0000080	hsa-miR-24-3p	hsa-miR-24-3p
hsa-miR-339-5p	MIMAT0000764	hsa-miR-339-5p	hsa-miR-339-5p
hsa-miR-374a-5p	MIMAT0000727	hsa-miR-374a-5p	hsa-miR-374a-5p
hsa-miR-422a	MIMAT0001339	hsa-miR-422a	hsa-miR-422a
hsa-miR-432-3p	MIMAT0002815	hsa-miR-432-3p	hsa-miR-432-3p
hsa-miR-543	MIMAT0004954	hsa-miR-543	hsa-miR-543
hsa-miR-586	MIMAT0003252	hsa-miR-586	hsa-miR-586
hsa-miR-590-5p	MIMAT0003258	hsa-miR-590-5p	hsa-miR-590-5p
hsa-miR-9-3p	MIMAT0000442	hsa-miR-9-3p	hsa-miR-9-3p
hsa-miR-9-5p	MIMAT0000441	hsa-miR-9-5p	hsa-miR-9-5p

Table G.3 The 24 miRNAs of interest targeted 2551 genes in 146 different pathways according to KEGG, data generated from DIANA miRPath v2.0. The lists of 24 miRNAs of interest were inputted into the DIANA miRPath prediction tool where a posteriori analysis was performed. The significance levels between all possible miRNA pathway pairs according to KEGG were calculated using enrichment analysis. The previously calculated significance levels were combined with this to provide a merged p-value for each pathway by applying Fisher's combined probability method.

KEGG pathway	p-value	#genes	#miRNAs
Prion diseases	<1E-16	3	3
ECM-receptor interaction	<1E-16	15	6
TGF-beta signalling pathway	<1E-16	42	9
MAPK signalling pathway	<1E-16	98	10
Pathways in cancer	<1E-16	117	10
PI3K-Akt signalling pathway	<1E-16	121	11
Focal adhesion	1.11E-16	74	10
Prostate cancer	1.11E-16	43	11
Transcriptional misregulation in cancer	9.24E-13	68	11
Wnt signalling pathway	2.42E-12	55	11
Endometrial cancer	5.94E-11	24	9
Glioma	8.23E-11	25	8
Regulation of actin cytoskeleton	1.41E-10	69	8
Neurotrophin signalling pathway	1.68E-10	46	9
Hepatitis B	2.62E-10	44	11
Renal cell carcinoma	4.26E-10	26	6
Insulin signalling pathway	2.49E-09	49	11
Chronic myeloid leukaemia	3.54E-09	27	8
Amoebiasis	5.18E-09	20	5
p53 signalling pathway	8.19E-09	25	7
ErbB signalling pathway	1.10E-08	32	8
Small cell lung cancer	1.56E-08	38	10
Hypertrophic cardiomyopathy (HCM)	2.47E-08	29	7
Glycosaminoglycan biosynthesis - chondroitin sulfate	2.73E-07	4	4
B cell receptor signalling pathway	3.78E-07	25	7
T cell receptor signalling pathway	1.08E-06	27	4
mTOR signalling pathway	3.02E-06	25	8
Dilated cardiomyopathy	1.11E-05	31	9
Melanoma	1.50E-05	25	7
Acute myeloid leukaemia	1.61E-05	21	7
Non-small cell lung cancer	3.22E-05	18	7
HTLV-I infection	4.30E-05	47	7
Cytokine-cytokine receptor interaction	6.96E-05	32	6

Pathogenic Escherichia coli infection	7.38E-05	8	1
Colorectal cancer	0.000181	24	6
Long-term potentiation	0.000186	25	4
Axon guidance	0.000288	38	4
Basal cell carcinoma	0.001142	18	6
Circadian rhythm	0.001693	15	5
Arrhythmogenic right ventricular cardiomyopathy (ARVC)	0.002041	12	3
Valine, leucine and isoleucine biosynthesis	0.002189	2	7
Ubiquitin mediated proteolysis	0.003648	33	5
GnRH signalling pathway	0.00863	20	4
Adipocytokine signalling pathway	0.009211	12	4
Dorso-ventral axis formation	0.009752	7	4
Endocytosis	0.012588	35	3
mRNA surveillance pathway	0.012739	23	3
Lysine degradation	0.015693	10	5
Pancreatic cancer	0.017541	19	4
Gap junction	0.022004	14	3
VEGF signalling pathway	0.02785	17	3
Adherens junction	0.031416	27	5
Jak-STAT signalling pathway	0.04341	23	4
Protein digestion and absorption	0.053215	10	3
Fc epsilon RI signalling pathway	0.055219	9	2
Thyroid cancer	0.058518	10	5
HIF-1 signalling pathway	0.065032	14	2
Mucin type O-Glycan biosynthesis	0.066994	7	5
Melanogenesis	0.069544	14	3
Biosynthesis of unsaturated fatty acids	0.086606	4	1
Dopaminergic synapse	0.089544	30	3
Osteoclast differentiation	0.09518	32	4
Phosphatidylinositol signalling system	0.096817	25	5
RNA transport	0.13389	13	3
Biotin metabolism	0.134585	1	2
GABAergic synapse	0.157337	12	3
Chemokine signalling pathway	0.171029	32	3
ABC transporters	0.17257	6	2
Type II diabetes mellitus	0.181815	5	3
Cholinergic synapse	0.210517	27	4
Inositol phosphate metabolism	0.213264	14	4
Cell cycle	0.215188	14	3
Renin-angiotensin system	0.240273	5	1
Gastric acid secretion	0.248511	16	4
Bacterial invasion of epithelial cells	0.293373	20	4
Hedgehog signalling pathway	0.29584	12	3
Calcium signalling pathway	0.379276	8	1

Amphetamine addiction	0.408419	18	3
Protein processing in endoplasmic reticulum	0.42342	8	1
Viral carcinogenesis	0.438084	27	3
RNA degradation	0.46417	11	3
Hepatitis C	0.465413	10	1
Endocrine and other factor-regulated calcium reabsorption	0.488316	12	2
Viral myocarditis	0.504112	8	4
Apoptosis	0.514354	9	3
Long-term depression	0.531543	16	3
Pancreatic secretion	0.663237	12	2
Aldosterone-regulated sodium reabsorption	0.668861	10	3
Herpes simplex infection	0.691523	25	3
Epstein-Barr virus infection	0.707393	13	1
Vascular smooth muscle contraction	0.719352	5	2
Retrograde endocannabinoid signalling	0.726176	13	2
Toll-like receptor signalling pathway	0.726836	18	3
Tight junction	0.761025	17	2
Glutamatergic synapse	0.798927	20	2
Shigellosis	0.835699	14	2
Oocyte meiosis	0.864453	12	2
Chagas disease (American trypanosomiasis)	0.900815	6	1
Sphingolipid metabolism	0.934722	6	1
African trypanosomiasis	0.93694	3	1
Fanconi anemia pathway	0.958664	2	1
Other glycan degradation	0.968731	2	3
Amyotrophic lateral sclerosis (ALS)	0.969045	5	1
Measles	0.970755	9	1
Terpenoid backbone biosynthesis	0.979777	7	2
Salivary secretion	0.980074	5	1
RIG-I-like receptor signalling pathway	0.98462	5	1
Glycerophospholipid metabolism	0.988557	8	1
Notch signaling pathway	0.989326	4	1
Butanoate metabolism	0.99052	4	1
NOD-like receptor signalling pathway	0.99096	9	2
Glycosaminoglycan biosynthesis - keratan sulfate	0.993582	3	3
Sulfur relay system	0.993763	2	2
NF-kappa B signalling pathway	0.993981	6	2
Serotonergic synapse	0.994442	8	2
Influenza A	0.995537	15	2
Maturity onset diabetes of the young	0.995979	4	1
Carbohydrate digestion and absorption	0.997374	5	1
One carbon pool by folate	0.997636	5	2
Cardiac muscle contraction	0.998475	2	1
Circadian entrainment	0.998884	6	1

Nicotinate and nicotinamide metabolism	0.998966	2	1
Leukocyte transendothelial migration	0.99939	8	1
Fructose and mannose metabolism	0.999642	4	1
Legionellosis	0.999699	4	1
Nucleotide excision repair	0.999877	2	1
Valine, leucine and isoleucine degradation	0.999898	1	1
Pentose phosphate pathway	0.999953	4	2
Alcoholism	0.999968	9	1
Taurine and hypotaurine metabolism	0.99997	1	1
Folate biosynthesis	0.999977	1	1
Pantothenate and CoA biosynthesis	0.999992	3	1
Type I diabetes mellitus	0.999994	4	1
Vasopressin-regulated water reabsorption	0.999998	5	1
Glycosylphosphatidylinositol(GPI)-anchor biosynthesis	0.999998	3	1
Glycosphingolipid biosynthesis - globo series	0.999999	1	1
DNA replication	0.999999	2	1
Fat digestion and absorption	1	3	1
Graft-versus-host disease	1	3	1
Galactose metabolism	1	3	1
Fatty acid elongation	1	1	1
Tyrosine metabolism	1	2	1
D-Glutamine and D-glutamate metabolism	1	1	1
Lipoic acid metabolism	1	1	1
Metabolism of xenobiotics by cytochrome P450	1	1	1
Phagosome	1	6	1

Table G.4 Complete list of miRNAs of interest predicted from DIANA-miRPath v2.0 and crossed checked in TargetScan. Table showing Gene, conserved miRNAs from the 24 miRNAs of interest, the position in the gene, seed match and the probability of conserved targeting (P_{CT}).

Gene	Conserved miRNA seed regions in 3'UTR	Position in Gene 3'→5'	Seed Match	P_{CT}
ITGA9	miR-125a-5p	281-287	7mer-m8	0.91
	miR-148b	402-408	7mer-1A	0.85
	miR-152	402-408	7mer-1A	< 0.1
ITGA5	miR-148b	187-193, 902-909	7mer-m8, 8mer	0.39, 0.71
	miR-152	187-193, 902-909	7mer-m8, 8mer	0.39, 0.71
COL3A1	let-7 b/c/d/e	408-415	8mer	0.95
ITGA11	let-7 b/c/d/e	784-790	7mer-A1	0.91
	miR-148b	1082-1089	8mer	0.86
	miR-152	1082-1089	8mer	0.86
COL2A1	miR-148b	82-89	8mer	0.80
COL4A2	let-7 b/c/d/e	49-55	7mer-A1	0.95
	miR-9	107-113	7mer-m8	0.79
COL1A1	let-7 b/c/d/e	789-795	7mer-m8	0.89
COL4A6	let-7 b/c/d/e	265-272	8mer	0.95
COL5A2	let-7 b/c/d/e	1051-1058	8mer	0.95
COL4A1	miR-148b	266-273	8mer	0.61
	miR-152	266-273	8mer	0.61
	miR-590-5p	194-200	7mer-m8	0.22
	let-7 b/c/d/e	88-94	7mer-A1	0.85
LAMA4	miR-148b	41-47	7mer-A1	0.78
	miR-152	41-47	7mer-A1	0.78
SOS2	miR-148b	257-263, 300-307	7mer-m8, 8 mer	0.48, 0.78
	miR-152	257-263, 300-307	7mer-m8, 8 mer	0.48, 0.78
	miR-145-5p	25-31	7mer-A1	0.58
FGF12	miR-9	174-180	7mer-m8	0.54
CHUK	let-7 b/c/d/e	495-501	7mer-m8	0.44
KRAS	miR-155	205-211	7mer-m8	0.23
FGF9	miR-155	717-724	8mer	0.34
	miR-9	1067-1073	7mer-m8	0.72
NGF	let-7 b/c/d/e	65-61	8mer	0.95
RASGRF1	miR-125a-5p	1228-1234	7mer-m8	0.91
RELA	miR-155	1406-1413	8mer	0.59
FGFR1	miR-125a-5p	417-423	7mer-m8	0.23
ROCK1	miR148-b	867-873, 1414-1420	7mer-m8, 7mer-A1	0.93
	miR152	867-873, 1414-1420	7mer-m8, 7mer-A1	0.86
	miR-145	1357-1363	7mer-A1	> 0.99
ITGB8	miR-145	4500-4507	8mer	0.77

	miR-221	227-233	7mer-A1	0.86
	miR-152	290-296	7mer-A1	0.83
	miR-148b	290-296	7mer-A1	0.83
	let-7 b/c/d/e	1606-1612	7mer-m8	0.91
COL4A5	let-7 b/c/d/e	165-171	7mer-A1	0.79
RAF1	miR-125a-5p	641-648	8mer	< 0.1
PIK3R3	miR-152	202-209	8mer	0.58
	miR-148b	202-209	8mer	0.58
	miR-9	495-501	7mer-m8	0.91
	miR-24	1548-1555	8mer	0.43
PDK1	miR-155	2525-2532	8mer	< 0.1
COL1A2	let-7 b/c/d/e	378-385	8mer	0.95
PPP2CB	miR-132	262-268	7mer-m8	0.23
COL11A1	let-7 b/c/d/e	748-754	7mer-A1	0.84
PTEN	miR-152	2254-2260, 3151-3158	7mer-m8, 8mer	0.86, 0.88
	miR-148b	2254-2260, 3151-3158	7mer-m8, 8mer	0.86, 0.88
RPS6KB1	miR-145	819-826	8mer	0.59
	miR-24	1652-1685	7mer-A1	0.17
PPP2CA	miR125a-5p	476-482	7mer-A1	0.81
GSK3B	miR-132	2665-2671	7mer-A1	0.27
	miR-9	3645-3651	7mer-m8	0.72
	miR-24	4111-4118	8mer	0.37
TSC1	let-7 b/c/d/e	720-726	7mer-m8	0.89
PDGFRA	miR-24	2116-2123	8mer	0.42
PPP2R5E	miR-132	956-962	7mer-m8	0.27
	miR-148b	3465-3472	8mer	< 0.1
	miR-152	3465-3472	8mer	< 0.1
MYB	miR-155	15-21	7mer-m8	0.23
PRKAA2	miR-125a-5p	3542-3549	8mer	0.26
	miR-146a	3943-3950	8mer	< 0.1
	let b/c/d/e	6617-66624	8mer	0.95
CREB5	miR-9	4013-4019, 5055-5061	7mer-m8	0.70, 0.68
	miR-132	5493-6499	7mer-m8	0.28
	miR-145	4393-4400	8mer	0.62
YWHAG	miR-132	232-238	7mer-m8	0.44
	miR-125a-5p	940-947	8mer	0.47
	miR-221	2737-2743	7mer-m8	0.10
	miR-145	1993-1999	7mer-A1	0.59
CREB1	miR-155	157-163	7mer-A1	0.56
	miR-125a-5p	5078-5084, 5900-5906	7mer-m8	0.57, 0.78
ANGPT2	miR-145	331-338	8mer	0.91
	miR-125a-5p	495-501	7mer-A1	0.53
CDKN1B	miR-221	201-208, 274-281	8mer	0.68
	miR-24	1253-1260	8mer	0.84
	miR-148b	128-134	7mer-A1	N/A
	miR-152	128-134	7mer-A1	N/A
YWHAB	miR-148b	1698-1705	8mer	0.86
		1698-1705	8mer	0.86

GNB1	miR-145	28-34	7mer-A1	0.51
PPP2R5C	miR-125a-5p	1262-1268	7mer-m8	0.73
	miR-132	2232-2238	7mer-m8	0.33
CDK6	miR-148b	2270-2277	8mer	0.66
	miR-152	2270-2277	8mer	0.66
	miR-145 let-7 b/c/d/e	2388-2395, 9872-9878 854-860	8mer, 7mer-m8 7mer-m8	0.76, 0.65 0.83
GHR	let-7 b/c/d/e	2246-2252	7mer-A1	0.95
EIF4E	miR-9	69-69	7mer-m8	0.92
CCNE2	miR-9	677-684	8mer	0.61
PPP2R2A	miR-9	1404-1410	7mer-A1	0.58
	miR-221	452-458	7mer-A1	0.35
	let-7 b/c/d/e	745-751	7mer-m8	0.80
PIK3R1	miR-221	522-529	8mer	0.67
	miR-590-5p	861-867	7mer-m8	0.51
	miR-155	3718-3724	7mer-m8	0.23
YWHAZ	miR-155	1353-1360	8mer	0.46
KITLG	miR-132	18-24	7mer-A1	0.28
	miR-9	1647-1654	8mer	< 0.1
INSR	let-7 b/c/d/e	2393-2400	8mer	0.96
PRKAA1	miR-148b	2069-2076	8mer	0.75
	miR-152	2069-2076	8mer	0.75
FGF2	miR-148b	3114-3121	8mer	< 0.1
	miR-152	3114-3121	8mer	< 0.1
BCL2L1	let-7 b/c/d/e	945-952	8mer	0.81
CREB3L2	miR-9	1253-1259	7mer-A1	0.82
FOXO3	miR-132	162-169	8mer	0.77
	miR-155	1497-1503	7mer-m8	0.23
	miR-9	3175-3181	7mer-m8	0.86
PKN2	miR-145	205-211	7mer-A1	0.66
	miR-155	1969-1976	8mer	0.20
	let-7 b/c/d/e	1228-1234	7mer-A1	0.83
CDKN1A	let-7 b/c/d/e	943-950	8mer	0.82
	miR-132	1365-1371	7mer-m8	0.12
SGK3	miR-132	287-293, 332-338	7mer-m8	0.55, 0.22
	miR-9	998-1004	7mer-A1	0.72
	miR-155	249-256	8mer	0.45
CSF1R	miR-24	215-221, 584-590	7mer-m8, 7mer-A1	0.46, 0.17
	miR-155	763-770	8mer	0.21
OSMR	let-7 b/c/d/e	756-763	8mer	0.95
CSF1	miR-148b	801-807, 902-909	7mer-m8, 8mer	0.72, <
	miR-152	801-807, 902-909	7mer-m8, 8mer	0.1 0.72, < 0.1
GNG5	let-7 b/c/d/e	149-155	7mer-m8	0.96
TEK	miR-148b	894-901	8mer	0.29
	miR-152	894-901	8mer	0.29
BCL2L11	miR-24	442-449, 2678-2685	8mer	0.82, 0.84

	miR-221	4052-4059	8mer	0.68
	miR-148b	3996-4002, 4094-4101	7mer-A1, 8mer	0.76, 0.89
	miR-152	3996-4002, 4094-4101	7mer-A1, 8mer	0.76, 0.89
	miR-9	1927-1934	8mer	0.90
EFNA1	miR-145	731-737	7mer-m8	0.59
	miR-9	273-279	7mer-A1	0.80
INHBB	miR-148b	1459-1466	8mer	0.86
	miR-152	1459-1466	8mer	0.86
	miR-145	1370-1376	7mer-m8	0.61
	miR-9	1575-1852	8mer	0.91
BMPR1B	miR-125a-5p	141-148	8mer	< 0.1
PITX2	miR-590-5p	278-284	7mer-m8	0.50
SMAD3	miR-145	1397-1404, 3925-3931	8mer, 7mer-m8	0.85, 0.60
ID4	miR-9	1201-1207, 1248-1254, 2714-2721	7mer-m8, 7mer-A1, 8mer	0.71, 0.68, < 0.1
ACVR1	miR-148b	449-455	7mer-m8	0.66
	miR-152	449-455	7mer-m8	0.66
	miR-155	304-310	7mer-A1	0.38
SKP1	miR-148b	51-57	7mer-m8	0.92
	miR-152	51-57	7mer-m8	0.92
	miR-145	420-427	8mer	0.55
	miR-221	521-528	8mer	0.10
ZFYVE16	miR-221	882-889	8mer	0.63
E2F5	miR-132	18-25	8mer	< 0.1
	let-7 b/c/d/e	27-33	7mer-m8	0.84
	miR-132	18-25	8mer	< 0.1
SMAD5	miR-145	261-268	8mer	0.82
	miR-148b	532-538	7mer-m8	0.32
	miR-152	532-538	7mer-m8	0.32
	miR-132	1036-1043	8mer	0.10
	miR-155	830-836	7mer-A1	0.40
	miR-24	2166-2172	7mer-m8	0.41
ACVR2A	miR-145	40-46	7mer-m8	0.37
	miR-155	559-565	7mer-m8	0.23
	let-7 b/c/d/e	589-595	7mer-A1	0.88
GDF6	miR-148b	1825-1831	7mer-m8	0.89
	miR-152	1825-1831	7mer-m8	0.89
	miR-155	1994-2001	8mer	0.70
	let-7 b/c/d/e	2094-2101	8mer	0.96
ACVR1C	let-7 b/c/d/e	90-97	8mer	0.96
	miR-125a-5p	1965-1972	8mer	0.35
	miR-9	6759-6765	7mer-A1	0.76
GDF5	miR-132	508-515	8mer	0.14
TGFB2	miR-145	284-290, 2098-2105	7mer-A1, 8mer	0.94, 0.36
	miR-590-5p	1282-1289	8mer	0.78
	miR-148b	2300-2307	8mer	0.89
	miR-152	2300-2307	8mer	0.89
EP300	miR-132	1065-1072	8mer	0.65

LTBP1	miR-148b	34-40	7mer-m8	0.62
	miR-152	34-40	7mer-m8	0.61
SMAD7	miR-590-5p	1122-1129	8mer	0.80
NOG	miR-148b	172-178	7mer-m8	0.58
	miR-152	172-178	7mer-m8	0.58
BMPR2	miR-125a-5p	6570-6576	7mer-m8	0.81
	miR-590-5p	7554-7561, 7739-7745	8mer, 7mer-m8	< 0.1, 0.51
ACTB	miR-145	145-152	8mer	0.75
SHC1	miR-9	209-215, 1465-1471	7mer-m8	0.75, 0.90
COL24A1	let-7 b/c/d/e	485-491	7mer-m8	0.91
VCL	miR-590-5p	283-289, 1908-1915	7mer-m8, 8mer	0.51, 0.36
	miR-9	1680-1686	7mer-A1	0.82
CAV2	miR-148b	750-756	7mer-m8	0.44
	miR-152	750-756	7mer-m8	0.44
	miR-145	1806-1813	8mer	0.55
PPP1R12	miR-148b	1202-1208	7mer-m8	0.63
	miR-152	1202-1208	7mer-m8	0.63
SRC	miR-9	419-425	7mer-A1	0.77
PAK4	miR-9	22-29	8mer	0.95
	miR-145	294-300	7mer-A1	0.91
	miR-24	470-477	8mer	0.76
VAV3	miR-125a-5p	235-241	7mer-A1	0.74
	miR-155	1357-1364	8mer	< 0.1
	let-7 b/c/d/e	1549-1555	7mer-A1	0.95
	miR-9	2032-2039	8mer	0.95
MYLK	miR-155	179-185	7mer-A1	0.71
	miR-9	1017-1023	7mer-A1	0.75
	miR-24	485-491	7mer-A1	0.17
XIAP	miR-146a	2795-2802	8mer	< 0.1
	miR-155	3253-3259	7mer-m8	0.23
PPP1CB	miR-148b	64-70	7mer-m8	0.91
	miR-152	64-70	7mer-m8	0.91
FOS	miR-221	203-210	8mer	0.62
	miR-155	325-332	8mer	0.55
NTF3	miR-221	52-59	8mer	0.66
	miR-590-5p	133-139	7mer-m8	0.50
GNA12	miR-132	2521-2527	7mer-A1	0.28
IL1R1	miR-24	2916-2922	7mer-A1	0.17
RASA2	miR-145	24-31	8mer	0.88
	miR-9	2497-2503	7mer-A1	0.62
	miR-125a-5p	627-633	7mer-A1	0.81
	miR-590-5p	1369-1376	8mer	0.53
ELK4	miR-145	3369-3676, 6526-6533	8mer	0.47, 0.89
	let-7 b/c/d/e	2556-2562	7mer-m8	0.89
	miR-221	8492-8498	7mer-A1	0.48
MAP3K3	miR-9	560-567, 1804-1810	7mer-m8	0.79, 0.35
	miR-145	760-766	7mer-m8	0.36

	miR-125a-5p	597-603	7mer-A1	0.54
	let-7 b/c/d/e	1201-1207	7mer-A1	0.88
	miR-132	1576-1583	8mer	0.74
MAP2K7	miR-125a-5p	644-650	7mer-m8	0.88
	miR-9	758-764, 1385-1391	7mer-m8	0.88,0.56
CACNB4	miR-221	5624-5271, 6086-6092	8mer, 7mer-A1	0.44, 0.35
	miR-155	2250-2256	7mer-m8	0.23
	let-7 b/c/d/e	3640-3646	7mer-m8	0.48
DUSP6	miR-9	423-429	7mer-A1	0.82
	miR-145	1018-1025	8mer	0.90
	miR-125a-5p	952-958	7mer-A1	0.81
MAP4K3	let-7 b/c/d/e	1056-1063	8mer	0.94
RPS6KA1	miR-125a-5p	777-783	7mer-m8	0.75
GADD45A	miR-148b	32-39	8mer	0.64
	miR-152	32-39	8mer	0.64
MAP3K4	miR-148b	384-391	8mer	0.79
	miR-152	384-391	8mer	0.79
MAP3K1	miR-9	2183-2189	7mer-m8	0.80
	let-7 b/c/d/e	2152-2159	8mer	0.94
MAP3K13	let-7 b/c/d/e	848-855	8mer	0.71
TAB2	let-7 b/c/d/e	160-166	7mer-A1	0.87
	miR-155	818-825	8mer	0.49
BDNF	miR-155	271-278	8mer	0.93
MAP3K11	miR-145	56-62	7mer-A1	0.71
	miR-125a-5p	271-278	8mer	0.93
TAOK1	miR-24	1216-1223, 4409-4416	8mer	0.81, 0.44
	let-7 b/c/d/e	2787-2793	7mer-m8	0.74
	miR-145	3493-3499, 4794-4801	8mer	0.65, 0.47
	miR-221	5695-5701	7mer-m8	0.10
	miR-155	7492-7498	7mer-A1	0.37
FGF11	miR-24	388-395	8mer	0.58
	let-7 b/c/d/e	1192-1199	8mer	0.94
PPP3CA	miR-145	736-743	8mer	0.76
	miR-590-5p	1129-1135	7mer-m8	0.50
	let-7 b/c/d/e	638-644	7mer-A1	0.81
NLK	miR-24	411-417	7mer-A1	0.17
	miR-221	32-38	7mer-m8	0.10
	miR-148b	879-885	7mer-m8	0.59
	miR-152	879-885	7mer-m8	0.59
	let-7 b/c/d/e	1116-1133	7mer-m8	0.90
	miR-132	1349-1355	7mer-A1	0.27
CASP3	let-7 b/c/d/e	317-324	8mer	0.95
RASGRP1	let-7 b/c/d/e	493-500	8mer	0.95
RAPGEF2	miR-145	1043-1049	7mer-m8	0.65
	miR-155	1731-1738	8mer	0.15
PPM1A	miR-125a-5p	2583-2589	7mer-m8	0.85
CACNB1	miR-125a-5p	1168-1175	8mer	0.84
CACNA1	miR-24	2361-2368	8mer	0.35

CACNAE	let-7 b/c/d/e	1368-1374	7mer-A1	0.91
	miR-9	2032-2038	7mer-m8	0.70
DUSP8	miR-590-5p	1650-1657	8mer	0.81
	miR-9	479-584	7mer-m8	0.38
	miR-24	401-407	7mer-m8	0.74
	miR-148b	1790-1796	7mer-m8	0.39
	miR-152	1790-1796	7mer-m8	0.39
PPP3R1	miR-221	189-195, 343-349	7mer-A1, 7mer-m8	0.47, 0.10
FAS	let-7 b/c/d/e	879-886	8mer	0.73
RPS6KA3	let-7 b/c/d/e	4432-4438	7mer-m8	0.94
	miR-155	312-318	7mer-m8	0.23
	miR-590-5p	4486-4492	7mer-m8	0.50
	miR-145	3929-3935	7mer-m8	0.44
MAPK12	miR-125a-5p	378-385	8mer	0.75
CACNB2	miR-125a-5p	1164-1170	7mer-A1	0.55
	miR-145	1279-1285	7mer-A1	0.75
	miR-9	1510-1516	7mer-m8	0.52
MEF2C	miR-590-5p	192-198	7mer-m8	0.45
	miR-9	3788-3795	8mer	0.89
	let-7 b/c/d/e	3889-3895, 3906-3912	7mer-A1	0.82, 0.79
IL1A	miR-24	105-111	7mer-m8	0.46
MAP2K4	miR-145	340-346	7mer-A1	0.53
SRF	miR-9	153-159	7mer-A1	0.58
	miR-125a-5p	2055-2061	7mer-A1	0.37
DUSP1	let-7 b/c/d/e	433-439	7mer-A1	0.95
MAPK10	miR-590-5p	604-610	7mer-m8	0.45
	miR-221	705-711	7mer-m8	0.10
PDGFRB	miR-24	232-239	8mer	0.56
	miR-9	1763-1770	8mer	0.95
CACNB3	miR-125a-5p	338-345	8mer	0.76